UNIVERSIDADE FEDERAL DO PARANÁ

TALITA HELEN BOMBARDELLI GOMIG LAZAROTTO

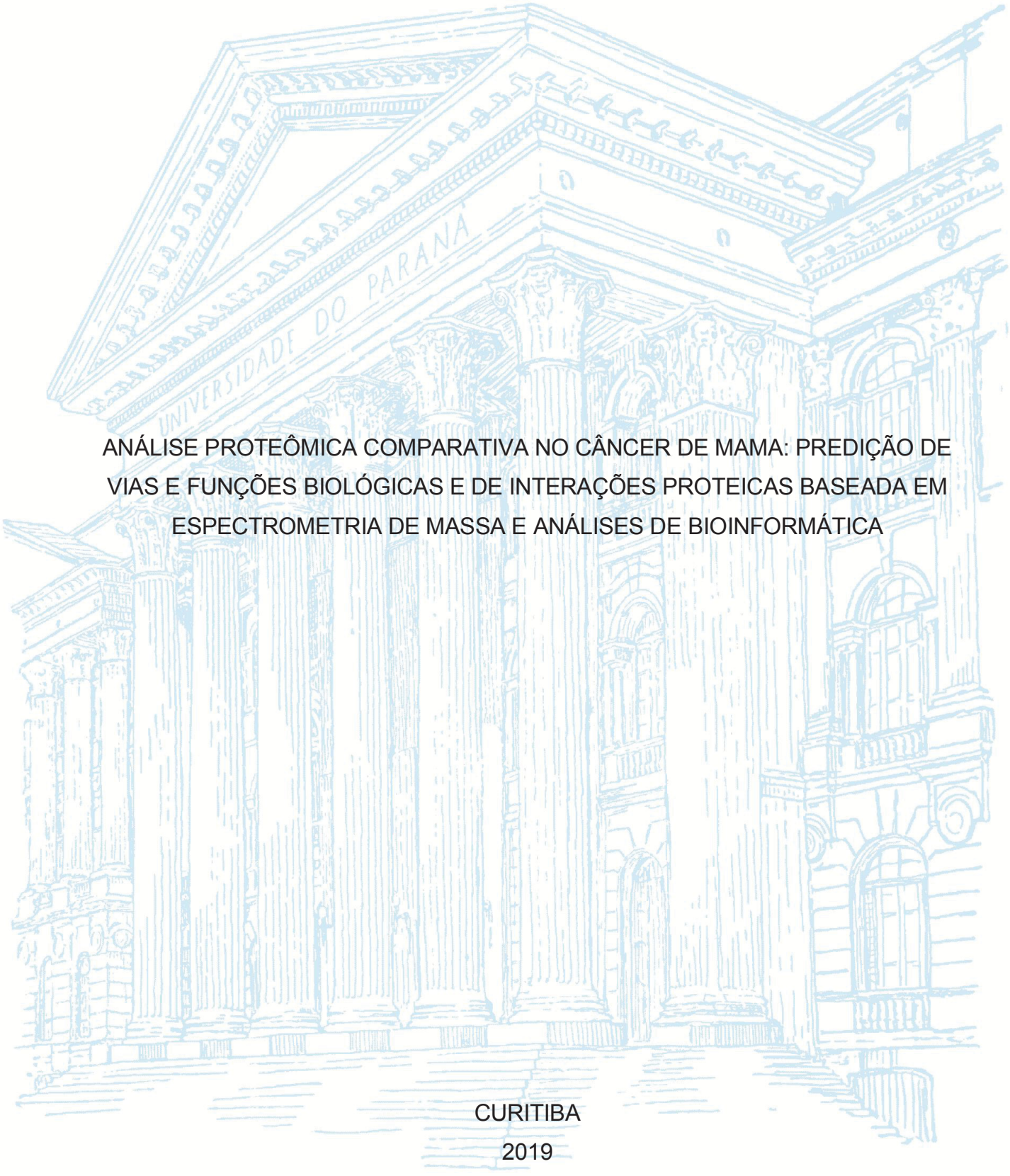

ANÁLISE PROTEÔMICA COMPARATIVA NO CÂNCER DE MAMA: PREDIÇÃO DE VIAS E FUNÇÕES BIOLÓGICAS E DE INTERAÇÕES PROTEICAS BASEADA EM ESPECTROMETRIA DE MASSA E ANÁLISES DE BIOINFORMÁTICA

CURITIBA

2019

TALITA HELEN BOMBARDELLI GOMIG LAZAROTTO

ANÁLISE PROTEÔMICA COMPARATIVA NO CÂNCER DE MAMA: PREDIÇÃO DE VIAS E FUNÇÕES BIOLÓGICAS E DE INTERAÇÕES PROTEICAS BASEADA EM ESPECTROMETRIA DE MASSA E ANÁLISES DE BIOINFORMÁTICA

Tese apresentada ao curso de Pós-Graduação em Genética, Setor de Ciências Biológicas, Universidade Federal do Paraná, como requisito parcial à obtenção do título de Doutor em Genética.

Orientador: Prof. Dr. Iglenir João Cavalli

Coorientador(a): Prof(a). Dr(a). Enilze Maria de Souza Fonseca Ribeiro

CURITIBA

2019

Universidade Federal do Paraná. Sistema de Bibliotecas.
Biblioteca de Ciências Biológicas.
(Carla Fabiane Rasmussen – CRB/9-940)

Lazarotto, Talita Helen Bombardelli Gomig.
Análise proteômica comparativa no câncer de mama: predição de vias e funções biológicas e de interações proteicas baseadas em espectometria de massa e análises de bioinformática. / Talita Helen Bombardelli Gomig Lazarotto. – Curitiba, 2019.
274 p. : il.

Orientador: Iglenir João Cavalli.
Coorientadora: Enilze Maria de Souza Fonseca Ribeiro.

Tese (Doutorado) – Universidade Federal do Paraná, Setor de Ciências Biológicas. Programa de Pós-Graduação em Genética.

1. Mamas - Câncer. 2. Proteômica. 3. Bioinformática. I. Título. II. Cavalli, Iglenir João. III. Ribeiro, Enilze Maria de Souza Fonseca. IV. Universidade Federal do Paraná. Setor de Ciências Biológicas. Programa de Pós-Graduação em Genética.

CDD(20.ed.)5614.5999449

MINISTÉRIO DA EDUCAÇÃO
SETOR DE CIENCIAS BIOLOGICAS
UNIVERSIDADE FEDERAL DO PARANÁ
PRÓ-REITORIA DE PESQUISA E PÓS-GRADUAÇÃO
PROGRAMA DE PÓS-GRADUAÇÃO GENÉTICA - 40001016006P1

TERMO DE APROVAÇÃO

Os membros da Banca Examinadora designada pelo Colegiado do Programa de Pós-Graduação em GENÉTICA da Universidade Federal do Paraná foram convocados para realizar a arguição da tese de Doutorado de **TALITA HELEN BOMBARDELLI GOMIG LAZAROTTO** intitulada: **ANÁLISE PROTEÔMICA COMPARATIVA NO CÂNCER DE MAMA: PREDIÇÃO DE VIAS E FUNÇÕES BIOLÓGICAS E DE INTERAÇÕES PROTEICAS BASEADA EM ESPECTROMETRIA DE MASSA E ANÁLISES DE BIOINFORMÁTICA**, que após terem inquirido a aluna e realizada a avaliação do trabalho, são de parecer pela sua aprovação no rito de defesa.

A outorga do título de doutor está sujeita à homologação pelo colegiado, ao atendimento de todas as indicações e correções solicitadas pela banca e ao pleno atendimento das demandas regimentais do Programa de Pós-Graduação.

CURITIBA, 22 de Fevereiro de 2019.

IGLENIR JOÃO CAVALLI
Presidente da Banca Examinadora

JAQUELINE CARVALHO DE OLIVEIRA
Avaliador Interno (UNIVERSIDADE FEDERAL DO PARANÁ)

FABIO PASSETTI
Avaliador Externo (FUNDAÇÃO OSWALDO CRUZ, INSTITUTO CARLOS CHAGAS, CURITIBA-PR,)

SHEILA MARIA BROCHADO WINNISCHOFER
Avaliador Externo (UNIVERSIDADE FEDERAL DO PARANÁ)

ANA CLAUDIA BONATTO
Avaliador Interno (UNIVERSIDADE FEDERAL DO PARANÁ)

AGRADECIMENTOS

Primeiramente, à Deus, por cada oportunidade e por todos em minha vida.

Aos meus orientadores, pelos ensinamentos transmitidos e construídos em nossos dez anos de convivência, e pela oportunidade de crescimento pessoal e profissional que têm proporcionado. Agradeço pela confiança em mim e em meu trabalho desde os tempos da Iniciação Científica e, em especial, pela dedicação para com minha formação e pela grande amizade que permanece.

A todos os professores, pesquisadores, técnicos e demais profissionais que contribuíram de variadas formas para o meu aprendizado e para a execução deste e de outros estudo dos quais participei. À todas as instituições envolvidas e seus integrantes e, em particular, aos pacientes que aceitaram participar dessa e de outras pesquisas científicas, à equipe médica e aos funcionários dos hospitais. E ao apoio financeiro das agências de fomento, CAPES, CNPq e Fundação Araucária.

Aos membros da banca, pelo aceite em participar da defesa de tese e por contribuírem com seus conhecimentos e reflexões.

Aos integrantes do Laboratório de Citogenética Humana e Oncogenética, antigos e atuais, pela amizade, apoio e convivência. Em especial, às pessoas que dedicaram seu tempo e seus esforços para me ajudar em experimentos e interpretações de resultados. De forma singular, agradeço com muito carinho às amizades concretizadas ao longo desses anos... Sem vocês, a rotina de trabalho e a vida não seriam as mesmas. Obrigada por partilharem de tantos momentos, histórias, loucuras e desafios.

À minha família de amigos, pelos momentos de descontração, encontros, conversas e risadas, especialmente por se fazerem presentes mesmo em minhas ausências. Agradeço a compreensão e o apoio de sempre.

Em especial e com muito amor e carinho, agradeço aos meus familiares e à minha família, pela parceria e por todo o suporte, incentivo e confiança em meus passos ao longo desses anos de dedicação à pesquisa. Obrigada pelo amor e carinho, e por cada exemplo, oportunidade e ensinamento propiciados. A gratidão por ter vocês em minha vida é imensurável.

A tudo e a todos que contribuíram, direta ou indiretamente, afetiva ou profissionalmente, para a minha formação e conclusão deste trabalho, meus sinceros agradecimentos!

*“First, **think.***

*Second, **believe.***

*Third, **dream.***

*And finally, **dare.**”*

Walt Disney

RESUMO

O câncer de mama é o mais comum em mulheres no mundo e o segundo mais incidente em mulheres no Brasil, após o câncer de pele não melanoma. Em homens, é uma malignidade pouco frequente representando cerca de 1,8% dos casos de câncer de mama em geral. Tecnologias de alta resolução aliadas à bioinformática têm sido utilizadas como estratégias de estudo para auxiliar no diagnóstico, na seleção da terapia e no prognóstico do câncer. Nesse contexto, as análises de proteoma e interatoma consistem em importantes abordagens para evidenciar os principais processos biológicos associados à tumorigênese, uma vez que níveis de expressão proteica alterados podem influenciar vias celulares críticas e redes de interações, e comprometer a homeostase do ambiente tecidual, contribuindo para o desenvolvimento do câncer. Neste estudo, a espectrometria de massa baseada na quantificação livre de marcação, seguida da anotação/enriquecimento funcional e da predição de redes de interação proteína-proteína, foi realizada para obter um panorama do proteoma diferencial e seu contexto biológico funcional no câncer de mama feminino e masculino. Os níveis de expressão proteica dos tumores primários de mama foram avaliados simultaneamente aos linfonodos axilares metastáticos e tecidos mamários não tumorais para identificar as proteínas diferencialmente expressas entre esses tecidos. Análises *in sílico* dos dados proteômicos foram utilizadas para identificar as vias de sinalização e metabólicas, funções e processos biológicos mais relevantes, bem como redes de interação que envolvem proteínas com alteração de expressão. Os dados referentes à análise do câncer de mama feminino demonstraram um alto nível de similaridade no perfil proteômico de ambos os tecidos mamários não tumorais (contralateral e adjacente) e entre os malignos (tumor primário de mama e linfonodo axilar metastático). O contexto biológico geral dessa análise incluiu as vias de LXR/RXR, óxido nítrico, eNOS, eIF2 e sirtuínas; metabolismo de ácidos graxos; estresse oxidativo; funções relacionadas ao tumor; e o processo metastático; além de funções biológicas agrupadas nos *hallmarks* clássicos do câncer e em fenótipos de estresse, processos metabólicos e vias de sinalização. O proteoma comparativo do câncer de mama masculino, por sua vez, evidenciou várias proteínas diferencialmente expressas entre os tecidos analisados. Em geral, essa análise identificou as vias de sinalização de granzima B, sirtuínas, eIF2, citoesqueleto de actina, eNOS, cálcio e resposta de fase aguda relacionadas às proteínas com alteração de expressão. A análise proteômica comparativa adicional, realizada entre os tecidos de tumor mamário masculino e o de uma paciente do sexo feminino com o mesmo subtipo da doença e parâmetros clinicopatológicos similares, indicou um relevante conjunto de proteínas diferencialmente expressas, envolvido principalmente em processos relacionados ao câncer e na transdução de sinal. Ao todo, este estudo revela perfis proteômicos diferenciais em processos associados e interconectados de sinalização no câncer de mama feminino e masculino e fornece fontes de dados relevantes para a pesquisa do câncer, as quais podem contribuir para procedimentos clínicos no câncer de mama. Para isso, abordagens complementares e estudos de validação são recomendados para confirmar o potencial de proteínas individuais e/ou de vias como marcadores biológicos na tumorigênese mamária.

Palavras-chave: Câncer de mama. Proteômica. LFQ-MS. Bioinformática.

ABSTRACT

Breast cancer is the most common cancer in women worldwide and the second most incident in women in Brazil, after non-melanoma skin cancer. In men, it is a rare malignancy accounting for about 1.8% of overall breast cancer cases. High-throughput technologies allied to bioinformatics have been used as study strategies to assist in the diagnosis, therapy selection, and prognosis of cancer. In this context, proteome and interactome analyses consist in important approaches to highlight the main biological processes associated with tumorigenesis, since the protein levels altered expression can influence critical cellular pathways and interactive networks, and compromise the tissue environment homeostasis contributing to cancer development. In this study, the mass spectrometry-based label-free quantification followed by functional annotation/enrichment and protein-protein interaction networks prediction were performed to obtain a landscape of the differential proteome and its functional biological context in the female and male breast cancer. Protein expression levels of the primary breast tumors were evaluated simultaneously with the corresponding metastatic axillary lymph nodes and the non-tumor breast tissues to identify the differentially expressed proteins among these tissues. *In silico* analyses of the proteomic data were used to identify the most relevant signaling and metabolic pathways, biological functions and processes as well as interaction networks related to the deregulated proteins. Data from female breast cancer analysis demonstrated a high level of similarity in the proteome profile of both non-tumor breast tissues (contralateral and adjacent) and between the malignant ones (primary breast tumor and axillary metastatic lymph nodes). The general biological context of this analysis included the pathways of LXR/RXR, nitric oxide, eNOS, eIF2 and sirtuins; fatty acid metabolism; oxidative stress; tumor-related functions; metastatic process; and to biological roles grouped into the classic hallmarks of cancer and in stress phenotypes, metabolic processes and signaling pathways. The comparative proteome of male breast cancer, on the other hand, highlights various differentially expressed proteins among the tissues analyzed. In general, this analysis identified the signaling pathways of granzyme B, sirtuins, eIF2, actin cytoskeleton, eNOS, calcium and acute phase response related to the deregulated proteins. The additional proteomic comparative analysis, performed between the tissues of the male breast tumor and the ones of a female patient matched for the breast cancer subtype and similar clinico-pathological parameters, indicated an interesting set of differentially expressed proteins, which were mainly involved in cancer-related biological processes and signal transduction. Altogether, this study reveals differential proteomic profiles in cancer associated and interconnected signaling processes in female and male breast cancers and provides relevant data sources for the cancer research, which can ultimately contributes to the clinical approaches in the breast cancer. Therefore, complementary approaches and validation studies are recommended to confirm the potential of individual proteins and/or pathways and cellular processes as biological markers in breast tumorigenesis.

Keywords: Breast cancer. Proteomics. LFQ-MS. Bioinformatics.

LISTA DE FIGURAS

REVISÃO BIBLIOGRÁFICA

MATERIAL E MÉTODOS

CAPITULO I

SUBITEM 6.1

SUBITEM 6.2

SUBITEM 6.3

CAPITULO II

LISTA DE QUADROS

REVISÃO BIBLIOGRÁFICA

MATERIAL E MÉTODOS

LISTA DE TABELAS

CAPITULO I

SUBITEM 6.1

SUBITEM 6.3

CAPÍTULO II

LISTA DE SIGLAS

1D-SDS-PAGE – *One-Dimensional SDS-Polyacrylamide Gel Electrophoresis*
2D-PAGE – *Two-Dimensional Polyacrylamide Gel Electrophoresis*
ABC – Bicarbonato De Amônio
ACN – Acetonitrila
AF – Ácido Fórmico
AGC – *Automatic Gain Control*
AJCC – *American Joint Committee on Cancer*
ANOVA – Análise de Variância
ANT – *Adjacent non-tumor breast tissue*
APCI – *Atmospheric Pressure Chemical Ionization*
APS – Persulfato de Amônio
BC – *Breast Cancer*
CAPES – Coordenação de Aperfeiçoamento de Pessoal de Nível Superior
CDI – Carcinoma Ductal Invasor
CDIS – Carcinoma Ductal *In Situ*
CDM – Centro de Doenças da Mama
CID – *Collision-Induced Dissociation*
CLI – Carcinoma Lobular Invasor
CLIS – Carcinoma Lobular *In Situ*
CNA – *Copy-Number Alterations*
COSMIC – *Catalogue Of Somatic Mutations In Cancer*
CPTAC – *Clinical Proteomic Tumor Analysis Consortium*
CSC – *Cancer Stem Cells*
DAVID – *Database for Annotation, Visualization and Integrated Discovery*
DDA – *Data Dependent Acquisition*
Deps – *Differentially Expressed Proteins*
DIA – *Data Independent Acquisition*
DMSO – Dimetilsulfóxido
DTT – Ditiotreitol
EASE – *Expression Analysis Systematic Explorer*
EMC – *Extracellular matrix*
EMT – *Epithelial–Mesenchymal Transition*
ESI – *Electrospray Ionization*
FASP – *Filter-Aided Sample Preparation*
FBC – *Female Breast Cancer*

FC – *Fold Change*

FDR – *False Discovery Rate*

FPT – *Female-primary breast tumor*

FT-ICR – *Fourier Transform Ion Cyclotron Resonance*

GO – *Gene Ontology*

HC – Hospital das Clínicas

HCL – *Hierarchical Cluster Analysis*

HER2 – Receptor de fator de crescimento epidérmico 2

HNSG – Hospital Nossa Senhora das Graças

HPLC – *High-Performance Liquid Chromatography*

IAA – Iodoacetamida

IARC – *International Agency for Research on Cancer*

IDC – *Invasive Ductal Carcinoma*

INCA – Instituto Nacional de Câncer

IPA – *Ingenuity Pathway Analysis*

kDa – Kilodalton

KEGG – *Kyoto Encyclopedia of Genes and Genomes*

Ki67 – Antígeno marcador de proliferação celular

LabCHO – Laboratório de Citogenética Humana e Oncogenética

LC-ESI-MS/MS – *Liquid Chromatography-Electrospray Ionization-Tandem Mass Spectrometry*

LC-MS/MS – *Liquid Chromatography-Tandem Mass Spectrometry*

LFQ – *Label-Free Quantification*

LFQ-MS – *Label-Free Quantification-Mass Spectrometry*

LN – Linfonodo axilar metastático

log2 FC – *Logarithmized Fold Change*

MALDI – *Matrix-Assisted Laser Desorption/Ionization*

MaSCs – *Mammary Stem Cells*

MBC – *Male Breast Cancer*

MEC – Matriz Extracelular

MLN – *Male-axillary metastatic lymph node*

MNT – *Male-non-tumor breast tissue*

MPT – *Male-primary breast tumor*

MS – *Mass Spectrometry*

MS – Ministério da Saúde

MS1 – *Mass Spectrum*

MS2 – *In Tandem Mass Spectrum*

MSigDB – *Molecular Signatures Database*

NA – Tecido mamário não tumoral adjacente

NAF – *Nipple Aspirate Fluid*

NaN – *Not a Number*

NCT – Tecido mamário não tumoral contralateral

NMWL – *Nominal Molecular Weight Limit*

NT – Tecidos mamários não tumorais

OMS – Organização Mundial da Saúde

p.p.m – Partes por milhão

PANTHER – *Protein ANalysis THrough Evolutionary Relationships*

PCA – *Principal Component Analysis*

P-MBC – Paciente do sexo masculino

PPI – *Protein-Protein Interaction*

PT – *Primary breast tumor*

RE – Receptor de Estrogênio

ROS – *Reactive Oxygen Species*

RP – Receptor de Progesterona

SDS – Dodecil sulfato de sódio

SELDI – *Surface-Enhanced Laser Desorption/Ionization*

SIM – Sistema de Informações sobre Mortalidade

STRING – *Search Tool for the Retrieval of Interacting Genes/Proteins*

SUS – Sistema Único de Saúde

TCGA – *The Cancer Genome Atlas*

TEM – Transição Epitelial-Mesenquimal

TEMED – Tetrametiletilenodiamina

TFA – Ácido Trifluoroacético

TME – Transição Mesenquimal-Epitelial

TOF – *Time-of-Flight*

TP – Tumor primário de mama

Tris-HCl – Tris(hidroximetil)aminometano-Hidrocloreto

UA – Ureia

UFPR – Universidade Federal do Paraná

UICC – *Union for International Cancer Control*

v. – Versão/*Version*

WHO – *World Health Organization*

SUMÁRIO

1 INTRODUÇÃO

A glândula mamária humana apresenta grande complexidade em sua arquitetura e funcionalidade. Redes interconectadas de sinalização, incluindo interações entre os diversos tipos celulares que a compõe, são fundamentais para o desenvolvimento, manutenção e funcionalidade da mesma. Essa complexidade é de relevância para a suscetibilidade a doenças mamárias, incluindo o câncer (NAVARRETE et al., 2005).

O câncer de mama apresenta elevada incidência e mortalidade entre as mulheres, sendo estimado como o principal tipo de câncer que acomete a população feminina no mundo (IARC/WHO, 2019). No Brasil, é o segundo tipo de câncer mais incidente em mulheres, após o câncer de pele não melanoma (INCA/MS, 2017), constituindo um importante problema de saúde pública e justificando a realização de estudos que possam contribuir para novas abordagens diagnósticas, terapêuticas e prognósticas.

Em homens, o câncer de mama é pouco frequente representando cerca de 1,8% dos casos da doença no mundo (FITZMAURICE et al., 2017) e estimativas inferiores a 1% na população brasileira (INCA/MS, 2019). O diagnóstico do câncer de mama masculino é frequentemente realizado em estágios avançados da doença, impactando no prognóstico e sobrevida desses pacientes (CUTULI et al., 2010).

A tumorigênese mamária é de etiologia multifatorial, ou seja, diversos fatores contribuem para a malignidade, com alterações em níveis moleculares distintos, incluindo o genômico, transcriptômico, proteômico e interatômico; entre estes ressalta-se o aumento exponencial de complexidade (CHAKRABORTY et al., 2018). Particularmente, alterações envolvendo o proteoma, definido como o conjunto de proteínas expresso pelo genoma, e suas interações proteicas, que constituem o interatoma, têm sido amplamente descritas no câncer de mama (TENGA; LAZAR, 2014; SUMAN et al., 2016; REN et al., 2018).

A complexidade da tumorigênese mamária está relacionada às diversas vias metabólicas e de sinalização envolvidas em processos celulares que determinam a transformação e progressão de células normais em malignas. Além disso, as diversas funções celulares são reguladas por interações macromoleculares, particularmente com outras proteínas (CAFARELLI et al., 2017), ampliando o repertório de alterações moleculares no câncer. As interações proteicas podem

informar sobre a regulação de vias biológicas, indicando suas complexas funções celulares e o impacto de alterações ou do mal funcionamento dessas interações na biologia da célula, as quais têm sido descritas como causas de várias doenças, incluindo o câncer (KESKIN et al., 2016).

Diversas abordagens “ômicas” têm sido utilizadas para acessar a complexidade dos sistemas biológicos em diferentes níveis moleculares. Neste contexto, destacam-se as estratégias proteômica e interatômica, que têm fornecido informações sobre vias e moléculas envolvidas no câncer de mama (DUTTA et al., 2012; PANIS et al., 2014; TENGA; LAZAR, 2014; TYANOVA; ALBRECHTSEN; et al., 2016). Paralelamente às abordagens experimentais, métodos computacionais aplicáveis às ciências biomoleculares também têm sido desenvolvidos, permitindo a análise e interpretação biológica de grandes quantidades de dados (DE LAS RIVAS; DE LUIS, 2004).

Estudos integrando abordagens proteômicas e interatômicas têm ampliado a compreensão dos mecanismos subjacentes ao desenvolvimento do câncer e podem identificar importantes moléculas como biomarcadores de doenças. A identificação de proteínas cuja modulação da expressão exerce efeitos promotores ou supressores da progressão tumoral consiste numa relevante estratégia para o estabelecimento de marcadores moleculares da tumorigênese mamária, uma vez que também constitui a informação inicial para a elucidação dos mecanismos de regulação subsequentes que podem explicar os níveis proteicos observados. A compreensão das complexas redes que controlam a expressão destas proteínas e suas vias de atuação, por sua vez, pode contribuir com novas possibilidades para intervenções terapêuticas, ressaltando a relevância dessa abordagem no câncer de mama.

Neste contexto, o presente estudo consistiu na análise proteômica comparativa de tecidos tumorais (tumor primário de mama e linfonodo axilar metastático) e não tumorais (mama contralateral e adjacente) correspondentes de pacientes diagnosticados com câncer de mama através de técnicas de espectrometria de massa de alta resolução integrada à análise *in sílico* das proteínas diferencialmente expressas. Dois grupos amostrais foram separadamente analisados: o primeiro consistiu em amostras provenientes de pacientes do sexo feminino, cujos resultados são apresentados no capítulo I, e o segundo compreendeu amostras de um paciente do sexo masculino e de uma paciente do

sexo feminino, conforme descrito no capítulo II. Em ambas as análises, objetivou-se a obtenção do proteoma diferencial entre os tecidos tumorais e não tumorais e do contexto biológico relacionado às proteínas diferencialmente expressas, enfatizando vias e funções biológicas bem como interações proteicas relevantes na tumorigênese mamária e que possam constituir alvos de interesse para estudos futuros no câncer de mama.

2 REVISÃO BIBLIOGRÁFICA

2.1 A GLÂNDULA MAMÁRIA HUMANA

A glândula mamária humana apresenta composição heterogênea e um complexo ciclo de desenvolvimento em decorrência das flutuações hormonais às quais está exposta. O tecido mamário é composto por diversos tipos celulares que formam complexas redes de interações essenciais para o seu desenvolvimento e funções fisiológicas normais (POLYAK; KALLURI, 2010).

Anatomicamente, a glândula mamária feminina apresenta um compartimento glandular/epitelial, constituído por um sistema ramificado de ductos e lóbulos, que são revestidos por células epiteliais e um estroma de tecido conectivo e adiposo, com alta vascularização (HONDERMARCK, 2003; PELLACANI et al., 2019) (FIGURA 1). A glândula mamária masculina difere da feminina e é constituída principalmente por tecido adiposo e poucos ductos e estroma (IUANOW et al., 2011).

FIGURA 1 – ESTRUTURA DA GLÂNDULA MAMÁRIA FEMININA

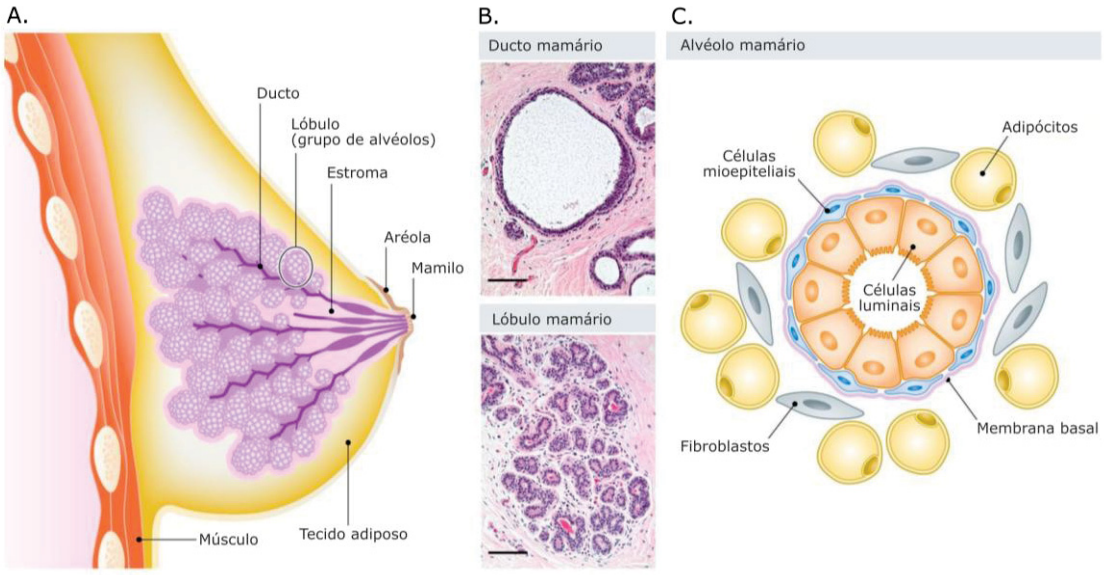

FONTE: Adaptado de PELLACANI et al. (2019).
LEGENDA: A. Diagrama representando as estruturas anatômicas da glândula mamária. B. Cortes histológicos corados com hematoxilina-eosina indicando ductos e lóbulos mamários, aumento de 100 µm. C. Diagrama representando os tipos celulares que compõem a estrutura ducto-lobular da glândula mamária e o estroma circundante.

Histologicamente, ductos e lóbulos mamários maduros são revestidos por células epiteliais luminais e mioepiteliais e encontram-se imersos em um estroma composto por diversos tipos celulares, os quais fornecem suporte ao desenvolvimento e funcionalidade da glândula mamária (HASSIOTOU; GEDDES, 2013) (FIGURA 2).

FIGURA 2 – COMPOSIÇÃO HISTOLÓGICA DA GLÂNDULA MAMÁRIA

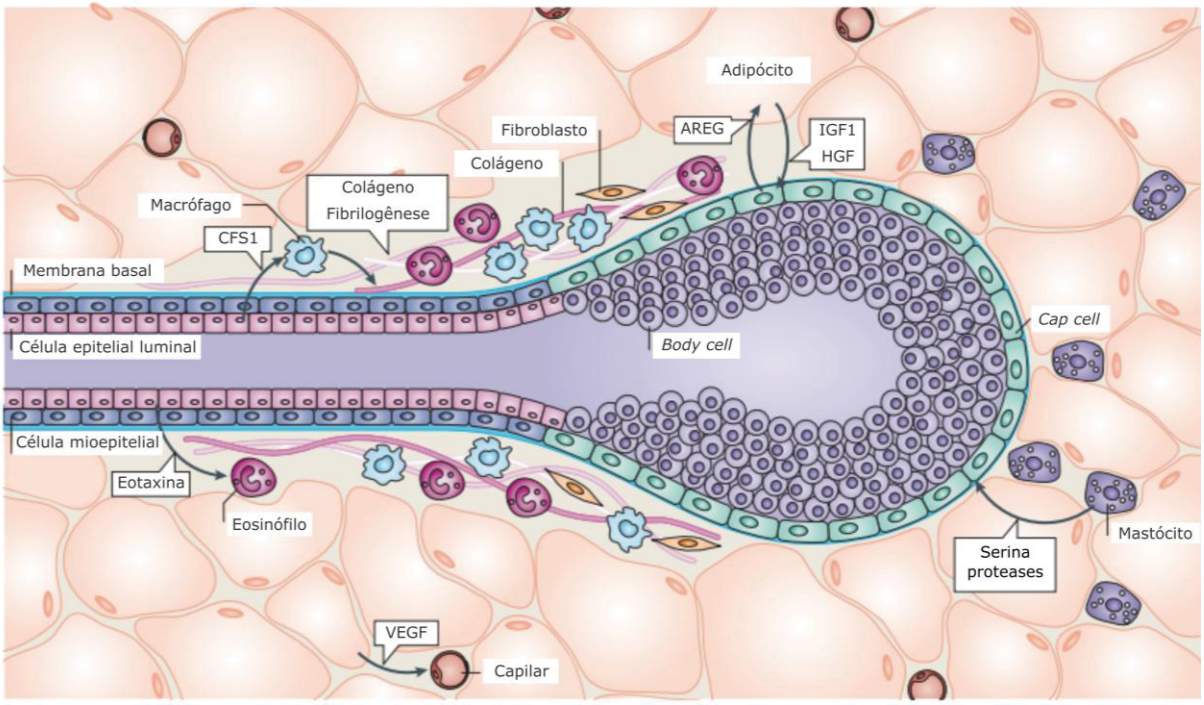

FONTE: Adaptado de GJOREVSKI; NELSON (2011).
LEGENDA: CSF1 – Fator estimulador de colônia de macrófagos, IGF-1 – Fator de crescimento semelhante à insulina tipo 1, HGF – Fator de crescimento de hepatócito, AREG – Anfiregulina, VEGF – Fator de crescimento endotelial vascular. Algumas das substâncias que são utilizadas para a comunicação entre as células do tumor e seu microambiente, e que contribuem para diversos aspectos da tumorigênese, estão destacadas nos balões retangulares.

Estruturas ducto-lobulares possuem um revestimento interno formado por células luminais, que podem ser ductais ou alveolares, sendo as últimas com potencial de diferenciação em células secretoras de leite (lactócitos) durante o período de lactação; a camada exterior apresenta células mioepiteliais contráteis e uma pequena população de células-tronco mamárias (*mammary stem cells*, MaSCs) (VISVADER, 2009; GJOREVSKI; NELSON, 2011), que possui função na reposição celular, morfogênese e homeostase da estrutura ducto-lobular, envolvendo diversificadas interações com o microambiente celular (VISVADER; STINGL, 2014; FENG et al., 2018). As células mioepiteliais, por sua vez, influenciam importantes

processos celulares relacionados à organização tecidual da glândula mamária e produzem a membrana basal, que forma uma barreira física entre os compartimentos celular e estromal (POLYAK; KALLURI, 2010).

Envolvendo lóbulos e ductos há um complexo estroma que corresponde a mais de 80% do volume da mama e apresenta tipos celulares distintos (RONNOV-JESSEN et al., 1996), como fibroblastos, adipócitos, vasos sanguíneos e linfáticos, fibras nervosas e células do sistema imune, além de células mesenquimais, que são altamente responsivas à sinalização hormonal do microambiente (GJOREVSKI; NELSON, 2011; HASSIOTOU; GEDDES, 2013).

A proliferação e diferenciação do epitélio mamário apresentam um controle dinâmico, incluindo sinalização hormonal, de células circundantes bem como de componentes do microambiente, como fatores de crescimento (PAGE et al., 1999; HONDERMARCK, 2003). A alta responsividade do epitélio mamário a sinais locais e sistêmicos constitui uma característica de relevância para a estrutura e função da glândula mamária (VISVADER; STINGL, 2014). Essas interações permitem o remodelamento cíclico, característico do tecido mamário (HONDERMARCK, 2003).

O epitélio ducto-lobular é constantemente remodelado durante o ciclo reprodutivo da mulher. O desenvolvimento da glândula mamária, iniciado na fase embrionária e morfologicamente quiescente até a fase da puberdade, ocorre através de sucessivos remodelamentos em sua estrutura ducto-lobular a cada ciclo menstrual, agregando modificações estruturais características do tecido mamário maduro; este atinge o remodelamento completo e a maturidade funcional durante o período de gravidez/ lactação (HASSIOTOU; GEDDES, 2013). O desenvolvimento da glândula mamária desde a formação dos placódios mamários (espessamentos ectodérmicos) até a involução na menopausa é detalhadamente descrito na literatura (GJOREVSKI; NELSON, 2011; MACIAS; HINCK, 2012; HASSIOTOU; GEDDES, 2013).

2.2 O CÂNCER DE MAMA

2.2.1 Aspectos epidemiológicos do câncer de mama

O câncer constitui uma importante questão de saúde pública mundial, apresentando altos índices de incidência, mortalidade, impacto socioeconômico,

entre outros aspectos indicados pela Organização Mundial da Saúde (OMS) (*World Health Organization,* WHO) e pelo Instituto Nacional de Câncer/ Ministério da Saúde (INCA/MS). Os dados estimados mundialmente pelo projeto GLOBOCAN 2018, da Agência Internacional para Pesquisa em Câncer (*International Agency for Research on Cancer,* IARC)/ WHO, indicaram a ocorrência de 18,1 milhões de novos casos de câncer e 9,6 milhões de mortes causadas pela doença no ano de 2018 (BRAY et al., 2018). Dados completos sobre as estimativas globais do câncer estão descritos por Bray et al (2018) e disponíveis na plataforma interativa *Global Cancer Observatory* (CGO) (<http://gco.iarc.fr/>), da IARC/ WHO.

Para a população feminina, as estimativas mundiais do projeto GLOBOCAN 2018 indicaram a predominância do câncer de mama sobre os demais tipos de cânceres. A incidência estimada para 2018 foi de cerca de 2,1 milhões de novos casos, sendo 46,3 casos a cada 100 mil mulheres, seguido do câncer colorretal com cerca de 823 mil novos casos estimados e taxa de 16,3 casos a cada 100 mil mulheres. Nesse mesmo ano foram previstas cerca de 627 mil mortes e taxa de mortalidade de 13 casos a cada 100 mil mulheres, quase o dobro do estimado para o segundo tipo de neoplasia mais frequente em mulheres, o câncer colorretal, para o qual foram previstas 7,2 mortes a cada 100 mil mulheres (IARC/WHO, 2019). O câncer de mama também foi o mais prevalente, sendo estimados aproximadamente 6,9 milhões de sobreviventes após cinco anos do diagnóstico (considerados a partir do ano de 2018) (IARC/WHO, 2019).

No Brasil, o INCA/MS (2017) estimou para cada ano do biênio 2018-2019 a ocorrência de 59.700 novos casos de câncer de mama na população feminina, com um risco estimado de 56,33 casos a cada 100 mil mulheres. Dados do Sistema de Informações sobre Mortalidade (SIM)/ Sistema Único de Saúde (SUS), indicaram mais de 16 mil mortes causadas pela doença no ano de 2016, último ano para o qual as informações encontram-se disponíveis (DATASUS/MS, 2019).

Particularmente, na população masculina o câncer de mama apresentou incidência global de 1,8% (44.000/2.422.000) no ano de 2015, considerando dados estimados para a doença em ambos os sexos (FITZMAURICE et al., 2017). Anteriormente, em homens, a doença representava menos de 1% dos casos de câncer de mama (femininos e masculinos) no mundo (KORDE et al., 2010). No Brasil, a incidência do câncer de mama em homens é inferior a 1% (INCA/MS, 2019).

Portanto, os panoramas epidemiológicos mundial e nacional ressaltam a relevância do investimento em pesquisas básicas e avançadas no câncer de mama, sob estratégias variadas que proporcionem uma melhor compreensão dos mecanismos subjacentes à tumorigênese mamária e aprimorem o diagnóstico, terapêutica e prognóstico, permitindo a identificação, desenvolvimento e implementação de novas abordagens clínicas.

2.2.2 Aspectos etiológicos do câncer de mama

Em geral, a etiologia do câncer é complexa e envolve diversos fatores biológicos, comportamentais e ambientais. Nesse sentido, os fatores de risco para o desenvolvimento do câncer de mama podem ser considerados sob dois aspectos: fatores inerentes e extrínsecos ao indivíduo. Os primeiros constituem parâmetros independentes do modo de vida das pessoas, como idade, sexo, ancestralidade e predisposição genética. Já fatores extrínsecos são condicionados pelo estilo de vida, incluindo hábitos alimentares, prática de atividades físicas, uso prolongado de contraceptivos hormonais, terapia de reposição hormonal, entre outros (KAMINSKA et al., 2015).

Em ambos os sexos, para os diversos tipos de câncer, a idade representa um importante fator de risco uma vez que os tumores resultam do acúmulo de alterações moleculares nas células durante as divisões celulares. A predisposição genética também reflete a maior suscetibilidade em desenvolver a doença, sendo relevantes a história familial de câncer de mama (especialmente envolvendo parentes de primeiro grau afetados) e de ovário; e a presença de mutações em genes de suscetibilidade e de alto risco, como *BRCA1* e *BRCA2;* além de outras condições hereditárias como as síndromes de Li-Fraumeni e de Cowden (AMERICAN CANCER SOCIETY, 2017). Alterações envolvendo *BRCA2* e genes como *PTEN*, *TP53* e *CHEK2*, bem como a síndrome de Klinefelter (XXY), têm sido descritas no câncer de mama masculino (KORDE et al., 2010).

Períodos específicos do desenvolvimento fisiológico feminino são enfatizados na etiologia do câncer de mama. A menarca antes dos 12 anos e a menopausa após os 55 anos são reconhecidamente relacionadas ao aumento no risco de desenvolvimento da doença (INCA/MS, 2017). A nuliparidade e a primeira gravidez após os 30 anos bem como o uso de alguns anticoncepcionais e da

reposição hormonal na menopausa também constituem fatores de risco (INCA/MS, 2017). Terapias hormonais com o uso de estrógenos em homens (para o tratamento do câncer de próstata, por exemplo) também aumentam o risco de desenvolver a doença (AMERICAN CANCER SOCIETY, 2019). Neste contexto, ressalta-se que o tempo de exposição hormonal ao estrogênio influencia a proliferação do epitélio mamário, possibilitando novas oportunidades para o surgimento e acúmulo de alterações nas células (OLDENBURG et al., 2007).

Além disso, em mulheres, aspectos como a densidade da glândula mamária e a densidade mineral dos ossos também têm sido relacionados como fatores de risco para o desenvolvimento do câncer de mama (AMERICAN CANCER SOCIETY, 2017). Outra importante fonte de estrogênio endógeno é o tecido adiposo, correlacionando o peso corporal ao câncer de mama (KEY et al., 2003). Estudos demonstram que o ganho de peso e a obesidade na adolescência (resultante do excesso no consumo de alimentos calóricos, com altos níveis de proteína animal e baixo consumo de frutas e vegetais) aliado a pouca ou nenhuma atividade física, influenciam o período da menarca (BERKEY et al., 2000). Em homens, a obesidade e a falta de atividades físicas também são apresentadas como fatores de risco para a doença (RUDDY; WINER, 2013).

Diversos estudos têm indicado que o consumo de bebidas alcoólicas aumenta o risco de desenvolver o câncer de mama em ambos os sexos (AMERICAN CANCER SOCIETY, 2017; AMERICAN CANCER SOCIETY, 2019). O aumento nos níveis de estrogênio e de andrógenos é um dos mecanismos que relacionam o álcool a essa doença (SINGLETARY; GAPSTUR, 2001).

As mudanças no estilo de vida das mulheres, acompanhado da industrialização e do desenvolvimento econômico, em conjunto com os padrões reprodutivos femininos (intervalo de tempo entre a menarca e a primeira gestação) têm sido descritos como fatores de risco que contribuem para o aumento nas taxas de câncer de mama (COLDITZ; BOHLKE, 2015). Além disso, alterações nos turnos de trabalho para o período da noite, no qual há exposição à luz artificial, têm sido consensualmente descritas como um importante fator de risco para o desenvolvimento do câncer, incluindo o de mama (AMERICAN CANCER SOCIETY, 2017). A exposição à luz no período noturno interrompe a produção de melanina, um hormônio que regula o sono e que apresenta função na prevenção do crescimento e desenvolvimento de tumores (STEVENS et al., 2014).

A exposição a fatores ambientais como a radiação ionizante, os poluentes ambientais (ex. pesticidas organoclorados) e substâncias como o dietilestilbestrol (estrogênio não esteroide) também podem conferir risco em relação ao câncer de mama (AMERICAN CANCER SOCIETY, 2017). Outros fatores relacionados à doença no sexo masculino incluem doenças hepáticas e condições testiculares (remoção parcial ou total dos testículos) (AMERICAN CANCER SOCIETY, 2019).

Por outro lado, condições relacionadas a hábitos de vida saudáveis são consideradas como fatores protetivos, como dietas alimentares equilibradas e a prática de exercícios físicos regulares. Estudos indicam a atividade física como um fator modificável sob o qual pode-se intervir para diminuir o risco de câncer de mama (LIU et al., 2016). A gravidez e a amamentação por um longo período de tempo também conferem proteção (OLDENBURG et al., 2007), e estão relacionadas às mudanças na composição celular da glândula mamária (HASSIOTOU; GEDDES, 2013).

2.2.3 Classificação do câncer de mama

Inicialmente, o termo “câncer” designa um conjunto de mais de 100 tipos diferentes de doenças comumente caracterizadas pelo crescimento descontrolado de células anormais com potencial invasivo, cuja origem é de natureza multifatorial (INCA/MS, 2018).

O câncer de mama compreende diferentes tipos de neoplasias malignas, sendo caracterizado como uma doença heterogênea, que apresenta variados aspectos clínicos e histopatológicos bem como alterações moleculares distintas. Tumores mamários apresentam características e composição celulares variáveis que implicam em morfologias distintas e comportamentos biológicos diferentes em termos de agressividade, curso e resposta à terapia (VAN 'T VEER et al., 2002; CAMPBELL; POLYAK, 2007).

Diferentes abordagens são utilizadas para classificar o câncer de mama. A classificação histopatológica é baseada na heterogeneidade morfológica da doença. A maioria das neoplasias malignas de mama possui origem epitelial (superior a 95% dos casos) e é denominada carcinoma (TOMASKOVIC-CROOK et al., 2009). Tumores derivados de tecidos conjuntivos, os sarcomas, são raramente observados na mama (HONDERMARCK, 2003).

A maioria dos carcinomas tem sua origem em células dos ductos e lóbulos da glândula mamária, resultando no desenvolvimento de tumores ductais e lobulares, que podem ser *in situ* (proliferação de células atípicas localmente delimitada pela membrana basal) ou invasivos (disseminação das células tumorais para tecidos adjacentes e distantes) (FIGURA 3). Tumores mucinosos, inflamatórios, medulares, tubulares, papilares e filoides compreendem casos de menor frequência (GUIMARÃES, 2008).

FIGURA 3 – ASPECTOS HISTOLÓGICOS DE TUMORES *IN SITU* E INVASIVOS

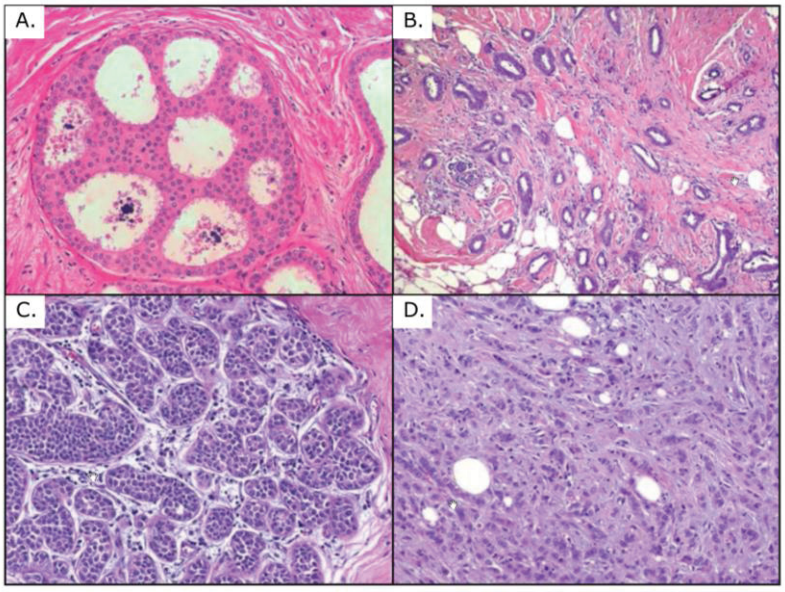

FONTE: Adaptado de SGROI (2010).
LEGENDA: Cortes histológicos corados com hematoxilina-eosina evidenciando A. Carcinoma lobular *in situ* (CLIS). B. Carcinoma ductal *in situ* (CDIS). C. Carcinoma lobular invasor (CLI). D. Carcinoma ductal invasor (CDI).

Entre os tipos histológicos do câncer de mama, estudos indicam o carcinoma ductal invasivo (CDI) com prevalência entre 60% e 83% dos diagnósticos (EHEMAN et al., 2009; SGROI, 2010; MENEZES DE MEDEIROS et al., 2016). Trata-se de um grupo de tumores cujo diagnóstico é feito por exclusão, isto é, quando a lesão não se enquadra nos critérios que definem os tipos especiais de carcinomas mamários (lobular invasivo, tubular, cribiforme, metaplástico, apócrino, mucinoso, papilar, micropapilar, entre outros), motivo pelo qual tem sido proposta a alteração da terminologia CDI não especificado de outra forma (NOS – *not otherwise specified*) para “carcinomas invasivos de tipo não especial” (NST – *no special type*) (SINN; KREIPE, 2013).

Outros parâmetros histológicos também utilizados na classificação de tumores mamários incluem o grau de diferenciação celular, o pleomorfismo nuclear, as atividades mitóticas e a formação do túbulo/glândula. Estes permitem determinar tumores de grau I (bem diferenciado, células com baixa atividade mitótica e similares ao fenótipo normal), grau II (moderadamente diferenciado e com características intermediárias) e grau III (pouco diferenciado, com células de fenótipos distintos do tecido normal e que tendem a crescer e se disseminar de forma agressiva) (OLDENBURG et al., 2007).

De ampla aplicação clínica, a heterogeneidade do câncer de mama pode ser ilustrada pelo estadiamento clínico da doença, baseado em exames físicos e de imagem (TURASHVILI; BROGI, 2017). Este é realizado pelo sistema de classificação TNM de tumores malignos, padrão mundialmente reconhecido para determinar a extensão da disseminação do câncer e preconizado pela *American Joint Committee on Cancer*/ *Union for International Cancer Control* (AJCC/ UICC), que utiliza como parâmetros: o tamanho do tumor primário (T), a presença/ ausência de metástase em linfonodos regionais (N) e a presença / ausência de metástase(s) à distância (M) (SOBIN et al., 2009).

Ao sistema tradicional de classificação somou-se a classificação molecular e, com o advento de novas tecnologias experimentais e computacionais, diversos estudos demonstraram a existência de subtipos intrínsecos do câncer de mama com base em seus perfis moleculares, incluindo o *status* dos receptores de estrogênio (RE) e de progesterona (RP), amplificação do receptor de fator de crescimento epidérmico 2 (ERBB2, também conhecido como HER2), nível de expressão do antígeno marcador de proliferação celular Ki-67, receptor de andrógeno (RA), entre outros. Os estudos de Perou et al. (2000), Sorlie et al. (2001; 2003), Farmer et al. (2005) e Prat et al. (2010) descrevem distintos perfis moleculares associando-os a diferentes subtipos do câncer de mama.

Inicialmente, a análise de perfis de expressão gênica baseados em microarranjo resultou na distinção de pelo menos quatro subtipos de câncer de mama: luminal/ RE+, correspondente à linhagem luminal; tipo basal (basal-*like*), podendo incluir a linhagem mioepitelial; HER2+, com superexpressão de HER2; e semelhante ao normal (normal-*like*) (PEROU et al., 2000). Esses dados foram posteriormente validados e ampliados, resultando na classificação adicional de tumores luminal A (tumores de baixo grau, RP+ e HER2-) e B (tumores de grau

elevado, RP+/- , HER2+/- e alto escore de Ki-67) (SORLIE et al., 2001; SORLIE et al., 2003). Estudos adicionais acrescentaram mais dois subtipos distintos: molecular apócrino, que apresenta aumento da sinalização de andrógenos, RA+, RE- e características apócrinas, como citoplasma abundantemente eosinofílico e nucléolo proeminente, podendo apresentar superexpressão ou amplificação de HER2 (FARMER et al., 2005); e claudina baixa, caracterizado pela ausência ou baixa expressão de marcadores luminais e expressão elevada de marcadores relacionados à transição epitelial-mesenquimal (TEM) (PRAT et al., 2010).

Na prática clínica, para o diagnóstico do subtipo da doença tem sido utilizada a classificação imunoistoquímica, estabelecida em 2013 na 13ª Conferência Internacional de Saint Gallen (GOLDHIRSCH et al., 2013) (QUADRO 1) e inalterada em edições posteriores do evento (2015 e 2017).

QUADRO 1 – DEFINIÇÕES CLÍNICOPATOLÓGICAS DOS SUBTIPOS MOLECULARES DO CÂNCER DE MAMA

Subtipo intrínseco	**Definição clinicopatológica**	
	Subtipo do câncer de mama	**Parâmetros imunoistoquímicos**
Luminal A	Luminal A-*like*	ER+ e PR+ (>20%*) HER2- Ki-67 baixo (<14%**)
Luminal B	Luminal B-*like* HER2-	ER+ HER2- Ki-67 alto (>14%) e/ou PR- ou baixo (<20%)
	Luminal B-*like* HER2+	ER+ HER2 superexpresso/ amplificado Presença de Ki-67 Ausência ou presença de PR
ERBB2 superexpresso	HER2+ (não luminal)	ER e PR ausentes HER2 superexpresso/ amplificado
Basal-like	Triplo negativo (ductal)	ER e PR ausentes HER2-

FONTE: Adaptado de Goldhirsch et al. (2013).
NOTA: * Percentual estabelecido no estudo de Prat et al. (2013)[1] para definir o subtipo luminal A.
** O limite entre Ki-67 alto e baixo varia entre os laboratórios, sendo o valor <14% aqui descrito definido com base em um único laboratório (Cheang et al., 2009[2]).
LEGENDA: ERBB2 – Receptor de fator de crescimento epidérmico 2 (também conhecido como HER2), ER – receptor de estrogênio, PR – receptor de progesterona, Ki-67 – antígeno marcador de proliferação celular Ki-67.

---

[1] Prat A. et al. Prognostic significance of progesterone receptor-positive tumor cells within immunohistochemically defined luminal A breast cancer. **J Clin Oncol**, v. 31, p. 203-209, 2013.

[2] Cheang M. C. U. et al. Ki67 index, HER2 status, and prognosis of patients with luminal B breast cancer. **J Natl Cancer Inst**, v. 101, p. 736-750, 2009.

Informações detalhadas sobre as classificações do câncer de mama são apresentadas por Feng et al. (2018). As implicações terapêuticas relacionadas aos subtipos do câncer de mama são descritas na literatura (GOLDHIRSCH et al., 2013; DE LA MARE et al., 2014).

2.2.4 A tumorigênese mamária

O câncer de mama é uma doença complexa causada pelo acúmulo de alterações moleculares responsáveis por determinar a progressão de células normais, através de estágios hiperplásicos e displásicos, em um câncer invasivo e, finalmente, em uma doença metastática (GARNIS et al., 2004).

O modelo mais comum para o desenvolvimento do carcinoma mamário propõe que um tumor invasivo se origina nas unidades lóbulo-ductais terminais e progride através de estágios de doença benigna da mama, adquirindo alterações celulares, com excessiva proliferação e atipia (CICHON et al., 2010).

Inicialmente, o epitélio mamário apresenta alterações que evoluem para as primeiras lesões estruturalmente evidentes, as hiperplasias intraductais. Estas avançam a um estado de atipia celular e de oclusão dos ductos, resultando em um carcinoma intraductal *in situ* (CIS). O tumor pode permanecer como CIS ou progredir a carcinoma localmente invasivo (CI), no qual a membrana basal é rompida e as células epiteliais invadem o estroma circundante (VILLANUEVA et al., 2018), com possibilidade de metástase para vários órgãos, como pulmões, ossos e fígado (CICHON et al., 2010; BOMBONATI; SGROI, 2011). A figura 4 ilustra as etapas da tumorigênese mamária utilizando como exemplo o câncer de mama ductal.

FIGURA 4 – ALTERAÇÕES EPITELIAIS NA PROGRESSÃO DO CARCINOMA MAMÁRIO

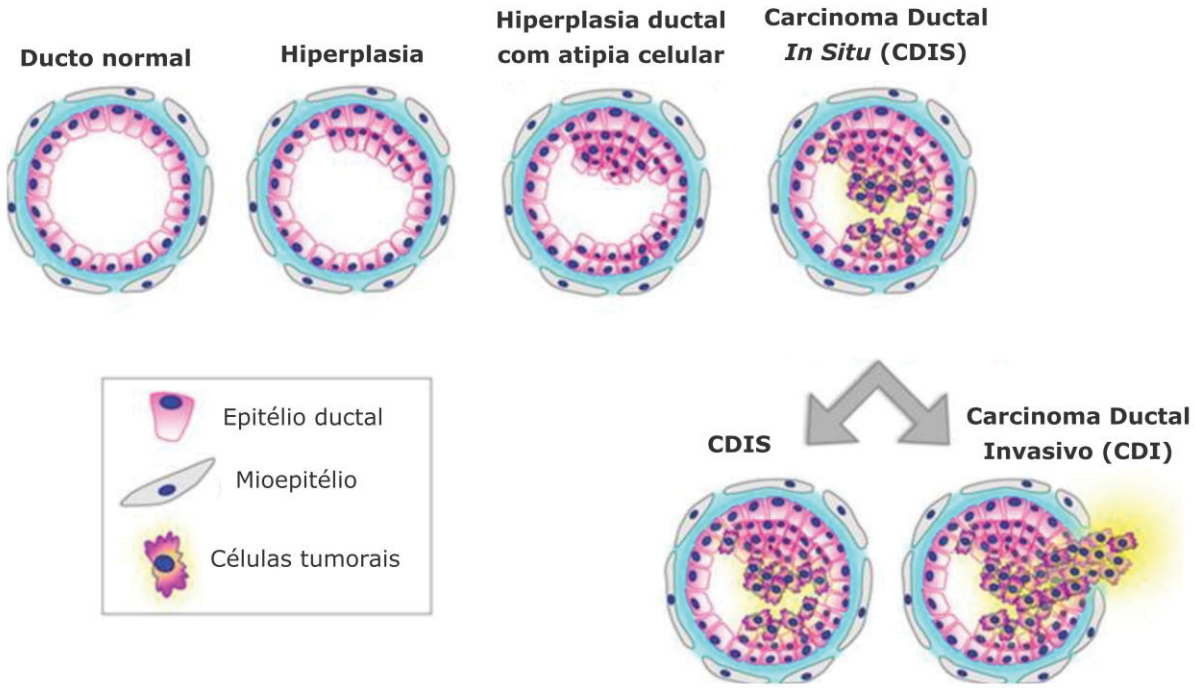

FONTE: Adaptado de VILLANUEVA et al. (2018).
LEGENDA: CDIS – Carcinoma ductal *in situ*, CDI – carcinoma ductal invasor.

A metástase compreende a última etapa da progressão do tumor primário e consiste na disseminação das células tumorais do sítio primário para determinados órgãos, sendo constituída por uma sequência de eventos altamente regulados. A cascata invasão-metástase inclui a invasão local dessas células no estroma circundante, intravasão destas na circulação sistêmica e posterior extravasão nos órgãos-alvo, com a posterior formação de micrometástases, que podem expandir e resultar no desenvolvimento de tumores nos sítios secundários (DING et al., 2017). A afinidade por determinados sítios metastáticos está relacionada às propriedades intrínsecas das células tumorais, à sinalização de citocinas, aos fatores do microambiente tumoral a ser colonizado, entre outros aspectos (BEN-BARUCH, 2009). Os processos envolvidos na metástase são detalhadamente descritos na literatura (JIN; MU, 2015). A figura 5 representa as etapas da cascata invasão-metástase.

FIGURA 5 – CASCATA INVASÃO-METÁSTASE NA TUMORIGÊNESE MAMÁRIA

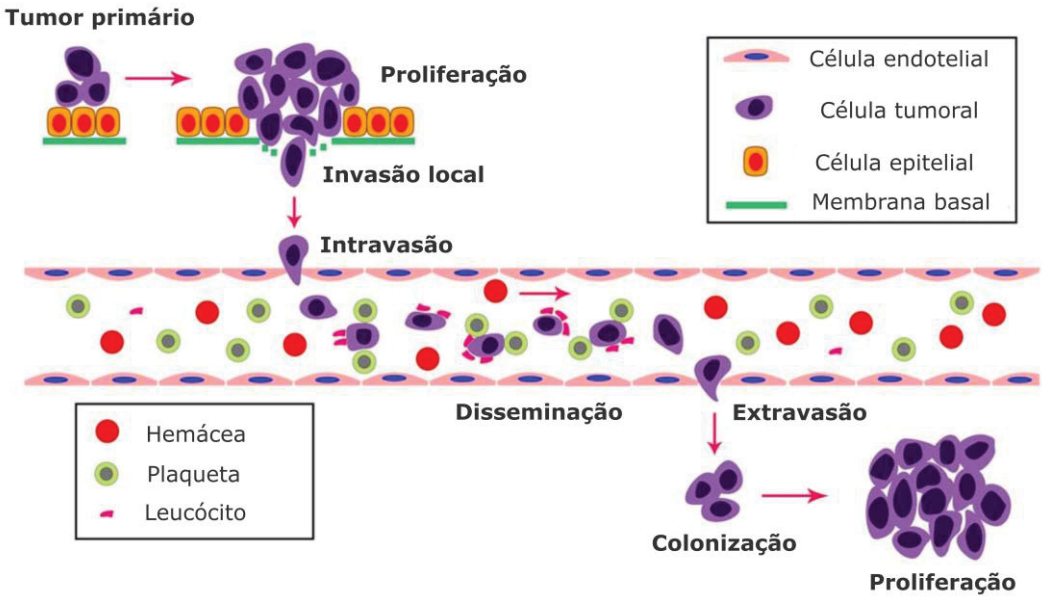

FONTE: Adaptado de DING et al. (2017).

Entre os processos envolvidos na metástase, destacam-se as transições entre os fenótipos celulares epitelial e mesenquimal, necessárias para a aquisição das propriedades funcionais de cada tipo celular. A TEM está relacionada à expressão de marcadores mesenquimais, como a vimentina, N-caderina, fibronectina e integrina αVβ6, e resulta na perda da polaridade das células epiteliais e no aumento da mobilidade celular, conferindo capacidade invasiva às células tumorais; o processo inverso, a transição mesenquimal-epitelial (TME), ocorre quando marcadores epiteliais passam a ser expressos em células com fenótipo mesenquimal, incluindo a E-caderina, desmoplaquina, citoqueratinas e ocludina, permitindo a aquisição de características epiteliais que possibilitam o desenvolvimento dos tumores nos sítios metastáticos (CREIGHTON et al., 2013). As transições entre esses fenótipos celulares constitui um fenômeno de notável relevância na pesquisa do câncer, uma vez que representam uma etapa-chave na disseminação dos tumores e um importante ponto para intervenção terapêutica.

Diversos tipos celulares e moléculas biológicas estão relacionados à tumorigênese mamária. Nesse sentido, o microambiente tumoral, composto por uma população heterogênea de células que conferem volume e suporte às células tumorais, tem sido relacionado à promoção da angiogênese, proliferação, invasão e metástase, bem como à resistência terapêutica (BUSSARD et al., 2016). Entre os

tipos celulares estromais descritos na progressão tumoral se destacam as células endoteliais (vasos sanguíneos e linfáticos), pericitos, fibroblastos e várias células derivadas da medula óssea, como macrófagos, neutrófilos, mastócitos, células-tronco mesenquimais, entre outras (JOYCE; POLLARD, 2009) (FIGURA 6). Diversas funções relacionadas à tumorigênese podem ser proporcionadas pela atuação conjunta das células que compõem o microambiente tumoral, indicando-o como um importante alvo para intervenções terapêuticas (JOYCE; POLLARD, 2009).

FIGURA 6 – MICROAMBIENTE DO TUMOR PRIMÁRIO E TUMORIGÊNESE

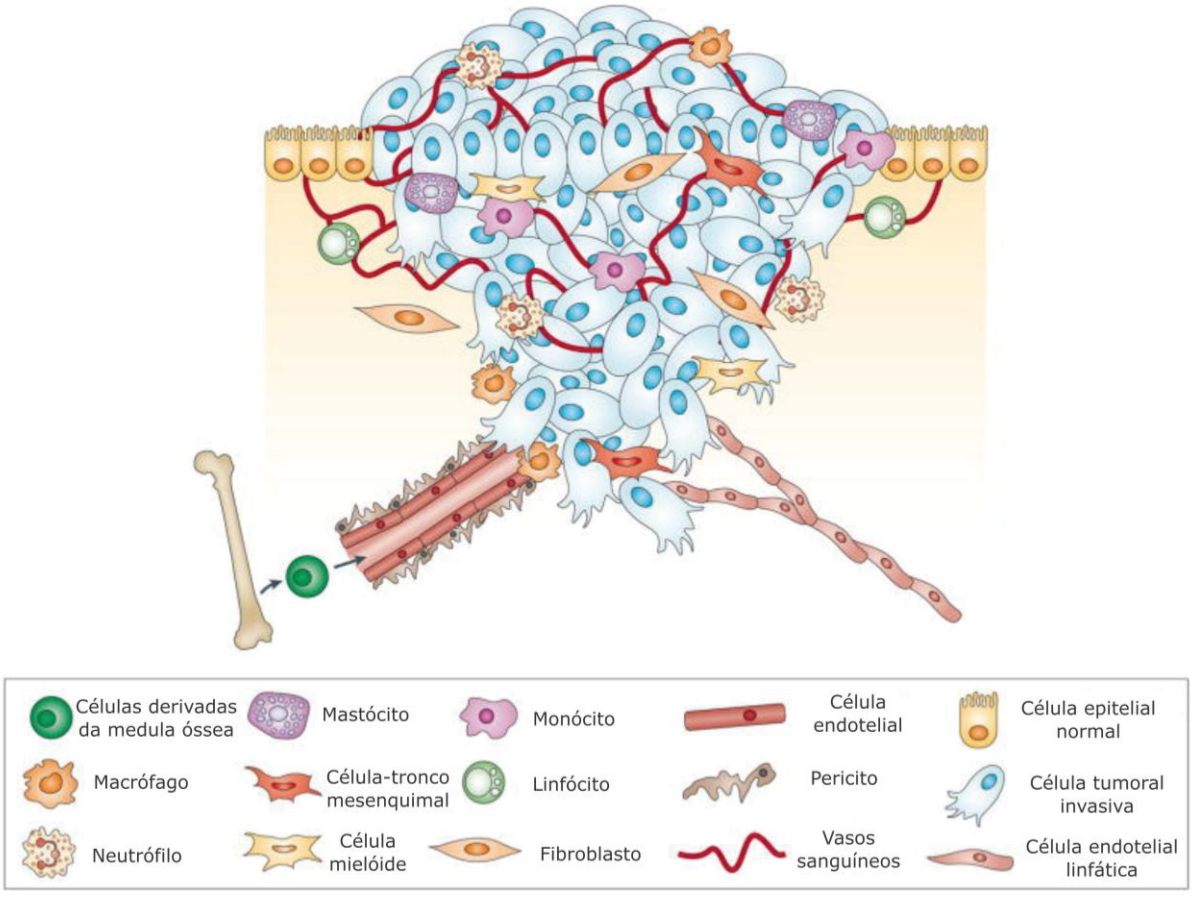

FONTE: Adaptado de JOYCE; POLLARD (2009).

No que se refere aos aspectos moleculares, o processo de desenvolvimento e progressão tumoral é influenciado por alterações em proteínas que desempenham funções em múltiplas vias e processos celulares envolvidos na aquisição do fenótipo maligno. Complexas redes de proteínas com interconexões de atividade regulam tais processos, assim, uma proteína anormal que tenha função-chave nestas redes pode afetar o fluxo de informações à jusante (CALVO et al., 2005; SOMIARI et al., 2005).

Entre as principais características adquiridas pelas células tumorais durante a tumorigênese, destacam-se os denominados *"hallmarks"* do câncer (HANAHAN; WEINBERG, 2011), representados na figura 7.

FIGURA 7 – CARACTERÍSTICAS COMUNS ADQUIRIDAS PELAS CÉLULAS TUMORAIS

FONTE: Adaptado de HANAHAN; WEINBERG (2011).

O repertório de células recrutadas pelo tumor, a partir do microambiente tumoral, contribui para a aquisição dessas características, adicionando maior complexidade ao câncer (HANAHAN; WEINBERG, 2011).

Esses *hallmarks* clássicos do câncer têm sido analisados sob diversas perspectivas, incluindo aspectos do metabolismo (LEWIS; ABDEL-HALEEM, 2013), microambiente tumoral (HANAHAN; COUSSENS, 2012), tipos de estresse celular (FIASCHI; CHIARUGI, 2012; URRA et al., 2016; WIGERUP et al., 2016), entre outros, complementando a gama de alterações fisiológicas, celulares e bioquímicas envolvidas na tumorigênese, além de ressaltar a importância desses *hallmarks* na pesquisa por biomarcadores do câncer.

Alterações em vias biológicas também têm sido descritas no desenvolvimento e progressão do câncer (VOGELSTEIN; KINZLER, 2004; SEVER; BRUGGE, 2015; SANCHEZ-VEGA et al., 2018). Particularmente, no câncer de mama são consideradas como principais vias as relacionadas às moléculas JAK-STAT, MAPK, NFκB, PI3K, receptor de estrogênio, TGFβ e de WNT (VELLOSO et

al., 2017). Várias alterações moleculares impactam em vias de sinalização que controlam aspectos relevantes da biologia celular, como o crescimento, divisão, apoptose e motilidade celular, e podem desencadear a progressão tumoral através de modificações no microambiente tumoral, capacidade angiogênica, inflamação, entre outros (SEVER; BRUGGE, 2015). Muitas das alterações na sinalização celular resultam em funções oncogênicas que refletem os *hallmarks* clássicos do câncer (GIANCOTTI, 2014).

A transformação maligna é relacionada a uma série de alterações em moléculas com função reconhecida na tumorigênese. Entre estas, se destacam as principais classes de genes relacionados ao câncer, como os oncogenes e os genes supressores de tumor. Diversos estudos descrevem a funcionalidade desses genes em vias biológicas e na sinalização celular do câncer de mama (CORZO et al., 2006; BOTLAGUNTA et al., 2008; RAJAGOPALAN et al., 2010).

A identificação e caracterização estrutural e funcional dos componentes envolvidos nas maquinarias celulares, e o entendimento de como estes interagem para realizar suas funções biológicas, são essenciais para compreender os processos relacionados à tumorigênese no nível molecular (HECK, 2008). Neste contexto, a abordagem proteômica se constitui numa relevante estratégia para a obtenção do perfil proteico relacionado ao contexto biológico do câncer.

2.3 A PROTEÔMICA COMO MÉTODO DE ESTUDO NO CÂNCER DE MAMA

Processos biológicos complexos geralmente envolvem a interconexão de genes, transcritos, proteínas, metabólitos e lipídios, cuja interpretação tem sido possível devido ao desenvolvimento de áreas como a genômica, transcriptômica, proteômica, metabolômica e lipidômica, às quais também se acrescenta a relevância da interatômica (MONTI et al., 2018) e outras técnicas “ômicas”.

Diversas abordagens têm sido desenvolvidas para acessar a complexidade dos sistemas biológicos em diferentes níveis moleculares. Tecnologias de alta resolução têm fornecido caracterizações mais detalhadas sobre o perfil molecular das amostras biológicas, permitindo uma maior compreensão acerca dos mecanismos regulatórios subjacentes aos processos patológicos (CHAKRABORTY et al., 2018). Paralelamente às abordagens experimentais, métodos computacionais aplicáveis às ciências biomoleculares também têm sido desenvolvidos, permitindo a

análise de grandes quantidades de dados (DE LAS RIVAS; DE LUIS, 2004). No câncer de mama, por exemplo, diversos estudos incluindo abordagens experimentais e bioinformáticas, em diferentes níveis moleculares, têm fornecido informações sobre biomarcadores da doença (CHA et al., 2010; HENEGHAN et al., 2010; TANAKA; OGISHIMA, 2015; WEN et al., 2015).

Com os avanços nas técnicas de alta resolução, o aumento na quantidade de informações geradas tem resultado na disponibilização de uma ampla gama de bancos de dados e plataformas de análise computacional descrita na literatura (GADALETA et al., 2011; PAVLOPOULOU et al., 2015). Neste contexto, destacam-se o projeto *The Cancer Genome Atlas* (TCGA), um banco de dados de ampla escala que contém a caracterização de alterações moleculares associadas com a iniciação e progressão de diversos tipos de câncer, incluindo o de mama; a plataforma *cBioPortal for Cancer Genomics*, acessível para explorar, visualizar e analisar dados multidimensionais do câncer, através de informações de diversos estudos publicados, incluindo o banco de dados TCGA; o banco de dados de mutações somáticas e seus efeitos no câncer denominado *Catalogue Of Somatic Mutations In Cancer* (COSMIC), que inclui dados da literatura avaliados manualmente por pesquisadores (FORBES et al., 2016); entre outros.

Entre as diversas abordagens “ômicas”, se destacam a proteômica e a interatômica, que têm fornecido informações relevantes sobre os mecanismos subjacentes à tumorigênese mamária (DUTTA et al., 2012; GROESSL et al., 2014; NABA et al., 2014; CONCOLINO et al., 2018).

2.3.1 A abordagem proteômica no câncer de mama

A abordagem proteômica se refere ao estudo do proteoma, termo que designa o conjunto de proteínas expresso pelo genoma sob determinadas condições fisiológicas (WILKINS et al., 1996). Em contraste com o genoma, o proteoma é dinâmico (SRINIVAS et al., 2002), refletindo o estado atual de funcionamento do sistema. Assim, as proteínas podem demonstrar com maior precisão os mecanismos genéticos intrínsecos das células e seus impactos sobre o microambiente tecidual, uma vez que são efetoras de processos celulares e caracterizam alvos terapêuticos mais acessíveis que os ácidos nucleicos (ANDERSSON et al., 2007). Nesse sentido, ressalta-se a importância da mensuração confiável e acurada das alterações

proteômicas em células anormais, como no contexto do câncer, para compreender os mecanismos envolvidos nos processos celulares (CHAKRABORTY et al., 2018).

No cenário pós-genômico, essa abordagem se consolida como uma estratégia de relevante potencial para a identificação de biomarcadores relacionados a doenças, como a superexpressão ou subexpressão de determinados peptídeos ou proteínas, com poder discriminatório entre os estados saudável e patológico no diagnóstico inicial e na determinação da progressão da doença (BAKRY et al., 2011). No câncer de mama, a proteômica tem fornecido importantes marcadores moleculares da tumorigênese (ZHANG; CHEN, 2010; SUMAN et al., 2016; PROCHAZKOVA et al., 2017; CHEN et al., 2018; MUELLER et al., 2018).

Além disso, os avanços tecnológicos têm contribuído para uma melhor caracterização de proteomas, sendo considerados como conjuntos de dados mais completos aqueles que são interpretados com ênfase nas propriedades relacionadas a questões biomédicas específicas, o que se observa em estudos mais recentes nos quais as etapas de verificação não apenas confirmam funções de proteínas individuais, mas objetivam discorrer sobre vias bioquímicas subjacentes a processos biológicos, por exemplo (MONTI et al., 2018). Em decorrência desses avanços, grandes quantidades de dados proteômicos têm sido depositadas em bancos de dados, ampliando a divulgação e acesso a dados para futuras análises.

2.3.2 A abordagem proteômica baseada na espectrometria de massa

A abordagem proteômica pode ser diferenciada pelo emprego ou não da técnica de espectrometria de massa (*mass spectrometry*, MS) na identificação das proteínas (GALVAO et al., 2011). Essa técnica é considerada de fundamental importância na bioquímica de proteínas e na análise proteômica, permitindo a detecção e a identificação de moléculas biológicas (GUNDRY et al., 2009) e alterações proteicas em misturas complexas (MONTI et al., 2018).

Em especial, a proteômica diferencial quantitativa, que se refere à análise comparativa do proteoma observado em dois ou mais grupos de amostras (MONTI et al., 2018), tem amplo emprego na investigação de doenças. No câncer, estudos baseados nesse método e em tecnologias de alta resolução têm indicado proteínas envolvidas na tumorigênese mamária (CORREA et al., 2017; CHEN et al., 2018).

Em geral, as etapas que compõem os protocolos de proteômica baseados em MS de alta resolução compreendem um módulo experimental, a análise dos espectros de massa e o processamento e interpretação dos dados proteômicos (LAZAR, 2017). Quanto à estratégia adotada na análise proteômica, são utilizadas abordagens *top-down*, *middle-down* e *bottom-up* (SWITZAR et al., 2013; GREGORICH et al., 2014), cujas etapas experimentais são ilustradas na figura 8.

FIGURA 8 – ESTRATÉGIAS PARA AS ANÁLISES PROTEÔMICAS

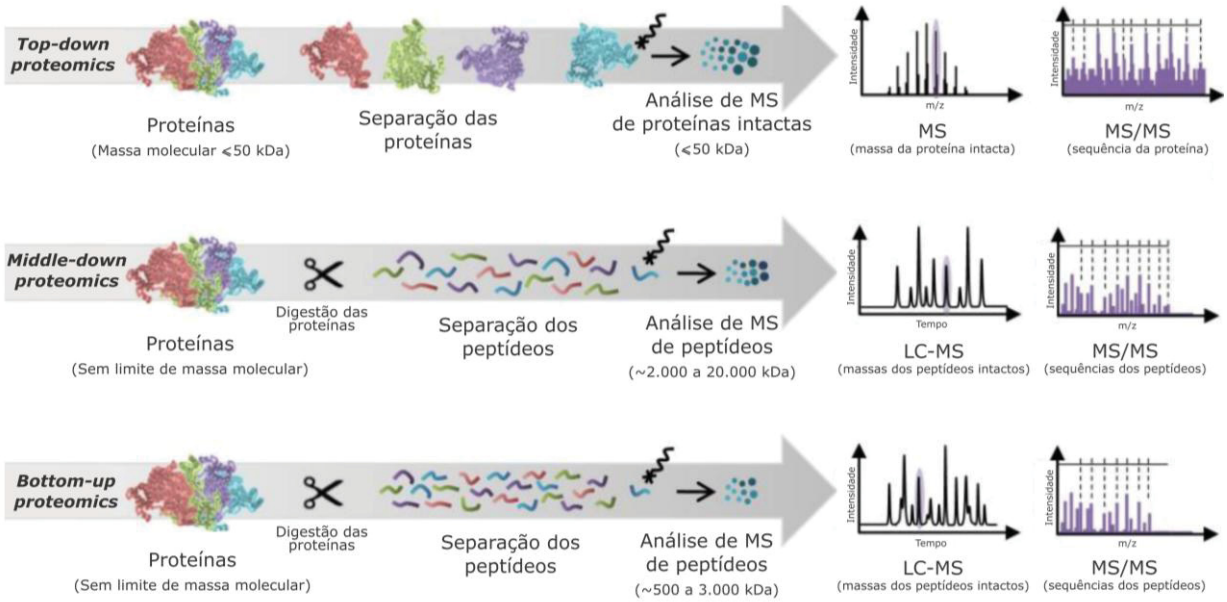

FONTE: Adaptado de SWITZAR et al. (2013).
LEGENDA: MS – Espectrometria de massa (*Mass Spectrometry*), LC-MS – cromatografia líquida acoplada à espectrometria de massa (*Liquid Chromatography-Mass Spectrometry*).

A estratégia *top-down* consiste na análise direta de proteínas intactas, o que diminui a complexidade das amostras por não proceder à digestão proteolítica, e preserva as informações relacionadas à integridade da proteína, como modificações pós-traducionais e variações de sequência decorrentes de mutações e eventos de *splicing* alternativo (ZHANG; GE, 2011). A proteômica sob as abordagens *middle-down* e *botton-up* requer a digestão prévia das proteínas para a obtenção de misturas de peptídeos, que serão analisadas sob faixas de amplitude de massa molecular distintas, sendo a última indicada para a análise de peptídeos menores.

Entre essas abordagens, a proteômica *bottom-up* caracteriza proteínas através da análise de seus peptídeos, sendo também denominada *shotgun* no caso

da análise de misturas de proteínas (em analogia ao sequenciamento genômico *shotgun*) (ZHANG et al., 2013). A proteômica *shotgun/ bottom-up* é aplicada a estudos no câncer (CHEN; YATES, 2007), e as etapas de extração proteica, digestão proteolítica, separação e análise de MS, entre outras considerações, descritas por Zhang et al. (2013).

Na MS, métodos variados de quantificação têm sido empregados para mensurar os níveis de expressão de peptídeos e proteínas nas amostras biológicas, incluindo a marcação de isótopos (ex.: SILAC, iTRAQ, etc.); a marcação metabólica; e a quantificação livre de marcação (*label-free quantification*, LFQ) (WALTHER; MANN, 2010), que apresenta o menor custo entre os métodos de quantificação utilizados em LC-MS/MS. Neste, a quantificação é realizada através do alinhamento (sobreposição) de corridas LC-MS/MS e posterior cálculo das diferenças de intensidade detectadas para um mesmo peptídeo em cada corrida (WALTHER; MANN, 2010). O desempenho da LFQ-MS tem sido demonstrado em estudos com diversos tipos de câncer, incluindo o de mama (PANIS et al., 2014; BERETOV et al., 2015; CORREA et al., 2017; LOBO et al., 2017; CHEN et al., 2018).

2.3.2.1 A espectrometria de massa

Os espectrômetros de massa são utilizados para mensurar a massa molecular de peptídeos e proteínas, através dos espectros de massa (MS1), e/ou para determinar características estruturais adicionais (como a sequência de aminoácidos ou os sítios e tipos de modificações pós-traducionais), através dos espectros de massa em tandem (MS2), que são resultantes da análise de íons precursores fragmentados (DOMON; AEBERSOLD, 2006).

O espectrômetro de massa é um instrumento analítico que permite mensurar a razão massa/carga (m/z) de íons em fase gasosa. Segundo a revisão detalhada de Ahmed (2008) sobre a utilidade dos espectrômetros de massa na análise proteômica, o primeiro destes instrumentos foi desenvolvido em 1899 por Sir JJ Thompson (o qual recebeu o Prêmio Nobel em Física em 1906). Entretanto, sua utilização como um método analítico de rotina na pesquisa proteômica foi possível em meados de 1980, quando foram incorporadas à MS as técnicas de ionização suave e, em seguida, os métodos de dessorção/ionização como a ionização/dessorção a laser assistida por matriz (*matrix-assisted laser*

desorption/ionization, MALDI) e a ionização por *eletrospray* (*electrospray ionization*, ESI). Estes últimos permitem volatilizar biomoléculas de dezenas de kDa em fase gasosa sem destruí-las, gerando íons de peptídeos intactos. Em particular, se destacam as tecnologias ESI em estudos proteômicos no câncer de mama (TYANOVA; ALBRECHTSEN; et al., 2016; CORREA et al., 2017).

De acordo com Ahmed (2008), um dos principais desafios da MS consiste na prévia separação de misturas complexas de proteínas ou peptídeos, a qual pode ser realizada através da eletroforese bidimensional em gel de poliacrilamida (2D-PAGE), com menor taxa de resolução, e por técnicas independentes de gel, como a cromatografia líquida de alta performance (*high-performance liquid chromatography*, HPLC) e os sistemas de eletroforese capilar, ambos acoplados ao sistema de MS.

Os principais componentes de um espectrômetro de massa compreendem a fonte de ionização, o analisador de massa e o sistema de detecção (RAUNIYAR et al., 2007; HAN et al., 2008). O campo eletromagnético gerado no sistema de vácuo faz com que as moléculas sejam carregadas eletricamente antes de sua ionização, o que permite a aceleração dos íons através das etapas subsequentes do sistema (WALTHER; MANN, 2010). Ao final, esse processo resulta em espectros de massa, nos quais a razão m/z é plotada contra o sinal de MS (que indica a intensidade de detecção), caracterizando o analito submetido ao processo de MS (WALTHER; MANN, 2010). A figura 9 representa a estrutura básica dos espectrômetros de massa, indicando as principais fontes de ionização e analisadores de massa. As especificações de cada componente e seus tipos são revisados por Ahmed (2008).

FIGURA 9 – COMPONENTES DOS ESPECTRÔMETROS DE MASSA

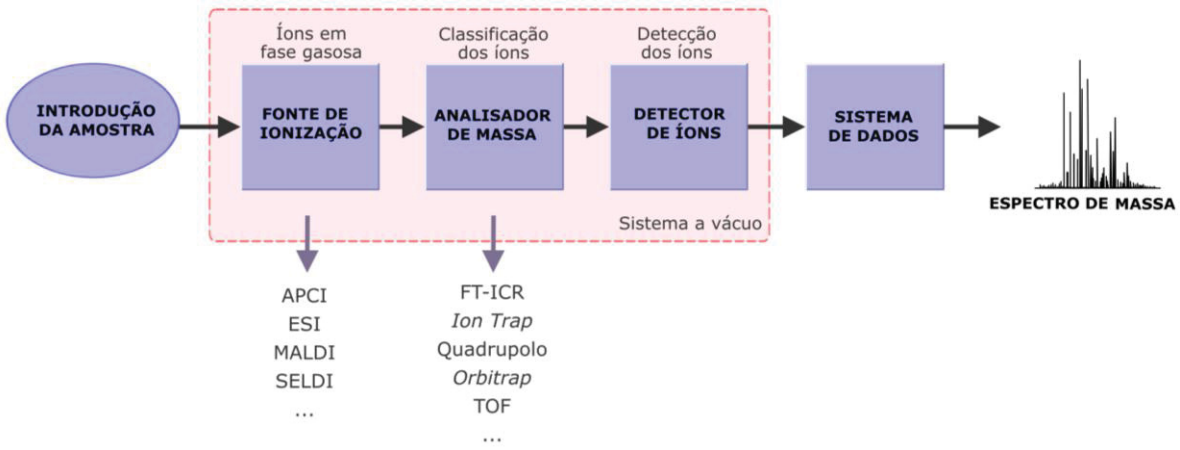

FONTE: Modificado de Rauniyar et al. (2007) e Ahmed (2008).
LEGENDA: APCI – Ionização química à pressão atmosférica (*Atmospheric Pressure Chemical Ionization*), ESI – ionização por *eletrospray* (*Electrospray Ionization*), MALDI – ionização/ dessorção a laser assistida por matriz (*Matrix Assisted Laser Desorption Ionization*) e SELDI – ionização/ dessorção de superfície estimulada por laser (*Surface-Enhanced Laser Desorption/Ionization*), FT-ICR – *Fourier Transform Ion Cyclotron Resonance*, TOF – *Time-of-Flight*.

Entre os métodos de ionização, destaca-se o *eletrospray* (ESI), que permite a MS de amostras em fase líquida, sendo possível o acoplamento direto (*online*) de sistemas de separação, como a HPLC, promovendo um aumento na sensibilidade da MS para misturas complexas (GUNDRY et al., 2009; WALTHER; MANN, 2010). A técnica *eletrospray* consiste na ionização do analito através da pulverização deste sob pressão atmosférica, produzindo íons precursores solvatados (gotículas contendo os peptídeos) e carregados (AHMED, 2008). O processo de evaporação reduz o raio da gotícula (dessolvatação), restando ao final somente os íons, geralmente carregados positivamente devido ao excesso de prótons (íons com múltiplos prótons). Esses íons precursores são subsequentemente transferidos para a região de alto vácuo do espectrômetro de massa (AHMED, 2008), onde serão analisados. A figura 10 representa o processo de ionização através de fontes ESI. Outros métodos de ionização também são utilizados na MS, conforme descrito por Ahmed (2008). As especificações técnicas e a análise através de ESI-MS são detalhadamente descritas na literatura (HO et al., 2003; UNIVERSITY OF BRISTOL, 2019).

FIGURA 10 – ESPECTROMETRIA DE MASSA BASEADA EM IONIZAÇÃO POR *ELETROSPRAY*

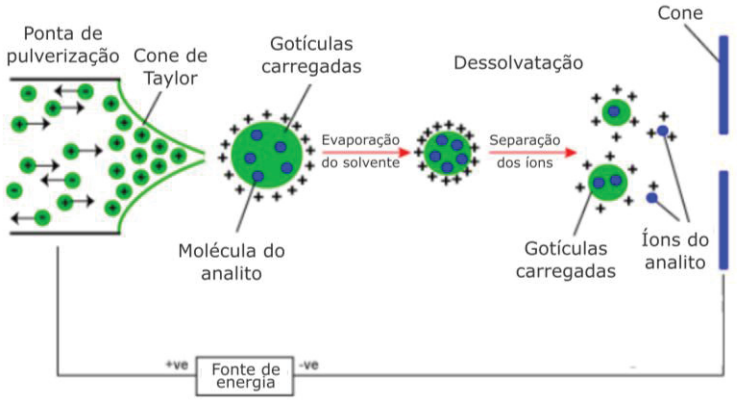

FONTE: Adaptado de *University of Bristol* (2019).

A combinação de diferentes fontes de ionização com vários tipos de analisadores de massa resulta em uma ampla variedade de espectrômetros de massa. Os cinco tipos de analisadores de massa mais frequentemente utilizados em proteômica são os analisadores quadrupolo (Q), *Ion Trap* (IT), *Time-of-Flight* (TOF), *Fourier Transform Ion-Cyclotron Resonance* (FT-ICR ou FT-MS) e *orbitrap* (OT) (HAAG, 2016). Instrumentos híbridos também foram desenvolvidos utilizando mais de um desses analisadores em sequência, ampliando as possibilidades de análise. A descrição da trajetória e análise dos íons em cada analisador de massa e a comparação entre as configurações dos principais espectrômetros de massa utilizados para aplicações proteômicas é descrita por Ahmed (2008).

Em adição à obtenção dos espectros de massa dos íons precursores (MS1), a técnica MS2 consiste em duas etapas sequenciais de análise de massa para se obter seletivamente a fragmentação de íons específicos (íons precursores) em uma mistura de peptídeos ionizados. A seleção dos íons a serem submetidos à MS2 pode ser realizada através dos métodos de aquisição de dados dependente (*data dependent acquisition*, DDA) ou independente (*data independent acquisition*, DIA). No primeiro, apenas os íons precursores de maior intensidade na etapa MS1, eluídos da LC em um determinado intervalo de tempo, são selecionados, fragmentados, analisados e quantificados; no segundo, os espectros de fragmentação de todos os peptídeos são adquiridos (KOOPMANS et al., 2018).

Segundo Ahmed (2009), o processo de MS2 é iniciado com a ativação (fragmentação) de um determinado íon precursor, que pode ser realizada através de diferentes métodos (definindo o tipo de produto de fragmentação). Entre os métodos

mais comuns, destaca-se a dissociação induzida por colisão (*collision-induced dissociation*, CID), no qual colisões entre o íon precursor e partículas de um gás inerte, como o hélio ou o nitrogênio a baixas pressões, induzem a fragmentação do íon (AHMED, 2009; WALTHER; MANN, 2010). Os fragmentos resultantes dessa etapa são analisados conforme sua razão m/z, gerando espectros de massa (denominados MS2), que consistem basicamente em uma lista de razões m/z para diferentes fragmentos que possibilita a identificação da sequência de aminoácidos do peptídeo (WALTHER; MANN, 2010).

Os espectros de massa obtidos pela MS contêm as informações referentes à massa e intensidade dos peptídeos e podem ser comparados com dados *in sílico* disponíveis em plataformas *online* para a identificação das proteínas em estudo (GALVAO et al., 2011). Para uma determinada proteína, vários peptídeos são mensurados, cada um contribuindo com um escore de identificação no banco de dados, resultando numa identificação proteica de alta confiabilidade (WALTHER; MANN, 2010). Neste contexto, a análise dos dados brutos de MS é detalhadamente descrita por Ahmed (2009) e Lazar (2017).

As principais plataformas computacionais e de bioinformática disponíveis para o processamento de dados de MS são descritas por Lazar (2017). Entre estas destacam-se os bancos de dados/programas: Andromeda, MASCOT, MaxQuant, SEQUEST, SwissProt, UniprotKB, X!Tandem, entre outros. Em particular, a plataforma de proteômica computacional MaxQuant integra vários algoritmos especificamente desenvolvidos para dados quantitativos de MS de alta resolução, os quais permitem determinar a precisão da massa e a acurácia dos peptídeos individualmente (COX; MANN, 2008). Essa plataforma realiza a detecção de picos nos dados brutos, a quantificação, o escore de peptídeos e reporta as proteínas identificadas através de tabelas (COX; MANN, 2008), além de possuir seu próprio recurso de busca de peptídeos, denominado Andromeda (COX et al., 2011).

Similar a outras plataformas de alta resolução, dados provenientes de experimentos baseados em LC-ESI-MS/MS demandam extensas análises de interpretação para extrair, a partir de resultados proteômicos, informações funcionais relacionadas a condições patológicas. Nesse sentido, Monti et al. (2018) ressaltam que esses dados têm apresentado função essencial no estudo de sistemas biológicos, tornando-se uma estratégia a ser empregada na identificação de proteínas relacionadas a doenças. Dessa forma, os principais objetivos de estudos

referentes à proteômica diferencial têm sido modificados da geração de longas listas de proteínas diferencialmente expressas com validações pontuais por técnicas independentes (ex. *Western Blotting*) para projetos amplos nos quais há geração de hipóteses e foco na interpretação funcional dos resultados (MONTI et al., 2018).

2.3.3 A interpretação biológica dos dados proteômicos

Monti et al. (2018) descrevem várias abordagens que permitem derivar aspectos funcionais de dados proteômicos, ressaltando que o comportamento de uma única proteína geralmente não reflete a complexidade dos mecanismos biológicos envolvidos na patogênese das doenças, uma vez que doenças complexas podem surgir em função da alteração de diversas proteínas e vias biológicas. Além disso, em vez de analisar as proteínas como unidades individuais, o estudo de suas interações é essencial para a obtenção de um panorama mais dinâmico e completo das funções celulares (MONTI et al., 2009).

Neste contexto, Lazar (2017) descreve como etapas da análise proteômica *in sílico* a anotação biológica, a identificação de categorias funcionais com maior representação (enriquecidas – $p<0,05$), a identificação de redes e interações proteína-proteína, o mapeamento das proteínas em vias biológicas e, por fim, a avaliação do comportamento dinâmico em uma estrutura de biologia de sistemas. A figura 11 contempla parte dos recursos de bioinformática que podem ser utilizados na análise de dados proteômicos.

FIGURA 11 – FLUXOGRAMA DE ANÁLISE DE DADOS PROTEÔMICOS EM LARGA ESCALA

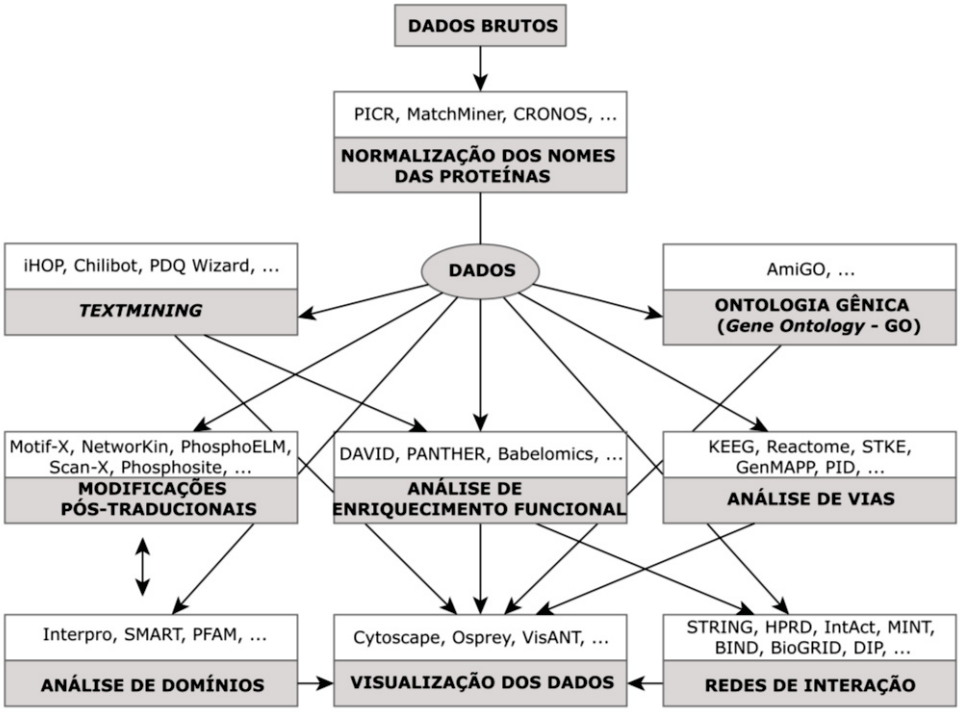

FONTE: Adaptado de Malik et al. (2010).

Malik et al. (2010), Laukens et al. (2015), Lazar (2017) e Monti et al. (2018) apresentam a variedade de programas e plataformas disponíveis para a análise de dados proteômicos, incluindo recursos que permitem a anotação e enriquecimento funcional, obtenção de redes de interação proteica, análise de vias biológicas, modificações pós-traducionais, motivos e domínios proteicos, entre outras aplicações.

2.3.3.1 As estratégias de anotação e enriquecimento funcional

A complexidade de interpretação dos dados proteômicos, os quais geralmente resultam em extensas listas de proteínas, tem sido amplamente discutida na literatura (MALIK et al., 2010; LAUKENS et al., 2015; LAZAR, 2017). Em muitos casos, essas listas são interpretadas de forma parcial, no contexto de questões específicas e hipóteses de pesquisa, sendo que a análise global dos dados é de grande relevância para a interpretação biológica das informações (LAUKENS et al., 2015).

A crescente quantidade de dados de MS ressalta a necessidade de estratégias para extrair as informações biologicamente relevantes dos estudos

proteômicos (MALIK et al., 2010). Paralelamente ao desenvolvimento das plataformas experimentais, diversos recursos e bancos de dados têm sido propostos para a interpretação biológica dos dados proteômicos.

Vários bancos de dados permitem inferir funções a genes ou proteínas, através de termos pertencentes a um vocabulário dinâmico e controlado que descreve um significado definido e supervisionado por especialistas (LAUKENS et al., 2015), reduzindo ambiguidades. Entre esses bancos, destaca-se a plataforma de ontologia gênica *Gene Ontology* (GO) (ASHBURNER et al., 2000; CONSORTIUM, 2017), que fornece três categorias amplas nas quais os genes são classificados: processos biológicos, funções moleculares e componentes celulares. Para ilustrar, alguns dos termos de GO obtidos para o oncogene *MYC*, de atuação reconhecida no câncer, compreendem os processos biológicos “processo metabólico” (GO:0008152), “processo celular” (GO:0009987) e “regulação biológica” (GO:0065007); bem como as funções moleculares de “ligação” (GO:0005488) e “atividade de regulação da transcrição” (GO:0140110).

De acordo com Malik et al. (2010), a análise de termos de GO constitui a etapa mais básica na caracterização bioinformática de conjuntos de dados proteômicos, também sendo de relevância determinar se esses termos são identificados em processos biológicos, funções ou compartimentos celulares específicos com base nas análises de enriquecimento funcional. Para a obtenção dessas informações, são utilizados recursos e plataformas que realizam as referidas análises. Em particular, essa abordagem tem sido utilizada para dados proteômicos no câncer de mama (CHA et al., 2010; LI, W. X. et al., 2017).

Análises de enriquecimento funcional comparam a frequência de anotações individuais dentro de um determinado conjunto de proteínas contra a frequência de anotação em uma lista de referência (listas de proteínas específicas ou informações provenientes do genoma completo), sendo a super-representação (enriquecimento) de um termo avaliado estatisticamente através de distribuição hipergeométrica ou teste exato de Fisher (LAUKENS et al., 2015). De forma simplificada, o valor de p para um termo super-representado é calculado a partir do número de proteínas da lista experimental em relação ao conjunto de referência informado ou proveniente do banco de dados utilizado pela plataforma de análise. O resultado dessa análise apresenta valores de p para cada termo obtido, cujo limite de significância ($p<0,05$) define se há a super-representação (enriquecimento). Considerando o elevado

número de termos funcionais, métodos de correção de testagem múltipla são aplicados (MALIK et al., 2010). Assim, as informações sobre termos super-representados em um conjunto de dados podem direcionar a interpretação biológica dos dados proteômicos.

Após a extração das informações acima referidas, análises de interações e vias biológicas podem se constituir nas próximas etapas de análise (MALIK et al., 2010). Segundo Lazar (2017), diversas plataformas computacionais estão disponíveis para mapear proteínas e seus genes codificadores em vias biológicas e redes de interação proteica. As interpretações baseadas em vias e interatomas são utilizadas em diversos estudos no câncer em geral e no de mama (ZHANG; CHEN, 2010; TENGA; LAZAR, 2014; TYANOVA; ALBRECHTSEN; et al., 2016; REN et al., 2018).

No que se refere às vias biológicas, Lazar (2017) sugere que vias biológicas e seus metabólitos podem apresentar-se alterados nos casos em que várias proteínas a elas relacionadas possuam expressão alterada, indicando moléculas de interesse para estudos adicionais. Neste contexto, importantes vias de sinalização envolvidas na tumorigênese podem ser melhor caracterizadas, fornecendo potenciais moléculas-alvo para intervenções terapêuticas.

2.3.3.2 A abordagem interatômica computacional

A interatômica, técnica que estuda a totalidade de interações proteína-proteína que ocorre na célula (o interatoma), complementa as informações fornecidas pela proteômica diferencial quantitativa e compreende uma etapa fundamental para estudar a relação funcional entre as proteínas e os processos biológicos (LIU; CHEN, 2012).

Como moléculas efetoras, as proteínas apresentam função-chave em virtualmente todos os processos que ocorrem dentro e entre as células (MOSCA et al., 2013), cuja sincronização e regulação são críticas para o funcionamento celular normal. A coordenação destas funções biológicas frequentemente é realizada por complexas redes de interações proteicas transitórias (STEIN et al., 2009; MOSCA et al., 2013), as quais, por sua vez, são reguladas por vários mecanismos (BERGGARD et al., 2007). Uma ampla gama de processos celulares, incluindo a

transdução de sinal, comunicação celular, replicação, transcrição e o transporte de proteínas são realizados via interações proteicas (KESKIN et al., 2016).

As redes de interação constituem um modelo com relevante potencial para formular as complexas relações responsáveis pelos processos celulares (BARABASI; OLTVAI, 2004). Segundo Monti et al. (2018), redes consistem em modelos matemáticos (gráficos, por exemplo) que representam a simplificação de um problema. Nelas, os “nós” podem representar diversos componentes (incluindo proteínas, DNA, RNA, metabólitos, entre outros) enquanto as interligações representam as interações (físicas ou funcionais) entre esses componentes (FASANO et al., 2016). Alterações envolvendo essas interações podem interferir nas propriedades da rede, o que pode resultar em alterações no fenótipo das células.

As abordagens centradas no estudo de redes de interação proteica têm sido amplamente empregadas (MOSCA et al., 2013) e diferentes métodos de detecção e de análise dessas interações são propostos na literatura (BERGGARD et al., 2007; IVANOV et al., 2011).

Todavia, a complexidade relacionada à obtenção de interatomas supera a dinamicidade dos proteomas. Neste contexto, Keskin et al. (2016) discorre sobre as dificuldades do estudo de interatomas considerando a heterogeneidade temporal e espacial bem como a dinamicidade das interações proteicas, as modificações químicas necessárias para a ocorrência destas, entre outros aspectos. Assim, são sugeridas análises através de métodos computacionais de predição/modelagem de interações proteicas como pré-requisitos para a obtenção de mapas completos das interações do proteoma (KESKIN et al., 2016). Segundo Liu e Chen (2012), métodos computacionais proporcionam alternativas promissoras para identificar relações entre macromoléculas e construir mapas de interações. Nesse sentido, Liu e Chen (2012) e Keskin et al. (2016) descrevem diversas abordagens experimentais e computacionais, bem como bancos de dados relacionados ao estudo de interações proteína-proteína.

No que se refere à obtenção e análise de interações proteicas como sistemas biológicos, recursos de bioinformática e plataformas de programação (incluindo *Cytoscape, Phyton*, R, MATLAB, entre outros) têm permitido a integração de informações disponíveis em bancos de dados de interações proteína-proteína com resultados experimentais (MONTI et al., 2018). Outras plataformas relevantes incluem o STRING, MINT, BioCarta, BioGrid, IntAct, entre outras. Além destas,

diversos bancos de dados fornecem informações sobre interações proteicas, entretanto deve-se considerar a redundância de informações, diferenças na forma com que as interações são anotadas e curadas, bem como as dificuldades na integração dos bancos de dados, sendo esta última um desafio de relevância para a obtenção de interatomas confiáveis (KESKIN et al., 2016).

Contudo, a análise das interações proteicas obtidas através de métodos computacionais constitui uma estratégia relevante para a seleção de alvos para validação com um contexto funcional melhor caracterizado, possibilitando a interpretação de dados proteômicos sob diversos aspectos de seu significado biológico.

3 OBJETIVOS

3.1 OBJETIVO GERAL

Analisar as proteínas diferencialmente expressas entre os tecidos tumorais (tumor primário de mama e linfonodo axilar metastático) e não tumorais (mama contralateral e adjacente) correspondentes de pacientes diagnosticados com câncer de mama no contexto de suas funções biológicas na tumorigênese mamária e fornecer informações sobre vias, processos biológicos e moléculas de interesse no câncer de mama.

3.2 OBJETIVOS ESPECÍFICOS

- Identificar e quantificar as proteínas expressas pelos tecidos tumorais (tumor primário de mama e linfonodo axilar metastático) e não tumorais (tecido mamário contralateral e adjacente ao tumor), correspondentes em pacientes do sexo feminino e um paciente do sexo masculino;
- Detectar diferenças significativas de expressão proteica entre os tecidos acima referidos;
- Comparar os conjuntos de proteínas diferencialmente expressas às informações disponíveis em bancos de dados relacionados ao câncer;
- Realizar análises de anotação e enriquecimento funcionais para as proteínas diferencialmente expressas;
- Obter e descrever redes de interação proteína-proteína envolvendo estas proteínas;
- Analisar o contexto biológico funcional das proteínas diferencialmente expressas, evidenciando vias e processos celulares de relevância na tumorigênese mamária.

4 MATERIAL E MÉTODOS

A análise proteômica comparativa descrita neste estudo foi realizada através das etapas representadas na figura 12.

FIGURA 12 – FLUXOGRAMA DA ANÁLISE PROTEÔMICA

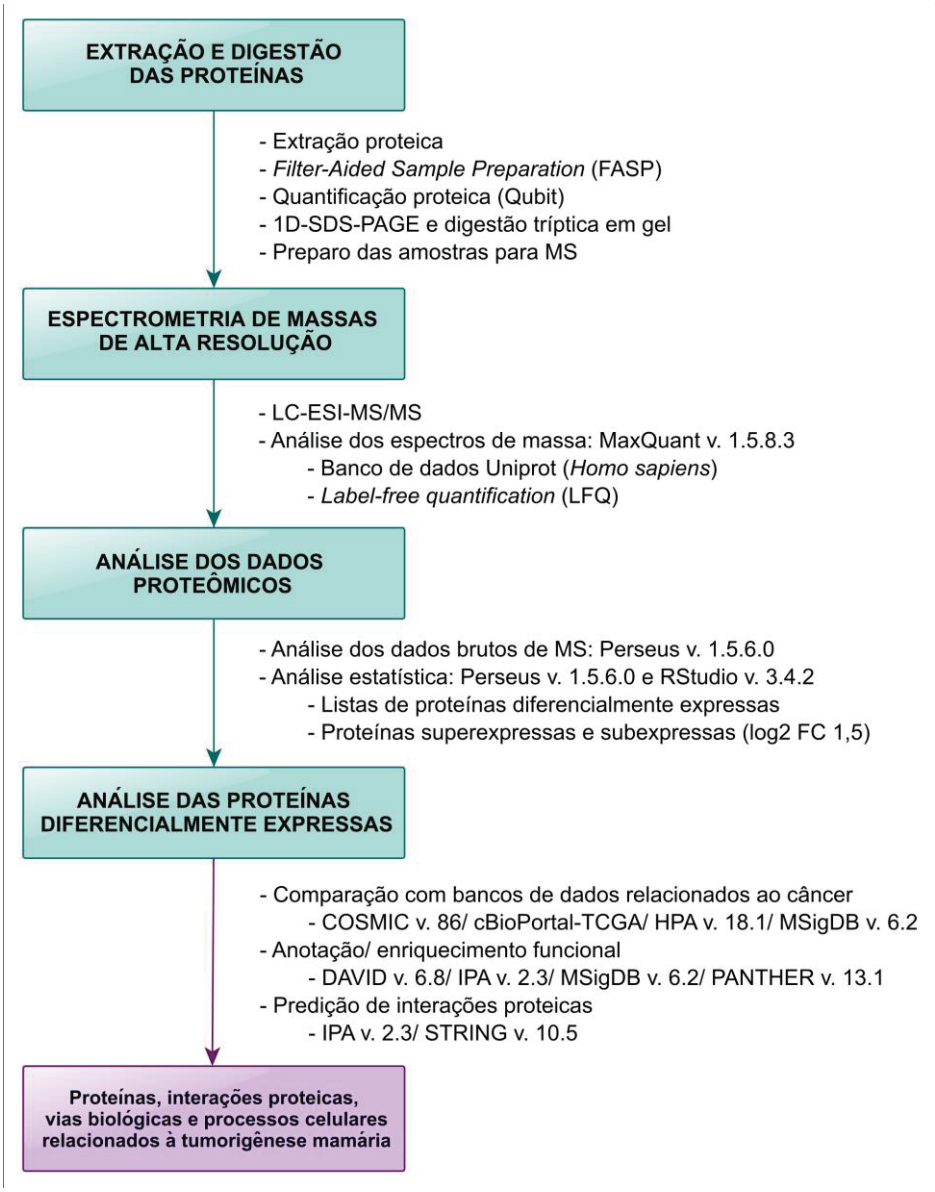

FONTE: O autor (2019).

LEGENDA: LC-ESI-MS/MS – Cromatografia líquida acoplada à espectrometria de massa com ionização por *eletrospray* (*Liquid Chromatography-Electrospray Ionization-MassSpectrometry*), MS – espectrometria de massa (*Mass Spectrometry*), FC – *fold change,* COSMIC – *Catalogue Of Somatic Mutations In Cancer*, TCGA – *The Cancer Genome Atlas*, HPA – *Human Protein Atlas*, MSigDB – *Molecular Signatures Database*, DAVID – *Database for Annotation, Visualization and Integrated Discovery*, IPA – *Ingenuity Pathway Analysis*, PANTHER – *Protein ANalysis THrough Evolutionary Relationships*, STRING – *Search Tool for the Retrieval of Interacting Genes/Proteins.*

4.1 CARACTERIZAÇÃO, COLETA E PROCESSAMENTO DAS AMOSTRAS

Este estudo pertence a um amplo projeto de pesquisa na área de genética dos tumores mamários, desenvolvido pelo Laboratório de Citogenética Humana e Oncogenética (LabCHO) do Departamento de Genética, Setor de Ciências Biológicas, Universidade Federal do Paraná (UFPR) e pelo Centro de Doenças da Mama (CDM) do Hospital Nossa Senhora das Graças. O estudo foi aprovado por Comitê de Ética (CONEP 7220/2003, Hospital Nossa Senhora das Graças).

As análises descritas nos capítulos apresentados foram realizadas com amostras de tecidos mamários tumorais e não tumorais de pacientes diagnosticadas com carcinoma ductal invasivo (CDI), provenientes do Hospital Nossa Senhora das Graças (HNSG) (Curitiba, Paraná, Brasil) e de um paciente do sexo masculino, com diagnóstico de CDI, atendido no Hospital das Clínicas (HC) (Curitiba, Paraná, Brasil). A inclusão dos pacientes foi realizada mediante a assinatura do Termo de Consentimento Livre e Esclarecido (ANEXO 1).

Dois grupos amostrais foram investigados separadamente através de análises proteômicas e *in sílico* em plataformas computacionais, descritas nos capítulos I e II do estudo.

O capítulo I consistiu na análise de amostras provenientes de sete pacientes do sexo feminino, sendo utilizados os seguintes tecidos: tumor primário de mama [TP, cuja sigla em inglês (PT) refere-se à *primary breast tumor*]; linfonodo axilar metastático (LN); e tecidos mamários não tumorais contralateral (NCT) e adjacente [NA, cuja sigla em inglês (ANT) refere-se à *adjacente non-tumor*]. O tecido NCT corresponde àquele retirado da mama oposta à acometida pelo câncer e 5 mm foram considerados como margem de segurança para a obtenção do tecido NA. O número amostral foi distinto para cada tecido em decorrência da disponibilidade de material biológico, cujos efeitos foram minimizados em função dos procedimentos estatísticos adotados.

O capítulo II descreve análises similares com amostras provenientes de um paciente do sexo masculino (P-MBC), incluindo os tecidos TP, LN e NA [referidos nesse capítulo como MPT (*male-primary breast tumor*), MLN (*male-axillary metastatic lymph node*) e MNT (*male-non-tumor breast tissue*). Posteriormente, o tecido TP foi comparado àquele proveniente de uma das pacientes do sexo feminino (referida como FPT – *female-primary breast tumor*) descrita no capítulo I, a qual

apresentou parâmetros clínicos e imunoistoquímicos semelhantes ao tumor masculino.

As informações clínicas e imunoistoquímicas dos pacientes descritos nos capítulos I e II, obtidas conforme os dados dos laudos anátomopatológicos, são apresentadas no quadro 2.

QUADRO 2 – CARACTERIZAÇÃO CLÍNICOPATOLÓGICA E IMUNOISTOQUÍMICA DOS PACIENTES

Código	Idade	Diagnóstico/ grau do tumor	Metástase	Imunoistoquímica				Amostras de tecido
				ER	PR	HER2	Ki-67	
P1	76	CDI - II	POS	SI	SI	SI	SI	TP, LN
P2	36	CDI - II	NEG	POS	POS	NEG (0)	10%	NCT, NA, TP
P3	63	CDI - II	POS	POS	POS	NEG (0)	28%	NCT, NA, TP
P4	39	CDI - II	NEG	NEG	NEG	NEG (0)	60%	NCT, NA, TP
P5	52	CDI - II	POS	SI	SI	SI	SI	NCT, NA, TP, LN
P6	67	CDI - III	POS	NEG	NEG	NEG (0)	80%	NCT, NA, TP, LN
P7**	59	CDI - III	POS	POS	POS	NEG (0)	45%	NCT, NA, TP, LN
P_MBC*	70	CDI - III	POS	POS	POS	(+2)	40%	NA, TP, LN

FONTE: O autor (2019).

NOTA: A análise das amostras das pacientes P1-P7 (sexo feminino) é descrita no capítulo I e dos pacientes indicados por "*" (sexo masculino) e "**" (sexo feminino) no capítulo II.

LEGENDA: Informações referentes ao diagnóstico e aos dados imunoistoquímicos dos pacientes cujas amostras de tecido foram analisadas neste estudo. RE – Receptor de estrogênio, RP – receptor de progesterona, HER2 – receptor de fator de crescimento epidérmico 2 (também denominado ERBB2), Ki67 – antígeno marcador de proliferação celular, SI – sem informação, P1-P7 – código das pacientes do sexo feminino, P_MBC – paciente do sexo masculino, CDI – carcinoma ductal invasivo, POS – positivo, NEG – negativo [+2 – resultado duvidoso e encaminhado para complementação pela técnica de hibridização *in situ* por fluorescência (*fluorescence in situ hybridization,* FISH), porém sem este resultado no prontuário], TP – tumor primário, LN – linfonodo axilar metastático, NCT – tecido mamário não tumoral contralateral, NA – tecido mamário não tumoral adjacente.

A coleta das amostras foi realizada durante a intervenção cirúrgica para a retirada do tumor e a reconstrução estética. O material biológico foi armazenado em tubos contendo a solução de estabilização *RNAlater* (*Thermo Fisher Scientific*). O processamento das amostras foi realizado no fluxo laminar para a remoção de resquícios de vasos sanguíneos e gordura, descartados posteriormente. As amostras foram dispostas sobre Placas de Petri e fragmentadas com o auxílio de pinças e tesouras estéreis, sendo estocadas a -80°C, embebidas em solução de *RNAlater*, para a futura extração das proteínas.

4.2 EXTRAÇÃO E DIGESTÃO DAS PROTEÍNAS

4.2.1 Obtenção dos extratos proteicos

A extração das proteínas foi realizada através das lises química (reagentes) e mecânica (homogeneização), conforme a adaptações de protocolos descritos para a proteômica baseada em LC-ESI-MS/MS (OSTASIEWICZ et al., 2010; TYANOVA; ALBRECHTSEN; et al., 2016).

Para cada amostra, 50 mg de tecido foram homogeneizados em 500 µL solução de dodecil sulfato de sódio (SDS) 4%, tris(hidroximetil)aminometano-hidrocloreto (Tris-HCl) 0,1 M pH 7,6 e ditiotreitol (DTT) 0,1 M, sendo a proporção de 100 µL de tampão para cada 10 mg de tecido. Nessa etapa, microtubos de 1,5 mL foram utilizados para permitir a adequada maceração do tecido através da agitação de esferas (*beads*) durante a homogeneização no disruptor de células *TissueLyser II* (Qiagen Corp. MD, EUA), a qual foi realizada por 3 minutos em frequência oscilatória de 25 Hz. Posteriormente, as amostras foram aquecidas a 95ºC, em banho seco, por 5 minutos. As etapas de homogeneização e aquecimento foram repetidas três vezes para a completa dissolução dos tecidos e consequente solubilização das proteínas. Após, o banho ultrassônico foi utilizado por aproximadamente 1 hora para diminuir a viscosidade dos extratos proteicos. A centrifugação foi realizada em duas etapas de 10 minutos a 4ºC e 20.000 x g, sendo os *pellets* resultantes descartados. A coleta dos sobrenadantes foi realizada com o auxílio de seringa e agulha, evitando a contaminação com resquícios de gordura. Os extratos proteicos obtidos foram congelados a -80ºC, sendo sua quantificação realizada nos dias subsequentes.

4.2.2 Preparo das amostras pelo método FASP

Previamente à quantificação das proteínas, o método de preparo de amostra mediante filtração (*filter-aided sample preparation*, FASP) (WISNIEWSKI et al., 2009), foi utilizado para eliminar o SDS dos extratos proteicos. Esse reagente foi adicionado à amostra na lise química e tem sido empregado na obtenção de extratos proteicos, no entanto, pode interferir na digestão enzimática das proteínas e na espectrometria de massa por ser ionizável e possivelmente mais abundante que alguns peptídeos (ZHOU et al., 2012).

A técnica FASP consistiu numa sequência de lavagens com soluções baseadas em ureia (UA) 8M em Tris-HCl 100 mM pH 8,8 [acrescida de DTT ou iodoacetamida (IAA)] e em bicarbonato de amônio (ABC) 50 mM, com centrifugações a 14.000 x g por 15 minutos a 20ºC. Para cada amostra, cerca de 40 uL de extrato proteico foi adicionado em filtros de ultracentrifugação do tipo Amicon 30kDa (Merck-Millipore, MA, USA), os quais possuem um filtro de membrana com limite de massa molecular específico (*nominal molecular weight limit* - NMWL), permitindo a purificação de componentes macromoleculares e a remoção de SDS, e um tubo acoplado para a coleta do material filtrado.

Inicialmente foram realizadas três etapas de homogeneização da amostra, com auxílio de micropipeta, em 200 µL de solução contendo UA 8M e DTT 10 mM, com posterior centrifugação e descarte do líquido filtrado. O DTT auxilia na redução das pontes dissulfeto, as quais contribuem para a formação da estrutura terciária das proteínas e impedem a exposição dos sítios de ligação da enzima tripsina, comprometendo a digestão enzimática das proteínas.

Após, foram adicionados 100 µL de solução contendo UA e iodoacetamida 50 mM ao conteúdo do filtro, com homogeneização sob agitação a 600 rpm por 1 minuto e incubação no escuro por 20 minutos, permitindo a alquilação dos resíduos de cisteína das proteínas, prevenindo a reoxidação das mesmas. Posteriormente, os filtros foram centrifugados e o líquido filtrado foi descartado.

Em seguida, foram realizadas duas etapas de homogeneização, com auxílio de micropipeta, com 100 µL de solução UA, centrifugação e descarte do líquido filtrado. E, por fim, duas etapas de homogeneização, com auxílio de micropipeta, em 100 µL de solução ABC, centrifugação e descarte do líquido filtrado.

Nesta etapa, aproximadamente 2 µL foram coletados de cada extrato proteico (contidos nos filtros) para a mensuração da concentração de proteínas por fluorometria através do método Qubit (Qubit® 2.0 Fluorometer, Life Technologies), verificando-se o volume necessário de tripsina para realizar a digestão enzimática, a qual pode ser realizada em solução ou em gel. Na primeira, na qual há adição de tripsina diluída em solução ABC nos filtros contendo o extrato proteico, incubação por 18 horas a 37ºC e posterior eluição dos peptídeos através de centrifugações a 14.000 x g por 10 minutos a 20ºC. Na segunda, o processo de digestão enzimática ocorre nas bandas proteicas obtidas após a prévia eletroforese unidimensional em gel de poliacrilamida, na presença de SDS (1D-SDS-PAGE), e os peptídeos são eluídos do gel 1D. No presente estudo, a etapa de digestão em gel foi incorporada ao protocolo para promover uma maior remoção de potenciais interferentes na LC-ESI-MS/MS, como gordura e resquícios de reagentes utilizados na lise química. Assim, o conteúdo dos filtros foi coletado e armazenado a -80ºC, para posterior utilização na 1D-SDS-PAGE e digestão enzimática.

4.2.3 Corrida eletroforética 1D-SDS-PAGE

Géis unidimensionais de poliacrilamida de empilhamento e de resolução (separação) a 10% foram utilizados para uma breve corrida eletroforética (previamente à digestão enzimática das proteínas). O primeiro foi composto por acrilamida 0,9%, Tris-HCl 120 mM pH 6.8, SDS 10%, persulfato de amônio (APS) 0,075% e tetrametiletilenodiamina (TEMED) 0,07%. O gel para a separação das proteínas, por sua vez, conteve acrilamida 0,9%, Tris-HCl 400 mM pH 6.8, SDS 10%, APS 0,075% e TEMED 0,07%.

As amostras foram aplicadas em triplicatas no gel 1D, ampliando a obtenção de peptídeos ao final da digestão enzimática, sendo aplicados 25 µg de proteína em cada replicata em tampão de amostra 4X. A corrida eletroforética foi realizada a 10 mA/ gel e foi mantida até que as proteínas alcançassem aproximadamente 1 cm após a entrada no gel de resolução, evitando a completa separação destas conforme o parâmetro massa molecular. Em seguida, os géis foram corados com azul de Coomassie (Coomassie R-250) 0,1% por 1 hora, em agitador orbital. A descoloração do gel foi realizada por 18 horas em solução contendo metanol 30% e ácido acético 10%.

Após, os géis foram dispostos sobre placas de vidro e as bandas contendo os extratos proteicos foram excisadas com o auxílio de lâminas de bisturi. Cada banda foi individualmente cortada em fragmentos de aproximadamente 1 mm x 1 mm, posteriormente acondicionados em microtubos para o preparo das amostras para a MS.

4.2.4 Digestão enzimática das proteínas e preparo para LC-ESI-MS/MS

Para cada amostra, os géis foram descorados por duas vezes em 300 µL de solução de descoloração, etanol e ABC 1:1 (*v:v*), sob agitação a 800 rpm, por 10 minutos a 25ºC, descartando-se o líquido. Posteriormente, estes foram mantidos sob as mesmas condições em 300 µL de solução de descoloração por 18 horas.

Após o descarte do líquido, foram realizadas duas etapas de desidratação do gel em 300 µL de etanol 100%, sob agitação a 800 rpm, por 10 minutos a 25ºC, com posterior evaporação do líquido mediante centrifugação em equipamento *speed vac* a uma pressão aproximada de 5 mbar (centrífuga SPD131DDA com armadilha refrigerada RVT4104, *Thermo Fisher Scientific*) por 7 minutos. A redução das proteínas foi realizada com 300 µL de solução de DTT 10 mM, ABC 50 mM sob agitação a 800 rpm, por 1 hora a 56ºC, e posterior descarte do líquido. Em seguida, a alquilação das proteínas foi efetuada com 300 µL de solução contendo iodacetamida 50 mM, ABC 50 mM sob agitação a 800 rpm, no escuro, por 45 minutos a 25ºC, descartando-se o líquido. Após, foi realizada uma nova etapa de lavagem com desidratação do gel por 10 minutos com etanol 100% (conforme acima), seguida pela adição de 300 µL de solução ABC, agitação a 800 rpm, por 20 minutos a 25ºC, e posterior descarte do líquido; esta lavagem foi repetida. A evaporação do líquido foi realizada mediante centrifugação em *speed vac* conforme descrito anteriormente.

Ao final desse processo, cada amostra foi incubada com 150 µL de solução de tripsina em ABC (proporção de 12,5 ng/µL de tripsina) por 20 minutos a 4ºC, sendo posteriormente removido o excesso de tripsina e acrescentado ABC em volume suficiente para cobrir a quantidade de gel. O período de digestão enzimática foi de 18 horas a 37ºC. Após, os peptídeos foram acidificados com ácido trifluoroacético (TFA) 0,5% de concentração final, homogeneizados no vórtex e coletados para um novo microtubo (uma vez que o líquido pode conter peptídeos).

Em seguida, os peptídeos foram extraídos por duas vezes em 200 µL de solução de acetonitrila (ACN) 30% e TFA 3% e duas vezes em 200 µL de ACN 100%, sendo cada etapa realizada sob agitação a 800 rpm, por 10 minutos a 25ºC, e posterior coleta do sobrenadante. Por fim, os peptídeos foram submetidos à centrifugação *speed vac* a 45 ºC por aproximadamente 120 minutos.

As etapas subsequentes consistiram na purificação e armazenamento dos peptídeos em *Stage-Tips* C18, as quais consistem em ponteiras de 200 µL com uma porção de membrana C18 inserida em seu interior (ISHIHAMA et al., 2006). A funcionalidade dessas ponteiras requer a prévia ativação da membrana C18 com 100 µL de metanol, seguida de centrifugação a 1.000 x g por 2 minutos, e equilíbrio com 200 µL de solução de ácido fórmico (AF) 0,1% e centrifugação a 1.000 x g por 6 minutos.

Os peptídeos (secos através de *speed vac*) foram ressuspensos em 100 µL de solução AF e foram transferidos para a membrana de C18, mediante centrifugação a 1.000 x g pelo tempo necessário para passagem da amostra pela membrana de C18. Em seguida, os *Stage-Tips* C18 foram lavados duas vezes com 200 µL de solução AF e centrifugados a 1.000 x g por 6 minutos a cada lavagem, sendo posteriormente armazenados a 4ºC até o momento da eluição.

A etapa de eluição é realizada previamente à LC-MS/MS, sendo necessário realizar uma lavagem inicial dos *Stage-Tips* C18 com 200 µL de solução AF e centrifugação a 1.000 x g por 6 minutos, descartando-se o líquido. Após, para cada *Stage-Tip* C18, a eluição é realizada duas vezes com 20 µL de solução AF 0,1%, ACN 80% em novos microtubos. A posterior centrifugação em *speed vac* por aproximadamente 10 minutos a 25ºC permite a evaporação da ACN. Ao final, os peptídeos foram ressuspensos em 20 µL de solução de AF 0,1%, dimetilsulfóxido (DMSO) 5%, mensurados pela fluorescência do triptofano (PAJOT, 1976; WISNIEWSKI; GAUGAZ, 2015) e transferidos para uma placa de 96 poços e então para o auto-amostrador do cromatógrafo.

4.3 ANÁLISE DE ESPECTROMETRIA DE MASSA DE ALTA RESOLUÇÃO

4.3.1 LC-ESI-MS/MS

Os peptídeos referentes a cada extrato foram analisados por nanocromatografia líquida acoplada à espectrometria de massa com ionização por eletrospray. Os experimentos de LFQ-MS foram realizados na plataforma de espectrometria de massa do ICC/Fiocruz-PR através do cromatógrafo EASY-nLC 1000 (*Thermo Fisher Scientific*) diretamente conectado ao espectrômetro de massas LTQ Orbitrap XL ETD (*Thermo Fisher Scientific*), o qual possui uma fonte de ionização por nanoeletrospray.

Para cada amostra, 5 µL (equivalente a cerca de 5 µg de peptídeos) foram injetados no sistema de cromatografia. A cromatografia ocorreu em coluna analítica de fase reversa, com dimensões de 15 cm de comprimento e 75 µm de diâmetro interno, empacotada com partículas de C18 de 3 µm de diâmetro (ReproSil-Pur 120, Dr. Maisch). As amostras foram separadas com um gradiente linear de 5 a 40% de ACN, 0,1% de AF e 5% de DMSO durante 240 minutos a um fluxo de 250 nL/min. Em seguida, os peptídeos foram ionizados através de nanoeletrospray e injetados no espectrômetro de massas. Os parâmetros adotados na ionização incluíram: voltagem e corrente do spray de 2,7 kV e de 100 µA, respectivamente; voltagem e temperatura do capilar de transferência de 35 V e de 175ºC, respectivamente; e voltagem das lentes de 100 V.

Os espectros dos precursores, modo MS (*full scan MS*) foram adquiridos no analisador *Orbitrap*, com resolução de 60.000, intervalo de m/z compreendendo 300 a 1.600, valor de *automatic gain control* (AGC) definido para 1x10E6 e tempo máximo de injeção de 1000 ms. Em seguida, os 10 íons mais abundantes foram selecionados para a fragmentação sequencial por dissociação induzida por CID no analisador *Ion Trap*, modo MS2, segundo o modo de aquisição de dados DDA. Na seleção de íons para MS2 foram adotados os seguintes parâmetros: valor de AGC definido para 3x104, tempo de preenchimento máximo de 150 ms e limite de sinal mínimo de 100 contagens. A fragmentação dos íons precursores foi realizada com energia de colisão normalizada de 35%, janela de isolamento de 2 m/z, tempo de ativação de 30 ms e tempo de permanência de um íon na lista de exclusão dinâmica de 90 s; a opção *lock mass* (401,922718 m/z) foi utilizada para melhorar a acurácia

de massa dos peptídeos, com erro abaixo de 0,5 p.p.m (partes por milhão). Íons de carga única e íons sem estado de carga definido não foram submetidos a MS2.

4.3.2 Análise dos espectros de massa

Os espectros de massa foram analisados no programa MaxQuant versão 1.5.8.3 (COX; MANN, 2008), sendo a identificação das proteínas realizada através do recurso de busca configurado para o banco de dados Uniprot (UNIPROT CONSORTIUM, 2018) espécie *Homo sapiens*, versão de 24 de maio de 2017, contendo 70.939 entradas, assumindo a digestão enzimática das proteínas por tripsina. A oxidação de metionina e a acetilação N-terminal de proteínas foram especificadas como modificações variáveis e a carbamidometilação de cisteína como modificação fixa. O mínimo de sete aminoácidos foi assumido para a identificação dos peptídeos. As identificações de peptídeos e proteínas foram aceitas para uma taxa de falso positivo (*false discovery rate,* FDR) menor ou igual a 1%. A opção de quantificação livre de marcação (*label-free quantification* - LFQ) foi adotada na quantificação das proteínas. Considerando o princípio da máxima parcimônia, proteínas com peptídeos similares, cuja distinção não foi realizada com base nos espectros de MS2, foram agrupadas e representadas como uma única identificação (não foram consideradas neste estudo). As identificações e quantificações no programa MaxQuant resultaram na obtenção da tabela "proteinGroups.txt", posteriormente analisada no programa Perseus versão 1.5.6.0 (TYANOVA; TEMU; et al., 2016).

Ao todo, três análises foram realizadas separadamente no programa MaxQuant, gerando tabelas de identificações e quantificações proteicas ("proteinGroups.txt") para: os dados descritos no capítulo I (amostras das pacientes do sexo feminino), adotando a opção de sobreposição entre corridas (*match between runs*) que agrupa as quantificações das triplicatas técnicas em um único dado de intensidade LFQ por amostra; e as análises apresentadas no capítulo II, sendo geradas duas tabelas (uma referente às amostras do paciente masculino e outra para as amostras dos tumores masculino e feminino), ambas sem sobreposição entre corridas para permitir a obtenção de informações sobre as quantificações em cada replicata técnica, possibilitando a posterior análise de variância entre os tecidos.

4.4 ANÁLISE DOS DADOS PROTEÔMICOS

A análise dos dados proteômicos foi realizada separadamente para cada arquivo “proteinGroups.txt” gerado pelo programa MaxQuant. Em geral, conforme indicado no fluxograma da figura 12, foram adotados os mesmos procedimentos para o processamento de dados e testes estatísticos nas análises descritas nos capítulos I e II. O contexto biológico referente às proteínas diferencialmente expressas foi analisado através de diferentes plataformas online, ressaltando variados recursos para a interpretação biológica de dados proteômicos.

4.4.1 Processamento dos dados proteômicos brutos

A análise inicial dos dados de MS foi realizada no programa Perseus utilizando as informações contidas no arquivo “proteinGroups.txt”. Os valores de intensidade LFQ foram considerados na quantificação da expressão proteica obtida em cada amostra.

Inicialmente, as identificações categorizadas como potenciais contaminantes (*contaminants*), peptídeos reversos (*reverse*) e peptídeos identificados a partir de apenas um sítio modificado (*only identified by site*) foram removidas. Nesta etapa, recomenda-se uma avaliação prévia da reprodutibilidade das replicatas biológicas/ técnicas, a qual pode ser realizada através da correlação de Pearson.

Em seguida, as amostras foram agrupadas de acordo com os tecidos aos quais pertencem (PT, LN, NCT, NA, etc.) e os valores de intensidade foram transformados em logaritmo de base 2 [log2 (x)], resultando na incorporação de designações “NaN” (*not a number)* onde não foram quantificados valores de intensidade LFQ. Dessa forma, possibilitou-se a seleção de proteínas a partir de quantidades mínimas de valores válidos observados por tecido. Para os dados analisados no capítulo I foram selecionados no mínimo 70% de valores válidos para cada tecido, conforme recomendações para o programa (ROBLES et al., 2014); de forma equivalente, para o capítulo II, foram selecionadas proteínas que apresentaram valores válidos em no mínimo duas replicatas técnicas. Esta etapa resultou numa redução substancial dos dados proteômicos, possibilitando uma maior robustez aos resultados obtidos.

Os valores de intensidade LFQ foram normalizados pelo método *width adjustment* previamente à substituição de valores inválidos (NaN), conforme descrito para dados de LFQ-MS (KARPIEVITCH et al., 2012). Esta última foi realizada utilizando os parâmetros recomendados para o programa (*width*, 0.3; *down-shift*, 1.8), atribuindo-se valores que representam sinais das proteínas de menor abundância, conforme a distribuição normal.

Com estes novos conjuntos de dados, a correlação de Pearson foi utilizada para avaliar a reprodutibilidade entre as amostras, sendo também observados os padrões de distribuição das mesmas (e de seus proteomas) na análise de componente principal (*principal component analysis*, PCA) e nos *heatmaps* gerados na análise de *clusterização* hierárquica.

As matrizes contendo os dados proteômicos de cada análise foram exportadas para a plataforma R, na qual os testes estatísticos foram realizados. Posteriormente, os dados referentes às proteínas diferencialmente expressas foram novamente importados para o programa Perseus, no qual foram geradas novas análises de *clusterização* hierárquica.

4.4.2 Análise estatística dos dados proteômicos

As análises estatísticas foram desenvolvidas na plataforma R, através de testes codificados manualmente, e no programa Perseus.

O programa RStudio versão 3.4.2 (<http://www.R-project.org>) foi utilizado para as análises proteômicas comparativas dos capítulos I e II (análise referente às amostras do paciente do sexo masculino). Nestas, para cada proteína, o teste de Bartlett foi inicialmente aplicado para avaliar a homogeneidade entre as variâncias observadas entre os tecidos. Proteínas cuja variância apresentou-se homogênea ($p>0.05$) foram, então, submetidas à análise de variância (ANOVA *one-way*), considerando $p<0,05$ e FDR de 0,05, utilizando o método de correção de múltiplas hipóteses de Benjamini-Hochberg. As proteínas diferencialmente expressas identificadas por ANOVA foram analisadas através do pós-teste de Duncan para identificar os pares de tecidos cuja diferença entre as médias de expressão das proteínas apresentou-se significativa. Dessa forma, listas de proteínas diferencialmente expressas foram obtidas para comparações a cada dois tecidos, as quais encontram-se descritas em cada capítulo.

O programa Perseus foi utilizado para realizar a análise estatística entre os tumores dos pacientes masculino (P_MBC) e feminino (P7), sendo adotado o teste *t* de *Student* no nível de significância de 5% (p-valor). A análise dessa lista de proteínas diferencialmente expressa está descrita no capítulo II.

As análises estatísticas resultaram na obtenção de listas de proteínas diferencialmente expressas entre os tecidos analisados, sendo desconsideradas as identificações que continham mais de uma proteína como possibilidade de identificação, uma vez que essas identificações não permitem inferir com precisão a identidade da proteína em questão.

Para cada lista de proteínas diferencialmente expressas, o valor de diferença entre as médias de expressão (*fold change,* FC) de 1,5 foi estabelecido para considerar superexpressão (≥ 1,5) ou subexpressão (≤ 1,5), mantendo-se os dados em log2. Portanto, utilizou-se o limite de log2 FC de 1,5 como parâmetro para avaliar proteínas com maior ou menor diferença de expressão entre os tecidos.

4.5 ANÁLISE *IN SÍLICO* DAS PROTEÍNAS DIFERENCIALMENTE EXPRESSAS

As proteínas diferencialmente expressas entre os tecidos analisados em cada capítulo foram analisadas em várias plataformas e bancos de dados.

Inicialmente, em todas as análises o projeto *Cancer Gene Census* (COSMIC versão 86, n= 699 genes) (<https://cancer.sanger.ac.uk/census>) foi utilizado para a obtenção de informações referentes a genes relacionados ao câncer. Informações também foram obtidas através do recurso de classificação funcional "*Gene families"*, disponível no banco de dados *Molecular Signatures Database* (MSigDB) versão 6.2 (LIBERZON et al., 2011; LIBERZON et al., 2015).

Comparações quantitativas e qualitativas entre listas de proteínas foram realizadas com o auxílio da plataforma *Interactivenn* (HEBERLE et al., 2015) (<http://www.interactivenn.net/>), que permite a confecção de diagramas de Venn com até seis conjuntos de dados.

No que se refere ao contexto biológico e às interações proteicas envolvendo as proteínas diferencialmente expressas, optou-se por realizar as análises de classificação e/ou enriquecimento funcional com o conjunto de proteínas que apresentou log2 FC de 1,5. As siglas dos genes codificadores dessas proteínas foram utilizadas para a obtenção dos resultados através das seguintes plataformas:

- *Database for Annotation, Visualization and Integrated Discovery* (DAVID) versão 6.8 (HUANG DA et al., 2009) (<https://david.ncifcrf.gov/>): Banco de dados biológicos integrado com recursos analíticos desenvolvidos para extrair sistematicamente os significados biológicos de amplas listas de proteínas e genes. O conjunto de recursos de anotação funcional permite a obtenção de termos biológicos (particularmente para termos de ontologia gênica – GO) e vias de bancos de dados como o *Kyoto Encyclopedia of Genes and Genomes* (KEGG) e *Reactome* enriquecidos (especificamente associados), bem como o agrupamento de anotações redundantes (*functional annotation clustering*) e outras funcionalidades. As anotações/ enriquecimento funcional são realizadas através do teste exato de Fisher modificado em escore EASE (*Expression Analysis Systematic Explorer*), o qual confere um ajuste mais conservativo ao primeiro (HOSACK et al., 2003).
- *Ingenuity® Pathway Analysis* (IPA) (*IPA-Ingenuity® Systems, QIAGEN Bioinformatics*) versão 2.3 (KRAMER et al., 2014): Plataforma comercial *online* que permite a análise de dados derivados de técnicas de alta resolução, incluindo experimentos de proteômica que geram listas de proteínas ou genes. Essa plataforma foi utilizada considerando os valores de FC para as proteínas diferencialmente expressas além das siglas de seus genes codificadores, permitindo a identificação de vias, funções, doenças, redes de interação molecular, reguladores *upstream* e biomarcadores envolvendo as proteínas identificadas. Para muitos desses aspectos, valores de z-score foram obtidos, indicando seu estado de ativação/ inibição em um tecido em relação ao outro. Os valores de p relacionados a vias e funções biológicas são estimados através do teste exato de Fisher e o FDR é baseado no método de Benjamini-Hochberg.
- MSigDB versão 6.2 (LIBERZON et al., 2015) (<http://software.broadinstitute.org/gsea/msigdb/annotate.jsp>): O recurso *online "Investigate Gene Sets"* foi utilizado para avaliar a sobreposição de dados entre o conjunto de dados informado e as coleções de grupos de genes (*gene sets*) disponíveis no banco de dados, incluindo *hallmarks* (LIBERZON et al., 2015), termos de ontologia gênica (termos GO), vias conforme as plataformas KEGG e *Reactome*, e módulos do câncer (SEGAL et al.,

2004). As coleções analisadas podem apresentar até 100 sobreposições, sendo os valores de p determinados através de distribuição hipergeométrica e o FDR pelo método de Benjamini-Hochberg.

- *Protein ANalysis THrough Evolutionary Relationships* (PANTHER) versão 13.1 (THOMAS et al., 2003; MI et al., 2017) (<http://www.pantherdb.org/>): Sistema de classificação que utiliza abordagens filogenéticas para categorizar proteínas e genes de acordo com suas famílias e subfamílias (proteínas evolutivamente relacionadas), termos GO e vias.
- *Search Tool for the Retrieval of Interacting Genes/Proteins* (STRING) versão 10.5 (SZKLARCZYK et al., 2017) (<https://string-db.org/>): Banco de dados que integra informações de interações preditas entre proteínas, sendo associações diretas (físicas) ou indiretas (funcionais), apresentando significados biológicos. As interações preditas derivam de diversas fontes, incluindo análises experimentais e sistemáticas de co-expressão, exploração de termos na literatura científica (*textmining*) e em bancos de dados, entre outros. Para cada interação proteína-proteína, um valor de escore é atribuído, representando a confiabilidade dessa predição, que indica a probabilidade de uma determinada interação possuir significado biológico conforme as fontes de dados consideradas.
    - TCGA (<https://cancergenome.nih.gov/>), *UCSC Xena* e *cBioPortal for Cancer Genomics* (<http://www.cbioportal.org/>): O TCGA consiste num banco de dados que contém informações publicamente disponibilizadas sobre o panorama de alterações genômicas envolvidas em diversos tipos de câncer. A plataforma *UCSC Xena* compreende um recurso de integração e exploração de dados “ômicos” e anotações fenotípicas e clínicas associadas, contendo conjuntos de dados de vários bancos de dados, incluindo o TCGA. O cBioPortal, por sua vez, compreende uma plataforma interativa que permite a visualização e análise de conjuntos de dados genômicos do câncer em larga escala, incluindo os estudos disponibilizados pelo TCGA. Nele, os perfis moleculares provenientes de tecidos e linhagens tumorais são organizados em perfis genômicos que descrevem alterações genéticas, epigenéticas, transcriptômicas e proteômicas, reduzindo a complexidade dos dados (GAO et al., 2014).

5 DESCRIÇÃO DOS CAPÍTULOS

A análise proteômica comparativa está descrita em dois capítulos: I – pacientes do sexo feminino diagnosticadas com CDI; e II – paciente do sexo masculino diagnosticado com CDI, cuja amostra de tumor mamário também foi comparada à de uma paciente do sexo feminino que apresentou dados clínicos e imunoistoquímicos similares, conforme descrito no subitem 4.1 da sessão “Material e Métodos”.

O capítulo I (item 6) é subdividido em três subitens:

- 6.1 – Artigo submetido à revista *Journal of Proteomics*, intitulado *“**Quantitative label-free mass spectrometry using contralateral and adjacent breast tissues reveal differentially expressed proteins and their predicted impacts on pathways and cellular functions in breast cancer**”* e com formatação de acordo com as normas indicadas pela revista. Esse artigo contempla a análise principal deste capítulo e descreve as proteínas diferencialmente expressas entre tecidos malignos e não tumorais bem como vias e funções biológicas, redes de interação proteica, reguladores *upstream*, biomarcadores descritos no câncer, entre outros aspectos, objetivando analisar o contexto biológico de atuação das proteínas que apresentaram alterações significativas de expressão no câncer de mama. O material suplementar deste artigo encontra-se disponível em GOMIG et al., 2019a.

- 6.2 – Artigo de dados (*Data in Brief*) submetido conjuntamente ao artigo acima, intitulado ***“High-throughput mass spectrometry and bioinformatics analysis of breast cancer proteomic data”***, e elaborado para apresentar os principais dados que fundamentam a análise acima descrita. Esse artigo contém a lista de proteínas diferencialmente expressas entre os tecidos avaliados, resultados das análises de *clusterização* hierárquica para os conjuntos de proteínas de cada comparação realizada e os resultados brutos obtidos da análise no programa IPA (QIAGEN Inc.). O material suplementar deste artigo encontra-se disponível em GOMIG et al., 2019b.

- 6.3 – Análise complementar ao subitem 6.1, intitulada **"Análise proteômica comparativa entre tecidos malignos e não tumorais de pacientes com câncer de mama"**, que consiste na descrição das proteínas comumente identificadas como diferencialmente expressas nas comparações entre o tumor primário de mama e ambos os tecidos não tumorais bem como entre o linfonodo axilar metastático e ambos os tecidos não tumorais. Essas proteínas foram analisadas no contexto de suas funções biológicas em processos e vias envolvidas no desenvolvimento e progressão do câncer, objetivando destacar proteínas que podem distinguir o tumor primário e sítios metastáticos no linfonodo axilar da condição saudável (a qual pode ser avaliada independentemente do tipo de tecido não tumoral utilizado como controle, NCT ou NA). A análise também objetivou a predição de processos e vias biológicas bem como de redes de interação proteica que podem ter relevância na tumorigênese mamária e que, através de estudos adicionais, possam ser avaliados como potenciais biomarcadores do câncer de mama. O material suplementar deste subitem é apresentado no apêndice 1 e a bibliografia encontra-se nas referências gerais do estudo.

O capítulo II (item 7) apresenta o artigo submetido à revista *The International Journal of Biochemistry & Cell Biology*, intitulado ***"Integrated analysis of label-free quantitative proteomics and bioinformatics reveal insights into signaling pathways in male breast cancer"*** e com formatação de acordo com as normas indicadas pela revista. Esse artigo descreve as proteínas diferencialmente expressas identificadas entre os tecidos malignos e não tumoral e seus contextos biológicos, sendo também avaliado o proteoma diferencial entre os tumores masculino e feminino e seu respectivo contexto biológico. As análises apresentadas neste artigo objetivam destacar as principais proteínas com alteração significativa de expressão no câncer de mama masculino e, entre outros aspectos, indicar seu envolvimento em vias de sinalização que podem ter função no desenvolvimento do câncer de mama, fornecendo informações para ampliar o conhecimento dos mecanismos moleculares subjacentes a essa doença em homens e alvos de interesse para a investigação como potenciais biomarcadores do câncer de mama masculino, mediante estudos adicionais. O material suplementar deste artigo é apresentado no apêndice 2.

6 CAPÍTULO I

6.1 QUANTITATIVE LABEL-FREE MASS SPECTROMETRY USING CONTRALATERAL AND ADJACENT BREAST TISSUES REVEAL DIFFERENTIALLY EXPRESSED PROTEINS AND THEIR PREDICTED IMPACTS ON PATHWAYS AND CELLULAR FUNCTIONS IN BREAST CANCER

Graphical abstract

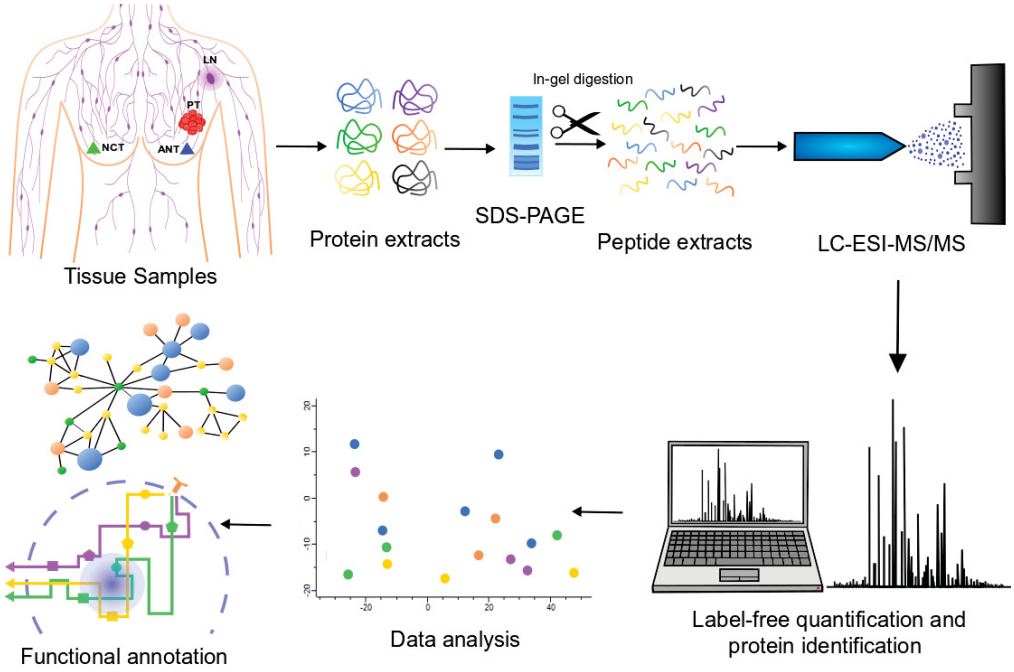

Highlights

- High similarity in the proteome of the contralateral and adjacent non-tumor tissues.
- DEPs of malignant tissues were related to LXR/RXR, eNOS, sirtuins and eIF2 pathways.
- Networks around NFkB, ERK1/2 and Akt were predicted for DEPs of primary tumor tissue.
- Cellular motility-related processes were observed to DEPs of lymph node tissue.

Quantitative label-free mass spectrometry using contralateral and adjacent breast tissues reveal differentially expressed proteins and their predicted impacts on pathways and cellular functions in breast cancer

Talita Helen Bombardelli Gomig[1]; Iglenir João Cavalli[1]; Ricardo Lehtonen Rodrigues de Souza[1]; Evelyn Vieira[1]; Aline Castro Rodrigues Lucena[2]; Michel Batista[2,3]; Kelly Cavalcanti Machado[3]; Fabricio Klerynton Marchini[2,3]; Fabio Albuquerque Marchi[4]; Rubens Silveira Lima[5]; Cícero de Andrade Urban[5]; Luciane Regina Cavalli[6,7]; Enilze Maria de Souza Fonseca Ribeiro[1]

[1] Genetics Department, Federal University of Parana, Curitiba, Brazil;
[2] Functional Genomics Laboratory, Carlos Chagas Institute, Fiocruz, Curitiba, Parana, Brazil;
[3] Mass Spectrometry Facility - RPT02H, Carlos Chagas Institute, Fiocruz, Curitiba, Parana, Brazil;
[4] International Research Center (CIPE) - A.C. Camargo Cancer Center, São Paulo, SP, Brazil;
[5] Breast Disease Center, Hospital Nossa Senhora das Graças, Curitiba, Brazil;
[6] Research Institute Pele Pequeno Principe, Curitiba, Brazil;
[7] Lombardi Comprehensive Cancer Center, Georgetown University, USA.

Corresponding author*:* Enilze Maria de Souza Fonseca Ribeiro, Centro Politécnico, Setor de Ciências Biológicas, Departamento de Genética - Caixa Postal 19071, Laboratório de Citogenética Humana e Oncogenética, CEP: 81531-990 - Curitiba/Parana, Brazil.
Tel: +55 4133611549, e-mail: enilzeribeiro@gmail.com

Abstract

Proteins play an essential role in the biological processes associated with cancer. Their altered expression levels can deregulate critical cellular pathways and interactive networks. In this study, the mass spectrometry-based label-free quantification followed by functional annotation was performed to investigate the most significant deregulated proteins among tissues of primary breast tumor (PT) and axillary metastatic lymph node (LN) and corresponding non-tumor tissues contralateral (NCT) and adjacent (ANT) from patients diagnosed with invasive ductal carcinoma. A total of 462 proteins was observed as differentially expressed (DEPs) among the groups analyzed. A high level of similarity was observed in the proteome profile of both non-tumor breast tissues and DEPs (n=12) were mainly predicted in the RNA metabolism. The DEPs among the malignant and non-tumor breast tissues [n=396 (PTxNCT) and n=410 (LNxNCT)] were related to pathways of the LXR/RXR, NO, eNOS, eIF2 and sirtuins, tumor-related functions, fatty acid metabolism and oxidative stress. Remarkable similarity was observed between both malignant tissues, which the DEPs were related to metastatic capabilities. Altogether, our findings revealed differential proteomic profiles that affected cancer associated and interconnected signaling processes. Validation studies are recommended to demonstrate the potential of individual proteins and/or pathways as biological markers in breast cancer.

Keywords: Breast cancer; proteomics; contralateral breast tissue; label-free mass spectrometry; bioinformatics analysis.

Significance

The proteomic analysis of this study revealed high similarity in the proteomic profile of the contralateral and adjacent non-tumor breast tissues. Significant differences were identified among the proteome of the malignant and non-tumor tissue groups of the same patients, providing relevant insights into the hallmarks, signaling pathways, biological functions, and interactive protein networks that act during tumorigenesis and breast cancer progression. These proteins are suggested as targets of relevant interest to be explored as potential biological markers related to tumor development and metastatic progression in the breast cancer disease.

Introduction

The biological processes that occur during the malignant cell transformation involve a cascade of molecular events tightly regulated by the availability of interconnected proteins. Protein changes include alterations in their expression levels, post-translational modifications, interrupted or abnormal activities and aberrant localization. In addition, their upstream regulators and downstream targets can be disrupted as a result of deregulations of cell signaling pathways and interaction networks [1]. Therefore, changes of proteome and interactome may affect the biological cellular functions and compromise the tissue environment homeostasis contributing to cancer development. The mapping of DEPs in biological pathways and networks has been widely performed in many types of tumor, including breast [2-5]. DEPs can be used as protein signatures of breast cancer contributing to biomarker research [6, 7].

Omics-based technologies allied to bioinformatics and computational science has been used as sensitive tools to assist in the diagnosis, therapies, and prognosis of cancer. Proteomics' methods have been employed to identify the protein content of tissues in specific physiological conditions. The use of mass spectrometry (MS)-based high-throughput proteomics in large-scale cancer studies has provided critical information regarding the deregulated proteins that are associated with the mammary tumorigenesis [8, 9]. Label-free quantification (LFQ) is one of the less expensive MS methods to detect differentially expressed proteins in complex biological specimens, such as solid tumors. The performance of LFQ approach have been demonstrated in several types of cancers [10, 11], including breast cancer [4, 12]. In the present study, we used this methodology, integrated with bioinformatics tools, to investigate cellular pathways, biological functions and interaction networks that could be associated with DEPs among paired non-tumor breast tissues (contralateral and adjacent), primary breast tumors and axillary metastatic lymph nodes samples.

Material and Methods

Patients and samples

This study was approved by the National Commission of Ethics in Research (CONEP number 7220)**.** Tissue samples were collected during the surgery procedure at Hospital Nossa Senhora das Graças in Curitiba, Paraná, Brazil, under patients´ signed informed consent. Samples were macrodissected for removal of fat, necrotic and other non-breast tissue areas and stored at -80^{o}C until protein extraction. In total, six contralateral (NCT) and six adjacent (ANT) (surgical 5 mm safety margin) non-tumor breast

tissues, seven primary tumor (PT) and four axillary metastatic lymph nodes (LN) were used for the LFQ-MS analysis. Clinico-pathological data were obtained in a decodified manner through the analysis of the pathology reports. The mean age was 56± 14.63 years old and all presented Invasive Ductal Carcinoma (IDC) (**Table 1**). The limited availability of biological samples resulted in an unequal number of tissue samples used in the proteomic analysis, as well as in different grade classification. However, appropriate statistical methods were applied to minimize the impact of these differences.

Contralateral disease-free breast samples were obtained when breast symmetrization was performed at the same time of tumor surgical removal. Therefore, all the paired samples of this study were from the same patient and shared the same physiological condition, allowing a reliable proteomic comparative analysis.

Sample preparation

The tissue samples were prepared for proteomic analysis according to standardized protocol adapted from Ostasiewicz and coworkers [13] and Tyanova and coworkers [9]. Briefly, the RNA later preserved samples were lysed in 4% SDS, 0.1 M Tris-HCl pH 7.6 and 0.1 M DTT (100 µL buffer per 10 mg tissue), homogenized in TissueLyser II sample disruptor (Qiagen Corp. MD, USA) at an oscillation frequency of 25 Hz for 3 min and heated to 95ºC. Homogenization and heating were repeated three times followed by sonication and centrifugation to remove cellular debris. In order to estimate protein concentration, an aliquot of each extract was added to 30-kDa Amicon Ultra filters (Merck-Millipore, MA, USA), washed three times with 8 M urea, 10 mM DTT, 0.1 M Tris-HCl pH 8,8 and twice with 50 mM ammonium bicarbonate (ABC). The concentration of protein extracts was obtained by the Qubit® 2.0 Fluorometer (Life Technologies). The unwashed protein extracts (25 µg) were separated in 1D-PAGE 10% (v/v) acrylamide gels, reduced with 10 mM DTT, alkylated with 50 mM iodacetamide and digested overnight with 12.5 ng/µl trypsin solution in ABC at 37°C. After that, the peptides were extracted twice with 30% acetonitrile (ACN), 3% trifluoroacetic acid (TFA) and twice with ACN, dried in a vacuum centrifuge and desalted with C18 Stage Tips.

NanoLC-ESI-MS/MS analysis and protein identification

Peptide mixtures were separated by online nanoscale capillary liquid chromatography and analyzed by nanoelectrospray tandem mass spectrometry (nanoESI MS/MS) in triplicate. The runs were performed on EASY-nLC 1000 chromatograph (Thermo Scientific) coupled to an LTQ Orbitrap XL ETD (Thermo Scientific) mass spectrometer (mass spectrometry facility RPT02H/Carlos Chagas Institute – Fiocruz Parana). The chromatography followed using a flow of 250 nL/min, with a 240 min linear gradient from 5 to 40% MeCN (ACN), 0.1% formic acid, 5% dimethyl sulfoxide (DMSO).

The separation was carried out in a C18 reversed-phase (RP) analytical column, with 15 cm length, 75 µm ID, packed with 3 µm C18 particles (ReproSil-Pur 120, Dr. Maisch). Full MS was acquired in the Orbitrap analyzer with a resolution of 60,000, m/z window of 300 to 1,600, enabling preview scan. MS2 analysis was performed in a data dependent acquisition (DDA) mode, where the ten most intense ions were subjected to collision-induced fragmentation (CID) fragmentation in the ion trap analyzer. A dynamic exclusion list of 90 s was applied, and the lock mass option was enabled for the m/z 401.922718. The spray voltage used was 2.7 kV, spray current 100 µA, capillary voltage 35 V, tube lens 100 V, and capillary heater 175°C. The mass spectra were analyzed with MaxQuant software version 1.5.8.3 [14]. Trypsin was set as the enzyme and the search was done against human UniProt protein database (UniProtKB [15] 24 May 2017, 70,939 entries) for protein identification. Oxidation of methionine and acetylation of protein N-terminal were set as variable modification and carbamidomethylation of cysteine as fixed modification. For peptide identification, at least seven amino acids were required. An FDR of 1% was independently applied for both peptide and protein identification. LFQ and match between runs options were enabled. The mass spectrometry proteomics data have been deposited to the ProteomeXchange Consortium via the PRIDE [16] partner repository with the dataset identifier PXD012431.

Data analysis

Protein expression was established based on the normalized spectral label-free protein intensity (LFQ intensity). Data was processed using the Perseus software version 1.5.6.0 [17]. Proteins that were identified based only on modified peptides (named “only identified by site”) as well as potential contaminants and reverse peptides were removed from the proteomic analysis. The LFQ intensity values were logarithmized (log2 (x)). Samples were grouped according to the following tissues: NCT, ANT, PT and LN. Reproducibility of biological replicates was accessed by Pearson’s correlation coefficients based on LFQ intensities.

Proteins quantified in at least 70% of samples for each tissue were selected to statistical analysis and a principal component analysis (PCA) and histogram plots were performed with log2-LFQ intensity values. Normalization was performed by width adjustment and missing values were imputed by values from the normal distribution (width, 0.3; down-shift, 1.8) to simulate signals from low abundant proteins, as recommended by Perseus developers [18]. Data was export for further analysis in R.

Bioinformatic analyses

Statistical analyses were performed in RStudio version 3.4.2 (http://www.R-project.org), using in-house scripts. ANOVA test with FDR cut-off 0.05 was applied to

proteins that presented homogeneous variances, accessed by Bartlett's test ($p<0.05$). The Duncan's test was carried out to identify significant differences in the mean values among the samples' pairs.

Changes in protein expression were based on log2 fold-change cutoff of 1.5 (equivalent to fold-change 2.8), aiming to obtain the largest differences among the tissues. The following groups of comparisons were evaluated: NCTxANT, PTxNCT, PTxANT, LNxNCT, LNxANT, and PTxLN. Quantitative comparisons among the groups were performed using the Interactivenn tool (http://www.interactivenn.net/) [19].

The 462 DEPs were investigated in the cBioPortal for Cancer Genomics platform (http://www.cbioportal.org/) in order to identify molecular changes described in the breast cancer data from The Cancer Genome Atlas (TCGA) Data Portal. A cohort of 613 breast primary tumor samples was defined as case list of samples based on the "phenotypes" dataset from TCGA Breast Cancer (BRCA) (available in the UCSC Xena Functional Genomics Browser, https://xena.ucsc.edu/), according to the following parameters: female gender; primary tumor; infiltrating ductal carcinoma histological type; no history of neoadjuvant treatment; and initial pathologic diagnosis at 36-76 years old, in the years 2000 to 2013. A single study query was performed in the cBioPortal platform using the study "Breast Invasive Carcinoma (TCGA, Provisional)" and the user-defined case list of samples abovementioned to investigate four genomic profiles: mutations, putative copy-number alterations (CNA) from GISTIC 2.0, mRNA expression (RNA Seq V2 RSEM, z-score= 2.0) and protein expression (mass spectrometry by the Clinical Proteomic Tumor Analysis Consortium, CPTAC; z-score = 2.0). The genes encoding the 462 DEPs were set as user-defined list for analysis against the TCGA breast cancer cohort.

Functional relevance of the DEPs at 1.5 log2 fold change was investigated using the "Investigate Gene Sets" web-based tool provided by the Broad Institute (http://software.broadinstitute.org/gsea/msigdb/annotate.jsp). The hypergeometric distribution was applied to examine the overlap between the input data (gene symbol of the DEPs) and the gene sets of the Molecular Signatures Database (MSigDB) version 6.2 [20, 21]. Hallmarks that summarize and represent specific well-defined biological states or processes [22] and biological process (Gene Ontology terms) were identified for the deregulated expressed proteins with FDR<0.05. Functional classes were also obtained from the MSigDB, according to the "Gene families" tool. The Cancer Gene Census of the Catalogue Of Somatic Mutations In Cancer (COSMIC) version 86 [23] was used for the identification of genes known to be involved in oncogenesis. Core Analysis tool of the Ingenuity Pathway Analysis software version 2.3 (QIAGEN Inc., https://www.qiagen bioinformatics.com/products/ ingenuity-pathway-analysis) [24] was employed to identify the most relevant signaling and metabolic pathways, diseases, biological functions and interaction networks affected by the deregulated proteins. Upstream regulator and

biomarker analyses were also performed by IPA's tools. Analyses through IPA allowed to determine the overall activation/inhibition status of biological processes and upstream regulators based on z-score from fold change values of DEPs and to evaluate predicted protein interactions.

Results and Discussion

Protein expression alterations identified by LFQ-MS

In this study, we investigated the LFQ intensities as a measurement of protein expression levels in paired breast tissue samples from the same patient. To the best of our knowledge, this is the first comprehensive study where the tissue from NCT is simultaneously compared to ANT, PT and LN tissue samples (from the same patient) using a high-throughput mass spectrometry protein quantification. Of particular interest is the analysis of non-tumor breast tissue obtained from the healthy contralateral breast of the patient (NCT), since the majority of the reported proteomic comparative studies using contralateral samples has been mainly restricted to nipple aspirate fluid (NAF) samples [25, 26]. Although the tumor tissues represents a small fraction of the tumor, tissue samples were complex and could be informative to access the heterogeneity and the main biological processes involved in the tumor biology [27].

Tissue specimens for all the seven breast cancer patients of this study were successfully analyzed using LFQ-MS, according to the flowchart of **Figure 1.** A total of 3,320 proteins were identified across all samples' groups (NCT, ANT, PT and LN). A number of 1,032 proteins that were quantified in at least 70% of each group were selected for the statistical analyses. An approximate Gaussian distribution of LFQ intensity values was observed in the histogram plots (**Supplementary File S1**). High reproducibility on the LQF intensities was observed in the biological replicates of all groups. The mean values of the Pearson correlation coefficients were r=0.9035 ±0.0298 in NCT; r=0.8935 ±0.0494 in ANT; r=0.8172 ±0.0672 in PT and r=0.8089 ±0.0611 in LN. The correlation analyses among all the groups are described in the **Supplementary File S2**. In the comparative analyses among the six groups evaluated **(**NCTxANT, PTxNCT, PTxANT, LNxNCT, LNxANT and PTxLN) a remarkable similarity was observed between the NCT and ANT (r=0.9017 ±0.0297) and between the PT and LN (r=0.8052 ±0.0674) groups.

Principal Component Analysis (PCA) analysis clustered the samples' groups, discriminating the non-tumor tissues (ANT and NCT) from the malignant ones (PT and LN) **(Figure 2A)**. A total of 462 differentially expressed proteins (DEPs) ($p<0.05$, FDR<0.05) was observed among the six comparative's groups (see Supplementary File S1 in [28]), which, as the PCA, were distinctly grouped in the hierarchical cluster analysis

(HCL) (Perseus v.1.5.6.0) **(Figure 2B)**. Interestingly, this clustering did not show any obvious distinction between the NCT and ANT groups and/or PT and LN tissue groups. HCL was also performed separately for each group comparison (see Figure 1 in [28]), where also can be noted that both NCT and ANT presented similar proteomic profiles and distinct clusters from the malignant tissues in all the comparison´s performed (PTxNCT, PTxANT, LNxNCT and LNxANT). The DEPs from PTxLN analysis grouped some PT and LN samples in the same cluster, evidencing the similarities among the proteome profiles of the malignant tissues.

The analysis of the 462 genes encoding the identified DEPs using the Cancer Gene Census (COSMIC) and the "Gene families" tool from MSigDB revealed known cancer associated oncogenes, tumor suppressors, transcription factors, kinases and others **(Table 2),** such as the *HNRNPA2B1, HSP90AA1, NPM1, TNC* and *RPL5* genes.

cBioPortal analysis of the differentially expressed proteins and the TCGA breast cancer cohort

The cancer-related molecular changes described for these 462 genes were explored in the cBioPortal platform using a cohort of 613 primary breast tumor samples from TCGA database (defined based on clinico-pathological data similar to the patients of the present study). Regarding the limited availability of protein expression data in the TCGA cohort, the mRNA expression and CNA profiles were also applied in the cBioPortal analysis. In general, a high frequency of gene alteration was observed in this analysis, which highlights their involvement in breast cancer development and progression (**Supplementary File S3**).

The cancer genomics datasets analyzed across the samples and genes revealed that the majority of the proteins at 1.5 log2 fold change identified in our study presented alterations in their profiles of protein and mRNA expression (up-regulation/ down-regulation) CNA (amplification/ deep deletion) and mutation (missense/ truncating/ inframe).

Particularly, 51 DEPs had the same protein expression levels (up-regulated or down-regulated) in the TCGA cohort, 43 of which with correspondent mRNA expression and CNA alterations. In addition, 89 DEPs presented a similar protein expression levels in at least one sample of the TCGA cohort; 61 of these proteins showed a correspondent mRNA expression and CNA alterations. These genomic profiles were also consistent with the protein expression levels of 107 DEPs, which did not have the protein expression available or presented divergent proteomics data. Altogether, most of the proteins predicted in relevant functional annotations had a compatible profiling in the TCGA cohort analyzed. Some of the main DEPs and their results from the cBioPortal analysis are

described in **table 3**. Complete OncoPrint graphical summary is shown in the **Supplementary File S3**.

The cBioPortal analysis provided an overview of the cancer-related genes and their molecular changes in a large cohort of primary breast cancer samples. The alterations reported in the OncoPrint data and the fold change values of the DEPs reinforces the relevance of deregulated proteins in the breast tumorigenesis and could help to guide further studies in the breast cancer research. In this context, we highlight that all the proteins discussed below presented the protein expression and mRNA expression and/ or CNA profiles compatible with the protein expression levels quantified in this study. It reinforces the potential of these proteins as biomarkers in breast cancer.

Comparative proteomic analysis of non-tumor breast tissues

High similarity in the protein expression profiles was observed in the comparison of non-tumor breast tissues groups (NCTxANT). Only 1.2% (12/1032) of the proteins identified in these groups were observed with significant differences in expression, however in general, they presented with low fold change values (log2-FC<1.5) (see Supplementary File S1 in [28]).

The enrichment analysis using MSigDB revealed MYC and E2F targets as relevant regulators of the DEPs observed in this group comparison **(Table 4)**. The most relevant functions (GO terms – biological process) were related to RNA metabolism, with DEPs encoded by the *FBL* and *NOP56* genes associated to the processing and modification of RNA and the ones by the *FUS, DDX6* and *SYNCRIP* genes to the RNA metabolic process. Due the high similarity of the non-tumor proteomic profiles and no proteins at 1.5 log2 fold change, IPA's analysis was not performed in these groups' datasets.

Despite of some statistically significant differences, we point out to the remarkable similarity in the protein expression levels that was observed in both non-tumor breast tissues analyzed, reinforcing that the ANT, once the surgical safety margin is considered, expresses a typically non-tumor proteome profile, without relevant protein changes when compared to the contralateral disease-free breast (NCT). Therefore, both tissues could independently be considered as references of non-tumor breast tissue for proteomic studies.

Comparative proteomic analysis of malignant versus non-tumor breast tissues

The comparative analysis among the malignant and non-tumor tissues was performed combined and separately for each comparative's group: PTxNCT, PTxANT, LNxNCT and LNxANT.

A total of 32.8% (339/1032) DEPs were commonly observed among all the malignant *versus* non-tumor tissue comparisons, with 45.1% (153/339) at 1.5 log2-fold change; sixty three and 90 of these proteins were up and down-regulated, respectively, in

the malignant tissues compared to the non-tumor breast tissues. The top 15 DEPs observed with the largest fold change values (≥ 1.5 and ≤ -1.5) among these groups are shown in **Figure 3A.** Tenascin-C (*TNC*), an extracellular matrix glycoprotein, was the up-regulated protein observed with the highest fold change in the comparison of these groups (3.38 log2-folds in PTxNCT and 4.33 log2-folds in LNxNCT), with expression levels gradually increasing as the lesions progressed (from NCT and ANT to PT to LN). This findings support the studies in colorectal and breast tumors, where high expression levels of tenascin-C has been associated with tumorigenic phenotypes and tumor progression [29, 30]. Other identified proteins, on the other hand, presented a gradual decrease in their expression from the non-tumor breast tissues to the malignant ones, with the lowest levels observed in the lymph node samples. Among these proteins are included the ones encoded by the *COL6A6*, *FABP4, LIPE, MGLL* and *SORBS1* genes; these proteins presented fold change values between -4.3 and -6.5 in PTxNCT and LNxNCT groups' comparisons.

Ninety-four of the 153 (61.4%) DEPs observed among the malignant and non-tumor tissue groups, were identified in the IPA database analysis to be associated with cancer and other types of diseases, 41 of which were also commonly DEPs among the PTxNCT, PTxANT, LNxNCT and LNxANT individual groups' comparisons **(Figure 3B).** Among these proteins, it is included the ones encoded by the *FABP4* and *TNC* genes.

In LN samples, DEPs encoded by *SERPINA1, SERPINA3* and *TF* genes could be investigated as potential biomarkers of tumor progression. These proteins presented LFQ intensities remarkable different among the PTxNCT and LNxNCT groups' comparisons, with expression levels gradually decreasing from NCT and ANT to PT to LN. The protein encoded by the oncogene *MYH9,* on the other hand, was up-regulated only in PTxNCT groups' analysis, but its expression levels in LNs were also increased compared to non-tumor breast tissues (log2-FC<1.5), so further studies are required to access their potential to discriminate PTs from metastatic sites, as the LNs.

Interestingly, as we reported above, the comparisons of PT and/or LN groups with NCT or ANT, showed a high number of common DEPs proteins (n= 375 for PTxNCT and PTxANT, and n= 407 for LNxNCT and LNxANT). These data confirms the similarity in the protein expression profiles of both non-tumor tissues.

All the DEPs observed among the PTxNCT (n= 396), PTxANT (n= 405), LNxNCT (n= 410) and LNxANT (n= 435) groups of samples were identified in the enrichment analysis of MSigDB to be involved in critical cancer associated "hallmarks", including MYC targets, MTORC1 signaling, xenobiotic metabolism and E2F targets. **Table 5** presents the main DEPs related to hallmarks observed in PTxNCT and LNxNCT groups' analysis. Similar results were identified in the ANT groups' comparisons.

The IPA's analysis from the DEPs among the PTxNCT and PTxANT and the LNxNCT and LNxANT groups' comparisons revealed similar data. Therefore, the results

below were discussed based on the PTxNCT and LNxNCT data (unique results for each group comparison were first presented followed by common data). The general IPA's data (canonical pathways, disease/ function annotations and networks) are presented in the Supplementary File S2 in [28].

Canonical pathways, interaction networks and upstream regulators of the DEPs from PTxNCT groups' comparison

In the PTxNCT groups' comparison, IPA's analysis identified a total of 91 canonical pathways statistically significant ($p<0.05$), 31.9% (29/91) of them were cell signaling pathways. The activated/ inhibited pathways in this group were also identified for the DEPs from LNxNCT groups' comparison and were presented later.

In the breast tumor context, the IPA's "disease and function" analysis also revealed a total of 100 DEPs significantly associated with the "breast cancer" disease. The top-15 up-regulated proteins in the PTxNCT, ranked by the fold change, included those encoded by the *TNC, CSE1L, KRT18, DSP, PARP1, DHX15, KRT19, CKAP4, PRKDC, HSP90AA1, RPL4, EPRS, EFTUD2, CRABP2* and *TYMP* genes and the top-15 down-regulated by the *CES1, AKR1C1, LIPE, ANK1, SLC4A1, MCAM, MGLL, AKR1C3, COL4A2, TNS1*, *CRYAB, LTF, FBLN5, RRAS* and *NID2* genes. Several DEPs among malignant and non-tumor breast tissues that presented the largest fold change values in our study were not described in breast cancer IPA's database and could play a role in malignant transformation. Further studies will be conducted by our research group to elucidate the biological function of the most relevant DEPs in mammary tumorigenesis.

IPA's networks analysis from the DEPs observed in this group (PTxNCT) revealed important biological interactions with recognized players in oncogenesis, such as NFkB, ERK1/2 and AKT. The top three interactive networks with a minimum score of 35 are presented in **Figure 4.** The Nuclear factor-κB (NF-κB), a component of the network shown in **Figure 4A,** is from a family of transcription factors that plays an essential role in immune and inflammatory responses [31]. Several upstream and downstream regulators of this factor are mediated by the NFkB signaling, such as *APOH*, *CAT, HSPD1, LTF, NAMPT* and *PLG* encoded proteins with deregulated expression, suggesting that this complex is probably impaired in the tumors studied. Another targeted network involves proteins that regulate the ERK1/2 pathway **(Figure 4B),** composed of mitogen-activated protein (MAP) kinases that play a role in the Ras-Raf-MEK-ERK signal transduction cascade [32]. Their DEPs partners were encoded by *ILK, ITGA6* and *TNC* genes as well as the ones from the PI3K family. Last, is the network involving the AKT protein (AKT/PBK) **(Figure 4C),** a serine/threonine protein kinase that participates in signaling pathways regulating many cellular functions, including cell growth, apoptosis and survival [33]. Relevant genes involved in the AKT activation, such as *HSP90* members, *MGLL,*

PARP1 and *PRKDC* were observed encoding DEPs in the malignant tissues of this study. Many DEPs observed in these networks were enriched in relevant hallmarks mentioned above, such as encoded by *APOA1, CAT, GAPDH, HSPD1, PLG, PON1, PRKDC* and *NPM1* genes. Further studies in the proteins composing these identified networks and their interactions can lead to the identification of potential tumor targets with relevance to breast cancer.

IPA analysis was also performed to predict the activation/inhibition of upstream regulators according to the DEPs observed in PTxNCT groups' comparison. A total of 206 upstream regulators were discovered at $p<0.05$, 12.6% (26/206) of them were predicted with activation/inhibition z-score values. The main activated regulators observed include the transcription factors MYC and SATB1 and the mature microRNA, miR-146a-5p **(Figure 5A-C).** MYC was the key upstream regulator of at least 15 proteins, including the ones encoded by *FBL, HSP90AA1, HSPD1, NOP56* and *NPM1* genes, also observed in the MYC targets hallmark. MYC is a central signaling hub that regulates expression of targets in multiple pathways and cellular processes, such as cell death, proliferation, differentiation, stress mechanisms and drug resistance [34]. In addition, SATB1 and miR-146a-5p were predicted as increased in malignant tissues; first by mediating the activation of *HSP90AA1, HSPA8* and *ILF3* genes and second by indirectly inhibiting the expression of *CAT, CFH, LTF* and *PGLYRP2* genes. Another important regulator predicted by our data was the *TP53* gene **(Figure 5D)** that acts as a transcription factor inhibiting the expression of several genes, such as the ones of our study, *APOE, CAT* and *XPO1*. In summary, this upstream regulator analysis revealed the relationship of known cancer driver genes with the proteins identified in our study, highlighting their relevance in cancer research.

Canonical pathways, interaction networks and upstream regulators of the DEPs from LNxNCT groups' comparison

In the LNxNCT groups' comparison, IPA's analysis predicted DEPs to be involved in 100 canonical pathways ($p<0.05$), 35% (35/100) of them related to cell signaling pathways **(Table 6).** The pathways activated only in this group included the ones associated with cellular motility, such as: the regulation of actin-based motility by Rho, a small GTPase with a recognized role in cell migration and whose signaling pathways were activated in LN samples; the remodeling of epithelial adherens junctions, which indicates changes in the cellular morphogenesis and the occurrence of epithelial–mesenchymal transitions (EMT) [35]; the actin nucleation by ARP-WASP, a complex that contributes to nucleate branched actin filaments which is important for lamellipodial protrusion and endocytosis [36]; and the Fcγ receptor-mediated phagocytosis in macrophages and monocytes which is also related to actin cytoskeleton rearrangements [37]. The proteins

encoded by *ACTR2, ACTR3*, *ARPC2* and *ARPC3* genes were commonly observed in these pathways, in addition to *ACTB, EZR, GNA11*, *RRAS* and *RAC2* encoded proteins.

In the LNxNCT groups' comparison, IPA analysis predicted three networks with score threshold of 35 involving the DEPs, including the lipid metabolism, small molecule biochemistry, vitamin and mineral metabolism; cellular response to therapeutics, infectious diseases and neurological disease; and RNA post-transcriptional modification, cancer and organismal injury and abnormalities (see Supplementary File S2 in [28]). A total of 188 upstream regulators were identified ($p<0.05$) for DEPs from this groups' analysis, 15.9% (30/188) of them with activation z-score. The main activated/ inhibited upstream regulators presented similar regulatory networks to the figure 5, reinforcing that the observed DEPs affected interactions among relevant known cancer genes.

Canonical pathways and main biological functions affected by the DEPs from PTxNCT and LNxNCT groups' comparisons

Fourteen pathways based on activation/inhibition z-score values were commonly observed in the PTxNCT and LNxNCT groups' comparisons **(Table 7).** The LXR/RXR activation pathway was the most inhibited biological process predicted from DEPs observed in the malignant breast tissues. The liver X receptors (LXR) act as sensors of cholesterol homeostasis, fatty acid and glucose metabolism and can also modulate cellular immune responses [38, 39]. In the PT and LN samples, DEPs related to LXR/RXR activation were down-regulated, which may suggest that these proteins play a central role in lipid-related processes in cancer, as observed in colon, breast and prostate carcinomas [10, 40, 41]. The apolipoproteins A1, B, E and H (encoded by *APOA1, APOB, APOE* and *APOH* genes) and the associated antioxidant enzyme paraoxonase 1 (encoded by *PON1* gene) were the main proteins involved in lipid-related functions in this study, and are reported to be present with lower expression levels in cancer [42], which supports our findings. The activation of LXR/RXR pathway drives the transcription of genes involved in cholesterol efflux and reduced cholesterol influx [38]. Cholesterol levels in the cells are closely associated with the hyperproliferation of tumor cells, whereas lower levels affect cell growth, inducing cell death [38]. This suggests that low cholesterol efflux and elevated lipid content in tumor cells could contribute to tumor growth. *APOE* is also a potent metastatic suppressor gene, whose expression is increased under the activation of the LXR/RXR pathway [43]. Therefore, based on our data, the down-regulated expression of the protein apolipoprotein E (observed in both the PT and LN lesions) may be central in inhibiting this pathway.

The reactive oxygen species (ROS) were also identified among the pathways to be affected by the DEPs observed in both the PTxNCT and LNxNCT groups' comparisons. Oxidants present roles in inflammation, immune regulation and stress-related responses [44]. Under pathological conditions, the uncontrolled synthesis of ROS induces the

oxidative stress and cytotoxicity, disrupting cellular functions and contributing to initiate and amplify the malignant phenotype [44, 45]. Nitric oxide (NO) is a type of ROS mainly produced by endothelial nitric oxide synthase (eNOS) [46]. The expression of eNOS has been related in many types of tumors, including breast [47]. In cancer, different levels of NO have been reported to promote or inhibit the growth tumor and metastasis [46, 47]. In the malignant tissues analyzed in our study, we observed down-regulated expression of proteins involved in the eNOS signaling and NO synthesis in comparison to the expression observed in non-tumor breast tissues. Up-regulated chaperones HSP90 were predicted in this signaling pathway. HSP90 plays a key role for maintaining the activity of many signaling proteins, including eNOS activation and, consequently, modulation of NO and O_2^- levels in the cell [48]. In our data, five chaperones were up-regulated in malignant tissues compared to the non-tumor breast tissues, including the members encoded by *HSP90AA1* and *HSP90B1* genes.

Signaling by eukaryotic translation initiation factor 2 (eIF2) and sirtuins were the most activated pathways predicted to malignant tissues. The eIF2 signaling is important to protein synthesis and their activation was described in different colorectal cancer cell lines, associated to up-regulated proteins [49]. Among them, we highlight the proteins encoded by *RPL5*, a tumor suppressor gene [50], *HSPA5*, an important player in cancer progression [51] and *RRAS*, a critical regulator of the tumor vascularization [52]. Sirtuins belongs to the class III histone deacetylase enzymes NAD^+-dependent (SIRT1-SIRT7 members in mammals) that play a role in many cellular processes [53]. In tumor microenvironment, sirtuins signaling is associated to cellular responses to stress, hypoxia, angiogenesis, inflammation, and EMT process [54]. In this study, up-regulated proteins in sirtuin signaling pathway were related to *IDH2, NAMPT, PARP1, PRKDC and TRIM28* genes.

The actin cytoskeleton signaling, which plays a crucial role in cell motility [55] confers to the malignant cancer cells the ability to invade adjacent tissues and blood/ lymph vessels, and ultimately to metastasize [56]. Interestingly, this pathway was predicted as inhibited in PT in contrast to their activation in LN samples, suggesting DEPs that could play a role in metastasis. In both malignant tissues, we observed the up-regulation of proteins encoded by *ACTB* and *EZR* genes and the down-regulation of proteins encoded by the *KNG1* and *RRAS* genes. On the other hand, myosin-9 (*MYH9),* was observed only in PT samples. In LN tissue, we highlight the actin-related proteins encoded by *ACTR2, ACTR3*, *ARPC2* and *ARPC3* genes that plays a role in cellular migration [57] and Ras-related C3 botulinum toxin substrate 2 (RAC2), a GTPase associated to metastasis [58].

We also evaluate the IPA's "disease and function" to further understand the biological role of protein expression alterations and its impact on the tumor

microenvironment. **Table 8** shows some of the main functions found for up and down-regulated proteins in the IPA's analysis from PTxNCT and LNxNCT groups' comparison.

The fatty acid metabolism was the most inhibited biological function predicted to be affected in the malignant tissues studied. Alterations in fatty acid metabolism are known to occur in many types of cancers, including breast, with high concentration of lipids reported to be present in tumor cells [59-61]. In the PTxNCT and LNxNCT groups' comparisons, IPA's analysis predicted various lipid-related functions inhibited in malignant tissues, such as lipid secretion and transport. Fatty acid metabolism and LXR/RXR activation pathway shared several down-regulated proteins, indicating the interconnection of DEPs in many biological processes. The immune response functions were predicted as inhibited in malignant tissues according to the IPA and most of their related DEPs were down-regulated in PT and LN samples compared to non-tumor breast tissues. Importantly, apolipoprotein E (*APOE*) was highlighted in many biological processes related to cancer in our study.

Despite of decreased NO synthesis, the function of the generation of ROS and oxidative stress response were predicted as activated in the malignant tissues analyzes. DEPs encoded by *AGT, CAT* and *NAMPT* genes and specific members of aldehyde dehydrogenases (encoded by *ALDH2* and *ALDH3A2* genes) were associated to ROS according to the IPA. Reduced antioxidant activity of catalase (*CAT*) leads to accumulation of peroxides H_2O_2 that may enhance DNA damage and promote neoplastic transformation [62]. In malignant tissues, catalase was found among the top-15 down-regulated cancer-related genes according IPA's Biomarker Analysis (see **Figure 3B**). On the other hand, high expression levels of nicotinamide phosphoribosyltransferase (*NAMPT*) have been reported in tumors, as in our study, and its inhibition results in a decreased cellular NAD level and cell growth, enhancing the susceptibility to oxidative stress [63].

Interestingly, we found relevant functions specifically associated with tumor cells, including decreased cell death and increased proliferation, invasion and migration in malignant tissues, as expected. These biological processes integrate the recognized hallmarks of cancer [64]. The proteins encoded by *CAT, CSE1L* and *ILK* genes were associated to all of these functions. In addition, we observed alterations in proteins that are well known in cancer and act in most of the described functions above [65-70], including those up-regulated encoded by the *EZR, HDGF, HNRNPA2B1, HSP90AA1, HSPA5, ILF3, NPM1, PARP1, PRKDC, TNC* and *TRIM28* genes and down-regulated encoded by the *AGT, APOE, MCAM and S100A10* genes.

Comparative analysis of malignant tissues

The proteomic profile of the malignant tissues (PT and LN samples) presented high similarity: only 6.3% (65/1032) of the proteins were differentially expressed with statistical

significance. Of these, only 22% (14/65) were at 1.5 log2-fold change (see Supplementary File S1 in [28]).

The functional classes of the 65 DEPs observed among these groups, according to the “Gene families” tool of MSigDB, identified the oncogenes *CTNNB1, DDX6, SEPT6* and *SEPT9*, the tumor suppressor *SDHB* and the transcription factors *CCT4, CTNNB1* and *PSMC5*. Functional enrichment analysis of these 65 DEPs showed among the top 10 enriched hallmarks, the EMT, apoptosis and KRAS and mTORC1 signaling pathways **(Table 9).** These pathways are known to be critical regulators of the metastatic ability, playing important roles in cell growth, differentiation, survival, migration, and cytoskeletal changes [71]. In many of these hallmarks, proteins encoded by *BGN, COL1A2* and *MGLL* genes were related to invasive breast cancer according to the IPA’s “disease and function” data. These proteins presented a gradual decrease in their expression from the non-tumor breast tissues to the malignant ones, with the lowest levels observed in the lymph node samples.

Biglycan (*BGN*) is a small leucine-rich proteoglycan of the extracellular matrix and plays a role in neoplastic transformation. Despite the described up-regulated expression of biglycan in many types of tumors [72, 73], in our study, we did not identify significant difference in the expression of this protein in the PT samples when compared to the non-tumor breast tissues. In contrast, the LN samples showed the lowest levels of biglycan in all groups’ comparisons (-3.17 log2 fold change), suggesting a role in cancer progression.

Collagen alpha-2(I) chain (*COL1A2*) belongs to type I collagen, an important member of collagen family that play a key role in extracellular matrix structure and its deregulation has been reported in several types of cancer [74]. In our study, collagen alpha-2(I) chain was found related to advanced stages of disease (TNM stages II and III) and to Rho protein signal transduction, an important signaling to metastasis. Its decreased expression levels in LN samples (and their gradual decrease from NCT and ANT to PT to LN) is consistent to findings that suggest *COL1A2* as a potential tumor suppressor in human colorectal cancer (CRC), which down-regulated levels in primary CRC compared to adjacent non-tumor tissues were correlated to invasion and lymph node metastasis [75].

Monoglyceride lipase (*MGLL*) is a lipase that catalyzes the conversion of monoacylglycerides to free fatty acids (FFA) and glycerol. Evidences suggest that *MGLL* is related to metastasis behavior through the production of signaling lipids including monoacylglycerol (MAGs), FFA, and secondary lipid metabolites which contribute to cancer cell proliferation and aggressiveness [76]. Our study corroborates with previous studies that described reduced or absent levels of MGLL mRNA and protein expression in multiple human malignances, particularly in colon, lung and breast cancers. On the other hand, its overexpression was reported in functional studies to suppress colony formation

in several types of cancer cell lines, where its function was associated with cell cycle progression [77].

Other genes associated with the enriched hallmarks included the *SERPINA1* and *SEPT6*. *SERPINA1* encodes the protein alpha-1-antitrypsin and has been described in breast cancer cell lines associated with their metastatic capabilities, such as conferring cell movement, migratory capacity, invasion and colony formation by the tumor cells [78]. In PTxLN groups' analysis, alpha-1-antitrypsin was observed up-regulated in PT compared to LN. It also was presented as potential metastasis biomarker in **Figure 3B**, highlighting their differential expression levels in LN samples. *SEPT6,* on other hand, encodes the septin-6 that belongs to a family of GTP-binding proteins related to actin cytoskeleton dynamics and changes in their expression levels are reported in several types of cancer [79]. In our study, septin-6 was found down-regulated in the PT when compared to the LN samples. Considering its role in cellular motility-related pathways observed in our study, including the actin cytoskeleton signaling, its increased expression levels in the metastatic samples agree with its described function.

Biological processes (GO terms) enriched from PTxLN groups' analysis in MSigDB identified most of deregulated genes encoded DEPs related to regulation of immune system process (*AMBP, APOD, CFB, COL1A2* and *RAC2* genes) and negative regulation of protein metabolic process (*AMBP, APOD, BGN, ITIH1* and *SERPINA1* genes). In addition, *RAC2*, related to metastasis, was also enriched in positive regulations of cellular component organization and response to stimulus; and *SERPINA1* was found associated with many processes, including proteolysis, vesicle-mediated transport and protein metabolism.

IPA's analysis conducted for the 65 DEPs from PTxLN groups' comparison identified three relevant cancer biomarkers: *APOD, CFB* and *SERPINA1*. These genes were observed in important hallmarks, pathways and biological processes.

Thirteen significant pathways were observed in PTxLN groups' comparison (activation/inhibition z-score values not available) in which *APOD* and *SERPINA1* genes were related to LXR/RXR and FXR/RXR activation, production of NO and ROS, signaling by IL-12 and clathrin-mediated endocytosis signaling. *CFB* gene was identified in complement system and acute phase response signaling and *COL1A2* gene in intrinsic prothrombin activation pathway.

In addition, IPA's network analysis identify one interactive network associated with cancer, organismal injury and abnormalities, and reproductive system disease (score= 32), composed of deregulated proteins encoded by *APOD, BGN, CFB, COL1A2, MGLL* and *RAC2* genes and was related to *CTNNB1* [80] and *TGFB1* [81] known cancer-related genes **(Figure 6).** Quantification of DEPs in the tissues across the breast cancer progression can elucidate potential targets to discriminate the LN metastasis and

contribute to propose a landscape of deregulated proteins beyond the mammary tumorigenesis.

Conclusion

The proteomic profiles of the contralateral and adjacent non-tumor breast tissues studied showed high level of similarity, indicating that these tissues can equally be considered as non-tumor breast tissues for proteomic comparative studies.

A high number of differentially expressed proteins (DEPs) was observed among the malignant and non-tumor tissue groups, involving proteins in biological functions and signaling pathways critically affected in cancer. Further analysis of these DEPs can reveal proteins with potential biomarker value for cancer development.

A high level of similarity was also observed among the proteome profiles of the primary tumors and the axillary metastatic lymph nodes' groups of samples, suggesting that common proteins play a role in both stages of the disease progression. The DEPs observed among the PT and LN groups, highlighted their involvement in specific stages of tumorigenesis, potentially associated with early and late stages of the disease progression, respectively.

The DEPs observed among the groups of breast tissues compared in this study also presented molecular changes in their protein, mRNA, CNA and mutation profiles, according to the cBioPortal analysis, reinforcing the differential proteome profiling in breast cancer. The involvement of these proteins in cancer associated signaling pathways and biological functions contribute to the understanding of their interacted networks and to the identification of potential tumor' biomarkers. In addition, it reveals the complex dimension of their interconnected signaling pathways that can impact in cell transformation and breast cancer progression.

Acknowledgments

The authors would like to thank Federal University of Paraná, Hospital das Clínicas (Curitiba/BR) and Program for Technological Development in Tools for Health-PDTIS-FIOCRUZ for providing the technical infrastructure and professional assistance.

Financial support

This study was financed by the Coordenação de Aperfeiçoamento de Pessoal de Nível Superior - Brasil (CAPES) - Finance Code 001 and the CNPq/ Araucaria Research Foundation of Parana State (PRONEX/2012).

Conflict of interest statement: None declared.

References

[1] K.R. Calvo, L.A. Liotta, E.F. Petricoin, Clinical proteomics: from biomarker discovery and cell signaling profiles to individualized personal therapy, Bioscience reports 25(1-2) (2005) 107-25.

[2] J. Brandi, I. Dando, E.D. Pozza, G. Biondani, R. Jenkins, V. Elliott, K. Park, G. Fanelli, L. Zolla, E. Costello, A. Scarpa, D. Cecconi, M. Palmieri, Proteomic analysis of pancreatic cancer stem cells: Functional role of fatty acid synthesis and mevalonate pathways, Journal of proteomics 150 (2017) 310-322.

[3] L. Chang, J. Ni, J. Beretov, V.C. Wasinger, J. Hao, J. Bucci, D. Malouf, D. Gillatt, P.H. Graham, Y. Li, Identification of protein biomarkers and signaling pathways associated with prostate cancer radioresistance using label-free LC-MS/MS proteomic approach, Scientific reports 7 (2017) 41834.

[4] S. Correa, C. Panis, R. Binato, A.C. Herrera, L. Pizzatti, E. Abdelhay, Identifying potential markers in Breast Cancer subtypes using plasma label-free proteomics, Journal of proteomics 151 (2017) 33-42.

[5] H. Xie, W. Wang, F. Sun, K. Deng, X. Lu, H. Liu, W. Zhao, Y. Zhang, X. Zhou, K. Li, Y. Hou, Proteomics analysis to reveal biological pathways and predictive proteins in the survival of high-grade serous ovarian cancer, Scientific reports 7(1) (2017) 9896.

[6] N.Q. Liu, C. Stingl, M.P. Look, M. Smid, R.B. Braakman, T. De Marchi, A.M. Sieuwerts, P.N. Span, F.C. Sweep, B.K. Linderholm, A. Mangia, A. Paradiso, L.Y. Dirix, S.J. Van Laere, T.M. Luider, J.W. Martens, J.A. Foekens, A. Umar, Comparative proteome analysis revealing an 11-protein signature for aggressive triple-negative breast cancer, Journal of the National Cancer Institute 106(2) (2014) djt376.

[7] I.J. Suarez-Arroyo, Y.R. Feliz-Mosquea, J. Perez-Laspiur, R. Arju, S. Giashuddin, G. Maldonado-Martinez, L.A. Cubano, R.J. Schneider, M.M. Martinez-Montemayor, The proteome signature of the inflammatory breast cancer plasma membrane identifies novel molecular markers of disease, American journal of cancer research 6(8) (2016) 1720-40.

[8] A. Cohen, E. Wang, K.A. Chisholm, R. Kostyleva, M. O'Connor-McCourt, D.M. Pinto, A mass spectrometry-based plasma protein panel targeting the tumor microenvironment in patients with breast cancer, Journal of proteomics 81 (2013) 135-47.

[9] S. Tyanova, R. Albrechtsen, P. Kronqvist, J. Cox, M. Mann, T. Geiger, Proteomic maps of breast cancer subtypes, Nature communications 7 (2016) 10259.

[10] J. Beretov, V.C. Wasinger, E.K. Millar, P. Schwartz, P.H. Graham, Y. Li, Proteomic Analysis of Urine to Identify Breast Cancer Biomarker Candidates Using a Label-Free LC-MS/MS Approach, PloS one 10(11) (2015) e0141876.

[11] C. Panis, L. Pizzatti, A.C. Herrera, S. Correa, R. Binato, E. Abdelhay, Label-free proteomic analysis of breast cancer molecular subtypes, Journal of proteome research 13(11) (2014) 4752-72.

[12] M.D. Lobo, F.B. Moreno, G.H. Souza, S.M. Verde, R.A. Moreira, A.C. Monteiro-Moreira, Label-Free Proteome Analysis of Plasma from Patients with Breast Cancer: Stage-Specific Protein Expression, Frontiers in oncology 7 (2017) 14.

[13] P. Ostasiewicz, D.F. Zielinska, M. Mann, J.R. Wisniewski, Proteome, phosphoproteome, and N-glycoproteome are quantitatively preserved in formalin-fixed paraffin-embedded tissue and analyzable by high-resolution mass spectrometry, Journal of proteome research 9(7) (2010) 3688-700.

[14] J. Cox, M. Mann, MaxQuant enables high peptide identification rates, individualized p.p.b.-range mass accuracies and proteome-wide protein quantification, Nature biotechnology 26(12) (2008) 1367-72.

[15] T.U. Consortium, UniProt: the universal protein knowledgebase, Nucleic acids research 45(D1) (2017) D158-D169.

[16] J.A. Vizcaino, A. Csordas, N. Del-Toro, J.A. Dianes, J. Griss, I. Lavidas, G. Mayer, Y. Perez-Riverol, F. Reisinger, T. Ternent, Q.W. Xu, R. Wang, H. Hermjakob, 2016 update of the PRIDE database and its related tools, Nucleic acids research 44(22) (2016) 11033.

[17] S. Tyanova, T. Temu, P. Sinitcyn, A. Carlson, M.Y. Hein, T. Geiger, M. Mann, J. Cox, The Perseus computational platform for comprehensive analysis of (prote)omics data, Nature methods 13(9) (2016) 731-40.

[18] M.S. Robles, J. Cox, M. Mann, In-vivo quantitative proteomics reveals a key contribution of post-transcriptional mechanisms to the circadian regulation of liver metabolism, PLoS genetics 10(1) (2014) e1004047.

[19] H. Heberle, G.V. Meirelles, F.R. da Silva, G.P. Telles, R. Minghim, InteractiVenn: a web-based tool for the analysis of sets through Venn diagrams, BMC bioinformatics 16 (2015) 169.

[20] V.K. Mootha, C.M. Lindgren, K.F. Eriksson, A. Subramanian, S. Sihag, J. Lehar, P. Puigserver, E. Carlsson, M. Ridderstrale, E. Laurila, N. Houstis, M.J. Daly, N. Patterson, J.P. Mesirov, T.R. Golub, P. Tamayo, B. Spiegelman, E.S. Lander, J.N. Hirschhorn, D. Altshuler, L.C. Groop, PGC-1alpha-responsive genes involved in oxidative phosphorylation are coordinately downregulated in human diabetes, Nature genetics 34(3) (2003) 267-73.

[21] A. Subramanian, P. Tamayo, V.K. Mootha, S. Mukherjee, B.L. Ebert, M.A. Gillette, A. Paulovich, S.L. Pomeroy, T.R. Golub, E.S. Lander, J.P. Mesirov, Gene set enrichment analysis: a knowledge-based approach for interpreting genome-wide expression profiles, Proceedings of the National Academy of Sciences of the United States of America 102(43) (2005) 15545-50.

[22] A. Liberzon, C. Birger, H. Thorvaldsdottir, M. Ghandi, J.P. Mesirov, P. Tamayo, The Molecular Signatures Database (MSigDB) hallmark gene set collection, Cell systems 1(6) (2015) 417-425.

[23] S.A. Forbes, D. Beare, N. Bindal, S. Bamford, S. Ward, C.G. Cole, M. Jia, C. Kok, H. Boutselakis, T. De, Z. Sondka, L. Ponting, R. Stefancsik, B. Harsha, J. Tate, E. Dawson, S. Thompson, H. Jubb, P.J. Campbell, COSMIC: High-Resolution Cancer Genetics Using the Catalogue of Somatic Mutations in Cancer, Current protocols in human genetics 91 (2016) 10 11 1-10 11 37.

[24] A. Kramer, J. Green, J. Pollard, Jr., S. Tugendreich, Causal analysis approaches in Ingenuity Pathway Analysis, Bioinformatics 30(4) (2014) 523-30.

[25] J.L. Noble, R.S. Dua, G.R. Coulton, C.M. Isacke, G.P. Gui, A comparative proteinomic analysis of nipple aspiration fluid from healthy women and women with breast cancer, Eur J Cancer 43(16) (2007) 2315-20.

[26] T.M. Pawlik, D.H. Hawke, Y. Liu, S. Krishnamurthy, H. Fritsche, K.K. Hunt, H.M. Kuerer, Proteomic analysis of nipple aspirate fluid from women with early-stage breast cancer using isotope-coded affinity tags and tandem mass spectrometry reveals differential expression of vitamin D binding protein, BMC cancer 6 (2006) 68.

[27] N.W. Bateman, T.P. Conrads, Recent advances and opportunities in proteomic analyses of tumour heterogeneity, The Journal of pathology 244(5) (2018) 628-637.

[28] I.J.C. T.H.B. Gomig, R.L.R. Souza, A.C.R. Lucena, M. Batista, K.C. Machado, F.K. Marchini, F.A. Marchi, R.S. Lima, C.A. Urban, L.R. Cavalli, E.M.S.F. Ribeiro. , High-throughput mass spectrometry and bioinformatics analysis of breast cancer proteomic data, Data in brief (in press).

[29] K.S. Midwood, T. Hussenet, B. Langlois, G. Orend, Advances in tenascin-C biology, Cellular and molecular life sciences : CMLS 68(19) (2011) 3175-99.

[30] M. Li, F. Peng, G. Li, Y. Fu, Y. Huang, Z. Chen, Y. Chen, Proteomic analysis of stromal proteins in different stages of colorectal cancer establishes Tenascin-C as a stromal biomarker for colorectal cancer metastasis, Oncotarget 7(24) (2016) 37226-37237.

[31] B. Hoesel, J.A. Schmid, The complexity of NF-kappaB signaling in inflammation and cancer, Molecular cancer 12 (2013) 86.

[32] R. Roskoski, Jr., ERK1/2 MAP kinases: structure, function, and regulation, Pharmacological research 66(2) (2012) 105-43.

[33] G. Song, G. Ouyang, S. Bao, The activation of Akt/PKB signaling pathway and cell survival, Journal of cellular and molecular medicine 9(1) (2005) 59-71.

[34] Y. Fallah, J. Brundage, P. Allegakoen, A.N. Shajahan-Haq, MYC-Driven Pathways in Breast Cancer Subtypes, Biomolecules 7(3) (2017).

[35] M. Takeichi, Dynamic contacts: rearranging adherens junctions to drive epithelial remodelling, Nature reviews. Molecular cell biology 15(6) (2014) 397-410.

[36] M. Rodnick-Smith, Q. Luan, S.L. Liu, B.J. Nolen, Role and structural mechanism of WASP-triggered conformational changes in branched actin filament nucleation by Arp2/3 complex, Proceedings of the National Academy of Sciences of the United States of America 113(27) (2016) E3834-43.

[37] M. Diakonova, G. Bokoch, J.A. Swanson, Dynamics of cytoskeletal proteins during Fcgamma receptor-mediated phagocytosis in macrophages, Molecular biology of the cell 13(2) (2002) 402-11.

[38] F. Bovenga, C. Sabba, A. Moschetta, Uncoupling nuclear receptor LXR and cholesterol metabolism in cancer, Cell metabolism 21(4) (2015) 517-26.

[39] C.Y. Lin, L.L. Vedin, K.R. Steffensen, The emerging roles of liver X receptors and their ligands in cancer, Expert opinion on therapeutic targets 20(1) (2016) 61-71.

[40] K. Davalieva, S. Kiprijanovska, I. Maleva Kostovska, S. Stavridis, O. Stankov, S. Komina, G. Petrusevska, M. Polenakovic, Comparative Proteomics Analysis of Urine Reveals Down-Regulation of Acute Phase Response Signaling and LXR/RXR Activation Pathways in Prostate Cancer, Proteomes 6(1) (2017).

[41] H. Tang, S. Mirshahidi, M. Senthil, K. Kazanjian, C.S. Chen, K. Zhang, Down-regulation of LXR/RXR activation and negative acute phase response pathways in colon adenocarcinoma revealed by proteomics and bioinformatics analysis, Cancer biomarkers : section A of Disease markers 14(5) (2014) 313-24.

[42] M. Irshad, R. Dubey, Apolipoproteins and their role in different clinical conditions: an overview, Indian journal of biochemistry & biophysics 42(2) (2005) 73-80.

[43] A. El Roz, J.M. Bard, S. Valin, J.M. Huvelin, H. Nazih, Macrophage apolipoprotein E and proliferation of MCF-7 breast cancer cells: role of LXR, Anticancer research 33(9) (2013) 3783-9.

[44] S. Kumari, A.K. Badana, M.M. G, S. G, R. Malla, Reactive Oxygen Species: A Key Constituent in Cancer Survival, Biomarker insights 13 (2018) 1177271918755391.

[45] S.S. Sabharwal, P.T. Schumacker, Mitochondrial ROS in cancer: initiators, amplifiers or an Achilles' heel?, Nature reviews. Cancer 14(11) (2014) 709-21.

[46] L. Zhang, M. Zeng, B.M. Fu, Inhibition of endothelial nitric oxide synthase decreases breast cancer cell MDA-MB-231 adhesion to intact microvessels under physiological flows, American journal of physiology. Heart and circulatory physiology 310(11) (2016) H1735-47.

[47] S.K. Choudhari, M. Chaudhary, S. Bagde, A.R. Gadbail, V. Joshi, Nitric oxide and cancer: a review, World journal of surgical oncology 11 (2013) 118.

[48] C. Cortes-Gonzalez, J. Barrera-Chimal, M. Ibarra-Sanchez, M. Gilbert, G. Gamba, A. Zentella, M.E. Flores, N.A. Bobadilla, Opposite effect of Hsp90alpha and Hsp90beta on eNOS ability to produce nitric oxide or superoxide anion in human embryonic kidney cells, Cellular physiology and biochemistry : international journal of experimental cellular physiology, biochemistry, and pharmacology 26(4-5) (2010) 657-68.

[49] A.A. Mathieu, E. Ohl-Seguy, M.L. Dubois, D. Jean, C. Jones, F. Boudreau, F.M. Boisvert, Subcellular proteomics analysis of different stages of colorectal cancer cell lines, Proteomics 16(23) (2016) 3009-3018.

[50] T. Teng, C.A. Mercer, P. Hexley, G. Thomas, S. Fumagalli, Loss of tumor suppressor RPL5/RPL11 does not induce cell cycle arrest but impedes proliferation due to reduced ribosome content and translation capacity, Molecular and cellular biology 33(23) (2013) 4660-71.

[51] Y.W. Chang, C.F. Tseng, M.Y. Wang, W.C. Chang, C.C. Lee, L.T. Chen, M.C. Hung, J.L. Su, Deacetylation of HSPA5 by HDAC6 leads to GP78-mediated HSPA5 ubiquitination at K447 and suppresses metastasis of breast cancer, Oncogene 35(12) (2016) 1517-28.

[52] J. Sawada, T. Urakami, F. Li, A. Urakami, W. Zhu, M. Fukuda, D.Y. Li, E. Ruoslahti, M. Komatsu, Small GTPase R-Ras regulates integrity and functionality of tumor blood vessels, Cancer cell 22(2) (2012) 235-49.

[53] N.J. German, M.C. Haigis, Sirtuins and the Metabolic Hurdles in Cancer, Current biology : CB 25(13) (2015) R569-83.

[54] A. Chalkiadaki, L. Guarente, The multifaceted functions of sirtuins in cancer, Nature reviews. Cancer 15(10) (2015) 608-24.

[55] M.F. Olson, E. Sahai, The actin cytoskeleton in cancer cell motility, Clinical & experimental metastasis 26(4) (2009) 273-87.

[56] H. Yamaguchi, J. Condeelis, Regulation of the actin cytoskeleton in cancer cell migration and invasion, Biochimica et biophysica acta 1773(5) (2007) 642-52.

[57] H.E. Rauhala, S. Teppo, S. Niemela, A. Kallioniemi, Silencing of the ARP2/3 complex disturbs pancreatic cancer cell migration, Anticancer research 33(1) (2013) 45-52.

[58] S. Joshi, A.R. Singh, M. Zulcic, L. Bao, K. Messer, T. Ideker, J. Dutkowski, D.L. Durden, Rac2 controls tumor growth, metastasis and M1-M2 macrophage differentiation in vivo, PloS one 9(4) (2014) e95893.

[59] E. Currie, A. Schulze, R. Zechner, T.C. Walther, R.V. Farese, Jr., Cellular fatty acid metabolism and cancer, Cell metabolism 18(2) (2013) 153-61.

[60] M.E. Monaco, Fatty acid metabolism in breast cancer subtypes, Oncotarget 8(17) (2017) 29487-29500.

[61] M. Omabe, M. Ezeani, K.N. Omabe, Lipid metabolism and cancer progression: The missing target in metastatic cancer treatment, Journal of Applied Biomedicine 13(1) (2015) 47-59.

[62] T.K. Er, M.F. Hou, E.M. Tsa, J.N. Lee, L.Y. Tsai, Differential expression of manganese containing superoxide dismutase in patients with breast cancer in Taiwan, Annals of clinical and laboratory science 34(2) (2004) 159-64.

[63] R. Xu, Z. Yuan, L. Yang, L. Li, D. Li, C. Lv, Inhibition of NAMPT decreases cell growth and enhances susceptibility to oxidative stress, Oncology reports 38(3) (2017) 1767-1773.

[64] D. Hanahan, R.A. Weinberg, Hallmarks of cancer: the next generation, Cell 144(5) (2011) 646-74.

[65] T. Cabezon, J.E. Celis, I. Skibshoj, J. Klingelhofer, M. Grigorian, P. Gromov, F. Rank, J.H. Myklebust, G.M. Maelandsmo, E. Lukanidin, N. Ambartsumian, Expression of S100A4 by a variety of cell types present in the tumor microenvironment of human breast cancer, International journal of cancer 121(7) (2007) 1433-44.

[66] P. Czerwinska, S. Mazurek, M. Wiznerowicz, The complexity of TRIM28 contribution to cancer, Journal of biomedical science 24(1) (2017) 63.

[67] A.R. Green, D. Caracappa, A.A. Benhasouna, A. Alshareeda, C.C. Nolan, R.D. Macmillan, S. Madhusudan, I.O. Ellis, E.A. Rakha, Biological and clinical significance of PARP1 protein expression in breast cancer, Breast cancer research and treatment 149(2) (2015) 353-62.

[68] G. Loubeau, R. Boudra, S. Maquaire, C. Lours-Calet, C. Beaudoin, P. Verrelle, L. Morel, NPM1 silencing reduces tumour growth and MAPK signalling in prostate cancer cells, PloS one 9(5) (2014) e96293.

[69] C.M. Lowy, T. Oskarsson, Tenascin C in metastasis: A view from the invasive front, Cell adhesion & migration 9(1-2) (2015) 112-24.

[70] C.J. Tai, C.H. Hsu, S.C. Shen, W.R. Lee, M.C. Jiang, Cellular apoptosis susceptibility (CSE1L/CAS) protein in cancer metastasis and chemotherapeutic drug-induced apoptosis, Journal of experimental & clinical cancer research : CR 29 (2010) 110.

[71] D. Silvera, A. Ernlund, R. Arju, E. Connolly, V. Volta, J. Wang, R.J. Schneider, mTORC1 and -2 Coordinate Transcriptional and Translational Reprogramming in Resistance to DNA Damage and Replicative Stress in Breast Cancer Cells, Molecular and cellular biology 37(5) (2017).

[72] X. Gu, Y. Ma, J. Xiao, H. Zheng, C. Song, Y. Gong, X. Xing, Up-regulated biglycan expression correlates with the malignancy in human colorectal cancers, Clinical and experimental medicine 12(3) (2012) 195-9.

[73] F. Jacobsen, J. Kraft, C. Schroeder, C. Hube-Magg, M. Kluth, D.S. Lang, R. Simon, G. Sauter, J.R. Izbicki, T.S. Clauditz, A.M. Luebke, A. Hinsch, W. Wilczak, C. Wittmer, F. Buscheck, D. Hoflmayer, S. Minner, M.C. Tsourlakis, H. Huland, M. Graefen, L. Budaus, I. Thederan, G. Salomon, T. Schlomm, N. Melling, Up-regulation of Biglycan is Associated with Poor Prognosis and PTEN Deletion in Patients with Prostate Cancer, Neoplasia 19(9) (2017) 707-715.

[74] J. Li, Y. Ding, A. Li, Identification of COL1A1 and COL1A2 as candidate prognostic factors in gastric cancer, World journal of surgical oncology 14(1) (2016) 297.

[75] Y. Yu, D. Liu, Z. Liu, S. Li, Y. Ge, W. Sun, B. Liu, The inhibitory effects of COL1A2 on colorectal cancer cell proliferation, migration, and invasion, Journal of Cancer 9(16) (2018) 2953-2962.

[76] W. Zhu, Y. Zhao, J. Zhou, X. Wang, Q. Pan, N. Zhang, L. Wang, M. Wang, D. Zhan, Z. Liu, X. He, D. Ma, S. Liu, Monoacylglycerol lipase promotes progression of hepatocellular carcinoma via NF-kappaB-mediated epithelial-mesenchymal transition, Journal of hematology & oncology 9(1) (2016) 127.

[77] H. Sun, L. Jiang, X. Luo, W. Jin, Q. He, J. An, K. Lui, J. Shi, R. Rong, W. Su, C. Lucchesi, Y. Liu, M.S. Sheikh, Y. Huang, Potential tumor-suppressive role of monoglyceride lipase in human colorectal cancer, Oncogene 32(2) (2013) 234-41.

[78] R.H. Law, Q. Zhang, S. McGowan, A.M. Buckle, G.A. Silverman, W. Wong, C.J. Rosado, C.G. Langendorf, R.N. Pike, P.I. Bird, J.C. Whisstock, An overview of the serpin superfamily, Genome biology 7(5) (2006) 216.

[79] S. Mostowy, P. Cossart, Septins: the fourth component of the cytoskeleton, Nature reviews. Molecular cell biology 13(3) (2012) 183-94.

[80] S. Tanabe, T. Kawabata, K. Aoyagi, H. Yokozaki, H. Sasaki, Gene expression and pathway analysis of CTNNB1 in cancer and stem cells, World journal of stem cells 8(11) (2016) 384-395.

[81] M.H. Barcellos-Hoff, R.J. Akhurst, Transforming growth factor-beta in breast cancer: too much, too late, Breast cancer research : BCR 11(1) (2009) 202.

Figures

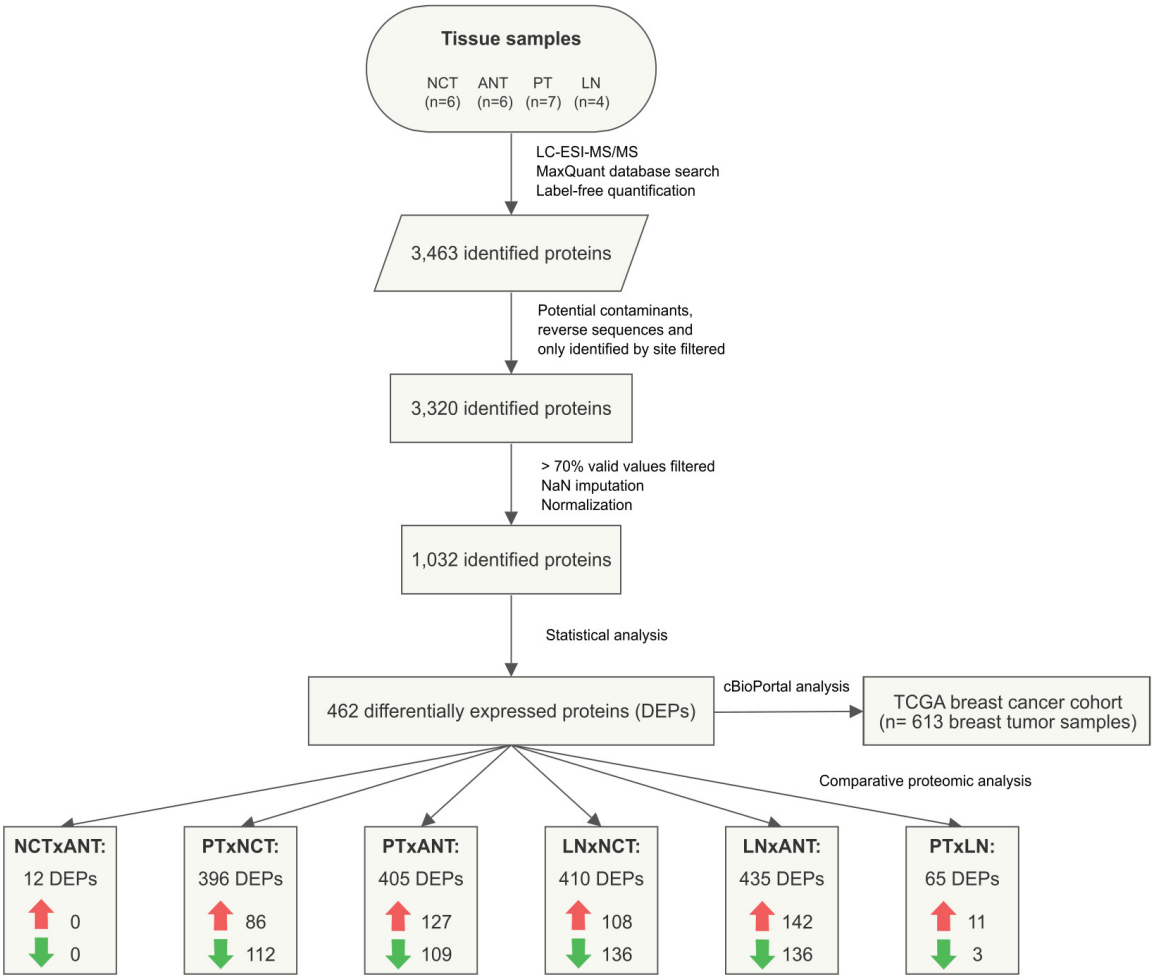

Figure 1. Flowchart and data analysis of the proteomic profiles of breast cancer comparing the non-tumor breast tissues [contralateral (NCT) and adjacent (ANT)], primary breast tumor (PT) and axillary metastatic lymph node (LN) samples. Tissue samples were separately evaluated for protein expression by LC-ESI-MS/MS. Proteomic data were label-free quantified and identified using appropriated databases and statistical methods. Differentially expressed proteins (DEPs) were analyzed in the cBioPortal for Cancer Genomics to evaluate the molecular changes related to these proteins/ genes in a cohort of tumor breast samples from TCGA database. Lists of DEPs were generated for each groups' comparisons: NCTxANT, PTxNCT, PTxANT, LNxNCT, LNxANT and PTxLN. Up-regulated (red arrows) and down-regulated (green arrows) proteins were comparatively annotated/ enriched according to the gene sets of the Molecular Signatures Database (MSigDB v. 6.2) and Ingenuity Pathway Analysis v. 2.3.

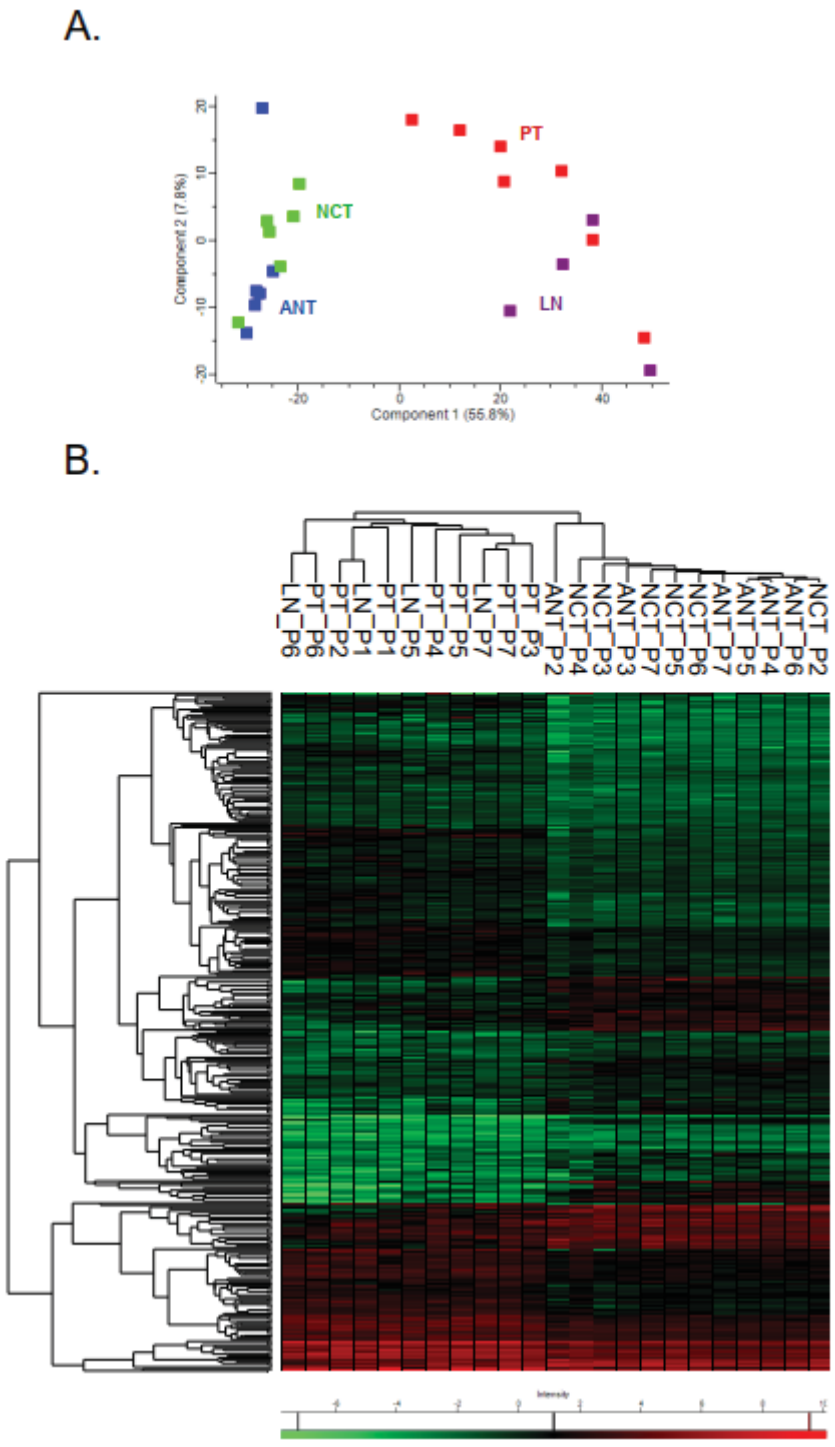

Figure 2. Principal Component Analysis (PCA) and hierarchical clustering analysis. **A.** The PCA plot represents 1,032 identified proteins for the tissue samples analyzed: NCT – contralateral non-tumor breast tissue (green), ANT – adjacent non-tumor breast tissue (blue), PT – primary breast tumor (red) and LN – axillary metastatic lymph node (purple). **B.** Heatmap hierarchical clustering from differentially expressed proteins (n=462) identified across all samples' groups. Clustering of samples was performed in Perseus v. 1.5.6.0.

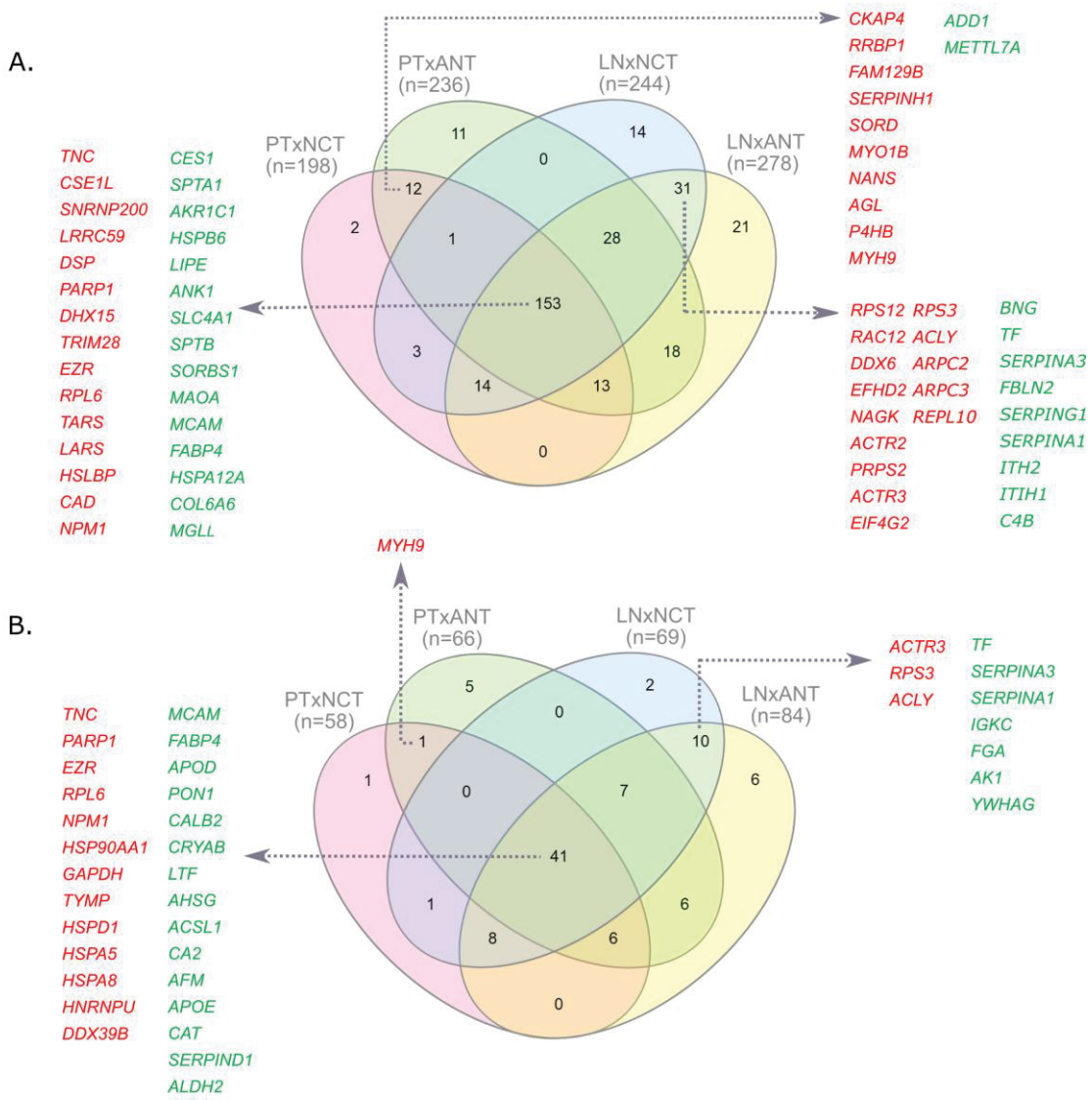

Figure 3. Venn Diagrams showing the differentially expressed proteins observed among the comparisons of the PTxNCT, PTxANT, LNxNCT and LNxANT groups of samples. **A.** Number of up-regulated and down-regulated proteins observed among each group comparison. **B.** Biomarkers predicted to be involved in cancer identified by the IPA's Biomarker Analysis. Genes encoding DEPs with the most significant differences of expression (largest log2 fold change values) are highlighted in red (up-regulated) and in green (down-regulated).

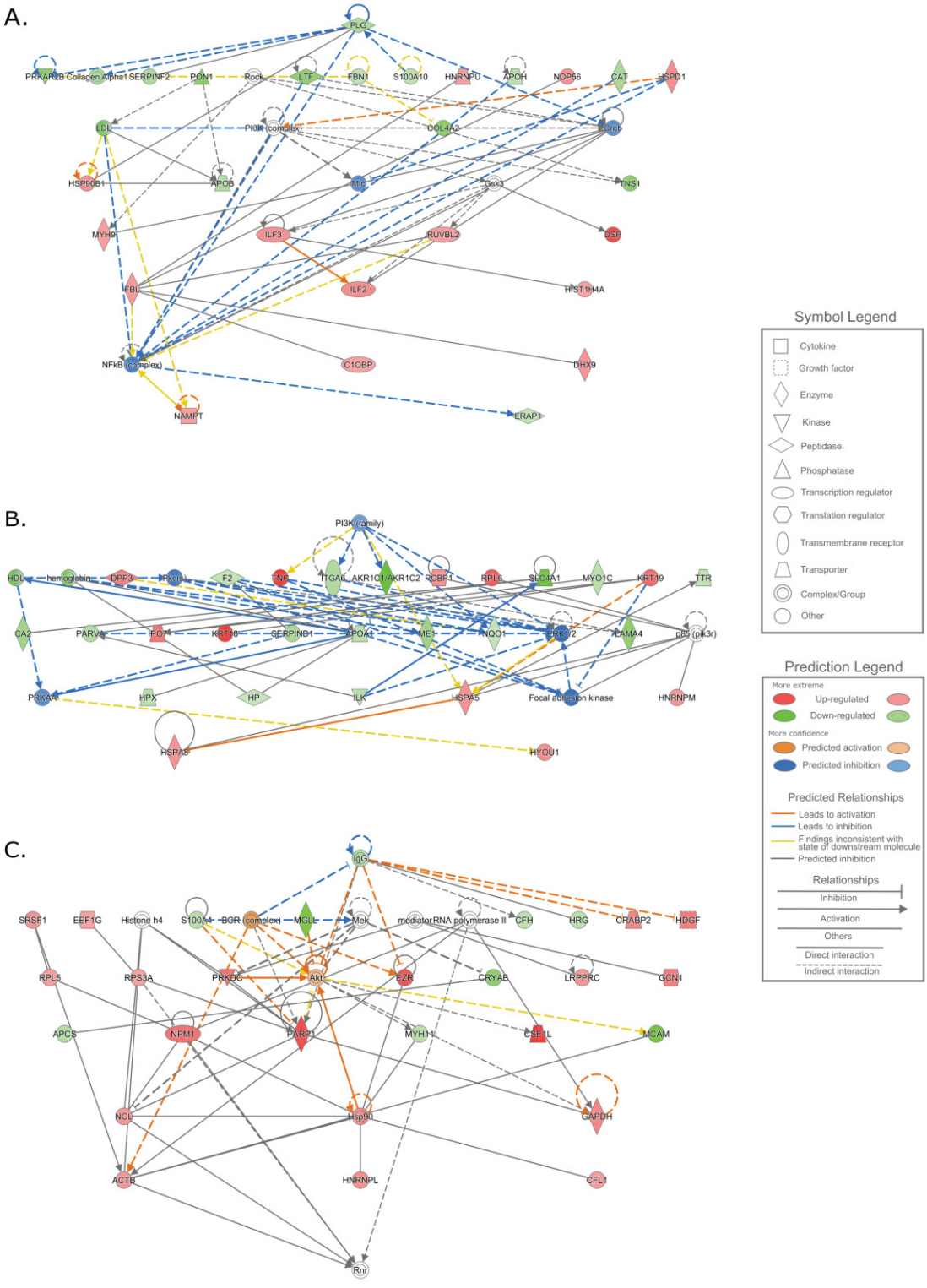

Figure 4. Predicted top protein interactive networks of the differentially expressed proteins observed among the PT and NCT samples, related to **A.** Organismal injury and abnormalities, cell death and survival and cancer related network; **B.** Endocrine system disorders, organismal injury and abnormalities and cancer related network; **C.** Cellular movement, cell death and survival, hematological system development and function related network.

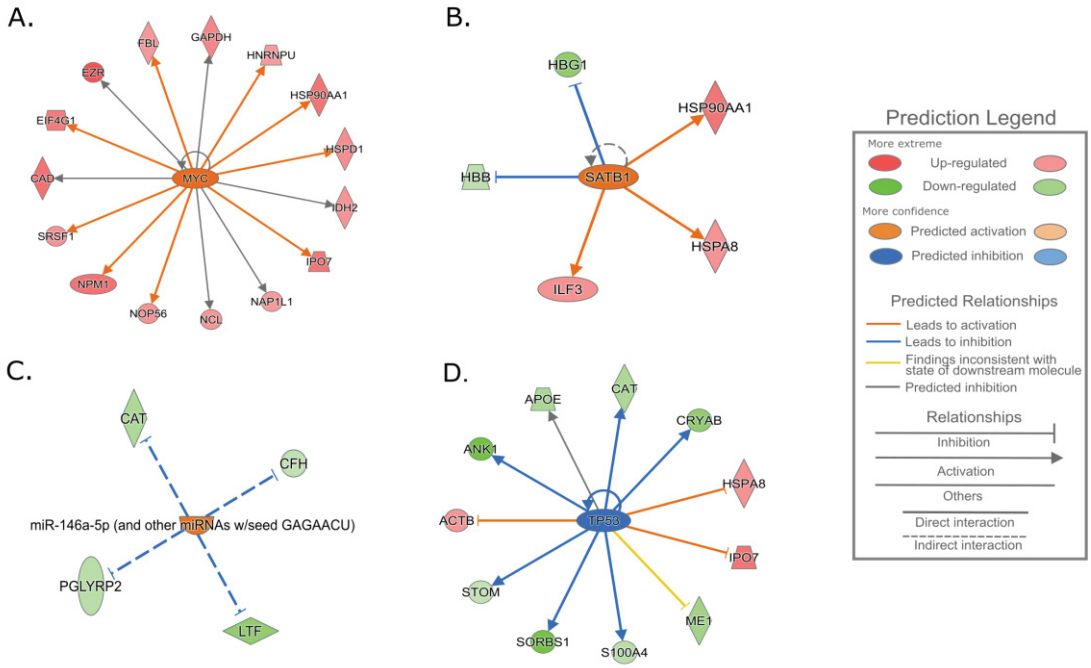

Figure 5. Upstream regulators for differentially expressed proteins in primary breast tumor samples. IPA's Upstream Regulator Analysis revealed four mainly regulators for up and down-regulated proteins from PTxNCT groups' comparison, including **A.** MYC; **B.** TP53; **C.** SATB1; **D.** mir-146a-5p.

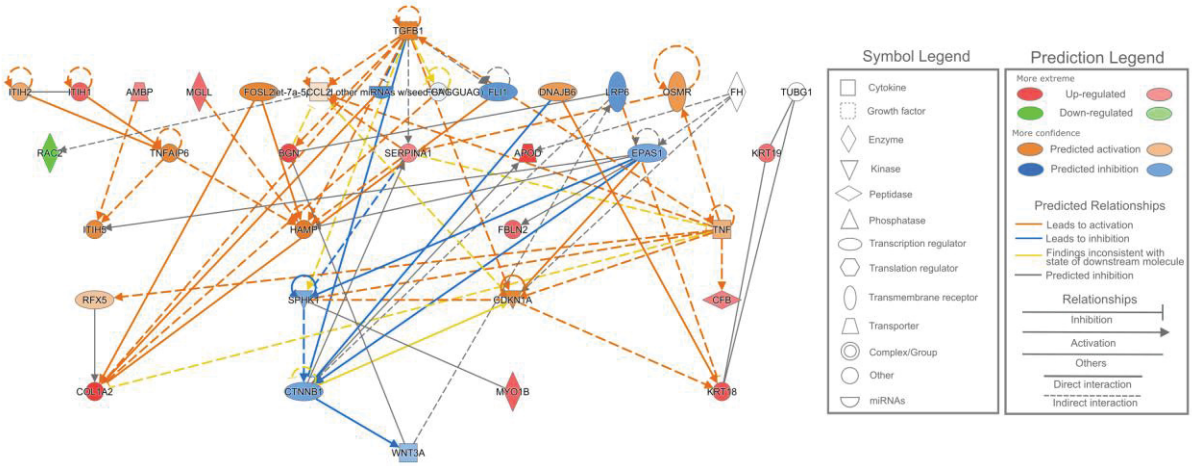

Figure 6. Predictive protein interactive network of the differentially expressed proteins observed among the malignant tissues (PTxLN), related to cancer, organismal injury and abnormalities, and reproductive system disease.

Tables

Table 1. Clinico-pathological data of patients and type of samples obtained from each patient.

Patient code	Age	Histopatology/ Tumor grade	LN metastasis	Tissue samples
P1	76	IDC/ II	+	PT, LN
P2	36	IDC/ II	–	NCT, ANT, PT
P3	63	IDC/ II	+	NCT, ANT, PT
P4	39	IDC/ II	–	NCT, ANT, PT
P5	52	IDC/ II	+	NCT, ANT, PT, LN
P6	67	IDC/ III	+	NCT, ANT, PT, LN
P7	59	IDC/ III	+	NCT, ANT, PT, LN

IDC - Invasive ductal carcinoma; PT – primary breast tumor tissue; LN – axillary metastatic lymph node; NCT– contralateral non-tumor breast tissue; ANT – adjacent non-tumor breast tissue; "+" indicate diagnosis of metastasis.

Table 2. Functional classes of genes encoding the differentially expressed proteins among all the groups of breast tissues studied (COSMIC v. 86 and MSigDB v. 6.2).

Functional class	Gene symbol
Tumor Suppressors	*FBLN2, RPL5, RPL10, FUS, SFPQ, TPM3*
Oncogenes	*DDX6, FUS, GNA11, HNRNPA2B1, HS90AA1, IDH2, MYH11, MYH9, NPM1, SFPQ, TPM3, TNC, XPO1*
Protein Kinases	*DCLK1, ILK, PRKDC, TRIM28*
Transcription Factors	*ANP32A, CSRP1, ILF2, ILF3, PRS8, TNC, TRIM28*
Cytokines and Growth Factors	*AGT, CAT, CTSG, C3, C5, HDGF, NAMPT, TNC, TYMP*
Cell Differentiation Markers	*AMPN, ITGA1, ITGA6, MCAM, NT5E, SLC4A1*

Table 3. Proteomic data of the main differentially expressed proteins and their genomic profiles obtained in the cBioPortal analysis using a TCGA cohort of 613 primary breast tumor samples.

Protein name	Gene symbol	*Our proteomic data*		*Genomic profiles from cBioPortal platform (TCGA data)*			
		PTxNCT fold change	LNxNCT fold change	Protein expression	mRNA expression	CNA	Mutations
Beta-2-glycoprotein 1	*APOH*	Down	Down	Down	Up	Deep deletion	Yes
Collagen alpha-6(VI) chain	*COL6A6*	Down	Down	Down	Up	Deep deletion	Yes
Cytoskeleton-associated protein 4	*CKAP4*	Up	-	Up	Up	Amplification	Yes
Desmoplakin	*DSP*	Up	Up	Up	Up	Amplification	Yes
Ezrin	*EZR*	Up	Up	Up	Up	Amplification	Yes
Guanine nucleotide-binding protein subunit alpha-11	*GNA11*	-	Down	Up	Down	Deep deletion	Yes
Nucleolar protein 56	*NOP56*	Up	Up	Up	Down	Amplification	Yes
Poly [ADP-ribose] polymerase 1	*PARP1*	Up	Up	Down	Up	Amplification	Yes
Tenascin	*TNC*	Up	Up	Up	Up	Amplification	Yes
14-3-3 protein gamma	*YWHAG*	-	Down	Up	Down	Deep deletion	-

Differentially expressed proteins out of the 1.5 log2 fold change in our study and data not available for TCGA samples are represented by "-".

Table 4. Top-enriched hallmark gene sets for the differentially expressed proteins observed among non-tumor breast tissue samples (NCTxANT) (MSigDB v. 6.2).

Hallmark gene set	FDR q-value	Gene symbol
MYC Targets	5.74E-08	*FBL, IMPDH2, NOP56, SSB, SYNCRIP*
Unfolded Protein Response	9.73E-03	*FUS, NOP56*
E2F Targets	2.01E-02	*NOP56, SYNCRIP*

NCT– contralateral non-tumor breast tissue; ANT – adjacent non-tumor breast tissue; FDR – false discovery rate.

Table 5. Top-enriched hallmark gene sets for differentially expressed proteins observed among the malignant and contralateral non-tumor breast tissue samples (PTxNCT and LNxNCT) (MSigDB v. 6.2).

Hallmark gene set	PTxNCT FDR q-value	LNxNCT FDR q-value	Gene symbol
MYC Targets	1.04E-56	2.75E-64	*AKR1C1, APOA1, APOD, APOE, CAT, CES1, CFB, COL1A2, FBL, HNRNPU, HSPD1, LIPE, LTF, MAOA, MGLL, NAP1L1, NOP56, NPM1, PGLYRP2, PLG, PON1, S100A10, SRSF1*
MTORC1 Signaling	1.37E-21	4.27E-25	*ACTR2, ACTR3, CACYBP, EPRS, GAPDH, GBE1, HSP90B1, HSPA5, HSPD1, ME1*
Adipogenesis	2.97E-19	6.14E-18	*ACADS, ALDH2, APOE, CAT, FABP4, GBE1, LIPE, ME1, MGLL, RETSAT*
Coagulation	3.08E-15	7.10E-23	*APOA1, C9, CFB, CFD, CFH, CFI, F12, F2, FBN1, PLG, SERPINC1, TF*
Xenobiotic Metabolism	1.38E-13	6.14E-18	*AKR1C3, ALDH2, APOE, CAT, CES1, CFB, FAH, ITIH4, MAOA, PLG, RETSAT*
Complement	-	2.06E-13	*C9, CA2, CFB, CFH, COL4A2, F2, HSPA5, LTF, ME1, PLG, SERPINA1*
Fatty Acid Metabolism	3.63E-13	7.41E-12	*ACADS, ACSL1, ALAD, CA2, HSP90AA1, MAOA, ME1, MGLL, RETSAT, S100A10*
Unfolded Protein Response	7.81E-12	1.06E-11	*EIF4A1, EIF4G1, HSP90B1, HSPA5, HYOU1, IARS, NOP56, NPM1, TARS*
Oxidative Phosphorylation	1.31E-11	-	*IDH2, LRPPRC, RETSAT*
E2F Targets	1.18E-10	1.91E-10	*CSE1L, ILF3, IPO7, NAP1L1, NOP56, PRKDC, SRSF1, XPO1*
Heme Metabolism	1.18E-10	1.91E-10	*ALAD, ANK1, CA2, CAT, HBB, HBD, HDGF, SLC4A1, SPTA1, SPTB, TNS1*

Proteins with the highest fold change values are presented through their gene symbols.
PT – primary breast tumor tissue; NCT– contralateral non-tumor breast tissue; LN – axillary metastatic lymph node; FDR – false discovery rate.

Table 6. Top-canonical pathways identified to be affected by the differentially expressed proteins observed among the axillary metastatic lymph node samples and contralateral non-tumor breast tissue samples (LNxNCT) (IPA v. 2.3).

Ingenuity canonical pathways	p-value	z-score	Gene symbol
RhoGDI Signaling	5.89E-03	-2.449	*ACTB, ACTR2, ACTR3, ARPC2, ARPC3, EZR, GNA11*
Agrin Interactions at Neuromuscular Junction	1.66E-04	-0.447	*ACTB, ITGA1, ITGA6, LAMB1, RAC2, RRAS*
Integrin Signaling	6.03E-05	0.302	*ACTB, ACTR2, ACTR3, ARPC2, ARPC3, ILK, ITGA6, PARVA, RAC2, RRAS*
Ephrin Receptor Signaling	1.29E-03	0.707	*ACTR2, ACTR3, ARPC2, ARPC3, GNA11, RAC2, RRAS, SORBS1*
Actin Nucleation by ARP-WASP Complex	5.89E-04	1.342	*ACTR2, ACTR3, ARPC2, ARPC3, RRAS*
Rac Signaling	3.02E-03	1.342	*ACTR2, ACTR3, ANK1, ARPC2, ARPC3, RRAS*
fMLP Signaling in Neutrophils	1.70E-02	1.342	*ACTR2, ACTR3, ARPC2, ARPC3, RRAS*
Remodeling of Epithelial Adherens Junctions	1.26E-03	2	*ACTB, ACTR2, ACTR3, ARPC2, ARPC3*
Regulation of Actin-based Motility by Rho	6.46E-04	2.449	*ACTB, ACTR2, ACTR3, ARPC2, ARPC3, RAC2*
RhoA Signaling	3.80E-03	2.449	*ACTB, ACTR2, ACTR3, ARPC2, ARPC3, EZR*
Signaling by Rho Family GTPases	3.47E-02	2.449	*ACTB, ACTR2, ACTR3, ARPC2, ARPC3, EZR, GNA11*
Fcγ Receptor-mediated Phagocytosis in Macrophages and Monocytes	1.41E-04	2.646	*ACTB, ACTR2, ACTR3, ARPC2, ARPC3, EZR, RAC2*

Table 7. Top- canonical pathways identified to be affected by the differentially expressed proteins observed among the malignant tissues *versus* contralateral non-tumor breast tissue samples (PTxNCT and LNxNCT) (IPA v. 2.3).

Ingenuity canonical pathways	PTxNCT p-value	PTxNCT z-score	LNxNCT p-value	LNxNCT z-score	Gene symbol
LXR/RXR Activation	3.98E-15	-4.123	1.58E-18	-4.583	*AGT, AHSG, AMBP, APOA1, APOB, APOD, APOE, APOH, C4A/C4B**, FGA**, GC, HPX, ITIH4, KNG1, ORM1, ORM2, PCYOX1, PON1, SERPINA1**, SERPINF2, TF**, TTR*
GP6 Signaling Pathway	2.00E-03	-2.449	5.37E-03	-2.449	*COL1A2, COL4A2, COL6A6, FGA**, FGB*, LAMA4, LAMB1*
Production of Nitric Oxide and Reactive Oxygen Species in Macrophages	7.08E-04	-2.121	6.17E-04	-2.333	*APOA1, APOB, APOD, APOE, CAT, ORM1, ORM2, PON1, SERPINA1**
eNOS Signaling	6.17E-03	-2	1.58E-02	-2	*KNG1, HSPA5, HSPA8, HSP90AA1, HSP90B1, PRKAR2B*
Acute Phase Response Signaling	1.58E-18	-1.508	3.98E-25	-1.604	*AGT, AHSG, AMBP, APCS, APOA1, APOH, C4A/C4B**, C4BPA, CFB, CRABP2, F2, FGA**, FGB*, HNRNPK, HP, HPX, HRG, ITIH2**, ITIH4, ORM1, ORM2, PLG, RRAS, SERPINA1**, SERPINA3**, SERPIND1, SERPINF2, SERPING1**, TF**, TTR*
Intrinsic Prothrombin Activation Pathway	3.02E-06	-1.342	9.55E-06	-1.342	*COL1A2, KNG1, F2, F12, FGA**, FGB*, SERPIC1*
PPARα/RXRα Activation	6.76E-03	-0.816	1.70E-02	-1.342	*APOA1, GNA11**, GOT2*, HSP90AA1, HSP90B1, PRKAR2B, RRAS*
Actin Cytoskeleton Signaling	1.70E-03	-0.378	8.91E-05	1.265	*ACTB, ACTR2**, ACTR3**, ARPC2**, ARPC3**, CFL1*, EZR, F2, KNG1, MYH11, MYH9*, RAC2**, RRAS*
Nitric Oxide Signaling in the Cardiovascular System	2.29E-02	0	4.27E-02	0	*KNG1, HSP90AA1, HSP90B1, PRKAR2B*
PI3K/AKT Signaling	3.47E-02	0	1.74E-02	-0.447	*ILK, HSP90AA1, HSP90B1, RRAS, YWHAG**
Coagulation System	3.98E-11	0.333	7.94E-12	0.632	*F2, F12, FGA**, FGB*, KNG1, PLG, SERPINA1**, SERPINA5, SERPINC1, SERPIND1, SERPINF2*
Complement System	5.62E-08	0.816	3.16E-13	0.333	*C1QBP, C1QC, C4A/C4B**, C4BPA, C8A**, C8B, CFB, CFD, CFH, CFI, SERPING1**

Ingenuity canonical pathways	PTxNCT p-value	PTxNCT z-score	LNxNCT p-value	LNxNCT z-score	Gene symbol
EIF2 Signaling	9.33E-06	1.134	1.58E-11	1.897	*ACTB, EIF3A, EIF4A1, EIF4G1, EIF4G2**, HSPA5, RPL10**, RPL13, RPL18A, RPL24, RPL3, RPL4, RPL5, RPL6, RPL7A, RPL9, RPS12**, RPS17, RPS24, RPS3**, RPS3A, RPS4X, RPSA, RRAS*
Sirtuin Signaling Pathway	2.34E-02	1.134	5.89E-02[+]	1.134	*ACLY**, GOT2*, IDH2*, NAMPT*, PARP1, PRKDC, TRIM28, TUBA1B, XRCC5**, XRCC6***

[+] Sirtuin Signaling Pathway was predicted from LNxNCT groups' comparison at the significance limit of the p-value.
DEPs predicted in the canonical pathways only for PTxNCT (*) or LNxNCT (**) groups' analysis.

Table 8. Biological functions identified to be affected by the differentially expressed proteins observed among the malignant tissues *versus* contralateral non-tumor breast tissue samples (PTxNCT and LNxNCT) (IPA v. 2.3).

Biological function	PTxNCT p-value	PTxNCT z-score	LNxNCT p-value	LNxNCT z-score	Gene symbol
Fatty Acid Metabolism	2.15E-05	-2.474	2.15E-04	-2.266	*ACLY**, ACSL1, AGT, AKR1C1/AKR1C2, AKR1C3, APOA1, APOB, APOE, APOH, EPHX1*, F2, HSPA8, KNG1, LTF, ME1, PON1*
Immune Response of Cells	5.75E-04	-2.099	2.66E-04	-1.98	*AGT, AHSG, ANPEP**, APCS, APOE, CFH, GAPDH, HSP90B1, IGHA1, IGHA2, IGHG3, IGKC**, NPM1*
Cell Death of Tumor Cell Lines	8.89E-04	-1.231	3.08E-06	-0.892	*ADH5**, API5**, APOB, APOE, CAT, CFH, CRABP2, CRYAB, CSE1L, CTSG**, CYB5A**, DHX9, DSP, EIF4G2**, EZR, FAM129B*, GAPDH, GBE1, GNA11**, HNRNPH1**, HNRNPK**, HSPA5, HSPA8, HSPD1, ILF2, ILK, ITGA6, KANK2**, LMNB1**, MAOA, NAMPT*, NCL, NPM1, NT5E**, P4HB*, PARP1, PARVA, PLG, PRKAR2B, PRKDC, SERPINA3**, SFPQ**, SRSF1, TF**, TNC, TRIM28, TYMP, XPO1**, XRCC5**, XRCC6**, YWHAG***
Migration of Tumor Cell Lines	5.02E-06	0.357	4.95E-07	0.248	*AGT, ANPEP**, ARPC2**, ASPH, C1QBP, CAT, CSE1L, DSP, EZR, F2, FBLN2**, FBLN5, FGA**, GNA11**, HDGF, HNRNPA2B1, HNRNPK**, HSP90AA1, ILF3, ILK, IPO7, ITGA6, KNG1, KRT19*, MCAM, MYH9*, NCL, NPM1, PARVA, RUVBL2, S100A10, SERPINA1**, SERPINA5, TNC, TPM3***
Invasion of Tumor Cell Lines	7.21E-06	0.402	2.15E-04	0.353	*ASPH, CAT, CFH, CSE1L, DSP, EZR, F2, FAM129B*, FBLN2**, FBLN5, HDGF, HNRNPA2B1, HSP90AA1, ILF3, ILK, IPO7, KNG1, KRT19*, MCAM, NAMPT*, NPM1, PARVA, PLG, RPSA**, S100A10, SERPINA1**, TNC*
Generation of Reactive Oxygen Species	2.97E-06	0.996	1.06E-04	0.631	*AGT, ALDH2, CAT, CFH, CRYAB, F2, HBA1/HBA2, ITGA6, NAMPT**
Cell Proliferation of Tumor Cell Lines	1.82E-04	1.786	8.26E-06	2.572	*ACLY**, ACTB, AGT, AKR1C3, APOB, ASPH, C1QBP, CACYBP, CAT, CSE1L, CTSG**, DCLK1, EZR, F12, F2, FAM129B*, FBLN2**, FUS**, GAPDH, HDGF, HNRNPA2B1, HNRNPK**, HSP90AA1, HSPA5, HSPB6, IDH2*, IGKC**, ILF2, ILF3, ILK, IPO7, ITGA1**, KNG1, KRT19*, MGLL, NAMPT*, NCL, NPM1, PARP1, PLG, PRKAR2B, PRPS2**, S100A10, SFPQ**, SNRNP200, TNC, TPM1**, TRIM28, UBA6**, XPO1**, XRCC5**, XRCC6**, YWHAG***

Differentially expressed proteins predicted in the canonical pathways only for PTxNCT (*) or LNxNCT (**) groups' analysis.

Table 9. Top-enriched hallmark gene sets for differentially expressed proteins observed among the malignant tissue samples (PTxLN) (MSigDB v. 6.2).

Hallmark gene set	FDR q-value	Gene symbol
Coagulation	2.11E-11	*APOA1, C3, C8B, CFB, GSN, ITIH1, SERPINA1, SERPING1, TF*
MYC Targets	1.14E-08	*CCT3, CCT4, CCT7, PRPS2, PSMC4, PSMD3, RUVBL2, TCP1*
Apical Junction	7.01E-06	*ACTN1, ACTN4, CTNND1, JUP, RAC2, VCL*
Complement	8.27E-05	*C3, CFB, ITIH1, SERPINA1, SERPING1*
Epithelial-Mesenchymal Transition	8.27E-05	*BGN, COL1A2, FBLN2, FLNA, SERPINH1*
Mitotic Spindle	8.27E-05	*ACTN4, FLNA, GSN, SEPT9, VCL*
Apoptosis	5.94E-04	*BGN, CTNNB1, GSN, LMNA*
Adipogenesis	8.70E-04	*C3, FAH, MGLL, SDHB*
KRAS Signaling Up	8.70E-04	*APOD, CFB, JUP, SERPINA3*
MTORC1 Signaling	8.70E-04	*ACTR2, PSMC4, PSMD12, SERPINH1*

6.2 DATA ARTICLE (*DATA IN BRIEF*)

Title: High-throughput mass spectrometry and bioinformatics analysis of breast cancer proteomic data

Authors: Talita Helen Bombardelli Gomig[1]; Iglenir João Cavalli[1]; Ricardo Lehtonen Rodrigues de Souza[1]; Aline Castro Rodrigues Lucena[2]; Michel Batista[2,3]; Kelly Cavalcanti Machado[3]; Fabricio Klerynton Marchini[2,3]; Fabio Albuquerque Marchi[4]; Rubens Silveira Lima[5]; Cícero de Andrade Urban[5]; Luciane Regina Cavalli[6,7]; Enilze Maria de Souza Fonseca Ribeiro[1]

Affiliations:

[1] Genetics Department, Federal University of Parana, Curitiba, Brazil;

[2] Functional Genomics Laboratory, Carlos Chagas Institute, Fiocruz, Curitiba, Parana, Brazil;

[3] Mass Spectrometry Facility - RPT02H, Carlos Chagas Institute, Fiocruz, Curitiba, Parana, Brazil;

[4] International Research Center (CIPE) - A.C. Camargo Cancer Center, São Paulo, SP, Brazil;

[5] Breast Disease Center, Hospital Nossa Senhora das Graças, Curitiba, Brazil;

[6] Research Institute Pele Pequeno Principe, Curitiba, Brazil;

[7] Lombardi Comprehensive Cancer Center, Georgetown University, USA.

Contact email: enilzeribeiro@gmail.com (E.M.S.F. Ribeiro)

Abstract

Data present here describe a comparative proteomic analysis among the malignant [primary breast tumor (PT) and axillary metastatic lymph nodes (LN)], and the non-tumor [contralateral (NCT) and adjacent (ANT)] breast tissues. Protein identification and quantification were performed through label-free mass spectrometry using a nano-liquid chromatography coupled to an electrospray ionization-mass spectrometry (nLC-ESI-

MS/MS).The mass spectrometry proteomics data have been deposited to the ProteomeXchange Consortium via the PRIDE [1] partner repository with the dataset identifier PXD012431. A total of 462 differentially expressed proteins was identified among these tissues and was analyzed in six groups' comparisons (named NCTxANT, PTxNCT, PTxANT, LNxNCT, LNxANT and PTxLN). Proteins at 1.5 log2 fold change were submitted to the Ingenuity® Pathway Analysis (IPA) software version 2.3 (QIAGEN Inc.) to identify biological pathways, disease and function annotation, and interaction networks related to cancer biology. The detailed data present here provides information about the proteome alterations and their role on breast tumorigenesis. This information can lead to novel biological insights on cancer research. For further interpretation of these data, please see our research article 'Quantitative label-free mass spectrometry using contralateral and adjacent breast tissues reveal differentially expressed proteins and their predicted impacts on pathways and cellular functions in breast cancer' [2].

Specifications Table

Subject area	Biology
More specific subject area	Cancer proteomics
Type of data	Table
How data was acquired	Nanoliquid chromatography coupled to the nanoelectrospray mass spectrometry (LC-ESI-MS/MS)
Data format	Raw and analyzed data, figures
Experimental factors	Samples of tumor and non-tumor tissues from breast cancer patients were collected in the same surgery procedure and stored in RNA later solution
Experimental features	Protein extracts were isolated from tissue samples and analyzed in the LC-ESI-MS/MS using the label-free quantification (LFQ) method to obtain the protein expression levels of each condition. Statistical tests revealed the differentially expressed proteins (DEPs) among the tissues. The lists of DEPs were submitted to Ingenuity® Pathway Analysis (IPA) software.
Data source location	Hospital Nossa Senhora das Graças, Curitiba, Paraná, Brazil.
Data accessibility	The mass spectrometry proteomics data have been deposited to the ProteomeXchange Consortium via the PRIDE partner repository with the dataset identifier PXD012431. HCL and IPA's analyses are in this article.
Related research article	T.H.B. Gomig, I.J. Cavalli, R.L.R. Souza, A.C.R. Lucena, M. Batista, K.C. Machado, F.K. Marchini, F.A. Marchi, R.S. Lima, C.A. Urban, L.R. Cavalli, E.M.S.F. Ribeiro. Quantitative label-free mass spectrometry using contralateral and adjacent breast tissues reveal differentially expressed proteins and their predicted impacts on pathways and cellular functions in breast cancer, Journal of Proteomics, 199C (2019), 1-14 [2].

Value of the Data

- A differential proteome between tumor and non-tumor tissues is described, highlighting the use of a valuable biological sample as control, the contralateral non-tumor breast tissue.
- The non-tumor breast tissues (NCT e ANT) present high similarity in the proteome profiling.
- The common alterations in the proteomes of malignant tissues (PT and LN) point out to cancer associated proteins and pathways that can be explored in tumor progression studies.
- The complete lists of differential expressed proteins and their biological context are a rich source of potential targets to be investigated in further studies.

Data

The differential proteomic profiling of the breast cancer-related tissues was obtained using a high throughput mass spectrometry platform and appropriate statistical methods. A total of 462 identified proteins presented significant differences in the protein expression among these tissues (Supplementary File S1). Six different comparisons were performed: contralateral non-tumor breast tissue versus adjacent non-tumor breast tissue (NCTxANT); primary breast tumor versus contralateral non-tumor breast tissue (PTxNCT); primary breast tumor versus adjacent non-tumor breast tissue (PTxANT); axillary metastatic lymph node versus contralateral non-tumor breast tissue (LNxNCT); axillary metastatic lymph node versus adjacent non-tumor breast tissue (LNxANT); and primary breast tumor versus axillary metastatic lymph node (PTxLN). The differentially expressed proteins of each group' comparison were distinctly grouped by hierarchical cluster analysis using the Perseus software version 1.5.6.0 (Fig. 1). Proteins at 1.5 log2 fold change were analyzed with IPA's tools to identify significant canonical pathways, biological functions, diseases and interaction networks for each group' comparison (Supplementary File S2). A detailed data interpretation is available on [2].

Experimental Design, Material and Methods

Protein Extraction e Digestion

Tissue samples were collected during the surgical procedure at Hospital Nossa Senhora das Graças at Curitiba, Parana, Brazil, and stored in RNA later solution. The

samples were prepared as described in [2], according to a protocol adapted from Ostasiewicz and coworkers [3] and Tyanova and coworkers [4]. Briefly, the samples were lysed in 4% SDS, 0.1 M Tris-HCl pH 7.6 and 0.1 M DTT and homogenized in TissueLyser II sample disruptor (Qiagen Corp. MD, USA), followed by heating to 95 °C for 5 minutes. Samples were submitted to ultrasonic bath, centrifuged to remove cellular debris and processed by filter-aided sample preparation (FASP) method [5]. Proteins were briefly separated in a 1D-PAGE 10% (v/v) acrylamide gel, reduced with 10 mM DTT, alkylated with 50 mM iodacetamide and digested for 18 h with 12.5 ng/µl trypsin at 37 °C. The resulting peptides were processed to LC-ESI-MS/MS.

LC-ESI-MS/MS

Tryptic peptides were separated by online EASY-nLC 1000 chromatograph (Thermo Scientific) and analyzed in the LTQ Orbitrap XL ETD (Thermo Scientific). The runs were performed in triplicate for each sample. Full MS was acquired in the Orbitrap analyzer and the MS2 analysis in the ion trap analyzer, using the CID fragmentation in a DDA mode. The acquired data were analyzed in the MaxQuant software version 1.5.8.3 [6] through the Andromeda search engine [7] and the human UniProt protein database (UniProtKB [8] 24 May 2017, 70,939 entries). Raw data have been deposited to the ProteomeXchange Consortium via PRIDE [1] partner repository with the dataset identifier PXD012431. The parameters of LC-ESI-MS/MS and MaxQuant analysis are further detailed in the research article [2].

Data analysis

The “proteinGroups.txt” file generated by MaxQuant software was processed and analyzed in Perseus v. 1.5.6.0 [9]. Distinct tissue samples were categorized in their respective groups, including PT, LN, NCT and ANT tissues. The LFQ intensity values (that represent the protein expression levels) were log2-transformed and only proteins quantified in at least 70% of samples for each tissue were used for further analysis. Normalization was performed by width adjustment previously to the imputation of the missing values (downshift = 1.8 and width = 0.3) [10], [11]. This processed data were exported to the R platform and analyzed in RStudio version 3.4.2 (http://www.R-project.org), using in-house scripts containing the Bartlett's test, ANOVA and Duncan's test, all at significance level of 5%. Proteins that presented homogeneous variances (accessed by Bartlett's test) were submitted to ANOVA's test at $p < 0.05$ and FDR of 0.05. The resulting differentially expressed proteins were analyzed to identify significant differences in the mean values among the samples' pairs (Duncan's test), providing lists of the differential proteome for the six groups' comparisons (NCTxANT, PTxNCT, PTxANT, LNxNCT, LNxANT and PTxLN). Euclidean distances were

used for hierarchical cluster analyses performed with the differentially expressed proteins for each group' comparison. The 1.5 fold change cutoff was applied into the log2 data.

Ingenuity Pathway Analysis

Proteins at 1.5 log2 fold change of each comparative group were separately analyzed in the IPA software version 2.3 (QIAGEN Inc.) [12]. The NCTxANT group comparison was not included considering that no protein was observed at this cutoff. The gene symbols of the differentially expressed proteins and their fold change values were uploaded in IPA. The Core Analysis was performed under the following parameters: the expression fold change was set as the type of Core Analysis; direct and indirect relationships were consider to generate the networks; the prediction of these networks included the endogenous chemicals, 35 molecules per network and a total of 25 networks enabled per analysis; the confidence considers only relationships based on experimentally observed data; only the human species as well as all tissues and cell lines were set in this analysis. The cutoff values applied to all datasets included fold change ≥1.5 for up-regulated and ≤-1.5 for down-regulated proteins. Adjusted p values (Benjamini-Hochberg, FDR) of <0.05 were considered significant. Based on the IPA's analysis, significant canonical pathways, biological functions and diseases, and interaction networks were algorithmically generated, including z-score values for predict the activation status of these processes.

Funding

This study was financed by the Coordenação de Aperfeiçoamento de Pessoal de Nível Superior - Brasil (CAPES) - Finance Code 001 and the CNPq/Araucaria Research Foundation of Parana State (PRONEX/2012).

Acknowledgments

Federal University of Paraná, Hospital das Clínicas (Curitiba/BR) and Program for Technological Development in Tools for Health-PDTIS-FIOCRUZ for providing the technical infrastructure and professional assistance.

Conflict of interest

The authors declare that they have no known competing financial interests or personal relationships that could have appeared to influence the work reported in this paper.

References

[1] J.A. Vizcaíno, A. Csordas, N. del-Toro, J.A. Dianes, J. Griss, I. Lavidas, G. Mayer, Y. Perez-Riverol, F. Reisinger, T. Ternent, Q.W. Xu, R. Wang, H. Hermjakob, 2016 update of the PRIDE database and related tools, Nucleic Acids Res 44(D1) (2016) 447-456.

[2] T.H.B. Gomig, I.J. Cavalli, R.L.R. Souza, A.C.R. Lucena, M. Batista, K.C. Machado, F.K. Marchini, F.A. Marchi, R.S. Lima, C.A. Urban, L.R. Cavalli, E.M.S.F. Ribeiro. Quantitative label-free mass spectrometry using contralateral and adjacent breast tissues reveal differentially expressed proteins and their predicted impacts on pathways and cellular functions in breast cancer, Journal of Proteomics, in press.

[3] P. Ostasiewicz, D.F. Zielinska, M. Mann, J.R. Wisniewski, Proteome, phosphoproteome, and N-glycoproteome are quantitatively preserved in formalin-fixed paraffin-embedded tissue and analyzable by high-resolution mass spectrometry, Journal of proteome research 9(7) (2010) 3688-3700.

[4] S. Tyanova, R. Albrechtsen, P. Kronqvist, J. Cox, M. Mann, T. Geiger, Proteomic maps of breast cancer subtypes, Nature communications 7 (2016) 10259.

[5] J.R. Wiśniewski, A. Zougman, N. Nagaraj, M. Mann, Universal sample preparation method for proteome analysis, Nat Methods 6(5) (2009) 359–362.

[6] J. Cox, M. Mann, MaxQuant enables high peptide identification rates, individualized p.p.b.-range mass accuracies and proteome-wide protein quantification, Nature biotechnology 26(12) (2008) 1367-1372.

[7] J. Cox, N. Neuhauser, A. Michalski, R.A. Scheltema, J.V. Olsen, M. Mann, Andromeda: A Peptide Search Engine Integrated into the MaxQuant Environment, Journal of Proteome Research 10(4) (2011) 1794-1805.

[8] T.U. Consortium, UniProt: the universal protein knowledgebase, Nucleic acids research 45(D1) (2017) D158-D169.

[9] S. Tyanova, T. Temu, P. Sinitcyn, A. Carlson, M.Y. Hein, T. Geiger, M. Mann, J. Cox, The Perseus computational platform for comprehensive analysis of (prote)omics data, Nature methods 13(9) (2016) 731-40.

[10] S.J. Deeb, R.C. D'Souza, J. Cox, M. Schmidt-Supprian, M. Mann, Super-SILAC allows classification of diffuse large B-cell lymphoma subtypes by their protein expression profiles, Mol Cell Proteomics 11(5) (2012) 77–89.

[11] M.S. Robles, J. Cox, M. Mann, In-vivo quantitative proteomics reveals a key contribution of post-transcriptional mechanisms to the circadian regulation of liver metabolism, PLoS genetics 10(1) (2014) e1004047.

[12] A. Kramer, J. Green, J. Pollard, Jr., S. Tugendreich, Causal analysis approaches in Ingenuity Pathway Analysis, Bioinformatics 30(4) (2014) 523-30.

Figure

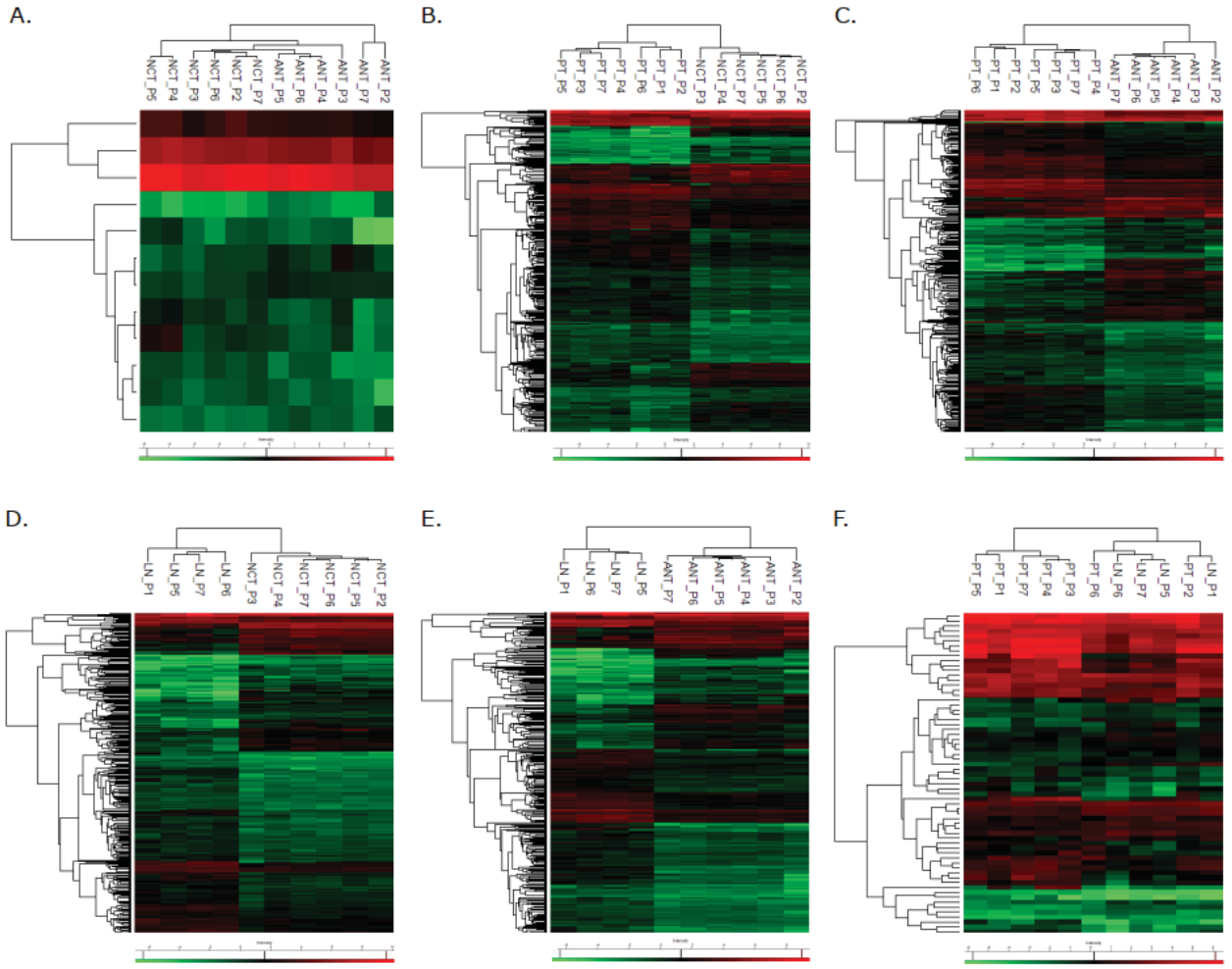

Fig. 1. Hierarchical clustering analysis of the differentially expressed proteins for all the groups' comparisons: A. NCTxANT; B. PTxNCT; C. PTxANT; D. LNxNCT; E. LNxANT; F. TPxLN. NCT - non tumor contralateral breast tissue, ANT - non tumor adjacent breast tissue, PT - primary breast tissue, LN - axillary metastatic lymph node; P1-P7 indicate the patients.

6.3 ANÁLISE PROTEÔMICA COMPARATIVA ENTRE TECIDOS MALIGNOS E NÃO TUMORAIS DE PACIENTES COM CÂNCER DE MAMA

Resumo gráfico

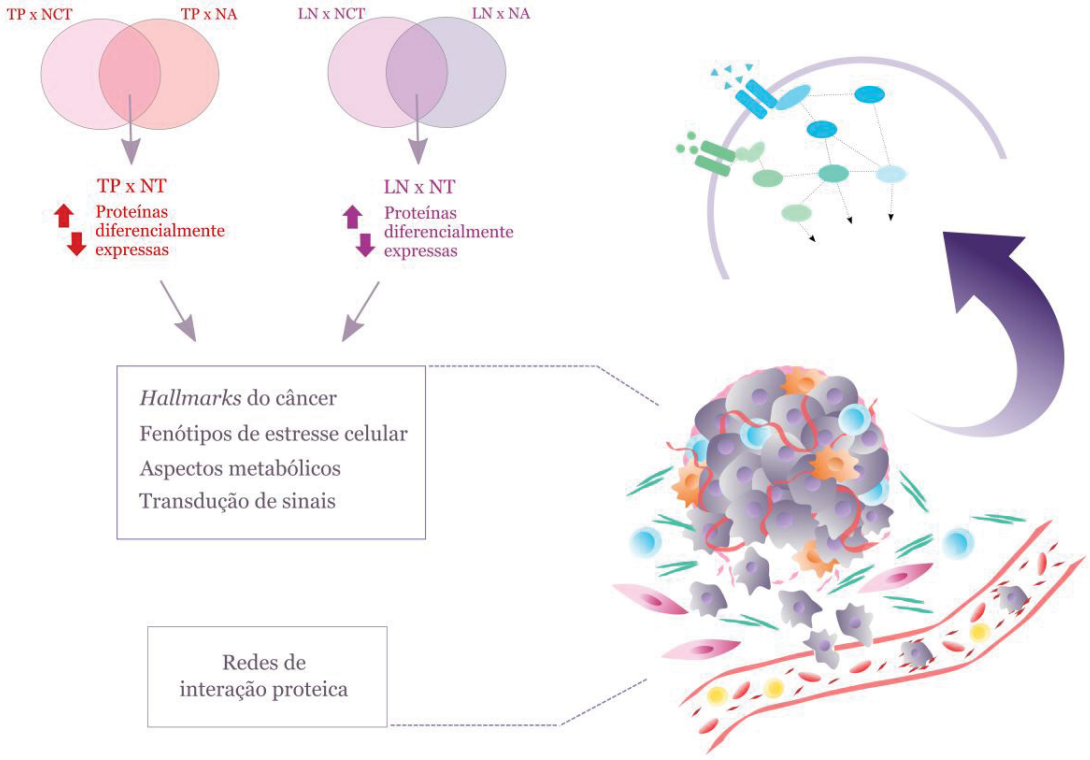

1 Introdução

Métodos proteômicos são amplamente utilizados no estudo comparativo entre amostras tumorais e não tumorais, proporcionando a identificação de proteínas com funções relevantes na tumorigênese mamária. Estudos baseados no perfil proteômico da mama contralateral têm sido restritos à amostras do aspirado do fluido mamilar (PAWLIK et al., 2006; NOBLE et al., 2007), o que evidencia a relevância de abordagens utilizando o tecido mamário não tumoral contralateral como amostra biológica.

Neste sentido, para ampliar o conhecimento do proteoma desse tecido e das possíveis alterações nos níveis de expressão proteica relacionadas à transformação maligna de células mamárias, a presente análise complementa a abordagem proteômica descrita nos subitens 6.1 e 6.2 deste estudo ao avaliar, separada e conjuntamente, as proteínas que diferem o tumor primário de mama (TP) e o linfonodo axilar metastático (LN) da condição não tumoral (NT), a qual compreende os tecidos da mama contralateral (NCT) e adjacente NA). Dessa forma, pretende-se evidenciar as diferenças proteômicas com potencial para distinguir a condições tumoral e não tumoral independentemente do controle sadio (NCT e/ou NA).

Segundo as informações apresentadas nos subitens 6.1 e 6.2, os perfis proteômicos dos tecidos NCT e NA são similares o suficiente para permitir que sejam interpretados como um único proteoma. Dessa forma, as comparações envolvendo esses tecidos apresentaram resultados em sua grande maioria semelhantes (subitem 6.1). Assim, a presente análise avalia conjuntamente o perfil proteômico diferencial identificado nas comparações TP x NCT e TP x NA bem como em LN x NCT e LN x NA, para a obtenção um panorama geral do contexto biológico relacionado às proteínas diferencialmente expressas entre as condições tumoral e não tumoral do tecido mamário, contribuindo para futuros estudos no câncer de mama.

2 Material e Métodos

A presente análise foi realizada a partir dos dados proteômicos obtidos para as pacientes P1 a P7, referentes aos subitens 6.1 e 6.2 deste estudo. Para compor a apresentação desta análise proteômica complementar, as listas de proteínas diferencialmente expressas referentes às comparações TP x NCT, TP x NA, LN x NCT e LN x NA foram extraídas do material suplementar S1 referente ao subitem 6.2.

As proteínas diferencialmente expressas nessas comparações foram analisadas através de diagramas de Venn para a obtenção de um proteoma diferencial que discrimine os tecidos TP e, separadamente, LN em relação a ambos os tecidos não tumorais, NCT e NA (conjuntamente referidos pela sigla NT). As proteínas identificadas na intersecção de cada diagrama foram definidas como os conjuntos de dados a serem analisados, os quais foram designados pelas siglas TP x NT e LN x NT. Os diagramas foram gerados através da plataforma *InteractiVenn.*

A análise de enriquecimento funcional foi realizada utilizando as siglas dos genes que codificam as proteínas diferencialmente expressas para cada conjunto de dados. A sobreposição destes com as informações disponíveis na plataforma MSigDB v. 62 foi realizada através do recurso *online* "*Investigate Gene Sets*" (http://software.broadinstitute.org/gsea/msigdb/annotate.jsp), que utiliza a distribuição hipergeométrica para o cálculo do valor de p e o método de correção de múltiplas hipóteses de Benjamini-Hochberg para determinar o valor de FDR. Até 100 sobreposições significativas ($p<0,05$ e $FDR<0,05$) para cada coleção de genes foram identificadas nessa análise, sendo descritas as principais relacionadas ao câncer. As coleções de genes investigadas incluíram: *hallmarks* (LIBERZON et al., 2015), processos biológicos (conforme os termos de GO), vias KEGG e *Reactome*, além de módulos do câncer.

As interações proteína-proteína (*protein-protein interaction,* PPI) foram preditas através da plataforma STRING v. 10.5, utilizando as siglas dos genes que codificam as proteínas superexpressas e subexpressas ($p<0,05$, log2 FC de 1,5) e

os seguintes parâmetros: fonte de dados incluindo "*textmining*", "*experiments*", "*databases*" e "*co‑expression*"; e escore de interações mínimo de 0,70 (o qual representa interações de alta confiabilidade). A *clusterização* funcional das interações proteicas foi realizada através do método *MCL clustering*, um algoritmo de *clusterização* não supervisionado para gráficos (como as redes de interação) e que apresenta maior robustez (BROHEE; VAN HELDEN, 2006), constituindo a opção recomendada pela plataforma para essa análise. Segundo a plataforma STRING, a informação utilizada para realizar a *clusterização* consiste nos escores globais de interação entre as proteínas, de modo que proteínas com altos valores de escore apresentam maior probabilidade de permanecerem em um mesmo *cluster*.

3 Resultados

A presente análise demonstra um grande percentual de proteínas em comum entre as comparações TP x NCT e TP x NA, bem como entre LN x NCT e LN x NA, conforme mencionado no subitem 6.1. Particularmente, 94,7% (375/396) das proteínas diferencialmente expressas identificadas em TP x NCT e 92,6% (375/405) em TP x NA foram comuns entre ambas as comparações; e em relação ao tecido LN, as proteínas comuns compreenderam 99,3% (407/410) dos dados em LN x NCT e 93,6% (407/435) em LN x NA. Essas informações preliminares sugerem proteínas que podem ser utilizadas para discriminar os tecidos TP e LN em relação à condição NT, independente do tecido mamário utilizado como controle (NCT ou NA).

Os conjuntos de dados proteômicos e os procedimentos computacionais utilizados na presente análise encontram-se descritos na figura 1. Os conjuntos de dados TP x NT (n= 375) e LN x NT (n=407) foram analisados separadamente e o contexto biológico relacionado às proteínas foi apresentado de forma conjunta para evidenciar os principais processos e moléculas preditos na tumorigênese mamária.

3.1 Análise proteômica comparativa entre o tumor primário de mama e os tecidos não tumorais

3.1.1 Proteínas diferencialmente expressas comuns às comparações TP x NCT e TP x NA

A análise proteômica comparativa referente à comparação TP x NT indicou 375 proteínas diferencialmente expressas, sendo 179 no limite de log2 FC de 1,5. As proteínas que apresentaram as maiores diferenças de expressão (valores de FC acima ou abaixo do limite estabelecido em 1,5 vezes) são descritas na tabela 1.

Previamente à análise de enriquecimento funcional, as proteínas superexpressas e subexpressas ($p<0,05$, log2 FC de 1,5; n= 179) foram avaliadas quanto ao perfil de expressão nos diferentes tecidos. A análise de *clusterização* hierárquica resultou na distinção entre TP e NT (FIGURA 2) e em 15 *clusters* com padrões de expressão proteica definidos (FIGURA 3 e MATERIAL SUPLEMENTAR 1A). As maiores diferenças de expressão foram observadas nos *clusters* 1, 4 e 7, compreendendo proteínas superexpressas no TP em relação ao NT, e nos *clusters* 9, 11 e 14, envolvendo proteínas subexpressas no TP.

3.1.2 Enriquecimento funcional e redes de interação em TP x NT

A análise de enriquecimento funcional, realizada com o conjunto de proteínas superexpressas e subexpressas ($p<0,05$, log2 FC de 1,5; n= 179), identificou *hallmarks* de relevância no câncer (TABELA 2); principais processos biológicos com base em termos GO (TABELA 3); diversas vias das plataformas KEGG e Reactome (TABELA 4); e vários módulos de genes relacionados ao câncer (TABELA 5).

A plataforma STRING foi utilizada para a predição de interações entre as proteínas superexpressas e subexpressas entre esses tecidos ($p<0,05$, log2 FC de 1,5; n= 179). A rede de interações obtida apresentou-se estatisticamente significativa ($p<1,0E-16$) e com interações de alta confiabilidade, para as quais foram obtidos potenciais *clusters* funcionais, conforme representado na figura 4.

3.2 Análise proteômica comparativa entre o linfonodo axilar metastático e os tecidos não tumorais

3.2.1 Proteínas diferencialmente expressas comuns às comparações LN x NCT e LN x NA

A análise dos proteomas dos tecidos LN e NT resultou na identificação de 407 proteínas diferencialmente expressas em comum entre as comparações LN x NCT e LN x NA, 226 das quais apresentaram valores de log2 FC de 1,5. As proteínas que apresentaram as maiores diferenças de expressão (valores de FC acima ou abaixo do limite estabelecido em 1,5 vezes) para ambas as comparações são descritas na tabela 6.

Para este conjunto de dados, o perfil de expressão das proteínas superexpressas e subexpressas ($p<0,05$, FC de 1,5; n= 226) foi avaliado através da análise de *clusterização* hierárquica e resultou num dendograma que indica a distinção entre esses tecidos (FIGURA 5) e 15 *clusters* com padrões de expressão proteica definidos (FIGURA 6 e MATERIAL SUPLEMENTAR 1B), sendo as maiores diferenças de expressão observadas nos *clusters* 5, 6 e 7, que incluem proteínas superexpressas no LN em relação a NT, e nos *clusters* 10 e 11, que envolvem proteínas subexpressas no LN.

3.2.2 Enriquecimento funcional e redes de interação em LN x NT

A análise de enriquecimento funcional utilizando os dados das proteínas superexpressas e subexpressas ($p<0,05$, FC de 1,5; n= 226) resultou na identificação de *hallmarks* relacionados à tumorigênese (TABELA 7); processos biológicos de acordo com termos de GO (TABELA 8); diversas vias das plataformas KEGG e Reactome (TABELA 9); e módulos de genes relacionados ao câncer (TABELA 10).

Além disso, interações entre as proteínas superexpressas e subexpressas entre esses tecidos ($p<0,05$, FC de 1,5; n= 226) foram analisadas através da plataforma STRING. Como resultado, obteve-se uma rede com

interações significativas (p<1,0E-16), de alta confiabilidade e com potenciais *clusters* funcionais (FIGURA 7).

3.3 Análise de enriquecimento funcional e aspectos relacionados ao câncer

De acordo com os resultados obtidos para ambos os conjuntos de dados, TP x NT e LN x NT, diversos aspectos biológicos de importância no desenvolvimento do câncer podem ser relacionados às proteínas diferencialmente expressas no câncer de mama, sendo os principais sumarizados na tabela 11.

4 Discussão

4.1 Análise do proteoma diferencial entre tecidos malignos e tecidos não tumorais no câncer de mama

Alterações em diversos mecanismos regulatórios e moléculas cooperam para a aquisição de fenótipos progressivamente malignos, entre as quais se destaca a alteração nos níveis de expressão proteica. Neste contexto, a presente análise descreve as principais proteínas diferencialmente expressas e seus contextos biológicos no processo da tumorigênese.

Inicialmente, ressalta-se a alta similaridade no proteoma expresso pelos tecidos NCT e NA, refletindo em conjuntos de proteínas diferencialmente expressas similares entre as comparações TP x NCT e TP x NA e entre LN x NCT e LN x NA (percentual de proteínas em comum superior a 90% para cada comparação). Assim, os conjuntos TP x NT e LN x NT, abordados na presente análise, indicam proteínas e aspectos biológicos cuja diferença de expressão foi significativa independentemente do tecido não tumoral utilizado como controle, o que pode fornecer um melhor direcionamento das pesquisas proteômicas no câncer de mama, uma vez que ambos os tecidos são bons controles em estudos comparativos.

Entre as comparações TP x NT e LN x NT também foram identificadas diversas proteínas em comum. Essa similaridade resultou na obtenção de vários aspectos biológicos similares na análise de enriquecimento funcional, fornecendo um panorama sobre as vias e processos biológicos que podem ser influenciados pela alteração do proteoma na tumorigênese mamária.

Com base no enriquecimento funcional de *hallmarks* (MSigDB), processos e vias biológicas bem como de módulos do câncer, foi possível elencar os principais aspectos relacionados à tumorigênese e as proteínas cuja alteração nos níveis de expressão pode ser relevante na doença. Estes, por sua vez, podem ser relacionados aos *hallmarks* clássicos do câncer, a fenótipos característicos de estresse celular, ao metabolismo de moléculas e à transdução de sinais, além de outros aspectos que também compreendem a biologia do câncer. As proteínas que apresentaram as maiores diferenças de expressão (nível de significância de 5%) foram relacionadas a esses aspectos e posteriormente discutidas no contexto do câncer e do câncer de mama.

4.2 Contexto biológico relacionado às proteínas diferencialmente expressas entre os tecidos malignos e não tumorais no câncer de mama

4.2.1 Proteínas diferencialmente expressas e hallmarks clássicos do câncer

Muitas das proteínas apresentadas nesta análise estão relacionadas aos *hallmarks* clássicos do câncer, descritos por Hanahan e Weinberg (2011). As categorias funcionais identificadas são referentes à apoptose, angiogênese, invasão e metástase, inflamação, e instabilidade genômica e mutação. Mecanismos envolvidos nesses processos contribuem para o desenvolvimento e/ou progressão tumoral (CORY; ADAMS, 2002). Portanto, a identificação de moléculas a eles relacionadas é de fundamental importância no estudo do câncer.

Na tumorigênese, a resistência à morte celular é considerada uma característica típica das células tumorais, sendo a multiplicidade de mecanismos a ela relacionados um reflexo da diversidade de sinais indutores pelos quais as células estão sujeitas no processo de transformação maligna (HANAHAN;

WEINBERG, 2011). Entre as proteínas relacionadas à apoptose, se destaca a queratina do citoesqueleto 18, tipo II, ou citoqueratina 18 (*KRT18*), com função na resistência a fatores de estresse que podem desencadear a apoptose (KARANTZA, 2011).

A angiogênese compreende um processo complexo, em múltiplas etapas, cujo mecanismo molecular envolve uma extensa comunicação entre células, fatores solúveis e componentes da matriz extracelular (MEC) (GUPTA; QIN, 2003) e que constitui um importante mecanismo para a progressão tumoral. Na presente análise, a β2-glicoproteína 1 (*APOH*) foi relacionada à angiogênese. Propriedades anti-angiogênicas têm sido descritas para essa proteína (SAKAI et al., 2007; YU et al., 2008; CHIU et al., 2016), de modo que baixos níveis de expressão nos tecidos malignos, como observado neste estudo, podem ser compatíveis com a angiogênese e a progressão tumoral.

A invasão e a metástase constituem um *hallmark* de relevância na tumorigênese e são descritas como principais propriedades celulares na cascata invasão-metástase a adesão célula-célula, adesão célula-MEC, migração celular, TEM, redes moleculares do microambiente tumoral e as células-tronco do câncer (*cancer stem cells*, CSC) (JIANG et al., 2015). Diversas proteínas diferencialmente expressas foram identificadas nessas propriedades.

Em relação a esses aspectos, o citoesqueleto e a MEC desempenham funções essenciais na manutenção da homeostase e integridade tecidual, com variadas funções na invasão e metástase (FIFE et al., 2014; PICKUP et al., 2014). Interações envolvendo células e MEC são essenciais para controlar a iniciação e progressão tumoral e têm se constituído em importantes alvos para o direcionamento terapêutico (VENNING et al., 2015). Diversas proteínas participam como receptores das redes de sinalização que envolvem a MEC, incluindo proteoglicanos, glicoproteínas, integrinas, entre outras classes.

Em relação a essas interações, as proteínas observadas permitiram a identificação das vias de integrinas de superfície celular, de LCAM1 (molécula de adesão celular L1) e de semaforinas, as quais possuem relação com a progressão da tumorigênese. As integrinas compõem a classe predominante de proteínas

receptoras de superfície celular, estão envolvidas na adesão célula-MEC e são responsivas a diversos estímulos que permitem controlar a adesão celular, proliferação, sobrevivência, diferenciação e migração, apresentando função essencial na promoção de fenótipos malignos em diversos tipos de câncer (SEGUIN et al., 2015). A molécula L1CAM, por sua vez, consiste numa glicoproteína de superfície celular que possui múltiplas funções pró-angiogênicas (ANGIOLINI; CAVALLARO, 2017), de motilidade e de invasão (ALTEVOGT et al., 2016). Já as semaforinas compreendem proteínas extracelulares de sinalização consideradas reguladoras-chave da morfologia e motilidade em diferentes tipos celulares, incluindo células tumorais (ALTO; TERMAN, 2017).

Outro mecanismo alterado na tumorigênese compreende a adesão celular. Neste contexto, além da adesão focal, diferentes tipos de junção celular foram relacionados às proteínas diferencialmente expressas, como as junções aderentes e de oclusão. Aspectos funcionais distintos são regulados por moléculas relacionadas a esses componentes, os quais têm sido descritos na promoção da mobilidade celular e na metástase (KNIGHTS et al., 2012; SEONG et al., 2013).

Aspectos relacionados ao citoesqueleto e à MEC, bem como suas interações através de moléculas envolvidas na intercomunicação e adesão célula-MEC possuem relação com outro processo dinâmico e indispensável para a cascata invasão-metástase, a TEM, reconhecida como um evento necessário à progressão tumoral.

Com base nas proteínas diferencialmente expressas envolvidas nos aspectos acima referidos bem como em informações da literatura, pode-se indicar que as principais proteínas relacionadas aos processos de invasão e metástase são codificadas pelos genes *AKR1C1, ARPC2, ARPC3, BGN, COL1A2, EZR, FBLN2, FBN1, ITGA6, LAMB1, MYH9* e *MYH11, RRAS* e *TNC*. Essas proteínas são indicadas na progressão de diferentes tipos de tumores, sendo os genes *COL1A2, FBLN2, LMNB1, MYH11* e *TNC* descritas em assinaturas moleculares da metástase (RAMASWAMY et al., 2003; ALBINI et al., 2008).

Outro aspecto de relevância na tumorigênese e que pode ser amplamente relacionado ao processo de invasão e metástase consiste na resposta à injúria,

que envolve a ativação transiente de programas celulares que resultam na migração e proliferação de células epiteliais bem como no remodelamento da MEC circundante (GURTNER et al., 2008). As vias e funções envolvidas nesse processo geralmente são alteradas no câncer e promovem a ativação da resposta à injúria de forma autossustentável, coincidindo com a aquisição de fenótipos celulares que permitem a invasão e a metástase (ELLISEN, 2017). Observou-se que diversas proteínas mencionadas acima foram comumente identificadas na resposta à injúria, reforçando seu potencial de atuação na progressão do câncer. Entre essas proteínas, se destacam as codificadas pelos genes *ACTB, COL1A2, ILK, MCAM, MYH9, RAC2, TNC* e *TPM1*.

A inflamação, por sua vez, compreende um importante *hallmark* clássico do câncer, influenciando outras características das células tumorais ao fornecer moléculas bioativas ao microambiente tumoral, que atuam na promoção da angiogênese, invasão e metástase, entre outras funções (HANAHAN; WEINBERG, 2011). Nesta análise, as proteínas relacionadas à inflamação também foram observadas em outros processos referentes ao câncer, indicando que seus níveis de expressão podem ter relação com o desenvolvimento da doença através de mecanismos variados. Entre as principais proteínas, estão as codificadas pelos genes *APOD, AHSG, FABP4* e *MGLL*.

Outro *hallmark* clássico do câncer a ser relacionado compreende a instabilidade genômica e mutação, com destaque para as categorias funcionais referentes à via de p53, ciclo celular e reparo de DNA. De acordo com Hanahan e Weinberg (2011), vantagens seletivas conferidas pelo acúmulo de mutações permitem o crescimento e eventual predomínio de subpopulações celulares no microambiente tumoral. Nesse sentido, genótipos favoráveis à progressão do tumor são adquiridos, em parte, pela atuação dos sistemas de manutenção do genoma, como o reparo de danos ao DNA, e por alterações envolvendo moléculas sinalizadoras no ciclo celular, como a proteína p53, considerada “guardiã do genoma” e descrita na tumorigênese mamária (MULLER; VOUSDEN, 2014). Nesta análise, a via de p53 foi relacionada à proteína S100-A10 (*S100A10*), pertencente à família de proteínas S100 ligantes de cálcio e associadas à anexina-

2, cujas funções são envolvidas na divisão celular, motilidade, síntese de proteínas, permeabilidade da membrana, secreção, entre outras (CANCEMI et al., 2018).

No que se refere ao ciclo celular, além de proteínas envolvidas com sua regulação, também foram identificadas as fases mitóticas G2/M e seu respectivo ponto de checagem. É importante ressaltar que a maioria das proteínas relacionadas a esses processos apresentou superexpressão nos tecidos malignos em relação aos não tumorais, com destaque para as proteínas codificadas pelos genes *HSP90AA1, LMNB1, NPM1* e *TNC* no ciclo celular; e *HNRNPU, HSPA8, ILF3, NCL* e *SRSF1* no ponto de checagem de G2/M. Entre estes, *LMNB1, NCL, NPM1* e *TNC* são reconhecidos em mecanismos que envolvem o ciclo celular e a tumorigênese (GRINSTEIN et al., 2006; CAMPS et al., 2014; ZHAO et al., 2015; CAI et al., 2018), reforçando sua importância para estudos adicionais no câncer de mama.

Além disso, também foram observadas proteínas envolvidas na resposta a danos no DNA, incluindo vias de reparo relacionadas à quebra de dupla fita. Em geral, somente proteínas superexpressas nos tecidos malignos em relação aos não tumorais foram relacionadas a esses processos. A superexpressão de proteínas de reparo tem sido descrita em diversos tipos de câncer, sendo sugerido seu envolvimento na estabilização do genoma das células malignas, permitindo a aquisição de fenótipos invasivos e metastáticos (SARASIN; KAUFFMANN, 2008). As proteínas mais comumente observadas nesses aspectos são codificadas pelos genes *PRKDC, XRCC5* e *XRCC6*, os quais estão diretamente envolvidos em vias de reparo de quebra de dupla fita (WANG et al., 2013; DAVIS et al., 2014).

4.2.2 Proteínas diferencialmente expressas e os fenótipos de estresse celular

Os tumores estão sujeitos a diversos tipos de estresse celular durante seu desenvolvimento. Para ilustrar essa questão, fenótipos de estresse foram descritos como *hallmarks* adicionais do câncer, de forma complementar e em concordância com os clássicos (LUO et al., 2009). Esses fenótipos podem auxiliar na compreensão dos mecanismos moleculares subjacentes aos processos e

respostas fisiológicas envolvidos na dinâmica de manutenção e progressão do tumor, bem como na evolução do microambiente tumoral (LUO et al., 2009).

Na presente análise, além da resposta geral ao estresse, também foram obtidos processos que podem ser categorizados nesses *hallmarks* adicionais do câncer, incluindo o desdobramento de proteínas, espécies reativas de oxigênio e hipóxia.

Diversas proteínas foram relacionadas à resposta ao estresse, processo biológico que também apresenta genes alterados em variados tipos de câncer, constituindo-se como um módulo do câncer, de acordo com a banco de dados MSigDB. Entre as principais proteínas relacionadas ao estresse, estão as codificadas pelos genes *AKR1C3, ANK1, FABP4, FBLN2, KRT18, MAOA* e *RAC2.*

O desdobramento de proteínas, também denominado de estresse proteotóxico, está relacionado à homeostase do proteoma e é comum em células tumorais como resultado da extrema aneuploidia, da variação do número de cópias e de alterações transcricionais, as quais comprometem a dosagem das subunidades proteicas em diferentes complexos e aumentam o estresse nas vias de chaperonas (LUO et al., 2009). As principais proteínas identificadas nesse processo são codificadas pelos genes *CRYAB, IARS, NPM1* e *TARS.* Em especial, também foram observadas proteínas da família *heat shock*, incluindo as codificadas pelos genes *HSP90B1, HSPA5, HSPA8* e *HSPD1*. As proteínas chaperonas *heat shock* pertencem a uma das principais vias de resposta ao estresse proteotóxico, promovendo o adequado dobramento das proteínas (LUO et al., 2009). Alterações na expressão de proteínas dessa família são comumente descritas no câncer, sendo observados níveis elevados dessas proteínas em vários tipos de tumores, com função na adaptação das células tumorais (DAI et al., 2012).

A produção de espécies reativas de oxigênio (*reactive oxygen species*, ROS), resultante de diversas reações metabólicas na célula, também é uma condição de estresse celular. Embora baixos níveis de ROS sejam utilizados pela célula na transdução de sinais, sua concentração elevada está relacionada ao metabolismo acelerado das células tumorais e à manutenção da alta taxa

proliferativa dos tumores (SOSA et al., 2013). Os efeitos do aumento do estresse oxidativo e das ROS impactam sobre os *hallmarks* clássicos do câncer (FIASCHI; CHIARUGI, 2012). Nesta análise, a proteína catalase (*CAT*) foi identificada na via de ROS.

Outro fator que gera estresse celular é a hipóxia, uma condição de baixa concentração de oxigênio, comum na maioria dos tumores e que desencadeia a ampliação da vascularização, a alteração do metabolismo das células tumorais e a aquisição do fenótipo TEM, promovendo a mobilidade celular e a metástase (MUZ et al., 2015). As principais proteínas identificadas com relação à hipóxia são codificadas pelos genes *BGN, GBE1, HSPA5, MYH9* e *PGM1*.

4.2.3 Proteínas diferencialmente expressas e aspectos metabólicos

Várias proteínas diferencialmente expressas foram categorizadas funcionalmente em processos envolvendo o metabolismo de moléculas como ácidos graxos, mRNA, proteínas, além do metabolismo de xenobióticos. Alterações nos níveis de expressão dessas proteínas podem influenciar funções relacionadas a esses aspectos metabólicos e contribuir para o desenvolvimento e progressão tumoral.

O metabolismo de lipídios participa do controle de vários processos celulares comumente alterados no câncer, como a apoptose, crescimento celular, proliferação, diferenciação, motilidade, homeostase de membranas celulares, além de atuar na inflamação, resposta a quimioterápicos e resistência a drogas (HUANG; FRETER, 2015). Alterações no metabolismo de ácidos graxos, os quais constituem importantes moléculas de sinalização, são descritas no câncer de mama (MONACO, 2017). Nesta análise, a maioria das proteínas identificadas nesse processo foram subexpressas nos tecidos malignos em relação aos não tumorais, sendo destacadas as codificadas pelos genes *ACSL1, HSP90AA1, MAOA* e *MGLL.*

Os metabolismos de mRNA e de proteínas, por sua vez, estão relacionados às diversas reações químicas que envolvem essas moléculas e fornecem um panorama das proteínas que podem ter função nos processos pós-

transcricionais e traducionais. A tradução de mRNA é um dos processos que mais consome energia na célula, está fortemente correlacionada com a atividade metabólica desta e, portanto, desempenha funções importantes no crescimento e proliferação celulares (TOPISIROVIC; SONENBERG, 2011). Assim, a tradução de mRNA apresenta relevante contribuição para o desenvolvimento do câncer (LINDQVIST et al., 2018). Nesta análise, diversas proteínas foram identificadas em processos relacionados ao mRNA e à tradução, sendo a maioria superexpressa nos tecidos malignos em relação aos não tumorais, em teoria, corroborando com a intensa atividade metabólica das células tumorais.

No que se refere especificamente à molécula de mRNA, foram observadas as proteínas codificadas pelos genes *SNRNP200, DHX15* e por vários membros da família de ribonucleoproteínas heterogêneas (hnRNPs), que atuam na biogênese dos telômeros, reparo de DNA, transcrição e tradução, *splicing* de RNA e na sinalização celular, além do potencial envolvimento nos processos de apoptose, angiogênese, invasão e TEM (HAN et al., 2013). Outras duas classes de proteínas com importância no câncer incluem proteínas ribossomais das subunidades 40S e 60S, cuja função na tumorigênese inclui a apoptose, ciclo celular, proliferação celular, transformação maligna, migração e invasão, entre outras (XU et al., 2016).

Muitas proteínas identificadas no metabolismo de mRNA também foram observadas no metabolismo de proteínas, incluindo as proteínas ribossomais das subunidades 40S e 60S e as codificadas pelos genes *EIF4A1* e *EIF4G1*, que desempenham funções importantes no câncer (ALI et al., 2017). Outras proteínas principais incluem as codificadas pelos genes *APOD, EZR, FABP4, NOP56* e *PRKDC*.

Por fim, outro processo metabólico identificado nesta análise compreende o metabolismo de xenobióticos, que consiste em etapas através das quais as células metabolizam, eliminam e detoxificam drogas e substâncias estranhas ao organismo (xenobióticos), através da atuação de diferentes enzimas (OMIECINSKI et al., 2010). Em geral, as proteínas envolvidas no metabolismo de drogas e xenobióticos e seus níveis de expressão desempenham funções importantes na

tumorigênese e na resposta a drogas (LI, Y. et al., 2017). Nesta análise, a maioria das proteínas relacionadas ao metabolismo de xenobióticos apresentou subexpressão nos tecidos tumorais em relação aos não tumorais, incluindo principalmente as codificadas pelos genes *AKR1C1, AKR1C3, CAT, MAOA* e *MGLL,* as quais ampliam o repertório de moléculas envolvidas na detoxificação celular e que podem ter função na tumorigênese.

4.2.4 Proteínas diferencialmente expressas e a transdução de sinais

Diferentes vias e moléculas relacionadas à sinalização celular foram identificadas a partir das proteínas diferencialmente expressas. Estas também foram relacionadas aos processos mencionados anteriormente, corroborando a relevância para estudos futuros no câncer de mama.

A progressiva transformação de células fenotipicamente normais em malignas envolve alterações em redes e vias interconectadas de sinalização (SEVER; BRUGGE, 2015). Nesta análise, as vias de sinalização identificadas foram relacionadas às moléculas mTORC1, PI3K-AKT-mTOR, IL2-STAT5, PDGF, Hedgehog e KRAS. Além destas, também se destacam a resposta ao estrogênio e a homeostase de íons cálcio, cuja transdução de sinais tem função na tumorigênese, e as vias em câncer (KEGG).

Entre essas vias, a sinalização mediada por mTORC1 está relacionada à via de sinalização de mTOR (complexo de rapamicina em mamíferos), uma serina/treonina quinase conservada que atua como efetora *downstream* da via PI3K-AKT e existe em dois complexos proteicos principais nas células, mTORC1 e mTORC2 (POPULO et al., 2012). A ativação de mTORC1 promove a conversão dos nutrientes disponíveis em biomassa para a síntese de proteínas, lipídios e nucleotídeos, moléculas fundamentais para o crescimento e a proliferação celulares (ILAGAN; MANNING, 2016). Em geral, mTOR possui função central na regulação de muitos processos celulares essenciais, incluindo desde a síntese de proteínas até a autofagia, e alterações envolvendo sua transdução de sinal são relevantes na progressão tumoral (SAXTON; SABATINI, 2017). Nesta análise, a maioria das proteínas relacionadas à mTORC1 apresentaram aumento de

expressão nos tecidos malignos em relação aos não tumorais. Em geral, as principais proteínas identificadas nessa via são codificadas pelos genes *CACYBP, EPRS, GAPDH, GBE1, HSPD1* e *ME1*.

A sinalização mediada por IL-2 (interleucina-2) e seu alvo *downstream* STAT5 (transdutores de sinal e ativadores da transcrição – *signal transducers and activators of transcription*) está relacionada ao crescimento, diferenciação e regulação da morte celular em células do sistema imune (NELSON, 2002). Em geral, a sinalização de IL-2 pode resultar na ativação de diferentes moléculas efetoras, que são responsáveis por mediar a sobrevivência, proliferação, diferenciação, ativação, produção de citocinas, entre outras habilidades, pelos diferentes tipos de células imunes (JIANG et al., 2016). Na presente análise, a sinalização IL2-STAT5 foi relacionada às proteínas codificadas pelos genes *CA2, CKAP4, FAH* e *ITGA6.*

Em relação à sinalização de PDGF (fator de crescimento derivado de plaquetas – *platelet-derived growth factor*), diversas proteínas alteradas impactam na regulação de sua transdução de sinal e de suas funções no crescimento e sobrevivência de diversos tipos celulares bem como no câncer (FAROOQI; SIDDIK, 2015). A sinalização de receptores PDGF contribui para múltiplos processos associados ao câncer, incluindo o estímulo para a proliferação celular, desenvolvimento de fibroblastos no microambiente tumoral, angiogênese, entre outros (OSTMAN; HELDIN, 2007). As proteínas identificadas na sinalização de PDGF apresentaram expressão diminuída nos tecidos malignos em relação aos não tumorais, sendo as principais codificadas pelos genes *COL1A2, PLG* e *PRKAR2B*.

Proteínas relacionadas à resposta ao estrogênio, por sua vez, indicam moléculas envolvidas na transdução de sinais relacionada a seus receptores, a qual tem importância na tumorigênese mamária. Esse hormônio tem função regulatória em uma ampla gama de processos biológicos, promovendo a sobrevivência e proliferação celulares bem como a intercomunicação com vias de fatores de crescimento (ROTHENBERGER et al., 2018). Particularmente, no que se refere aos efeitos da sinalização do estrogênio na expressão gênica, um estudo

de meta-análise identificou genes de resposta precoce (3-4h) e tardia (24h) ao estrogênio, sendo as principais funções dos primeiros relacionadas à sinalização celular e proliferação e dos demais à divisão celular, reparo de DNA e recombinação; e as funções dos genes de resposta tardia especificamente relacionadas ao câncer de mama (JAGANNATHAN; ROBINSON-RECHAVI, 2011). Nesta análise, as principais proteínas identificadas na resposta precoce e/ou tardia ao estrogênio são codificadas pelos genes *CALB2, KRT18, KRT19, LTF* e *PRKAR2B* e fornecem informações adicionais sobre as moléculas potencialmente envolvidas na sinalização do estrogênio no câncer de mama.

No que se refere ao Ca^{2+}, a transdução de sinal o envolvendo remete a importantes vias na progressão tumoral, cuja função determina o destino/comportamento da célula, sendo que alterações em seus níveis e, consequentemente, em sua sinalização, são relacionadas a todos os *hallmarks* clássicos do câncer (STEWART et al., 2015). Níveis alterados de Ca^{2+} podem auxiliar as células tumorais na evasão da morte celular (VANHOUTEN et al., 2010), sinalizar a hipóxia e induzir a proliferação de células endoteliais, migração e angiogênese (XU et al., 2018), e estão relacionados à TEM (DAVIS et al., 2014). A maioria das proteínas relacionadas ao Ca^{2+} apresentou subexpressão nos tecidos malignos em relação aos não tumorais, sendo as principais codificadas pelos genes *ACSL1, CALB2, CFD, LTF, PLG* e *S100A10*.

Nesta análise também foram identificadas proteínas em vias relacionadas ao câncer, segundo o banco de dados KEGG, incluindo as codificadas pelos genes *COL4A2, HSP90AA1, HSP90B1, ITGA6, LAMA4, LAMB1* e *RAC2*. Essas proteínas foram observadas em vários processos no contexto da tumorigênese acima descrito.

4.3 Interações proteicas preditas entre as proteínas diferencialmente expressas

As interações entre proteínas podem auxiliar na descrição e restringir a função de uma proteína por vários fatores: sua estrutura tridimensional pode ter significado biológico apenas no contexto de complexos multiproteicos; suas

atuações moleculares podem ser reguladas por ligações cooperativas ou alostéricas; e seu contexto celular pode ser controlado por múltiplas interações de transporte, “sequestro” e sinalização (SZKLARCZYK et al., 2015). Neste contexto, a obtenção de um panorama de interações proteicas auxilia na interpretação biológica dos possíveis efeitos da expressão diferencial das proteínas na tumorigênese mamária.

O agrupamento das proteínas em *clusters* distintos indicou grupos de proteínas que podem desempenhar funções em vias e processos biológicos em comum e que cujas interações diretas (físicas) ou indiretas (funcionais) podem representar alvos de relevância para estudos futuros.

Nesta análise, as redes de interação obtidas para os conjuntos de dados TP x NT e LN x NT resultou em diversas interações proteína-proteína, com destaque para as que apresentaram 10 ou mais interações, as quais envolveram variados *clusters* e proteínas distintas, como as codificadas pelos genes *DHX9, EFTUD2, EPRS, HNRNPA2B1, HSP90AA1, RPL5* e *RPL7A*.

Outras interações foram observadas envolvendo relevantes proteínas mencionadas nos contextos biológicos descritos anteriormente, como as codificadas pelos genes *ACTB, ACTR2, ACTR3, AGT DHX15, EZR, FABP4, MAOA, MCAM, MYH11, NOP56, PARP1, PLG, S100A10, SNRNP200, SPTA1, SPTB*, entre outros.

Considerando o caráter essencialmente descritivo da abordagem interatômica desta análise, sugere-se uma avaliação mais detalhada das interações proteicas de interesse em outros bancos de dados de PPI, aprimorando a seleção de alvos para estudos. Entre as principais plataformas nas quais essas interações podem ser investigadas, destacam-se: *Agile Protein Interaction Data Analyzer* (APID), *Biological General Repository for Interaction Datasets* (BioGrid), *Database of Interacting Proteins* (DIP), *Genome-scale Integrated Analysis of gene Networks in Tissues* (GIANT), *HumanBase, Human Protein Reference Database* (HPRD), *IntAct Molecular Interaction Database* (IntAct), *Integrated Interactions Database* (IID), *Interologous Interaction Database* (I2D), *Mentha, Molecular*

interaction Database (Mint), *SPECific Tissue/Tumor Related PPI networks Analyzer* (Spectra), entre outras.

4.4 Proteínas diferencialmente expressas e o câncer de mama

Várias proteínas foram relacionadas a aspectos de relevância no câncer e apresentaram diferença estatisticamente significativa com consideráveis valores de FC. Essas proteínas representam algumas das moléculas de interesse para estudos adicionais. Estas e outras proteínas envolvidas nas mesmas vias e processos biológicos bem como em interações proteicas diretas e indiretas, podem constituir alvos de relevância para a pesquisa no câncer de mama.

Entre as proteínas diferencialmente expressas que apresentaram as maiores diferenças de expressão e que foram preditas em mais de um aspecto relacionado ao câncer, são destacadas as codificadas pelos genes *CKAP4, DHX15, DSP, EZR, KRT18, KRT19, NOP56, PRKDC, RPL6, SNRNP200, TNC* e *TRIM28*, superexpressas nos tecidos malignos em relação aos não tumorais; e *AKR1C1, ANK1, APOD, CES1, COL1A2, COL6A6, FABP4, FAH, MAOA, MCAM, MGLL* e *SPTA1*, subexpressas nos tecidos malignos em relação aos não tumorais. Além disso, também se destacam *PLG, CA2, RAC2* e *SERPING1*, cujas proteínas foram relacionadas a maior variedade de processos na análise de enriquecimento funcional.

Segundo os dados obtidos na análise realizada através do *cBioPortal for Cancer Genomics*, descrita no subitem 6.1, a maioria dessas proteínas apresentou níveis de expressão compatíveis (superexpressão ou subexpressão no tumor primário de mama) com os observados no estudo, reforçando a relevância e credibilidade dos dados aqui apresentados.

Em relação a estudos da literatura, as proteínas acima destacadas que são amplamente descritas no câncer incluem as codificadas pelos genes *APOD, EZR, KRT18, KRT19, PLG, PRKDC, MGLL, TNC* e *TRIM28* (MIDWOOD; SCHWARZBAUER, 2002; NOMURA et al., 2010; CLUCAS; VALDERRAMA, 2014; KOTULA et al., 2015; CZERWINSKA et al., 2017).

Entre essas proteínas, a ezrina (*EZR*) consiste num membro da família ERM (Ezrina-Radixina-Moesina) de proteínas associada ao citoesqueleto, que estão envolvidas em múltiplos aspectos da migração celular (CLUCAS; VALDERRAMA, 2014). No câncer de mama, a atuação dessa proteína foi observada na adesão focal e na dinâmica de invadopodia (protrusões da membrana plasmática ricas em filamentos de actina), processos relacionados à metástase (HOSKIN et al., 2015).

O plasminogênio (*PLG*) tem sua importância descrita no câncer com base na atividade dos receptores de plasminogênio e da proteína plasmina, a qual está envolvida na resposta à injúria, angiogênese e invasão celular e é sintetizada através da ligação do plasminogênio, seu precursor, à superfície celular, processo regulado por várias moléculas, incluindo os receptores de plasminogênio (DIDIASOVA et al., 2014). Alterações nos componentes do sistema plasminogênio/plasmina podem resultar no crescimento tumoral e na metástase (KWAAN; MCMAHON, 2009).

A tenascina-C, que compõe a MEC, está relacionada à modulação da adesão celular, angiogênese, progressão tumoral e indução de múltiplas vias oncogênicas de sinalização, como a via de Wnt (MIDWOOD; SCHWARZBAUER, 2002), além de apresentar funções na resposta à injúria tecidual e, consequentemente, na tumorigênese (MIDWOOD; OREND, 2009). No câncer de mama, essa proteína é descrita na promoção do crescimento tumoral e invasão (HANCOX et al., 2009).

O fator de transcrição intermediário 1-beta (*TRIM28*) está envolvido em diversos processos intracelulares relacionados ao câncer, incluindo a resposta de danos no DNA, degradação de p53, regulação da transcrição gênica, manutenção da pluripotência, indução à TEM, entre outros que conferem complexidade à sua contribuição no desenvolvimento do câncer (CZERWINSKA et al., 2017). No câncer de mama, sua função tem sido demonstrada na agressividade tumoral, capacidade de autorrenovação, crescimento do tumor, invasão e migração, TEM e quimioresistência (DAMINENI et al., 2017).

Outras proteínas destacadas nesta análise que apresentam funções estudadas no câncer de mama incluem o membro C1 da família 1 de alfa-ceto redutase (*AKR1C1)*, envolvido no catabolismo e sinalização mediada por progesterona e no crescimento tumoral desencadeado a esse hormônio (JI et al., 2004); a proteína adaptadora do citoesqueleto ankirina-1 (*ANK1*), com função na resposta ao dano no DNA (HALL et al., 2016); a proteína 4 de ligação a ácidos graxos (*FABP4*), envolvida no transporte de ácidos graxos e descrita na proliferação do tumor bem como na indução das cascatas de sinalização mediadas por AKT e MAPK (GUAITA-ESTERUELAS et al., 2017); a enzima monoamina oxidase-A (*MAOA*) e a glicoproteína de superfície celular MUC18, também conhecida como molécula de adesão celular de melanoma (*MCAM*) ou *cluster* de diferenciação 146 (*CD146*), ambas envolvidas na indução do processo de TEM e de metástase (ZENG et al., 2012; BHARTI et al., 2018); entre outras. Além dessas, as proteínas codificadas pelos genes *APOD* e *COL6A6* também são mencionadas em estudos no câncer de mama (SOILAND et al., 2007; YEH et al., 2018).

Outras proteínas, apesar da escassez de informações em relação às suas funções no câncer de mama, têm sido descritas no câncer em geral e/ou em tipos específicos da doença, como as codificadas pelos genes *CA2, CKAP4, COL1A2, DHX15, DSP, NOP56, RAC2* e *RPL6.*

Entre estas, as proteínas da família anidrase carbônica, à qual pertence a anidrase carbônica II (*CA2*), desempenham função no controle do pH do microambiente tumoral e estão envolvidas na sobrevivência e proliferação celular, sendo os membros IX e XII considerados como alvos para terapias no câncer (MBOGE et al., 2018). A desmoplaquina (*DSP*) constitui um dos componentes dos desmossomos, junções intercelulares que unem mecanicamente as células e estabilizam a estrutura dos tecidos e são relacionados ao câncer (ZHOU et al., 2017). A proteína Rac2 (*RAC2*) compõe a família de GTPases Rac, cuja atividade é relacionada à tumorigênese e metástase e à funções celulares essenciais, incluindo motilidade, adesão e proliferação (WERTHEIMER et al., 2012). A proteína ribossomal L6 (*RPL6)* consiste num regulador essencial da resposta de

dano ao DNA, via proteína PARP, cuja inibição impede o recrutamento de proteínas que desempenham função nesse processo, como a proteína 1 de ligação a p53 (*TP53BP1)* e a proteína associada ao reparo BRCA1 (*BRCA1*), além de resultar em defeitos no ponto de checagem G2/M, reparo de dano no DNA e na sobrevivência celular (YANG et al., 2018).

Por fim, embora outros membros estejam relacionados ao câncer, informações para as proteínas codificadas pelos genes *CES1, FAH, SERPING1, SNRNP200, SPTA1* apresentam-se escassas ou ausentes no câncer de mama.

Em geral, as proteínas aqui descritas apresentam potencial para serem melhor avaliadas no câncer de mama, objetivando compreender e demonstrar sua função na tumorigênese e sua relevância em discriminar a condição maligna da não tumoral na glândula mamária.

5 Considerações finais

A presente análise forneceu informações complementares às descritas no subitem 6.1 deste estudo, indicando proteínas que apresentam diferença significativa de expressão nos tecidos malignos em relação a ambos os não tumorais e que, portanto, têm potencial para discriminar a tumorigênese mamária independente do tecido considerado como controle saudável.

O contexto biológico descrito nessa análise representa as principais vias, funções e processos biológicos que podem ser influenciados pela alteração no proteoma da glândula mamária em decorrência do processo de tumorigênese. Entre os principais aspectos relacionados ao câncer, se destacam os *hallmarks* clássicos, condições de estresse típicas de células tumorais, o metabolismo de diversas moléculas e vias de sinalização com função reconhecida na tumorigênese. A predição de interações proteicas, por sua vez, evidenciou a complexidade de interconexões moleculares subjacentes ao câncer de mama, além de contribuir para análises preliminares de seu interatoma. Nesse sentido, são sugeridas abordagens *in sílico* complementares para a definição de alvos para a validação no câncer de mama.

Dessa forma, as proteínas analisadas fornecem informações que podem auxiliar no direcionamento da pesquisa no câncer de mama e evidenciar vias e funções biológicas bem como moléculas de interesse para estudos proteômicos adicionais que possam avaliar a relevância destas na tumorigênese mamária e seu potencial de utilização na prática clínica.

Referências

A bibliografia descrita nesta análise encontra-se nas referências gerais do estudo.

Figuras

FIGURA 1 – FLUXOGRAMA REPRESENTANDO AS ETAPAS DE ANÁLISE DAS PROTEÍNAS DIFERENCIALMENTE EXPRESSAS

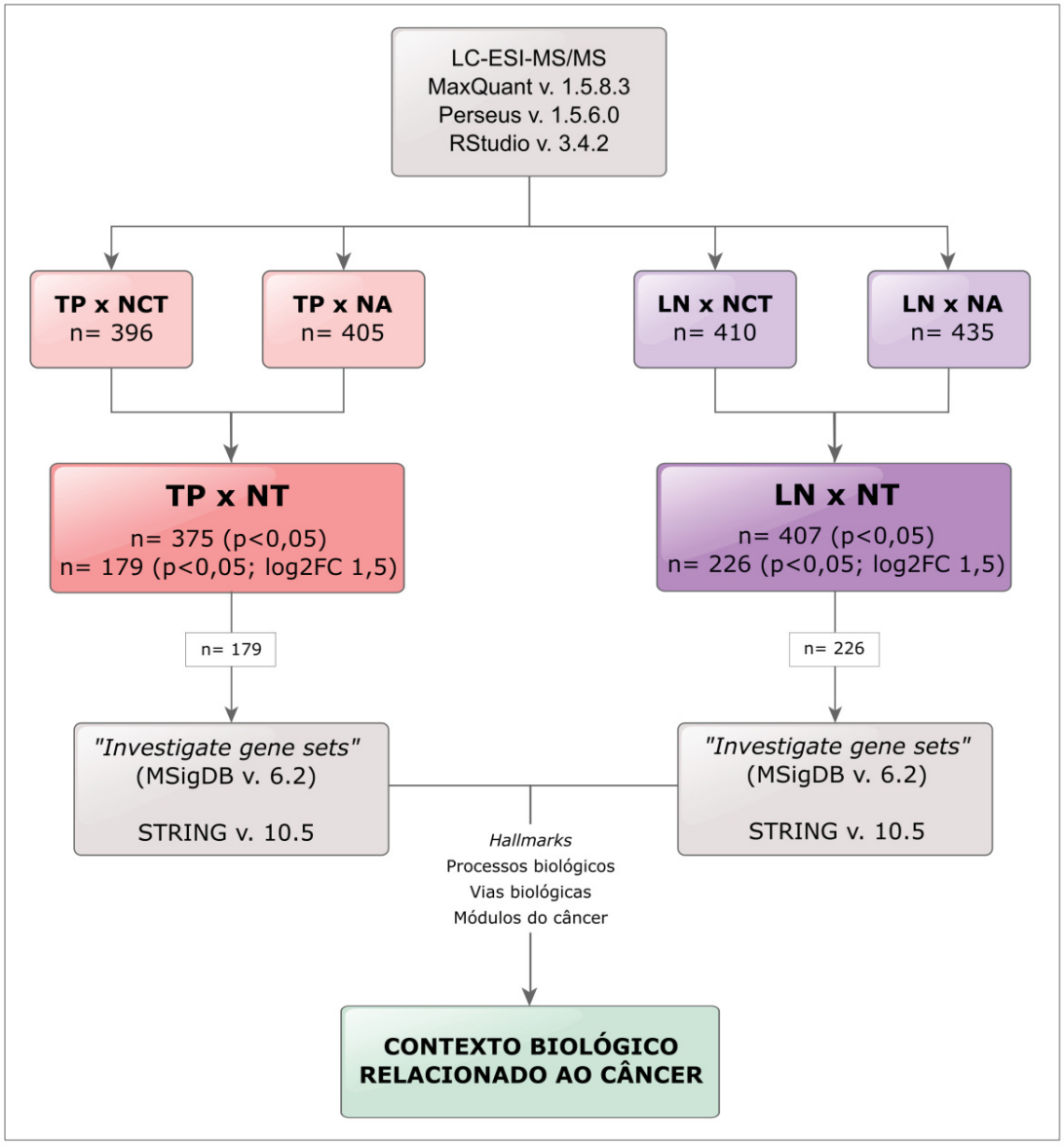

FONTE: O autor (2019).
NOTA: O conjunto de proteínas diferencialmente expresso é designado pela letra “n”.
LEGENDA: LC-ESI-MS/MS – cromatografia líquida acoplada à espectrometria de massa com ionização por *eletrospray*; v. – versão; TP – tumor primário de mama; NCT – tecido não tumoral contralateral; NA – tecido não tumoral adjacente; LN – linfonodo axilar metastático; NT – tecidos não tumorais; log2FC – *Fold Change* em logaritmo de base 2; MSigDB – *Molecular Signatures Database;* STRING - *Search Tool for the Retrieval of Interacting Genes/Proteins*.

FIGURA 2 – ANÁLISE DE *CLUSTERIZAÇÃO* HIERÁRQUICA DAS PROTEÍNAS SUPEREXPRESSAS E SUBEXPRESSAS NA COMPARAÇÃO TP x NT

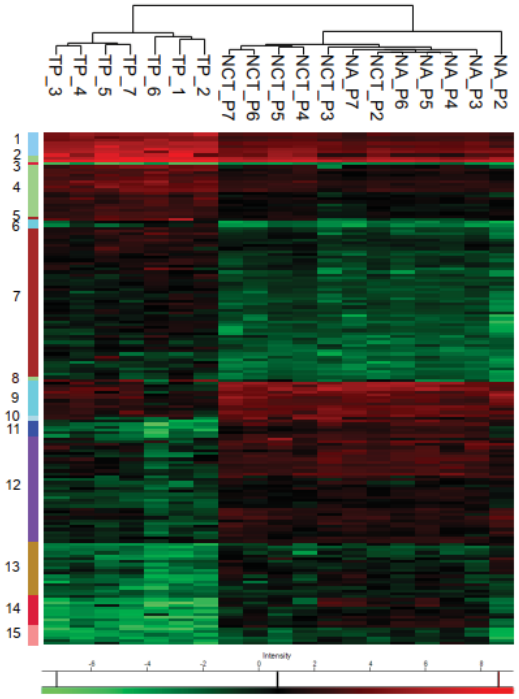

FONTE: O autor (2019).
NOTA: Os *clusters* obtidos estão indicados e enumerados na lateral esquerda do *heatmap.*
LEGENDA: TP – Tumor primário de mama, NCT – tecido mamário não tumoral contralateral, NA – tecido mamário não tumoral adjacente, P1-P7 – códigos das pacientes.

FIGURA 3 – PADRÃO DE EXPRESSÃO DOS PRINCIPAIS *CLUSTERS* DE PROTEÍNAS DIFERENCIALMENTE EXPRESSAS NA COMPARAÇÃO TP x NT

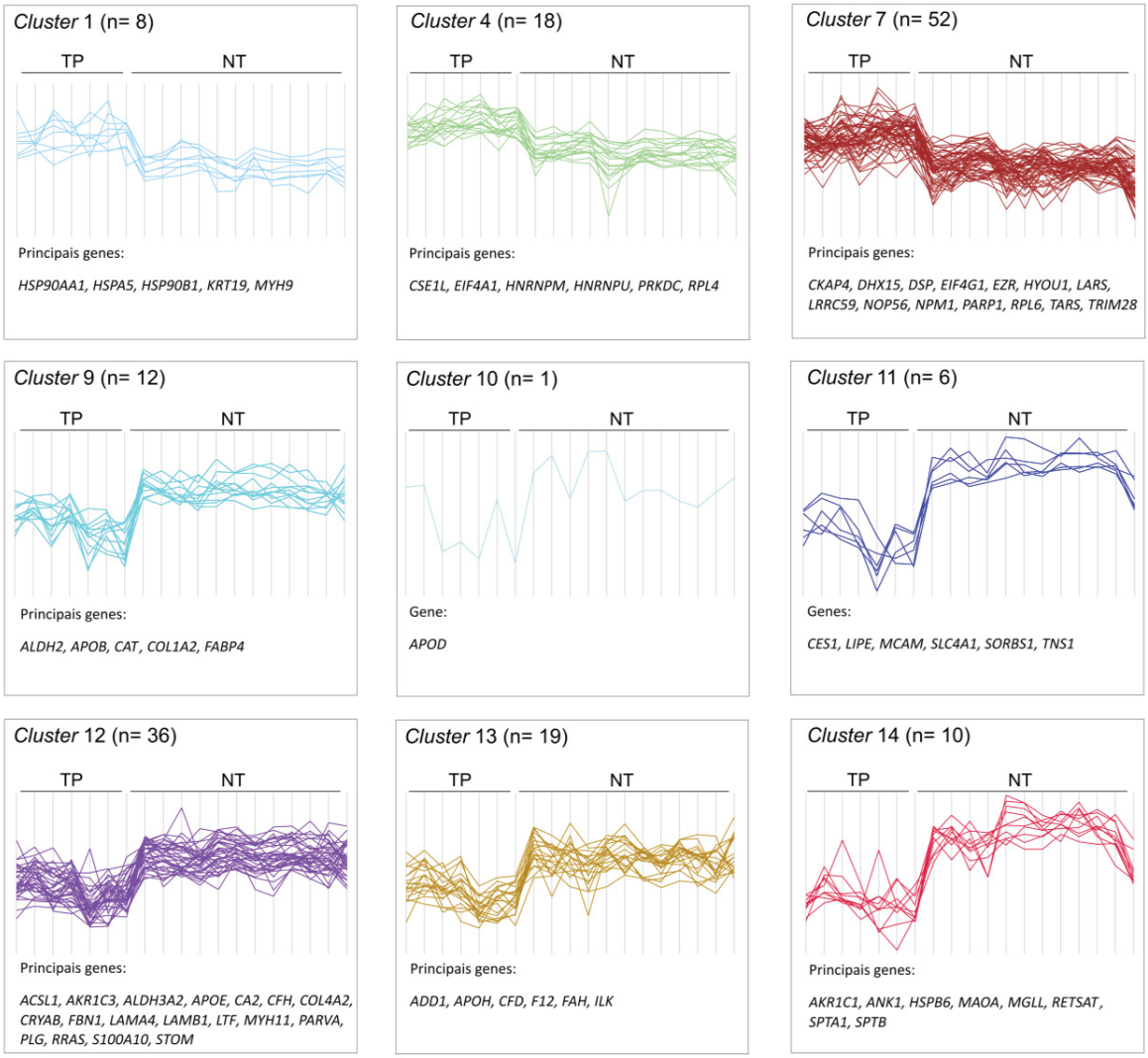

FONTE: O autor (2019).
NOTA: As principais proteínas dos *clusters* estão representadas abaixo de cada gráfico pela sigla de seus genes codificadores.
LEGENDA: TP – tumor primário de mama, NT – tecidos mamários não tumorais.

FIGURA 4 – REDE DE INTERAÇÕES PREDITAS ENTRE OS GENES QUE CODIFICAM AS PROTEÍNAS SUPEREXPRESSAS E SUBEXPRESSAS NA COMPARAÇÃO TP x NT

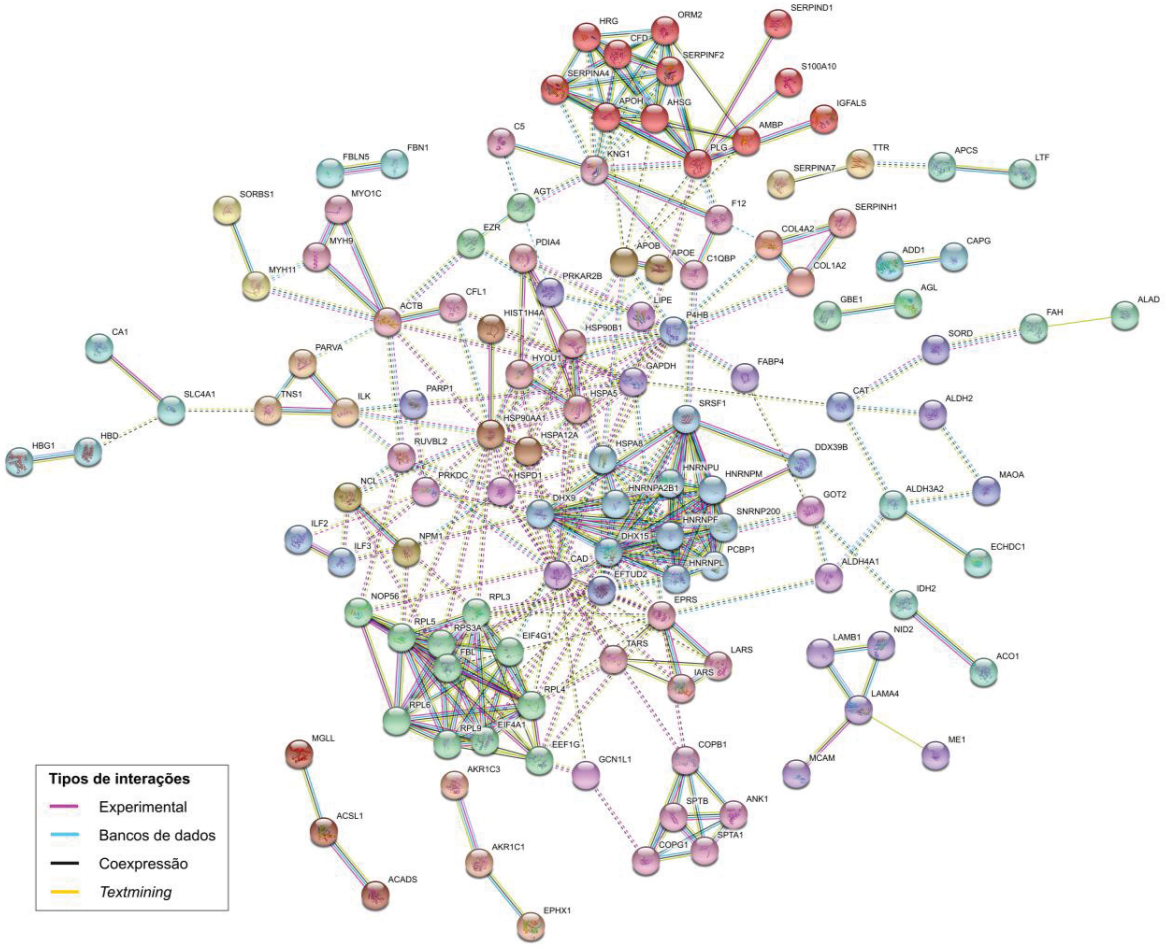

FONTE: O autor (2019).

NOTA: *Clusters* funcionais estão indicados em cores distintas e a inter-relação entre *clusters* distintos é representada por linhas pontilhadas.

FIGURA 5 – ANÁLISE DE *CLUSTERIZAÇÃO* HIERÁRQUICA DAS PROTEÍNAS DIFERENCIALMENTE EXPRESSAS NA COMPARAÇÃO LN x NT

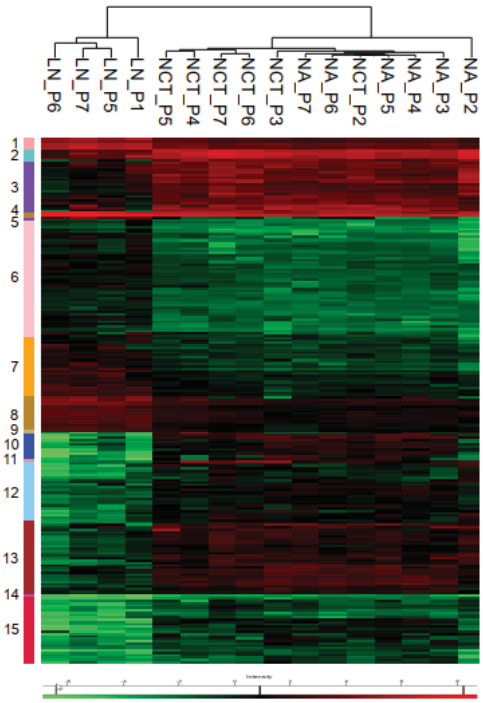

FONTE: O autor (2019).
NOTA: Os *clusters* obtidos estão indicados e enumerados na lateral esquerda do *heatmap.*
LEGENDA: LN – Linfonodo axilar metastático, NCT – tecido mamário não tumoral contralateral, NA – tecido mamário não tumoral adjacente, P1-P7 – códigos das pacientes.

FIGURA 6 – PADRÃO DE EXPRESSÃO DOS PRINCIPAIS *CLUSTERS* DE PROTEÍNAS DIFERENCIALMENTE EXPRESSAS NA COMPARAÇÃO LN x NT

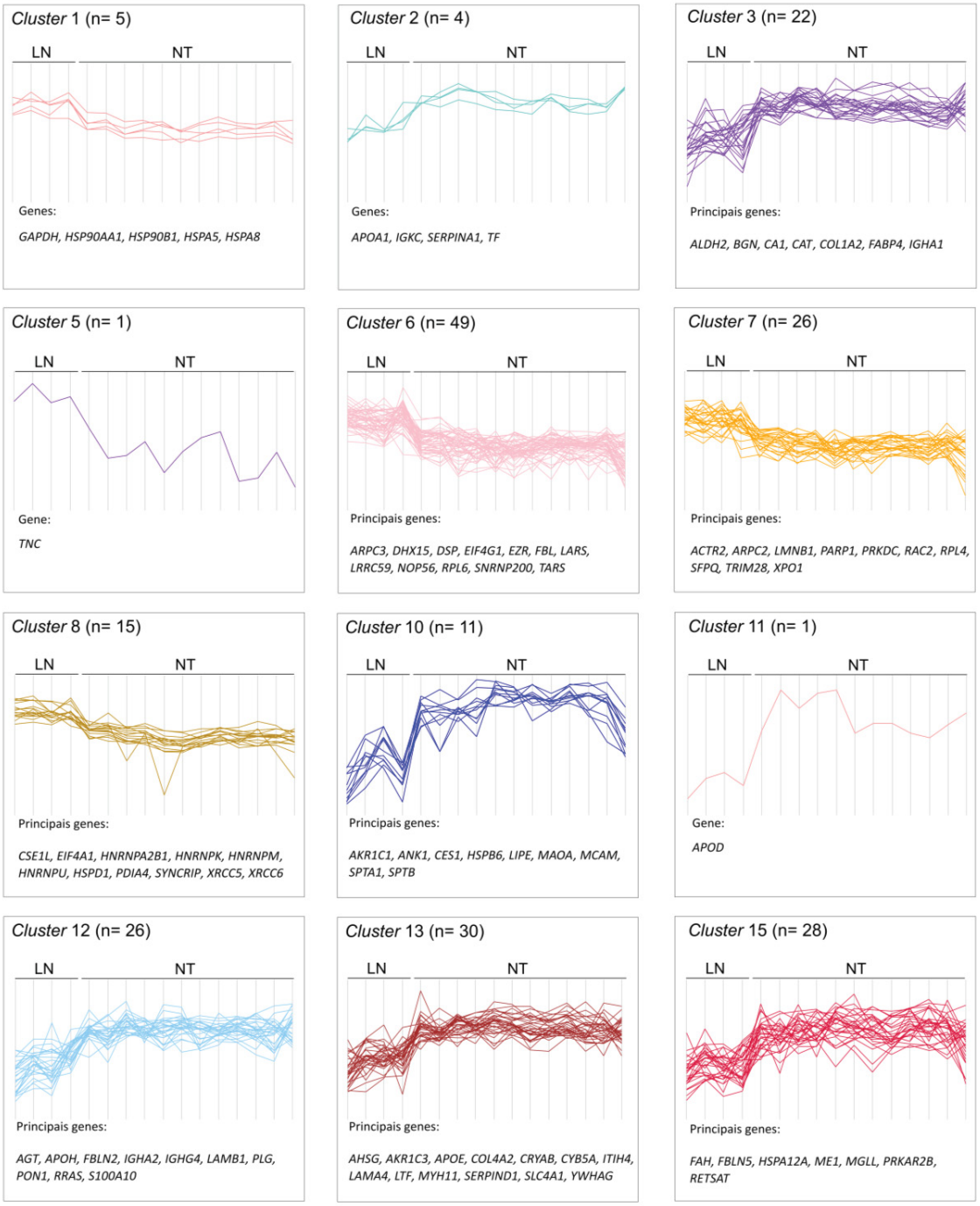

FONTE: O autor (2019).
NOTA: As principais proteínas dos clusters estão representadas abaixo de cada gráfico pela sigla de seus genes codificadores.
LEGENDA: LN – Linfonodo axilar metastático, NT – tecidos mamários não tumorais.

FIGURA 7 – REDE DE INTERAÇÕES PREDITAS ENTRE OS GENES QUE CODIFICAM AS PROTEÍNAS SUPEREXPRESSAS E SUBEXPRESSAS NA COMPARAÇÃO LN x NT

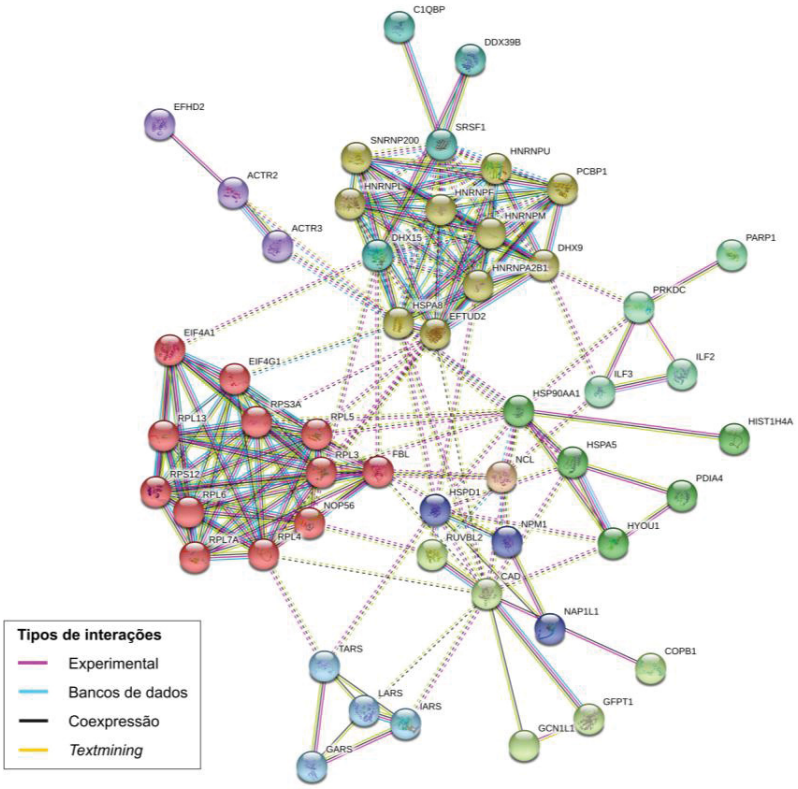

FONTE: O autor (2019).
NOTA: *Clusters* funcionais estão indicados em cores distintas e a inter-relação entre *clusters* distintos é representada por linhas pontilhadas.

Tabelas

TABELA 1 – PROTEÍNAS DIFERENCIALMENTE EXPRESSAS COM OS MAIORES E MENORES VALORES DE *FOLD CHANGE* NA COMPARAÇÃO TP x NT

Nome da proteína	Sigla do gene	FC TPxNCT	FC TPxNA	q-valor ANOVA
Tenascina	*TNC*	3,377 ↑	4,768 ↑	3,94E-04
Exportina-2	*CSE1L*	3,324 ↑	3,439 ↑	4,74E-04
Queratina do citoesqueleto 18, tipo II	*KRT18*	3,227 ↑	4,706 ↑	1,40E-03
Helicase ribonucleoproteína pequena nuclear U5 de 200 kDa	*SNRNP200*	3,207 ↑	3,437 ↑	4,56E-06
Proteína 59 contendo repetições ricas em leucina	*LRRC59*	3,042 ↑	3,218 ↑	4,39E-05
Desmoplaquina	*DSP*	2,956 ↑	4,299 ↑	1,64E-04
Poli [ADP-ribose] polimerase 1	*PARP1*	2,917 ↑	3,330 ↑	1,39E-07
RNA helicase DHX15 dependente de ATP, fator de splicing de pré-mRNA	*DHX15*	2,880 ↑	3,176 ↑	7,85E-06
Fator intermediário de transcrição 1-beta	*TRIM28*	2,830 ↑	3,482 ↑	1,53E-06
Ezrina	*EZR*	2,823 ↑	3,183 ↑	9,40E-08
Proteína L6 ribossômica 60S	*RPL6*	2,661 ↑	3,269 ↑	1,32E-07
Treonina - tRNA ligase, citoplasmática	*TARS*	2,554 ↑	3,186 ↑	3,18E-05
Leucina - tRNA ligase, citoplasmática	*LARS*	2,450 ↑	2,517 ↑	1,72E-05
Queratina do citoesqueleto 19, tipo I	*KRT19*	2,403 ↑	4,084 ↑	2,19E-03
Proteína 4 associada ao citoesqueleto	*CKAP4*	2,383 ↑	2,462 ↑	1,95E-05
Carboxilesterase do fígado 1	*CES1*	-5,770 ↓	-6,003 ↓	2,04E-06
Cadeia alfa da espectrina eritrocítica 1	*SPTA1*	-5,672 ↓	-5,897 ↓	5,03E-05
Família Aldo-keto redutase 1, membro C1	*AKR1C1*	-5,656 ↓	-5,627 ↓	2,53E-07
Proteína *heat shock* beta-6	*HSPB6*	-5,631 ↓	-6,477 ↓	1,63E-07
Lipase sensível a hormônios	*LIPE*	-5,233 ↓	-5,088 ↓	2,79E-07
Anquirina-1	*ANK1*	-5,049 ↓	-4,948 ↓	1,86E-04
Proteína de transporte de ânion banda 3	*SLC4A1*	-4,983 ↓	-4,874 ↓	1,47E-04
Cadeia beta da espectrina eritrocítica	*SPTB*	-4,883 ↓	-4,693 ↓	5,93E-05
Sorbina e proteína 1 contendo o domínio SH3	*SORBS1*	-4,743 ↓	-5,069 ↓	1,36E-07
Amina oxidase A [contendo flavina]	*MAOA*	-4,723 ↓	-5,232 ↓	4,19E-06
Glicoproteína de superfície celular MUC18	*MCAM*	-4,536 ↓	-4,593 ↓	1,24E-06
Proteína de ligação a ácidos graxos, adipócitos	*FABP4*	-4,430 ↓	-4,391 ↓	6,36E-06
Proteína 12A *heat shock* de 70 kDa	*HSPA12A*	-4,400 ↓	-4,713 ↓	1,32E-07
Lipase monoglicerídeo	*MGLL*	-4,327 ↓	-4,243 ↓	4,86E-07
Apolipoproteína D	*APOD*	-4,153 ↓	-2,337 ↓	1,38E-04

FONTE: O autor (2019).
NOTA: Proteínas ordenadas conforme os maiores (↑) e menores (↓) valores de *fold change*. O ajuste do valor de p foi realizado pelo método de Benjamini-Hochberg (q-valor).
LEGENDA: FC – *Fold change,* TP – tumor primário de mama, NCT – tecido mamário não tumoral contralateral, NA – tecido mamário não tumoral adjacente.

TABELA 2 – PRINCIPAIS *HALLMARKS* IDENTIFICADOS PARA OS GENES QUE CODIFICAM AS PROTEÍNAS SUPEREXPRESSAS E SUBEXPRESSAS NA COMPARAÇÃO TP x NT

Hallmark	**q-valor (FDR)**	**Sigla dos genes**
Alvos de MYC	6,78E-21	*C1QBP, CAD, DHX15, EIF4A1, EPRS, FBL, GOT2, HDGF, HNRNPA2B1, HNRNPU, HSPD1, IARS, ILF2, NOP56, NPM1, PCBP1, RPL6, RUVBL2, SRSF1, TRIM28*
Metabolismo de xenobióticos	9,16E-13	*AKR1C3, ALDH2, APOE, BLVRB, CA2, CAT, CES1, EPHX1, FAH, HRG, MAOA, PLG, RETSAT*
Metabolismo de ácidos graxos	1,38E-11	*ACADS, ACSL1, ALAD, ALDH3A2, CA2, EPHX1, HSP90AA1, MAOA, ME1, MGLL, RETSAT, S100A10*
Sinalização MTORC1	2,81E-09	*CACYBP, EPRS, GAPDH, GBE1, HSP90B1, HSPA5, HSPD1, ME1, NAMPT, SERPINH1, SORD*
Resposta ao desdobramento de proteínas	3,82E-09	*EIF4A1, EIF4G1, HSP90B1, HSPA5, HYOU1, IARS, NOP56, NPM1, TARS*
Transição epitelial-mesenquimal	5,29E-06	*CAPG, COL1A2, COL4A2, FBLN5, FBN1, NID2, SERPINH1, TNC*
Resposta tardia ao estrogênio	5,29E-06	*ALDH3A2, BLVRB, CA2, IDH2, KRT19, LTF, PRKAR2B, SORD*
Peroxissomo	1,34E-05	*ACSL1, CAT, IDH2, RETSAT, TTR*
Complemento	5,06E-05	*CA2, CFH, COL4A2, HSPA5, LTF, ME1, PLG*
Coagulação	5,85E-05	*CFD, CFH, F12, FBN1, HRG, PLG*
Junção apical	3,40E-04	*ACTB, CALB2, FBN1, MYH9, PARVA, RRAS*
Alvos E2F	3,40E-04	*CSE1L, ILF3, IPO7, NOP56, PRKDC, SRSF1*
Hipóxia	3,40E-04	*GAPDH, GBE1, HDLBP, HSPA5, MYH9*
Sinalização IL2-STAT5	3,40E-04	*CA2, CAPG, CKAP4, FAH, ITGA6, MYO1C*
Ponto de checagem G2M	2,35E-03	*HNRNPU, HSPA8, ILF3, NCL, SRSF1*
Glicólise	2,35E-03	*AGL, GOT2, HDLBP, HSPA5, ME1*
Via de p53	2,35E-03	*EPHX1, RETSAT, S100A10, STOM*
Resposta precoce ao estrogênio	1,39E-02	*BLVRB, CALB2, KRT18, KRT19*
Angiogênese	1,45E-02	*APOH*
Sinalização de Hedgehog	1,45E-02	*MYH9, PLG*
Via de espécies reativas de oxigênio	2,54E-02	*CAT*
Apoptose	3,91E-02	*ADD1, KRT18, RETSAT*

FONTE: O autor (2019).
LEGENDA: FDR – Taxa de falso positivo (*false discovery rate*).

TABELA 3 – PRINCIPAIS PROCESSOS BIOLÓGICOS IDENTIFICADOS PARA AS PROTEÍNAS SUPEREXPRESSAS E SUBEXPRESSAS NA COMPARAÇÃO TP x NT

Processo Biológico (GO)	**q-valor (FDR)**	**Sigla dos genes**
Regulação da resposta ao estresse	4,44E-16	*AGT, AHSG, AMBP, APCS, APOD, APOE, APOH, C1QBP, C4BPA, C5, CFH, CRYAB, DDX39B, EZR, F12, ABP4, FBLN5, GAPDH, HRG, HSP90AA1, HSP90B1, HSPA5, HSPA8, HSPD1, HYOU1, KNG1, LTF, MGLL, NPM1, P4HB, PGLYRP2, PLG, PRKDC, SERPINF2, STOM, TRIM28*
Processo metabólico de mRNA	9,10E-13	*C1QBP, DDX39B, DHX9, EFTUD2, EIF4A1, EIF4G1, HNRNPA2B1, HNRNPF, HNRNPL, HNRNPM, HNRNPU, HSPA8, RPL6, PCBP1, RPL3, RPL4, RPL5, RPL9, RPS3A, DHX15, SNRNP200, SRSF1*
Regulação negativa* do processo metabólico de proteínas	3,95E-12	*AGT, AHSG, AMBP, APCS, APOD, APOE, C4BPA, C5, CRYAB, EPRS, EZR, FABP4, GAPDH, HNRNPA2B1, HRG, ILF3, ILK, KNG1, NPM1, PON1, PRKAR2B, PRKDC, SERPINA4, SERPINA7, SERPIND1, SERPINF2, SERPINH1*
Processo do sistema imunológico	7,57E-12	*ACTB, ADD1, APCS, APOB, C1QBP, C4BPA, C5, CFD, CFH, COL1A2, EPRS, F12, GAPDH, HSP90AA1, HSP90B1, HSPD1, IGHA2, IGHG2, IGHG3, IGHG4, IGKV3-20, ILF2, ILF3, IPO7, ITGA6, LTF, MYH9, MYO1C, PARP1, PGLYRP2, PRKDC, RAB6A, RRAS, SPTA1, TRIM28*
Regulação pós-transcricional da expressão gênica	2,63E-10	*ACO1, ANP32A, C1QBP, DDX39B, DHX9, EIF4A1, EIF4G1, EPRS, GAPDH, HNRNPA2B1, HNRNPU, HSPA8, IARS, ILF3, LARS, LRPPRC, NPM1*
Resposta à injúria	9,39E-10	*ACTB, APOD, APOH, C1QBP, COL1A2, DSP, F12, HBD, HBG1, HRG, ILK, KNG1, MCAM, MYH9, PLG, PRKAR2B, SERPIND1, TNC*
Regulação da resposta inflamatória	1,03E-08	*AGT, AHSG, APCS, APOD, APOE, C1QBP, C4BPA, C5, CFH, F12, FABP4, MGLL, PGLYRP2*
Regulação da morte celular	2,96E-08	*AGT, AKR1C3, APOE, APOH, C1QBP, CAT, CFL1, CRYAB, FAM129B, HRG, HSP90B1, HSPA5, HSPD1, HYOU1, ILK, ITGA6, KNG1, KRT18, LTF, NCL, NPM1, P4HB, PRKDC, RPS3A*
Processamento de mRNA	7,47E-08	*C1QBP, DDX39B, DHX15, DHX9, EFTUD2, HNRNPA2B1, HNRNPF, HNRNPL, HNRNPM, HNRNPU, HSPA8, PCBP1, SNRNP200, SRSF1*
Processo de oxidação e redução	1,00E-07	*ACADS, ACO1, AGL, AKR1C1, AKR1C3, ALDH2, ALDH3A2, ALDH4A1, ASPH, BLVRB, CAT, GAPDH, GBE1, IDH2, MAOA, ME1, RETSAT, SORD*

FONTE: O autor (2019).
NOTA: * Regulação negativa se refere a qualquer processo capaz de cessar, prevenir ou reduzir a frequência, taxa ou extensão das reações químicas e vias envolvendo uma proteína.
LEGENDA: FDR – Taxa de falso positivo (*false discovery rate*).

TABELA 4 – PRINCIPAIS VIAS BIOLÓGICAS IDENTIFICADAS PARA AS PROTEÍNAS SUPEREXPRESSAS E SUBEXPRESSAS NA COMPARAÇÃO TP x NT

Vias biológicas	q-valor FDR	Sigla dos genes
KEGG		
Cascatas de coagulação e do complemento	1,25E-09	*C4BPA, C5, CFD, CFH, F12, KNG1, PLG, SERPIND1, SERPINF2*
Spliceossomo	1,73E-07	*DDX39B, DHX15, EFTUD2, HNRNPM, HNRNPU, HSPA8, PCBP1, SNRNP200, SRSF1*
Adesão focal	4,09E-07	*ACTB, COL1A2, COL4A2, COL6A6, ILK, ITGA6, LAMA4, LAMB1, PARVA, TNC*
Interação de receptores ECM	1,76E-06	*COL1A2, COL4A2, COL6A6, ITGA6, LAMA4, LAMB1, TNC*
Metabolismo de ácidos graxos	3,86E-04	*ACADS, ACSL1, ALDH2, ALDH3A2*
Regulação do citoesqueleto de actina	2,61E-03	*ACTB, CFL1, EZR, ITGA6, MYH9, RRAS*
Vias em câncer	1,25E-02	*COL4A2, HSP90AA1, HSP90B1, ITGA6, LAMA4, LAMB1*
Junção *tight*	1,25E-02	*ACTB, MYH11, MYH9, RRAS*
Metabolismo de xenobióticos pelo citocromo p450	1,61E-02	*AKR1C1, AKR1C3, EPHX1*
Reactome		
Splicing de mRNA	1,30E-08	*DHX9, EFTUD2, HNRNPA2B1, HNRNPF, HNRNPL, HNRNPM, HNRNPU, PCBP1, SNRNP200, SRSF1*
Processamento de mRNA	1,30E-07	*DHX9, EFTUD2, HNRNPA2B1, HNRNPF, HNRNPL, HNRNPM, HNRNPU, PCBP1, SNRNP200, SRSF1*
Resposta ao Ca^{2+} citosólico plaquetário elevado	4,78E-06	*CFD, CFL1, HRG, HSPA5, KNG1, PLG, SERPINF2*
Metabolismo de mRNA	1,15E-05	*EIF4A1, EIF4G1, HSPA8, RPL3, RPL4, RPL5, RPL6, RPL9, RPS3A*
Metabolismo de proteínas	3,99E-05	*ACTB, EEF1G, EIF4A1, EIF4G1, HSPD1, NOP56, RPL3, RPL4, RPL5, RPL6, RPL9, RPS3A*
Interações de semaforinas	2,21E-04	*CFL1, HSP90AA1, MYH11, MYH9, RRAS*
Interações de integrinas da superfície celular	4,14E-04	*COL1A2, COL4A2, FBN1, LAMB1, TNC*
Resposta ao desdobramento de proteínas	4,14E-04	*ADD1, HDGF, HSP90B1, HSPA5, HYOU1*
Interações L1CAM	5,26E-04	*ANK1, EZR, LAMB1, SPTA1, SPTB*
Organização da matriz extracelular	5,37E-04	*COL1A2, COL4A2, P4HB, PLG, SERPINH1*
Sinalização por PDGF	1,77E-02	*COL1A2, COL4A2, PLG, PRKAR2B*
Interações da matriz celular extracelular	1,77E-02	*ILK, PARVA*

FONTE: O autor (2019).
LEGENDA: FDR – Taxa de falso positivo (*false discovery rate*).

TABELA 5 – PRINCIPAIS MÓDULOS DO CÂNCER IDENTIFICADOS PARA AS PROTEÍNAS SUPEREXPRESSAS E SUBEXPRESSAS NA COMPARAÇÃO TP x NT

Número do módulo	Descrição do módulo	q-valor FDR	Sigla dos genes
84	Resposta imune (humoral) e inflamatória	1,29E-13	*ACSL1, APOD, APOE, CAPG, CES1, CFD, COL1A2, CRYAB, FABP4, IGHG3, ITGA6, KRT18, KRT19, LTF, MGLL, MYH11, NAMPT, ORM2, STOM, TYMP*
47	Matriz extracelular e colágenos	2,38E-07	*AKR1C1, CKAP4, COL1A2, COL4A2, CRYAB, FBN1, LAMB1, MCAM, SERPINH1, TNC*
357	Filamentos intermediários e queratinas	3,17E-07	*AKR1C1, AKR1C3, CA2, DSP, ITGA6, KRT19, MAOA*
117	Sinalização	3,17E-07	*AFM, AGT, APCS, APOB, APOD, APOH, CA1, CA2, F12, KNG1, LTF, PLG, PON1, SERPINA7, SERPIND1, SERPINF2*
33	Genes de resposta ao estresse/ imune	3,97E-07	*AKR1C3, ANK1, ASPH, CAPG, CFD, EFTUD2, FABP4, ITGA6, KRT18, MAOA, PAFAH1B3, SERPINA7*
355	Dobramento de proteínas	8,40E-07	*CRYAB, HSP90B1, HSPA5, HSPA8, HSPD1*
252	Fatores de transcrição e fatores nucleares	3,49E-06	*CSE1L, DHX9, DSP, HNRNPF, ILF2, ILF3, IPO7, PRKDC, SRSF1*
305	Metabolismo de ácidos graxos e CoA	6,26E-06	*ACO1, ALDH2, ALDH3A2, IDH2*
324	Ligação a íons de cálcio/ metal	6,96E-06	*ACSL1, CA2, CALB2, FBN1, LTF, S100A10*
183	*Splicing* de RNA	3,90E-05	*HNRNPA2B1, HNRNPF, HNRNPU, PCBP1, SRSF1*
438	Filamentos intermediários e microtúbulos	4,79E-05	*DSP, KRT19, LAMB1, MYH11, TNC*
247	Metabolismo de xenobióticos	8,51E-05	*AKR1C1, EPHX1, MGLL*
373	Oxirredutases	4,57E-04	*ALDH3A2, GOT2, MAOA*
130	Complemento	5,17E-04	*C4BPA, C5, CFH*
573	Reguladores do ciclo celular e transportadores de carboidratos	6,60E-04	*AMBP, HSP90B1, TNC*
64	Receptores de membrana	9,69E-04	*AGT, APOB, APOE, APOH, MCAM, NAMPT, SLC4A1, STOM, TNC*
524	Ligação ao citoesqueleto de actina	1,05E-03	*CFL1, MYH11, MYH9*
122	Moléculas de adesão	1,11E-03	*FBN1, LAMA4, LAMB1, MCAM, TNC*
195	*Clusters* de expressão de	1,31E-03	*EFTUD2, GC, HYOU1, MYO1C, TYMP*

Número do módulo	Descrição do módulo	q-valor FDR	Sigla dos genes
	câncer de mama		
131	Fatores da coagulação sanguínea	1,34E-03	*F12, PLG, SERPIND1*
124	Transcrição	2,41E-03	*HNRNPA2B1, HNRNPF, HNRNPL, HNRNPU*
244	Resposta a danos no DNA	3,49E-03	*HNRNPU, HSPA8, HSPD1, IARS, ILF2*

FONTE: O autor (2019).
LEGENDA: FDR – Taxa de falso positivo (*false discovery rate*).

TABELA 6 – PROTEÍNAS DIFERENCIALMENTE EXPRESSAS COM OS MAIORES E MENORES VALORES DE *FOLD CHANGE* NA COMPARAÇÃO LN x NT

Nome da proteína	Sigla do gene	FC LNxNCT	FC LNxNA	q-valor ANOVA
Tenascina	*TNC*	4,336 ↑	5,728 ↑	3,94E-04
Poli [ADP-ribose] polimerase 1	*PARP1*	3,782 ↑	4,194 ↑	1,39E-07
Helicase ribonucleoproteína pequena nuclear U5 de 200 kDa	*SNRNP200*	3,705 ↑	3,934 ↑	4,56E-06
Exportina-2	*CSE1L*	3,600 ↑	3,715 ↑	4,74E-04
RNA helicase DHX15 dependente de ATP, fator de *splicing* de pré-mRNA	*DHX15*	3,459 ↑	3,755 ↑	7,85E-06
Ezrina	*EZR*	3,329 ↑	3,688 ↑	9,40E-08
Proteína 59 contendo repetições ricas em leucina	*LRRC59*	2,972 ↑	3,149 ↑	4,39E-05
Fator intermediário de transcrição 1-beta	*TRIM28*	2,840 ↑	3,492 ↑	1,53E-06
Treonina-tRNA ligase, citoplasmática	*TARS*	2,835 ↑	3,467 ↑	3,18E-05
Proteína CAD	*CAD*	2,823 ↑	3,379 ↑	8,16E-04
Proteína L6 ribossômica 60S	*RPL6*	2,804 ↑	3,412 ↑	1,32E-07
Proteína nucleolar 56	*NOP56*	2,583 ↑	3,826 ↑	5,06E-05
Subunidade catalítica da proteína quinase dependente de DNA	*PRKDC*	2,549 ↑	3,104 ↑	1,26E-06
Proteína de ligação à calciciclina	*CACYBP*	2,506 ↑	2,408 ↑	1,13E-04
Leucina-tRNA ligase, citoplasmática	*LARS*	2,412 ↑	2,480 ↑	1,72E-05
Apolipoproteína D	*APOD*	-6,548 ↓	-4,731 ↓	1,38E-04
Família Aldo-keto redutase 1, membro C1	*AKR1C1*	-6,542 ↓	-6,513 ↓	2,53E-07
Lipase sensível a hormônios	*LIPE*	-6,534 ↓	-6,389 ↓	2,79E-07
Carboxilesterase do fígado 1	*CES1*	-6,177 ↓	-6,410 ↓	2,04E-06
Lipase monoglicerídeo	*MGLL*	-6,155 ↓	-6,071 ↓	4,86E-07
Sorbina e proteína 1 contendo o domínio SH3	*SORBS1*	-5,952 ↓	-6,278 ↓	1,36E-07
Proteína de ligação a ácidos graxos, adipócitos	*FABP4*	-5,747 ↓	-5,707 ↓	6,36E-06
Cadeia de colágeno alfa-6 (VI)	*COL6A6*	-5,697 ↓	-4,293 ↓	1,01E-02
Proteína 12A *heat shock* de 70 kDa	*HSPA12A*	-5,150 ↓	-5,463 ↓	1,32E-07
Cadeia beta da espectrina eritrocítica	*SPTB*	-5,106 ↓	-4,916 ↓	5,93E-05
Proteína *heat shock* beta-6	*HSPB6*	-4,873 ↓	-5,720 ↓	1,63E-07
Cadeia de colágeno alfa-2 (I)	*COL1A2*	-4,744 ↓	-4,376 ↓	2,30E-04
Cadeia alfa da espectrina eritrocítica 1	*SPTA1*	-4,721 ↓	-4,945 ↓	5,03E-05
Glicoproteína de superfície celular MUC18	*MCAM*	-4,561 ↓	-4,619 ↓	1,24E-06
Fumarilacetoacetase	*FAH*	-4,558 ↓	-4,567 ↓	4,37E-05

FONTE: O autor (2019).
NOTA: Proteínas ordenadas conforme os maiores (↑) e menores (↓) valores de FC. O ajuste do valor de p foi realizado pelo método de Benjamini-Hochberg (q-valor).
LEGENDA: FC – *Fold change,* LN – linfonodo axilar metastático, NCT – tecido mamário não tumoral contralateral, NA – tecido mamário não tumoral adjacente.

TABELA 7 – PRINCIPAIS *HALLMARKS* IDENTIFICADOS PARA AS PROTEÍNAS SUPEREXPRESSAS E SUBEXPRESSAS NA COMPARAÇÃO LN x NT

Hallmark	**q-valor FDR**	**Sigla dos genes**
Alvos de MYC	9,41E-31	*C1QBP, CAD, DHX15, EIF4A1, EIF4G2, EPRS, FBL, HDGF, HNRNPA2B1, HNRNPU, HSPD1, IARS, ILF2, IMPDH2, NAP1L1, NOP56, NPM1, PCBP1, PRPS2, RPL6, RPS3, RUVBL2, SNRPD3, SRSF1, SYNCRIP, TRIM28, XPO1, XRCC6*
Coagulação	8,27E-21	*APOA1, C8B, C9, CFB, CFD, CFH, CFI, CSRP1, F12, F2, FBN1, FGA, HRG, ITIH1, PLG, SERPINA1, SERPINC1, SERPING1, TF*
Metabolismo de xenobióticos	2,79E-15	*AKR1C3, ALDH2, APOE, BLVRB, CA2, CAT, CES1, CFB, CYB5A, FAH, HRG, ITIH1, ITIH4, MAOA, PLG, RETSAT*
Complemento	4,53E-14	*C1QC, C9, CA2, CFB, CFH, COL4A2, CSRP1, F2, HSPA5, ITIH1, LTF, ME1, PLG, SERPINA1, SERPINC1, SERPING1*
Resposta ao desdobramento de proteínas	2,07E-09	*EIF4A1, EIF4G1, FUS, HSP90B1, HSPA5, HYOU1, IARS, NOP56, NPM1, TARS*
Sinalização MTORC1	2,28E-09	*ACLY, ACTR2, ACTR3, CACYBP, EPRS, GAPDH, GBE1, HSP90B1, HSPA5, HSPD1, ME1, PGM1*
Alvos E2F	2,78E-08	*CSE1L, ILF3, IPO7, LMNB1, NAP1L1, NOP56, PRKDC, SRSF1, SYNCRIP, XPO1, XRCC6*
Metabolismo de ácidos graxos	3,30E-08	*ACADS, ACSL1, ALAD, CA2, HSP90AA1, MAOA, ME1, MGLL, RETSAT, S100A10*
Transição epitelial-mesenquimal	2,39E-07	*BGN, CAPG, COL1A2, COL4A2, FBLN2, FBLN5, FBN1, NID2, TNC, TPM1*
Ponto de checagem G2M	2,39E-07	*HNRNPU, HSPA8, ILF3, LMNB1, NCL, SFPQ SRSF1, SYNCRIP, UPF1, XPO1*
Hipóxia	2,32E-05	*BGN, GAPDH, GBE1, HDLBP, HSPA5, NAGK, PGM1*
Junção apical	1,80E-04	*ACTB, ARPC2, CALB2, FBN1, PARVA, RAC2, RRAS*
Resposta tardia ao estrogênio	1,80E-04	*BLVRB, CA2, LTF, PRKAR2B, SERPINA1, SERPINA3, SERPINA5*
Peroxissomo	4,54E-04	*ACSL1, CAT, RETSAT, TTR*
Glicólise	1,12E-03	*CYB5A, GFPT1, HDLBP, HSPA5, ME1, ME2*
Sinalização IL2-STAT5	1,12E-03	*CA2, CAPG, FAH, ITGA6, MYO1C, SERPINC1*
Via de p53	1,12E-03	*AK1, RETSAT, RPS12, S100A10, STOM*

Hallmark	**q-valor FDR**	**Sigla dos genes**
Angiogênese	1,65E-03	*APOH, SERPINA5*
Sinalização PI3K-AKT-MTOR	3,89E-03	*ACTR2, ACTR3, ARPC3, HSP90B1*
Sinalização KRAS	6,19E-03	*APOD, CA2, CFB, CFH, SERPINA3*
Via de espécies reativas de oxigênio	4,13E-02	*CAT*

FONTE: O autor (2019).
LEGENDA: FDR – Taxa de falso positivo (*false discovery rate*).

TABELA 8 – PRINCIPAIS PROCESSOS BIOLÓGICOS IDENTIFICADOS PARA AS PROTEÍNAS SUPEREXPRESSAS E SUBEXPRESSAS NA COMPARAÇÃO LN x NT

Processo biológico (GO)	**q-valor FDR**	**Sigla dos genes**
Processo metabólico de mRNA	3,20E-26	*C1QBP, DDX39B, DDX6, DHX15, DHX9, EFTUD2, EIF4A1, EIF4G1, FUS, HNRNPA2B1, HNRNPF, HNRNPH1, HNRNPK, HNRNPL, HNRNPM, HNRNPU, HSPA8, PCBP1, RPL10, RPL13, RPL24, RPL3, RPL4, RPL5, RPL6, RPL7A, RPS12, RPS17, RPS3, RPS3A, RPSA, SFPQ, SNRNP200, SNRPD3, SRSF1, SYNCRIP, UPF1*
Regulação da resposta ao estresse	7,97E-26	*AGT, AHSG, AMBP, APCS, APOA1, APOD, APOE, APOH, C1QBP, C4B, C4BPA, C5, C6, C8B, C9, CFB, CFH, CFI, CRYAB, DDX39B, EZR, F12, F2, FABP4, FBLN5, FGA, GAPDH, HNRNPK, HP, HPX, HRG, HSP90AA1, HSP90B1, HSPA5, HSPA8, HSPD1, HYOU1, KNG1, LTF, MGLL, NPM1, PGLYRP2, PLG, PRKDC, RPS3, SERPINC1, SERPINF2, SERPING1, SFPQ, STOM, TRIM28*
Processo do sistema imunológico	2,93E-25	*ACTB, ACTR2, ACTR3, APCS, APOB, ARPC2, ARPC3, C1QBP, C1QC, C4B, C4BPA, C5, C6, C8B, C9, CFB, CFD, CFH, CFI, COL1A2, CTSG, EPRS, F12, F2, FGA, GAPDH, HNRNPK, HP, HSP90AA1, HSP90B1, HSPD1, IGHA1, IGHA2, IGHG2, IGHG3, IGHG4, IGKC, IGKV3-20, ILF2, ILF3, IMPDH2, IPO7, ITGA1, ITGA6, LTF, MYO1C, PARP1, PGLYRP2, PRKDC, RAB6A, RPS17, RRAS, SERPING1, SPTA1, SYNCRIP, TRIM28, XRCC5*
Regulação negativa* do processo metabólico de proteínas	7,33E-23	*AGT, AHSG, AMBP, APCS, APOD, APOE, BGN, C4B, C4BPA, C5, CRYAB, EPRS, EZR, F2, FABP4, FGA, GAPDH, HNRNPA2B1, HRG, ILF3, ILK, ITIH1, ITIH2, ITIH4, KNG1, NPM1, PON1, PRKAR2B, PRKDC, RPS3, SERPINA1, SERPINA3, SERPINA4, SERPINA5, SERPINA7, SERPINC1, SERPIND1, SERPINF2, SERPING1, SYNCRIP, UPF1, YWHAG*
Resposta à injúria	7,63E-18	*ACTB, APOA1, APOD, APOH, C1QBP, COL1A2, CSRP1, DSP, F12, F2, FGA, GNA11, HBD, HBG1, HRG, ILK, KNG1, MCAM, PLG, PRKAR2B, RAC2, SERPINA1, SERPINA5, SERPINC1, SERPIND1, SERPING1, TNC, TPM1*
Regulação da resposta inflamatória	1,33E-17	*AGT, AHSG, APCS, APOA1, APOD, APOE, C1QBP, C4B, C4BPA, C5, C6, C8B, C9, CFB, CFH, CFI, F12, FABP4, MGLL, PGLYRP2, SERPINC1, SERPING1*
Resposta de fase aguda	1,59E-16	*AHSG, APCS, F2, FGA, HNRNPK, HP, ITIH4, ORM1, ORM2, SERPINA1, SERPINA3, SERPINF2*
Regulação pós-transcricional da expressão gênica	4,75E-15	*ACO1, ANP32A, C1QBP, DDX39B, DDX6, DHX9, EIF4A1, EIF4G1, EIF4G2, EPRS, GAPDH, HNRNPA2B1, HNRNPU, HSPA8, IARS, ILF3, LARS, LRPPRC, NPM1, RPS3, SYNCRIP, UPF1, XPO1*

Processo biológico (GO)	q-valor FDR	Sigla dos genes
Regulação da resposta de defesa	6,34E-14	*AGT, AHSG, APCS, APOA1, APOD, APOE, C1QBP, C4B, C4BPA, C5, C6, C8B, C9, CFB, CFH, CFI, F12, FABP4, HPX, HSP90B1, HSPD1, LTF, MGLL, PGLYRP2, SERPINC1, SERPING1, STOM*

FONTE: O autor (2019).
NOTA: * Regulação negativa se refere a qualquer processo capaz de cessar, prevenir ou reduzir a frequência, taxa ou extensão das reações químicas e vias envolvendo uma proteína.
legenda: fdr – taxa de falso positivo (*false discovery rate*).

TABELA 9 – PRINCIPAIS VIAS BIOLÓGICAS IDENTIFICADAS PARA AS PROTEÍNAS SUPEREXPRESSAS E SUBEXPRESSAS NA COMPARAÇÃO LN x NT

Vias biológicas	q-valor FDR	Sigla dos genes
KEGG		
Cascatas de coagulação e do complemento	4,23E-32	*C1QC, C4B, C4BPA, C5, C6, C8B, C9, CFB, CFD, CFH, CFI, F12, F2, FGA, KNG1, PLG, SERPINA1, SERPINA5, SERPINC1, SERPIND1, SERPINF2, SERPING1*
Spliceossomo	2,64E-09	*DDX39B, DHX15, EFTUD2, HNRNPK, HNRNPM, HNRNPU, HSPA8, PCBP1, SNRNP200, SNRPD3, SRSF1*
Adesão focal	1,80E-08	*ACTB, COL1A2, COL4A2, COL6A6, ILK, ITGA1, ITGA6, LAMA4, LAMB1, PARVA, RAC2, TNC*
Interação de receptores ECM	3,32E-07	*COL1A2, COL4A2, COL6A6, ITGA1, ITGA6, LAMA4, LAMB1, TNC*
Regulação do citoesqueleto de actina	2,45E-05	*ACTB, ARPC2, ARPC3, EZR, F2, ITGA1, ITGA6, RAC2, RRAS*
União de extremidades não homólogas (NHEJ)	5,72E-04	*PRKDC, XRCC5, XRCC6*
Metabolismo de ácidos graxos	9,64E-03	*ACADS, ACSL1, ALDH2*
Vias em câncer	9,72E-03	*COL4A2, HSP90AA1, HSP90B1, ITGA6, LAMA4, LAMB1, RAC2*
Metabolismo de drogas – outras enzimas	1,43E-02	*CES1, IMPDH2, TYMP*
Junções aderentes	3,58E-02	*ACTB, RAC2, SORBS1*
Reactome		
Metabolismo de mRNA	6,62E-14	*ANP32A, DDX6, EIF4A1, EIF4G1, HSPA8, RPL10, RPL13, RPL24, RPL3, RPL4, RPL5, RPL6, RPL7A, RPS12, RPS17, RPS3, RPS3A, RPSA, XPO1*
Splicing de RNA	6,62E-14	*DHX9, EFTUD2, FUS, HNRNPA2B1, HNRNPF, HNRNPH1, HNRNPK, HNRNPL, HNRNPM, HNRNPU, PCBP1, SNRNP200, SNRPD3, SRSF1*
Processamento de mRNA	5,69E-12	*DHX9, EFTUD2, FUS, HNRNPA2B1, HNRNPF, HNRNPH1, HNRNPK, HNRNPL, HNRNPM, HNRNPU, PCBP1, SNRNP200, SNRPD3, SRSF1*
Resposta ao Ca2 citosólico plaquetário elevado	3,63E-11	*APOA1, CFD, FGA, HRG, HSPA5, KNG1, PLG, SERPINA1, SERPINF2, SERPING1, TF*
Metabolismo de proteínas	5,60E-10	*ACTB, EIF4A1, EIF4G1, F2, HSPD1, NOP56, RPL10, RPL13, RPL24, RPL3, RPL4, RPL5, RPL6, RPL7A, RPS12, RPS17, RPS3, RPS3A, RPSA*

Vias biológicas	q-valor FDR	Sigla dos genes
Interações de integrinas da superfície celular	3,45E-06	*COL1A2, COL4A2, FBN1, FGA, ITGA1, LAMB1, TNC*
Interações L1CAM	8,97E-05	*ANK1, EZR, ITGA1, LAMB1, SPTA1, SPTB*
Interações de semaforinas	4,11E-04	*HSP90AA1, ITGA1, MYH11, RAC2, RRAS*
Reparo de quebra de dupla fita	3,07E-03	*PRKDC, XRCC5, XRCC6*
Fases mitóticas G2-M	8,83E-03	*HSP90AA1, PRKAR2B, XPO1, YWHAG*
Organização da matriz extracelular	1,11E-02	*COL1A2, COL4A2, CTSG, PLG*
Ciclo celular	1,42E-02	*HIST1H4A, HSP90AA1, LMNB1, NPM1, PRKAR2B, RUVBL2, XPO1, YWHAG*
Interações da matriz celular extracelular	2,25E-02	*ILK, PARVA*
Sinalização por PDGF	3,05E-02	*COL1A2, COL4A2, PLG, PRKAR2B*

FONTE: O autor (2019).
LEGENDA: FDR – Taxa de falso positivo (*false discovery rate*).

TABELA 10 – PRINCIPAIS MÓDULOS DO CÂNCER IDENTIFICADOS PARA AS PROTEÍNAS SUPEREXPRESSAS E SUBEXPRESSAS NA COMPARAÇÃO LN x NT

Número do módulo	Descrição do módulo	q-valor FDR	Sigla dos genes
114	Biossíntese de proteínas e ribossomos	1,23E-15	*ARPC2, ARPC3, CES1, EIF4A1, HSPA8, IMPDH2, LRPPRC, NAP1L1, NCL, NPM1, PCBP1, RPL10, RPL13, RPL24, RPL4, RPL6, RPL7A, RPS3, RPS3A, RPSA, YWHAG*
130	Complemento	2,58E-14	*C4B, C4BPA, C5, C6, C9, CFB, CFH, CFI, SERPING1*
84	Resposta imune (humoral) e inflamatória	1,34E-13	*ACSL1, APOD, APOE, C1QC, CAPG, CES1, CFD, COL1A2, CRYAB, FABP4, IGHG3, IGKC, ITGA6, LTF, MGLL, MYH11, ORM2, RAC2, SERPINA1, SERPING1, STOM, TYMP*
117	Sinalização	2,55E-10	*AFM, AGT, APCS, APOA1, APOB, APOD, APOH, CA1, CA2, CFB, F12, HP, KNG1, LTF, PLG, PON1, RAC2, SERPINA5, SERPINA7, SERPINC1, SERPIND1, SERPINF2*
47	Matriz extracelular e colágenos	1,43E-09	*AKR1C1, APOA1, BGN, COL1A2, COL4A2, CRYAB, FBLN2, FBN1, LAMB1, MCAM, SERPING1, TNC, TPM1*
252	Fatores de transcrição e fatores nucleares	2,64E-09	*CSE1L, DHX9, DSP, HNRNPF, ILF2, ILF3, IPO7, LMNB1, NAP1L1, PRKDC, SFPQ, SRSF1, XRCC5*
183	*Splicing* de RNA	1,17E-08	*HNRNPA2B1, HNRNPF, HNRNPH1, HNRNPU, PCBP1, SFPQ, SNRPD3, SRSF1*
93	Oxidoredutases	1,86E-08	*AKR1C1, AKR1C3, ALDH4A1, BLVRB, CAT, GC, IMPDH2, MAOA, PDIA4, TTR*
33	Genes de resposta ao estresse/ imune	7,14E-08	*AKR1C3, ANK1, ASPH, C8B, CAPG, CFD, EFTUD2, FABP4, FBLN2, ITGA6, ITIH1, MAOA, RAC2, SERPINA7*
131	Fatores da coagulação sanguínea	1,09E-07	*F12, F2, FGA, PLG, SERPINC1, SERPIND1*
324	Ligação a íons de cálcio/ metal	1,84E-07	*ACSL1, CA2, CALB2, FBLN2, FBN1, LTF, S100A10, TF*
355	Dobramento de proteínas	2,31E-06	*CRYAB, HSP90B1, HSPA5, HSPA8, HSPD1*
357	Filamentos intermediários e queratinas	1,94E-05	*AKR1C1, AKR1C3, CA2, DSP, ITGA6, MAOA*
244	Resposta a danos no DNA	2,90E-05	*DDX6, HNRNPU, HSPA8, HSPD1, IARS, ILF2, XRCC5, XRCC6*
195	*Clusters* de expressão de	5,39E-05	*EFTUD2, GC, HYOU1, ME2, MYO1C,*

Número do módulo	Descrição do módulo	q-valor FDR	Sigla dos genes
	câncer de mama		*RPL10, TYMP*
438	Filamentos intermediários e microtúbulos	1,17E-04	*DSP, LAMB1, LMNB1, MYH11, TNC*
122	Moléculas de adesão	3,65E-04	*BGN, FBN1, LAMA4, LAMB1, MCAM, TNC*
392	Processamento de rRNA e reparo de DNA	4,38E-04	*NCL, NPM1, XPO1*
573	Reguladores do ciclo celular e transportadores de carboidratos	1,14E-03	*AMBP, HSP90B1, TNC*
64	Receptores de membrana	1,18E-03	*AGT, APOB, APOE, APOH, C9, CFI, MCAM, SLC4A1, STOM, TNC*
221	Metabolismo de ácidos graxos	1,89E-03	*ACSL1, ALDH2, BLVRB*
76	Resposta inflamatória	3,00E-03	*C4B, C5, MGLL, ORM1*
247	Metabolismo de xenobióticos	3,39E-03	*AKR1C1, MGLL*

FONTE: O autor (2019).
LEGENDA: FDR – Taxa de falso positivo (*false discovery rate*).

TABELA 11 – PROCESSOS RELACIONADOS AO CÂNCER E PROTEÍNAS SUPEREXPRESSAS E SUBEXPRESSAS NOS TECIDOS MALIGNOS EM RELAÇÃO AOS NÃO TUMORAIS

Processos no câncer	**Enriquecimento funcional**	**Sigla dos genes**
Angiogênese	*Hallmarks* (TP x NT e LN x NT)	*APOH*↓
Apoptose	*Hallmarks* (TP x NT)	*ADD1*↓*, *KRT18*↑, *RETSAT*↓
Estresse celular		
Resposta ao estresse	Processos biológicos (TP x NT e LN x NT) Módulos do câncer (TP x NT e LN x NT)	*AGT*↓, *AHSG*↓, *AKR1C3*↓, *AMBP*↓, *ANK1*↓, *APCS*↓, *APOA1*↓, *APOD*↓, *APOE*↓, *APOH*↓, *ASPH*↓, *C1QBP*↑, *C4B*↓**, *C4BPA*↓, *C5*↓, *C6*↓**, *C8B*↓, *C9*↓, *CAPG*↑, *CFB*↓, *CFD*↓, *CFH*↓, *CFI*↓, *CRYAB*↓, *DDX39B*↑, *EFTUD2*↑, *EZR*↑, *F12*↓, *F2*↓, *FABP4*↓, *FBLN2*↓**, *FBLN5*↓, *FGA*↓**, *GAPDH*↑, *HNRNPK*↑**, *HP*↓, *HPX*↓, *HRG*↓, *HSP90AA1*↑, *HSP90B1*↑, *HSPA5*↑, *HSPA8*↑, *HSPD1*↑, *HYOU1*↑, *ITGA6*↓, *ITIH1*↓**, *KNG1*↓, *KRT18*↑*, *LTF*↓, *MAOA*↓, *MGLL*↓, *NPM1*↑, *P4HB*↑*, *PAFAH1B3*↑*, *PGLYRP2*↓, *PLG*↓, *PRKDC*↑, *RAC2*↑**, *RPS3*↑**, *SERPINA7*↓, *SERPINC1*↓, *SERPINF2*↓, *SERPING1*↓**, *SFPQ*↑**, *STOM*↓, *TRIM28*↑
Hipóxia	*Hallmarks* (TP x NT e LN x NT)	*BGN*↓**, *GAPDH*↑, *GBE1*↓, *HDLBP*↑, *HSPA5*↑, *MYH9*↑*, *NAGK*↑**, *PGM1*↓**
Desdobramento de Proteínas	*Hallmarks* (TP x NT e LN x NT) Vias *Reactome* (TP x NT) Módulos do câncer (TP x NT e LN x NT)	*ADD1*↓*, *CRYAB*↓, *EIF4A1*↑, *EIF4G1*↑, *FUS*↑**, *HDGF*↑, *HSP90B1*↑, *HSPA5*↑, *HSPA8*↑, *HSPD1*↑, *HYOU1*↑, *IARS*↑, *NOP56*↑, *NPM1*↑, *TARS*↑
Espécies reativas de Oxigênio	*Hallmarks* (TP x NT e LN x NT)	*CAT*↓
Glicólise	*Hallmarks* (TP x NT e LN x NT)	*AGL*↑*, *CYB5A*↓**, *GFPT1*↑**, *GOT2*↑*, *HDLBP*↑, *HSPA5*↑, *ME1*↓, *ME2*↑**
Homeostase do cálcio	Vias *Reactome* (TP x NT e LN x NT) Módulos do câncer (TP x NT e LN x NT)	*ACSL1*↓, *APOA1*↓, *CA2*↓, *CALB2*↓, *CFD*↓, *CFL1*↑*, *FBLN2*↓**, *FBN1*↓, *FGA*↓**, *HRG*↓, *HSPA5*↑, *KNG1*↓, *LTF*↓, *PLG*↓, *S100A10*↓, *SERPINA1*↓**, *SERPINF2*↓, *SERPING1*↓**, *TF*↓**

Processos no câncer	Enriquecimento funcional	Sigla dos genes
Inflamação	Processos biológicos (TP x NT e LN x NT) Módulos do câncer (LN x NT)	*AGT*↓, *AHSG*↓, *APCS*↓, *APOA1*↓, *APOD*↓, *APOE*↓, *C1QBP*↑, *C4B*↓**, *C4BPA*↓, *C5*↓, *C6*↓**, *C8B*↓, *C9*↓, *CFB*↓, *CFH*↓, *CFI*↓, *F12*↓, *FABP4*↓, *MGLL*↓, *ORM1*↓ , *PGLYRP2*↓, *SERPINC1*↓, *SERPING1*↓**
Instabilidade genômica e mutação		
Ciclo celular	*Hallmarks* (TP x NT e LN x NT) Vias *Reactome* (LN x NT) Módulos do câncer (TP x NT e LN x NT)	*AMBP*↓, *HIST1H4A*↑, *HNRNPU*↑, *HSP90AA1*↑, *HSP90B1*↑, *HSPA8*↑, *ILF3*↑, *LMNB1*↑**, *NCL*↑, *NPM1*↑, *PRKAR2B*↓, *RUVBL2*↑, *SFPQ*↑**, *SRSF1*↑, *SYNCRIP*↑**, *TNC*↑, *UPF1*↑**, *XPO1*↑**, *YWHAG*↓**
Danos ao DNA e reparo	Vias KEGG e *Reactome* (LN x NT) Módulos do câncer (TP x NT e LN x NT)	*DDX6*↑**, *HNRNPU*↑, *HSPA8*↑, *HSPD1*↑, *IARS*↑, *ILF2*↑, *NCL*↑, *NPM1*↑, *PRKDC*↑, *XPO1*↑**, *XRCC5*↑**, *XRCC6*↑**
Via de p53	*Hallmarks* (TP x NT e LN x NT)	*AK1*↓**, *EPHX1*↓*, *RETSAT*↓, *RPS12*↑**, *S100A10*↓, *STOM*↓
Invasão e metástase		
Citoesqueleto	Vias KEGG (TP x NT e LN x NT) Módulos do câncer (TP x NT e LN x NT)	*ACTB*↑, *AKR1C1*↓, *AKR1C3*↓, *ARPC2*↑**, *ARPC3*↑**, *CA2*↓, *CFL1*↑*, *DSP*↑, *EZR*↑, *F2*↓, *ITGA1*↓**, *ITGA6*↓, *KRT19*↑*, *LAMB1*↓, *LMNB1*↑**, *MAOA*↓, *MYH11*↓, *MYH9*↑*, *RAC2*↑**, *RRAS*↓, *TNC*↑
Matriz extracelular	Vias *Reactome* (TP x NT e LN x NT) Módulos do câncer (TP x NT e LN x NT)	*AKR1C1*↓, *APOA1*↓, *BGN*↓**, *CKAP4*↑*, *COL1A2*↓, *COL4A2*↓, *CRYAB*↓, *CTSG*↓**, *FBLN2*↓**, *FBN1*↓, *LAMB1*↓, *MCAM*↓, *P4HB*↑*, *PLG*↓, *SERPING1*↓**, *SERPINH1*↑*, *TNC*↑, *TPM1*↓**
Interações célula-matriz	Vias KEGG (TP x NT e LN x NT) Vias *Reactome* (TP x NT e LN x NT)	*ANK1*↓, *CFL1*↑*, *COL1A2*↓, *COL4A2*↓, *COL6A6*↓, *EZR*↑, *FBN1*↓, *FGA*↓**, *HSP90AA1*↑, *ILK*↓, *ITGA1*↓**, *ITGA6*↓, *LAMA4*↓, *LAMB1*↓, *MYH11*↓, *MYH9*↑*, *PARVA*↓, *RAC2*↑**, *RRAS*↓, *SPTA1*↓, *SPTB*↓, *TNC*↑
Adesão celular	*Hallmarks* (TP x NT e LN x NT) Vias KEGG (TP x NT e LN x NT) Módulos do câncer (TP x NT e LN x NT)	*ACTB*↑, *ARPC2*↑**, *BGN*↓**, *CALB2*↓, *COL1A2*↓, *COL4A2*↓, *COL6A6*↓, *FBN1*↓, *ILK*↓, *ITGA1*↓**, *ITGA6*↓, *LAMA4*↓, *LAMB1*↓, *MCAM*↓, *MYH11*↓, *MYH9*↑*, *PARVA*↓, *RAC2*↑**, *RRAS*↓, *SORBS1*↓, *TNC*↑

Processos no câncer	Enriquecimento funcional	Sigla dos genes
Transição epitelial-mesenquimal	*Hallmarks* (TP x NT e LN x NT)	*BGN*↓**, *CAPG*↑, *COL1A2*↓, *COL4A2*↓, *FBLN2*↓**, *FBLN5*↓, *FBN1*↓, *NID2*↓, *SERPINH1*↑*, *TNC*↑, *TPM1*↓**
Metabolismo de ácidos graxos	*Hallmarks* (TP x NT e LN x NT) Vias KEGG (TP x NT e LN x NT) Módulos do câncer (TP x NT e LN x NT)	*ACADS*↓, *ACO1*↓, *ACSL1*↓, *ALAD*↓, *ALDH2*↓, *ALDH3A2*↓*, *BLVRB*↓, *CA2*↓, *EPHX1*↓*, *HSP90AA1*↑, *IDH2*↑*, *MAOA*↓, *ME1*↓, *MGLL*↓, *RETSAT*↓, *S100A10*↓
Metabolismo de mRNA		
Metabolismo de mRNA (em geral)	Processos biológicos (TP x NT e LN x NT) Vias *Reactome* (TP x NT e LN x NT)	*ANP32A*↑, *C1QBP*↑, *DDX39B*↑, *DDX6*↑**, *DHX15*↑, *DHX9*↑, *EFTUD2*↑, *EIF4A1*↑, *EIF4G1*↑, *FUS*↑**, *HNRNPA2B1*↑, *HNRNPF*↑, *HNRNPH1*↑**, *HNRNPK*↑**, *HNRNPL*↑, *HNRNPM*↑, *HNRNPU*↑, *HSPA8*↑, *PCBP1*↑, *RPL10*↑**, *RPL13*↑**, *RPL24*↑**, *RPL3*↑, *RPL4*↑, *RPL5*↑, *RPL6*↑, *RPL7A*↑**, *RPL9*↑*, *RPS12*↑**, *RPS17*↑**, *RPS3*↑**, *RPS3A*↑, *RPSA*↑**, *SFPQ*↑**, *SNRNP200*↑, *SNRPD3*↑**, *SRSF1*↑, *SYNCRIP*↑**, *UPF1*↑**
Processamento e *splicing* de mRNA	Processo biológico (TP x NT) Vias KEGG (TP x NT e LN x NT) Vias *Reactome* (TP x NT e LN x NT)	*C1QBP*↑, *DDX39B*↑, *DHX15*↑, *DHX9*↑, *EFTUD2*↑, *FUS*↑**, *HNRNPA2B1*↑, *HNRNPF*↑, *HNRNPH1*↑**, *HNRNPK*↑**, *HNRNPL*↑, *HNRNPM*↑, *HNRNPU*↑, *HSPA8*↑, *PCBP1*↑, *RAC2*↑**, *SNRNP200*↑, *SNRPD3*↑**, *SRSF1*↑, *TNC*↑
Metabolismo de proteínas	Processos biológicos (TP x NT e LN x NT) Vias *Reactome* (TP x NT e LN x NT)	*ACTB*↑, *AGT*↓, *AHSG*↓, *AMBP*↓, *APCS*↓, *APOD*↓, *APOE*↓, *BGN*↓**, *C4B*↓**, *C4BPA*↓, *C5*↓, *CRYAB*↓, *EEF1G*↑*, *EIF4A1*↑, *EIF4G1*↑, *EPRS*↑, *EZR*↑, *F2*↓, *FABP4*↓, *FGA*↓**, *GAPDH*↑, *HNRNPA2B1*↑, *HRG*↓, *HSPD1*↑, *ILF3*↑, *ILK*↓, *ITIH1*↓**, *ITIH2*↓**, *ITIH4*↓, *KNG1*↓, *NOP56*↑, *NPM1*↑, *PON1*↓, *PRKAR2B*↓, *PRKDC*↑, *RPL10*↑**, *RPL13*↑**, *RPL24*↑**, *RPL3*↑, *RPL4*↑, *RPL5*↑, *RPL6*↑, *RPL7A*↑**, *RPL9*↑*, *RPS12*↑**, *RPS17*↑**, *RPS3*↑**, *RPS3A*↑, *RPSA*↑**, *SERPINA1*↓**, *SERPINA3*↓**, *SERPINA4*↓, *SERPINA5*↓, *SERPINA7*↓, *SERPINC1*↓, *SERPIND1*↓, *SERPINF2*↓, *SERPING1*↓**, *SERPINH1*↑*, *SYNCRIP*↑**, *UPF1*↑**, *YWHAG*↓**

Processos no câncer	Enriquecimento funcional	Sigla dos genes
Metabolismo de xenobióticos	*Hallmarks* (TP x NT e LN x NT) Vias KEGG (TP x NT e LN x NT) Módulos do câncer (TP x NT e LN x NT)	*AKR1C1↓, AKR1C3↓, ALDH2↓, APOE↓, BLVRB↓, CA2↓, CAT↓, CES1↓, CFB↓, CYB5A↓**, EPHX1↓*, FAH↓, HRG↓, IMPDH2↑**, ITIH1↓**, ITIH4↓, MAOA↓, MGLL↓, PLG↓, RETSAT↓, TYMP↑*
Oxidação-redução	Processos biológicos (TP x NT) Módulos do câncer (TP x NT e LN x NT)	*ACADS↓, ACO1↓, AGL↑*, AKR1C1↓, AKR1C3↓, ALDH2↓, ALDH3A2↓*, ALDH4A1↓, ASPH↓, BLVRB↓, CAT↓, GAPDH↑, GBE1↓, GC↓, GOT2↑*, IDH2↑*, IMPDH2↑**, MAOA↓, ME1↓, PDIA4↑, RETSAT↓, SORD↑*, TTR↓*
Peroxissomo	*Hallmarks* (TP x NT e LN x NT)	*ACSL1↓, CAT↓, RETSAT↓, TTR↓*
Regulação pós-transcricional da expressão gênica	Processos biológicos (TP x NT e LN x NT)	*ACO1↓, ANP32A↑, C1QBP↑, DDX39B↑, DDX6↑**, DHX9↑, EIF4A1↑, EIF4G1↑, EIF4G2↑**, EPRS↑, GAPDH↑, HNRNPA2B1↑, HNRNPU↑, HSPA8↑, IARS↑, ILF3↑, LARS↑, LRPPRC↑, NPM1↑, RPS3↑**, SYNCRIP↑**, UPF1↑**, XPO1↑***
Resposta ao estrogênio	*Hallmarks* (TP x NT e LN x NT)	*ALDH3A2↓*, BLVRB↓, CA2↓, CALB2↓, IDH2↑*, KRT18↑*, KRT19↑*, LTF↓, PRKAR2B↓, SERPINA1↓**, SERPINA3↓**, SERPINA5↓, SORD↑**
Resposta à injúria	Processos biológicos (TP x NT e LN x NT)	*ACTB↑, APOA1↓, APOD↓, APOH↓, C1QBP↑, COL1A2↓, CSRP1↓**, DSP↑, F12↓, F2↓, FGA↓**, GNA11↓**, HBD↓, HBG1↓, HRG↓, ILK↓, KNG1↓, MCAM↓, MYH9↑*, PLG↓, PRKAR2B↓, RAC2↑**, SERPINA1↓**, SERPINA5↓, SERPINC1↓, SERPIND1↓, SERPING1↓**, TNC↑, TPM1↓***
Sinalização celular		
Sinalização	Módulos do câncer (TP x NT e LN x NT)	*AFM↓, AGT↓, APCS↓, APOA1↓, APOB↓, APOD↓, APOH↓, CA1↓, CA2↓, CFB↓, F12↓, HP↓, KNG1↓, LTF↓, PLG↓, PON1↓, RAC2↑**, SERPINA5↓, SERPINA7↓, SERPINC1↓, SERPIND1↓, SERPINF2↓*
Hedgehog	*Hallmarks* (TP x NT)	*MYH9↑*, PLG↓*
IL2-STAT5	*Hallmarks* (TP x NT e LN x NT)	*CA2↓, CAPG↑, CKAP4↑*, FAH↓, ITGA6↓, MYO1C↓, SERPINC1↓*
KRAS**	*Hallmarks* (LN x NT)	*APOD↓, CA2↓, CFB↓, CFH↓, SERPINA3↓***
MTORC1	*Hallmarks* (TP x NT e LN x NT)	*ACLY↑**, ACTR2↑**, ACTR3↑**, CACYBP↑, EPRS↑, GAPDH↑, GBE1↓, HSP90B1↑, HSPA5↑, HSPD1↑, ME1↓, NAMPT↑*, PGM1↓**, SERPINH1↑*, SORD↑**

Processos no câncer	Enriquecimento funcional	Sigla dos genes
PDGF	Processos biológicos (TP x NT e LN x NT)	*COL1A2↓, COL4A2↓, PLG↓, PRKAR2B↓*
PI3K-AKT-MTOR**	*Hallmarks* (LN x NT)	*ACTR2↑**, ACTR3↑**, ARPC3↑**, HSP90B1↑*
Sistema de coagulação	*Hallmarks* (TP x NT e LN x NT) Vias KEGG (TP x NT e LN x NT) Módulos do câncer (TP x NT e LN x NT)	*APOA1↓, C1QC↓, C4B↓, C4BPA↓, C5↓, C6↓, C8B↓, C9↓, CFB↓, CFD↓, CFH↓, CFI↓, CSRP1↓, F12↓, F2↓, FBN1↓, FGA↓, HRG↓, ITIH1↓, KNG1↓, PLG↓, SERPINA1↓, SERPINA5↓, SERPINC1↓, SERPIND1↓, SERPINF2↓, SERPING1↓, TF↓*
Sistema complemento	*Hallmarks* (TP x NT e LN x NT) Vias KEGG (TP x NT e LN x NT) Módulos do câncer (TP x NT e LN x NT)	*C1QC↓**, C4B↓**, C4BPA↓, C5↓, C6↓**, C8B↓, C9↓, CA2↓, CFB↓, CFD↓, CFH↓, CFI↓, COL4A2↓, CSRP1↓**, F12↓, F2↓, FGA↓**, HSPA5↑, ITIH1↓**, KNG1↓, LTF↓, ME1↓, PLG↓, SERPINA1↓**, SERPINA5↓, SERPINC1↓, SERPIND1↓, SERPINF2↓, SERPING1↓**
Sistema imune	Processos biológicos (TP x NT e LN x NT) Módulos do câncer (TP x NT e LN x NT)	*ACSL1↓, ACTB↑, ACTR2↑**, ACTR3↑**, ADD1↓*, APCS↓, APOB↓, APOD↓, APOE↓, ARPC2↑**, ARPC3↑**, C1QBP↑, C1QC↓**, C4B↓**, C4BPA↓, C5↓, C6↓**, C8B↓, C9↓, CAPG↑, CES1↓, CFB↓, CFD↓, CFH↓, CFI↓, COL1A2↓, CRYAB↓, CTSG↓**, EPRS↑, F12↓,F2↓, FABP4↓, FGA↓**, GAPDH↑, HNRNPK↑**, HP↓, HSP90AA1↑, HSP90B1↑, HSPD1↑, IGHA1↓, IGHA2↓, IGHG2↓, IGHG3↓, IGHG4↓, IGKC↓**, IGKV3-20↓, ILF2↑, ILF3↑, IMPDH2↑**, IPO7↑, ITGA1↓**, ITGA6↓, KRT18↑*, KRT19↑*, LTF↓, MGLL↓, MYH11↓, MYH9↑*, MYO1C↓, NAMPT↑*, ORM2↓, PARP1↑, PGLYRP2↓, PRKDC↑, RAB6A↑, RAC2↑**, RPS17↑**, RRAS↓, SERPINA1↓**, SERPING1↓**, SPTA1↓, STOM↓, SYNCRIP↑**, TRIM28↑, TYMP↑, XRCC5↑**
Vias em câncer	Vias KEGG (TP x NT e LN x NT)	*COL4A2↓, HSP90AA1↑, HSP90B1↑, ITGA6↓, LAMA4↓, LAMB1↓, RAC2↑**

FONTE: O autor (2019).
NOTA: Proteínas superexpressas ou subexpressas (log2 *fold change* de 1,5) somente na comparação TP x NT estão indicadas com "*" e somente na comparação LN x NT com "**".
LEGENDA: TP – Tumor primário de mama, LN – linfonodo axilar metastático, NT – tecidos mamários não tumorais.

7 CAPÍTULO II

INTEGRATED ANALYSIS OF LABEL-FREE QUANTITATIVE PROTEOMICS AND BIOINFORMATICS REVEAL INSIGHTS INTO SIGNALING PATHWAYS IN MALE BREAST CANCER

Graphical Abstract

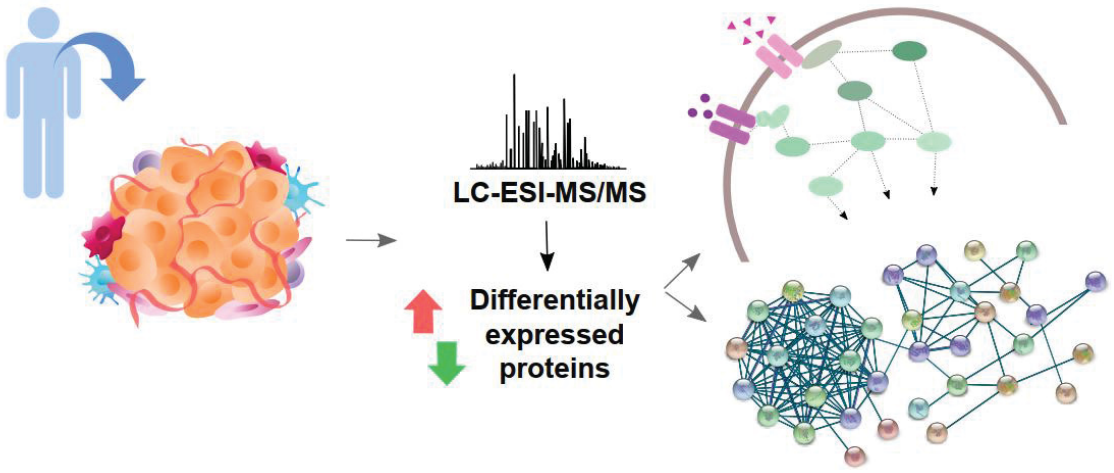

Highlights

- High-throughput proteomic profiling of a male breast cancer case;
- Deregulated proteins were into signaling pathways related to the cancer development;
- Male and female breast tumors presented distinct proteomes;
- DEPs between male and female breast tumors were linked to known cancer-related drives.
- Our study provides a landscape of proteomic data for the male breast cancer research.

Integrated analysis of label-free quantitative proteomics and bioinformatics reveal insights into signaling pathways in male breast cancer

Talita Helen Bombardelli Gomig[a*]; Amanda Moletta Gontarski[a*]; Iglenir João Cavalli[a]; Ricardo Lehtonen Rodrigues de Souza[a]; Aline Castro Rodrigues Lucena[b]; Michel Batista[b,c]; Kelly Cavalcanti Machado[c]; Fabricio Klerynton Marchini[b,c]; Fabio Albuquerque Marchi[d]; Rubens Silveira Lima[e]; Cícero de Andrade Urban[e]; Luciane Regina Cavalli[f,g]; Enilze Maria de Souza Fonseca Ribeiro[a]

* These authors contributed equally to this study.

[a] Genetics Department, Federal University of Parana, Curitiba, Brazil;
[b] Functional Genomics Laboratory, Carlos Chagas Institute, Fiocruz, Curitiba, Parana, Brazil;
[c] Mass Spectrometry Facility - RPT02H, Carlos Chagas Institute, Fiocruz, Curitiba, Parana, Brazil;
[d] International Research Center (CIPE) - A.C. Camargo Cancer Center, São Paulo, SP, Brazil;
[e] Breast Disease Center, Hospital Nossa Senhora das Graças, Curitiba, Brazil;
[f] Research Institute Pelé Pequeno Príncipe, Curitiba, Brazil;
[g] Lombardi Comprehensive Cancer Center, Georgetown University, USA.

Corresponding author*:* Enilze Maria de Souza Fonseca Ribeiro, Centro Politécnico, Setor de Ciências Biológicas, Departamento de Genética - Caixa Postal 19071, Laboratório de Citogenética Humana e Oncogenética, CEP: 81531-990 - Curitiba/Paraná, Brazil.
Tel: +55 4133611549, e-mail: enilzeribeiro@gmail.com

Abstract

Male breast cancer (MBC) is a rare malignancy that accounts for about 1.8% of all breast cancer cases. In contrast to the high number of the “omics” studies in breast cancer in women, only recently molecular approaches have been performed in MBC research. High-throughput proteomics based methodologies are promisor strategies to characterize the MBC proteomic signatures and their association with clinico-pathological parameters. In this study, we performed an integrated analysis of label-free quantification-mass spectrometry (LFQ-MS) and bioinformatics to obtain the proteomic profiling of a MBC case. Protein expression levels of the primary tumor were evaluated simultaneously with the corresponding axillary metastatic lymph nodes and the adjacent non-tumor breast tissue to identify differentially expressed proteins (DEPs) among these tissues. An additional proteomic comparative analysis was performed with a breast tumor of a female patient. A number of Ingenuity Pathway Analysis (IPA) and functional annotation tools were used to further analyze the DEPs. Data from MBC case presented the signaling pathways of granzyme B, sirtuins, eIF2, actin cytoskeleton, eNOS, acute phase response and calcium as affected by the DEPs. The main upstream regulators of the DEPs included *MYC, PI3K SMARCA4* and cancer-related chemical drugs. The proteomic comparison between the male and female tumors revealed an interesting set of DEPs, which were mainly involved in cancer-related biological processes and signal transduction. Our study highlights deregulated proteins and signaling pathways in the male breast tumorigenesis and provides a relevant data source for the MBC research that can help the therapeutic strategies for its management.

Keywords: Male breast cancer; proteomics; label-free mass spectrometry; bioinformatics analysis; signaling pathways.

Abbreviations

BC, breast cancer; COSMIC, Cancer Gene Census of the Catalogue of Somatic Mutations in Cancer; DAVID, Database for Annotation, Visualization and Integrated Discovery; DEP, differentially expressed protein; FBC, female breast cancer; FPT, female-primary breast tumor; HCL, hierarchical cluster analysis; IDC, invasive ductal carcinoma; IPA, Ingenuity Pathway Analysis; KEGG, Kyoto Encyclopedia of Genes and Genomes; LFQ, label-free

quantification; MBC, male breast cancer; MLN, male-axillary metastatic lymph node; MNT, male-non-tumor breast tissue; MPT, male-primary breast tumor; MS, mass spectrometry; MSigDB, Molecular Signatures Database; PANTHER, Protein ANalysis THrough Evolutionary Relationships; STRING, Search Tool for the Retrieval of Interacting Genes/Proteins.

1 Introduction

Breast cancer (BC) is the most commonly incident type of cancer among women in the world. A systematic analysis for the global cancer burden revealed an incidence of 2,4 million cases of BC in 2015, 1.8% (44/2,422 thousands) of which represented the male breast cancer (MBC) cases (Fitzmaurice et al., 2017). Although breast cancer is rare in men, it is a relevant cause of morbidity and mortality in male population. In 2015, it accounted for about 10,000 deaths worldwide (Fitzmaurice et al., 2017). MBC is usually diagnosed later than in female cases, often in later stages and with axillary lymph node metastasis, which leads to worse prognosis and lower survival rates when compared to the female breast cancer (FBC) (Cutuli et al., 2010).

Despite of the general similarities in the male and female breast tumorigenesis, differences in the epidemiology, risk factors, diagnosis, pathology, treatment and prognosis have been reported in MBC (Korde et al., 2010). The low incidence of MBC associated with the limited number of studies comparing the genetic alterations between the FBC and MBC in the literature, compromises the understanding of the molecular landscape of these tumors, which impairs their appropriated clinical management and treatment. The specific molecular portrait of these tumors, which characterizes them as a unique tumor type, can reflect into distinct treatment choices and clinical outcomes (Callari et al., 2011).

A number of approaches have been employed to identify and characterize these unique MBC biology (Chen et al., 2013; Fentiman, 2016; Humphries et al., 2017; Kornegoor et al., 2012; Shaaban et al., 2012; Syrine et al., 2017; Yuan et al., 2016), including few studies in proteomics, as recently reviewed (Zografos et al., 2016). Considering the recognized and critical role of protein interactions in many cellular processes and their impact in the pathophysiologic conditions associated to diseases, the interactome analysis is a promising approach to reveal the specific molecular

characteristics and cellular process that are involved in the MBC biology. In this sense, a systematic high-throughput protein analysis integrated with bioinformatics tools can contribute to the discovery of novel potential biomarkers and druggable targets (Manna et al., 2010), that can ultimately contribute to the tailored of specific and more efficient forms of treatment to MBC.

In the present study, we performed an integrated analysis of label-free quantification-mass spectrometry (LFQ-MS) and bioinformatics to obtain the proteomic profiling of a MBC case of the luminal B subtype. Protein expression levels of the primary tumor were evaluated simultaneously with the corresponding axillary metastatic lymph nodes and the adjacent non-tumor breast tissue to identify differentially expressed proteins (DEPs) among these tissues. An additional proteomic comparative analysis was performed in a luminal B subtype of a female patient. All DEPs were analyzed for their biological functions in signaling pathways and interaction networks to obtain a “snapshot” of the deregulated biological processes that could be impacted by their expression deregulation in male breast tumorigenesis. These analyses provided novel proteomic markers that can be further studied to validate their potential use as molecular markers of the MBC.

2 Material and Methods

2.1 Patients

The MBC samples were from a 70-years-old Brazilian man treated at Hospital das Clínicas at Curitiba, Parana, Brazil, in 2016, diagnosed with Invasive Ductal Carcinoma (IDC), Nottingham histologic grade III, tumor dimensions of 5.3 x 3.0 x 1.0 cm, luminal B subtype [as defined by immunohistochemistry using the four surrogate markers, ER (score 5), PR (score 3), HER2 (score +2) and Ki-67<14%] with positivity for lymph node metastasis. The karyotype and *BRCA2* status were not available.

A sample of primary breast tumor tissue of a 59-years-old woman patient, that undergo surgery at the Hospital Nossa Senhora das Graças at Curitiba, Parana, Brazil, in the same year, with matching diagnosis (IDC, grade III, luminal B subtype and positivity for lymph node metastasis) was used to compare the primary breast tumor proteomic profiles in both sexes.

The tissue samples [male-primary breast tumor (MPT), male-adjacent non-tumor tissue (MNT), male-axillary metastatic lymph node (MLN) and female-primary breast tumor (FPT)] were collected during the same surgery procedure and immediately stored in RNA later for the experimental analysis. Samples were macrodissected for removal of fat, blood vessels and other non-breast tissue areas, and stored at -80ºC until proteomic analysis. This study was approved by the National Commission of Ethics in Research (CONEP number 7220). The patients voluntarily agreed to participate in the study through an informed consent.

2.2 Protein preparation and in-gel tryptic digestion

Whole proteins were extracted from the breast tissues using adapted protocols from liquid chromatography-electrospray ionization-tandem mass spectrometry (LC-ESI-MS/MS) (Ostasiewicz et al., 2010; Tyanova et al., 2016a). The protein extracts were obtained from homogenization with 4% SDS, 0.1 M Tris-HCl pH 7.6 and 0.1 M DTT (100 µL buffer per 10 mg tissue) in TissueLyser II sample disruptor (Qiagen Corp. MD, USA) at an oscillation frequency of 25 Hz for 3 min and heated to 95ºC. Homogenization and heating were repeated three times followed by sonication and centrifugation to remove cellular debris. The quantification of protein extracts was performed in the Qubit® 2.0 Fluorometer (Life Technologies) after employing the FASP method (Wisniewski et al., 2009), in which aliquots of the extracts were added to 30-kDa Amicon Ultra filters (Merck-Millipore, MA, USA), washed three times with 8 M urea, 10 mM DTT, 0.1 M Tris-HCl pH 8,8 and twice with 50 mM ammonium bicarbonate (ABC). After quantification, the unwashed protein extracts (25 µg) were separated in 1D-PAGE 10% (v/v) acrylamide gels, reduced with 10 mM DTT, alkylated with 50 mM iodacetamide and digested overnight with 12.5 ng/µL trypsin solution in ABC at 37°C. The peptides were extracted twice with 30% acetonitrile (ACN), 3% trifluoroacetic acid (TFA) and twice with ACN, dried in a vacuum centrifuge and desalted with C18 Stage Tips.

2.3 Label-free protein quantification by mass spectrometry

Label-free quantitative mass spectrometry experiments were conducted in triplicate with an EASY-nLC 1000 chromatograph (Thermo Scientific) coupled to an LTQ Orbitrap XL ETD (Thermo Scientific) mass spectrometer (mass spectrometry facility RPT02H/Carlos Chagas Institute – Fiocruz Parana). In the chromatography, the peptides were eluted from the column at a constant flow of 250 nL/min, with a 240 min linear

gradient from 5 to 40% MeCN (ACN), 0.1% formic acid, 5% dimethyl sulfoxide (DMSO). The separation was carried out in a C18 reversed-phase (RP) analytical column, with 15 cm length, 75 µm ID, packed with 3 µm C18 particles (ReproSil-Pur 120, Dr. Maisch). The Orbitrap analyzer acquired the full MS with a resolution of 60,000, m/z window of 300 to 1,600, enabling preview scan. MS2 analysis was performed in a data dependent acquisition (DDA) mode, where the ten most intense ions were subjected to collision-induced fragmentation (CID) fragmentation in the ion trap analyzer. A dynamic exclusion list of 90 s was applied, and the lock mass option was enabled for the m/z 401.922718. The spray voltage used was 2.7 kV, spray current 100 µA, capillary voltage 35 V, tube lens 100 V, and capillary heater 175°C. Mass spectra data was analyzed in the MaxQuant software version 1.5.8.3 (Cox and Mann, 2008) and protein identification was performed against human uniprot protein database (UniProtKB, 24 May 2017, 70,939 entries). Trypsin was set as the enzyme, oxidation of methionine and acetylation of protein N-terminal were set as variable modification and carbamidomethylation of cysteine as fixed modification. For peptide identification, at least seven amino acids were required. An FDR of 1% was independently applied for both peptide and protein identification. LFQ and match between runs options were enabled. The mass spectrometry proteomics data have been deposited to the ProteomeXchange Consortium via the PRIDE (Vizcaino et al., 2016) partner repository with the dataset identifier PXD012453.

2.4 Data analysis

Protein data was processed using the Perseus software version 1.5.6.0 (Tyanova et al., 2016b). The proteomic analyses of the MBC case (MPT, MNT and MLN specimens) and the male and female tissue comparisons (MPT *vs.* FPT) were performed separately. Tissue samples were evaluated in technical triplicates and the LFQ intensity values were used to refer to protein expression. Proteins that were identified based only on modified peptides (named “only identified by site”), potential contaminants, and reverse peptides were removed from data. LFQ intensity values were log2-transformed and filtered so that for each protein, at least two technical replicates for each tissue sample contained valid values. Data normalization was performed by width adjustment. The remaining missing values were imputed by random numbers drawn from a normal distribution (width, 0.3; down-shift, 1.8) to simulate signals from low abundant proteins (Robles et al., 2014). Based on LFQ intensity values, the reproducibility of technical replicates was accessed by

Pearson's correlation coefficients. Hierarchical cluster analysis (HCL) was employed to analyze the protein expression patters among the tissue samples.

Data of the MBC case was export for further analysis in R Platform. The RStudio version 3.4.2 (http://www.R-project.org) and in-house scripts were used to perform the statistical analysis. Proteins with statistically significant differences among the tissues were obtained from ANOVA test ($p<0.05$, $FDR<0.05$) applied to proteins that presented homogeneous variances (accessed by the Bartlett's test). Duncan's post hoc test was carried out to provide lists of DEPs according to the tissue samples' pairs comparisons: MPT x MNT, MLN x MNT and MPT x MLN. Proteomic analysis of the MPT x FPT group' comparison was performed in the Perseus software using the Student's t-test (Benjamini-Hochberg FDR of 0.05). In both analyses, up and down-regulated proteins were defined based on the log2 fold-change cutoff of 1.5.

2.5 Bioinformatic analysis

Functional groups of the DEPs were investigated using the "Gene families" tool of the Molecular Signatures Database (MSigDB) version 6.2 (Liberzon et al., 2015) and were compared with genes listed in the Cancer Gene Census project of the Cancer Gene Census of the Catalogue Of Somatic Mutations In Cancer (COSMIC) database version 86 (Forbes et al., 2016) to identify proteins that play a role in cancer and could be involved in male breast cancer.

A fold change filtering (minimum of 1.5 log2-transformed values) was applied to define the DEPs with the most differences in the protein expression levels among the tissue samples. These proteins were subjected to bioinformatics analysis tools for functional annotation, enrichment analysis and to obtain protein interactions networks, as follow: Gene List Analysis tool of the Protein Analysis THrough Evolutionary Relationships (PANTHER) classification system version 13.1 (Thomas et al., 2003) was used to categorize DEPs according to their protein classes and gene ontology (GO) terms to identify the molecular functions and biological processes; Database for Annotation, Visualization and Integrated Discovery (DAVID) version 6.8 (Huang da et al., 2009) was employed to further characterize the GO terms and pathways according to the Kyoto Encyclopedia of Genes and Genomes (KEGG) (Kanehisa et al., 2016); Core Analysis tool of the Ingenuity Pathway Analysis software version 2.3 (QIAGEN Inc., https://www.qiagenbioinformatics.com/products/ ingenuity-pathway-analysis) (Kramer et al., 2014) and its Ingenuity Pathways Knowledge Base were used to identify the most

relevant signaling pathways and interaction networks affected by the deregulated proteins, with predictions of the activation/inhibition status based on z-score from fold changes of DEPs; and the Search Tool for the Retrieval of Interacting Genes/Proteins (STRING) database version 10.5 (Szklarczyk et al., 2017) to evaluate the protein-protein interaction networks of the DEPs based on evidences from “textmining”, “experiments”, “databases” and “co-expression” interaction sources, minimum interaction scores of 0.7 (high confidence) and the STRING k-Means clustering algorithm.

3 Results

3.1 Proteomic characterization of the male breast cancer (MBC) patient: MPT x MNT, MLN x MNT and MPT x MLN groups’ comparisons

The malignant (MPT and MLN) and non-tumor (MNT) tissues from the male patient were analyzed from technical triplicates, previously checked for reproducibility by Pearson’s correlation, which showed a high correlation score (from >0.93 to >0.98) among the technical triplicates (**Supplementary File 1A**). The hierarchical cluster analysis (HCL) revealed a differential proteomic profile clustering among the MPT and MLN compared to the MNT sample (**Supplementary File 1A).** The LFQ-MS quantification identified a total of 675 DEPs among these tissue samples. A total of 31 oncogenes and 9 tumor suppressors were identified among the genes encoding these DEPs (**Table 1**).

The DEPs were identified in three groups’ comparisons: MPT x MNT, MLN x MNT, and MPT x MLN (**Fig. 1**). Similar patterns of protein expression were observed between the proteomic profiles of the MPT x MNT and MLN x MNT [both of the malignant tissues were part of the same major cluster as shown by the HCL (see **Supplementary File 1A**)]. Considering this similarity, we reported the data from the MLN x MNT tissues’ comparison in the **Supplementary File 2**. From the general 675 DEPs observed among the tissues, 283 (42%) were commonly deregulated among all the groups’ comparisons (MPT x MNT, MLN x MNT and MPT x MLN). Of these, 124 DEPs presented expression levels gradually increased from MNT to MPT to MLN samples. On the other hand, 101 DEPs were gradually decreased among these tissue samples. In summary, we observed 225 DEPs that were commonly deregulated among all the tissue samples from MBC case and showed a pattern of increased/ decreased expression levels throughout the tumor

progression (MNT to MPT to MLN samples) (**Supplementary File 1B**). STRING protein-protein interaction revealed that 62.2% (140/225) of these DEPs could interact and form strong protein networks, with high confidence scores (at minimum of 0.70) and functional clusters (**Fig. 2**).

3.1.1 Primary breast tumor (MPT) versus *non-tumor breast tissue (MNT) analysis*

In MPT x MNT tissues' comparison, 597 DEPs were identified, 234 (39.2%, 234/597) of which with 1.5 log2-fold change values (124 up-regulated and 110 down-regulated in the MPT sample). The up and down-regulated expressed proteins and their respective fold change values in this comparison are shown in **Supplementary File 3A.** Brief results of the PANTHER and DAVID analyses involving these 234 DEPs are presented in **Supplementary File 3B**.

The IPA's analyses were also performed with the up-regulated and down-regulated expressed proteins from the MPT x MNT tissues' comparison. According to the Ingenuity Pathways Knowledge Base, the "disease and function annotation" revealed that most of the identified 234 DEPs were observed to be involved in cancers in general (96.2%, 225/234), and particularly in breast cancer (32.9%, 77/234) (**Table 2)**.

The enrichment of Ingenuity canonical pathways for these 234 DEPs identified 22 of the 95 significant pathways (23.1%, 22/95) related to biological signaling processes, four of which were predicted as activated and two as inhibited in MPT sample when compared to the MNT sample (**Table 3**). According to the MSigDB, six of these DEPs are encoded by oncogenes (*HNRNPA2B1, HSP90AA1, HSP90AB1, MYH11, MYH9*, and *NUMA1*); three by cytokines and growth factors (*AGT, C5, CAT*); two by kinases (*ILK, PRKDC*) and one by transcription factor and a cell differentiation marker (*STAT1* and *CD36,* respectively).

The top-scored interaction protein network generated by IPA's tools involved 32 DEPs related to RNA post-transcriptional modification, molecular transport, and RNA trafficking (**Fig. 3A**). In addition, we observed two cancer-related networks of DEPs from this comparison, composed of 41 predicted proteins. The main functions of the proteins in the first network were related to cell death and survival, cell cycle, and cancer (**Fig. 3B**) and in the second were related to cardiovascular disease, organismal injury and abnormalities, and cancer (**Fig. 3C**). Many of the proteins involved in these networks were reported in cancer and breast cancer annotations, as well as in the signaling pathways mentioned above.

The IPA's tools provides an additional upstream regulator analysis, which predicted a total of 193 upstream regulators ($p<0.05$) for these DEPs. The main upstream regulators and their targets are described in **Supplementary File 3C**. The DEPs involved in the main signaling pathways, biological functions and protein interaction networks were predicted as target of these regulators. Among the main regulators, it is included the *MYC* oncogene and the tumor suppressors *PIK3R1* and *SMARCA4*.

3.1.2 Primary breast tumor (MPT) versus axillary metastatic lymph node (MLN) analysis

In MPT x MLN tissues' comparison 370 DEPs were identified, 25 (6.76%, 25/370) of which with 1.5 log2-fold change values (18 up-regulated and 7 down-regulated in the MPT sample). The up and down-regulated expressed proteins and their respective fold change values in this comparison are shown in **Supplementary File 4A.** PANTHER and DAVID analyses of these 25 DEPs are presented in **Supplementary File 4B.**

According to the Ingenuity Pathways Knowledge Base, the "disease and function annotation" analysis for the DEPs from MPT x MLN tissues' comparison indicated only the *POSTN* and *TNC* genes as involved in the invasive ductal breast carcinoma.

The enrichment pathway analysis of these DEPs, using the IPA's tools, showed their involvement in 25 significant canonical pathways, none of which with the activation/inhibition z-score available. Two of these pathways were related to signaling via granzyme A and calcium. In the first pathway was identified the DEP encoded by *H1F0* gene and in second, *CALR* and *MYH11* genes.

A top-scored protein interaction network from the DEPs observed in this comparison is presented in **Fig. 4** and its main functions were related to cellular and tissue development and connective tissue development and function. The DEPs predicted in this network were also reported in the disease annotation mentioned above and in the calcium signaling pathway.

In addition, a total of 59 significant upstream regulators were predicted by IPA's tools. The main regulators are reported in **Supplementary File 4C.** The DEPs predicted as their regulation targets were involved in diseases, signaling pathways and protein interactions obtained in the IPA's analyses.

3.2 Comparative proteomic analysis between the primary tumor of the male (MPT) versus *female (FPT) tissues' comparison*

To determine whether there was a difference in proteomic profiling of the MBC case studied in relation to the FBC, we performed a comparative proteome analysis between the MPT tissue of the MBC patient with the FPT of the FBC patient, matched for the breast cancer subtype and other clinico-pathological parameters. The reproducibility of technical replicates in the proteomic analysis was obtained in the Perseus software and is reported in the **Supplementary File 5A**.

The comparison between the MPT and FPT tissue samples resulted in 447 DEPs, 102 of which were in the 1.5 log2 fold change cutoff (42 up-regulated and 60 down-regulated in the male MPT tissue) (**Supplementary File 5B)**. According to the MSigDB, among the genes encoding all the DEPs from MPT x FPT, 13 were identified as oncogenes and two as tumor suppressor genes (**Table 4).**

In order to explore the relationship among these identified 447 DEPs, protein-protein interactions were analyzed in the STRING database. A strong network was predicted involving 66.2% (296/447) of these DEPs, with the highest confidence scores (at minimum of 0.90) and functional clusters (**Fig. 5**). The DEPs with more expressive fold change values were involved in relevant interactions, including the ones encoded by *CD36, FABP4, FLOT1, HSPA2, OGN, SLC9A3R1, SORD, THBS1, TNXB* and *USO1* genes.

Compared to the data of the MBC case, 54 of the DEPs at 1.5 log2 fold change were also differentially expressed in the MPT x MNT tissues' comparison (30 of these were also common to the MPT x MLN tissues' comparison). Among these DEPs, the 10 most up-regulated in the MPT compared to the FPT sample are encoded by *CYB5A, CYB5R1, HACD3, HSPA2, IARS2, ISOC2, MCCC2, SORD, THBS1* and *USO1* genes; and the 10 most down-regulated are encoded by *CD36, CRYAB, DHRS2, FABP4, HBD, LUM, OGN, PLIN1, PTGIS* and *TNXB* genes.

The functional annotation analyses performed in PANTHER and DAVID were employed to further comprise the biological context of the DEPs from the MPT x FPT tissues' comparison (**Supplementary File 5C**). The functional enrichment analysis of the DEPs into 1.5 log2 fold change performed in DAVID platform provided a biological landscape for the main deregulated proteins between the male and female breast tumors (**Supplementary File 5D**). The main cancer-related processes and their DEPs, and the

main signaling pathways related to these DEPs were reported in the **tables 5** and **6**, respectively. These proteins presented the largest fold change values and were involved in biological processes and KEGG pathways of relevance in the tumor biology; thus, they could be suggested as potential candidates to further studies in the MBC research.

4 Discussion

4.1 Differential expressed proteins observed among the groups' comparisons of this study

In this study, proteome profiling of a MBC case revealed a higher number of DEPs among the malignant (MPT and MLN) and corresponding non-tumor (MNT) sample, totalizing 675 general DEPs. The HCL analysis reinforces the differences among these tissues. Importantly, many DEPs were accessed using any of the malignant tissues compared to the MNT sample, which indicate that the primary tumor and metastatic sites shared most of their proteomes.

Interestingly, in the MBC case proteomic analysis was possible to identify a high number of commonly deregulated proteins that presented a gradual increase/ decrease from MNT to MPT to MLN samples, totaling 225 of the 675 identified DEPs. Relevant DEPs were observed into the 1.5 log2 fold change cutoff in the MPT x MNT and MPT x MLN groups' comparisons and in relevant signaling pathways. These DEPs provide an overview of deregulated processes involved in the male breast tumorigenesis and indicate biological functions and proteins of interest to additional studies. It may help to improve the knowledge about the MBC and ultimately the therapeutic strategies for its management.

A total of 447 DEPs was observed between the MPT x FPT tissues' comparison. The HCL analysis allowed highlighting the differential proteome between the male and female breast tumors. Many of these DEPs were common to the 675 DEPs from MBC case and some of them were also observed in the signaling pathways from the IPA's analyses. Interestingly, some DEPs from MPT x FPT tissues' comparison were also differentially expressed in the groups' comparisons of the MBC case, reinforcing their potential involvement in the male breast tumorigenesis.

According to the COSMIC and MSigDB databases, several DEPs identified in this study belong to functional classes of cancer-related genes, such as oncogenes and tumor suppressors, suggesting the involvement of these proteins in cancer development. Among

the oncogenes and tumor suppressors observed in the 675 general DEPs identified in the MBC case, the proteins encoded by *COL1A1, FH, HNRNPA2B1, HSP90AA1, KTN1, LCP1, MSN, MYH11, NONO, SDHB* and *SEPT9* genes were also observed in the list of the DEPs identified between the MPT x FPT tissues' comparison. The plastin-2 (*LCP1*) was shown to be relevant in the MBC due to its fold change values and its responsiveness to testosterone in androgen receptor (AR)-positive prostate and breast cancer cells (Lin et al., 2000). Importantly, the heat shock protein HSP 90-alpha (*HSP90AA1*), an isoform of heat shock 90 that increase its expression levels in the presence of cellular stress (Zuehlke et al., 2015), and myosin-11 (*MYH11*), a major contractile protein able to convert chemical energy into mechanical energy in presence of ATP (Wang et al., 2014), were observed in a number of the signaling pathways predicted in this study.

4.2 Protein network analysis of the identified differentially expressed proteins

A landscape of protein interactions involving the DEPs identified in this study suggests relevant and specific functional protein links to be further explored in the MBC research. According to the STRING database, the two predicted protein-protein interaction networks (with the 225 general DEPs observed among the MBC tissues and the 447 DEPs from MPT x FPT tissues' comparisons) presented high confidence scores and highlighted the biological connectivity of the identified DEPs into relevant processes in cancer biology. Fifty-nine DEPs were commonly observed in both of these networks including the ones encoded by *ACADSB, DCN, IARS2, LCP1, LUM, OGN, SERPIND1, TF* and *TTR* genes.

The protein networks generated by the IPA's analyses revealed relevant interaction partners among the DEPs observed in the groups' comparisons from the MBC patient (MPT x MNT and MPT x MLN). Interestingly, protein-protein interactions predicted in STRING database were also observed in these networks, suggesting that alterations in the expression levels of the DEPs identified in this study could affect the intricate connections that regulate several biological processes around recognized players in cancer development, such as the splicing factor U2AF 65 kDa subunit (*U2AF2*) (Silipo et al., 2015) and PI3K complex (Wong et al., 2010); *PARP1* (Rojo et al., 2012) and *NPM1* (Box et al., 2016); factor nuclear kappa B (NFkB) complex (Dolcet et al., 2005); *TP53* (Miller et al., 2005) and *TNF* (Bertazza and Mocellin, 2010).

4.3 Most affected signaling pathways by the differentially expressed proteins

IPA analysis conducted with the DEPs at 1.5 log2 fold change among the MBC tissues' comparisons identified distinct canonical signaling pathways. In the MPT x MNT tissues' comparison, 22 signaling pathways were identified as significant, some of them were associated with z-score activation values, allowing their prediction of activity status in the MPT compared to the MNT sample. On the other hand, the low number of DEPs in the MPT x MLN tissues' comparison resulted in the identification of two signaling associated pathways, without z-score predictions.

A number of the DEPs involved in the general signaling pathways identified in this study were among the largest fold change values observed for MBC case, including the ones encoded by *BPGM, CD36, CRABP2, CRYAB, FKBP4, GOT2, HSPH1, KRT18, MAOA, RPL6* and *STAT1* genes (in the MPT x MNT tissues' comparison) and *CARL, H1F0* and *MYH11* (MPT x MLN tissues' comparison). In addition, some of the DEPs identified in these signaling pathways were also differentially expressed between the male and female breast tumors, such as the ones encoded by *CES1, CRYAB, NSF, PRKDC* and *SERPIND1* genes.

The IPA analysis for the MPT x MNT tissues' comparison predicted the signaling pathways mediated by granzyme B, sirtuins, eIF2 and actin cytoskeleton as activated signaling in MPT compared to the MNT sample, while the ones related to eNOS and acute phase response (APR) were predicted as inhibited in the MPT tissue.

Granzymes belong to a group of cell death-inducing serine proteases that are released in cytotoxic granules of cytotoxic T lymphocytes (CTL) and natural killer (NK) cells (Lieberman, 2010). The signaling via both of granzymes A and B were identified in the MPT x MNT tissues' comparison, which were among the up-regulated DEPs observed in the MPT sample. Particularly, the granzyme B pathway was the most activated pathway in the MPT x MNT tissues' comparison, which could be mediated by the overexpression of proteins encoded by *LNMB1*, *NUMA1*, *PARP1* and *PRKDC* genes. Concordantly, the poly (ADP-ribose) polymerase-1 (*PARP1*) is described as a preferred substrate for several 'suicidal' proteases, including granzymes, and its proteolysis produces specific fragments recognized as PARP1-signature fragments, which represents biomarkers for specific patterns of protease activity in cell death programs (Chaitanya et al., 2010). Further, the DNA-dependent protein kinase catalytic subunit (*PRKDC*) has been described as substrate of granzyme B (Backes et al., 2005). Both of these proteins are known to be

overexpressed in breast cancer, as identified in the MPT compared to the MNT tissue. In addition, *PARP1* and *PRKDC* were also observed in the MPT x FPT tissues' comparison.

Sirtuins (SIRTs) are members of the highly conserved NAD(+)-dependent class III histone deacetylase family and are stress-responsive proteins that drive several cellular processes, such as the cell cycle progression, genome integrity, cell death and cell growth (O'Callaghan and Vassilopoulos, 2017). Sirtuins has been described with pivotal roles in the tumor metabolism by integrate cellular stress and nutrient status of tumor cells with coordinated metabolic outputs (German and Haigis, 2015). Among the DEPs involved in the sirtuins signaling, the ones encoded by *PARP1* and *PRKDC* were observed in our study. PARP acts in the DNA repair and maintenance of genomic integrity, and is also a NAD+ dependent enzyme (as the SIRT enzymes) involved in the same biological processes as SIRTs (Canto et al., 2013), thus PARPs and SIRTs may compete for the limiting NAD+ substrate (Houtkooper and Auwerx, 2012). Furthermore, SIRTs members interact with other proteins involved in the DNA repair and allow the efficient recruitment of double-strand break (DSB) repair proteins, such as the protein kinase DNA-activated, catalytic (*PRKDC*), a key mediator of the NHEJ pathway of DSB repair (Bosch-Presegue and Vaquero, 2011). Concordantly, protein-protein interaction between *PARP* and *PRKDC* was predicted in the IPA's network associated to cell death and survival, cell cycle, and cancer. In addition, the bisphosphoglycerate mutase *(BPGM*) and aspartate aminotransferase, mitochondrial (*GOT2*) were also related to sirtuins signaling and showed a largest fold change in the MPT x MNT tissues' comparison. These proteins are involved in the glycolysis and amino acid metabolism (Amelio et al., 2014; Oslund et al., 2017), processes critically involved in cell growth.

The eukaryotic translation initiation factors (eIFs), such as eIF2, act in the translation process and when deregulated can trigger the oncogenic progression (Ali et al., 2017). The protein eIF2 acts under stresses conditions, such as the proteotoxic stress (unfolded proteins) in the endoplasmic reticulum (ER stress), amino acid deprivation and exposition to oxidants, leading to impaired expression genes (Harding et al., 2003). In our data, all DEPs observed associated to the eIF2 signaling were up-regulated in MPT compared to the MNT tissue.

Another pathway predicted as activated in MPT compared to the MNT tissue was related to the actin cytoskeleton signaling, which involves a major network of proteins that affect cell growth, polarity, motility and survival, key networks for metastasis development (Stevenson et al., 2012). The main DEPs observed in association to this pathway included

ezrin (*EZR*), that regulate the local invasion and metastasis (Mak et al., 2012); fibronectin (*FN1*), associated with epithelial-mesenchymal transition (EMT) and invasive/ metastatic phenotypes (Li et al., 2017) and the myosins 9 and 11 (*MYH9* and *MYH11*, respectively), that are actin-dependent molecular motors involved in the cell contractility, endocytosis, vesicle trafficking, protein/RNA localization and cell signaling (Ouderkirk and Krendel, 2014). Among the myosins identified in this study, the myosin-11 presented differential expression in all the groups of tissues analyzed (MPT x MNT, MPT x MLN and MPT x FPT). This protein is involved in intracellular transport, cell migration, adhesion, signal transduction and has been associated to poor prognosis in breast cancer (Wang et al., 2014). In this study, this protein was related to the actin cytoskeleton signaling as well as to the signaling involving epithelial adherens junctions and tight junctions, in which the myosin-9 also plays a function. These cellular junctions contribute to the maintenance and integrity of normal adhesion, and when deregulated are associated to EMT, cancer progression and metastasis (Knights et al., 2012).

On the other hand, the endothelial nitric oxide synthase (eNOS) signaling was the most inhibited pathway in MPT compared to the MNT tissue. eNOS catalyzes the synthesis of nitric oxide (NO), a short-lived and pleiotropic molecule that acts as a signal transducer involved in numerous critical physiological processes (Burke et al., 2013). Different levels of NO in the tumor microenvironment present dichotomous effects in cancer biology, including apoptosis, cellular proliferation, migration, invasion and angiogenesis, and can promote or inhibit the growth tumor and metastasis (Burke et al., 2013; Choudhari et al., 2013; Zhang et al., 2016). In this study, the main DEPs involved in the eNOS signaling were the members of heat shock proteins (*HSPA5, HSPA8, HSPA9, HSP90AA1, HSP90AB1*), which were up-regulated in MPT compared to the MNT sample. These proteins are a large family of chaperones that acts in the protein folding and maturation protecting them from oxidative and thermal stresses, hypoxia and degradation, and are strongly implicated in cancer development and progression (Chatterjee and Burns, 2017).

Importantly, the proteins encoded by *HSP90AA1* and *HSP90AB1* genes act in several pivotal roles in the cancer development through other relevant signaling pathways identified in this study, such as the ones involving the aryl hydrocarbon receptor (AhR) (Feng et al., 2013), glucocorticoid receptor (Vilasco et al., 2011) and nitric oxide (NO) (Rizi et al., 2017).

Last, the acute phase response (APR), which associated DEPs observed down-regulated in the MPT when compared to the MNT sample, consists in a rapid reprogramming of gene expression and metabolism due to the inflammatory cytokine signaling (Venteclef et al., 2011). The DEPs observed in this pathway, including the cytokines angiotensinogen (*AGT*) and complement C5 (*C5*). The heparin cofactor II (*SERPIND1*), a serine proteinase inhibitor identified in this pathway, was also observed as a DEP in MPT x FPT tissues' comparison. This protein plays a role in the cell motility, invasion, filopodium dynamics and metastatic colonization (Liao et al., 2015). In breast cancer, however, its expression pattern remains unclear.

Importantly, in addition to the signaling pathways aforementioned, the DEPs from MPT x FPT tissues' comparison were also observed in the aldosterone signaling in epithelial cells (*CRYAB*), xenobiotic metabolism signaling (*CES1*) and in the tight junction signaling (*NSF*), which are relevant pathways that could impact in the cancer development directly or through their downstream effectors (Ashton et al., 2015; Martin and Jiang, 2009; Zanger and Schwab, 2013).

In the MPT x MLN tissues' comparison the significant signaling pathways affected by its DEPs were related to granzyme A, as discussed above, and to calcium.

The calcium signaling pathway was related to the proteins calreticulin (*CARL*) and myosin-11 (*MYH11*), which also were part of the IPA's networks involving the p53 protein (*TP53* gene) and tumor necrosis factor (TNF) and were also differentially expressed in the MPT x FPT tissues' comparison. Calreticulin has an important impact in the cancer development and their expression levels affects the cell proliferation, differentiation and angiogenic capacity, and its interaction with integrins impact on cell adhesion and ultimately in the metastasis (Lu et al., 2015)

Furthermore, an additional analysis using the DAVID platform was performed to explore the biological context of the DEPs observed between the MPT x FPT tissues' comparison since several of the main DEPs in this comparison did not appear in the signaling pathways aforementioned.

A selected number of 54 of these DEPs, were able to distinguish the MPT and FPT tissues. The main biological functions related to these DEPs included the cell adhesion-related processes, apoptosis, cellular stress response (proteotoxic stress and hypoxia), oxidation-reduction process and gene expression regulation. In addition, signal transduction involving known cancer-related drives, such as NFκβ, MAPK, p53, PI3K-Akt, Rho, TGFβ, Wnt were among the ones enriched for the DEPs. Our data also highlight the

proteins encoded by *AGR2, AHNAK, CD36, CRYAB, DCN, HSPA2, LCP1, PFN1, PRKDC, PTGIS, SLC9A3R1, THBS1, TNC* and *TNXB* genes as DEPs between the male and female breast tumors. Some of these proteins were previously described in cancer, most specifically in prostate cancer, which could indicate specific protein alterations in male associated cancers (Bu et al., 2011; Firlej et al., 2011; Lin et al., 2000; Rohde et al., 2005).

4.4 Upstream regulator analysis of the differentially expressed proteins

In addition to the pathways and their related DEPs, IPA's analyses allowed predicting the upstream regulators involved in the expression levels of the proteins identified in this study. Important cancer-related molecules were observed as potential regulators for the DEPs, such as MYC, CD3, CEBPB, PI3K complex, SMARCA4 and the anti-cancer chemical drugs 5-fluorouracil, dexamethasone, sirolimus (rapamycin) and tretinoin. Many of the relevant DEPs discussed in the groups' comparisons (MPT x MNT, MPT x MLN and MPT x FPT) above were related to these molecules.

5 Conclusion

The present study provides a new bioinformatics insight into MBC at a system biology level by integrating the LFQ-MS protein quantification method and functional annotation analysis. This integration lead to the identification of the main signaling pathways and interaction networks affected by the deregulated proteins observed among the malignant and non-tumor tissues of the reported MBC case. Our findings highlight the granzyme B and eNOS signaling as the most activated and inhibited pathways, respectively, observed in this reported case

The DEPs observed between the primary tumors of the male and female breast cancer could indicate cellular processes associated to the breast cancer biology in men.

Altogether, our data showed an overview of the MBC proteome landscape, which can contribute to improve the knowledge of the breast tumorigenesis in men, guiding further research in focused biomarkers. Relevant DEPs from all the groups' comparisons of this study were observed involved in several critical cellular processes and interaction

networks, highlighting their relevance in the MBC biology and their potential application in its clinical management.

Conflict of interest statement: None declared.

Acknowledgments

The authors would like to thank Federal University of Paraná, Hospital das Clínicas (Curitiba/BR), Hospital Nossa Senhora das Graças (Curitiba/BR) and Program for Technological Development in Tools for Health-PDTIS-FIOCRUZ for providing the technical infrastructure and professional assistance.

Financial support

This study was financed by the Coordenação de Aperfeiçoamento de Pessoal de Nível Superior - Brasil (CAPES) - Finance Code 001 and the CNPq/ Araucaria Research Foundation of Parana State (PRONEX/2012).

References

Ali, M.U., Ur Rahman, M.S., Jia, Z., Jiang, C., 2017. Eukaryotic translation initiation factors and cancer. Tumour biology : the journal of the International Society for Oncodevelopmental Biology and Medicine 39(6), 1010428317709805.

Amelio, I., Cutruzzola, F., Antonov, A., Agostini, M., Melino, G., 2014. Serine and glycine metabolism in cancer. Trends in biochemical sciences 39(4), 191-198.

Ashton, A.W., Le, T.Y., Gomez-Sanchez, C.E., Morel-Kopp, M.C., McWhinney, B., Hudson, A., Mihailidou, A.S., 2015. Role of Nongenomic Signaling Pathways Activated by Aldosterone During Cardiac Reperfusion Injury. Mol Endocrinol 29(8), 1144-1155.

Backes, C., Kuentzer, J., Lenhof, H.P., Comtesse, N., Meese, E., 2005. GraBCas: a bioinformatics tool for score-based prediction of Caspase- and Granzyme B-cleavage sites in protein sequences. Nucleic acids research 33(Web Server issue), W208-213.

Bertazza, L., Mocellin, S., 2010. The dual role of tumor necrosis factor (TNF) in cancer biology. Current medicinal chemistry 17(29), 3337-3352.

Bosch-Presegue, L., Vaquero, A., 2011. The dual role of sirtuins in cancer. Genes & cancer 2(6), 648-662.

Box, J.K., Paquet, N., Adams, M.N., Boucher, D., Bolderson, E., O'Byrne, K.J., Richard, D.J., 2016. Nucleophosmin: from structure and function to disease development. BMC molecular biology 17(1), 19.

Bu, H., Bormann, S., Schafer, G., Horninger, W., Massoner, P., Neeb, A., Lakshmanan, V.K., Maddalo, D., Nestl, A., Sultmann, H., Cato, A.C., Klocker, H., 2011. The anterior gradient 2 (AGR2) gene is overexpressed in prostate cancer and may be useful as a urine sediment marker for prostate cancer detection. The Prostate 71(6), 575-587.

Burke, A.J., Sullivan, F.J., Giles, F.J., Glynn, S.A., 2013. The yin and yang of nitric oxide in cancer progression. Carcinogenesis 34(3), 503-512.

Callari, M., Cappelletti, V., De Cecco, L., Musella, V., Miodini, P., Veneroni, S., Gariboldi, M., Pierotti, M.A., Daidone, M.G., 2011. Gene expression analysis reveals a different transcriptomic landscape in female and male breast cancer. Breast cancer research and treatment 127(3), 601-610.

Canto, C., Sauve, A.A., Bai, P., 2013. Crosstalk between poly(ADP-ribose) polymerase and sirtuin enzymes. Molecular aspects of medicine 34(6), 1168-1201.

Chaitanya, G.V., Steven, A.J., Babu, P.P., 2010. PARP-1 cleavage fragments: signatures of cell-death proteases in neurodegeneration. Cell communication and signaling : CCS 8, 31.

Chatterjee, S., Burns, T.F., 2017. Targeting Heat Shock Proteins in Cancer: A Promising Therapeutic Approach. International journal of molecular sciences 18(9).

Chen, X., Liu, X., Zhang, L., Li, S., Shi, Y., Tong, Z., 2013. Poorer survival of male breast cancer compared with female breast cancer patients may be due to biological differences. Japanese journal of clinical oncology 43(10), 954-963.

Choudhari, S.K., Chaudhary, M., Bagde, S., Gadbail, A.R., Joshi, V., 2013. Nitric oxide and cancer: a review. World journal of surgical oncology 11, 118.

Cox, J., Mann, M., 2008. MaxQuant enables high peptide identification rates, individualized p.p.b.-range mass accuracies and proteome-wide protein quantification. Nature biotechnology 26(12), 1367-1372.

Cutuli, B., Le-Nir, C.C., Serin, D., Kirova, Y., Gaci, Z., Lemanski, C., De Lafontan, B., Zoubir, M., Maingon, P., Mignotte, H., de Lara, C.T., Edeline, J., Penault-Llorca, F., Romestaing, P., Delva, C., Comet, B., Belkacemi, Y., 2010. Male breast cancer. Evolution of treatment and prognostic factors. Analysis of 489 cases. Critical reviews in oncology/hematology 73(3), 246-254.

Dolcet, X., Llobet, D., Pallares, J., Matias-Guiu, X., 2005. NF-kB in development and progression of human cancer. Virchows Archiv : an international journal of pathology 446(5), 475-482.

Feng, S., Cao, Z., Wang, X., 2013. Role of aryl hydrocarbon receptor in cancer. Biochimica et biophysica acta 1836(2), 197-210.

Fentiman, I.S., 2016. Male breast cancer is not congruent with the female disease. Critical reviews in oncology/hematology 101, 119-124.

Firlej, V., Mathieu, J.R., Gilbert, C., Lemonnier, L., Nakhle, J., Gallou-Kabani, C., Guarmit, B., Morin, A., Prevarskaya, N., Delongchamps, N.B., Cabon, F., 2011. Thrombospondin-1 triggers cell migration and development of advanced prostate tumors. Cancer research 71(24), 7649-7658.

Fitzmaurice, C., Allen, C., Barber, R.M., Barregard, L., Bhutta, Z.A., Brenner, H., Dicker, D.J., Chimed-Orchir, O., Dandona, R., Dandona, L., Fleming, T., Forouzanfar, M.H., Hancock, J., Hay, R.J., Hunter-Merrill, R., Huynh, C., Hosgood, H.D., Johnson, C.O., Jonas, J.B., Khubchandani, J., Kumar, G.A., Kutz, M., Lan, Q., Larson, H.J., Liang, X., Lim, S.S., Lopez, A.D., MacIntyre, M.F., Marczak, L., Marquez, N., Mokdad, A.H., Pinho, C., Pourmalek, F., Salomon, J.A., Sanabria, J.R., Sandar, L., Sartorius, B., Schwartz, S.M., Shackelford, K.A., Shibuya, K., Stanaway, J., Steiner, C., Sun, J., Takahashi, K., Vollset, S.E., Vos, T., Wagner, J.A., Wang, H., Westerman, R., Zeeb, H., Zoeckler, L.,

Abd-Allah, F., Ahmed, M.B., Alabed, S., Alam, N.K., Aldhahri, S.F., Alem, G., Alemayohu, M.A., Ali, R., Al-Raddadi, R., Amare, A., Amoako, Y., Artaman, A., Asayesh, H., Atnafu, N., Awasthi, A., Saleem, H.B., Barac, A., Bedi, N., Bensenor, I., Berhane, A., Bernabe, E., Betsu, B., Binagwaho, A., Boneya, D., Campos-Nonato, I., Castaneda-Orjuela, C., Catala-Lopez, F., Chiang, P., Chibueze, C., Chitheer, A., Choi, J.Y., Cowie, B., Damtew, S., das Neves, J., Dey, S., Dharmaratne, S., Dhillon, P., Ding, E., Driscoll, T., Ekwueme, D., Endries, A.Y., Farvid, M., Farzadfar, F., Fernandes, J., Fischer, F., TT, G.H., Gebru, A., Gopalani, S., Hailu, A., Horino, M., Horita, N., Husseini, A., Huybrechts, I., Inoue, M., Islami, F., Jakovljevic, M., James, S., Javanbakht, M., Jee, S.H., Kasaeian, A., Kedir, M.S., Khader, Y.S., Khang, Y.H., Kim, D., Leigh, J., Linn, S., Lunevicius, R., El Razek, H.M.A., Malekzadeh, R., Malta, D.C., Marcenes, W., Markos, D., Melaku, Y.A., Meles, K.G., Mendoza, W., Mengiste, D.T., Meretoja, T.J., Miller, T.R., Mohammad, K.A., Mohammadi, A., Mohammed, S., Moradi-Lakeh, M., Nagel, G., Nand, D., Le Nguyen, Q., Nolte, S., Ogbo, F.A., Oladimeji, K.E., Oren, E., Pa, M., Park, E.K., Pereira, D.M., Plass, D., Qorbani, M., Radfar, A., Rafay, A., Rahman, M., Rana, S.M., Soreide, K., Satpathy, M., Sawhney, M., Sepanlou, S.G., Shaikh, M.A., She, J., Shiue, I., Shore, H.R., Shrime, M.G., So, S., Soneji, S., Stathopoulou, V., Stroumpoulis, K., Sufiyan, M.B., Sykes, B.L., Tabares-Seisdedos, R., Tadese, F., Tedla, B.A., Tessema, G.A., Thakur, J.S., Tran, B.X., Ukwaja, K.N., Uzochukwu, B.S.C., Vlassov, V.V., Weiderpass, E., Wubshet Terefe, M., Yebyo, H.G., Yimam, H.H., Yonemoto, N., Younis, M.Z., Yu, C., Zaidi, Z., Zaki, M.E.S., Zenebe, Z.M., Murray, C.J.L., Naghavi, M., 2017. Global, Regional, and National Cancer Incidence, Mortality, Years of Life Lost, Years Lived With Disability, and Disability-Adjusted Life-years for 32 Cancer Groups, 1990 to 2015: A Systematic Analysis for the Global Burden of Disease Study. JAMA oncology 3(4), 524-548.

Forbes, S.A., Beare, D., Bindal, N., Bamford, S., Ward, S., Cole, C.G., Jia, M., Kok, C., Boutselakis, H., De, T., Sondka, Z., Ponting, L., Stefancsik, R., Harsha, B., Tate, J., Dawson, E., Thompson, S., Jubb, H., Campbell, P.J., 2016. COSMIC: High-Resolution Cancer Genetics Using the Catalogue of Somatic Mutations in Cancer. Current protocols in human genetics 91, 10 11 11-10 11 37.

German, N.J., Haigis, M.C., 2015. Sirtuins and the Metabolic Hurdles in Cancer. Current biology : CB 25(13), R569-583.

Harding, H.P., Zhang, Y., Zeng, H., Novoa, I., Lu, P.D., Calfon, M., Sadri, N., Yun, C., Popko, B., Paules, R., Stojdl, D.F., Bell, J.C., Hettmann, T., Leiden, J.M., Ron, D., 2003. An integrated stress response regulates amino acid metabolism and resistance to oxidative stress. Molecular cell 11(3), 619-633.

Houtkooper, R.H., Auwerx, J., 2012. Exploring the therapeutic space around NAD+. The Journal of cell biology 199(2), 205-209.

Huang da, W., Sherman, B.T., Lempicki, R.A., 2009. Systematic and integrative analysis of large gene lists using DAVID bioinformatics resources. Nature protocols 4(1), 44-57.

Humphries, M.P., Sundara Rajan, S., Honarpisheh, H., Cserni, G., Dent, J., Fulford, L., Jordan, L.B., Jones, J.L., Kanthan, R., Litwiniuk, M., Di Benedetto, A., Mottolese, M., Provenzano, E., Shousha, S., Stephens, M., Kulka, J., Ellis, I.O., Titloye, A.N., Hanby, A.M., Shaaban, A.M., Speirs, V., 2017. Characterisation of male breast cancer: a descriptive biomarker study from a large patient series. Scientific reports 7, 45293.

Kanehisa, M., Sato, Y., Kawashima, M., Furumichi, M., Tanabe, M., 2016. KEGG as a reference resource for gene and protein annotation. Nucleic acids research 44(D1), D457-462.

Knights, A.J., Funnell, A.P., Crossley, M., Pearson, R.C., 2012. Holding Tight: Cell Junctions and Cancer Spread. Trends in cancer research 8, 61-69.

Korde, L.A., Zujewski, J.A., Kamin, L., Giordano, S., Domchek, S., Anderson, W.F., Bartlett, J.M., Gelmon, K., Nahleh, Z., Bergh, J., Cutuli, B., Pruneri, G., McCaskill-Stevens, W., Gralow, J., Hortobagyi, G., Cardoso, F., 2010. Multidisciplinary meeting on male breast cancer: summary and research recommendations. Journal of clinical oncology : official journal of the American Society of Clinical Oncology 28(12), 2114-2122.

Kornegoor, R., Verschuur-Maes, A.H., Buerger, H., Hogenes, M.C., de Bruin, P.C., Oudejans, J.J., van der Groep, P., Hinrichs, B., van Diest, P.J., 2012. Molecular subtyping of male breast cancer by immunohistochemistry. Modern pathology : an official journal of the United States and Canadian Academy of Pathology, Inc 25(3), 398-404.

Kramer, A., Green, J., Pollard, J., Jr., Tugendreich, S., 2014. Causal analysis approaches in Ingenuity Pathway Analysis. Bioinformatics 30(4), 523-530.

Li, C.L., Yang, D., Cao, X., Wang, F., Hong, D.Y., Wang, J., Shen, X.C., Chen, Y., 2017. Fibronectin induces epithelial-mesenchymal transition in human breast cancer MCF-7 cells via activation of calpain. Oncology letters 13(5), 3889-3895.

Liao, W.Y., Ho, C.C., Hou, H.H., Hsu, T.H., Tsai, M.F., Chen, K.Y., Chen, H.Y., Lee, Y.C., Yu, C.J., Lee, C.H., Yang, P.C., 2015. Heparin co-factor II enhances cell motility and promotes metastasis in non-small cell lung cancer. The Journal of pathology 235(1), 50-64.

Liberzon, A., Birger, C., Thorvaldsdottir, H., Ghandi, M., Mesirov, J.P., Tamayo, P., 2015. The Molecular Signatures Database (MSigDB) hallmark gene set collection. Cell systems 1(6), 417-425.

Lieberman, J., 2010. Granzyme A activates another way to die. Immunological reviews 235(1), 93-104.

Lin, C.S., Lau, A., Yeh, C.C., Chang, C.H., Lue, T.F., 2000. Upregulation of L-plastin gene by testosterone in breast and prostate cancer cells: identification of three cooperative androgen receptor-binding sequences. DNA and cell biology 19(1), 1-7.

Lu, Y.C., Weng, W.C., Lee, H., 2015. Functional roles of calreticulin in cancer biology. BioMed research international 2015, 526524.

Mak, H., Naba, A., Varma, S., Schick, C., Day, A., SenGupta, S.K., Arpin, M., Elliott, B.E., 2012. Ezrin phosphorylation on tyrosine 477 regulates invasion and metastasis of breast cancer cells. BMC cancer 12, 82.

Manna, S.K., Patterson, A.D., Yang, Q., Krausz, K.W., Li, H., Idle, J.R., Fornace, A.J., Jr., Gonzalez, F.J., 2010. Identification of noninvasive biomarkers for alcohol-induced liver disease using urinary metabolomics and the Ppara-null mouse. Journal of proteome research 9(8), 4176-4188.

Martin, T.A., Jiang, W.G., 2009. Loss of tight junction barrier function and its role in cancer metastasis. Biochimica et biophysica acta 1788(4), 872-891.

Miller, L.D., Smeds, J., George, J., Vega, V.B., Vergara, L., Ploner, A., Pawitan, Y., Hall, P., Klaar, S., Liu, E.T., Bergh, J., 2005. An expression signature for p53 status in human breast cancer predicts mutation status, transcriptional effects, and patient survival. Proceedings of the National Academy of Sciences of the United States of America 102(38), 13550-13555.

O'Callaghan, C., Vassilopoulos, A., 2017. Sirtuins at the crossroads of stemness, aging, and cancer. Aging cell 16(6), 1208-1218.

Oslund, R.C., Su, X., Haugbro, M., Kee, J.M., Esposito, M., David, Y., Wang, B., Ge, E., Perlman, D.H., Kang, Y., Muir, T.W., Rabinowitz, J.D., 2017. Bisphosphoglycerate mutase controls serine pathway flux via 3-phosphoglycerate. Nature chemical biology 13(10), 1081-1087.

Ostasiewicz, P., Zielinska, D.F., Mann, M., Wisniewski, J.R., 2010. Proteome, phosphoproteome, and N-glycoproteome are quantitatively preserved in formalin-fixed paraffin-embedded tissue and analyzable by high-resolution mass spectrometry. Journal of proteome research 9(7), 3688-3700.

Ouderkirk, J.L., Krendel, M., 2014. Non-muscle myosins in tumor progression, cancer cell invasion, and metastasis. Cytoskeleton (Hoboken) 71(8), 447-463.

Rizi, B.S., Achreja, A., Nagrath, D., 2017. Nitric Oxide: The Forgotten Child of Tumor Metabolism. Trends in cancer 3(9), 659-672.

Robles, M.S., Cox, J., Mann, M., 2014. In-vivo quantitative proteomics reveals a key contribution of post-transcriptional mechanisms to the circadian regulation of liver metabolism. PLoS genetics 10(1), e1004047.

Rohde, M., Daugaard, M., Jensen, M.H., Helin, K., Nylandsted, J., Jaattela, M., 2005. Members of the heat-shock protein 70 family promote cancer cell growth by distinct mechanisms. Genes & development 19(5), 570-582.

Rojo, F., Garcia-Parra, J., Zazo, S., Tusquets, I., Ferrer-Lozano, J., Menendez, S., Eroles, P., Chamizo, C., Servitja, S., Ramirez-Merino, N., Lobo, F., Bellosillo, B., Corominas, J.M., Yelamos, J., Serrano, S., Lluch, A., Rovira, A., Albanell, J., 2012. Nuclear PARP-1 protein overexpression is associated with poor overall survival in early breast cancer. Annals of oncology : official journal of the European Society for Medical Oncology 23(5), 1156-1164.

Shaaban, A.M., Ball, G.R., Brannan, R.A., Cserni, G., Di Benedetto, A., Dent, J., Fulford, L., Honarpisheh, H., Jordan, L., Jones, J.L., Kanthan, R., Maraqa, L., Litwiniuk, M., Mottolese, M., Pollock, S., Provenzano, E., Quinlan, P.R., Reall, G., Shousha, S., Stephens, M., Verghese, E.T., Walker, R.A., Hanby, A.M., Speirs, V., 2012. A comparative biomarker study of 514 matched cases of male and female breast cancer reveals gender-specific biological differences. Breast cancer research and treatment 133(3), 949-958.

Silipo, M., Gautrey, H., Tyson-Capper, A., 2015. Deregulation of splicing factors and breast cancer development. Journal of molecular cell biology 7(5), 388-401.

Stevenson, R.P., Veltman, D., Machesky, L.M., 2012. Actin-bundling proteins in cancer progression at a glance. Journal of cell science 125(Pt 5), 1073-1079.

Syrine, A., Lhem, B., Meher, N., Olfa, A., Aida, G., Hatem, B., Hamouda, B., Khaled, R., Amor, G., 2017. Prognostic implications of the intrinsic molecular subtypes in male breast cancer. Journal of B.U.ON. : official journal of the Balkan Union of Oncology 22(2), 377-382.

Szklarczyk, D., Morris, J.H., Cook, H., Kuhn, M., Wyder, S., Simonovic, M., Santos, A., Doncheva, N.T., Roth, A., Bork, P., Jensen, L.J., von Mering, C., 2017. The STRING database in 2017: quality-controlled protein-protein association networks, made broadly accessible. Nucleic acids research 45(D1), D362-D368.

Thomas, P.D., Campbell, M.J., Kejariwal, A., Mi, H., Karlak, B., Daverman, R., Diemer, K., Muruganujan, A., Narechania, A., 2003. PANTHER: a library of protein families and subfamilies indexed by function. Genome research 13(9), 2129-2141.

Tyanova, S., Albrechtsen, R., Kronqvist, P., Cox, J., Mann, M., Geiger, T., 2016a. Proteomic maps of breast cancer subtypes. Nature communications 7, 10259.

Tyanova, S., Temu, T., Sinitcyn, P., Carlson, A., Hein, M.Y., Geiger, T., Mann, M., Cox, J., 2016b. The Perseus computational platform for comprehensive analysis of (prote)omics data. Nature methods 13(9), 731-740.

Venteclef, N., Jakobsson, T., Steffensen, K.R., Treuter, E., 2011. Metabolic nuclear receptor signaling and the inflammatory acute phase response. Trends in endocrinology and metabolism: TEM 22(8), 333-343.

Vilasco, M., Communal, L., Mourra, N., Courtin, A., Forgez, P., Gompel, A., 2011. Glucocorticoid receptor and breast cancer. Breast cancer research and treatment 130(1), 1-10.

Vizcaino, J.A., Csordas, A., Del-Toro, N., Dianes, J.A., Griss, J., Lavidas, I., Mayer, G., Perez-Riverol, Y., Reisinger, F., Ternent, T., Xu, Q.W., Wang, R., Hermjakob, H., 2016. 2016 update of the PRIDE database and its related tools. Nucleic acids research 44(22), 11033.

Wang, R.J., Wu, P., Cai, G.X., Wang, Z.M., Xu, Y., Peng, J.J., Sheng, W.Q., Lu, H.F., Cai, S.J., 2014. Down-regulated MYH11 expression correlates with poor prognosis in stage II and III colorectal cancer. Asian Pacific journal of cancer prevention : APJCP 15(17), 7223-7228.

Wisniewski, J.R., Zougman, A., Nagaraj, N., Mann, M., 2009. Universal sample preparation method for proteome analysis. Nature methods 6(5), 359-362.

Wong, K.K., Engelman, J.A., Cantley, L.C., 2010. Targeting the PI3K signaling pathway in cancer. Current opinion in genetics & development 20(1), 87-90.

Yuan, Y., Liu, L., Chen, H., Wang, Y., Xu, Y., Mao, H., Li, J., Mills, G.B., Shu, Y., Li, L., Liang, H., 2016. Comprehensive Characterization of Molecular Differences in Cancer between Male and Female Patients. Cancer cell 29(5), 711-722.

Zanger, U.M., Schwab, M., 2013. Cytochrome P450 enzymes in drug metabolism: regulation of gene expression, enzyme activities, and impact of genetic variation. Pharmacology & therapeutics 138(1), 103-141.

Zhang, L., Zeng, M., Fu, B.M., 2016. Inhibition of endothelial nitric oxide synthase decreases breast cancer cell MDA-MB-231 adhesion to intact microvessels under physiological flows. American journal of physiology. Heart and circulatory physiology 310(11), H1735-1747.

Zografos, E., Gazouli, M., Tsangaris, G., Marinos, E., 2016. The Significance of Proteomic Biomarkers in Male Breast Cancer. Cancer genomics & proteomics 13(3), 183-190.

Zuehlke, A.D., Beebe, K., Neckers, L., Prince, T., 2015. Regulation and function of the human HSP90AA1 gene. Gene 570(1), 8-16.

Figures

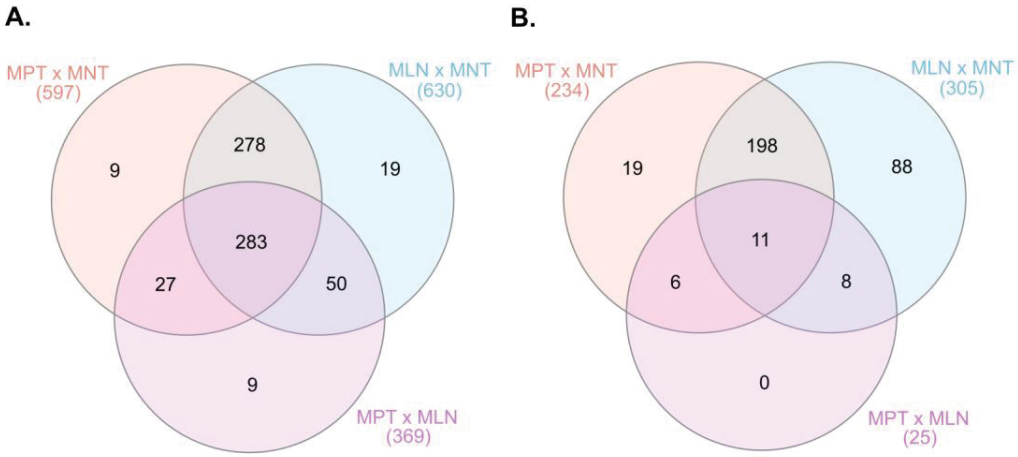

Fig. 1. Venn diagrams of the differentially expressed proteins observed among the comparisons of the MPT x MNT, MLN x MNT and MPT x MLN groups of samples of the male patient. **A.** Number of all proteins identified as differentially expressed among the groups' comparison. **B.** Number of up-regulated and down-regulated proteins (log2-fold change cut-off 1.5) observed among each group comparison.

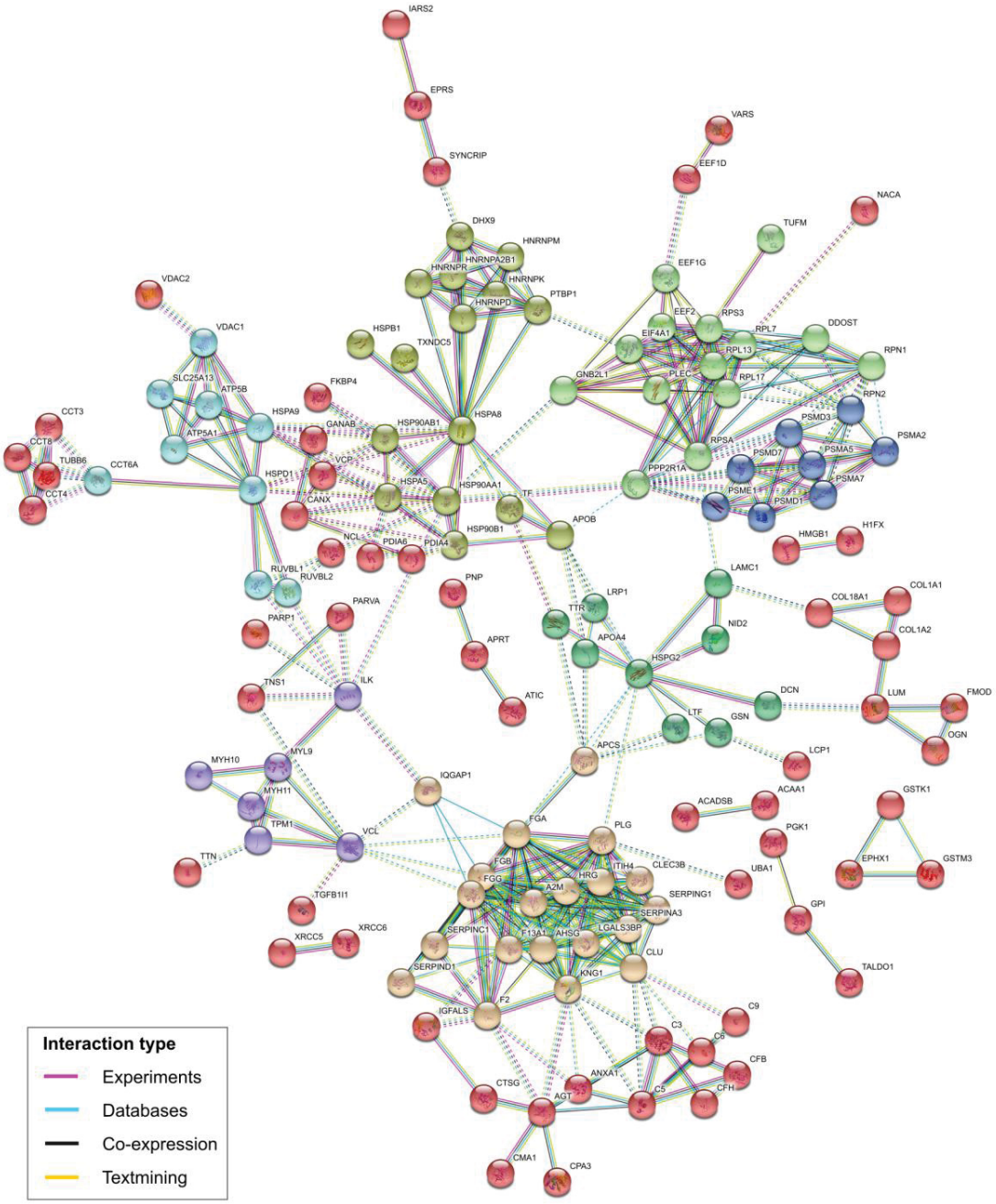

Fig. 2. Protein-protein interactions of the 225 differentially expressed proteins presenting gradual increased/decreased expression levels from MNT to MPT to MLN, predicted by STRING database v. 10.5. The colors of the nodes correspond to different clusters and inter-cluster edges are represented by dashed-lines.

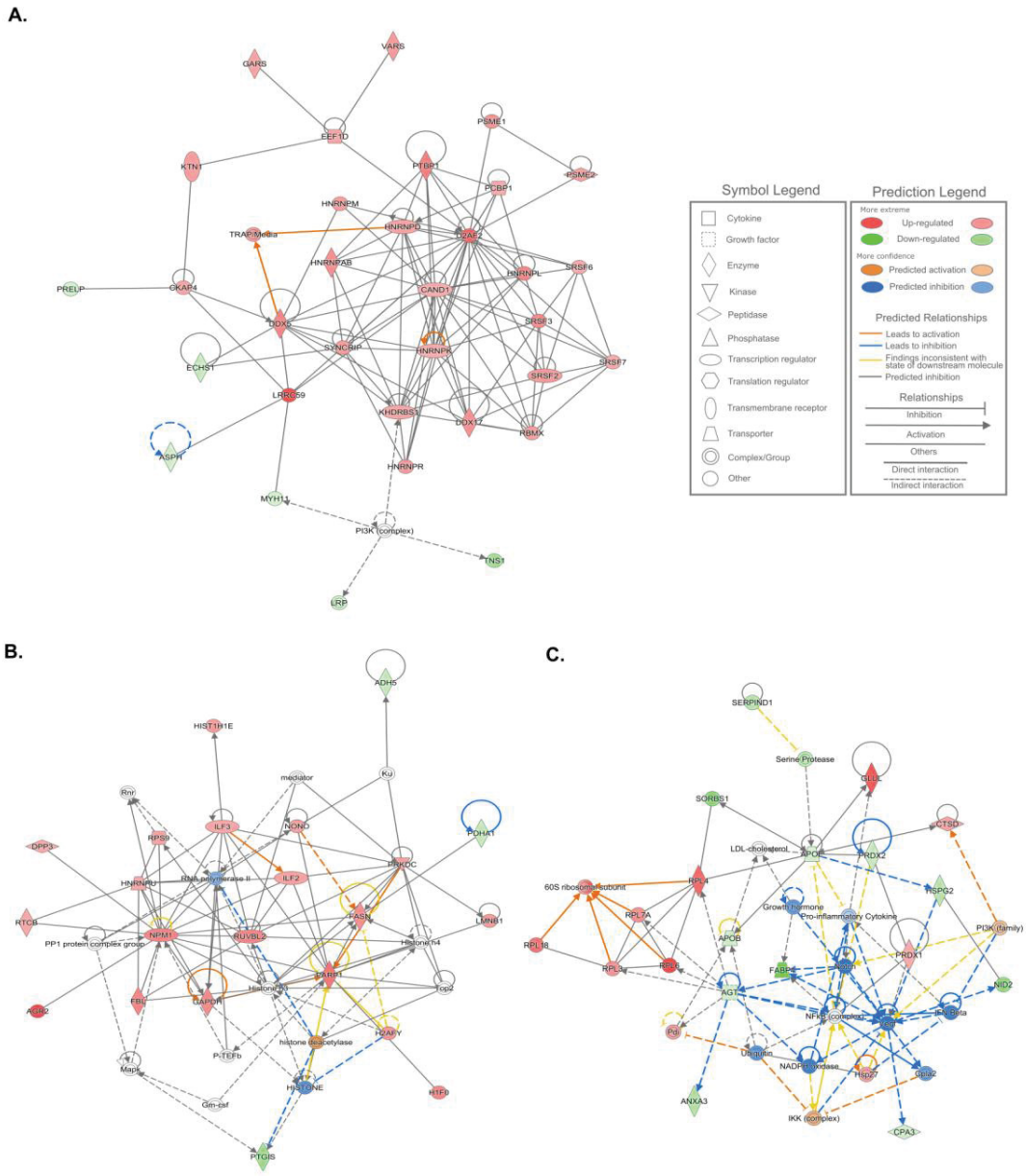

Fig. 3. Predicted protein interactive networks of the differentially expressed proteins observed among the MPT and MNT tissue samples, which are related to A. RNA post-transcriptional modification, molecular transport, and RNA trafficking; B. Cell death and survival, cell cycle, and cancer; C. Cardiovascular disease, organismal injury and abnormalities, and cancer.

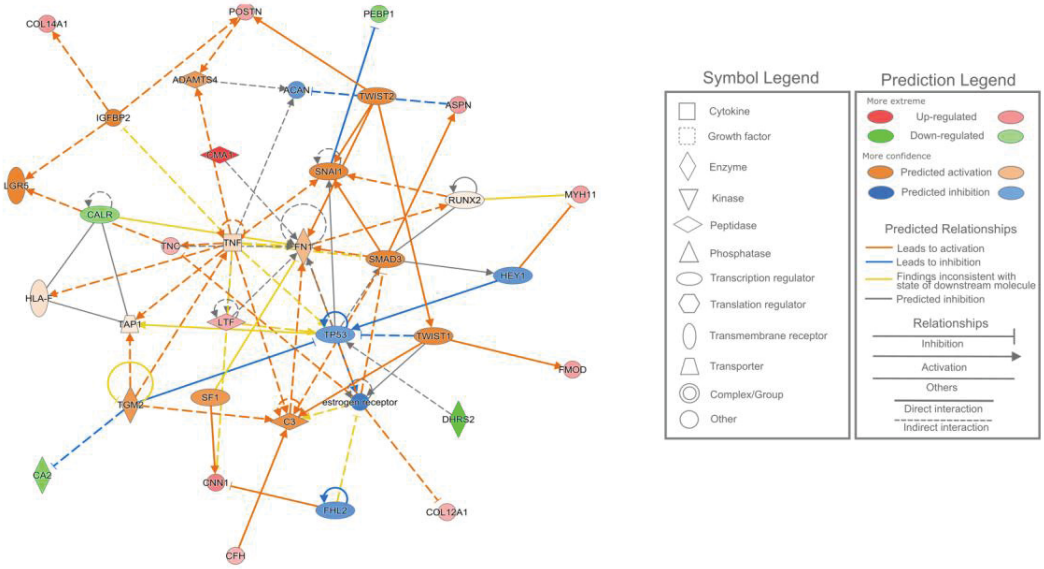

Fig. 4. Predicted protein interactive network of the differentially expressed proteins observed among the MPT and MLN tissue samples, related to cellular development, connective tissue development and function, and tissue development.

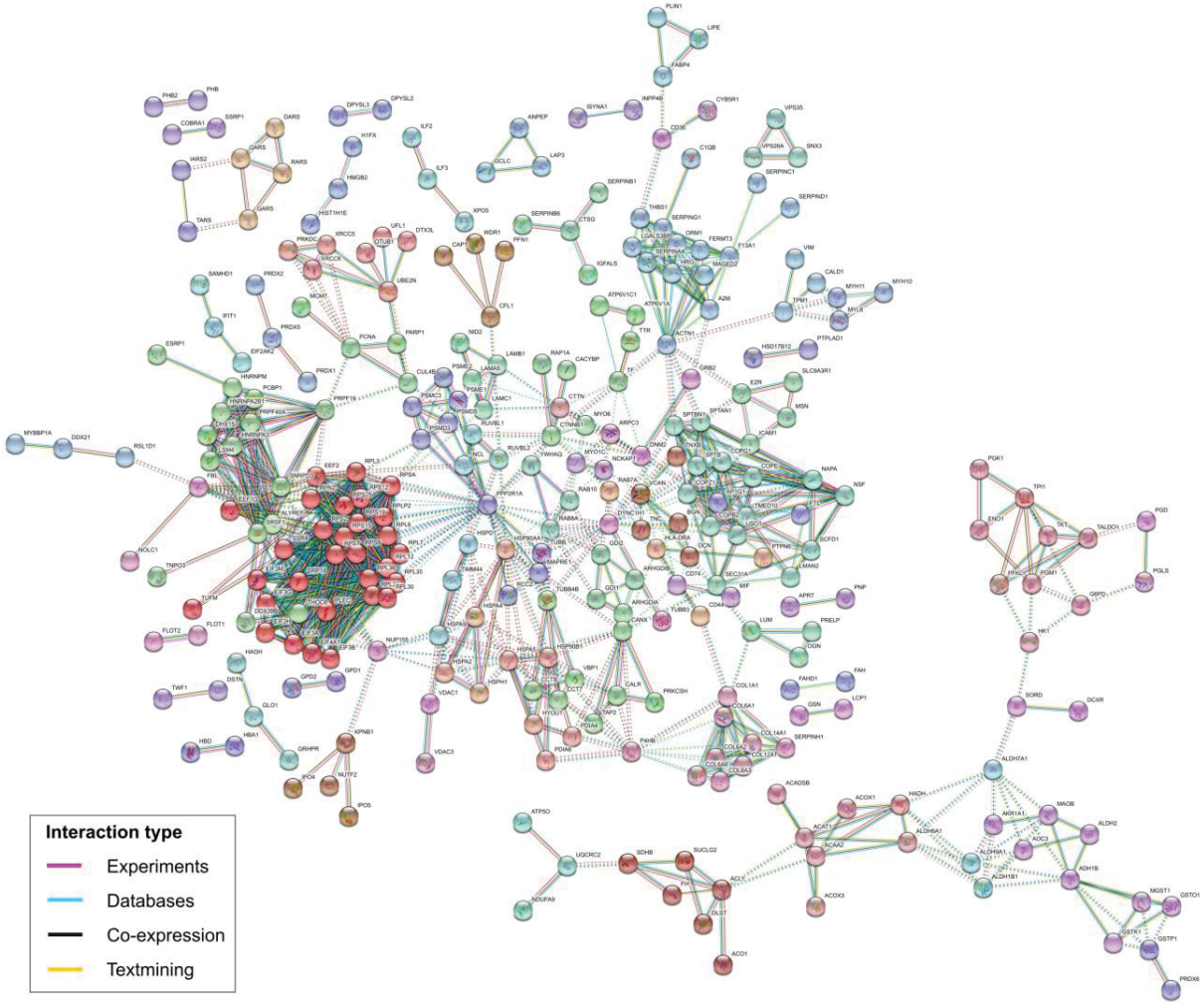

Fig. 5. Protein-protein interactions of the 447 differentially expressed proteins between male and female primary breast tumors, predicted by STRING database v. 10.5. The colors of the nodes correspond to different clusters and inter-cluster edges are represented by dashed-lines.

Tables

Table 1. Functional classes identified for the 675 differentially expressed proteins of the male breast cancer case (COSMIC v. 86 and MSigDB v. 6.2).

Functional class	Gene symbol
Tumor suppressors	*ATP1A1, CLTC, FH, MYH9, PPP2R1A, RPL5, SDHA, SDHB, SFPQ*
Oncogenes	*ATIC, ATP1A1, CALR, CLTC, COL1A1, DDX5, GNAS, HNRNPA2B1, HSP90AA1, HSP90AB1, IDH1, IDH2, KTN1, LASP1, LCP1, MSN, MYH11, MYH9, NACA, NONO, NPM1, NUMA1, PICALM, RPN1, SEPT9, SFPQ, SND1, SRSF2, SRSF3, TPM4, XPO1*
Protein kinases	*DCLK1, EIF2AK2, ILK, PRKACB, PRKDC, TTN*
Transcription factors	*C14orf166, CAND1, CBX3, CCT4, CORO1A, CRIP2, CSRP1, ENO1, HMGB1, HMGB2, ILF2, ILF3, PSMC5, PURA, SND1, STAT1, TGFB1I1*
Cytokines and growth factors	*AGT, C3, C5, CAT, CMA1, CTSG, GPI, NAMPT, OGN, TNC, TYMP*
Cell differentiation markers	*BCAM, CD14, CD36, ITGB1, LAMP1, LRP1, MCAM, SLC4A1*

Table 2. Differentially expressed proteins into the “Cancer” and “Breast cancer” annotations according to the Ingenuity Pathways Knowledge Base (IPA v. 2.3).

Disease	p-value	Gene symbol
Cancer	3.24E-06	*A1BG, ABHD14B, ACAA2, ACACB, ACADM, ACADS, ACADSB, ACO1, ACOT1, ACSL1, AEBP1, AFM, AGR2, AGT, AHSG, ALDH1A1, ALDH2, ALDH6A1, ALDOA, ANXA3, AP1G1, APOB, APOD, APOE, ARCN1, ASPH, ASS1, BLVRB, BPGM, C1S, C5, CA1, CA2, CACYBP, CALB2, CAND1, CAPG, CAT, CAV1, CAVIN1, CAVIN3, CBX3, CD36, CES1, CFH, CKAP4, CKB, CLEC3B, CNN1, COL12A1, COL18A1, COPB1, COPG1, CPA3, CRABP2, CRYAB, CSE1L, CSTA, CTSD, CYB5R1, DDX17, DDX39B, DDX5, DHRS2, DHX15, DPP3, DSP, ECHS1, ECI1, EEF1D, EFHD1, EFTUD2, EHD2, ETFB, EZR, F2, FABP4, FAH, FASN, FBL, FBN1, FGG, FKBP4, FMOD, FN1, GAPDH, GARS, GDI1, GLUL, GOT2, GPD1, GPD2, GPX3, H1F0, H2AFY, HADH, HBD, HDLBP, HIST1H1E, HNRNPA2B1, HNRNPAB, HNRNPD, HNRNPK, HNRNPL, HNRNPM, HNRNPR, HNRNPU, HP, HRG, HSP90AA1, HSP90AB1, HSPA12A, HSPA5, HSPA8, HSPA9, HSPB1, HSPD1, HSPG2, HSPH1, HYOU1, IGFALS, ILF2, ILF3, ILK, ITIH4, KHDRBS1, KNG1, KRT18, KTN1, LAMC1, LBP, LDHB, LMAN2, LMNB1, LRG1, LRP1, LRPPRC, LRRC59, LTF, MAOA, MCAM, MCCC2, MDH2, ME1, MTHFD1, MYH11, MYH9, MYO1C, NID2, NNMT, NNT, NONO, NPM1, NSF, NUMA1, OGN, ORM1, P4HB, PARP1, PARVA, PCBP1, PCYOX1, PDHA1, PDIA3, PGM1, PHB, PHGDH, PKM, PLG, PLIN1, PLIN4, PON1, POSTN, PRDX1, PRDX2, PRELP, PRKAR2B, PRKDC, PRPF8, PSME1, PSME2, PTBP1, PTGIS, RBMX, RBP4, RETSAT, RNPEP, RPL13, RPL18, RPL3, RPL4, RPL6, RPL7A, RPS9, RRBP1, RTCB, RUVBL2, SELENBP1, SERPIND1, SERPINF2, SLC25A1, SLC4A1, SLC9A3R1, SNRNP200, SORBS1, SORD, SPTBN1, SRSF2, SRSF6, SRSF7, STAT1, SYNCRIP, THBS1, TNC, TNS1, TNXB, TRAP1, TUBB, TUBB4B, TYMP, U2AF2, UGDH, UGP2, VARS*
Breast cancer	1.00E-06	*ACAA2, ACACB, ACOT1, AGR2, AGT, ALDH1A1, ALDOA, APOB, APOE, CAV1, CBX3, CES1, CKAP4, CKB, CNN1, COL12A1, CRABP2, CRYAB, CSE1L, CTSD, DDX39B, DHRS2, DHX15, DSP, EFTUD2, FASN, FBN1, FN1, GLUL, H2AFY, HNRNPM, HNRNPR, HP, HSP90AA1, HSP90AB1, HSPA5, HSPB1, HSPD1, HSPG2, ILF2, ILF3, ITIH4, KRT18, LBP, LRP1, LTF, MCAM, MYH11, MYH9, NID2, OGN, ORM1, P4HB, PARP1, PARVA, PCYOX1, PHB, PKM, PLG, POSTN, PRDX2, PRKDC, RBMX, RPL4, RTCB, SLC4A1, SLC9A3R1, STAT1, THBS1, TNC, TNS1, TNXB, TUBB, TUBB4B, TYMP, U2AF2, UGDH*

Table 3. Canonical signaling pathways predicted from the differentially expressed proteins between the primary breast tumor and non-tumor breast tissue of the male breast cancer case (IPA v. 2.3).

Ingenuity canonical pathways	p-value	Ratio	Gene symbol
Acute Phase Response Signaling**	1.58E-12	1.07E-01	*AGT, AHSG, C1S, C5, CRABP2, F2, FGG, FN1, HNRNPK, HP, HRG, ITIH4, LBP, ORM1, PLG, RBP4, SERPIND1, SERPINF2*
Aldosterone Signaling in Epithelial Cells	7.41E-07	7.19E-02	*CRYAB, HSP90AA1, HSP90AB1, HSPA12A, HSPA5, HSPA8, HSPA9, HSPB1, HSPD1, HSPH1, PDIA3, TRAP1*
Granzyme B Signaling*	3.09E-05	2.5E-01	*LMNB1, NUMA1, PARP1, PRKDC*
eNOS Signaling**	1.58E-04	5.45E-02	*CAV1, HSP90AA1, HSP90AB1, HSPA5, HSPA8, HSPA9, KNG1, PRKAR2A, PRKAR2B*
IL-12 Signaling and Production in Macrophages	3.24E-04	5.56E-02	*APOB, APOD, APOE, ORM1, PCYOX1, PON1, RBP4, STAT1*
Clathrin-mediated Endocytosis Signaling	6.03E-04	4.55E-02	*APOB, APOD, APOE, F2, HSPA8, ORM1, PCYOX1, PON1, RBP4*
eIF2 Signaling*	9.77E-04	4.25E-02	*HSPA5, PTBP1, RPL13, RPL18, RPL3, RPL4, RPL6, RPL7A, RPS9*
Aryl Hydrocarbon Receptor Signaling	1.17E-03	5.15E-02	*ALDH1A1, ALDH2, ALDH6A1, CTSD, HSP90AA1, HSP90AB1, HSPB1*
Caveolar-mediated Endocytosis Signaling	1.51E-03	7.04E-02	*ARCN1, CAV1, CAVIN1,COPB1, COPG1*
NO Signaling in the Cardiovascular System	1.78E-03	5.56E-02	*CAV1, HSP90AA1, HSP90AB1, KNG1, PRKAR2A, PRKAR2B*
Sertoli Cell-Sertoli Cell Junction Signaling	4.57E-03	4.05E-02	*ILK, PRKAR2A, PRKAR2B, SORBS1, SPTBN1, TUBB, TUBB4B*
Glucocorticoid Receptor Signaling	6.92E-03	2.98E-02	*AGT, FGG, FKBP4, HSP90AA1, HSP90AB1, HSPA5, HSPA8, HSPA9, KRT18, STAT1*
ILK Signaling	8.13E-03	3.63E-02	*DSP, FN1, ILK, KRT18, MYH11, MYH9, PARVA*
Actin Cytoskeleton Signaling*	1.62E-02	3.17E-02	*EZR, F2, FN1, KNG1, LBP, MYH11, MYH9*
Xenobiotic Metabolism Signaling	1.62E-02	2.93E-02	*ALDH1A1, ALDH2, ALDH6A1, CAT, CES1, HSP90AA1, HSP90AB1, MAOA*
Granzyme A Signaling	1.70E-02	1.18E-01	*H1F0, HIST1H1E*
Sirtuin Signaling Pathway*	1.95E-02	2.83E-02	*BPGM, GOT2, H1F0, HIST1H1E, LDHB, PARP1, PDHA1, PRKDC*
Gap Junction Signaling	2.63E-02	3.14E-02	*CAV1, PDIA3, PRKAR2A, PRKAR2B, TUBB, TUBB4B*
Epithelial Adherens Junction Signaling	2.75E-02	3.5E-02	*MYH9, MYH11, SORBS1, TUBB, TUBB4B*
Sonic Hedgehog Signaling	4.57E-02	6.9E-02	*PRKAR2A, PRKAR2B*
Tight Junction Signaling	4.79E-02	3.01E-02	*MYH9, MYH11, NSF, PRKAR2A, PRKAR2B*

Note: Signaling pathways predicted as activated (*) and inhibited (**) in PT compared to the NT sample, according to the z-score values. The ratio refers to the number of the DEPs that map to the pathway listed divided by the total number of molecules that define the canonical pathway from IPA.

Table 4. Functional classes identified for the 447 differentially expressed proteins between the male and female breast tumors (COSMIC v. 86 and MSigDB v. 6.2).

Functional class	Gene symbol
Tumor suppressors	*ATP1A1, DNM2, FBLN2, FH, NDRG1, PPP2R1A, PTPN6, SDHB*
Oncogenes	*ATP1A1, CALR, CD74, COL1A1, CTNNB1, HNRNPA2B1, HSP90AA1, KTN1, LCP1, MSI2, MSN, MYH11, NONO, SEPT9, TNC, TOP1*
Protein kinases	*EIF2AK2, PRKDC, TRIM28, TWF1*
Transcription factors	*CAND1, CRIP2, TNNB1, NO1, HMGB2, ILF2, ILF3, MYBBP1A, PURA, SSRP1, TRIM28*
Cytokines and growth factors	*CTSG, MIF, OGN, TNC*
Cell differentiation markers	*ANPEP, CD36, CD44, CD74, ICAM1, LAMP2, MRC2, SLC3A2, SLC4A1*

Table 5. Main biological processes according to the enriched GO terms ($p<0.05$) from the differentially expressed proteins between the male and female breast tumors (DAVID v. 6.8).

Biological functions	Gene symbol
Actin cytoskeleton	*LCP1, PALLD, PFN1, SLC9A3R1, TNXB,*
Cell adhesion	*AGR2, AHNAK, CD36, PFN1, THBS1, TNC, TNXB, USO1, VAPB*
Angiogenesis	*BGN, DCN, PTGIS, THBS1*
Apoptosis	*AGR2, CACYBP, CD36, CRYAB, DHRS2, GLO1, PRKDC, PTGIS, SLC9A3R1, THBS1*
Cell cycle	*HSPA2, PHGDH, PRKDC, THBS1*
Cell proliferation	*DHRS2, SLC9A3R1, THBS1, TNC*
DNA repair	*HIST1H4A, PRKDC*
Extracellular matrix (ECM)	*BGN, DCN, LCP1, LUM, PRKDC, THBS1, TNC, TNXB, TTR,*
ECM-receptor interaction	*CD36, THBS1, TNC, TNXB*
Gene expression	*AGR2, CRYAB, DCN, FABP4, GLO1, HIST1H4A, LUM, PFN1, PHGDH, TNC*
Hypoxia	*CRYAB, PTGIS, THBS1*
Oxidation-reduction process	*CYB5A, CYB5R1, DHRS2, PHGDH, PTGIS, SORD*
Migration process	*LCP1, PALLD, PFN1, SLC9A3R1, TNC*
Proteotoxic stress	*AGR2, CRYAB, HSPA2, SEC63, THBS1, VAPB*
Xenobiotic metabolism	*ATP1A1, CES1, DHRS2, SORD*
Wound healing	*DNC, LCP1, TNC*

Table 6. Main signaling pathways according to the enriched KEGG pathways ($p<0.05$) from the differentially expressed proteins between the male and female breast tumors (DAVID v. 6.8).

Signaling pathway	Gene symbol
EGFR receptor signaling pathway	*AGR2*
I-kappaB kinase/ NF-kappaB signaling	*CD36, HACD3*
MAPK signaling pathway	*HSPA2*
Nitric oxide mediated signal transduction	*CD36, THBS1*
p53 signaling pathway	*THBS1*
PI3K-Akt signaling pathway	*THBS1, TNC, TNXB*
Rac protein signal transduction	*HACD3*
Rho protein signal transduction	*HACD3*
TFG-beta signaling pathway	*DCN, THBS1*
Wnt signaling pathway	*CACYBP, PFN1, SLC9A3R1*

8 CONCLUSÃO

Neste estudo, a espectrometria de massa com quantificação livre de marcação (LFQ-MS) permitiu a identificação de proteínas com diferenças significativas de expressão entre amostras de tecidos que representam a glândula mamária saudável (NCT e NA) e a progressão da tumorigênese mamária, incluindo os sítios primário e metastático da doença (TP e LN). Assim, com base nos valores de intensidade LFQ das proteínas nos diferentes tecidos, foi possível avaliar o padrão de expressão destas em diferentes grupos comparativos.

Os resultados observados permitiram descrever o proteoma diferencial entre os tecidos analisados, destacando-se no capítulo I: a alta similaridade no nível proteômico entre ambos os tecidos não tumorais, refletindo em conjuntos de proteínas diferencialmente expressas semelhantes quando comparados aos tecidos malignos (TP e/ou LN); e os perfis proteômicos similares entre estes últimos, indicando que sítios primários e metastáticos compartilham alterações de expressão proteica, que podem ter função na progressão tumoral. No capítulo II foram observadas similaridades entre os proteomas dos tecidos malignos e relevantes diferenças significativas de expressão proteica entre os tumores masculino e feminino, as quais, por sua vez, podem indicar alvos para o estudo no câncer de mama masculino.

As plataformas computacionais e seus recursos de anotação/ enriquecimento funcional e de predição de redes de interação proteica permitiram a identificação dos contextos biológicos de atuação das proteínas diferencialmente expressas e de suas interações proteicas, ressaltando aspectos e moléculas relevantes na tumorigênese mamária.

Assim, para cada grupo amostral, as análises proteômicas comparativas forneceram um panorama do proteoma diferencial do câncer de mama (feminino e masculino), contribuindo para elucidar o repertório proteômico bem como vias, funções e processos biológicos de relevância para estudos adicionais no câncer de mama.

9 PERSPECTIVAS

Este estudo fornece um repertório de moléculas, interações, vias, funções e processos biológicos que podem ser investigados mais profundamente no câncer de mama objetivando a obtenção de marcadores moleculares que possam discriminar o tecido tumoral e, consequentemente, auxiliar na abordagem clínica do paciente.

Com os dados proteômicos obtidos, serão selecionados alvos de interesse para a validação da expressão proteica bem como de possíveis interações preditas entre proteínas (e outras moléculas) e reguladores *upstream*, contribuindo para elucidar mecanismos moleculares subjacentes ao contexto biológico de atuação de determinadas proteínas diferencialmente expressas no câncer de mama.

Dessa forma, pretende-se utilizar diversas técnicas moleculares e ensaios funcionais para analisar e compreender o panorama de alvos que regulam e são regulados por proteínas consideradas de relevância neste estudo, avaliando o impacto funcional de alterações na disponibilidade desses componentes em vias biológicas e/ou processos celulares importantes no desenvolvimento e progressão tumoral. Estudos de interatoma baseados em coimunoprecipitação e espectrometria de massa serão realizados por nosso grupo de pesquisa para avaliar as proteínas que interagem diretamente com as de interesse.

Considerando este estudo como a etapa de implementação da abordagem proteômica de alta resolução no LabCHO, novos estudos baseados nesse método serão desenvolvidos para avaliar o perfil proteômico dos subtipos moleculares do câncer de mama (em tecidos e linhagens celulares), fornecendo proteínas diferencialmente expressas e seu contexto biológico para ampliar a compreensão das diferenças proteômicas e seu impacto funcional frente à heterogeneidade molecular da doença e fundamentar outros estudos desenvolvidos por nosso grupo de pesquisa.

REFERÊNCIAS

AHMED, F. E. Utility of mass spectrometry for proteome analysis: part I. Conceptual and experimental approaches. **Expert Rev Proteomics,** v. 5, n. 6, p. 841-64, Dec 2008. ISSN 1744-8387 (Electronic)
1478-9450 (Linking). Disponível em: < http://www.ncbi.nlm.nih.gov/pubmed/19086863 >.

_____. Utility of mass spectrometry for proteome analysis: part II. Ion-activation methods, statistics, bioinformatics and annotation. **Expert Rev Proteomics,** v. 6, n. 2, p. 171-97, Apr 2009. ISSN 1744-8387 (Electronic)
1478-9450 (Linking). Disponível em: < http://www.ncbi.nlm.nih.gov/pubmed/19385944 >.

ALBINI, A.; MIRISOLA, V.; PFEFFER, U. Metastasis signatures: genes regulating tumor-microenvironment interactions predict metastatic behavior. **Cancer Metastasis Rev,** v. 27, n. 1, p. 75-83, Mar 2008. ISSN 0167-7659 (Print)
0167-7659 (Linking). Disponível em: < http://www.ncbi.nlm.nih.gov/pubmed/18046511 >.

ALI, M. U. ET AL. Eukaryotic translation initiation factors and cancer. **Tumour Biol,** v. 39, n. 6, p. 1010428317709805, Jun 2017. ISSN 1423-0380 (Electronic)
1010-4283 (Linking). Disponível em: < http://www.ncbi.nlm.nih.gov/pubmed/28653885 >.

ALTEVOGT, P.; DOBERSTEIN, K.; FOGEL, M. L1CAM in human cancer. **Int J Cancer,** v. 138, n. 7, p. 1565-76, Apr 1 2016. ISSN 1097-0215 (Electronic)
0020-7136 (Linking). Disponível em: < http://www.ncbi.nlm.nih.gov/pubmed/26111503 >.

ALTO, L. T.; TERMAN, J. R. Semaphorins and their Signaling Mechanisms. **Methods Mol Biol,** v. 1493, p. 1-25, 2017. ISSN 1940-6029 (Electronic)
1064-3745 (Linking). Disponível em: < http://www.ncbi.nlm.nih.gov/pubmed/27787839 >.

AMERICAN CANCER SOCIETY. **Breast Cancer Facts & Figures 2017-2018.** , Atlanta, 2017. Disponível em: < https://www.cancer.org/content/dam/cancer-org/research/cancer-facts-and-statistics/breast-cancer-facts-and-figures/breast-cancer-facts-and-figures-2017-2018.pdf >.

AMERICAN CANCER SOCIETY. **Breast Cancer in Men - Risk Factors for Breast Cancer in Men**, April 27, 2018, 2019. Disponível em: < https://www.cancer.org/cancer/breast-cancer-in-men/causes-risks-prevention/risk-factors.html >.

ANDERSSON, T. ET AL. Automating MALDI sample plate loading. **J Proteome Res,** v. 6, n. 2, p. 894-6, Feb 2007. ISSN 1535-3893 (Print)
1535-3893 (Linking). Disponível em: < http://www.ncbi.nlm.nih.gov/pubmed/17269747 >.

ANGIOLINI, F.; CAVALLARO, U. The Pleiotropic Role of L1CAM in Tumor Vasculature. **Int J Mol Sci,** v. 18, n. 2, Jan 26 2017. ISSN 1422-0067 (Electronic)
1422-0067 (Linking). Disponível em: < http://www.ncbi.nlm.nih.gov/pubmed/28134764 >.

ASHBURNER, M. ET AL. Gene ontology: tool for the unification of biology. The Gene Ontology Consortium. **Nat Genet,** v. 25, n. 1, p. 25-9, May 2000. ISSN 1061-4036 (Print)
1061-4036 (Linking). Disponível em: < http://www.ncbi.nlm.nih.gov/pubmed/10802651 >.

BAKRY, R. ET AL. Protein profiling for cancer biomarker discovery using matrix-assisted laser desorption/ionization time-of-flight mass spectrometry and infrared imaging: a review. **Anal Chim Acta,** v. 690, n. 1, p. 26-34, Mar 25 2011. ISSN 1873-4324 (Electronic)
0003-2670 (Linking). Disponível em: < http://www.ncbi.nlm.nih.gov/pubmed/21414433 >.

BARABASI, A. L.; OLTVAI, Z. N. Network biology: understanding the cell's functional organization. **Nat Rev Genet,** v. 5, n. 2, p. 101-13, Feb 2004. ISSN 1471-0056 (Print)
1471-0056 (Linking). Disponível em: < http://www.ncbi.nlm.nih.gov/pubmed/14735121 >.

BEN-BARUCH, A. Site-specific metastasis formation: chemokines as regulators of tumor cell adhesion, motility and invasion. **Cell Adh Migr,** v. 3, n. 4, p. 328-33, Oct-Dec 2009. ISSN 1933-6926 (Electronic)
1933-6918 (Linking). Disponível em: < http://www.ncbi.nlm.nih.gov/pubmed/19550136 >.

BERETOV, J. ET AL. Proteomic Analysis of Urine to Identify Breast Cancer Biomarker Candidates Using a Label-Free LC-MS/MS Approach. **PLoS One,** v. 10, n. 11, p. e0141876, 2015. ISSN 1932-6203 (Electronic)
1932-6203 (Linking). Disponível em: < http://www.ncbi.nlm.nih.gov/pubmed/26544852 >.

BERGGARD, T.; LINSE, S.; JAMES, P. Methods for the detection and analysis of protein-protein interactions. **Proteomics,** v. 7, n. 16, p. 2833-42, Aug 2007. ISSN 1615-9853 (Print)
1615-9853 (Linking). Disponível em: < http://www.ncbi.nlm.nih.gov/pubmed/17640003 >.

BERKEY, C. S. ET AL. Relation of childhood diet and body size to menarche and adolescent growth in girls. **Am J Epidemiol,** v. 152, n. 5, p. 446-52, Sep 1 2000. ISSN 0002-9262 (Print)
0002-9262 (Linking). Disponível em: < http://www.ncbi.nlm.nih.gov/pubmed/10981459 >.

BHARTI, R. ET AL. Differential expression of IL-6/IL-6R and MAO-A regulates invasion/angiogenesis in breast cancer. **Br J Cancer,** v. 118, n. 11, p. 1442-1452, May 2018. ISSN 1532-1827 (Electronic)
0007-0920 (Linking). Disponível em: < http://www.ncbi.nlm.nih.gov/pubmed/29695771 >.

BOMBONATI, A.; SGROI, D. C. The molecular pathology of breast cancer progression. **J Pathol,** v. 223, n. 2, p. 307-17, Jan 2011. ISSN 1096-9896 (Electronic)
0022-3417 (Linking). Disponível em: < http://www.ncbi.nlm.nih.gov/pubmed/21125683 >.

BOTLAGUNTA, M. ET AL. Oncogenic role of DDX3 in breast cancer biogenesis. **Oncogene,** v. 27, n. 28, p. 3912-22, Jun 26 2008. ISSN 1476-5594 (Electronic)
0950-9232 (Linking). Disponível em: < http://www.ncbi.nlm.nih.gov/pubmed/18264132 >.

BRAY, F. ET AL. Global cancer statistics 2018: GLOBOCAN estimates of incidence and mortality worldwide for 36 cancers in 185 countries. **CA Cancer J Clin,** v. 68, n. 6, p. 394-424, Nov 2018. ISSN 1542-4863 (Electronic)
0007-9235 (Linking). Disponível em: < http://www.ncbi.nlm.nih.gov/pubmed/30207593 >.

BROHEE, S.; VAN HELDEN, J. Evaluation of clustering algorithms for protein-protein interaction networks. **BMC Bioinformatics,** v. 7, p. 488, Nov 6 2006. ISSN 1471-2105 (Electronic)
1471-2105 (Linking). Disponível em: < http://www.ncbi.nlm.nih.gov/pubmed/17087821 >.

BUSSARD, K. M. ET AL. Tumor-associated stromal cells as key contributors to the tumor microenvironment. **Breast Cancer Res,** v. 18, n. 1, p. 84, Aug 11 2016. ISSN 1465-542X (Electronic)
1465-5411 (Linking). Disponível em: < http://www.ncbi.nlm.nih.gov/pubmed/27515302 >.

CAFARELLI, T. M. ET AL. Mapping, modeling, and characterization of protein-protein interactions on a proteomic scale. **Curr Opin Struct Biol,** v. 44, p. 201-210, Jun 2017. ISSN 1879-033X (Electronic)
0959-440X (Linking). Disponível em: < http://www.ncbi.nlm.nih.gov/pubmed/28575754 >.

CAI, J. ET AL. Tenascin-C Modulates Cell Cycle Progression to Enhance Tumour Cell Proliferation through AKT/FOXO1 Signalling in Pancreatic Cancer. **J Cancer,** v. 9, n. 23, p. 4449-4462, 2018. ISSN 1837-9664 (Print)
1837-9664 (Linking). Disponível em: < http://www.ncbi.nlm.nih.gov/pubmed/30519351 >.

CALVO, K. R.; LIOTTA, L. A.; PETRICOIN, E. F. Clinical proteomics: from biomarker discovery and cell signaling profiles to individualized personal therapy. **Biosci Rep,** v. 25, n. 1-2, p. 107-25, Feb-Apr 2005. ISSN 0144-8463 (Print)

0144-8463 (Linking). Disponível em: < http://www.ncbi.nlm.nih.gov/pubmed/16222423 >.

CAMPBELL, L. L.; POLYAK, K. Breast tumor heterogeneity: cancer stem cells or clonal evolution? **Cell Cycle,** v. 6, n. 19, p. 2332-8, Oct 1 2007. ISSN 1551-4005 (Electronic)
1551-4005 (Linking). Disponível em: < http://www.ncbi.nlm.nih.gov/pubmed/17786053 >.

CAMPS, J. ET AL. Loss of lamin B1 results in prolongation of S phase and decondensation of chromosome territories. **FASEB J,** v. 28, n. 8, p. 3423-34, Aug 2014. ISSN 1530-6860 (Electronic)
0892-6638 (Linking). Disponível em: < http://www.ncbi.nlm.nih.gov/pubmed/24732130 >.

CANCEMI, P. ET AL. A multiomics analysis of S100 protein family in breast cancer. **Oncotarget,** v. 9, n. 49, p. 29064-29081, Jun 26 2018. ISSN 1949-2553 (Electronic)
1949-2553 (Linking). Disponível em: < http://www.ncbi.nlm.nih.gov/pubmed/30018736 >.

CHA, S. ET AL. In situ proteomic analysis of human breast cancer epithelial cells using laser capture microdissection: annotation by protein set enrichment analysis and gene ontology. **Mol Cell Proteomics,** v. 9, n. 11, p. 2529-44, Nov 2010. ISSN 1535-9484 (Electronic)
1535-9476 (Linking). Disponível em: < http://www.ncbi.nlm.nih.gov/pubmed/20739354 >.

CHAKRABORTY, S. ET AL. Onco-Multi-OMICS Approach: A New Frontier in Cancer Research. **Biomed Res Int,** v. 2018, p. 9836256, 2018. ISSN 2314-6141 (Electronic). Disponível em: < http://www.ncbi.nlm.nih.gov/pubmed/30402498 >.

CHEN, E. I.; YATES, J. R., 3RD. Cancer proteomics by quantitative shotgun proteomics. **Mol Oncol,** v. 1, n. 2, p. 144-59, Sep 2007. ISSN 1878-0261 (Electronic)
1574-7891 (Linking). Disponível em: < http://www.ncbi.nlm.nih.gov/pubmed/18443658 >.

CHEN, L. ET AL. Label-Free Quantitative Proteomic Screening of Candidate Plasma Biomarkers for the Prognosis of Breast Cancer with Different Lymph Node Statuses. **Proteomics Clin Appl,** v. 12, n. 3, p. e1700117, May 2018. ISSN 1862-8354 (Electronic)
1862-8346 (Linking). Disponível em: < http://www.ncbi.nlm.nih.gov/pubmed/29384592 >.

CHIU, W. C. ET AL. beta2-Glycoprotein I Inhibits Vascular Endothelial Growth Factor-Induced Angiogenesis by Suppressing the Phosphorylation of Extracellular Signal-Regulated Kinase 1/2, Akt, and Endothelial Nitric Oxide Synthase. **PLoS One,** v. 11, n. 8, p. e0161950, 2016. ISSN 1932-6203 (Electronic)
1932-6203 (Linking). Disponível em: < http://www.ncbi.nlm.nih.gov/pubmed/27579889 >.

CICHON, M. A. ET AL. Microenvironmental influences that drive progression from benign breast disease to invasive breast cancer. **J Mammary Gland Biol Neoplasia,** v. 15, n. 4, p. 389-97, Dec 2010. ISSN 1573-7039 (Electronic)
1083-3021 (Linking). Disponível em: < http://www.ncbi.nlm.nih.gov/pubmed/21161341 >.

CLUCAS, J.; VALDERRAMA, F. ERM proteins in cancer progression. **J Cell Sci,** v. 127, n. Pt 2, p. 267-75, Jan 15 2014. ISSN 1477-9137 (Electronic)
0021-9533 (Linking). Disponível em: < http://www.ncbi.nlm.nih.gov/pubmed/24421310 >.

COLDITZ, G. A.; BOHLKE, K. Preventing breast cancer now by acting on what we already know. **NPJ Breast Cancer,** v. 1, p. 15009, 2015. ISSN 2374-4677 (Print)
2374-4677 (Linking). Disponível em: < http://www.ncbi.nlm.nih.gov/pubmed/28721366 >.

CONCOLINO, A. ET AL. Proteomics Analysis to Assess the Role of Mitochondria in BRCA1-Mediated Breast Tumorigenesis. **Proteomes,** v. 6, n. 2, Mar 27 2018. ISSN 2227-7382 (Print)
2227-7382 (Linking). Disponível em: < http://www.ncbi.nlm.nih.gov/pubmed/29584711 >.

CONSORTIUM, G. O. Expansion of the Gene Ontology knowledgebase and resources. **Nucleic Acids Res,** v. 45, n. D1, p. D331-D338, Jan 4 2017. ISSN 1362-4962 (Electronic)
0305-1048 (Linking). Disponível em: < http://www.ncbi.nlm.nih.gov/pubmed/27899567 >.

CORREA, S. ET AL. Identifying potential markers in Breast Cancer subtypes using plasma label-free proteomics. **J Proteomics,** v. 151, p. 33-42, Jan 16 2017. ISSN 1876-7737 (Electronic)
1874-3919 (Linking). Disponível em: < http://www.ncbi.nlm.nih.gov/pubmed/27498391 >.

CORY, S.; ADAMS, J. M. The Bcl2 family: regulators of the cellular life-or-death switch. **Nat Rev Cancer,** v. 2, n. 9, p. 647-56, Sep 2002. ISSN 1474-175X (Print)
1474-175X (Linking). Disponível em: < http://www.ncbi.nlm.nih.gov/pubmed/12209154 >.

CORZO, C. ET AL. The MYC oncogene in breast cancer progression: from benign epithelium to invasive carcinoma. **Cancer Genet Cytogenet,** v. 165, n. 2, p. 151-6, Mar 2006. ISSN 0165-4608 (Print)
0165-4608 (Linking). Disponível em: < http://www.ncbi.nlm.nih.gov/pubmed/16527609 >.

COX, J.; MANN, M. MaxQuant enables high peptide identification rates, individualized p.p.b.-range mass accuracies and proteome-wide protein quantification. **Nat Biotechnol,** v. 26, n. 12, p. 1367-72, Dec 2008. ISSN 1546-1696 (Electronic)
1087-0156 (Linking). Disponível em: < http://www.ncbi.nlm.nih.gov/pubmed/19029910 >.

COX, J. ET AL. Andromeda: a peptide search engine integrated into the MaxQuant environment. **J Proteome Res,** v. 10, n. 4, p. 1794-805, Apr 1 2011. ISSN 1535-3907 (Electronic)
1535-3893 (Linking). Disponível em: < http://www.ncbi.nlm.nih.gov/pubmed/21254760 >.

CREIGHTON, C. J.; GIBBONS, D. L.; KURIE, J. M. The role of epithelial-mesenchymal transition programming in invasion and metastasis: a clinical perspective. **Cancer Manag Res,** v. 5, p. 187-95, 2013. ISSN 1179-1322 (Print)
1179-1322 (Linking). Disponível em: < http://www.ncbi.nlm.nih.gov/pubmed/23986650 >.

CUTULI, B. ET AL. Male breast cancer. Evolution of treatment and prognostic factors. Analysis of 489 cases. **Crit Rev Oncol Hematol,** v. 73, n. 3, p. 246-54, Mar 2010. ISSN 1879-0461 (Electronic)
1040-8428 (Linking). Disponível em: < http://www.ncbi.nlm.nih.gov/pubmed/19442535 >.

CZERWINSKA, P.; MAZUREK, S.; WIZNEROWICZ, M. The complexity of TRIM28 contribution to cancer. **J Biomed Sci,** v. 24, n. 1, p. 63, Aug 29 2017. ISSN 1423-0127 (Electronic)
1021-7770 (Linking). Disponível em: < http://www.ncbi.nlm.nih.gov/pubmed/28851455 >.

DAI, C.; DAI, S.; CAO, J. Proteotoxic stress of cancer: implication of the heat-shock response in oncogenesis. **J Cell Physiol,** v. 227, n. 8, p. 2982-7, Aug 2012. ISSN 1097-4652 (Electronic)
0021-9541 (Linking). Disponível em: < http://www.ncbi.nlm.nih.gov/pubmed/22105155 >.

DAMINENI, S. ET AL. Expression of tripartite motif-containing protein 28 in primary breast carcinoma predicts metastasis and is involved in the stemness, chemoresistance, and tumor growth. **Tumour Biol,** v. 39, n. 4, p. 1010428317695919, Apr 2017. ISSN 1423-0380 (Electronic)
1010-4283 (Linking). Disponível em: < http://www.ncbi.nlm.nih.gov/pubmed/28381187 >.

DATASUS/MS. Sistema de Informações sobre Mortalidade/ Sistema Único de Saúde/ Ministério da Saúde. **Atlas de Mortalidade por Câncer**, 1996-2014, 2019. Disponível em: < https://mortalidade.inca.gov.br/MortalidadeWeb/ >.

DAVIS, A. J.; CHEN, B. P.; CHEN, D. J. DNA-PK: a dynamic enzyme in a versatile DSB repair pathway. **DNA Repair (Amst),** v. 17, p. 21-9, May 2014. ISSN 1568-7856 (Electronic)
1568-7856 (Linking). Disponível em: < http://www.ncbi.nlm.nih.gov/pubmed/24680878 >.

DE LA MARE, J. A. ET AL. Breast cancer: current developments in molecular approaches to diagnosis and treatment. **Recent Pat Anticancer Drug Discov,** v. 9, n. 2, p. 153-75, May 2014. ISSN 2212-3970 (Electronic)
1574-8928 (Linking). Disponível em: < http://www.ncbi.nlm.nih.gov/pubmed/24171821 >.

DE LAS RIVAS, J.; DE LUIS, A. Interactome data and databases: different types of protein interaction. **Comp Funct Genomics,** v. 5, n. 2, p. 173-8, 2004. ISSN 1531-6912 (Print)
1531-6912 (Linking). Disponível em: < http://www.ncbi.nlm.nih.gov/pubmed/18629062 >.

DIDIASOVA, M. ET AL. From plasminogen to plasmin: role of plasminogen receptors in human cancer. **Int J Mol Sci,** v. 15, n. 11, p. 21229-52, Nov 17 2014. ISSN 1422-0067 (Electronic)
1422-0067 (Linking). Disponível em: < http://www.ncbi.nlm.nih.gov/pubmed/25407528 >.

DING, D. ET AL. C-type lectins facilitate tumor metastasis. **Oncol Lett,** v. 13, n. 1, p. 13-21, Jan 2017. ISSN 1792-1074 (Print)
1792-1074 (Linking). Disponível em: < http://www.ncbi.nlm.nih.gov/pubmed/28123516 >.

DOMON, B.; AEBERSOLD, R. Mass spectrometry and protein analysis. **Science,** v. 312, n. 5771, p. 212-7, Apr 14 2006. ISSN 1095-9203 (Electronic)
0036-8075 (Linking). Disponível em: < http://www.ncbi.nlm.nih.gov/pubmed/16614208 >.

DUTTA, B. ET AL. A network-based, integrative study to identify core biological pathways that drive breast cancer clinical subtypes. **Br J Cancer,** v. 106, n. 6, p. 1107-16, Mar 13 2012. ISSN 1532-1827 (Electronic)
0007-0920 (Linking). Disponível em: < http://www.ncbi.nlm.nih.gov/pubmed/22343619 >.

EHEMAN, C. R. ET AL. The changing incidence of in situ and invasive ductal and lobular breast carcinomas: United States, 1999-2004. **Cancer Epidemiol Biomarkers Prev,** v. 18, n. 6, p. 1763-9, Jun 2009. ISSN 1538-7755 (Electronic)
1055-9965 (Linking). Disponível em: < http://www.ncbi.nlm.nih.gov/pubmed/19454615 >.

ELLISEN, L. W. A wound-healing program is hijacked to promote cancer metastasis. **J Exp Med,** v. 214, n. 10, p. 2813-2815, Oct 2 2017. ISSN 1540-9538 (Electronic)
0022-1007 (Linking). Disponível em: < http://www.ncbi.nlm.nih.gov/pubmed/28904109 >.

FARMER, P. ET AL. Identification of molecular apocrine breast tumours by microarray analysis. **Oncogene,** v. 24, n. 29, p. 4660-71, Jul 7 2005. ISSN 0950-9232 (Print)
0950-9232 (Linking). Disponível em: < http://www.ncbi.nlm.nih.gov/pubmed/15897907 >.

FAROOQI, A. A.; SIDDIK, Z. H. Platelet-derived growth factor (PDGF) signalling in cancer: rapidly emerging signalling landscape. **Cell Biochem Funct,** v. 33, n. 5, p. 257-65, Jul 2015. ISSN 1099-0844 (Electronic)
0263-6484 (Linking). Disponível em: < http://www.ncbi.nlm.nih.gov/pubmed/26153649 >.

FASANO, M.; MONTI, C.; ALBERIO, T. A systems biology-led insight into the role of the proteome in neurodegenerative diseases. **Expert Rev Proteomics,** v. 13, n. 9, p. 845-55, Sep 2016. ISSN 1744-8387 (Electronic)
1478-9450 (Linking). Disponível em: < http://www.ncbi.nlm.nih.gov/pubmed/27477319 >.

FENG, Y. ET AL. Breast cancer development and progression: Risk factors, cancer stem cells, signaling pathways, genomics, and molecular pathogenesis. **Genes Dis,** v. 5, n. 2, p. 77-106, Jun 2018. ISSN 2352-3042 (Electronic)
2352-3042 (Linking). Disponível em: < http://www.ncbi.nlm.nih.gov/pubmed/30258937 >.

FIASCHI, T.; CHIARUGI, P. Oxidative stress, tumor microenvironment, and metabolic reprogramming: a diabolic liaison. **Int J Cell Biol,** v. 2012, p. 762825, 2012. ISSN 1687-8884 (Electronic)
1687-8876 (Linking). Disponível em: < http://www.ncbi.nlm.nih.gov/pubmed/22666258 >.

FIFE, C. M.; MCCARROLL, J. A.; KAVALLARIS, M. Movers and shakers: cell cytoskeleton in cancer metastasis. **Br J Pharmacol,** v. 171, n. 24, p. 5507-23, Dec 2014. ISSN 1476-5381 (Electronic)
0007-1188 (Linking). Disponível em: < http://www.ncbi.nlm.nih.gov/pubmed/24665826 >.

FITZMAURICE, C. ET AL. Global, Regional, and National Cancer Incidence, Mortality, Years of Life Lost, Years Lived With Disability, and Disability-Adjusted Life-years for 32 Cancer Groups, 1990 to 2015: A Systematic Analysis for the Global Burden of Disease Study. **JAMA Oncol,** v. 3, n. 4, p. 524-548, Apr 1 2017. ISSN 2374-2445 (Electronic)
2374-2437 (Linking). Disponível em: < http://www.ncbi.nlm.nih.gov/pubmed/27918777 >.

FORBES, S. A. ET AL. COSMIC: High-Resolution Cancer Genetics Using the Catalogue of Somatic Mutations in Cancer. **Curr Protoc Hum Genet,** v. 91, p. 10 11 1-10 11 37, Oct 11 2016. ISSN 1934-8258 (Electronic)
1934-8258 (Linking). Disponível em: < http://www.ncbi.nlm.nih.gov/pubmed/27727438 >.

GADALETA, E.; LEMOINE, N. R.; CHELALA, C. Online resources of cancer data: barriers, benefits and lessons. **Brief Bioinform,** v. 12, n. 1, p. 52-63, Jan 2011. ISSN 1477-4054 (Electronic)
1467-5463 (Linking). Disponível em: < http://www.ncbi.nlm.nih.gov/pubmed/20348133 >.

GALVAO, E. R. ET AL. Breast cancer proteomics: a review for clinicians. **J Cancer Res Clin Oncol,** v. 137, n. 6, p. 915-25, Jun 2011. ISSN 1432-1335 (Electronic)
0171-5216 (Linking). Disponível em: < http://www.ncbi.nlm.nih.gov/pubmed/21465318 >.

GAO, J. ET AL. Collection, integration and analysis of cancer genomic profiles: from data to insight. **Curr Opin Genet Dev,** v. 24, p. 92-8, Feb 2014. ISSN 1879-0380 (Electronic)
0959-437X (Linking). Disponível em: < http://www.ncbi.nlm.nih.gov/pubmed/24584084 >.

GARNIS, C.; BUYS, T. P.; LAM, W. L. Genetic alteration and gene expression modulation during cancer progression. **Mol Cancer,** v. 3, p. 9, Mar 22 2004. ISSN 1476-4598 (Electronic)
1476-4598 (Linking). Disponível em: < http://www.ncbi.nlm.nih.gov/pubmed/15035667 >.

GIANCOTTI, F. G. Deregulation of cell signaling in cancer. **FEBS Lett,** v. 588, n. 16, p. 2558-70, Aug 19 2014. ISSN 1873-3468 (Electronic)
0014-5793 (Linking). Disponível em: < http://www.ncbi.nlm.nih.gov/pubmed/24561200 >.

GJOREVSKI, N.; NELSON, C. M. Integrated morphodynamic signalling of the mammary gland. **Nat Rev Mol Cell Biol,** v. 12, n. 9, p. 581-93, Aug 10 2011. ISSN 1471-0080 (Electronic)
1471-0072 (Linking). Disponível em: < http://www.ncbi.nlm.nih.gov/pubmed/21829222 >.

GOLDHIRSCH, A. ET AL. Personalizing the treatment of women with early breast cancer: highlights of the St Gallen International Expert Consensus on the Primary Therapy of Early Breast Cancer 2013. **Ann Oncol,** v. 24, n. 9, p. 2206-23, Sep 2013. ISSN 1569-8041 (Electronic)
0923-7534 (Linking). Disponível em: < http://www.ncbi.nlm.nih.gov/pubmed/23917950 >.

GOMIG, T. H. B. ET AL. Quantitative label-free mass spectrometry using contralateral and adjacent breast tissues reveal differentially expressed proteins and their predicted impacts on pathways and cellular functions in breast cancer, **J Proteomics**, v. 199, p. 1-14, May 2019a. ISSN 1876-7737. Disponível em: < https://www.ncbi.nlm.nih.gov/pubmed/30772490 >.

GOMIG, T. H. B. ET AL. High-throughput mass spectrometry and bioinformatics analysis of breast cancer proteomic data. **Data in Brief**, v. 25, Aug 2019b. Disponível em: < https://www.sciencedirect.com/science/article/pii/S2352340919304792 >.

GREGORICH, Z. R.; CHANG, Y. H.; GE, Y. Proteomics in heart failure: top-down or bottom-up? **Pflugers Arch,** v. 466, n. 6, p. 1199-209, Jun 2014. ISSN 1432-2013 (Electronic)
0031-6768 (Linking). Disponível em: < http://www.ncbi.nlm.nih.gov/pubmed/24619480 >.

GRINSTEIN, E. ET AL. Cell cycle-controlled interaction of nucleolin with the retinoblastoma protein and cancerous cell transformation. **J Biol Chem,** v. 281, n. 31, p. 22223-35, Aug 4 2006. ISSN 0021-9258 (Print)
0021-9258 (Linking). Disponível em: < http://www.ncbi.nlm.nih.gov/pubmed/16698799 >.

GROESSL, M. ET AL. Proteome profiling of breast cancer biopsies reveals a wound healing signature of cancer-associated fibroblasts. **J Proteome Res,** v. 13, n. 11, p. 4773-82, Nov 7 2014. ISSN 1535-3907 (Electronic)
1535-3893 (Linking). Disponível em: < http://www.ncbi.nlm.nih.gov/pubmed/25238572 >.

GUAITA-ESTERUELAS, S. ET AL. Exogenous FABP4 increases breast cancer cell proliferation and activates the expression of fatty acid transport proteins. **Mol Carcinog,** v. 56, n. 1, p. 208-217, Jan 2017. ISSN 1098-2744 (Electronic)
0899-1987 (Linking). Disponível em: < http://www.ncbi.nlm.nih.gov/pubmed/27061264 >.

GUIMARÃES, J. R. **Manual de oncologia**. 3. São Paulo: Libbs Farmacêutica, 2008.

GUNDRY, R. L. ET AL. Preparation of proteins and peptides for mass spectrometry analysis in a bottom-up proteomics workflow. **Curr Protoc Mol Biol,** v. Chapter 10, p. Unit10 25, Oct 2009. ISSN 1934-3647 (Electronic)
1934-3647 (Linking). Disponível em: < http://www.ncbi.nlm.nih.gov/pubmed/19816929 >.

GUPTA, M. K.; QIN, R. Y. Mechanism and its regulation of tumor-induced angiogenesis. **World J Gastroenterol,** v. 9, n. 6, p. 1144-55, Jun 2003. ISSN 1007-9327 (Print)
1007-9327 (Linking). Disponível em: < http://www.ncbi.nlm.nih.gov/pubmed/12800214 >.

GURTNER, G. C. ET AL. Wound repair and regeneration. **Nature,** v. 453, n. 7193, p. 314-21, May 15 2008. ISSN 1476-4687 (Electronic)
0028-0836 (Linking). Disponível em: < http://www.ncbi.nlm.nih.gov/pubmed/18480812 >.

HAAG, A. M. Mass Analyzers and Mass Spectrometers. **Adv Exp Med Biol,** v. 919, p. 157-169, 2016. ISSN 0065-2598 (Print)
0065-2598 (Linking). Disponível em: < http://www.ncbi.nlm.nih.gov/pubmed/27975216 >.

HALL, A. E. ET AL. The cytoskeleton adaptor protein ankyrin-1 is upregulated by p53 following DNA damage and alters cell migration. **Cell Death Dis,** v. 7, p. e2184, Apr

7 2016. ISSN 2041-4889 (Electronic). Disponível em: < http://www.ncbi.nlm.nih.gov/pubmed/27054339 >.

HAN, N.; LI, W.; ZHANG, M. The function of the RNA-binding protein hnRNP in cancer metastasis. **J Cancer Res Ther,** v. 9 Suppl, p. S129-34, Nov 2013. ISSN 1998-4138 (Electronic)
1998-4138 (Linking). Disponível em: < http://www.ncbi.nlm.nih.gov/pubmed/24516048 >.

HAN, X.; ASLANIAN, A.; YATES, J. R., 3RD. Mass spectrometry for proteomics. **Curr Opin Chem Biol,** v. 12, n. 5, p. 483-90, Oct 2008. ISSN 1367-5931 (Print)
1367-5931 (Linking). Disponível em: < http://www.ncbi.nlm.nih.gov/pubmed/18718552 >.

HANAHAN, D.; COUSSENS, L. M. Accessories to the crime: functions of cells recruited to the tumor microenvironment. **Cancer Cell,** v. 21, n. 3, p. 309-22, Mar 20 2012. ISSN 1878-3686 (Electronic)
1535-6108 (Linking). Disponível em: < http://www.ncbi.nlm.nih.gov/pubmed/22439926 >.

HANAHAN, D.; WEINBERG, R. A. Hallmarks of cancer: the next generation. **Cell,** v. 144, n. 5, p. 646-74, Mar 4 2011. ISSN 1097-4172 (Electronic)
0092-8674 (Linking). Disponível em: < http://www.ncbi.nlm.nih.gov/pubmed/21376230 >.

HANCOX, R. A. ET AL. Tumour-associated tenascin-C isoforms promote breast cancer cell invasion and growth by matrix metalloproteinase-dependent and independent mechanisms. **Breast Cancer Res,** v. 11, n. 2, p. R24, 2009. ISSN 1465-542X (Electronic)
1465-5411 (Linking). Disponível em: < http://www.ncbi.nlm.nih.gov/pubmed/19405959 >.

HASSIOTOU, F.; GEDDES, D. Anatomy of the human mammary gland: Current status of knowledge. **Clin Anat,** v. 26, n. 1, p. 29-48, Jan 2013. ISSN 1098-2353 (Electronic)
0897-3806 (Linking). Disponível em: < http://www.ncbi.nlm.nih.gov/pubmed/22997014 >.

HEBERLE, H. ET AL. InteractiVenn: a web-based tool for the analysis of sets through Venn diagrams. **BMC Bioinformatics,** v. 16, p. 169, May 22 2015. ISSN 1471-2105 (Electronic)
1471-2105 (Linking). Disponível em: < http://www.ncbi.nlm.nih.gov/pubmed/25994840 >.

HECK, A. J. Native mass spectrometry: a bridge between interactomics and structural biology. **Nat Methods,** v. 5, n. 11, p. 927-33, Nov 2008. ISSN 1548-7105 (Electronic)
1548-7091 (Linking). Disponível em: < http://www.ncbi.nlm.nih.gov/pubmed/18974734 >.

HENEGHAN, H. M. ET AL. Circulating microRNAs as novel minimally invasive biomarkers for breast cancer. **Ann Surg,** v. 251, n. 3, p. 499-505, Mar 2010. ISSN 1528-1140 (Electronic)
0003-4932 (Linking). Disponível em: < http://www.ncbi.nlm.nih.gov/pubmed/20134314 >.

HO, C. S. ET AL. Electrospray ionisation mass spectrometry: principles and clinical applications. **Clin Biochem Rev,** v. 24, n. 1, p. 3-12, 2003. ISSN 0159-8090 (Print)
0159-8090 (Linking). Disponível em: < http://www.ncbi.nlm.nih.gov/pubmed/18568044 >.

HONDERMARCK, H. Breast cancer: when proteomics challenges biological complexity. **Mol Cell Proteomics,** v. 2, n. 5, p. 281-91, May 2003. ISSN 1535-9476 (Print)
1535-9476 (Linking). Disponível em: < http://www.ncbi.nlm.nih.gov/pubmed/12775769 >.

HOSACK, D. A. ET AL. Identifying biological themes within lists of genes with EASE. **Genome Biol,** v. 4, n. 10, p. R70, 2003. ISSN 1474-760X (Electronic)
1474-7596 (Linking). Disponível em: < http://www.ncbi.nlm.nih.gov/pubmed/14519205 >.

HOSKIN, V. ET AL. Ezrin regulates focal adhesion and invadopodia dynamics by altering calpain activity to promote breast cancer cell invasion. **Mol Biol Cell,** v. 26, n. 19, p. 3464-79, Oct 1 2015. ISSN 1939-4586 (Electronic)
1059-1524 (Linking). Disponível em: < http://www.ncbi.nlm.nih.gov/pubmed/26246600 >.

HUANG, C.; FRETER, C. Lipid metabolism, apoptosis and cancer therapy. **Int J Mol Sci,** v. 16, n. 1, p. 924-49, Jan 2 2015. ISSN 1422-0067 (Electronic)
1422-0067 (Linking). Disponível em: < http://www.ncbi.nlm.nih.gov/pubmed/25561239 >.

HUANG DA, W.; SHERMAN, B. T.; LEMPICKI, R. A. Systematic and integrative analysis of large gene lists using DAVID bioinformatics resources. **Nat Protoc,** v. 4, n. 1, p. 44-57, 2009. ISSN 1750-2799 (Electronic)
1750-2799 (Linking). Disponível em: < http://www.ncbi.nlm.nih.gov/pubmed/19131956 >.

IARC/WHO. Global Cancer Observatory 2019. Disponível em: < http://gco.iarc.fr/ >.

ILAGAN, E.; MANNING, B. D. Emerging role of mTOR in the response to cancer therapeutics. **Trends Cancer,** v. 2, n. 5, p. 241-251, May 2016. ISSN 2405-8033 (Print)
2405-8025 (Linking). Disponível em: < http://www.ncbi.nlm.nih.gov/pubmed/27668290 >.

INCA/MS. **Estimativa 2018: incidência de câncer no Brasil. Instituto Nacional de Câncer José Alencar Gomes da Silva. Coordenação de Prevenção e**

Vigilância. Rio de Janeiro: INCA, 2017. 128 ISBN 978-85-7318-361-0 Disponível em: < http://www1.inca.gov.br/estimativa/2018/estimativa-2018.pdf >.

_____. **ABC do câncer: abordagens básicas para o controle do câncer / Instituto Nacional de Câncer José Alencar Gomes da Silva; organização Mario Jorge Sobreira da Silva.** . 4. Rio de Janeiro: INCA, 2018. Disponível em: < https://www.inca.gov.br/sites/ufu.sti.inca.local/files//media/document//livro-abc-4-edicao.pdf >.

_____. Tipos de Câncer. **Câncer de Mama**, 11/10/2018, 2019. Disponível em: < https://www.inca.gov.br/tipos-de-cancer/cancer-de-mama >.

ISHIHAMA, Y.; RAPPSILBER, J.; MANN, M. Modular stop and go extraction tips with stacked disks for parallel and multidimensional Peptide fractionation in proteomics. **J Proteome Res,** v. 5, n. 4, p. 988-94, Apr 2006. ISSN 1535-3893 (Print)
1535-3893 (Linking). Disponível em: < http://www.ncbi.nlm.nih.gov/pubmed/16602707 >.

IUANOW, E.; KETTLER, M.; SLANETZ, P. J. Spectrum of disease in the male breast. **AJR Am J Roentgenol,** v. 196, n. 3, p. W247-59, Mar 2011. ISSN 1546-3141 (Electronic)
0361-803X (Linking). Disponível em: < http://www.ncbi.nlm.nih.gov/pubmed/21343472 >.

IVANOV, A. S.; ZGODA, V. G.; ARCHAKOV, A. I. [Protein interactomics technologies]. **Bioorg Khim,** v. 37, n. 1, p. 8-21, Jan-Feb 2011. ISSN 0132-3423 (Print)
0132-3423 (Linking). Disponível em: < http://www.ncbi.nlm.nih.gov/pubmed/21460877 >.

JAGANNATHAN, V.; ROBINSON-RECHAVI, M. Meta-analysis of estrogen response in MCF-7 distinguishes early target genes involved in signaling and cell proliferation from later target genes involved in cell cycle and DNA repair. **BMC Syst Biol,** v. 5, p. 138, Aug 30 2011. ISSN 1752-0509 (Electronic)
1752-0509 (Linking). Disponível em: < http://www.ncbi.nlm.nih.gov/pubmed/21878096 >.

JI, Q. ET AL. Selective loss of AKR1C1 and AKR1C2 in breast cancer and their potential effect on progesterone signaling. **Cancer Res,** v. 64, n. 20, p. 7610-7, Oct 15 2004. ISSN 0008-5472 (Print)
0008-5472 (Linking). Disponível em: < http://www.ncbi.nlm.nih.gov/pubmed/15492289 >.

JIANG, T.; ZHOU, C.; REN, S. Role of IL-2 in cancer immunotherapy. **Oncoimmunology,** v. 5, n. 6, p. e1163462, Jun 2016. ISSN 2162-4011 (Print)
2162-4011 (Linking). Disponível em: < http://www.ncbi.nlm.nih.gov/pubmed/27471638 >.

JIANG, W. G. ET AL. Tissue invasion and metastasis: Molecular, biological and clinical perspectives. **Semin Cancer Biol,** v. 35 Suppl, p. S244-S275, Dec 2015. ISSN 1096-3650 (Electronic)
1044-579X (Linking). Disponível em: < http://www.ncbi.nlm.nih.gov/pubmed/25865774 >.

JIN, X.; MU, P. Targeting Breast Cancer Metastasis. **Breast Cancer (Auckl),** v. 9, n. Suppl 1, p. 23-34, 2015. ISSN 1178-2234 (Print)
1178-2234 (Linking). Disponível em: < http://www.ncbi.nlm.nih.gov/pubmed/26380552 >.

JOYCE, J. A.; POLLARD, J. W. Microenvironmental regulation of metastasis. **Nat Rev Cancer,** v. 9, n. 4, p. 239-52, Apr 2009. ISSN 1474-1768 (Electronic)
1474-175X (Linking). Disponível em: < http://www.ncbi.nlm.nih.gov/pubmed/19279573 >.

KAMINSKA, M. ET AL. Breast cancer risk factors. **Prz Menopauzalny,** v. 14, n. 3, p. 196-202, Sep 2015. ISSN 1643-8876 (Print)
1643-8876 (Linking). Disponível em: < http://www.ncbi.nlm.nih.gov/pubmed/26528110 >.

KARANTZA, V. Keratins in health and cancer: more than mere epithelial cell markers. **Oncogene,** v. 30, n. 2, p. 127-38, Jan 13 2011. ISSN 1476-5594 (Electronic)
0950-9232 (Linking). Disponível em: < http://www.ncbi.nlm.nih.gov/pubmed/20890307 >.

KARPIEVITCH, Y. V.; DABNEY, A. R.; SMITH, R. D. Normalization and missing value imputation for label-free LC-MS analysis. **BMC Bioinformatics,** v. 13 Suppl 16, p. S5, 2012. ISSN 1471-2105 (Electronic)
1471-2105 (Linking). Disponível em: < http://www.ncbi.nlm.nih.gov/pubmed/23176322 >.

KESKIN, O.; TUNCBAG, N.; GURSOY, A. Predicting Protein-Protein Interactions from the Molecular to the Proteome Level. **Chem Rev,** v. 116, n. 8, p. 4884-909, Apr 27 2016. ISSN 1520-6890 (Electronic)
0009-2665 (Linking). Disponível em: < http://www.ncbi.nlm.nih.gov/pubmed/27074302 >.

KEY, T. J. ET AL. Nutrition and breast cancer. **Breast,** v. 12, n. 6, p. 412-6, Dec 2003. ISSN 0960-9776 (Print)
0960-9776 (Linking). Disponível em: < http://www.ncbi.nlm.nih.gov/pubmed/14659114 >.

KNIGHTS, A. J. ET AL. Holding Tight: Cell Junctions and Cancer Spread. **Trends Cancer Res,** v. 8, p. 61-69, 2012. ISSN 0973-1040 (Print)
0973-1040 (Linking). Disponível em: < http://www.ncbi.nlm.nih.gov/pubmed/23450077 >.

KOOPMANS, F. ET AL. Comparative Analyses of Data Independent Acquisition Mass Spectrometric Approaches: DIA, WiSIM-DIA, and Untargeted DIA. **Proteomics,** v. 18, n. 1, Jan 2018. ISSN 1615-9861 (Electronic)
1615-9853 (Linking). Disponível em: < http://www.ncbi.nlm.nih.gov/pubmed/29134766 >.

KORDE, L. A. ET AL. Multidisciplinary meeting on male breast cancer: summary and research recommendations. **J Clin Oncol,** v. 28, n. 12, p. 2114-22, Apr 20 2010. ISSN 1527-7755 (Electronic)
0732-183X (Linking). Disponível em: < http://www.ncbi.nlm.nih.gov/pubmed/20308661 >.

KOTULA, E. ET AL. DNA-PKcs plays role in cancer metastasis through regulation of secreted proteins involved in migration and invasion. **Cell Cycle,** v. 14, n. 12, p. 1961-72, 2015. ISSN 1551-4005 (Electronic)
1551-4005 (Linking). Disponível em: < http://www.ncbi.nlm.nih.gov/pubmed/26017556 >.

KRAMER, A. ET AL. Causal analysis approaches in Ingenuity Pathway Analysis. **Bioinformatics,** v. 30, n. 4, p. 523-30, Feb 15 2014. ISSN 1367-4811 (Electronic)
1367-4803 (Linking). Disponível em: < http://www.ncbi.nlm.nih.gov/pubmed/24336805 >.

KWAAN, H. C.; MCMAHON, B. The role of plasminogen-plasmin system in cancer. **Cancer Treat Res,** v. 148, p. 43-66, 2009. ISSN 0927-3042 (Print)
0927-3042 (Linking). Disponível em: < http://www.ncbi.nlm.nih.gov/pubmed/19377918 >.

LAUKENS, K.; NAULAERTS, S.; BERGHE, W. V. Bioinformatics approaches for the functional interpretation of protein lists: from ontology term enrichment to network analysis. **Proteomics,** v. 15, n. 5-6, p. 981-96, Mar 2015. ISSN 1615-9861 (Electronic)
1615-9853 (Linking). Disponível em: < http://www.ncbi.nlm.nih.gov/pubmed/25430566 >.

LAZAR, I. M. Bioinformatics Resources for Interpreting Proteomics Mass Spectrometry Data. **Methods Mol Biol,** v. 1647, p. 267-295, 2017. ISSN 1940-6029 (Electronic)
1064-3745 (Linking). Disponível em: < http://www.ncbi.nlm.nih.gov/pubmed/28809010 >.

LEWIS, N. E.; ABDEL-HALEEM, A. M. The evolution of genome-scale models of cancer metabolism. **Front Physiol,** v. 4, p. 237, Sep 3 2013. ISSN 1664-042X (Print)
1664-042X (Linking). Disponível em: < http://www.ncbi.nlm.nih.gov/pubmed/24027532 >.

LI, W. X. ET AL. Comprehensive tissue-specific gene set enrichment analysis and transcription factor analysis of breast cancer by integrating 14 gene expression datasets. **Oncotarget,** v. 8, n. 4, p. 6775-6786, Jan 24 2017. ISSN 1949-2553 (Electronic)

1949-2553 (Linking). Disponível em: < http://www.ncbi.nlm.nih.gov/pubmed/28036274 >.

LI, Y. ET AL. Tumoral expression of drug and xenobiotic metabolizing enzymes in breast cancer patients of different ethnicities with implications to personalized medicine. **Sci Rep,** v. 7, n. 1, p. 4747, Jul 6 2017. ISSN 2045-2322 (Electronic)
2045-2322 (Linking). Disponível em: < http://www.ncbi.nlm.nih.gov/pubmed/28684774 >.

LIBERZON, A. ET AL. The Molecular Signatures Database (MSigDB) hallmark gene set collection. **Cell Syst,** v. 1, n. 6, p. 417-425, Dec 23 2015. ISSN 2405-4712 (Print)
2405-4712 (Linking). Disponível em: < http://www.ncbi.nlm.nih.gov/pubmed/26771021 >.

LIBERZON, A. ET AL. Molecular signatures database (MSigDB) 3.0. **Bioinformatics,** v. 27, n. 12, p. 1739-40, Jun 15 2011. ISSN 1367-4811 (Electronic)
1367-4803 (Linking). Disponível em: < http://www.ncbi.nlm.nih.gov/pubmed/21546393 >.

LINDQVIST, L. M. ET AL. Cross-talk between protein synthesis, energy metabolism and autophagy in cancer. **Curr Opin Genet Dev,** v. 48, p. 104-111, Feb 2018. ISSN 1879-0380 (Electronic)
0959-437X (Linking). Disponível em: < http://www.ncbi.nlm.nih.gov/pubmed/29179096 >.

LIU, Y. ET AL. Physical activity from menarche to first pregnancy and risk of breast cancer. **Int J Cancer,** v. 139, n. 6, p. 1223-30, Sep 15 2016. ISSN 1097-0215 (Electronic)
0020-7136 (Linking). Disponível em: < http://www.ncbi.nlm.nih.gov/pubmed/27130486 >.

LIU, Z. P.; CHEN, L. Proteome-wide prediction of protein-protein interactions from high-throughput data. **Protein Cell,** v. 3, n. 7, p. 508-20, Jul 2012. ISSN 1674-8018 (Electronic)
1674-800X (Linking). Disponível em: < http://www.ncbi.nlm.nih.gov/pubmed/22729399 >.

LOBO, M. D. ET AL. Label-Free Proteome Analysis of Plasma from Patients with Breast Cancer: Stage-Specific Protein Expression. **Front Oncol,** v. 7, p. 14, 2017. ISSN 2234-943X (Print)
2234-943X (Linking). Disponível em: < http://www.ncbi.nlm.nih.gov/pubmed/28210565 >.

LUO, J.; SOLIMINI, N. L.; ELLEDGE, S. J. Principles of cancer therapy: oncogene and non-oncogene addiction. **Cell,** v. 136, n. 5, p. 823-37, Mar 6 2009. ISSN 1097-4172 (Electronic)
0092-8674 (Linking). Disponível em: < http://www.ncbi.nlm.nih.gov/pubmed/19269363 >.

MACIAS, H.; HINCK, L. Mammary gland development. **Wiley Interdiscip Rev Dev Biol,** v. 1, n. 4, p. 533-57, Jul-Aug 2012. ISSN 1759-7692 (Electronic)
1759-7684 (Linking). Disponível em: < http://www.ncbi.nlm.nih.gov/pubmed/22844349 >.

MALIK, R. ET AL. From proteome lists to biological impact--tools and strategies for the analysis of large MS data sets. **Proteomics,** v. 10, n. 6, p. 1270-83, Mar 2010. ISSN 1615-9861 (Electronic)
1615-9853 (Linking). Disponível em: < http://www.ncbi.nlm.nih.gov/pubmed/20077408 >.

MBOGE, M. Y. ET AL. Carbonic Anhydrases: Role in pH Control and Cancer. **Metabolites,** v. 8, n. 1, Feb 28 2018. ISSN 2218-1989 (Print)
2218-1989 (Linking). Disponível em: < http://www.ncbi.nlm.nih.gov/pubmed/29495652 >.

MENEZES DE MEDEIROS, J. ET AL. Perfil epidemiológico e estudo de sobrevida dos pacientes com câncer de mama atendidos no Hospital Erasto Gaertner em Curitiba, PR. . **Revista Brasileira de Mastologia.,** v. 23, n. 3, p. 107-112, 2016. Disponível em: < http://www.mastology.org/wp-content/uploads/2016/06/MAS_v26n3_107-112.pdf >.

MI, H. ET AL. PANTHER version 11: expanded annotation data from Gene Ontology and Reactome pathways, and data analysis tool enhancements. **Nucleic Acids Res,** v. 45, n. D1, p. D183-D189, Jan 4 2017. ISSN 1362-4962 (Electronic)
0305-1048 (Linking). Disponível em: < http://www.ncbi.nlm.nih.gov/pubmed/27899595 >.

MIDWOOD, K. S.; OREND, G. The role of tenascin-C in tissue injury and tumorigenesis. **J Cell Commun Signal,** v. 3, n. 3-4, p. 287-310, Dec 2009. ISSN 1873-961X (Electronic)
1873-9601 (Linking). Disponível em: < http://www.ncbi.nlm.nih.gov/pubmed/19838819 >.

MIDWOOD, K. S.; SCHWARZBAUER, J. E. Tenascin-C modulates matrix contraction via focal adhesion kinase- and Rho-mediated signaling pathways. **Mol Biol Cell,** v. 13, n. 10, p. 3601-13, Oct 2002. ISSN 1059-1524 (Print)
1059-1524 (Linking). Disponível em: < http://www.ncbi.nlm.nih.gov/pubmed/12388760 >.

MONACO, M. E. Fatty acid metabolism in breast cancer subtypes. **Oncotarget,** v. 8, n. 17, p. 29487-29500, Apr 25 2017. ISSN 1949-2553 (Electronic)
1949-2553 (Linking). Disponível em: < http://www.ncbi.nlm.nih.gov/pubmed/28412757 >.

MONTI, C. ET AL. Proteomics turns functional. **J Proteomics**, Dec 13 2018. ISSN 1876-7737 (Electronic)
1874-3919 (Linking). Disponível em: < http://www.ncbi.nlm.nih.gov/pubmed/30553948 >.

MONTI, M. ET AL. Puzzle of protein complexes in vivo: a present and future challenge for functional proteomics. **Expert Rev Proteomics,** v. 6, n. 2, p. 159-69, Apr 2009. ISSN 1744-8387 (Electronic)
1478-9450 (Linking). Disponível em: < http://www.ncbi.nlm.nih.gov/pubmed/19385943 >.

MOSCA, R.; CEOL, A.; ALOY, P. Interactome3D: adding structural details to protein networks. **Nat Methods,** v. 10, n. 1, p. 47-53, Jan 2013. ISSN 1548-7105 (Electronic)
1548-7091 (Linking). Disponível em: < http://www.ncbi.nlm.nih.gov/pubmed/23399932 >.

MUELLER, C. ET AL. Protein biomarkers for subtyping breast cancer and implications for future research. **Expert Rev Proteomics,** v. 15, n. 2, p. 131-152, Feb 2018. ISSN 1744-8387 (Electronic)
1478-9450 (Linking). Disponível em: < http://www.ncbi.nlm.nih.gov/pubmed/29271260 >.

MULLER, P. A.; VOUSDEN, K. H. Mutant p53 in cancer: new functions and therapeutic opportunities. **Cancer Cell,** v. 25, n. 3, p. 304-17, Mar 17 2014. ISSN 1878-3686 (Electronic)
1535-6108 (Linking). Disponível em: < http://www.ncbi.nlm.nih.gov/pubmed/24651012 >.

MUZ, B. ET AL. The role of hypoxia in cancer progression, angiogenesis, metastasis, and resistance to therapy. **Hypoxia (Auckl),** v. 3, p. 83-92, 2015. ISSN 2324-1128 (Print)
2324-1128 (Linking). Disponível em: < http://www.ncbi.nlm.nih.gov/pubmed/27774485 >.

NABA, A. ET AL. Extracellular matrix signatures of human mammary carcinoma identify novel metastasis promoters. **Elife,** v. 3, p. e01308, Mar 11 2014. ISSN 2050-084X (Electronic)
2050-084X (Linking). Disponível em: < http://www.ncbi.nlm.nih.gov/pubmed/24618895 >.

NAVARRETE, M. A. ET AL. Assessment of the proliferative, apoptotic and cellular renovation indices of the human mammary epithelium during the follicular and luteal phases of the menstrual cycle. **Breast Cancer Res,** v. 7, n. 3, p. R306-13, 2005. ISSN 1465-542X (Electronic)
1465-5411 (Linking). Disponível em: < http://www.ncbi.nlm.nih.gov/pubmed/15987425 >.

NELSON, B. H. Interleukin-2 signaling and the maintenance of self-tolerance. **Curr Dir Autoimmun,** v. 5, p. 92-112, 2002. ISSN 1422-2132 (Print)
1422-2132 (Linking). Disponível em: < http://www.ncbi.nlm.nih.gov/pubmed/11826762 >.

NOBLE, J. L. ET AL. A comparative proteinomic analysis of nipple aspiration fluid from healthy women and women with breast cancer. **Eur J Cancer,** v. 43, n. 16, p. 2315-20, Nov 2007. ISSN 0959-8049 (Print)

0959-8049 (Linking). Disponível em: < http://www.ncbi.nlm.nih.gov/pubmed/17904354 >.

NOMURA, D. K. ET AL. Monoacylglycerol lipase regulates a fatty acid network that promotes cancer pathogenesis. **Cell,** v. 140, n. 1, p. 49-61, Jan 8 2010. ISSN 1097-4172 (Electronic)
0092-8674 (Linking). Disponível em: < http://www.ncbi.nlm.nih.gov/pubmed/20079333 >.

OLDENBURG, R. A. ET AL. Genetic susceptibility for breast cancer: how many more genes to be found? **Crit Rev Oncol Hematol,** v. 63, n. 2, p. 125-49, Aug 2007. ISSN 1040-8428 (Print)
1040-8428 (Linking). Disponível em: < http://www.ncbi.nlm.nih.gov/pubmed/17498966 >.

OMIECINSKI, C. J. ET AL. Xenobiotic metabolism, disposition, and regulation by receptors: from biochemical phenomenon to predictors of major toxicities. **Toxicol Sci,** v. 120 Suppl 1, p. S49-75, Mar 2010. ISSN 1096-0929 (Electronic)
1096-0929 (Linking). Disponível em: < http://www.ncbi.nlm.nih.gov/pubmed/21059794 >.

OSTASIEWICZ, P. ET AL. Proteome, phosphoproteome, and N-glycoproteome are quantitatively preserved in formalin-fixed paraffin-embedded tissue and analyzable by high-resolution mass spectrometry. **J Proteome Res,** v. 9, n. 7, p. 3688-700, Jul 2 2010. ISSN 1535-3907 (Electronic)
1535-3893 (Linking). Disponível em: < http://www.ncbi.nlm.nih.gov/pubmed/20469934 >.

OSTMAN, A.; HELDIN, C. H. PDGF receptors as targets in tumor treatment. **Adv Cancer Res,** v. 97, p. 247-74, 2007. ISSN 2162-5557 (Electronic)
0065-230X (Linking). Disponível em: < http://www.ncbi.nlm.nih.gov/pubmed/17419949 >.

PAGE, M. J. ET AL. Proteomic definition of normal human luminal and myoepithelial breast cells purified from reduction mammoplasties. **Proc Natl Acad Sci U S A,** v. 96, n. 22, p. 12589-94, Oct 26 1999. ISSN 0027-8424 (Print)
0027-8424 (Linking). Disponível em: < http://www.ncbi.nlm.nih.gov/pubmed/10535966 >.

PAJOT, P. Fluroescence of proteins in 6-M guanidine hydrochloride. A method for the quantitative determination of tryptophan. **Eur J Biochem,** v. 63, n. 1, p. 263-9, Mar 16 1976. ISSN 0014-2956 (Print)
0014-2956 (Linking). Disponível em: < http://www.ncbi.nlm.nih.gov/pubmed/4317 >.

PANIS, C. ET AL. Label-free proteomic analysis of breast cancer molecular subtypes. **J Proteome Res,** v. 13, n. 11, p. 4752-72, Nov 7 2014. ISSN 1535-3907 (Electronic)
1535-3893 (Linking). Disponível em: < http://www.ncbi.nlm.nih.gov/pubmed/25221861 >.

PAVLOPOULOU, A.; SPANDIDOS, D. A.; MICHALOPOULOS, I. Human cancer databases (review). **Oncol Rep,** v. 33, n. 1, p. 3-18, Jan 2015. ISSN 1791-2431 (Electronic)
1021-335X (Linking). Disponível em: < http://www.ncbi.nlm.nih.gov/pubmed/25369839 >.

PAWLIK, T. M. ET AL. Proteomic analysis of nipple aspirate fluid from women with early-stage breast cancer using isotope-coded affinity tags and tandem mass spectrometry reveals differential expression of vitamin D binding protein. **BMC Cancer,** v. 6, p. 68, Mar 16 2006. ISSN 1471-2407 (Electronic)
1471-2407 (Linking). Disponível em: < http://www.ncbi.nlm.nih.gov/pubmed/16542425 >.

PELLACANI, D. ET AL. Transcriptional regulation of normal human mammary cell heterogeneity and its perturbation in breast cancer. **EMBO J**, Jan 11 2019. ISSN 1460-2075 (Electronic)
0261-4189 (Linking). Disponível em: < http://www.ncbi.nlm.nih.gov/pubmed/30635333 >.

PEROU, C. M. ET AL. Molecular portraits of human breast tumours. **Nature,** v. 406, n. 6797, p. 747-52, Aug 17 2000. ISSN 0028-0836 (Print)
0028-0836 (Linking). Disponível em: < http://www.ncbi.nlm.nih.gov/pubmed/10963602 >.

PICKUP, M. W.; MOUW, J. K.; WEAVER, V. M. The extracellular matrix modulates the hallmarks of cancer. **EMBO Rep,** v. 15, n. 12, p. 1243-53, Dec 2014. ISSN 1469-3178 (Electronic)
1469-221X (Linking). Disponível em: < http://www.ncbi.nlm.nih.gov/pubmed/25381661 >.

POLYAK, K.; KALLURI, R. The role of the microenvironment in mammary gland development and cancer. **Cold Spring Harb Perspect Biol,** v. 2, n. 11, p. a003244, Nov 2010. ISSN 1943-0264 (Electronic)
1943-0264 (Linking). Disponível em: < http://www.ncbi.nlm.nih.gov/pubmed/20591988 >.

POPULO, H.; LOPES, J. M.; SOARES, P. The mTOR signalling pathway in human cancer. **Int J Mol Sci,** v. 13, n. 2, p. 1886-918, 2012. ISSN 1422-0067 (Electronic)
1422-0067 (Linking). Disponível em: < http://www.ncbi.nlm.nih.gov/pubmed/22408430 >.

PRAT, A. ET AL. Phenotypic and molecular characterization of the claudin-low intrinsic subtype of breast cancer. **Breast Cancer Res,** v. 12, n. 5, p. R68, 2010. ISSN 1465-542X (Electronic)
1465-5411 (Linking). Disponível em: < http://www.ncbi.nlm.nih.gov/pubmed/20813035 >.

PROCHAZKOVA, I.; LENCO, J.; BOUCHAL, P. Targeted Proteomics Driven Verification of Biomarker Candidates Associated with Breast Cancer Aggressiveness. **Methods Mol Biol,** v. 1788, p. 177-184, 2017. ISSN 1940-6029 (Electronic)

1064-3745 (Linking). Disponível em: < http://www.ncbi.nlm.nih.gov/pubmed/29196895 >.

RAJAGOPALAN, S. ET AL. Mapping the physical and functional interactions between the tumor suppressors p53 and BRCA2. **Proc Natl Acad Sci U S A,** v. 107, n. 19, p. 8587-92, May 11 2010. ISSN 1091-6490 (Electronic)
0027-8424 (Linking). Disponível em: < http://www.ncbi.nlm.nih.gov/pubmed/20421506 >.

RAMASWAMY, S. ET AL. A molecular signature of metastasis in primary solid tumors. **Nat Genet,** v. 33, n. 1, p. 49-54, Jan 2003. ISSN 1061-4036 (Print)
1061-4036 (Linking). Disponível em: < http://www.ncbi.nlm.nih.gov/pubmed/12469122 >.

RAUNIYAR, N.; STEVENS, S. M., JR.; PROKAI, L. Fourier transform ion cyclotron resonance mass spectrometry of covalent adducts of proteins and 4-hydroxy-2-nonenal, a reactive end-product of lipid peroxidation. **Anal Bioanal Chem,** v. 389, n. 5, p. 1421-8, Nov 2007. ISSN 1618-2642 (Print)
1618-2642 (Linking). Disponível em: < http://www.ncbi.nlm.nih.gov/pubmed/17805520 >.

REN, J.; WANG, B.; LI, J. Integrating proteomic and phosphoproteomic data for pathway analysis in breast cancer. **BMC Syst Biol,** v. 12, n. Suppl 8, p. 130, Dec 21 2018. ISSN 1752-0509 (Electronic)
1752-0509 (Linking). Disponível em: < http://www.ncbi.nlm.nih.gov/pubmed/30577793 >.

ROBLES, M. S.; COX, J.; MANN, M. In-vivo quantitative proteomics reveals a key contribution of post-transcriptional mechanisms to the circadian regulation of liver metabolism. **PLoS Genet,** v. 10, n. 1, p. e1004047, Jan 2014. ISSN 1553-7404 (Electronic)
1553-7390 (Linking). Disponível em: < http://www.ncbi.nlm.nih.gov/pubmed/24391516 >.

RONNOV-JESSEN, L.; PETERSEN, O. W.; BISSELL, M. J. Cellular changes involved in conversion of normal to malignant breast: importance of the stromal reaction. **Physiol Rev,** v. 76, n. 1, p. 69-125, Jan 1996. ISSN 0031-9333 (Print)
0031-9333 (Linking). Disponível em: < http://www.ncbi.nlm.nih.gov/pubmed/8592733 >.

ROTHENBERGER, N. J.; SOMASUNDARAM, A.; STABILE, L. P. The Role of the Estrogen Pathway in the Tumor Microenvironment. **Int J Mol Sci,** v. 19, n. 2, Feb 19 2018. ISSN 1422-0067 (Electronic)
1422-0067 (Linking). Disponível em: < http://www.ncbi.nlm.nih.gov/pubmed/29463044 >.

RUDDY, K. J.; WINER, E. P. Male breast cancer: risk factors, biology, diagnosis, treatment, and survivorship. **Ann Oncol,** v. 24, n. 6, p. 1434-43, Jun 2013. ISSN 1569-8041 (Electronic)

0923-7534 (Linking). Disponível em: < http://www.ncbi.nlm.nih.gov/pubmed/23425944 >.

SAKAI, T. ET AL. Plasmin-cleaved beta-2-glycoprotein 1 is an inhibitor of angiogenesis. **Am J Pathol,** v. 171, n. 5, p. 1659-69, Nov 2007. ISSN 0002-9440 (Print)
0002-9440 (Linking). Disponível em: < http://www.ncbi.nlm.nih.gov/pubmed/17872974 >.

SANCHEZ-VEGA, F. ET AL. Oncogenic Signaling Pathways in The Cancer Genome Atlas. **Cell,** v. 173, n. 2, p. 321-337 e10, Apr 5 2018. ISSN 1097-4172 (Electronic)
0092-8674 (Linking). Disponível em: < http://www.ncbi.nlm.nih.gov/pubmed/29625050 >.

SARASIN, A.; KAUFFMANN, A. Overexpression of DNA repair genes is associated with metastasis: a new hypothesis. **Mutat Res,** v. 659, n. 1-2, p. 49-55, Jul-Aug 2008. ISSN 0027-5107 (Print)
0027-5107 (Linking). Disponível em: < http://www.ncbi.nlm.nih.gov/pubmed/18308619 >.

SAXTON, R. A.; SABATINI, D. M. mTOR Signaling in Growth, Metabolism, and Disease. **Cell,** v. 168, n. 6, p. 960-976, Mar 9 2017. ISSN 1097-4172 (Electronic)
0092-8674 (Linking). Disponível em: < http://www.ncbi.nlm.nih.gov/pubmed/28283069 >.

SEGAL, E. ET AL. A module map showing conditional activity of expression modules in cancer. **Nat Genet,** v. 36, n. 10, p. 1090-8, Oct 2004. ISSN 1061-4036 (Print)
1061-4036 (Linking). Disponível em: < http://www.ncbi.nlm.nih.gov/pubmed/15448693 >.

SEGUIN, L. ET AL. Integrins and cancer: regulators of cancer stemness, metastasis, and drug resistance. **Trends Cell Biol,** v. 25, n. 4, p. 234-40, Apr 2015. ISSN 1879-3088 (Electronic)
0962-8924 (Linking). Disponível em: < http://www.ncbi.nlm.nih.gov/pubmed/25572304 >.

SEONG, J.; WANG, N.; WANG, Y. Mechanotransduction at focal adhesions: from physiology to cancer development. **J Cell Mol Med,** v. 17, n. 5, p. 597-604, May 2013. ISSN 1582-4934 (Electronic)
1582-1838 (Linking). Disponível em: < http://www.ncbi.nlm.nih.gov/pubmed/23601032 >.

SEVER, R.; BRUGGE, J. S. Signal transduction in cancer. **Cold Spring Harb Perspect Med,** v. 5, n. 4, Apr 1 2015. ISSN 2157-1422 (Electronic)
2157-1422 (Linking). Disponível em: < http://www.ncbi.nlm.nih.gov/pubmed/25833940 >.

SGROI, D. C. Preinvasive breast cancer. **Annu Rev Pathol,** v. 5, p. 193-221, 2010. ISSN 1553-4014 (Electronic)

1553-4006 (Linking). Disponível em: < http://www.ncbi.nlm.nih.gov/pubmed/19824828 >.

SINGLETARY, K. W.; GAPSTUR, S. M. Alcohol and breast cancer: review of epidemiologic and experimental evidence and potential mechanisms. **JAMA,** v. 286, n. 17, p. 2143-51, Nov 7 2001. ISSN 0098-7484 (Print)
0098-7484 (Linking). Disponível em: < http://www.ncbi.nlm.nih.gov/pubmed/11694156 >.

SINN, H. P.; KREIPE, H. A Brief Overview of the WHO Classification of Breast Tumors, 4th Edition, Focusing on Issues and Updates from the 3rd Edition. **Breast Care (Basel),** v. 8, n. 2, p. 149-54, May 2013. ISSN 1661-3791 (Print)
1661-3791 (Linking). Disponível em: < http://www.ncbi.nlm.nih.gov/pubmed/24415964 >.

SOBIN; GOSPODAROWICZ; WITTEKIND. **TNM classification of malignant tumours**. 7. Oxford, UK: Wiley Blackwell, 2009. ISBN 978-1-4443-3241-4. Disponível em: < http://www.inen.sld.pe/portal/documentos/pdf/educacion/13072015_TNM%20Classification.pdf >.

SOILAND, H. ET AL. Emerging concepts of apolipoprotein D with possible implications for breast cancer. **Cell Oncol,** v. 29, n. 3, p. 195-209, 2007. ISSN 1570-5870 (Print)
1570-5870 (Linking). Disponível em: < http://www.ncbi.nlm.nih.gov/pubmed/17452772 >.

SOMIARI, R. I. ET AL. Proteomics of breast carcinoma. **J Chromatogr B Analyt Technol Biomed Life Sci,** v. 815, n. 1-2, p. 215-25, Feb 5 2005. ISSN 1570-0232 (Print)
1570-0232 (Linking). Disponível em: < http://www.ncbi.nlm.nih.gov/pubmed/15652811 >.

SORLIE, T. ET AL. Gene expression patterns of breast carcinomas distinguish tumor subclasses with clinical implications. **Proc Natl Acad Sci U S A,** v. 98, n. 19, p. 10869-74, Sep 11 2001. ISSN 0027-8424 (Print)
0027-8424 (Linking). Disponível em: < http://www.ncbi.nlm.nih.gov/pubmed/11553815 >.

SORLIE, T. ET AL. Repeated observation of breast tumor subtypes in independent gene expression data sets. **Proc Natl Acad Sci U S A,** v. 100, n. 14, p. 8418-23, Jul 8 2003. ISSN 0027-8424 (Print)
0027-8424 (Linking). Disponível em: < http://www.ncbi.nlm.nih.gov/pubmed/12829800 >.

SOSA, V. ET AL. Oxidative stress and cancer: an overview. **Ageing Res Rev,** v. 12, n. 1, p. 376-90, Jan 2013. ISSN 1872-9649 (Electronic)
1568-1637 (Linking). Disponível em: < http://www.ncbi.nlm.nih.gov/pubmed/23123177 >.

SRINIVAS, P. R. ET AL. Proteomics for cancer biomarker discovery. **Clin Chem,** v. 48, n. 8, p. 1160-9, Aug 2002. ISSN 0009-9147 (Print)
0009-9147 (Linking). Disponível em: < http://www.ncbi.nlm.nih.gov/pubmed/12142368 >.

STEIN, A. ET AL. Dynamic interactions of proteins in complex networks: a more structured view. **FEBS J,** v. 276, n. 19, p. 5390-405, Oct 2009. ISSN 1742-4658 (Electronic)
1742-464X (Linking). Disponível em: < http://www.ncbi.nlm.nih.gov/pubmed/19712106 >.

STEVENS, R. G. ET AL. Breast cancer and circadian disruption from electric lighting in the modern world. **CA Cancer J Clin,** v. 64, n. 3, p. 207-18, May-Jun 2014. ISSN 1542-4863 (Electronic)
0007-9235 (Linking). Disponível em: < http://www.ncbi.nlm.nih.gov/pubmed/24604162 >.

STEWART, T. A.; YAPA, K. T.; MONTEITH, G. R. Altered calcium signaling in cancer cells. **Biochim Biophys Acta,** v. 1848, n. 10 Pt B, p. 2502-11, Oct 2015. ISSN 0006-3002 (Print)
0006-3002 (Linking). Disponível em: < http://www.ncbi.nlm.nih.gov/pubmed/25150047 >.

SUMAN, S. ET AL. Quantitative proteomics revealed novel proteins associated with molecular subtypes of breast cancer. **J Proteomics,** v. 148, p. 183-93, Oct 4 2016. ISSN 1876-7737 (Electronic)
1874-3919 (Linking). Disponível em: < http://www.ncbi.nlm.nih.gov/pubmed/27498393 >.

SWITZAR, L.; GIERA, M.; NIESSEN, W. M. Protein digestion: an overview of the available techniques and recent developments. **J Proteome Res,** v. 12, n. 3, p. 1067-77, Mar 1 2013. ISSN 1535-3907 (Electronic)
1535-3893 (Linking). Disponível em: < http://www.ncbi.nlm.nih.gov/pubmed/23368288 >.

SZKLARCZYK, D. ET AL. STRING v10: protein-protein interaction networks, integrated over the tree of life. **Nucleic Acids Res,** v. 43, n. Database issue, p. D447-52, Jan 2015. ISSN 1362-4962 (Electronic)
0305-1048 (Linking). Disponível em: < http://www.ncbi.nlm.nih.gov/pubmed/25352553 >.

SZKLARCZYK, D. ET AL. The STRING database in 2017: quality-controlled protein-protein association networks, made broadly accessible. **Nucleic Acids Res,** v. 45, n. D1, p. D362-D368, Jan 4 2017. ISSN 1362-4962 (Electronic)
0305-1048 (Linking). Disponível em: < http://www.ncbi.nlm.nih.gov/pubmed/27924014 >.

TANAKA, H.; OGISHIMA, S. Network biology approach to epithelial-mesenchymal transition in cancer metastasis: three stage theory. **J Mol Cell Biol,** v. 7, n. 3, p. 253-66, Jun 2015. ISSN 1759-4685 (Electronic)

1759-4685 (Linking). Disponível em: < http://www.ncbi.nlm.nih.gov/pubmed/26103982 >.

TENGA, M. J.; LAZAR, I. M. Proteomic study reveals a functional network of cancer markers in the G1-Stage of the breast cancer cell cycle. **BMC Cancer,** v. 14, p. 710, Sep 24 2014. ISSN 1471-2407 (Electronic)
1471-2407 (Linking). Disponível em: < http://www.ncbi.nlm.nih.gov/pubmed/25252636 >.

THOMAS, P. D. ET AL. PANTHER: a library of protein families and subfamilies indexed by function. **Genome Res,** v. 13, n. 9, p. 2129-41, Sep 2003. ISSN 1088-9051 (Print)
1088-9051 (Linking). Disponível em: < http://www.ncbi.nlm.nih.gov/pubmed/12952881 >.

TOMASKOVIC-CROOK, E.; THOMPSON, E. W.; THIERY, J. P. Epithelial to mesenchymal transition and breast cancer. **Breast Cancer Res,** v. 11, n. 6, p. 213, 2009. ISSN 1465-542X (Electronic)
1465-5411 (Linking). Disponível em: < http://www.ncbi.nlm.nih.gov/pubmed/19909494 >.

TOPISIROVIC, I.; SONENBERG, N. mRNA translation and energy metabolism in cancer: the role of the MAPK and mTORC1 pathways. **Cold Spring Harb Symp Quant Biol,** v. 76, p. 355-67, 2011. ISSN 1943-4456 (Electronic)
0091-7451 (Linking). Disponível em: < http://www.ncbi.nlm.nih.gov/pubmed/22123850 >.

TURASHVILI, G.; BROGI, E. Tumor Heterogeneity in Breast Cancer. **Front Med (Lausanne),** v. 4, p. 227, 2017. ISSN 2296-858X (Print)
2296-858X (Linking). Disponível em: < http://www.ncbi.nlm.nih.gov/pubmed/29276709 >.

TYANOVA, S. ET AL. Proteomic maps of breast cancer subtypes. **Nat Commun,** v. 7, p. 10259, Jan 4 2016. ISSN 2041-1723 (Electronic)
2041-1723 (Linking). Disponível em: < http://www.ncbi.nlm.nih.gov/pubmed/26725330 >.

TYANOVA, S. ET AL. The Perseus computational platform for comprehensive analysis of (prote)omics data. **Nat Methods,** v. 13, n. 9, p. 731-40, Sep 2016. ISSN 1548-7105 (Electronic)
1548-7091 (Linking). Disponível em: < http://www.ncbi.nlm.nih.gov/pubmed/27348712 >.

UNIPROT CONSORTIUM, T. UniProt: the universal protein knowledgebase. **Nucleic Acids Res,** v. 46, n. 5, p. 2699, Mar 16 2018. ISSN 1362-4962 (Electronic)
0305-1048 (Linking). Disponível em: < http://www.ncbi.nlm.nih.gov/pubmed/29425356 >.

UNIVERSITY OF BRISTOL. **High Performance Liquid Chromatography Mass Spectrometry (HPLC/MS)**, 27/04/2005, 2019. Disponível em: < http://www.bris.ac.uk/nerclsmsf/techniques/hplcms.html >.

URRA, H. ET AL. Endoplasmic Reticulum Stress and the Hallmarks of Cancer. **Trends Cancer,** v. 2, n. 5, p. 252-262, May 2016. ISSN 2405-8025 (Electronic)
2405-8025 (Linking). Disponível em: < http://www.ncbi.nlm.nih.gov/pubmed/28741511 >.

VAN 'T VEER, L. J. ET AL. Gene expression profiling predicts clinical outcome of breast cancer. **Nature,** v. 415, n. 6871, p. 530-6, Jan 31 2002. ISSN 0028-0836 (Print)
0028-0836 (Linking). Disponível em: < http://www.ncbi.nlm.nih.gov/pubmed/11823860 >.

VANHOUTEN, J. ET AL. PMCA2 regulates apoptosis during mammary gland involution and predicts outcome in breast cancer. **Proc Natl Acad Sci U S A,** v. 107, n. 25, p. 11405-10, Jun 22 2010. ISSN 1091-6490 (Electronic)
0027-8424 (Linking). Disponível em: < http://www.ncbi.nlm.nih.gov/pubmed/20534448 >.

VELLOSO, F. J. ET AL. The crossroads of breast cancer progression: insights into the modulation of major signaling pathways. **Onco Targets Ther,** v. 10, p. 5491-5524, 2017. ISSN 1178-6930 (Print)
1178-6930 (Linking). Disponível em: < http://www.ncbi.nlm.nih.gov/pubmed/29200866 >.

VENNING, F. A.; WULLKOPF, L.; ERLER, J. T. Targeting ECM Disrupts Cancer Progression. **Front Oncol,** v. 5, p. 224, 2015. ISSN 2234-943X (Print)
2234-943X (Linking). Disponível em: < http://www.ncbi.nlm.nih.gov/pubmed/26539408 >.

VILLANUEVA, H. ET AL. The Emerging Roles of Steroid Hormone Receptors in Ductal Carcinoma in Situ (DCIS) of the Breast. **J Mammary Gland Biol Neoplasia,** v. 23, n. 4, p. 237-248, Dec 2018. ISSN 1573-7039 (Electronic)
1083-3021 (Linking). Disponível em: < http://www.ncbi.nlm.nih.gov/pubmed/30338425 >.

VISVADER, J. E. Keeping abreast of the mammary epithelial hierarchy and breast tumorigenesis. **Genes Dev,** v. 23, n. 22, p. 2563-77, Nov 15 2009. ISSN 1549-5477 (Electronic)
0890-9369 (Linking). Disponível em: < http://www.ncbi.nlm.nih.gov/pubmed/19933147 >.

VISVADER, J. E.; STINGL, J. Mammary stem cells and the differentiation hierarchy: current status and perspectives. **Genes Dev,** v. 28, n. 11, p. 1143-58, Jun 1 2014. ISSN 1549-5477 (Electronic)
0890-9369 (Linking). Disponível em: < http://www.ncbi.nlm.nih.gov/pubmed/24888586 >.

VOGELSTEIN, B.; KINZLER, K. W. Cancer genes and the pathways they control. **Nat Med,** v. 10, n. 8, p. 789-99, Aug 2004. ISSN 1078-8956 (Print)
1078-8956 (Linking). Disponível em: < http://www.ncbi.nlm.nih.gov/pubmed/15286780 >.

WALTHER, T. C.; MANN, M. Mass spectrometry-based proteomics in cell biology. **J Cell Biol,** v. 190, n. 4, p. 491-500, Aug 23 2010. ISSN 1540-8140 (Electronic)
0021-9525 (Linking). Disponível em: < http://www.ncbi.nlm.nih.gov/pubmed/20733050 >.

WANG, Z. ET AL. Repairing DNA damage by XRCC6/KU70 reverses TLR4-deficiency-worsened HCC development via restoring senescence and autophagic flux. **Autophagy,** v. 9, n. 6, p. 925-7, Jun 1 2013. ISSN 1554-8635 (Electronic)
1554-8627 (Linking). Disponível em: < http://www.ncbi.nlm.nih.gov/pubmed/23518600 >.

WEN, J. ET AL. Genome-wide analysis of alternative transcripts in human breast cancer. **Breast Cancer Res Treat,** v. 151, n. 2, p. 295-307, Jun 2015. ISSN 1573-7217 (Electronic)
0167-6806 (Linking). Disponível em: < http://www.ncbi.nlm.nih.gov/pubmed/25913416 >.

WERTHEIMER, E. ET AL. Rac signaling in breast cancer: a tale of GEFs and GAPs. **Cell Signal,** v. 24, n. 2, p. 353-62, Feb 2012. ISSN 1873-3913 (Electronic)
0898-6568 (Linking). Disponível em: < http://www.ncbi.nlm.nih.gov/pubmed/21893191 >.

WIGERUP, C.; PAHLMAN, S.; BEXELL, D. Therapeutic targeting of hypoxia and hypoxia-inducible factors in cancer. **Pharmacol Ther,** v. 164, p. 152-69, Aug 2016. ISSN 1879-016X (Electronic)
0163-7258 (Linking). Disponível em: < http://www.ncbi.nlm.nih.gov/pubmed/27139518 >.

WILKINS, M. R. ET AL. Current challenges and future applications for protein maps and post-translational vector maps in proteome projects. **Electrophoresis,** v. 17, n. 5, p. 830-8, May 1996. ISSN 0173-0835 (Print)
0173-0835 (Linking). Disponível em: < http://www.ncbi.nlm.nih.gov/pubmed/8783009 >.

WISNIEWSKI, J. R.; GAUGAZ, F. Z. Fast and sensitive total protein and Peptide assays for proteomic analysis. **Anal Chem,** v. 87, n. 8, p. 4110-6, Apr 21 2015. ISSN 1520-6882 (Electronic)
0003-2700 (Linking). Disponível em: < http://www.ncbi.nlm.nih.gov/pubmed/25837572 >.

WISNIEWSKI, J. R. ET AL. Universal sample preparation method for proteome analysis. **Nat Methods,** v. 6, n. 5, p. 359-62, May 2009. ISSN 1548-7105 (Electronic)
1548-7091 (Linking). Disponível em: < http://www.ncbi.nlm.nih.gov/pubmed/19377485 >.

XU, M. ET AL. A temporal examination of calcium signaling in cancer- from tumorigenesis, to immune evasion, and metastasis. **Cell Biosci,** v. 8, p. 25, 2018. ISSN 2045-3701 (Print)
2045-3701 (Linking). Disponível em: < http://www.ncbi.nlm.nih.gov/pubmed/29636894 >.

XU, X.; XIONG, X.; SUN, Y. The role of ribosomal proteins in the regulation of cell proliferation, tumorigenesis, and genomic integrity. **Sci China Life Sci,** v. 59, n. 7, p. 656-72, Jul 2016. ISSN 1869-1889 (Electronic)
1674-7305 (Linking). Disponível em: < http://www.ncbi.nlm.nih.gov/pubmed/27294833 >.

YANG, C. ET AL. Ribosomal protein L6 (RPL6) is recruited to DNA damage sites in a poly (ADP-ribose) polymerase-dependent manner and regulates the DNA damage response. **J Biol Chem**, Dec 31 2018. ISSN 1083-351X (Electronic)
0021-9258 (Linking). Disponível em: < http://www.ncbi.nlm.nih.gov/pubmed/30598506 >.

YEH, M. H. ET AL. Extracellular Matrix-receptor Interaction Signaling Genes Associated with Inferior Breast Cancer Survival. **Anticancer Res,** v. 38, n. 8, p. 4593-4605, Aug 2018. ISSN 1791-7530 (Electronic)
0250-7005 (Linking). Disponível em: < http://www.ncbi.nlm.nih.gov/pubmed/30061226 >.

YU, P. ET AL. Beta2-glycoprotein I inhibits vascular endothelial growth factor and basic fibroblast growth factor induced angiogenesis through its amino terminal domain. **J Thromb Haemost,** v. 6, n. 7, p. 1215-23, Jul 2008. ISSN 1538-7836 (Electronic)
1538-7836 (Linking). Disponível em: < http://www.ncbi.nlm.nih.gov/pubmed/18452581 >.

ZENG, Q. ET AL. CD146, an epithelial-mesenchymal transition inducer, is associated with triple-negative breast cancer. **Proc Natl Acad Sci U S A,** v. 109, n. 4, p. 1127-32, Jan 24 2012. ISSN 1091-6490 (Electronic)
0027-8424 (Linking). Disponível em: < http://www.ncbi.nlm.nih.gov/pubmed/22210108 >.

ZHANG, F.; CHEN, J. Y. Discovery of pathway biomarkers from coupled proteomics and systems biology methods. **BMC Genomics,** v. 11 Suppl 2, p. S12, Nov 2 2010. ISSN 1471-2164 (Electronic)
1471-2164 (Linking). Disponível em: < http://www.ncbi.nlm.nih.gov/pubmed/21047379 >.

ZHANG, H.; GE, Y. Comprehensive analysis of protein modifications by top-down mass spectrometry. **Circ Cardiovasc Genet,** v. 4, n. 6, p. 711, Dec 2011. ISSN 1942-3268 (Electronic)
1942-3268 (Linking). Disponível em: < http://www.ncbi.nlm.nih.gov/pubmed/22187450 >.

ZHANG, Y. ET AL. Protein analysis by shotgun/bottom-up proteomics. **Chem Rev,** v. 113, n. 4, p. 2343-94, Apr 10 2013. ISSN 1520-6890 (Electronic)
0009-2665 (Linking). Disponível em: < http://www.ncbi.nlm.nih.gov/pubmed/23438204 >.

ZHAO, X. ET AL. Cell cycle-dependent phosphorylation of nucleophosmin and its potential regulation by peptidyl-prolyl cis/trans isomerase. **J Mol Biochem,** v. 4, p. 95-103, Nov 25 2015. ISSN 2241-0090 (Print)
2241-0090 (Linking). Disponível em: < http://www.ncbi.nlm.nih.gov/pubmed/27099843 >.

ZHOU, G. ET AL. The role of desmosomes in carcinogenesis. **Onco Targets Ther,** v. 10, p. 4059-4063, 2017. ISSN 1178-6930 (Print)
1178-6930 (Linking). Disponível em: < http://www.ncbi.nlm.nih.gov/pubmed/28860814 >.

ZHOU, J. Y. ET AL. Simple sodium dodecyl sulfate-assisted sample preparation method for LC-MS-based proteomics applications. **Anal Chem,** v. 84, n. 6, p. 2862-7, Mar 20 2012. ISSN 1520-6882 (Electronic)
0003-2700 (Linking). Disponível em: < http://www.ncbi.nlm.nih.gov/pubmed/22339560 >.

APÊNDICE 1

MATERIAL SUPLEMENTAR 1A – PADRÃO DE EXPRESSÃO DOS PRINCIPAIS *CLUSTERS* DE PROTEÍNAS DIFERENCIALMENTE EXPRESSAS NA COMPARAÇÃO TP x NT

Cluster	Número de proteínas	TP x NT*	Sigla dos genes
1	8	↑	*GAPDH, HSP90AA1, HSP90B1, HSPA5, HSPA8, KRT19, MYH9, P4HB*
2	2	↑	*ACTB, HIST1H4A*
3	1	↓	*DCLK1*
4	18	↑	*CFL1, CSE1L, DDX39B, DHX9, EEF1G, EIF4A1, HNRNPA2B1, HNRNPM, HNRNPU, HSPD1, IDH2, ILF2, LRPPRC, NCL, PDIA4, PRKDC, RPL4, SERPINH1*
5	1	↑	*KRT18*
6	2	↑	*CAD, SNRNP200*
7	52	↑	*AGL, ANP32A, C1QBP, CACYBP, CAPG, CKAP4, COPB1, COPG1, CRABP2, DHX15, DPP3, DSP, EFTUD2, EIF4G1, EPRS, EZR, FAM129B, FBL, GCN1, GOT2, HDGF, HDLBP, HNRNPF, HNRNPL, HYOU1, IARS, ILF3, IPO7, LARS, LRRC59, MYO1B, NAMPT, NANS, NOP56, NPM1, PAFAH1B3, PARP1, PCBP1, RAB6A, RPL3, RPL5, RPL6, RPL9, RPS3A, RRBP1, RUVBL2, SORD, SRSF1, TARS, TTLL12, TRIM28, TYMP*
8	1	↑	*TNC*
9	12	↓	*ALDH2, APOB, CA1, CAT, COL1A2, FABP4, GC, HBD, IGHG2, IGHG3, MYO1C, TTR*
10	1	↓	*APOD*
11	6	↓	*CES1, LIPE, MCAM, SLC4A1, SORBS1, TNS1*
12	36	↓	*ACO1, ACSL1, AGT, AHSG, AKR1C3, ALAD, ALDH3A2, AMBP, APCS, APOE, ASPH, BLVRB, C5, CA2, CFH, COL4A2, CRYAB, EPHX1, FAM213A, FBN1, HRG, IGHG4, IGKV3-20, KNG1, LAMA4, LAMB1, LTF, MYH11, NID2, ORM2, PARVA, PLG, RRAS, S100A10, SERPIND1, STOM*
13	19	↓	*ADD1, AFM, APOH, C4BPA, CFD, F12, FAH, FBLN5, HBG1, IGFALS, IGHA2, ILK, LRG1, METTL7A, PGLYRP2, PON1, SERPINA4, SERPINA7, SERPINF2*
14	10	↓	*AKR1C1, ANK1, CALB2, HSPA12A, HSPB6, MAOA, MGLL, RETSAT, SPTA1, SPTB*
15	6	↓	*ACADS, ALDH4A1, ECHDC1, GBE1, ME1, PRKAR2B*

LEGENDA: TP – Tumor primário de mama, NT – tecidos não tumorais. * Expressão no tumor primário de mama em relação aos tecidos não tumorais: superexpressão (↑) e subexpressão (↓).

MATERIAL SUPLEMENTAR 1B – PADRÃO DE EXPRESSÃO DOS PRINCIPAIS *CLUSTERS* DE PROTEÍNAS DIFERENCIALMENTE EXPRESSAS NA COMPARAÇÃO LN x NT

Cluster	**Número de proteínas**	**LN x NT***	**Sigla dos genes**
1	5	↑	*GAPDH, HSP90AA1, HSP90B1, HSPA5, HSPA8*
2	4	↓	*APOA1, IGKC, SERPINA1, TF*
3	22	↓	*ALDH2, APOB, BGN, C4B, CA1, CAT, COL1A2, FABP4, FGA, GC, HBD, HP, HPX, IGHA1, IGHG2, IGHG3, MYO1C, ORM1, SERPINA3, SERPINC1, SERPING1, TTR*
4	2	↑	*ACTB, HIST1H4A*
5	1	↑	*TNC*
6	49	↑	*ANP32A, API5, ARPC3, C1QBP, CACYBP, CAD, DDX6, DHX15, DSP, EFHD2, EFTUD2, EIF4G1, EIF4G2, EPRS, EZR, FBL, FUS, , GARS, GCN1, GFPT1, HDGF, HDLBP, HNRNPL, HYOU1, IARS, IMPDH2, IPO7, LARS, LRRC59, ME2, NAP1L1, NOP56, NPM1, RAB6A, RPL10, RPL24, RPL3, RPL5, RPL6, RPS12, RPS17, RPS3A, RUVBL2, SARS, SNRNP200, SNRPD3, SRSF1, TARS, UPF1*
7	26	↑	*ACLY, ACTR2, ACTR3, ARPC2, CAPG, COPB1, DHX9, HNRNPF, HNRNPH1, ILF2, ILF3, LMNB1, LRPPRC, NAGK, PARP1, PCBP1, PRKDC, PRPS2, RAC2, RPL13, RPL4, RPL7A, SFPQ, TRIM28, TYMP, XPO1*
8	15	↑	*CSE1L, DDX39B, EIF4A1, HNRNPA2B1, HNRNPK, HNRNPM, HNRNPU, HSPD1, NCL, PDIA4, RPS3, RPSA, SYNCRIP, XRCC5, XRCC6*
9	1	↓	*COL6A6*
10	11	↓	*AKR1C1, ANK1, CES1, HSPB6, LIPE, MAOA, MCAM, SORBS1, SPTA1, SPTB, TNS1*
11	1	↓	*APOD*
12	26	↓	*AFM, AGT, AK1, ALAD, AMBP, APOH, ASPH, C5, C9, CSRP1, CTSG, FAM213A, FBLN2, IGHA2, IGHG4, LAMB1, LRG1, PARVA, PLG, PON1, RRAS, S100A10, SERPINA4, SERPINF2, STOM, TPM1*
13	30	↓	*ACO1, ACSL1, AHSG, AKR1C3, APCS, APOE, BLVRB, CA2, CFB, CFH, COL4A2, CRYAB, CYB5A, F2, FBN1, HRG, IGKV3-20, ITIH1, ITIH2, ITIH4, KNG1, LAMA4, LTF, MYH11, NID2, ORM2, PGM1, SERPIND1, SLC4A1, YWHAG*
14	2	↓	*DCLK1, KANK2*
15	28	↓	*ACADS, ALDH4A1, C1QC, C4BPA, C6, C8B, CALB2, CFD, CFI, F12, FAH, FBLN5, GBE1, GNA11, HBG1, HSPA12A, IGFALS, ILK, ITGA1, ITGA6, ME1, MGLL, PGLYRP2, PRKAR2B, RETSAT, SERPINA5, SERPINA7*

LEGENDA: LN – Linfonodo axilar metastático, NT – tecidos não tumorais. * Expressão no linfonodo axilar metastático em relação aos tecidos não tumorais: superexpressão (↑) e subexpressão (↓).

APÊNDICE 2

Supplementary File 1. A. Reproducibility of the MBC samples' technical replicates. **B.** Differentially expressed proteins identified in all groups' comparisons from the MBC case (MPT x MNT, MLN x MNT, MPT x MLN) according to the ANOVA's test.

Supplementary File 2. A. Differentially expressed proteins into the log2 fold change values identified in the MLN x MNT tissues' comparison according to the ANOVA's test. **B.** Functional annotation of the differentially expressed proteins identified in the MLN x MNT tissues' comparison (PANTHER system classification). **C.** Signaling canonical pathways predicted from the differentially expressed proteins identified in the MLN x MNT tissues' comparison (IPA analysis). **D.** Differentially expressed proteins into the “Cancer” and “Breast cancer” annotations according to the Ingenuity Pathways Knowledge Base (IPA analysis). **E.** Predicted protein interactive networks of the differentially expressed proteins identified in the MLN x MNT tissues' comparison (IPA analysis). **F.** Main upstream regulators analysis of the differentially expressed proteins identified in the MLN x MNT tissues' comparison (IPA analysis).

Supplementary File 3. A. Differentially expressed proteins into the log2 fold change values identified for MPT x MNT tissues' comparison according to the ANOVA's test. **B.** Functional annotation of the differentially expressed proteins identified in the MPT x MNT tissues' comparison (PANTHER system classification). **C.** Main upstream regulators analysis of the differentially expressed proteins identified in the MPT x MNT tissues' comparison (IPA analysis).

Supplementary File 4. A. Differentially expressed proteins into the log2 fold change values identified for MPT x MLN tissues' comparison according to the ANOVA's test. **B.** Functional annotation of the differentially expressed proteins identified in the MPT x MLN tissues' comparison. **C.** Main upstream regulators analysis of the differentially expressed proteins identified in the MPT x MLN tissues' comparison (IPA analysis).

Supplementary File 5. A. Reproducibility of the technical replicates from MPT x FPT tissues' comparison. **B.** Differentially expressed proteins identified for MPT x FPT tissues' comparison according to the ANOVA's test. **C.** Functional annotation of the differentially expressed proteins in the MPT x FPT tissues' comparison. **D.** Functional enrichment analysis ($p>0.05$) through DAVID analysis of the main up-regulated and down-regulated proteins identified in the MPT x FPT tissues' comparison.

Supplementary File 1A. Reproducibility of the MBC samples' technical replicates.

I. Pearson correlation analysis among the non-tumor breast tissues, primary breast tumor and axillary metastatic lymph node samples of the male patient based on LFQ intensity values of the 962 identified proteins.
II. Hierarchical clustering analysis from the 675 differentially expressed proteins among the non-tumor breast tissue, primary tumor and axillary metastatic lymph node samples.

Legend: MPT - male-primary breast tumor; MNT - male-non-tumor breast tissue; MLN - male-axillary metastatic lymph node.

I.

Technical Replicates	MNT_1	MNT_2	MNT_3	MPT_1	MPT_2	MPT_3	MLN_1	MLN_2	MLN_3
MNT_1	-	0.9611	0.9630	0.6567	0.6534	0.6549	0.5590	0.5509	0.5601
MNT_2	0.9611	-	0.9616	0.6499	0.6470	0.6512	0.5542	0.5423	0.5542
MNT_3	0.9630	0.9616	-	0.6512	0.6497	0.6518	0.5534	0.5426	0.5571
MPT_1	0.6567	0.6499	0.6512	-	0.9862	0.9851	0.9475	0.9453	0.9383
MPT_2	0.6534	0.6470	0.6497	0.9862	-	0.9858	0.9414	0.9400	0.9345
MPT_3	0.6549	0.6512	0.6518	0.9851	0.9858	-	0.9437	0.9427	0.9362
MLN_1	0.5590	0.5542	0.5534	0.9475	0.9414	0.9437	-	0.9906	0.9759
MLN_2	0.5509	0.5423	0.5426	0.9453	0.9400	0.9427	0.9906	-	0.9755
MLN_3	0.5601	0.5542	0.5571	0.9383	0.9345	0.9362	0.9759	0.9755	-

II.

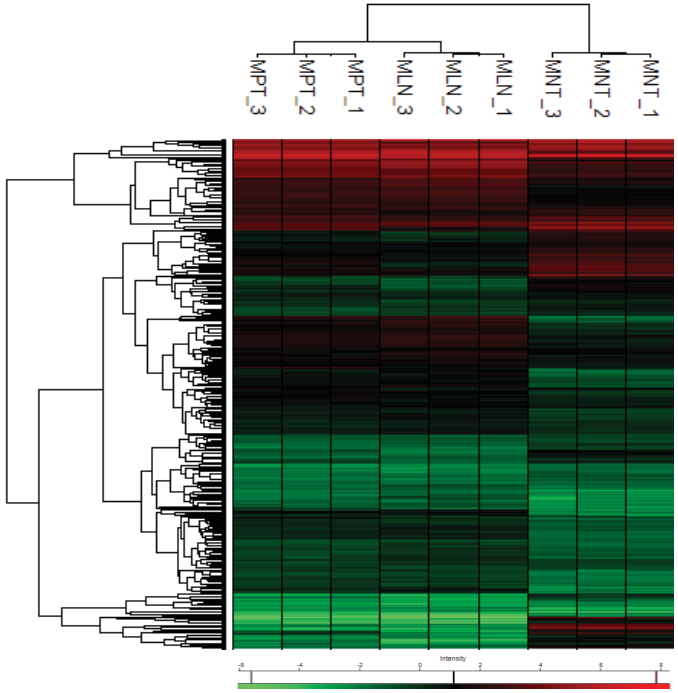

Supplementary File 1B. Differentially expressed proteins identified in all groups' comparisons from the MBC case (MPT x MNT, MLN x MNT, MPT x MLN) according to the ANOVA's test.

LFQ intensities were log2-transformed and normalized by width adjustment in Perseus v. 1.5.6.0. Fold changes were presented in log2 values (up-regulated and down-regulated proteins were highlighted in red and green, respectively).

* Proteins that presented a gradual increase or decrease in ther expression levels throughout the tumor progression (MNT to MPT to MLN samples). In this context, the fold change values of the MPT x MLN group' comparison indicate: negative values - higher expression levels in the MLN compared to the MPT sample; positive values - lower expression levels in the MLN sample.

Protein Name	Gene Symbol	MNT LFQ_mean	MPT LFQ_mean	MLN LFQ_mean	MPT x MNT fold change	MLN x MNT fold change	MPT x MLN fold change	Gradual ↑/↓ from MNT to MPT to MLN*	ANOVA p-value
Alpha-1B-glycoprotein	*A1BG*	2.1274	0.4713	0.4517	-1.6561	-1.6757	-	-	1.65E-03
Alpha-2-macroglobulin	*A2M*	5.4595	4.3128	3.2431	-1.1467	-2.2164	1.0697	↓	3.42E-06
Alpha/beta hydrolase domain-containing protein 11	*ABHD11*	-2.4499	-2.0277	-0.5992	-	1.8507	-1.4285	-	1.22E-02
Alpha/beta hydrolase domain-containing protein 14B	*ABHD14B*	0.5174	-1.6124	-1.2778	-2.1298	-1.7953	-	-	8.50E-06
3-ketoacyl-CoA thiolase, peroxisomal	*ACAA1*	-3.2105	-2.0180	-1.5373	1.1925	1.6732	-0.4807	↑	7.02E-05
3-ketoacyl-CoA thiolase, mitochondrial	*ACAA2*	1.2126	-0.8760	-0.8970	-2.0886	-2.1096	-	-	5.97E-06
Acetyl-CoA carboxylase 2;Biotin carboxylase	*ACACB*	0.7338	-3.8072	-3.7810	-4.5410	-4.5149	-	-	2.57E-04
Medium-chain specific acyl-CoA dehydrogenase, mitochondrial	*ACADM*	0.4431	-1.9845	-1.0689	-2.4277	-1.5120	-0.9157	-	5.06E-05
Short-chain specific acyl-CoA dehydrogenase, mitochondrial	*ACADS*	1.0767	-2.8929	-2.5097	-3.9696	-3.5864	-	-	1.53E-06
Short/branched chain specific acyl-CoA dehydrogenase, mitochondrial	*ACADSB*	-1.6947	0.2021	0.4542	1.8968	2.1490	-0.2522	↑	5.96E-07
Very long-chain specific acyl-CoA dehydrogenase, mitochondrial	*ACADVL*	1.7282	1.1758	1.1710	-0.5524	-0.5572	-	-	5.55E-05
Cytoplasmic aconitate hydratase	*ACO1*	1.3932	-0.1895	-0.4186	-1.5827	-1.8118	-	-	5.34E-06
Aconitate hydratase, mitochondrial	*ACO2*	1.3870	0.8925	1.5844	-0.4946	-	-0.6919	-	7.05E-03
Acyl-coenzyme A thioesterase 1	*ACOT1*	1.8228	-0.9927	-0.0417	-2.8155	-1.8645	-0.9510	-	8.08E-06
Long-chain-fatty-acid--CoA ligase 1	*ACSL1*	3.5536	-2.4079	-2.4161	-5.9615	-5.9697	-	-	2.22E-06
Alpha-actinin-1	*ACTN1*	3.0065	4.2385	3.7950	1.2321	0.7885	0.4436	-	5.32E-06
Alpha-actinin-4	*ACTN4*	2.3762	3.1367	3.0578	0.7605	0.6817	-	-	8.81E-05
Actin-related protein 2	*ACTR2*	-0.3669	0.3385	0.4920	0.7053	0.8588	-	-	1.23E-02
Actin-related protein 3	*ACTR3*	0.3873	1.2045	0.8330	0.8172	0.4456	0.3715	-	1.19E-03
Alcohol dehydrogenase class-3	*ADH5*	0.4225	-1.5999	-1.2975	-2.0224	-1.7200	-	-	3.39E-04
Adipocyte enhancer-binding protein 1	*AEBP1*	-0.8130	0.9414	0.2247	1.7544	1.0378	0.7166	-	6.59E-05
Afamin	*AFM*	0.8953	-1.0592	-1.6164	-1.9545	-2.5116	0.5571	↓	4.64E-05
Glycogen debranching enzyme;4-alpha-glucanotransferase;Amylo-alpha-1,6-glucosidase	*AGL*	-1.0734	0.1243	0.6580	1.1977	1.7314	-0.5337	↑	7.25E-05
Anterior gradient protein 2 homolog	*AGR2*	-2.1493	1.1504	1.0164	3.2997	3.1658	-	-	6.05E-06
Angiotensinogen;Angiotensin-1;Angiotensin-2;Angiotensin-3;Angiotensin-4;Angiotensin 1-9;Angioten	*AGT*	1.4353	-0.1363	-0.9917	-1.5716	-2.4271	0.8554	↓	2.63E-07
Adenosylhomocysteinase	*AHCY*	0.7595	1.9245	2.6085	1.1650	1.8489	-0.6839	↑	8.14E-07
Neuroblast differentiation-associated protein AHNAK	*AHNAK*	3.6849	3.3279	3.2975	-0.3570	-0.3874	-	-	6.21E-03
Alpha-2-HS-glycoprotein;Alpha-2-HS-glycoprotein chain A;Alpha-2-HS-glycoprotein chain B	*AHSG*	1.1837	-1.4220	-3.9872	-2.6057	-5.1709	2.5652	↓	4.35E-07
Apoptosis-inducing factor 1, mitochondrial	*AIFM1*	-0.1416	-0.6426	-0.5005	-0.5010	-0.3589	-	-	2.25E-02
Adenylate kinase 4, mitochondrial	*AK4*	0.3137	-2.2435	-3.2467	-2.5572	-3.5604	-	-	8.26E-04
Alcohol dehydrogenase [NADP(+)]	*AKR1A1*	-0.8542	-0.4976	-0.0383	0.3566	0.8159	-0.4593	↑	1.93E-05
Aflatoxin B1 aldehyde reductase member 2	*AKR7A2*	0.5199	-0.2169	-0.3530	-0.7369	-0.8730	-	-	2.06E-02
Retinal dehydrogenase 1	*ALDH1A1*	1.9275	0.3203	0.1418	-1.6072	-1.7857	0.1785	↓	8.89E-08
Aldehyde dehydrogenase X, mitochondrial	*ALDH1B1*	0.0703	-0.3124	-0.9843	-	-1.0545	0.6719	-	8.59E-03
Aldehyde dehydrogenase, mitochondrial	*ALDH2*	3.6553	1.5342	0.9643	-2.1212	-2.6910	0.5699	↓	4.99E-07
Methylmalonate-semialdehyde dehydrogenase [acylating], mitochondrial	*ALDH6A1*	0.1925	-2.4772	-2.3352	-2.6698	-2.5278	-	-	2.46E-04
4-trimethylaminobutyraldehyde dehydrogenase	*ALDH9A1*	2.4482	1.7597	1.6655	-0.6885	-0.7827	-	-	1.12E-04
Fructose-bisphosphate aldolase A;Fructose-bisphosphate aldolase	*ALDOA*	2.8319	4.5608	4.3895	1.7289	1.5576	-	-	6.19E-06
Fructose-bisphosphate aldolase C;Fructose-bisphosphate aldolase	*ALDOC*	1.6204	0.7722	0.0888	-	-1.5316	-	-	1.50E-02
Annexin A1;Annexin	*ANXA1*	3.8666	3.3100	2.7190	-0.5566	-1.1476	0.5910	↓	2.64E-05
Annexin A11	*ANXA11*	0.2264	-0.1251	-0.4952	-0.3515	-0.7216	0.3700	↓	1.99E-03
Annexin A2;Annexin;Putative annexin A2-like protein	*ANXA2*	5.0255	5.3236	4.8826	0.2982	-	0.4410	-	9.49E-03
Annexin;Annexin A3	*ANXA3*	0.1418	-2.6747	-2.6454	-2.8164	-2.7872	-	-	2.46E-04
Annexin A6;Annexin	*ANXA6*	3.8056	3.6011	3.7589	-0.2045	-	-	-	4.38E-02
Annexin A7	*ANXA7*	-0.3896	-0.4966	-0.1035	-	0.2861	-0.3932	-	1.39E-02
AP-1 complex subunit beta-1	*AP1B1*	-2.3633	-1.2686	-1.0845	1.0946	1.2787	-	-	5.05E-04
AP-1 complex subunit gamma-1	*AP1G1*	-2.5762	-0.9982	-1.1089	1.5780	1.4673	-	-	3.20E-05
AP-2 complex subunit alpha-1	*AP2A1*	-2.7381	-2.2341	-2.8555	0.5040	-	0.6214	-	1.95E-02
AP-2 complex subunit beta	*AP2B1*	0.3221	0.8445	0.6047	0.5224	-	-	-	4.77E-02
Serum amyloid P-component;Serum amyloid P-component(1-203)	*APCS*	2.7792	1.6725	0.5472	-1.1067	-2.2321	1.1253	↓	1.48E-06
Acylamino-acid-releasing enzyme	*APEH*	-0.6620	-1.1385	-0.8207	-0.4765	-0.1588	-0.3177	-	5.73E-04
Adipocyte plasma membrane-associated protein	*APMAP*	1.3387	0.0459	-0.2868	-1.2929	-1.6256	0.3327	↓	6.69E-07
Apolipoprotein A-I;Proapolipoprotein A-I;Truncated apolipoprotein A-I	*APOA1*	5.2728	4.4196	4.1812	-0.8532	-1.0916	-	-	6.51E-05
NAD(P)H-hydrate epimerase	*APOA1BP*	-2.5453	-1.2932	-1.1396	1.2521	1.4058	-	-	1.49E-03
Apolipoprotein A-IV	*APOA4*	2.7655	1.4481	0.7251	-1.3175	-2.0405	0.7230	↓	2.48E-06
Apolipoprotein B-100;Apolipoprotein B-48	*APOB*	3.1646	1.3936	0.1567	-1.7710	-3.0079	1.2369	↓	1.65E-07
Apolipoprotein D	*APOD*	1.0605	-0.9834	-2.1300	-2.0439	-3.1905	1.1466	↓	1.42E-05
Apolipoprotein E	*APOE*	0.8823	-0.7092	-0.9790	-1.5915	-1.8613	-	-	1.12E-04
Adenine phosphoribosyltransferase	*APRT*	-1.8936	-0.3706	0.0113	1.5230	1.9049	-0.3818	↑	1.73E-06
Coatomer subunit delta	*ARCN1*	-2.2693	-0.3386	-0.1878	1.9306	2.0815	-	-	2.51E-04
ADP-ribosylation factor 4	*ARF4*	-0.1004	0.1615	-0.2771	-	-	0.4386	-	3.38E-02
Rho GTPase-activating protein 1	*ARHGAP1*	0.6297	0.9427	0.9226	0.3130	0.2929	-	-	3.98E-02
Actin-related protein 2/3 complex subunit 2	*ARPC2*	0.1752	1.2154	0.9940	1.0402	0.8187	-	-	2.08E-04
Actin-related protein 2/3 complex subunit 3	*ARPC3*	-2.1029	-0.9614	-1.3502	1.1415	0.7527	-	-	1.25E-02
Actin-related protein 2/3 complex subunit 4	*ARPC4*	0.3661	1.4343	1.2894	1.0683	0.9234	-	-	6.41E-04
Aspartyl/asparaginyl beta-hydroxylase	*ASPH*	0.8701	-0.6635	-1.7129	-1.5336	-2.5830	1.0494	↓	7.73E-05
Asporin	*ASPN*	3.6409	2.6202	0.4874	-1.0207	-3.1535	2.1328	↓	2.14E-07
Argininosuccinate synthase	*ASS1*	0.5685	-4.5490	-4.9874	-5.1176	-5.5559	-	-	3.82E-07
Bifunctional purine biosynthesis protein PURH;Phosphoribosylaminoimidazolecarboxamide formyltra	*ATIC*	0.8362	1.1661	1.6919	0.3299	0.8556	-0.5257	↑	2.42E-04
Atlastin-3	*ATL3*	-0.0586	-0.8064	-1.3944	-0.7478	-1.3358	0.5880	↓	1.17E-04
Sodium/potassium-transporting ATPase subunit alpha-1	*ATP1A1*	-0.4380	-0.0304	0.0781	0.4076	0.5160	-	-	3.43E-03
Sarcoplasmic/endoplasmic reticulum calcium ATPase 2	*ATP2A2*	-0.6670	-1.0577	-1.1166	-0.3907	-0.4496	-	-	7.11E-04
ATP synthase subunit alpha, mitochondrial	*ATP5A1*	3.5133	4.5284	4.8904	1.0151	1.3772	-0.3621	↑	9.08E-07
ATP synthase subunit beta, mitochondrial;ATP synthase subunit beta	*ATP5B*	3.5509	4.5284	4.9152	0.9775	1.3643	-0.3869	↑	4.19E-06
ATP synthase subunit delta, mitochondrial	*ATP5D*	-1.5497	-1.5133	-2.5232	-	-0.9736	1.0099	-	2.78E-02
ATP synthase subunit d, mitochondrial	*ATP5H*	-1.5473	-1.8469	-0.6482	-0.2995	0.8991	-1.1986	-	5.63E-05
V-type proton ATPase subunit B, brain isoform	*ATP6V1B2*	-2.5404	-1.6347	-1.4911	0.9057	1.0493	-	-	1.18E-02
Basal cell adhesion molecule	*BCAM*	-0.7530	-1.6922	-1.1317	-0.9393	-0.3787	-0.5605	-	1.17E-03
Biglycan	*BGN*	4.0515	3.5046	3.4603	-0.5469	-0.5912	-	-	9.38E-03
Biliverdin reductase A	*BLVRA*	0.3015	0.8398	0.9243	0.5383	0.6228	-	-	7.50E-06
Flavin reductase (NADPH)	*BLVRB*	2.4902	0.3637	0.3085	-2.1264	-2.1816	-	-	5.31E-07
Bisphosphoglycerate mutase	*BPGM*	1.0392	-4.1536	-4.4148	-5.1928	-5.4540	-	-	2.52E-08
UPF0568 protein C14orf166	*C14orf166*	-2.0991	-0.9155	-0.4954	1.1836	1.6038	-	-	2.21E-04
Complement C1s subcomponent;Complement C1s subcomponent heavy chain;Complement C1s subc	*C1S*	-1.2571	-3.0649	-3.3103	-1.8078	-2.0532	-	-	1.90E-04
Complement C3;Complement C3 beta chain;C3-beta-c;Complement C3 alpha chain;C3a anaphylatoxin	*C3*	5.2650	4.5292	3.6872	-0.7358	-1.5778	0.8420	↓	7.79E-06
Complement C5;Complement C5 beta chain;Complement C5 alpha chain;C5a anaphylatoxin;Complen	*C5*	0.5269	-2.2444	-3.1069	-2.7713	-3.6338	0.8626	↓	1.94E-05
Complement component C6	*C6*	-0.6589	-2.1335	-3.3054	-1.4746	-2.6465	1.1719	↓	4.31E-07
Complement component C9;Complement component C9a;Complement component C9b	*C9*	1.2341	-0.2493	-0.9994	-1.4835	-2.2335	0.7500	↓	1.10E-05
Carbonic anhydrase 1	*CA1*	5.0484	1.7324	1.7200	-3.3160	-3.3284	-	-	1.22E-07
Carbonic anhydrase 2	*CA2*	3.0463	0.4364	2.3018	-2.6099	-0.7445	-1.8654	-	3.57E-07
Calcyclin-binding protein	*CACYBP*	-1.0595	1.2460	1.5421	2.3055	2.6016	-0.2961	↑	1.09E-07
Calretinin	*CALB2*	0.6328	-4.4251	-4.8767	-5.0579	-5.5095	-	-	9.60E-06
Caldesmon	*CALD1*	1.1324	1.2741	0.4808	-	-0.6516	0.7934	-	2.00E-04
Calreticulin	*CALR*	-0.2689	0.1178	1.7525	-	2.0213	-1.6347	-	5.77E-05
Cullin-associated NEDD8-dissociated protein 1	*CAND1*	1.3116	2.8206	2.6251	1.5090	1.3135	0.1955	-	1.42E-06
Calnexin	*CANX*	1.0715	2.5514	2.9265	1.4799	1.8549	-0.3750	↑	2.55E-06
Adenylyl cyclase-associated protein 1	*CAP1*	0.8354	1.5330	1.3791	0.6975	0.5437	-	-	1.04E-03
Macrophage-capping protein	*CAPG*	-0.7206	1.4330	1.6238	2.1535	2.3444	-0.1909	↑	6.80E-08
F-actin-capping protein subunit alpha-1	*CAPZA1*	0.8002	1.3886	1.4889	0.5884	0.6887	-	-	1.82E-04

Catalase	*CAT*	3.6991	1.5582	1.5014	-2.1409	-2.1977	-	-	2.46E-07
Caveolin-1	*CAV1*	2.2061	-1.8566	-1.9755	-4.0627	-4.1816	-	-	4.11E-06
Carbonyl reductase [NADPH] 1	*CBR1*	1.0251	0.1030	0.2002	-0.9222	-0.8249	-	-	6.48E-05
Chromobox protein homolog 3	*CBX3*	-2.2486	-0.2631	0.2724	1.9855	2.5210	-	-	1.19E-04
T-complex protein 1 subunit beta	*CCT2*	0.6180	1.5013	1.4102	0.8833	0.7922	-	-	1.50E-03
T-complex protein 1 subunit gamma	*CCT3*	0.3491	1.3694	1.6541	1.0203	1.3050	-0.2847	↑	5.94E-06
T-complex protein 1 subunit delta	*CCT4*	0.9158	1.4565	1.7318	0.5407	0.8160	-0.2753	↑	6.17E-04
T-complex protein 1 subunit epsilon	*CCT5*	0.0052	0.3595	0.4806	0.3543	0.4755	-	-	1.54E-02
T-complex protein 1 subunit zeta	*CCT6A*	0.4151	1.2086	1.5450	0.7936	1.1300	-0.3364	↑	2.94E-04
T-complex protein 1 subunit eta	*CCT7*	0.6045	0.9215	0.9792	0.3170	0.3747	-	-	6.20E-03
T-complex protein 1 subunit theta	*CCT8*	0.8249	1.5649	1.8674	0.7400	1.0425	-0.3025	↑	3.10E-06
Monocyte differentiation antigen CD14;Monocyte differentiation antigen CD14, urinary form;Monoc	*CD14*	-2.3265	-2.6286	-2.9852	-	-0.6588	-	-	1.46E-02
Platelet glycoprotein 4	*CD36*	3.3264	-3.9301	-3.6375	-7.2565	-6.9638	-	-	5.27E-08
CDK5 regulatory subunit-associated protein 3	*CDK5RAP3*	-3.1911	-2.6778	-2.3036	-	0.8875	-	-	3.97E-02
Liver carboxylesterase 1	*CES1*	1.9947	-1.2855	-1.8148	-3.2802	-3.8094	0.5293	↓	3.14E-06
Complement factor B	*CFB*	1.9764	0.8268	-0.1684	-1.1495	-2.1448	0.9952	↓	5.24E-06
Complement factor H	*CFH*	1.8955	0.2190	-1.3321	-1.6765	-3.2276	1.5511	↓	4.35E-06
Cofilin-1	*CFL1*	1.4329	2.6114	2.8536	1.1785	1.4207	-	-	2.44E-05
Cytoskeleton-associated protein 4	*CKAP4*	-0.1520	1.4944	1.1412	1.6463	1.2931	0.3532	-	2.90E-06
Creatine kinase B-type	*CKB*	1.2992	-1.6374	-1.7731	-2.9366	-3.0723	-	-	1.57E-05
Tetranectin	*CLEC3B*	0.6369	-1.1834	-1.7043	-1.8203	-2.3412	0.5209	↓	5.86E-05
Chloride intracellular channel protein 1	*CLIC1*	0.7232	1.7251	1.9727	1.0019	1.2495	-0.2476	↑	8.15E-06
Clathrin heavy chain;Clathrin heavy chain 1	*CLTC*	2.6071	3.9076	4.1145	1.3005	1.5075	-	-	1.82E-05
Clusterin;Clusterin beta chain;Clusterin alpha chain;Clusterin	*CLU*	2.0609	0.7905	0.3132	-1.2704	-1.7477	0.4773	↓	1.07E-06
Chymase	*CMA1*	1.0482	-0.2228	-4.4853	-1.2710	-5.5335	4.2625	↓	4.19E-05
Cytosolic non-specific dipeptidase	*CNDP2*	0.8007	1.7934	2.5796	0.9928	1.7789	-0.7861	↑	1.55E-05
Calponin-1;Calponin	*CNN1*	2.3538	-0.0842	-2.7271	-2.4380	-5.0809	2.6429	↓	8.57E-06
Bifunctional coenzyme A synthase;Phosphopantetheine adenylyltransferase;Dephospho-CoA kinase	*COASY*	-2.8186	-2.0146	-0.9187	0.8040	1.8999	-1.0959	↑	3.05E-05
Collagen alpha-1(XII) chain	*COL12A1*	2.2517	4.7556	3.0561	2.5039	0.8043	1.6995	-	8.88E-09
Collagen alpha-1(XIV) chain	*COL14A1*	3.7213	3.8950	1.7020	-	-2.0193	2.1930	-	2.88E-06
Collagen alpha-1(XVIII) chain;Endostatin	*COL18A1*	0.8185	-1.4648	-2.5465	-2.2833	-3.3649	1.0817	↓	4.24E-08
Collagen alpha-1(I) chain	*COL1A1*	3.0088	1.8647	0.4144	-1.1441	-2.5944	1.4503	↓	2.25E-04
Collagen alpha-2(I) chain	*COL1A2*	3.5030	2.1407	0.8211	-1.3624	-2.6819	1.3196	↓	1.05E-06
Collagen alpha-1(VI) chain	*COL6A1*	5.2775	5.2106	4.1513	-	-1.1262	1.0593	-	1.25E-04
Collagen alpha-2(VI) chain	*COL6A2*	4.4321	4.2314	3.2095	-	-1.2226	1.0219	-	4.37E-05
Collagen alpha-3(VI) chain	*COL6A3*	6.5381	7.0680	6.1335	0.5299	-0.4046	0.9345	-	8.39E-04
Coatomer subunit alpha;Xenin;Proxenin	*COPA*	0.5966	1.6767	1.9256	1.0801	1.3290	-0.2489	↑	3.11E-06
Coatomer subunit beta	*COPB1*	-0.9751	0.8973	1.1246	1.8724	2.0997	-	-	4.49E-06
Coatomer subunit beta	*COPB2*	-1.0934	0.1959	0.2678	1.2892	1.3611	-	-	1.09E-04
Coatomer subunit epsilon	*COPE*	-0.9112	0.0514	0.3343	0.9625	1.2455	-	-	8.61E-04
Coatomer subunit gamma-1	*COPG1*	-1.4863	0.6920	0.8275	2.1783	2.3138	-	-	1.40E-05
Coronin-1A;Coronin	*CORO1A*	-1.4657	-0.5782	-0.2904	0.8875	1.1754	-	-	4.16E-04
Coronin-1B	*CORO1B*	-1.3017	-1.7571	-1.6738	-0.4553	-0.3720	-	-	3.29E-02
Cytochrome c oxidase subunit 4 isoform 1, mitochondrial	*COX4I1*	-0.9943	-1.0083	-2.0879	-	-1.0936	1.0796	-	5.56E-04
Ceruloplasmin	*CP*	3.1347	1.9950	1.3086	-1.1397	-1.8262	0.6864	↓	2.18E-06
Mast cell carboxypeptidase A	*CPA3*	1.9123	0.3349	-3.2596	-1.5774	-5.1720	3.5946	↓	2.90E-08
Cellular retinoic acid-binding protein 2	*CRABP2*	-1.4784	1.4132	0.2527	2.8915	1.7310	1.1605	-	1.75E-03
Cysteine-rich protein 2	*CRIP2*	0.2767	-0.1845	0.0249	-0.4611	-	-	-	3.41E-02
Alpha-crystallin B chain	*CRYAB*	2.5615	-3.3989	-3.3540	-5.9603	-5.9154	-	-	3.25E-07
Citrate synthase;Citrate synthase, mitochondrial	*CS*	2.0720	1.9112	2.6668	-	0.5948	-0.7556	-	1.86E-03
Exportin-2	*CSE1L*	0.9154	2.7027	3.1500	1.7873	2.2345	-0.4472	↑	4.46E-06
Cysteine and glycine-rich protein 1	*CSRP1*	2.0081	0.7679	-0.3464	-1.2402	-2.3545	1.1143	↓	1.61E-06
Cystatin-A;Cystatin-A, N-terminally processed	*CSTA*	0.0320	-3.3106	-3.3851	-3.3426	-3.4171	-	-	2.34E-04
Catenin alpha-1	*CTNNA1*	-0.9254	0.2302	0.6067	1.1555	1.5320	-	-	3.52E-04
Catenin delta-1	*CTNND1*	-1.3851	-0.0238	-0.1589	1.3612	1.2261	-	-	3.66E-04
Cathepsin D;Cathepsin D light chain;Cathepsin D heavy chain	*CTSD*	1.3822	3.0030	3.0946	1.6208	1.7124	-	-	2.78E-06
Cathepsin G	*CTSG*	0.7956	-0.5105	-3.6005	-1.3061	-4.3961	3.0900	↓	1.15E-06
Cytochrome b5	*CYB5A*	1.8363	1.1150	0.5331	-0.7213	-1.3032	0.5819	↓	7.28E-04
NADH-cytochrome b5 reductase 1	*CYB5R1*	-0.2302	1.4042	2.1158	1.6344	2.3461	-0.7116	↑	2.82E-08
NADH-cytochrome b5 reductase 3;NADH-cytochrome b5 reductase 3 membrane-bound form;NADH-(	*CYB5R3*	2.4685	1.6582	1.7380	-0.8104	-0.7305	-0.0799	-	1.50E-07
Serine/threonine-protein kinase DCLK1	*DCLK1*	-2.9947	-4.0922	-4.7423	-1.0975	-1.7476	0.6501	↓	3.84E-04
Decorin	*DCN*	4.8487	3.5614	2.6302	-1.2872	-2.2185	0.9312	↓	1.56E-07
Dynactin subunit 1	*DCTN1*	-0.7151	-1.2346	-1.3939	-0.5196	-0.6789	-	-	8.14E-03
N(G),N(G)-dimethylarginine dimethylaminohydrolase 2	*DDAH2*	0.6017	-0.8427	-0.3443	-1.4444	-0.9460	-0.4984	-	3.74E-04
DNA damage-binding protein 1	*DDB1*	-0.5475	0.0350	0.1102	0.5825	0.6577	-	-	2.17E-02
Dolichyl-diphosphooligosaccharide--protein glycosyltransferase 48 kDa subunit	*DDOST*	0.5290	1.1914	1.6540	0.6624	1.1250	-0.4626	↑	3.12E-04
ATP-dependent RNA helicase DDX1	*DDX1*	-1.3784	-0.1390	0.3506	1.2394	1.7291	-0.4896	↑	1.98E-05
Probable ATP-dependent RNA helicase DDX17	*DDX17*	-0.7879	1.1929	1.4026	1.9808	2.1905	-	-	2.08E-03
Spliceosome RNA helicase DDX39B	*DDX39B*	0.3976	1.9550	2.2677	1.5574	1.8701	-0.3127	↑	4.92E-07
Probable ATP-dependent RNA helicase DDX5	*DDX5*	-2.3036	-0.1424	0.4547	2.1612	2.7583	-	-	5.14E-04
2,4-dienoyl-CoA reductase, mitochondrial	*DECR1*	0.8764	0.0789	0.3478	-0.7975	-0.5286	-0.2688	-	1.55E-04
Dehydrogenase/reductase SDR family member 2, mitochondrial	*DHRS2*	-2.7286	-1.1462	1.6987	1.5824	4.4273	-2.8449	↑	1.28E-05
Pre-mRNA-splicing factor ATP-dependent RNA helicase DHX15	*DHX15*	-1.6481	0.0145	0.1670	1.6626	1.8151	-	-	2.62E-04
ATP-dependent RNA helicase A	*DHX9*	0.2750	1.6877	1.9168	1.4127	1.6418	-0.2290	↑	2.11E-06
H/ACA ribonucleoprotein complex subunit 4	*DKC1*	-2.6715	-1.1739	-1.6745	1.4976	0.9970	-	-	2.58E-02
Acetyltransferase component of pyruvate dehydrogenase complex;Dihydrolipoyllysine-residue acetyl	*DLAT*	-0.8366	-1.8734	-1.5437	-1.0367	-0.7071	-0.3297	-	1.67E-04
Dihydrolipoyl dehydrogenase;Dihydrolipoyl dehydrogenase, mitochondrial	*DLD*	0.6664	0.0928	0.6414	-0.5736	-	-0.5486	-	5.57E-03
Dihydrolipoyllysine-residue succinyltransferase component of 2-oxoglutarate dehydrogenase comple	*DLST*	0.3807	-0.7589	-0.4531	-1.1397	-0.8338	-	-	1.02E-03
Dynamin-1-like protein	*DNM1L*	-1.9674	-0.9909	-0.5569	0.9765	1.4105	-	-	8.51E-03
Aspartyl aminopeptidase	*DNPEP*	-1.3525	-0.8128	-0.1670	-	1.1855	-	-	1.32E-02
Dipeptidyl peptidase 3	*DPP3*	-1.2255	0.3189	0.6763	1.5444	1.9018	-0.3574	↑	1.47E-05
Dihydropyrimidinase-related protein 2	*DPYSL2*	2.0209	1.6632	1.5987	-0.3577	-0.4222	-	-	2.51E-02
Dihydropyrimidinase-related protein 3	*DPYSL3*	1.5337	2.2299	1.2430	0.6962	-0.2907	0.9869	-	2.17E-05
Desmoplakin	*DSP*	-2.3338	0.2624	0.9284	2.5962	3.2623	-	-	3.44E-04
Cytoplasmic dynein 1 heavy chain 1	*DYNC1H1*	1.3246	0.9270	1.0821	-0.3976	-0.2425	-	-	1.43E-02
Delta(3,5)-Delta(2,4)-dienoyl-CoA isomerase, mitochondrial	*ECH1*	0.5711	-0.6142	-0.4246	-1.1853	-0.9958	-	-	8.60E-04
Enoyl-CoA hydratase, mitochondrial	*ECHS1*	1.9860	0.0975	0.2648	-1.8885	-1.7212	-	-	5.13E-05
Enoyl-CoA delta isomerase 1, mitochondrial	*ECI1*	-1.5809	0.2388	0.3379	1.8197	1.9188	-	-	4.40E-05
Proteasome-associated protein ECM29 homolog	*ECM29*	-2.7608	-1.7612	-1.5473	0.9996	1.2135	-	-	2.74E-03
Elongation factor 1-delta	*EEF1D*	0.2986	1.8765	2.3384	1.5779	2.0398	-0.4619	↑	1.03E-05
Elongation factor 1-gamma	*EEF1G*	0.7650	1.8264	2.1131	1.0613	1.3481	-0.2867	↑	1.59E-05
Elongation factor 2	*EEF2*	1.5948	3.0433	3.4179	1.4486	1.8231	-0.3746	↑	9.34E-08
EF-hand domain-containing protein D1	*EFHD1*	-1.6095	0.5111	1.0039	2.1205	2.6133	-0.4928	↑	1.05E-05
116 kDa U5 small nuclear ribonucleoprotein component	*EFTUD2*	-1.6382	0.2547	0.0454	1.8929	1.6836	-	-	5.81E-04
EH domain-containing protein 1	*EHD1*	-0.3444	-1.8350	-1.5233	-1.4905	-1.1789	-	-	7.18E-04
EH domain-containing protein 2	*EHD2*	4.3360	1.4223	1.2143	-2.9137	-3.1218	-	-	9.59E-08
EH domain-containing protein 4	*EHD4*	-0.0869	-0.7582	-0.6542	-0.6712	-0.5673	-	-	2.39E-05
Interferon-induced, double-stranded RNA-activated protein kinase	*EIF2AK2*	-2.9656	-1.8214	-0.7334	-	2.2322	-	-	1.20E-02
Eukaryotic translation initiation factor 3 subunit A	*EIF3A*	-1.3110	-0.4211	-0.1130	0.8899	1.1980	-	-	2.90E-04
Eukaryotic translation initiation factor 3 subunit L	*EIF3L*	-1.9689	-1.2410	-0.9884	0.7279	0.9805	-	-	1.99E-02
Eukaryotic initiation factor 4A-I	*EIF4A1*	1.2708	2.7644	2.9490	1.4936	1.6782	-0.1846	↑	1.07E-07
Eukaryotic initiation factor 4A-III;Eukaryotic initiation factor 4A-III, N-terminally processed	*EIF4A3*	-1.9222	-0.4313	-0.3426	1.4909	1.5796	-	-	3.98E-07
EMILIN-1	*EMILIN1*	0.3702	0.0448	-0.1900	-0.3254	-0.5602	0.2348	↓	2.78E-04
Alpha-enolase	*ENO1*	3.0798	4.1354	3.7672	1.0556	0.6874	0.3682	-	9.97E-05
Enolase-phosphatase E1	*ENOPH1*	-2.4804	-2.2957	-0.8616	-	1.6188	-1.4341	-	2.26E-04
Epoxide hydrolase 1	*EPHX1*	2.9077	1.6366	0.7861	-1.2711	-2.1216	0.8505	↓	2.50E-06
Bifunctional glutamate/proline--tRNA ligase;Glutamate--tRNA ligase;Proline--tRNA ligase	*EPRS*	-1.0629	-0.1484	0.6263	0.9145	1.6892	-0.7747	↑	1.43E-05
Endoplasmic reticulum aminopeptidase 1	*ERAP1*	-0.7699	-1.9385	-2.0251	-1.1685	-1.2552	-	-	3.17E-04
Erlin-2	*ERLIN2*	0.2627	-0.7239	-0.6366	-0.9866	-0.8993	-	-	4.80E-03

Endoplasmic reticulum resident protein 29	*ERP29*	-0.4073	0.3785	0.8898	0.7857	1.2970	-0.5113	↑	1.01E-04
S-formylglutathione hydrolase	*ESD*	-0.5547	-1.5996	-1.4946	-1.0449	-0.9398	-	-	1.95E-03
Extended synaptotagmin-1	*ESYT1*	1.7720	0.7571	0.9225	-1.0149	-0.8494	-	-	8.42E-05
Extended synaptotagmin-2	*ESYT2*	-2.8909	-3.7152	-4.5662	-0.8243	-1.6753	0.8511	↓	1.19E-03
Electron transfer flavoprotein subunit alpha, mitochondrial	*ETFA*	0.5007	-0.8766	-0.1289	-1.3773	-0.6295	-0.7477	-	4.24E-04
Electron transfer flavoprotein subunit beta	*ETFB*	0.9740	-1.0932	-0.3484	-2.0672	-1.3225	-0.7447	-	3.12E-05
Ezrin	*EZR*	-2.1635	-0.0784	0.6321	2.0851	2.7957	-	-	7.20E-03
Coagulation factor XIII A chain	*F13A1*	1.4560	0.6840	-0.6327	-0.7720	-2.0887	1.3167	↓	4.54E-06
Prothrombin;Activation peptide fragment 1;Activation peptide fragment 2;Thrombin light chain;Thro	*F2*	0.8241	-1.3182	-1.6662	-2.1423	-2.4903	0.3480	↓	4.02E-08
Fatty acid-binding protein, adipocyte	*FABP4*	4.4484	-1.4501	-1.6527	-5.8985	-6.1011	-	-	2.84E-07
Fumarylacetoacetase	*FAH*	1.3862	-1.7393	-2.1171	-3.1256	-3.5034	-	-	1.01E-05
Acylpyruvase FAHD1, mitochondrial	*FAHD1*	-2.7548	-2.5783	-1.8652	-	0.8897	-0.7132	-	2.98E-02
Redox-regulatory protein FAM213A	*FAM213A*	1.5102	-2.4306	-1.6723	-3.9408	-3.1824	-0.7583	-	8.36E-06
Phenylalanine--tRNA ligase beta subunit	*FARSB*	-1.3888	0.0911	0.0159	1.4799	1.4048	-	-	3.53E-05
Fatty acid synthase;[Acyl-carrier-protein] S-acetyltransferase;[Acyl-carrier-protein] S-malonyltransfer	*FASN*	5.0826	7.0661	8.2690	1.9835	3.1863	-1.2028	↑	8.32E-08
rRNA 2-O-methyltransferase fibrillarin	*FBL*	-1.0720	1.1000	0.8973	2.1720	1.9693	-	-	8.03E-06
Fibulin-1	*FBLN1*	1.1760	0.9668	-0.3748	-0.2092	-1.5508	1.3416	↓	2.57E-06
Fibulin-2	*FBLN2*	0.7209	-0.4982	-1.3368	-1.2190	-2.0577	0.8386	↓	7.06E-04
Fibrillin-1	*FBN1*	3.1729	0.9808	0.1689	-2.1921	-3.0040	0.8119	↓	3.59E-05
Fibrinogen alpha chain;Fibrinopeptide A;Fibrinogen alpha chain	*FGA*	4.0661	2.9448	1.8006	-1.1213	-2.2655	1.1442	↓	6.45E-07
Fibrinogen beta chain;Fibrinopeptide B;Fibrinogen beta chain	*FGB*	4.5556	3.3822	2.3081	-1.1734	-2.2474	1.0740	↓	4.95E-06
Fibrinogen gamma chain	*FGG*	4.8085	3.2972	2.4295	-1.5113	-2.3790	0.8676	↓	5.40E-07
Fumarate hydratase, mitochondrial	*FH*	0.5770	0.8941	1.4065	-	0.8295	-0.5124	-	4.00E-03
Peptidyl-prolyl cis-trans isomerase FKBP4;Peptidyl-prolyl cis-trans isomerase FKBP4, N-terminally pro	*FKBP4*	0.0301	3.1529	4.0059	3.1227	3.9758	-0.8530	↑	3.46E-10
FAD synthase;Molybdenum cofactor biosynthesis protein-like region;FAD synthase region	*FLAD1*	-4.9817	-3.7019	-3.2854	1.2798	1.6963	-0.4165	↑	1.84E-06
Protein flightless-1 homolog	*FLII*	-3.3578	-2.4176	-2.9755	0.9402	0.3824	0.5579	-	8.02E-04
Filamin-A	*FLNA*	4.7221	5.1691	4.5308	0.4470	-	0.6383	-	2.01E-03
Fibromodulin	*FMOD*	0.7103	-2.1584	-4.1646	-2.8687	-4.8750	2.0062	↓	1.78E-05
Fibronectin;Anastellin;Ugl-Y1;Ugl-Y2;Ugl-Y3	*FN1*	3.2214	4.7464	3.3456	1.5250	-	1.4008	-	3.57E-07
Fascin	*FSCN1*	0.8727	0.7709	-0.3632	-	-1.2359	1.1341	-	7.94E-05
Ferritin light chain	*FTL*	1.3827	2.8084	2.9146	1.4257	1.5319	-	-	1.35E-04
Glucose-6-phosphate 1-dehydrogenase	*G6PD*	1.1896	1.6067	1.1139	0.4171	-	0.4928	-	7.61E-04
Neutral alpha-glucosidase AB	*GANAB*	1.9116	2.9286	3.0964	1.0169	1.1848	-0.1678	↑	1.02E-07
Glyceraldehyde-3-phosphate dehydrogenase	*GAPDH*	3.4778	5.5608	5.5527	2.0830	2.0749	-	-	1.56E-05
Glycine--tRNA ligase	*GARS*	-1.9288	-0.3239	-0.6221	1.6050	1.3067	-	-	3.31E-05
Vitamin D-binding protein	*GC*	3.0011	1.7854	1.0065	-1.2157	-1.9946	0.7789	↓	2.91E-07
Rab GDP dissociation inhibitor alpha	*GDI1*	-1.1212	0.6636	0.6986	1.7849	1.8199	-	-	1.59E-04
Rab GDP dissociation inhibitor beta	*GDI2*	1.5563	2.2982	2.2587	0.7419	0.7025	-	-	5.45E-04
Lactoylglutathione lyase	*GLO1*	-1.2707	-1.9585	-1.2340	-0.6878	-	-0.7245	-	1.44E-02
Glutaredoxin-3	*GLRX3*	-1.6742	-2.6373	-2.4271	-0.9631	-0.7529	-	-	8.65E-03
Glutamine synthetase	*GLUL*	-1.2067	1.8061	2.0885	3.0128	3.2952	-	-	4.64E-06
Guanine nucleotide-binding protein G(i) subunit alpha-2	*GNAI2*	2.2444	1.2114	1.1128	-1.0330	-1.1316	-	-	9.79E-04
Guanine nucleotide-binding protein G(k) subunit alpha	*GNAI3*	-2.1995	-3.0566	-3.0790	-0.8571	-0.8795	-	-	3.23E-03
Guanine nucleotide-binding protein G(s) subunit alpha isoforms short;Guanine nucleotide-binding pr	*GNAS*	0.2171	-1.0748	-1.2133	-1.2919	-1.4304	-	-	1.43E-04
Guanine nucleotide-binding protein subunit beta-2-like 1;Guanine nucleotide-binding protein subunit	*GNB2L1*	-0.1677	0.7601	1.3246	0.9277	1.4922	-0.5645	↑	7.31E-04
Vesicle transport protein GOT1B	*GOLT1B*	-4.6596	-3.3332	-3.4647	1.3264	1.1950	-	-	6.41E-04
Aspartate aminotransferase, cytoplasmic	*GOT1*	-1.2241	-1.6578	-1.5922	-0.4338	-0.3681	-	-	2.53E-02
Aspartate aminotransferase, mitochondrial	*GOT2*	-1.1021	1.9629	2.6586	3.0650	3.7607	-0.6957	↑	1.24E-06
Glycerol-3-phosphate dehydrogenase [NAD(+)], cytoplasmic	*GPD1*	4.2765	-3.6608	-3.2919	-7.9373	-7.5684	-	-	2.36E-05
Glycerol-3-phosphate dehydrogenase 1-like protein	*GPD1L*	-1.1238	-1.8412	-1.3703	-0.7174	-0.2465	-0.4709	-	4.99E-04
Glycerol-3-phosphate dehydrogenase, mitochondrial	*GPD2*	-1.4381	0.0917	0.6423	1.5298	2.0804	-0.5506	↑	7.14E-07
Glucose-6-phosphate isomerase	*GPI*	2.7014	2.3541	1.9539	-0.3473	-0.7475	0.4002	↓	4.56E-04
Glutathione peroxidase;Glutathione peroxidase 3	*GPX3*	0.3461	-1.4208	-1.4885	-1.7669	-1.8346	-	-	8.68E-07
Gelsolin	*GSN*	2.9890	2.7440	2.5006	-0.2450	-0.4884	0.2434	↓	3.08E-03
Glutathione S-transferase kappa 1	*GSTK1*	-0.5620	0.7988	1.2228	1.3609	1.7849	-0.4240	↑	5.66E-07
Glutathione S-transferase Mu 3	*GSTM3*	-0.1602	0.5658	1.4627	0.7260	1.6229	-0.8968	↑	1.45E-04
Glutathione S-transferase omega-1	*GSTO1*	-0.5978	-0.4033	-0.8164	-	-	0.4132	-	1.87E-02
Glutathione S-transferase P	*GSTP1*	2.4460	1.9107	2.4446	-0.5354	-	-0.5339	-	2.04E-03
Histone H1.0;Histone H1.0, N-terminally processed	*H1F0*	-2.2492	-0.0541	-2.0838	2.1950	-	2.0296	-	5.98E-05
Histone H1x	*H1FX*	-1.8169	-0.3185	0.3642	1.4984	2.1811	-0.6827	↑	6.09E-05
Core histone macro-H2A.1;Histone H2A	*H2AFY*	0.7714	2.6676	2.9392	1.8961	2.1678	-	-	6.84E-06
Very-long-chain (3R)-3-hydroxyacyl-CoA dehydratase 3	*HACD3*	-0.9737	-0.0240	-0.0628	0.9497	0.9109	-	-	8.09E-03
Hydroxyacyl-coenzyme A dehydrogenase, mitochondrial	*HADH*	1.5491	-0.7814	-0.8059	-2.3306	-2.3551	-	-	2.56E-07
Trifunctional enzyme subunit alpha, mitochondrial;Long-chain enoyl-CoA hydratase;Long chain 3-hyd	*HADHA*	2.1939	2.2551	2.5327	-	0.3387	-0.2776	-	3.68E-03
Trifunctional enzyme subunit beta, mitochondrial;3-ketoacyl-CoA thiolase	*HADHB*	2.2191	2.0540	1.9002	-	-0.3189	-	-	2.02E-02
Hemoglobin subunit beta;LVV-hemorphin-7;Spinorphin	*HBB*	7.3422	5.8682	5.6443	-1.4740	-1.6978	-	-	1.20E-04
Hemoglobin subunit delta	*HBD*	4.0726	0.6782	0.4969	-3.3944	-3.5756	-	-	4.39E-07
Vigilin	*HDLBP*	-0.5045	1.1435	1.2119	1.6480	1.7164	-	-	1.68E-06
Heme-binding protein 2	*HEBP2*	-0.4428	-1.2396	-1.0016	-0.7969	-0.5588	-	-	7.57E-04
Histidine triad nucleotide-binding protein 1	*HINT1*	-0.6726	-0.7714	-1.3494	-	-0.6768	0.5780	-	2.06E-03
Histone H1.4	*HIST1H1E*	1.3525	3.1284	2.7652	1.7759	1.4127	0.3632	-	2.69E-05
Histone H4	*HIST1H4A*	4.3949	5.7922	5.9874	1.3973	1.5925	-	-	4.32E-05
Hexokinase-1	*HK1*	0.0970	0.5678	0.7853	0.4708	0.6883	-	-	1.32E-03
High mobility group protein B1	*HMGB1*	0.8856	1.7278	2.4397	0.8422	1.5541	-0.7119	↑	1.13E-03
High mobility group protein B2	*HMGB2*	-1.3636	-1.8441	-2.2828	-	-0.9192	-	-	3.73E-02
Heterogeneous nuclear ribonucleoprotein A0	*HNRNPA0*	-1.1497	0.0411	-0.0172	1.1908	1.1325	-	-	1.32E-03
Heterogeneous nuclear ribonucleoproteins A2/B1	*HNRNPA2B1*	1.7605	3.6290	4.0310	1.8684	2.2705	-0.4020	↑	2.21E-06
Heterogeneous nuclear ribonucleoprotein A/B	*HNRNPAB*	-2.0178	-0.0618	0.6043	1.9560	2.6220	-0.6661	↑	7.64E-07
Heterogeneous nuclear ribonucleoprotein D0	*HNRNPD*	-0.4755	1.1953	1.6322	1.6709	2.1077	-0.4369	↑	6.21E-06
Heterogeneous nuclear ribonucleoprotein F;Heterogeneous nuclear ribonucleoprotein F, N-terminall	*HNRNPF*	-2.3970	-1.3955	-1.6988	1.0014	0.6982	-	-	3.05E-02
Heterogeneous nuclear ribonucleoprotein H;Heterogeneous nuclear ribonucleoprotein H, N-terminal	*HNRNPH1*	0.4190	1.8560	1.6151	1.4370	1.1961	-	-	2.96E-05
Heterogeneous nuclear ribonucleoprotein K	*HNRNPK*	1.2137	2.7245	3.1825	1.5108	1.9689	-0.4581	↑	8.03E-09
Heterogeneous nuclear ribonucleoprotein L	*HNRNPL*	-2.2217	-0.0321	0.6497	2.1896	2.8714	-	-	9.81E-03
Heterogeneous nuclear ribonucleoprotein M	*HNRNPM*	-0.0239	1.7429	2.1221	1.7668	2.1461	-0.3792	↑	3.55E-07
Heterogeneous nuclear ribonucleoprotein R	*HNRNPR*	-1.0986	0.7117	0.9358	1.8102	2.0344	-0.2241	↑	6.04E-08
Heterogeneous nuclear ribonucleoprotein U	*HNRNPU*	0.9576	2.5463	2.7393	1.5887	1.7817	-	-	1.34E-05
Haptoglobin;Haptoglobin alpha chain;Haptoglobin beta chain	*HP*	2.5337	0.5639	-0.3585	-1.9698	-2.8923	0.9225	↓	6.22E-05
Hypoxanthine-guanine phosphoribosyltransferase	*HPRT1*	-0.5232	-0.6208	-0.0528	-	0.4705	-0.5680	-	3.81E-03
Histidine-rich glycoprotein	*HRG*	2.2502	0.6469	0.0558	-1.6033	-2.1944	0.5911	↓	1.39E-07
3-hydroxyacyl-CoA dehydrogenase type-2	*HSD17B10*	0.0835	0.4830	0.6408	0.3995	0.5573	-	-	9.23E-03
Very-long-chain 3-oxoacyl-CoA reductase	*HSD17B12*	-0.9438	-1.9416	-2.0038	-0.9978	-1.0600	-	-	3.10E-03
Peroxisomal multifunctional enzyme type 2;(3R)-hydroxyacyl-CoA dehydrogenase;Enoyl-CoA hydrata	*HSD17B4*	-0.0531	1.2132	1.0847	1.2664	1.1379	-	-	8.13E-06
Hydroxysteroid dehydrogenase-like protein 2	*HSDL2*	-1.0189	-1.6929	-1.5860	-0.6740	-0.5671	-	-	2.43E-02
Heat shock protein HSP 90-alpha	*HSP90AA1*	3.2094	5.3977	6.1426	2.1883	2.9332	-0.7449	↑	3.26E-06
Heat shock protein HSP 90-beta;Putative heat shock protein HSP 90-beta-3	*HSP90AB1*	2.2352	4.4685	5.1209	2.2333	2.8857	-0.6524	↑	2.57E-07
Endoplasmin	*HSP90B1*	2.5370	3.8510	4.9262	1.3139	2.3891	-1.0752	↑	2.26E-07
Heat shock 70 kDa protein 12A	*HSPA12A*	0.3873	-3.8718	-3.9580	-4.2591	-4.3453	-	-	5.67E-05
Heat shock-related 70 kDa protein 2	*HSPA2*	-1.8665	-1.3039	-1.2402	0.5626	0.6263	-	-	2.45E-03
Heat shock 70 kDa protein 4	*HSPA4*	-0.7943	-0.0234	0.3032	0.7710	1.0975	-	-	2.79E-03
78 kDa glucose-regulated protein	*HSPA5*	2.5182	4.1380	4.8827	1.6198	2.3645	-0.7447	↑	1.80E-08
Heat shock cognate 71 kDa protein	*HSPA8*	3.5477	5.2105	5.7345	1.6628	2.1868	-0.5240	↑	3.01E-07
Stress-70 protein, mitochondrial	*HSPA9*	1.3598	3.5990	4.4452	2.2392	3.0854	-0.8462	↑	3.73E-08
Heat shock protein beta-1	*HSPB1*	2.9881	4.6570	5.1939	1.6689	2.2058	-0.5368	↑	2.16E-06
60 kDa heat shock protein, mitochondrial	*HSPD1*	2.2468	4.3677	5.0749	2.1209	2.8281	-0.7073	↑	4.36E-07
10 kDa heat shock protein, mitochondrial	*HSPE1*	0.2211	1.5843	1.5184	1.3633	1.2974	-	-	1.56E-05
Basement membrane-specific heparan sulfate proteoglycan core protein;Endorepellin;LG3 peptide	*HSPG2*	3.9165	1.4272	0.4487	-2.4893	-3.4678	0.9785	↓	2.95E-07
Heat shock protein 105 kDa	*HSPH1*	-2.6217	0.4290	0.7817	3.0507	3.4035	-	-	1.14E-06
Hypoxia up-regulated protein 1	*HYOU1*	-1.1388	0.4269	0.3379	1.5657	1.4767	-	-	6.12E-05
Isoleucine--tRNA ligase, mitochondrial	*IARS2*	0.0064	1.3575	2.4591	1.3510	2.4527	-1.1017	↑	3.54E-06

Isocitrate dehydrogenase [NADP] cytoplasmic	*IDH1*	1.9913	0.7601	0.9667	-1.2312	-1.0246	-	-	1.29E-04
Isocitrate dehydrogenase [NADP], mitochondrial	*IDH2*	1.2559	2.6025	2.6553	1.3466	1.3994	-	-	6.51E-07
Isocitrate dehydrogenase [NAD] subunit alpha, mitochondrial	*IDH3A*	-0.2977	-0.7088	-0.1935	-0.4111	-	-0.5153	-	1.96E-04
Insulin-like growth factor-binding protein complex acid labile subunit	*IGFALS*	-1.8546	-3.4785	-4.2654	-1.6240	-2.4109	0.7869	↓	5.87E-05
Ig alpha-1 chain C region	*IGHA1*	2.5991	1.2397	0.6340	-1.3594	-1.9652	0.6057	↓	5.87E-05
Ig gamma-1 chain C region	*IGHG1*	5.6635	5.1612	6.2770	-0.5024	0.6135	-1.1159	-	4.05E-04
Ig gamma-4 chain C region	*IGHG4*	2.8549	1.3670	0.4826	-1.4879	-2.3723	0.8844	↓	1.11E-05
Ig mu chain C region;Ig mu heavy chain disease protein	*IGHM*	4.2658	3.1237	3.1870	-1.1422	-1.0789	-	-	9.03E-04
Ig heavy chain V-III region JON;Ig heavy chain V-III region WEA;Ig heavy chain V-III region TRO	*IGHV3-21*	0.8715	-1.1872	0.3057	-2.0587	-0.5658	-1.4929	-	9.84E-05
Ig kappa chain C region	*IGKC*	4.8141	4.3470	4.9623	-0.4671	-	-0.6152	-	7.28E-03
Ig kappa chain V-III region B6	*IGKV3D-20*	2.3964	0.8633	0.7732	-1.5330	-1.6231	-	-	6.33E-05
Interleukin enhancer-binding factor 2	*ILF2*	-0.0556	1.6223	1.7105	1.6779	1.7660	-	-	6.24E-05
Interleukin enhancer-binding factor 3	*ILF3*	-0.7598	0.8074	0.9704	1.5672	1.7302	-	-	4.65E-05
Integrin-linked protein kinase	*ILK*	-0.5639	-2.4023	-3.1419	-1.8384	-2.5779	0.7396	↓	7.20E-06
MICOS complex subunit MIC60	*IMMT*	-0.0581	0.3886	0.7091	0.4467	0.7672	-0.3205	↑	7.13E-04
Inosine-5-monophosphate dehydrogenase 2	*IMPDH2*	-1.1121	-0.1637	-0.1140	0.9483	0.9980	-	-	2.05E-02
Ras GTPase-activating-like protein IQGAP1	*IQGAP1*	1.9641	3.0197	3.2529	1.0556	1.2888	-0.2332	↑	2.93E-06
Isochorismatase domain-containing protein 1	*ISOC1*	-0.7003	-0.6207	0.0948	-	0.7952	-0.7155	-	2.08E-05
Isochorismatase domain-containing protein 2, mitochondrial	*ISOC2*	-2.2670	-1.4647	-0.7093	0.8023	1.5577	-0.7554	↑	6.82E-05
Inositol-3-phosphate synthase 1	*ISYNA1*	-2.5369	-3.1870	-2.6866	-0.6501	-	-0.5004	-	1.01E-02
Integrin beta-1	*ITGB1*	1.1347	-0.1164	-0.1361	-1.2510	-1.2708	-	-	5.64E-05
Inter-alpha-trypsin inhibitor heavy chain H1	*ITIH1*	1.4989	0.8098	1.1604	-0.6891	-0.3384	-0.3507	-	4.20E-03
Inter-alpha-trypsin inhibitor heavy chain H2	*ITIH2*	2.4268	1.3975	0.9912	-1.0293	-1.4356	0.4063	↓	2.28E-07
Inter-alpha-trypsin inhibitor heavy chain H4;70 kDa inter-alpha-trypsin inhibitor heavy chain H4;35 kD	*ITIH4*	2.3430	0.7080	-0.1934	-1.6350	-2.5364	0.9014	↓	7.94E-07
Junction plakoglobin	*JUP*	-0.3568	-0.2977	0.0693	-	0.4261	-0.3670	-	1.31E-02
BTB/POZ domain-containing protein KCTD12	*KCTD12*	0.3887	-0.1068	-0.6159	-0.4955	-1.0046	0.5091	↓	6.69E-04
KH domain-containing, RNA-binding, signal transduction-associated protein 1	*KHDRBS1*	-2.9218	-1.3215	-0.9233	1.6003	1.9986	-	-	1.64E-03
Kininogen-1;Kininogen-1 heavy chain;T-kinin;Bradykinin;Lysyl-bradykinin;Kininogen-1 light chain;Low	*KNG1*	2.2146	0.5840	-0.3921	-1.6305	-2.6067	0.9762	↓	2.87E-07
Keratin, type I cytoskeletal 18	*KRT18*	-1.9253	2.4561	2.8070	4.3813	4.7323	-	-	7.92E-06
Kinectin	*KTN1*	-1.8219	-0.1174	-0.4225	1.7045	1.3995	-	-	1.84E-05
Laminin subunit gamma-1	*LAMC1*	2.8354	-0.4616	-1.9305	-3.2971	-4.7659	1.4688	↓	8.64E-06
Lysosome-associated membrane glycoprotein 1	*LAMP1*	-1.0037	-1.9356	-2.2932	-0.9320	-1.2896	-	-	8.70E-03
Cytosol aminopeptidase	*LAP3*	1.0698	2.4773	3.1976	1.4075	2.1277	-0.7203	↑	4.18E-07
LIM and SH3 domain protein 1	*LASP1*	-0.3030	-0.6597	-0.0008	-0.3566	-	-0.6589	-	9.12E-03
Lipopolysaccharide-binding protein	*LBP*	-2.1570	-3.8189	-4.1528	-1.6619	-1.9958	-	-	1.28E-04
Plastin-2	*LCP1*	1.5234	2.4689	3.4928	0.9455	1.9694	-1.0239	↑	3.68E-07
L-lactate dehydrogenase A chain	*LDHA*	2.7045	3.9121	3.8878	1.2076	1.1833	-	-	3.42E-04
L-lactate dehydrogenase B chain;L-lactate dehydrogenase	*LDHB*	3.1512	1.6243	2.0426	-1.5269	-1.1086	-0.4183	-	7.66E-05
LETM1 and EF-hand domain-containing protein 1, mitochondrial	*LETM1*	-0.5160	0.0940	0.7513	0.6100	1.2673	-0.6573	↑	1.94E-04
Galectin-3;Galectin	*LGALS3*	2.3268	2.3016	1.6557	-	-0.6711	0.6459	-	7.75E-03
Galectin-3-binding protein	*LGALS3BP*	0.2368	1.1088	1.8695	0.8720	1.6327	-0.7607	↑	4.03E-06
Vesicular integral-membrane protein VIP36	*LMAN2*	-2.4150	-0.7556	-0.7202	1.6593	1.6948	-	-	4.38E-04
Prelamin-A/C;Lamin-A/C	*LMNA*	4.2983	4.9327	4.5904	0.6344	-	0.3423	-	8.07E-03
Lamin-B1	*LMNB1*	-1.0286	0.7844	0.9896	1.8130	2.0181	-	-	6.51E-05
Lon protease homolog, mitochondrial	*LONP1*	-0.8163	-0.4685	-0.0325	0.3479	0.7838	-0.4360	↑	3.57E-03
Leucine-rich alpha-2-glycoprotein	*LRG1*	-0.4564	-2.7778	-3.7323	-2.3214	-3.2759	-	-	4.42E-04
Prolow-density lipoprotein receptor-related protein 1;Low-density lipoprotein receptor-related prote	*LRP1*	-0.9453	-2.5693	-3.5181	-1.6239	-2.5728	0.9488	↓	6.13E-05
Leucine-rich PPR motif-containing protein, mitochondrial	*LRPPRC*	0.3761	1.8887	2.5998	1.5126	2.2237	-0.7111	↑	1.87E-10
Leucine-rich repeat-containing protein 47	*LRRC47*	-1.9064	-0.5811	-0.7690	1.3254	1.1374	-	-	3.48E-05
Leucine-rich repeat-containing protein 59	*LRRC59*	-1.9319	1.2951	1.4037	3.2270	3.3356	-	-	6.57E-08
Leukotriene A-4 hydrolase	*LTA4H*	-0.3753	-0.9391	-0.2452	-0.5637	-	-0.6939	-	3.87E-03
Lactotransferrin;Lactoferricin-H;Kaliocin-1;Lactoferroxin-A;Lactoferroxin-B;Lactoferroxin-C	*LTF*	2.3578	-3.6759	-5.4587	-6.0336	-7.8165	1.7829	↓	3.20E-07
Lumican	*LUM*	5.2356	4.7627	4.3527	-0.4729	-0.8829	0.4100	↓	1.58E-03
Amine oxidase [flavin-containing] A	*MAOA*	1.9006	-3.1677	-3.0711	-5.0683	-4.9717	-	-	1.85E-07
Amine oxidase [flavin-containing] B	*MAOB*	0.1244	-0.0923	-0.6201	-	-0.7445	0.5278	-	6.88E-03
Microtubule-associated protein;Microtubule-associated protein 4	*MAP4*	0.4738	0.0809	-0.3864	-0.3929	-0.8603	0.4673	↓	3.12E-04
S-adenosylmethionine synthase isoform type-2	*MAT2A*	-2.3362	-1.0381	-0.5495	1.2981	1.7867	-	-	2.43E-03
Matrin-3	*MATR3*	-0.4992	0.8778	0.9482	1.3770	1.4475	-	-	1.72E-05
Cell surface glycoprotein MUC18	*MCAM*	1.8194	-3.9521	-4.5274	-5.7715	-6.3468	-	-	3.32E-06
Methylcrotonoyl-CoA carboxylase beta chain, mitochondrial	*MCCC2*	-1.4150	0.4662	-1.1181	1.8812	-	1.5843	-	2.71E-05
Malate dehydrogenase, cytoplasmic	*MDH1*	2.2140	1.1024	1.3877	-1.1116	-0.8263	-	-	6.11E-04
Malate dehydrogenase, mitochondrial;Malate dehydrogenase	*MDH2*	2.1562	3.7563	3.7478	1.6001	1.5916	-	-	5.20E-06
NADP-dependent malic enzyme	*ME1*	-0.2062	-1.7249	-1.9242	-1.5187	-1.7180	-	-	1.01E-05
Microsomal glutathione S-transferase 1	*MGST1*	0.7474	-0.1052	-0.4015	-0.8527	-1.1489	-	-	1.18E-03
3-mercaptopyruvate sulfurtransferase;Sulfurtransferase	*MPST*	-1.3833	-2.7148	-2.1401	-1.3315	-0.7567	-0.5747	-	1.12E-03
Moesin	*MSN*	2.1149	2.3546	2.7754	-	0.6605	-0.4208	-	2.75E-03
C-1-tetrahydrofolate synthase, cytoplasmic;Methylenetetrahydrofolate dehydrogenase;Methenyltetr	*MTHFD1*	1.2189	-0.5599	-0.1058	-1.7789	-1.3247	-0.4542	-	4.45E-06
Major vault protein	*MVP*	0.3443	1.5622	0.8501	1.2180	0.5059	0.7121	-	4.88E-05
Myosin-10	*MYH10*	-0.0072	-0.3958	-1.3524	-0.3886	-1.3452	0.9566	↓	2.87E-04
Myosin-11	*MYH11*	3.4640	1.9041	-0.0918	-1.5598	-3.5558	1.9960	↓	1.29E-07
Myosin-14	*MYH14*	0.7663	0.5339	0.0531	-	-0.7132	0.4808	-	9.81E-04
Myosin-9	*MYH9*	3.9996	5.8962	5.5984	1.8966	1.5987	0.2979	-	4.16E-07
Myosin light polypeptide 6	*MYL6*	1.3919	2.5484	2.0698	1.1565	0.6779	0.4786	-	4.73E-06
Myosin regulatory light polypeptide 9	*MYL9*	0.0794	-0.8459	-1.7678	-0.9253	-1.8472	0.9219	↓	1.10E-05
Unconventional myosin-Ic	*MYO1C*	3.3706	1.2130	0.8485	-2.1576	-2.5221	0.3645	↓	3.90E-08
Myoferlin	*MYOF*	-0.2647	0.4892	-0.4907	-	-	0.9800	-	4.85E-02
Nascent polypeptide-associated complex subunit alpha, muscle-specific form;Nascent polypeptide-as	*NACA*	-0.6333	0.1846	0.7265	0.8179	1.3598	-0.5420	↑	1.26E-03
N-acetyl-D-glucosamine kinase	*NAGK*	-0.1834	0.7791	0.8594	0.9626	1.0429	-	-	5.58E-05
Nicotinamide phosphoribosyltransferase	*NAMPT*	-0.6949	-0.1270	-0.5113	0.5679	-	0.3843	-	1.90E-02
Sialic acid synthase	*NANS*	-0.9799	-0.3410	0.0876	0.6388	1.0675	-	-	5.73E-03
Nucleosome assembly protein 1-like 1	*NAP1L1*	-0.3429	0.3844	1.1645	0.7273	1.5074	-0.7801	↑	5.96E-06
Alpha-soluble NSF attachment protein	*NAPA*	-0.1341	0.3323	0.4367	0.4665	0.5708	-	-	1.16E-02
Nucleolin	*NCL*	1.4315	2.8661	3.4304	1.4347	1.9989	-0.5643	↑	2.22E-07
NADH dehydrogenase [ubiquinone] 1 alpha subcomplex subunit 9, mitochondrial	*NDUFA9*	-1.8507	-1.6506	-1.1087	-	0.7420	-0.5420	-	4.93E-03
NADH dehydrogenase [ubiquinone] iron-sulfur protein 3, mitochondrial	*NDUFS3*	-0.7285	-0.7118	-0.3504	-	0.3781	-0.3614	-	2.98E-02
NADH dehydrogenase [ubiquinone] flavoprotein 1, mitochondrial	*NDUFV1*	-2.8738	-3.6080	-2.7650	-0.7342	-	-0.8430	-	6.63E-03
NADH dehydrogenase [ubiquinone] flavoprotein 2, mitochondrial	*NDUFV2*	-2.7667	-2.3475	-1.7917	0.4193	0.9750	-0.5557	↑	7.60E-04
Nidogen-2	*NID2*	2.3346	-1.9316	-2.7235	-4.2663	-5.0581	0.7919	↓	1.17E-06
Protein NipSnap homolog 3A	*NIPSNAP3A*	-1.8081	-2.7980	-1.4706	-0.9899	-	-1.3275	-	1.24E-03
Nicotinamide N-methyltransferase	*NNMT*	-2.0795	0.0543	-1.6304	2.1338	-	1.6847	-	1.50E-04
NAD(P) transhydrogenase, mitochondrial	*NNT*	-0.1145	-1.8029	-1.0699	-1.6884	-0.9553	-0.7331	-	4.51E-04
Non-POU domain-containing octamer-binding protein	*NONO*	-1.3830	0.3358	0.3498	1.7188	1.7328	-	-	8.54E-06
Puromycin-sensitive aminopeptidase	*NPEPPS*	1.1588	1.4298	1.6270	-	0.4682	-	-	1.97E-02
Nucleophosmin	*NPM1*	-1.1842	1.0085	1.3060	2.1928	2.4902	-	-	4.53E-06
Vesicle-fusing ATPase	*NSF*	-0.9276	0.7123	0.5402	1.6399	1.4678	-	-	1.11E-04
Nuclear mitotic apparatus protein 1	*NUMA1*	-1.4829	0.1777	0.5041	1.6606	1.9870	-0.3264	↑	5.85E-06
2-oxoglutarate dehydrogenase, mitochondrial	*OGDH*	-0.1554	-1.5441	-1.3807	-1.3886	-1.2253	-	-	2.37E-03
Mimecan	*OGN*	5.0148	2.9127	0.7526	-2.1022	-4.2622	2.1600	↓	1.43E-06
Alpha-1-acid glycoprotein 1	*ORM1*	3.2234	1.1875	0.8735	-2.0358	-2.3498	-	-	1.46E-04
Ubiquitin thioesterase OTUB1	*OTUB1*	-0.2658	1.1947	1.1275	1.4605	1.3933	-	-	1.66E-05
Protein disulfide-isomerase	*P4HB*	2.3651	4.0196	4.0523	1.6545	1.6872	-	-	1.59E-06
Proliferation-associated protein 2G4	*PA2G4*	-0.8532	-0.4701	-0.7008	0.3831	-	-	-	2.35E-02
Palladin	*PALLD*	-1.1851	0.2897	-0.0821	1.4748	1.1030	0.3718	-	8.00E-06
Poly [ADP-ribose] polymerase 1	*PARP1*	-0.3357	2.1042	2.6797	2.4399	3.0154	-0.5755	↑	6.65E-06
Alpha-parvin	*PARVA*	0.8488	-1.3354	-1.7643	-2.1842	-2.6131	0.4289	↓	9.40E-07
Poly(rC)-binding protein 1	*PCBP1*	-0.6968	0.8153	0.9208	1.5121	1.6176	-	-	2.25E-06
Phosphoenolpyruvate carboxykinase [GTP], mitochondrial	*PCK2*	-1.6544	-1.6547	-0.9009	-	0.7535	-0.7539	-	9.99E-03
Prenylcysteine oxidase 1	*PCYOX1*	1.7375	0.1072	-0.6672	-1.6304	-2.4047	0.7743	↓	7.10E-07
Programmed cell death 6-interacting protein	*PDCD6IP*	0.7629	1.5288	1.6945	0.7659	0.9316	-	-	5.28E-04

Pyruvate dehydrogenase E1 component subunit alpha, somatic form, mitochondrial	*PDHA1*	-0.2887	-2.3811	-2.1680	-2.0924	-1.8793	-	-	9.57E-06
Protein disulfide-isomerase A3	*PDIA3*	2.2440	4.0449	3.6608	1.8008	1.4168	0.3840	-	5.01E-06
Protein disulfide-isomerase A4	*PDIA4*	0.4771	1.5657	2.1348	1.0886	1.6577	-0.5691	↑	8.53E-06
Protein disulfide-isomerase A6	*PDIA6*	0.8222	1.9123	2.6144	1.0900	1.7922	-0.7022	↑	4.62E-07
Pyridoxal kinase	*PDXK*	-0.1047	-1.5881	-1.4210	-1.4835	-1.3163	-	-	2.39E-04
Astrocytic phosphoprotein PEA-15	*PEA15*	-2.3105	-1.9560	-1.7003	-	0.6102	-	-	2.28E-02
Phosphatidylethanolamine-binding protein 1;Hippocampal cholinergic neurostimulating peptide	*PEBP1*	1.9676	2.0091	3.7814	-	1.8138	-1.7723	-	1.79E-05
ATP-dependent 6-phosphofructokinase, liver type	*PFKL*	0.4891	-0.4364	0.1754	-0.9255	-0.3138	-0.6118	-	2.10E-04
Profilin-1	*PFN1*	1.4136	2.0501	1.9851	0.6366	0.5715	-	-	1.69E-05
6-phosphogluconate dehydrogenase, decarboxylating	*PGD*	2.2959	1.4374	1.3215	-0.8584	-0.9744	-	-	1.15E-04
Phosphoglycerate kinase 1	*PGK1*	2.8898	4.2675	4.7255	1.3778	1.8358	-0.4580	↑	9.44E-07
6-phosphogluconolactonase	*PGLS*	-0.0951	0.0623	0.3496	-	0.4447	-0.2872	-	1.52E-03
Phosphoglucomutase-1	*PGM1*	1.7556	0.1862	0.0038	-1.5695	-1.7518	-	-	7.01E-05
Phosphoglucomutase-2	*PGM2*	-1.3467	-0.3734	-0.6170	0.9733	0.7297	-	-	7.51E-03
Membrane-associated progesterone receptor component 1	*PGRMC1*	-0.9258	-1.6026	-1.6372	-0.6768	-0.7114	-	-	1.39E-03
Membrane-associated progesterone receptor component 2	*PGRMC2*	0.0923	-0.8411	-0.6815	-0.9334	-0.7738	-	-	4.41E-04
Prohibitin	*PHB*	1.2827	2.8465	3.0430	1.5638	1.7603	-	-	9.47E-07
Prohibitin-2	*PHB2*	1.1992	2.5578	3.1636	1.3587	1.9645	-0.6058	↑	3.64E-06
D-3-phosphoglycerate dehydrogenase	*PHGDH*	1.9678	-0.8964	-1.5676	-2.8642	-3.5354	0.6712	↓	7.46E-08
Phosphatidylinositol-binding clathrin assembly protein	*PICALM*	-2.1119	-1.9310	-2.5316	-	-	0.6006	-	3.80E-02
Pyruvate kinase PKM;Pyruvate kinase	*PKM*	2.9453	5.0940	4.9225	2.1487	1.9772	-	-	1.63E-07
Plectin	*PLEC*	2.9829	4.0274	4.2546	1.0446	1.2717	-0.2272	↑	1.04E-06
Plasminogen;Plasmin heavy chain A;Activation peptide;Angiostatin;Plasmin heavy chain A, short form	*PLG*	1.9108	-0.4885	-1.9213	-2.3993	-3.8321	1.4328	↓	3.06E-05
Perilipin-1	*PLIN1*	4.4659	-2.8982	-2.4433	-7.3640	-6.9091	-0.4549	-	1.49E-10
Perilipin-3	*PLIN3*	-1.5425	-0.8102	-0.3030	0.7323	1.2395	-	-	5.61E-03
Perilipin-4	*PLIN4*	3.6374	-5.2592	-5.7818	-8.8965	-9.4192	-	-	1.50E-07
Plastin-3	*PLS3*	0.7458	1.1855	0.5458	-	-	0.6397	-	3.26E-02
Purine nucleoside phosphorylase	*PNP*	1.3906	1.7133	3.3444	0.3226	1.9537	-1.6311	↑	1.07E-07
Serum paraoxonase/arylesterase 1	*PON1*	0.6889	-1.6059	-3.2990	-2.2948	-3.9879	1.6931	↓	1.87E-07
Periostin	*POSTN*	2.6870	6.3962	6.6599	3.7092	3.9729	-0.2638	↑	1.29E-08
Inorganic pyrophosphatase	*PPA1*	-0.2710	0.1028	0.4841	-	0.7551	-	-	3.69E-02
Inorganic pyrophosphatase 2, mitochondrial	*PPA2*	-1.8031	-0.7757	-0.5804	1.0274	1.2227	-	-	3.52E-04
Peptidyl-prolyl cis-trans isomerase A;Peptidyl-prolyl cis-trans isomerase A, N-terminally processed;Pe	*PPIA*	2.9611	4.3352	4.5304	1.3741	1.5693	-	-	3.18E-05
Peptidyl-prolyl cis-trans isomerase B	*PPIB*	1.7647	2.5656	2.6666	0.8009	0.9019	-	-	3.92E-05
Serine/threonine-protein phosphatase 2A 65 kDa regulatory subunit A alpha isoform	*PPP2R1A*	0.4357	0.7772	1.1253	0.3416	0.6896	-0.3480	↑	2.49E-03
Peroxiredoxin-1	*PRDX1*	2.6855	4.1870	4.4239	1.5015	1.7384	-0.2369	↑	9.18E-07
Peroxiredoxin-2	*PRDX2*	3.9749	2.1224	2.2232	-1.8525	-1.7518	-	-	3.80E-06
Thioredoxin-dependent peroxide reductase, mitochondrial	*PRDX3*	1.2959	1.4397	1.9210	-	0.6250	-0.4813	-	3.09E-04
Peroxiredoxin-4	*PRDX4*	-0.5981	0.2999	1.5357	0.8979	2.1338	-1.2358	↑	1.22E-05
Peroxiredoxin-5, mitochondrial	*PRDX5*	0.2603	0.7309	0.9129	0.4706	0.6526	-	-	1.79E-03
Peroxiredoxin-6	*PRDX6*	3.4991	3.4340	4.1766	-	0.6775	-0.7426	-	2.16E-04
Prolargin	*PRELP*	4.8785	3.2139	3.8117	-1.6646	-1.0668	-0.5978	-	1.15E-05
Prolyl endopeptidase	*PREP*	-1.0630	-0.7195	-0.2312	0.3435	0.8318	-0.4883	↑	2.92E-04
cAMP-dependent protein kinase catalytic subunit beta	*PRKACB*	-1.0569	-2.4392	-1.7809	-1.3823	-0.7240	-0.6583	-	1.13E-03
cAMP-dependent protein kinase type II-alpha regulatory subunit	*PRKAR2A*	2.1199	-0.1883	-0.5626	-2.3082	-2.6825	-	-	1.65E-02
cAMP-dependent protein kinase type II-beta regulatory subunit	*PRKAR2B*	0.8785	-1.4201	-1.0323	-2.2986	-1.9108	-0.3878	-	9.31E-07
Protein kinase C delta-binding protein	*PRKCDBP*	0.4444	-1.5609	-2.9268	-2.0053	-3.3712	-	-	8.29E-03
DNA-dependent protein kinase catalytic subunit	*PRKDC*	-0.1922	1.5011	1.9272	1.6933	2.1195	-	-	1.03E-04
Pre-mRNA-processing-splicing factor 8	*PRPF8*	-1.8677	-0.2932	-0.2698	1.5745	1.5979	-	-	3.78E-06
Proteasome subunit alpha type-1;Proteasome subunit alpha type	*PSMA1*	0.0977	-0.2259	0.7835	-0.3236	0.6857	-1.0093	-	7.11E-04
Proteasome subunit alpha type;Proteasome subunit alpha type-2	*PSMA2*	-0.0398	0.2112	0.5527	0.2510	0.5925	-0.3415	↑	2.13E-03
Proteasome subunit alpha type-5	*PSMA5*	-0.1181	0.3661	0.8105	0.4842	0.9286	-0.4444	↑	5.26E-04
Proteasome subunit alpha type-7	*PSMA7*	0.6822	1.0574	1.3662	0.3752	0.6840	-0.3088	↑	2.57E-04
Proteasome subunit beta type-1	*PSMB1*	0.3038	0.6543	0.8283	0.3504	0.5245	-	-	6.91E-03
Proteasome subunit beta type-2	*PSMB2*	-1.2514	-0.8324	-0.5748	0.4190	0.6766	-	-	5.92E-03
Proteasome subunit beta type-5	*PSMB5*	-0.8838	-1.4095	-1.0725	-0.5257	-	-	-	3.24E-02
Proteasome subunit beta type-6	*PSMB6*	-1.5317	-2.1617	-1.9023	-0.6301	-0.3706	-0.2595	-	1.13E-03
26S protease regulatory subunit 4	*PSMC1*	-1.1746	-0.0257	-0.0102	1.1490	1.1644	-	-	5.95E-04
26S protease regulatory subunit 7	*PSMC2*	-1.7163	-1.9651	-1.4158	-	-	-0.5493	-	2.23E-02
26S protease regulatory subunit 6A	*PSMC3*	-1.1227	-1.3735	-0.7350	-	0.3876	-0.6385	-	7.69E-03
26S protease regulatory subunit 8	*PSMC5*	-1.0526	-0.2663	-0.1275	0.7863	0.9252	-	-	2.32E-03
26S proteasome non-ATPase regulatory subunit 1	*PSMD1*	-1.5322	-0.8460	-0.3631	0.6862	1.1691	-0.4829	↑	2.43E-04
26S proteasome non-ATPase regulatory subunit 11	*PSMD11*	0.1537	0.4238	0.6323	-	0.4787	-	-	3.83E-02
26S proteasome non-ATPase regulatory subunit 3	*PSMD3*	-1.3416	-0.7808	-0.1045	0.5608	1.2371	-0.6763	↑	2.33E-03
26S proteasome non-ATPase regulatory subunit 5	*PSMD5*	-1.0581	-1.8220	-1.8194	-0.7639	-0.7613	-	-	5.43E-03
26S proteasome non-ATPase regulatory subunit 6	*PSMD6*	-1.0103	-0.7619	-0.2766	-	0.7337	-0.4853	-	9.35E-03
26S proteasome non-ATPase regulatory subunit 7	*PSMD7*	-2.2423	-1.7413	-1.2678	0.5010	0.9745	-0.4735	↑	3.69E-03
Proteasome activator complex subunit 1	*PSME1*	0.4624	2.3759	2.9383	1.9134	2.4759	-0.5624	↑	3.27E-07
Proteasome activator complex subunit 2	*PSME2*	-0.9478	0.7647	1.1228	1.7125	2.0706	-	-	4.25E-05
Polypyrimidine tract-binding protein 1	*PTBP1*	-0.8922	1.3677	1.6058	2.2599	2.4980	-0.2381	↑	2.40E-07
Prostacyclin synthase	*PTGIS*	-0.6168	-4.2204	-3.8418	-3.6036	-3.2250	-0.3787	-	1.48E-08
Prostaglandin reductase 1	*PTGR1*	-2.2487	-2.6385	-3.1034	-0.3898	-0.8547	0.4649	↓	2.91E-03
Tyrosine-protein phosphatase non-receptor type 6	*PTPN6*	-3.6314	-2.8912	-1.7327	-	1.8986	-1.1585	-	5.07E-03
Polymerase I and transcript release factor	*PTRF*	3.8445	0.8655	0.3079	-2.9790	-3.5366	0.5575	↓	2.45E-07
Transcriptional activator protein Pur-alpha	*PURA*	-1.6122	-1.5098	-1.8242	-	-	0.3144	-	3.16E-02
Glycogen phosphorylase, brain form	*PYGB*	0.8348	0.2045	0.5159	-0.6303	-0.3189	-0.3114	-	9.54E-04
Alpha-1,4 glucan phosphorylase;Glycogen phosphorylase, liver form	*PYGL*	1.5454	0.0461	0.1640	-1.4993	-1.3814	-	-	4.17E-06
Dihydropteridine reductase	*QDPR*	0.6220	0.7836	2.0623	-	1.4403	-1.2787	-	1.08E-05
Ras-related protein Rab-10	*RAB10*	-1.5609	-2.0300	-2.4904	-	-0.9295	-	-	4.14E-02
Ras-related protein Rab-5B	*RAB5B*	-2.0866	-2.5703	-2.5991	-0.4837	-0.5125	-	-	1.06E-02
Ras-related protein Rab-8A	*RAB8A*	-1.5988	-2.4076	-2.5517	-0.8088	-0.9529	-	-	2.13E-02
UV excision repair protein RAD23 homolog B	*RAD23B*	-2.2477	-2.1681	-1.3347	-	0.9130	-0.8334	-	4.34E-02
GTP-binding nuclear protein Ran	*RAN*	1.1497	0.9083	2.2785	-	1.1289	-1.3702	-	6.12E-05
RNA-binding motif protein, X chromosome;RNA-binding motif protein, X chromosome, N-terminally p	*RBMX*	-1.5038	0.2185	0.1336	1.7223	1.6375	-	-	1.68E-04
Retinol-binding protein 4;Plasma retinol-binding protein(1-182);Plasma retinol-binding protein(1-181	*RBP4*	-1.8033	-4.7505	-5.3913	-2.9472	-3.5880	-	-	7.58E-04
All-trans-retinol 13,14-reductase	*RETSAT*	-0.0800	-3.0121	-3.2020	-2.9321	-3.1220	-	-	1.44E-05
Ribonuclease inhibitor	*RNH1*	0.8151	0.3684	0.1981	-0.4467	-0.6171	-	-	2.36E-02
Aminopeptidase B	*RNPEP*	-1.4811	0.5614	1.6734	2.0426	3.1546	-1.1120	↑	3.98E-05
60S ribosomal protein L10a	*RPL10A*	-0.1413	1.0403	1.3574	1.1816	1.4986	-	-	1.51E-03
60S ribosomal protein L12	*RPL12*	-0.2235	0.6725	0.7481	0.8960	0.9716	-	-	9.39E-04
60S ribosomal protein L13	*RPL13*	-1.6845	-0.0528	0.7723	1.6317	2.4568	-0.8252	↑	2.54E-05
60S ribosomal protein L14	*RPL14*	-0.8485	0.0820	-0.3975	0.9305	0.4510	0.4795	-	1.24E-03
60S ribosomal protein L17	*RPL17*	-0.4982	-0.1569	0.1941	0.3414	0.6924	-0.3510	↑	5.53E-03
60S ribosomal protein L18	*RPL18*	-1.7992	0.6932	1.0535	2.4924	2.8526	-	-	5.01E-05
60S ribosomal protein L23a	*RPL23A*	-0.2900	0.6136	0.8757	0.9036	1.1657	-	-	9.15E-04
60S ribosomal protein L24	*RPL24*	-1.4902	-0.6016	-0.1776	0.8886	1.3126	-	-	2.89E-03
60S ribosomal protein L27	*RPL27*	-0.3873	0.5166	0.1802	0.9039	0.5675	-	-	1.90E-03
60S ribosomal protein L3	*RPL3*	-1.3728	0.5731	-0.2382	1.9459	1.1345	0.8114	-	2.98E-06
60S ribosomal protein L31	*RPL31*	-1.1922	-0.7363	-1.4831	-	-	0.7468	-	4.10E-02
60S ribosomal protein L4	*RPL4*	-0.7083	1.9934	2.0225	2.7017	2.7308	-	-	2.82E-07
60S ribosomal protein L5	*RPL5*	-1.3192	-0.6674	0.1091	-	1.4283	-	-	1.22E-02
60S ribosomal protein L6	*RPL6*	-2.1260	1.2614	0.6111	3.3874	2.7371	0.6503	-	8.39E-06
60S ribosomal protein L7	*RPL7*	0.3712	1.0304	1.6836	0.6591	1.3124	-0.6533	↑	2.98E-04
60S ribosomal protein L7a	*RPL7A*	-0.7041	1.2934	0.8960	1.9975	1.6001	-	-	2.36E-02
60S ribosomal protein L9	*RPL9*	-0.5136	0.6038	0.6715	1.1174	1.1850	-	-	6.94E-04
60S acidic ribosomal protein P0	*RPLP0*	0.0649	1.4098	1.5141	1.3448	1.4492	-	-	2.86E-04
60S acidic ribosomal protein P2	*RPLP2*	-2.5938	-1.7711	-0.7285	-	1.8652	-	-	1.52E-02
Dolichyl-diphosphooligosaccharide--protein glycosyltransferase subunit 1	*RPN1*	1.2776	2.1613	2.4283	0.8837	1.1507	-0.2670	↑	3.96E-05
Dolichyl-diphosphooligosaccharide--protein glycosyltransferase subunit 2	*RPN2*	0.7111	1.6131	1.8250	0.9020	1.1139	-0.2119	↑	1.33E-05

40S ribosomal protein S10	*RPS10*	-0.5231	0.5369	0.8020	1.0600	1.3251	-	-	8.90E-05
40S ribosomal protein S13	*RPS13*	0.0770	1.1678	0.8601	1.0907	0.7831	-	-	5.94E-04
40S ribosomal protein S15a	*RPS15A*	-0.5554	0.1531	-0.4489	0.7086	-	0.6021	-	1.25E-02
40S ribosomal protein S19	*RPS19*	-0.9133	0.3090	0.3130	1.2223	1.2263	-	-	6.85E-03
40S ribosomal protein S2	*RPS2*	0.4333	1.2268	1.1907	0.7935	0.7574	-	-	3.24E-03
40S ribosomal protein S20	*RPS20*	0.1410	0.5603	0.6529	0.4194	0.5119	-	-	2.03E-02
40S ribosomal protein S3	*RPS3*	1.0427	2.1523	2.5579	1.1096	1.5152	-0.4056	↑	4.78E-05
40S ribosomal protein S3a	*RPS3A*	-1.5143	-0.3145	-0.4741	1.1999	1.0403	-	-	1.60E-02
40S ribosomal protein S7	*RPS7*	-1.6416	-0.3973	-0.5479	1.2443	1.0937	-	-	1.38E-04
40S ribosomal protein S8	*RPS8*	0.0491	0.9384	0.8724	0.8894	0.8233	-	-	1.17E-02
40S ribosomal protein S9	*RPS9*	0.1508	1.8094	1.9852	1.6586	1.8344	-	-	5.55E-06
40S ribosomal protein SA	*RPSA*	0.9464	2.0585	2.4535	1.1121	1.5072	-0.3950	↑	2.54E-05
Ribosome-binding protein 1	*RRBP1*	-1.5699	0.3034	1.2376	1.8733	2.8075	-0.9342	↑	1.41E-04
tRNA-splicing ligase RtcB homolog	*RTCB*	-1.2926	0.2525	0.5822	1.5451	1.8748	-	-	1.29E-03
Reticulon;Reticulon-4	*RTN4*	2.1518	1.5947	1.3405	-0.5571	-0.8113	0.2542	↓	5.02E-05
RuvB-like 1	*RUVBL1*	-0.4877	0.6553	1.1276	1.1430	1.6153	-0.4723	↑	5.43E-06
RuvB-like 2	*RUVBL2*	-1.7026	0.4851	0.9080	2.1877	2.6106	-0.4230	↑	4.56E-06
Deoxynucleoside triphosphate triphosphohydrolase SAMHD1	*SAMHD1*	0.4126	1.5340	1.3748	1.1213	0.9622	-	-	2.64E-05
SAP domain-containing ribonucleoprotein	*SARNP*	-3.5699	-2.2041	-2.2934	1.3659	1.2765	-	-	4.36E-02
Serine--tRNA ligase, cytoplasmic	*SARS*	-1.5758	-0.5031	0.1957	1.0727	1.7715	-0.6988	↑	2.65E-04
Succinate dehydrogenase [ubiquinone] flavoprotein subunit, mitochondrial	*SDHA*	-0.5211	-1.3959	-1.6785	-0.8748	-1.1573	-	-	3.27E-03
Succinate dehydrogenase [ubiquinone] iron-sulfur subunit, mitochondrial	*SDHB*	-1.5520	-2.5980	-2.1818	-1.0461	-0.6298	-0.4162	-	2.92E-04
Signal peptidase complex catalytic subunit SEC11;Signal peptidase complex catalytic subunit SEC11A;S	*SEC11A*	-1.3372	-1.9606	-2.1818	-0.6234	-0.8445	-	-	4.36E-03
Vesicle-trafficking protein SEC22b	*SEC22B*	-0.9576	-0.3832	-0.4396	0.5745	0.5181	-	-	3.07E-02
Protein transport protein Sec31A	*SEC31A*	-0.5912	0.5969	0.4448	1.1881	1.0360	-	-	3.85E-05
Translocation protein SEC63 homolog	*SEC63*	-2.4427	-1.4581	-1.7756	0.9846	-	-	-	4.77E-02
Selenium-binding protein 1	*SELENBP1*	3.0459	1.1404	0.8430	-1.9055	-2.2029	0.2974	↓	1.28E-09
Septin-11	*SEPT11*	0.4979	-0.3703	-1.4990	-0.8682	-1.9969	1.1287	↓	8.04E-08
Septin-2	*SEPT2*	0.8180	0.5020	0.2627	-	-0.5553	-	-	4.54E-02
Septin-9	*SEPT9*	0.0833	0.2365	0.6119	-	0.5285	-0.3754	-	2.56E-02
Alpha-1-antitrypsin;Short peptide from AAT	*SERPINA1*	5.6056	5.0780	4.9804	-0.5276	-0.6252	-	-	3.85E-03
Alpha-1-antichymotrypsin;Alpha-1-antichymotrypsin His-Pro-less	*SERPINA3*	3.2551	2.6684	2.3131	-0.5867	-0.9420	0.3553	↓	2.19E-05
Kallistatin	*SERPINA4*	-1.5138	-2.3113	-3.1261	-	-1.6122	-	-	7.71E-03
Plasma serine protease inhibitor	*SERPINA5*	-1.5488	-2.1817	-2.0525	-0.6329	-	-	-	4.94E-02
Leukocyte elastase inhibitor	*SERPINB1*	1.4532	0.9560	1.6282	-0.4972	0.1750	-0.6722	-	4.29E-05
Serpin B6	*SERPINB6*	0.7237	-0.1506	-0.2380	-0.8743	-0.9617	-	-	2.88E-05
Antithrombin-III	*SERPINC1*	3.4852	2.2513	1.4771	-1.2339	-2.0081	0.7742	↓	9.71E-07
Heparin cofactor 2	*SERPIND1*	1.7438	-0.8025	-1.5065	-2.5463	-3.2503	0.7040	↓	5.39E-08
Pigment epithelium-derived factor	*SERPINF1*	2.3878	2.2553	1.6081	-0.1325	-0.7797	0.6472	↓	2.79E-06
Alpha-2-antiplasmin	*SERPINF2*	0.4205	-2.2801	-2.6577	-2.7006	-3.0782	-	-	1.11E-03
Plasma protease C1 inhibitor	*SERPING1*	2.4909	1.4856	0.6461	-1.0053	-1.8448	0.8395	↓	9.22E-09
Serpin H1	*SERPINH1*	1.8932	3.1695	2.0560	1.2763	-	1.1135	-	1.21E-05
Splicing factor 3A subunit 1	*SF3A1*	-2.3383	-1.3295	-0.8489	1.0088	1.4895	-	-	9.81E-03
Splicing factor, proline- and glutamine-rich	*SFPQ*	0.3919	1.8633	1.9539	1.4714	1.5620	-	-	9.25E-05
Sideroflexin-1	*SFXN1*	-1.5558	-0.9528	-0.1805	0.6030	1.3753	-0.7723	↑	2.49E-03
SH3 domain-binding glutamic acid-rich-like protein	*SH3BGRL*	-0.6334	0.9192	0.8442	1.5526	1.4776	-	-	2.74E-06
Endophilin-B1	*SH3GLB1*	-2.2517	-3.2201	-3.4557	-0.9685	-1.2040	-	-	1.13E-02
Tricarboxylate transport protein, mitochondrial	*SLC25A1*	0.9369	-0.7725	-0.8359	-1.7094	-1.7728	-	-	3.68E-05
Mitochondrial dicarboxylate carrier	*SLC25A10*	-0.8484	-1.4966	-1.1796	-0.6482	-	-	-	1.64E-02
Calcium-binding mitochondrial carrier protein Aralar1	*SLC25A12*	-2.3481	-2.9705	-2.9513	-0.6224	-0.6032	-	-	7.32E-03
Calcium-binding mitochondrial carrier protein Aralar2	*SLC25A13*	-2.0581	-0.8481	-0.5396	1.2100	1.5185	-0.3085	↑	2.31E-05
Calcium-binding mitochondrial carrier protein SCaMC-1	*SLC25A24*	-2.2961	-2.1595	-1.8517	-	0.4444	-	-	2.76E-02
ADP/ATP translocase 3;ADP/ATP translocase 3, N-terminally processed	*SLC25A6*	1.5216	1.5544	1.3141	-	-0.2075	0.2404	-	3.07E-02
Band 3 anion transport protein	*SLC4A1*	3.5527	-1.7120	-3.0736	-5.2647	-6.6263	1.3616	↓	5.09E-07
Na(+)/H(+) exchange regulatory cofactor NHE-RF1	*SLC9A3R1*	-2.8018	0.4771	1.0017	3.2788	3.8035	-	-	8.36E-06
Staphylococcal nuclease domain-containing protein 1	*SND1*	0.4449	1.6320	1.9940	1.1870	1.5491	-0.3621	↑	4.10E-08
U5 small nuclear ribonucleoprotein 200 kDa helicase	*SNRNP200*	-2.3850	-0.4099	-0.0059	1.9751	2.3791	-	-	1.57E-04
Sorting nexin-2	*SNX2*	-0.5583	-1.3379	-1.3633	-0.7796	-0.8050	-	-	7.05E-03
Sorbin and SH3 domain-containing protein 1	*SORBS1*	1.1217	-3.3356	-4.0979	-4.4572	-5.2195	-	-	9.33E-06
Sorbitol dehydrogenase	*SORD*	-1.4568	2.1199	1.3943	3.5766	2.8511	0.7255	-	2.76E-07
Sepiapterin reductase	*SPR*	-1.5610	-1.3096	-0.2705	-	1.2905	-1.0390	-	2.64E-04
Spectrin alpha chain, non-erythrocytic 1	*SPTAN1*	3.1083	1.7296	2.0616	-1.3786	-1.0466	-0.3320	-	2.50E-05
Spectrin beta chain, non-erythrocytic 1	*SPTBN1*	2.9910	1.4154	1.4726	-1.5756	-1.5184	-	-	1.72E-06
Sulfide:quinone oxidoreductase, mitochondrial	*SQRDL*	-0.0665	1.1114	0.8478	1.1779	0.9142	-	-	2.64E-04
Signal recognition particle subunit SRP68	*SRP68*	-1.9496	-1.1965	-1.7949	0.7532	-	0.5984	-	3.45E-02
Serine/arginine-rich splicing factor 2	*SRSF2*	-2.0185	-0.2075	-0.3944	1.8110	1.6241	-	-	3.80E-04
Serine/arginine-rich splicing factor 3	*SRSF3*	-1.9598	0.1341	0.3935	2.0939	2.3533	-	-	3.90E-05
Serine/arginine-rich splicing factor 6	*SRSF6*	-1.7539	-0.2338	0.0059	1.5201	1.7597	-	-	1.43E-02
Serine/arginine-rich splicing factor 7	*SRSF7*	-1.9797	-0.4400	-0.2969	1.5397	1.6828	-	-	1.43E-03
Translocon-associated protein subunit alpha	*SSR1*	-2.0378	-0.5963	-0.6023	1.4416	1.4355	-	-	1.20E-04
Translocon-associated protein subunit delta	*SSR4*	-1.1430	-0.7621	-0.1867	-	0.9563	-0.5754	-	4.18E-03
Signal transducer and activator of transcription 1-alpha/beta;Signal transducer and activator of transc	*STAT1*	-1.6160	1.9952	2.7418	3.6113	4.3579	-0.7466	↑	1.49E-06
Stress-induced-phosphoprotein 1	*STIP1*	0.0167	1.4710	1.6141	1.4544	1.5974	-	-	1.41E-05
Succinyl-CoA ligase [ADP-forming] subunit beta, mitochondrial	*SUCLA2*	-0.5518	-1.4079	-1.8149	-0.8561	-1.2631	0.4070	↓	2.26E-04
Succinyl-CoA ligase [GDP-forming] subunit beta, mitochondrial	*SUCLG2*	-0.2014	-0.8605	-0.6337	-0.6591	-0.4323	-	-	1.74E-03
Heterogeneous nuclear ribonucleoprotein Q	*SYNCRIP*	0.0641	1.8336	2.2367	1.7695	2.1725	-0.4030	↑	1.16E-06
Transgelin	*TAGLN*	3.6600	3.5250	2.2252	-	-1.4347	1.2997	-	2.12E-04
Transgelin-2	*TAGLN2*	0.9782	2.3424	2.1031	1.3642	1.1249	-	-	1.26E-04
Transaldolase	*TALDO1*	1.5865	1.1796	0.9580	-0.4069	-0.6285	0.2216	↓	1.89E-04
Threonine--tRNA ligase, cytoplasmic	*TARS*	-1.3994	-0.5291	-0.3316	0.8703	1.0679	-	-	4.74E-05
T-complex protein 1 subunit alpha	*TCP1*	0.2923	0.9540	1.2270	0.6616	0.9347	-	-	3.80E-04
Serotransferrin	*TF*	5.4598	4.6124	4.0977	-0.8474	-1.3621	0.5147	↓	2.34E-04
Transforming growth factor beta-1-induced transcript 1 protein	*TGFB1I1*	-4.0819	-4.5850	-5.2515	-0.5031	-1.1696	0.6665	↓	7.93E-04
Transforming growth factor-beta-induced protein ig-h3	*TGFBI*	2.0923	2.6792	1.4971	0.5869	-0.5952	1.1820	-	1.60E-05
Protein-glutamine gamma-glutamyltransferase 2	*TGM2*	0.7534	0.6979	1.1621	-	0.4087	-0.4641	-	2.07E-03
Thrombospondin-1	*THBS1*	0.7646	3.1334	2.2863	2.3688	1.5217	0.8471	-	3.12E-07
Transketolase	*TKT*	3.1376	3.0938	2.9502	-	-0.1873	-	-	4.54E-02
Talin-1	*TLN1*	2.9640	2.8538	2.6206	-	-0.3434	0.2332	-	7.36E-03
Transmembrane emp24 domain-containing protein 10	*TMED10*	-0.6231	0.3828	0.1114	1.0059	0.7344	-	-	2.04E-03
Transmembrane protein 43	*TMEM43*	0.7428	0.5481	0.0565	-	-0.6863	0.4916	-	4.39E-03
Tenascin	*TNC*	0.5871	2.5731	0.8763	1.9860	0.2892	1.6968	-	3.48E-07
Tensin-1	*TNS1*	1.5678	-1.8431	-2.3624	-3.4109	-3.9302	0.5193	↓	4.31E-08
Tenascin-X	*TNXB*	1.3189	-3.6676	-4.6270	-4.9865	-5.9459	0.9594	↓	8.76E-07
Triosephosphate isomerase	*TPI1*	2.4839	3.7518	3.6485	1.2678	1.1646	-	-	3.98E-05
Tropomyosin alpha-1 chain	*TPM1*	1.4227	0.1711	-1.0312	-1.2516	-2.4540	1.2024	↓	8.46E-05
Tropomyosin alpha-4 chain	*TPM4*	0.6621	1.2861	0.3420	-	-	0.9440	-	3.65E-02
Translationally-controlled tumor protein	*TPT1*	-1.3790	-0.8819	-0.4729	0.4971	0.9061	-	-	6.71E-03
Heat shock protein 75 kDa, mitochondrial	*TRAP1*	-2.5908	-0.9483	-0.5966	1.6426	1.9943	-	-	3.99E-02
60 kDa SS-A/Ro ribonucleoprotein	*TROVE2*	-1.4639	-0.3816	-0.7369	1.0823	0.7270	0.3553	-	1.02E-05
Translin	*TSN*	-1.3666	-0.9571	-1.1635	0.4095	-	-	-	2.10E-02
Tubulin--tyrosine ligase-like protein 12	*TTLL12*	-1.1334	1.1320	2.8059	2.2654	3.9393	-1.6739	↑	5.08E-09
Titin	*TTN*	-0.3177	-1.0081	-1.2533	-0.6904	-0.9356	0.2452	↓	1.54E-04
Transthyretin	*TTR*	2.7590	1.7678	1.4575	-0.9912	-1.3015	0.3103	↓	4.72E-06
Tubulin beta chain	*TUBB*	2.1900	3.8437	4.1848	1.6537	1.9948	-	-	3.64E-05
Tubulin beta-4B chain	*TUBB4B*	3.5757	5.2204	5.4828	1.6447	1.9071	-	-	3.52E-06
Tubulin beta-6 chain	*TUBB6*	-0.2265	-1.4931	-2.7634	-1.2666	-2.5369	1.2703	↓	9.27E-08
Elongation factor Tu, mitochondrial	*TUFM*	1.3309	2.4493	2.7023	1.1184	1.3714	-0.2530	↑	2.53E-07
Thioredoxin domain-containing protein 5	*TXNDC5*	-1.5932	-0.7872	1.4591	0.8060	3.0523	-2.2464	↑	2.88E-06
Thymidine phosphorylase	*TYMP*	-1.3742	1.9053	1.9692	3.2796	3.3435	-	-	5.10E-05

Splicing factor U2AF 65 kDa subunit	*U2AF2*	-2.9283	-0.2138	-0.2659	2.7145	2.6624	-	-	4.00E-04
Ubiquitin-like modifier-activating enzyme 1	*UBA1*	1.7062	2.7288	3.1818	1.0226	1.4756	-0.4530	↑	7.04E-07
Ubiquitin-conjugating enzyme E2 N;Putative ubiquitin-conjugating enzyme E2 N-like	*UBE2N*	0.0116	0.1184	0.5086	-	0.4970	-0.3903	-	1.72E-02
Ubiquitin-conjugating enzyme E2 variant 1	*UBE2V1*	-0.0948	-0.0022	0.3389	-	0.4337	-0.3412	-	2.60E-02
UDP-glucose 6-dehydrogenase	*UGDH*	-0.2996	1.5473	1.7181	1.8469	2.0177	-	-	6.22E-05
UTP--glucose-1-phosphate uridylyltransferase	*UGP2*	2.4714	0.8641	0.7377	-1.6073	-1.7338	-	-	1.08E-07
Cytochrome b-c1 complex subunit 1, mitochondrial	*UQCRC1*	0.3573	0.0224	-0.2287	-0.3349	-0.5860	-	-	9.42E-03
Cytochrome b-c1 complex subunit 2, mitochondrial	*UQCRC2*	1.0276	1.4413	1.1470	0.4138	-	0.2943	-	1.79E-02
General vesicular transport factor p115	*USO1*	-0.9351	0.1219	-0.1215	1.0570	0.8137	-	-	3.18E-04
Ubiquitin carboxyl-terminal hydrolase;Ubiquitin carboxyl-terminal hydrolase 14	*USP14*	-1.0963	-0.4889	-0.1065	0.6074	0.9898	-	-	2.73E-03
Ubiquitin carboxyl-terminal hydrolase 5	*USP5*	-0.0851	1.2517	1.9549	1.3369	2.0400	-0.7031	↑	9.59E-06
Ubiquitin carboxyl-terminal hydrolase 7;Ubiquitin carboxyl-terminal hydrolase	*USP7*	-2.5853	-1.5270	-1.1071	1.0583	1.4782	-	-	2.12E-03
Vesicle-associated membrane protein-associated protein B/C	*VAPB*	-1.6181	-0.1894	-0.4464	1.4288	1.1717	-	-	1.49E-04
Valine--tRNA ligase	*VARS*	-1.6652	0.1034	1.1202	1.7686	2.7854	-1.0168	↑	1.90E-05
Synaptic vesicle membrane protein VAT-1 homolog	*VAT1*	1.5056	1.1588	1.0005	-	-0.5051	-	-	3.99E-02
Vinculin	*VCL*	3.2670	2.6322	2.1436	-0.6348	-1.1234	0.4886	↓	2.37E-06
Transitional endoplasmic reticulum ATPase	*VCP*	1.9196	2.7391	3.3752	0.8195	1.4555	-0.6360	↑	2.56E-06
Voltage-dependent anion-selective channel protein 1	*VDAC1*	1.6327	3.0610	3.4112	1.4283	1.7785	-0.3502	↑	1.30E-07
Voltage-dependent anion-selective channel protein 2	*VDAC2*	1.7834	2.2959	2.7222	0.5125	0.9388	-0.4264	↑	2.60E-04
Voltage-dependent anion-selective channel protein 3	*VDAC3*	0.5339	1.9125	2.0368	1.3786	1.5029	-	-	3.52E-04
Vimentin	*VIM*	6.2705	6.9550	6.6820	0.6845	0.4115	-	-	2.66E-03
Vacuolar protein sorting-associated protein 35	*VPS35*	0.8695	0.5475	0.9528	-0.3221	-	-0.4053	-	5.38E-03
Tryptophan--tRNA ligase, cytoplasmic;T1-TrpRS;T2-TrpRS	*WARS*	0.1960	0.5034	0.6372	0.3074	0.4412	-	-	2.93E-02
WD repeat-containing protein 1	*WDR1*	1.2668	1.9033	2.3254	0.6365	1.0586	-0.4221	↑	5.92E-05
Exportin-1	*XPO1*	-1.1337	0.0643	0.2791	1.1980	1.4129	-	-	2.63E-04
X-ray repair cross-complementing protein 5	*XRCC5*	0.8000	1.8095	2.2779	1.0095	1.4778	-0.4683	↑	7.54E-05
X-ray repair cross-complementing protein 6	*XRCC6*	1.1470	2.3779	2.9898	1.2308	1.8428	-0.6119	↑	1.52E-07
14-3-3 protein beta/alpha;14-3-3 protein beta/alpha, N-terminally processed	*YWHAB*	0.4680	0.8223	0.5976	0.3543	-	0.2246	-	1.46E-02
14-3-3 protein eta	*YWHAH*	0.2028	0.3833	-0.4275	-	-0.6304	0.8108	-	1.76E-02
14-3-3 protein theta	*YWHAQ*	0.1117	0.0032	0.5848	-	0.4731	-0.5816	-	1.79E-02
Zyxin	*ZYX*	-1.2323	-1.4022	-1.8590	-	-0.6267	0.4568	-	1.39E-03

Supplementary File 2A. Differentially expressed proteins into the log2 fold change values identified in the MLN x MNT tissues' comparison according to the ANOVA's test.
LFQ intensities were log2-transformed and normalized by width adjustment in Perseus v. 1.5.6.0. Fold changes were presented in log2 values (up-regulated and down-regulated proteins were highlighted in red and green, respectively).

Protein Name	Gene Symbol	MNT LFQ_mean	MPT LFQ_mean	MLN LFQ_mean	MLN x MNT fold change	ANOVA p-value
Alpha-1B-glycoprotein	*A1BG*	2.1273667	0.4712794	0.4516697	-1.6756970	1.65E-03
Alpha-2-macroglobulin	*A2M*	5.4595100	4.3127733	3.2430810	-2.2164290	3.42E-06
Alpha/beta hydrolase domain-containing protein 11	*ABHD11*	-2.4499187	-2.0277317	-0.5991934	1.8507253	1.22E-02
Alpha/beta hydrolase domain-containing protein 14B	*ABHD14B*	0.5174353	-1.6124077	-1.2778410	-1.7952763	8.50E-06
3-ketoacyl-CoA thiolase, peroxisomal	*ACAA1*	-3.2104950	-2.0179867	-1.5372723	1.6732227	7.02E-05
3-ketoacyl-CoA thiolase, mitochondrial	*ACAA2*	1.2126007	-0.8759514	-0.8970376	-2.1096383	5.97E-06
Acetyl-CoA carboxylase 2	*ACACB*	0.7338424	-3.8071660	-3.7810083	-4.5148508	2.57E-04
Medium-chain specific acyl-CoA dehydrogenase, mitochondrial	*ACADM*	0.4431139	-1.9845473	-1.0688760	-1.5119899	5.06E-05
Short-chain specific acyl-CoA dehydrogenase, mitochondrial	*ACADS*	1.0767380	-2.8929050	-2.5096593	-3.5863973	1.53E-06
Short/branched chain specific acyl-CoA dehydrogenase, mitochondrial	*ACADSB*	-1.6947300	0.2020742	0.4542427	2.1489727	5.96E-07
Cytoplasmic aconitate hydratase	*ACO1*	1.3932007	-0.1895427	-0.4186160	-1.8118166	5.34E-06
Acyl-coenzyme A thioesterase 1	*ACOT1*	1.8227813	-0.9926797	-0.0416841	-1.8644654	8.08E-06
Long-chain-fatty-acid--CoA ligase 1	*ACSL1*	3.5535703	-2.4078817	-2.4161427	-5.9697130	2.22E-06
Alcohol dehydrogenase class-3	*ADH5*	0.4225043	-1.5999213	-1.2975120	-1.7200163	3.39E-04
Afamin	*AFM*	0.8952869	-1.0592358	-1.6163593	-2.5116462	4.64E-05
Glycogen debranching enzyme	*AGL*	-1.0734283	0.1243061	0.6580078	1.7314361	7.25E-05
Anterior gradient protein 2 homolog	*AGR2*	-2.1493340	1.1504133	1.0164388	3.1657728	6.05E-06
Angiotensinogen	*AGT*	1.4353320	-0.1362981	-0.9917328	-2.4270648	2.63E-07
Adenosylhomocysteinase	*AHCY*	0.7595325	1.9245487	2.6084760	1.8489435	8.14E-07
Alpha-2-HS-glycoprotein	*AHSG*	1.1837283	-1.4219687	-3.9871997	-5.1709280	4.35E-07
Adenylate kinase 4, mitochondrial	*AK4*	0.3136558	-2.2435447	-3.2467423	-3.5603982	8.26E-04
Retinal dehydrogenase 1	*ALDH1A1*	1.9274803	0.3203192	0.1417759	-1.7857045	8.89E-08
Aldehyde dehydrogenase, mitochondrial	*ALDH2*	3.6553033	1.5341523	0.9642648	-2.6910386	4.99E-07
Methylmalonate-semialdehyde dehydrogenase [acylating], mitochondrial	*ALDH6A1*	0.1925467	-2.4772083	-2.3352423	-2.5277890	2.46E-04
Fructose-bisphosphate aldolase A	*ALDOA*	2.8319037	4.5608420	4.3894570	1.5575533	6.19E-06
Fructose-bisphosphate aldolase C	*ALDOC*	1.6203663	0.7722053	0.0887736	-1.5315927	1.50E-02
Annexin	*ANXA3*	0.1417565	-2.6746723	-2.6454050	-2.7871615	2.46E-04
Serum amyloid P-component	*APCS*	2.7792383	1.6724900	0.5471532	-2.2320852	1.48E-06
Adipocyte plasma membrane-associated protein	*APMAP*	1.3387423	0.0458863	-0.2868333	-1.6255757	6.69E-07
Apolipoprotein A-IV	*APOA4*	2.7655473	1.4480713	0.7250784	-2.0404690	2.48E-06
Apolipoprotein B-100	*APOB*	3.1646123	1.3936213	0.1566994	-3.0079130	1.65E-07
Apolipoprotein D	*APOD*	1.0605273	-0.9833878	-2.1299883	-3.1905156	1.42E-05
Apolipoprotein E	*APOE*	0.8823448	-0.7091507	-0.9789607	-1.8613054	1.12E-04
Adenine phosphoribosyltransferase	*APRT*	-1.8936040	-0.3705823	0.0112587	1.9048627	1.73E-06
Coatomer subunit delta	*ARCN1*	-2.2692520	-0.3386296	-0.1877606	2.0814914	2.51E-04
Aspartyl/asparaginyl beta-hydroxylase	*ASPH*	0.8701228	-0.6634710	-1.7129200	-2.5830428	7.73E-05
Asporin	*ASPN*	3.6409490	2.6202163	0.4874282	-3.1535208	2.14E-07
Argininosuccinate synthase	*ASS1*	0.5685268	-4.5490250	-4.9874080	-5.5559348	3.82E-07
Flavin reductase (NADPH)	*BLVRB*	2.4901637	0.3637450	0.3085455	-2.1816182	5.31E-07
Bisphosphoglycerate mutase	*BPGM*	1.0392277	-4.1535947	-4.4147870	-5.4540147	2.52E-08
UPF0568 protein C14orf166	*C14orf166*	-2.0991320	-0.9155474	-0.4953515	1.6037805	2.21E-04
Complement C1s subcomponent	*C1S*	-1.2571243	-3.0649203	-3.3102920	-2.0531677	1.90E-04
Complement C3	*C3*	5.2649933	4.5292250	3.6872240	-1.5777693	7.79E-06
Complement C5	*C5*	0.5269080	-2.2443813	-3.1069373	-3.6338454	1.94E-05
Complement component C6	*C6*	-0.6588544	-2.1334507	-3.3053780	-2.6465236	4.31E-07
Complement component C9	*C9*	1.2341440	-0.2493353	-0.9993612	-2.2335052	1.10E-05
Carbonic anhydrase 1	*CA1*	5.0484013	1.7323927	1.7200447	-3.3283567	1.22E-07
Calcyclin-binding protein	*CACYBP*	-1.0595199	1.2460227	1.5421263	2.6016462	1.09E-07
Calretinin	*CALB2*	0.6328267	-4.4251017	-4.8766890	-5.5095157	9.60E-06
Calreticulin	*CALR*	-0.2688514	0.1177904	1.7524807	2.0213320	5.77E-05
Calnexin	*CANX*	1.0715330	2.5514337	2.9264737	1.8549407	2.55E-06
Macrophage-capping protein	*CAPG*	-0.7205810	1.4329627	1.6238497	2.3444307	6.80E-08
Catalase	*CAT*	3.6990990	1.5582150	1.5014370	-2.1976620	2.46E-07
Caveolin-1	*CAV1*	2.2061240	-1.8565800	-1.9754650	-4.1815890	4.11E-06
Chromobox protein homolog 3	*CBX3*	-2.2486123	-0.2630711	0.2724186	2.5210310	1.19E-04
Platelet glycoprotein 4	*CD36*	3.3263533	-3.9301403	-3.6374753	-6.9638287	5.27E-08
Liver carboxylesterase 1	*CES1*	1.9946800	-1.2855133	-1.8147657	-3.8094457	3.14E-06
Complement factor B	*CFB*	1.9763533	0.8268206	-0.1684094	-2.1447627	5.24E-06
Complement factor H	*CFH*	1.8955007	0.2189654	-1.3321097	-3.2276103	4.35E-06
Creatine kinase B-type	*CKB*	1.2992493	-1.6373653	-1.7730723	-3.0723217	1.57E-05
Tetranectin	*CLEC3B*	0.6369099	-1.1833993	-1.7043250	-2.3412349	5.86E-05
Clathrin heavy chain	*CLTC*	2.6070680	3.9075547	4.1145447	1.5074767	1.82E-05
Clusterin	*CLU*	2.0608607	0.7904709	0.3131736	-1.7476870	1.07E-06
Chymase	*CMA1*	1.0482315	-0.2227559	-4.4852713	-5.5335028	4.19E-05
Cytosolic non-specific dipeptidase	*CNDP2*	0.8006636	1.7934180	2.5795567	1.7788931	1.55E-05
Calponin-1	*CNN1*	2.3537830	-0.0842368	-2.7270870	-5.0808700	8.57E-06
Bifunctional coenzyme A synthase	*COASY*	-2.8185743	-2.0145877	-0.9186964	1.8998780	3.05E-05
Collagen alpha-1(XIV) chain	*COL14A1*	3.7212867	3.8950080	1.7020303	-2.0192563	2.88E-06
Collagen alpha-1(XVIII) chain	*COL18A1*	0.8184561	-1.4648080	-2.5464623	-3.3649185	4.24E-08
Collagen alpha-1(I) chain	*COL1A1*	3.0087797	1.8647033	0.4143621	-2.5944175	2.25E-04
Collagen alpha-2(I) chain	*COL1A2*	3.5030327	2.1406623	0.8211111	-2.6819215	1.05E-06
Coatomer subunit beta	*COPB1*	-0.9750658	0.8972917	1.1246312	2.0996970	4.49E-06
Coatomer subunit gamma-1	*COPG1*	-1.4862567	0.6920393	0.8275461	2.3138027	1.40E-05
Ceruloplasmin	*CP*	3.1347433	1.9950077	1.3085823	-1.8261610	2.18E-06
Mast cell carboxypeptidase A	*CPA3*	1.9123297	0.3349454	-3.2596213	-5.1719510	2.90E-08
Cellular retinoic acid-binding protein 2	*CRABP2*	-1.4783579	1.4131590	0.2526711	1.7310290	1.75E-03
Alpha-crystallin B chain	*CRYAB*	2.5614527	-3.3988933	-3.3539940	-5.9154467	3.25E-07
Exportin-2	*CSE1L*	0.9154469	2.7027383	3.1499850	2.2345381	4.46E-06
Cysteine and glycine-rich protein 1	*CSRP1*	2.0080707	0.7678872	-0.3463881	-2.3544588	1.61E-06
Cystatin-A	*CSTA*	0.0319675	-3.3105913	-3.3851313	-3.4170989	2.34E-04
Catenin alpha-1	*CTNNA1*	-0.9253745	0.2301681	0.6066630	1.5320375	3.52E-04
Cathepsin D	*CTSD*	1.3821547	3.0030003	3.0945833	1.7124287	2.78E-06
Cathepsin G	*CTSG*	0.7955871	-0.5105142	-3.6005320	-4.3961191	1.15E-06
NADH-cytochrome b5 reductase 1	*CYB5R1*	-0.2302495	1.4041737	2.1158053	2.3460549	2.82E-08
Serine/threonine-protein kinase DCLK1	*DCLK1*	-2.9947040	-4.0922457	-4.7423000	-1.7475960	3.84E-04
Decorin	*DCN*	4.8486867	3.5614410	2.6302323	-2.2184543	1.56E-07
ATP-dependent RNA helicase DDX1	*DDX1*	-1.3784413	-0.1390039	0.3506143	1.7290556	1.98E-05
Probable ATP-dependent RNA helicase DDX17	*DDX17*	-0.7879003	1.1928513	1.4025917	2.1904920	2.08E-03
Spliceosome RNA helicase DDX39B	*DDX39B*	0.3976174	1.9550333	2.2676980	1.8700806	4.92E-07
Probable ATP-dependent RNA helicase DDX5	*DDX5*	-2.3036203	-0.1424269	0.4547050	2.7583254	5.14E-04
Dehydrogenase/reductase SDR family member 2, mitochondrial	*DHRS2*	-2.7286467	-1.1462392	1.6986643	4.4273110	1.28E-05
Pre-mRNA-splicing factor ATP-dependent RNA helicase DHX15	*DHX15*	-1.6480853	0.0144729	0.1670410	1.8151263	2.62E-04
ATP-dependent RNA helicase A	*DHX9*	0.2749934	1.6877340	1.9167817	1.6417883	2.11E-06
Dipeptidyl peptidase 3	*DPP3*	-1.2254843	0.3189383	0.6762967	1.9017810	1.47E-05
Desmoplakin	*DSP*	-2.3338403	0.2623712	0.9284350	3.2622753	3.44E-04
Enoyl-CoA hydratase, mitochondrial	*ECHS1*	1.9859820	0.0975179	0.2647617	-1.7212203	5.13E-05
Enoyl-CoA delta isomerase 1, mitochondrial	*ECI1*	-1.5809470	0.2387506	0.3378895	1.9188365	4.40E-05
Elongation factor 1-delta	*EEF1D*	0.2985854	1.8765270	2.3384050	2.0398196	1.03E-05
Elongation factor 2	*EEF2*	1.5947733	3.0433267	3.4179193	1.8231460	9.34E-08

EF-hand domain-containing protein D1	*EFHD1*	-1.6094537	0.5110793	1.0038935	2.6133471	1.05E-05
116 kDa U5 small nuclear ribonucleoprotein component	*EFTUD2*	-1.6382360	0.2546635	0.0453934	1.6836294	5.81E-04
EH domain-containing protein 2	*EHD2*	4.3360300	1.4223067	1.2142683	-3.1217617	9.59E-08
Interferon-induced, double-stranded RNA-activated protein kinase	*EIF2AK2*	-2.9656090	-1.8214030	-0.7334209	2.2321881	1.20E-02
Eukaryotic initiation factor 4A-I	*EIF4A1*	1.2708190	2.7644347	2.9490293	1.6782103	1.07E-07
Eukaryotic initiation factor 4A-III	*EIF4A3*	-1.9221903	-0.4312542	-0.3426216	1.5795688	3.98E-07
Enolase-phosphatase E1	*ENOPH1*	-2.4804280	-2.2957047	-0.8616077	1.6188203	2.26E-04
Epoxide hydrolase 1	*EPHX1*	2.9077487	1.6366227	0.7861162	-2.1216325	2.50E-06
Bifunctional glutamate/proline--tRNA ligase	*EPRS*	-1.0628956	-0.1484165	0.6262989	1.6891944	1.43E-05
Extended synaptotagmin-2	*ESYT2*	-2.8909207	-3.7151707	-4.5662280	-1.6753073	1.19E-03
Ezrin	*EZR*	-2.1635423	-0.0784337	0.6321236	2.7956659	7.20E-03
Coagulation factor XIII A chain	*F13A1*	1.4560487	0.6840134	-0.6326940	-2.0887426	4.54E-06
Prothrombin	*F2*	0.8241362	-1.3181690	-1.6661803	-2.4903165	4.02E-08
Fatty acid-binding protein, adipocyte	*FABP4*	4.4484050	-1.4500540	-1.6526987	-6.1011037	2.84E-07
Fumarylacetoacetase	*FAH*	1.3862380	-1.7393243	-2.1171123	-3.5033503	1.01E-05
Redox-regulatory protein FAM213A	*FAM213A*	1.5101690	-2.4306023	-1.6722683	-3.1824373	8.36E-06
Fatty acid synthase	*FASN*	5.0826363	7.0661360	8.2689500	3.1863137	8.32E-08
rRNA 2-O-methyltransferase fibrillarin	*FBL*	-1.0719948	1.0999787	0.8972601	1.9692548	8.03E-06
Fibulin-1	*FBLN1*	1.1759973	0.9667974	-0.3747738	-1.5507711	2.57E-06
Fibulin-2	*FBLN2*	0.7208974	-0.4981521	-1.3367960	-2.0576934	7.06E-04
Fibrillin-1	*FBN1*	3.1728610	0.9808016	0.1688750	-3.0039860	3.59E-05
Fibrinogen alpha chain	*FGA*	4.0661410	2.9448403	1.8006327	-2.2655083	6.45E-07
Fibrinogen beta chain	*FGB*	4.5555717	3.3821560	2.3081323	-2.2474393	4.95E-06
Fibrinogen gamma chain	*FGG*	4.8084983	3.2971623	2.4295367	-2.3789617	5.40E-07
Peptidyl-prolyl cis-trans isomerase FKBP4	*FKBP4*	0.0301403	3.1528810	4.0059153	3.9757751	3.46E-10
FAD synthase	*FLAD1*	-4.9817337	-3.7019430	-3.2854337	1.6963000	1.84E-06
Fibromodulin	*FMOD*	0.7103321	-2.1584037	-4.1646490	-4.8749811	1.78E-05
Ferritin light chain	*FTL*	1.3827163	2.8084113	2.9146460	1.5319297	1.35E-04
Glyceraldehyde-3-phosphate dehydrogenase	*GAPDH*	3.4777627	5.5607660	5.5526563	2.0748937	1.56E-05
Vitamin D-binding protein	*GC*	3.0011143	1.7854110	1.0064824	-1.9946319	2.91E-07
Rab GDP dissociation inhibitor alpha	*GDI1*	-1.1212111	0.6636495	0.6986414	1.8198525	1.59E-04
Glutamine synthetase	*GLUL*	-1.2067269	1.8060883	2.0884707	3.2951976	4.64E-06
Aspartate aminotransferase, mitochondrial	*GOT2*	-1.1020920	1.9629203	2.6585913	3.7606833	1.24E-06
Glycerol-3-phosphate dehydrogenase [NAD(+)], cytoplasmic	*GPD1*	4.2764917	-3.6608193	-3.2918613	-7.5683530	2.36E-05
Glycerol-3-phosphate dehydrogenase, mitochondrial	*GPD2*	-1.4380853	0.0916795	0.6422904	2.0803757	7.14E-07
Glutathione peroxidase	*GPX3*	0.3461173	-1.4207953	-1.4884887	-1.8346060	8.68E-07
Glutathione S-transferase kappa 1	*GSTK1*	-0.5620499	0.7988486	1.2228270	1.7848769	5.66E-07
Glutathione S-transferase Mu 3	*GSTM3*	-0.1602034	0.5658280	1.4626577	1.6228611	1.45E-04
Histone H1x	*H1FX*	-1.8169457	-0.3185082	0.3641945	2.1811402	6.09E-05
Core histone macro-H2A.1	*H2AFY*	0.7714439	2.6675703	2.9392450	2.1678011	6.84E-06
Hydroxyacyl-coenzyme A dehydrogenase, mitochondrial	*HADH*	1.5491393	-0.7814278	-0.8059173	-2.3550567	2.56E-07
Hemoglobin subunit beta	*HBB*	7.3421510	5.8681990	5.6443413	-1.6978097	1.20E-04
Hemoglobin subunit delta	*HBD*	4.0725790	0.6781733	0.4969436	-3.5756354	4.39E-07
Vigilin	*HDLBP*	-0.5044771	1.1434737	1.2118820	1.7163591	1.68E-06
Histone H4	*HIST1H4A*	4.3948587	5.7921527	5.9873630	1.5925043	4.32E-05
High mobility group protein B1	*HMGB1*	0.8855839	1.7278053	2.4397173	1.5541334	1.13E-03
Heterogeneous nuclear ribonucleoproteins A2/B1	*HNRNPA2B1*	1.7605333	3.6289653	4.0309877	2.2704543	2.21E-06
Heterogeneous nuclear ribonucleoprotein A/B	*HNRNPAB*	-2.0177573	-0.0617685	0.6042863	2.6220437	7.64E-07
Heterogeneous nuclear ribonucleoprotein D0	*HNRNPD*	-0.4755342	1.1953253	1.6321957	2.1077299	6.21E-06
Heterogeneous nuclear ribonucleoprotein K	*HNRNPK*	1.2136603	2.7244627	3.1825223	1.9688620	8.03E-09
Heterogeneous nuclear ribonucleoprotein L	*HNRNPL*	-2.2216857	-0.0321108	0.6497111	2.8713967	9.81E-03
Heterogeneous nuclear ribonucleoprotein M	*HNRNPM*	-0.0239437	1.7428893	2.1221297	2.1460734	3.55E-07
Heterogeneous nuclear ribonucleoprotein R	*HNRNPR*	-1.0985707	0.7116732	0.9358230	2.0343936	6.04E-08
Heterogeneous nuclear ribonucleoprotein U	*HNRNPU*	0.9575924	2.5463023	2.7393133	1.7817210	1.34E-05
Haptoglobin	*HP*	2.5337403	0.5639262	-0.3585478	-2.8922881	6.22E-05
Histidine-rich glycoprotein	*HRG*	2.2502317	0.6468936	0.0558019	-2.1944298	1.39E-07
Heat shock protein HSP 90-alpha	*HSP90AA1*	3.2094073	5.3976947	6.1425633	2.9331560	3.26E-06
Heat shock protein HSP 90-beta	*HSP90AB1*	2.2351950	4.4684907	5.1208630	2.8856680	2.57E-07
Endoplasmin	*HSP90B1*	2.5370460	3.8509590	4.9261723	2.3891263	2.26E-07
Heat shock 70 kDa protein 12A	*HSPA12A*	0.3873327	-3.8717680	-3.9579950	-4.3453277	5.67E-05
78 kDa glucose-regulated protein	*HSPA5*	2.5182010	4.1380207	4.8826983	2.3644973	1.80E-08
Heat shock cognate 71 kDa protein	*HSPA8*	3.5477120	5.2105167	5.7344953	2.1867833	3.01E-07
Stress-70 protein, mitochondrial	*HSPA9*	1.3598197	3.5989777	4.4451777	3.0853580	3.73E-08
Heat shock protein beta-1	*HSPB1*	2.9880967	4.6570270	5.1938677	2.2057710	2.16E-06
60 kDa heat shock protein, mitochondrial	*HSPD1*	2.2467923	4.3676670	5.0749280	2.8281357	4.36E-07
Basement membrane-specific heparan sulfate proteoglycan core protein	*HSPG2*	3.9165427	1.4271983	0.4487202	-3.4678224	2.95E-07
Heat shock protein 105 kDa	*HSPH1*	-2.6217060	0.4290357	0.7817440	3.4034500	1.14E-06
Isoleucine--tRNA ligase, mitochondrial	*IARS2*	0.0064470	1.3574680	2.4591200	2.4526730	3.54E-06
Insulin-like growth factor-binding protein complex acid labile subunit	*IGFALS*	-1.8545510	-3.4785157	-4.2654313	-2.4108803	5.87E-05
Ig alpha-1 chain C region	*IGHA1*	2.5991383	1.2397130	0.6339710	-1.9651674	5.87E-05
Ig gamma-4 chain C region	*IGHG4*	2.8548947	1.3669913	0.4825800	-2.3723147	1.11E-05
Ig kappa chain V-III region B6	*IGKV3D-20*	2.3963610	0.8633132	0.7732396	-1.6231214	6.33E-05
Interleukin enhancer-binding factor 2	*ILF2*	-0.0555838	1.6222750	1.7104603	1.7660441	6.24E-05
Interleukin enhancer-binding factor 3	*ILF3*	-0.7597621	0.8074046	0.9704017	1.7301639	4.65E-05
Integrin-linked protein kinase	*ILK*	-0.5639402	-2.4022983	-3.1418680	-2.5779278	7.20E-06
Isochorismatase domain-containing protein 2, mitochondrial	*ISOC2*	-2.2669983	-1.4646797	-0.7093096	1.5576888	6.82E-05
Inter-alpha-trypsin inhibitor heavy chain H4	*ITIH4*	2.3430227	0.7080326	-0.1934134	-2.5364361	7.94E-07
KH domain-containing, RNA-binding, signal transduction-associated protein 1	*KHDRBS1*	-2.9218337	-1.3215500	-0.9232728	1.9985609	1.64E-03
Kininogen-1	*KNG1*	2.2145587	0.5840359	-0.3921195	-2.6066782	2.87E-07
Keratin, type I cytoskeletal 18	*KRT18*	-1.9252607	2.4560843	2.8070383	4.7322990	7.92E-06
Laminin subunit gamma-1	*LAMC1*	2.8354123	-0.4616382	-1.9304633	-4.7658757	8.64E-06
Cytosol aminopeptidase	*LAP3*	1.0698197	2.4773100	3.1975617	2.1277420	4.18E-07
Lipopolysaccharide-binding protein	*LBP*	-2.1570057	-3.8189177	-4.1527883	-1.9957827	1.28E-04
Plastin-2	*LCP1*	1.5234320	2.4689050	3.4928377	1.9694057	3.68E-07
Galectin-3-binding protein	*LGALS3BP*	0.2368129	1.1087717	1.8695143	1.6327014	4.03E-06
Vesicular integral-membrane protein VIP36	*LMAN2*	-2.4149723	-0.7556293	-0.7201728	1.6947996	4.38E-04
Lamin-B1	*LMNB1*	-1.0285581	0.7844137	0.9895798	2.0181379	6.51E-05
Leucine-rich alpha-2-glycoprotein	*LRG1*	-0.4563952	-2.7778193	-3.7323277	-3.2759325	4.42E-04
Prolow-density lipoprotein receptor-related protein 1	*LRP1*	-0.9453462	-2.5692600	-3.5181093	-2.5727631	6.13E-05
Leucine-rich PPR motif-containing protein, mitochondrial	*LRPPRC*	0.3761265	1.8887000	2.5998440	2.2237175	1.87E-10
Leucine-rich repeat-containing protein 59	*LRRC59*	-1.9319187	1.2951047	1.4036853	3.3356040	6.57E-08
Lactotransferrin	*LTF*	2.3577610	-3.6758813	-5.4587493	-7.8165103	3.20E-07
Amine oxidase [flavin-containing] A	*MAOA*	1.9006087	-3.1676973	-3.0711047	-4.9717133	1.85E-07
S-adenosylmethionine synthase isoform type-2	*MAT2A*	-2.3361977	-1.0381262	-0.5495186	1.7866791	2.43E-03
Cell surface glycoprotein MUC18	*MCAM*	1.8194020	-3.9520980	-4.5273920	-6.3467940	3.32E-06
Malate dehydrogenase, mitochondrial	*MDH2*	2.1562147	3.7563140	3.7478497	1.5916350	5.20E-06
NADP-dependent malic enzyme	*ME1*	-0.2062243	-1.7249193	-1.9242437	-1.7180194	1.01E-05
Myosin-11	*MYH11*	3.4639690	1.9041430	-0.0918209	-3.5557899	1.29E-07
Myosin-9	*MYH9*	3.9996453	5.8962480	5.5983707	1.5987253	4.16E-07
Myosin regulatory light polypeptide 9	*MYL9*	0.0794047	-0.8459453	-1.7678003	-1.8472050	1.10E-05
Unconventional myosin-Ic	*MYO1C*	3.3706340	1.2130073	0.8485442	-2.5220898	3.90E-08
Nucleosome assembly protein 1-like 1	*NAP1L1*	-0.3429001	0.3843581	1.1645023	1.5074025	5.96E-06
Nucleolin	*NCL*	1.4314730	2.8661377	3.4304103	1.9989373	2.22E-07
Nidogen-2	*NID2*	2.3346410	-1.9316263	-2.7234867	-5.0581277	1.17E-06
Non-POU domain-containing octamer-binding protein	*NONO*	-1.3829817	0.3357859	0.3498126	1.7327943	8.54E-06

Nucleophosmin	*NPM1*	-1.1842370	1.0085388	1.3060003	2.4902373	4.53E-06
Nuclear mitotic apparatus protein 1	*NUMA1*	-1.4829060	0.1777351	0.5041392	1.9870452	5.85E-06
Mimecan	*OGN*	5.0148173	2.9126657	0.7526218	-4.2621955	1.43E-06
Alpha-1-acid glycoprotein 1	*ORM1*	3.2233620	1.1875423	0.8735183	-2.3498437	1.46E-04
Protein disulfide-isomerase	*P4HB*	2.3650857	4.0195913	4.0523197	1.6872340	1.59E-06
Poly [ADP-ribose] polymerase 1	*PARP1*	-0.3357313	2.1042050	2.6796830	3.0154143	6.65E-06
Alpha-parvin	*PARVA*	0.8488112	-1.3354060	-1.7642977	-2.6131089	9.40E-07
Poly(rC)-binding protein 1	*PCBP1*	-0.6967981	0.8153081	0.9208423	1.6176404	2.25E-06
Prenylcysteine oxidase 1	*PCYOX1*	1.7375093	0.1071543	-0.6671643	-2.4046737	7.10E-07
Pyruvate dehydrogenase E1 component subunit alpha, somatic form, mitochondrial	*PDHA1*	-0.2887027	-2.3811380	-2.1679630	-1.8792603	9.57E-06
Protein disulfide-isomerase A4	*PDIA4*	0.4770922	1.5657033	2.1348343	1.6577421	8.53E-06
Protein disulfide-isomerase A6	*PDIA6*	0.8222368	1.9122597	2.6144353	1.7921985	4.62E-07
Phosphatidylethanolamine-binding protein 1	*PEBP1*	1.9675840	2.0091243	3.7814273	1.8138433	1.79E-05
Phosphoglycerate kinase 1	*PGK1*	2.8897760	4.2675260	4.7255307	1.8357547	9.44E-07
Phosphoglucomutase-1	*PGM1*	1.7556270	0.1861590	0.0037989	-1.7518281	7.01E-05
Prohibitin	*PHB*	1.2827237	2.8464847	3.0430003	1.7602767	9.47E-07
Prohibitin-2	*PHB2*	1.1991573	2.5578237	3.1636283	1.9644710	3.64E-06
D-3-phosphoglycerate dehydrogenase	*PHGDH*	1.9677730	-0.8964086	-1.5676000	-3.5353730	7.46E-08
Pyruvate kinase PKM	*PKM*	2.9453197	5.0939760	4.9224767	1.9771570	1.63E-07
Plasminogen	*PLG*	1.9107620	-0.4885471	-1.9213373	-3.8320993	3.06E-05
Perilipin-1	*PLIN1*	4.4658663	-2.8981620	-2.4432707	-6.9091370	1.49E-10
Perilipin-4	*PLIN4*	3.6373500	-5.2591970	-5.7818400	-9.4191900	1.50E-07
Purine nucleoside phosphorylase	*PNP*	1.3906413	1.7132573	3.3443510	1.9537097	1.07E-07
Serum paraoxonase/arylesterase 1	*PON1*	0.6889262	-1.6059207	-3.2990087	-3.9879349	1.87E-07
Periostin	*POSTN*	2.6870187	6.3961687	6.6599243	3.9729057	1.29E-08
Peptidyl-prolyl cis-trans isomerase A	*PPIA*	2.9611043	4.3351983	4.5304333	1.5693290	3.18E-05
Peroxiredoxin-1	*PRDX1*	2.6854833	4.1870063	4.4239050	1.7384217	9.18E-07
Peroxiredoxin-2	*PRDX2*	3.9749357	2.1224147	2.2231710	-1.7517647	3.80E-06
Peroxiredoxin-4	*PRDX4*	-0.5980512	0.2998963	1.5357240	2.1337752	1.22E-05
cAMP-dependent protein kinase type II-alpha regulatory subunit	*PRKAR2A*	2.1198833	-0.1883300	-0.5625874	-2.6824707	1.65E-02
cAMP-dependent protein kinase type II-beta regulatory subunit	*PRKAR2B*	0.8785261	-1.4200583	-1.0323052	-1.9108313	9.31E-07
Protein kinase C delta-binding protein	*PRKCDBP*	0.4444214	-1.5608829	-2.9268233	-3.3712447	8.29E-03
DNA-dependent protein kinase catalytic subunit	*PRKDC*	-0.1922308	1.5010980	1.9272350	2.1194658	1.03E-04
Pre-mRNA-processing-splicing factor 8	*PRPF8*	-1.8676823	-0.2931586	-0.2698282	1.5978541	3.78E-06
Proteasome activator complex subunit 1	*PSME1*	0.4624360	2.3758780	2.9382990	2.4758630	3.27E-07
Proteasome activator complex subunit 2	*PSME2*	-0.9477663	0.7647163	1.1228200	2.0705863	4.25E-05
Polypyrimidine tract-binding protein 1	*PTBP1*	-0.8922164	1.3676657	1.6057640	2.4979804	2.40E-07
Prostacyclin synthase	*PTGIS*	-0.6167912	-4.2204283	-3.8417507	-3.2249594	1.48E-08
Tyrosine-protein phosphatase non-receptor type 6	*PTPN6*	-3.6313583	-2.8912200	-1.7327293	1.8986290	5.07E-03
Polymerase I and transcript release factor	*PTRF*	3.8444997	0.8654688	0.3079422	-3.5365574	2.45E-07
RNA-binding motif protein, X chromosome	*RBMX*	-1.5038313	0.2184772	0.1336368	1.6374681	1.68E-04
Retinol-binding protein 4	*RBP4*	-1.8032583	-4.7504700	-5.3912900	-3.5880317	7.58E-04
All-trans-retinol 13,14-reductase	*RETSAT*	-0.0800044	-3.0120643	-3.2020107	-3.1220063	1.44E-05
Aminopeptidase B	*RNPEP*	-1.4811417	0.5614425	1.6734340	3.1545757	3.98E-05
60S ribosomal protein L13	*RPL13*	-1.6845143	-0.0528309	0.7723319	2.4568463	2.54E-05
60S ribosomal protein L18	*RPL18*	-1.7991850	0.6932418	1.0534560	2.8526410	5.01E-05
60S ribosomal protein L4	*RPL4*	-0.7082869	1.9934340	2.0225383	2.7308252	2.82E-07
60S ribosomal protein L6	*RPL6*	-2.1259993	1.2613530	0.6110520	2.7370513	8.39E-06
60S ribosomal protein L7a	*RPL7A*	-0.7041110	1.2934230	0.8959760	1.6000870	2.36E-02
60S acidic ribosomal protein P2	*RPLP2*	-2.5937597	-1.7710817	-0.7285389	1.8652207	1.52E-02
40S ribosomal protein S3	*RPS3*	1.0426571	2.1522660	2.5578900	1.5152329	4.78E-05
40S ribosomal protein S9	*RPS9*	0.1508045	1.8094203	1.9852447	1.8344401	5.55E-06
40S ribosomal protein SA	*RPSA*	0.9463625	2.0585003	2.4535193	1.5071568	2.54E-05
Ribosome-binding protein 1	*RRBP1*	-1.5699190	0.3034175	1.2376140	2.8075330	1.41E-04
tRNA-splicing ligase RtcB homolog	*RTCB*	-1.2926379	0.2524910	0.5821734	1.8748113	1.29E-03
RuvB-like 1	*RUVBL1*	-0.4877091	0.6553021	1.1275814	1.6152905	5.43E-06
RuvB-like 2	*RUVBL2*	-1.7025903	0.4850787	0.9080327	2.6106230	4.56E-06
Serine--tRNA ligase, cytoplasmic	*SARS*	-1.5758433	-0.5031437	0.1957050	1.7715483	2.65E-04
Selenium-binding protein 1	*SELENBP1*	3.0458987	1.1403703	0.8429760	-2.2029227	1.28E-09
Septin-11	*SEPT11*	0.4978885	-0.3703101	-1.4990330	-1.9969215	8.04E-08
Kallistatin	*SERPINA4*	-1.5138171	-2.3113487	-3.1260533	-1.6122363	7.71E-03
Antithrombin-III	*SERPINC1*	3.4851947	2.2512810	1.4771137	-2.0080810	9.71E-07
Heparin cofactor 2	*SERPIND1*	1.7437940	-0.8024925	-1.5065330	-3.2503270	5.39E-08
Alpha-2-antiplasmin	*SERPINF2*	0.4204954	-2.2801463	-2.6577387	-3.0782341	1.11E-03
Plasma protease C1 inhibitor	*SERPING1*	2.4908853	1.4855670	0.6460976	-1.8447878	9.22E-09
Splicing factor, proline- and glutamine-rich	*SFPQ*	0.3919084	1.8632970	1.9539293	1.5620210	9.25E-05
Tricarboxylate transport protein, mitochondrial	*SLC25A1*	0.9369314	-0.7724900	-0.8358796	-1.7728109	3.68E-05
Calcium-binding mitochondrial carrier protein Aralar2	*SLC25A13*	-2.0580797	-0.8480613	-0.5395969	1.5184828	2.31E-05
Band 3 anion transport protein	*SLC4A1*	3.5527103	-1.7119653	-3.0736140	-6.6263243	5.09E-07
Na(+)/H(+) exchange regulatory cofactor NHE-RF1	*SLC9A3R1*	-2.8017610	0.4770815	1.0017050	3.8034660	8.36E-06
Staphylococcal nuclease domain-containing protein 1	*SND1*	0.4449238	1.6319617	1.9940170	1.5490932	4.10E-08
U5 small nuclear ribonucleoprotein 200 kDa helicase	*SNRNP200*	-2.3850117	-0.4099193	-0.0058725	2.3791392	1.57E-04
Sorbin and SH3 domain-containing protein 1	*SORBS1*	1.1216563	-3.3355603	-4.0978617	-5.2195180	9.33E-06
Sorbitol dehydrogenase	*SORD*	-1.4567897	2.1198560	1.3943383	2.8511280	2.76E-07
Spectrin beta chain, non-erythrocytic 1	*SPTBN1*	2.9909930	1.4153563	1.4726063	-1.5183867	1.72E-06
Serine/arginine-rich splicing factor 2	*SRSF2*	-2.0184907	-0.2075286	-0.3943808	1.6241099	3.80E-04
Serine/arginine-rich splicing factor 3	*SRSF3*	-1.9598023	0.1341418	0.3934567	2.3532590	3.90E-05
Serine/arginine-rich splicing factor 6	*SRSF6*	-1.7538633	-0.2337762	0.0058671	1.7597304	1.43E-02
Serine/arginine-rich splicing factor 7	*SRSF7*	-1.9796933	-0.4399577	-0.2968736	1.6828197	1.43E-03
Signal transducer and activator of transcription 1-alpha/beta	*STAT1*	-1.6160443	1.9952440	2.7418497	4.3578940	1.49E-06
Stress-induced-phosphoprotein 1	*STIP1*	0.0166503	1.4710463	1.6140840	1.5974337	1.41E-05
Heterogeneous nuclear ribonucleoprotein Q	*SYNCRIP*	0.0641388	1.8336157	2.2366500	2.1725112	1.16E-06
Thrombospondin-1	*THBS1*	0.7645540	3.1333877	2.2862923	1.5217383	3.12E-07
Tensin-1	*TNS1*	1.5678333	-1.8430547	-2.3623550	-3.9301883	4.31E-08
Tenascin-X	*TNXB*	1.3189193	-3.6676183	-4.6270300	-5.9459493	8.76E-07
Tropomyosin alpha-1 chain	*TPM1*	1.4227127	0.1711272	-1.0312409	-2.4539535	8.46E-05
Heat shock protein 75 kDa, mitochondrial	*TRAP1*	-2.5908477	-0.9482618	-0.5965958	1.9942519	3.99E-02
Tubulin--tyrosine ligase-like protein 12	*TTLL12*	-1.1334033	1.1320159	2.8058883	3.9392917	5.08E-09
Tubulin beta chain	*TUBB*	2.1899840	3.8437230	4.1848083	1.9948243	3.64E-05
Tubulin beta-4B chain	*TUBB4B*	3.5756913	5.2203887	5.4828243	1.9071330	3.52E-06
Tubulin beta-6 chain	*TUBB6*	-0.2264949	-1.4930803	-2.7634250	-2.5369301	9.27E-08
Thioredoxin domain-containing protein 5	*TXNDC5*	-1.5931980	-0.7872303	1.4591420	3.0523400	2.88E-06
Thymidine phosphorylase	*TYMP*	-1.3742422	1.9053313	1.9692480	3.3434902	5.10E-05
Splicing factor U2AF 65 kDa subunit	*U2AF2*	-2.9282993	-0.2138218	-0.2659393	2.6623600	4.00E-04
UDP-glucose 6-dehydrogenase	*UGDH*	-0.2995797	1.5472870	1.7180830	2.0176627	6.22E-05
UTP--glucose-1-phosphate uridylyltransferase	*UGP2*	2.4714373	0.8641431	0.7376516	-1.7337857	1.08E-07
Ubiquitin carboxyl-terminal hydrolase 5	*USP5*	-0.0851312	1.2517267	1.9548707	2.0400018	9.59E-06
Valine--tRNA ligase	*VARS*	-1.6652060	0.1033561	1.1201845	2.7853905	1.90E-05
Voltage-dependent anion-selective channel protein 1	*VDAC1*	1.6327347	3.0610150	3.4111857	1.7784510	1.30E-07
Voltage-dependent anion-selective channel protein 3	*VDAC3*	0.5338999	1.9124817	2.0367883	1.5028884	3.52E-04
X-ray repair cross-complementing protein 6	*XRCC6*	1.1470197	2.3778627	2.9897833	1.8427637	1.52E-07

Supplementary File 2B. Functional annotation of the differentially expressed proteins identified in the MLN x MNT tissues' comparison. According to the functional classification of the PANTHER system v. 13.1, based on the gene ontology (GO) terms: **A.** Protein class; **B.** Molecular function; **C.** Biological process. According to the functional enrichment analysis of the DAVID v. 6.8 database: **D.** Top enriched biological processes (GO terms, p<0.05); **E.** Top enriched KEGG pathways (p<0.05).

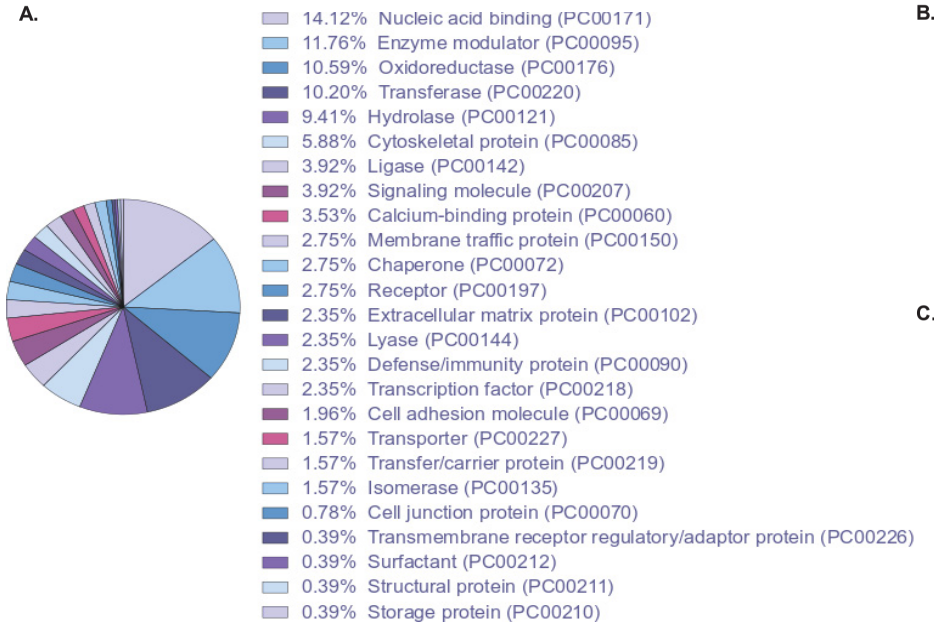

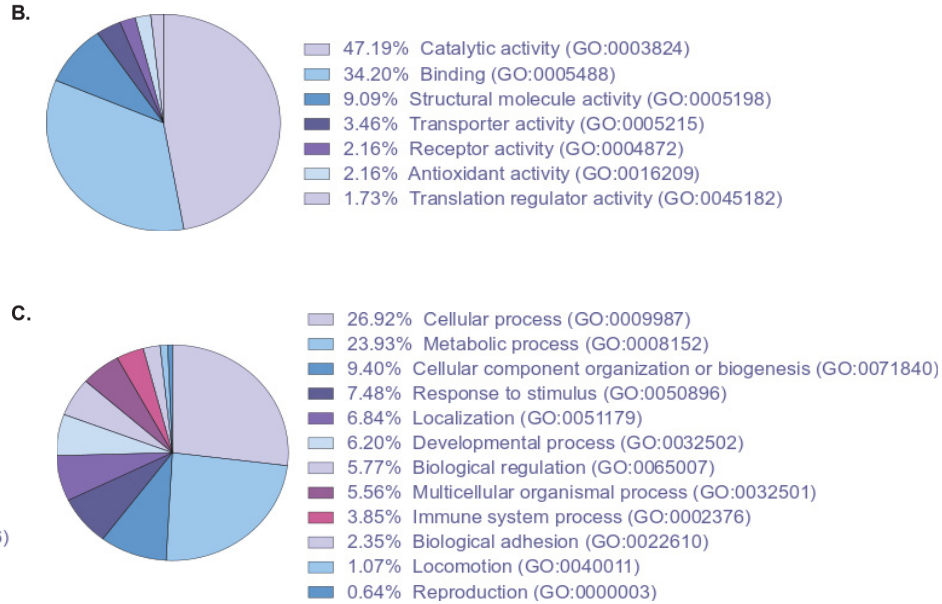

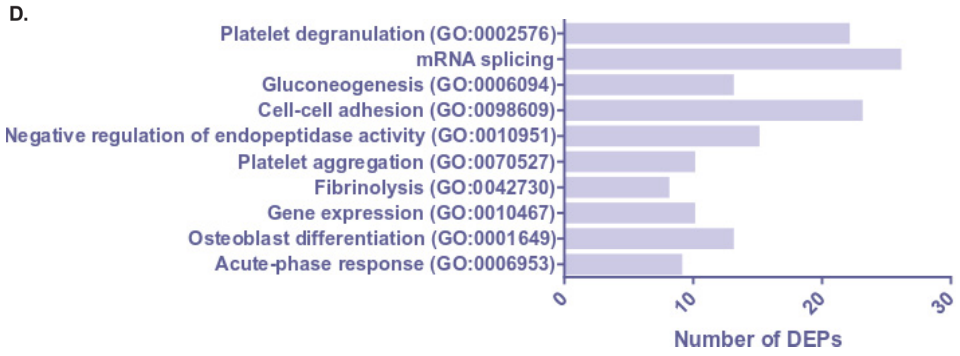

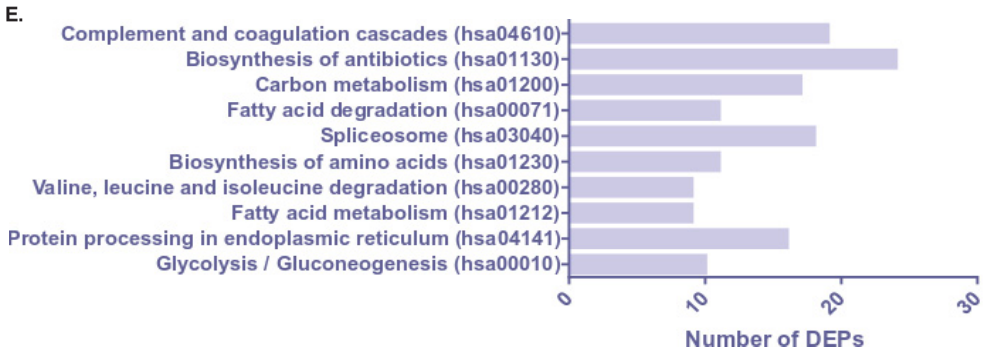

Supplementary File 2C. Signaling canonical pathways predicted from the differentially expressed proteins identified in the MLN x MNT tissues' comparison (IPA analysis).

Ingenuity Canonical Pathways	p-value	Ratio	z-score	Molecules
Acute Phase Response Signaling	1.26E-16	1.42E-01	-2.496	*SERPING1, C1S, AHSG, CP, F2, SERPINF2, HNRNPK, FGG, SERPIND1, PLG, HP, FTL, ORM1, APCS, ITIH4, CFB, FGB, HRG, LBP, FGA, CRABP2, A2M, AGT, RBP4*
Atherosclerosis Signaling	6.46E-09	1.13E-01	-	*APOE, APOA4, APOB, CMA1, CD36, PCYOX1, COL1A2, PON1, COL1A1, ORM1, COL18A1, CLU, APOD, RBP4*
Aldosterone Signaling in Epithelial Cells	1.78E-06	7.78E-02	-	*CRYAB, HSPH1, HSPA9, TRAP1, HSPD1, HSPA5, HSPA12A, HSPA8, HSP90B1, HSP90AB1, HSP90AA1, AHCY, HSPB1*
EIF2 Signaling	4.90E-06	6.60E-02	2.121	*PTBP1, RPL4, RPL13, EIF4A3, EIF4A1, RPS9, RPLP2, RPL6, EIF2AK2, HSPA5, RPS3, RPL7A, RPL18, RPSA*
Aryl Hydrocarbon Receptor Signaling	4.57E-05	7.35E-02	-1	*CTSD, ALDH2, HSP90B1, ALDH1A1, HSP90AB1, GSTM3, HSP90AA1, ALDH6A1, GSTK1, HSPB1*
Clathrin-mediated Endocytosis Signaling	5.50E-05	6.06E-02	-	*HSPA8, APOE, PON1, APOB, APOA4, ORM1, CLTC, PCYOX1, F2, CLU, RBP4, APOD*
IL-12 Signaling and Production in Macrophages	7.41E-05	6.94E-02	-	*APOE, PON1, APOB, APOA4, ORM1, PCYOX1, STAT1, CLU, RBP4, APOD*
Granzyme B Signaling	8.32E-05	2.50E-01	2	*PRKDC, NUMA1, LMNB1, PARP1*
eNOS Signaling	2.29E-04	6.06E-02	-1.89	*KNG1, HSPA8, HSP90B1, PRKAR2B, HSP90AB1, HSPA9, PRKAR2A, CAV1, HSP90AA1, HSPA5*
Sertoli Cell-Sertoli Cell Junction Signaling	3.31E-04	5.78E-02	-	*SPTBN1, PRKAR2B, TUBB6, TUBB4B, SORBS1, PRKAR2A, ILK, CTNNA1, TUBB, A2M*
Xenobiotic Metabolism Signaling	1.02E-03	4.40E-02	-	*ALDH2, HSP90B1, FTL, CES1, ALDH1A1, HSP90AB1, GSTM3, CAT, HSP90AA1, ALDH6A1, MAOA, GSTK1*
Nitric Oxide Signaling in the Cardiovascular System	1.35E-03	6.48E-02	0.378	*KNG1, HSP90B1, PRKAR2B, HSP90AB1, PRKAR2A, CAV1, HSP90AA1*
Epithelial Adherens Junction Signaling	1.58E-03	5.59E-02	-	*MYL9, MYH9, TUBB6, TUBB4B, SORBS1, CTNNA1, MYH11, TUBB*
Glucocorticoid Receptor Signaling	2.04E-03	3.87E-02	-	*HSPA8, HMGB1, HSP90B1, HSP90AB1, HSPA9, FKBP4, HSP90AA1, KRT18, HSPA5, STAT1, A2M, FGG, AGT*
GP6 Signaling Pathway	3.98E-03	5.34E-02	-2.646	*COL1A2, LAMC1, COL1A1, FGB, COL18A1, FGA, FGG*
Caveolar-mediated Endocytosis Signaling	4.57E-03	7.04E-02	-	*ARCN1, CAV1, COPB1, CAVIN1, COPG1*
Calcium Signaling	1.12E-02	4.04E-02	-	*MYL9, CALR, MYH9, PRKAR2B, PRKAR2A, TPM1, ASPH, MYH11*
Sirtuin Signaling Pathway	1.17E-02	3.53E-02	1.134	*PDHA1, PGK1, PRKDC, H1FX, XRCC6, GOT2, VDAC1, VDAC3, BPGM, PARP1*
Germ Cell-Sertoli Cell Junction Signaling	1.51E-02	4.14E-02	-	*TUBB6, TUBB4B, SORBS1, ILK, CTNNA1, TUBB, A2M*
Hypoxia Signaling in the Cardiovascular System	2.51E-02	5.48E-02	-	*P4HB, HSP90B1, HSP90AB1, HSP90AA1*
ILK Signaling	2.88E-02	3.63E-02	-0.816	*MYL9, PARVA, MYH9, ILK, KRT18, MYH11, DSP*
Renin-Angiotensin Signaling	3.80E-02	4.13E-02	-1	*PTPN6, PRKAR2B, PRKAR2A, STAT1, AGT*
Growth Hormone Signaling	4.07E-02	4.71E-02	-1	*PTPN6, IGFALS, STAT1, A2M*
Tight Junction Signaling	4.17E-02	3.61E-02	-	*MYL9, MYH9, PRKAR2B, PRKAR2A, CTNNA1, MYH11*
Neuregulin Signaling	4.27E-02	4.65E-02	-	*HSP90B1, HSP90AB1, DCN, HSP90AA1*

Supplementary File 2D. Differentially expressed proteins into the “Cancer” and “Breast cancer” annotations according to the Ingenuity Pathways Knowledge Base (IPA analysis).

Categories	Diseases or Functions Annotation	p-value	Molecules
Cancer, Organismal Injury and Abnormalities, Reproductive System Disease	Breast cancer	6.24E-08	*ACAA2, ACACB, ACOT1, AGR2, AGT, ALDH1A1, ALDOA, APOB, APOE, CAV1, CBX3, CES1, CKB, CLTC, CLU, CNDP2, CNN1, COL14A1, COL1A1, COL1A2, CP, CRABP2, CRYAB, CSE1L, CTSD, DCN, DDX39B, DHRS2, DHX15, DSP, EFTUD2, EIF2AK2, EIF4A1, EPRS, ESYT2, FASN, FBLN2, FBN1, FGA, GLUL, GSTM3, H2AFY, HBB, HNRNPM, HNRNPR, HP, HSP90AA1, HSP90AB1, HSP90B1, HSPA5, HSPB1, HSPD1, HSPG2, ILF2, ILF3, ITIH4, KRT18, LBP, LGALS3BP, LRP1, LTF, MCAM, MYH11, MYH9, NCL, NID2, OGN, ORM1, P4HB, PARP1, PARVA, PCYOX1, PGK1, PHB, PKM, PLG, POSTN, PRDX2, PRKDC, RBMX, RPL4, RTCB, SERPINC1, SFPQ, SLC4A1, SLC9A3R1, STAT1, THBS1, TNS1, TNXB, TPM1, TUBB, TUBB4B, TUBB6, TYMP, U2AF2, UGDH, VDAC3*
Cancer, Organismal Injury and Abnormalities	Cancer	1.34E-06	*A1BG, A2M, ABHD11, ABHD14B, ACAA1, ACAA2, ACACB, ACADM, ACADS, ACADSB, ACO1, ACOT1, ACSL1, AFM, AGL, AGR2, AGT, AHCY, AHSG, ALDH1A1, ALDH2, ALDH6A1, ALDOA, ALDOC, ANXA3, APCS, APMAP, APOA4, APOB, APOD, APOE, ARCN1, ASPH, ASPN, ASS1, BLVRB, BPGM, C1S, CA1, CACYBP, CALB2, CALR, CANX, CAPG, CAT, CAV1, CAVIN1, CAVIN3, CBX3, CD36, CES1, CFB, CFH, CKB, CLEC3B, CLTC, CLU, CMA1, CNDP2, CNN1, COASY, COL14A1, COL18A1, COL1A1, COL1A2, COPB1, COPG1, CP, CPA3, CRABP2, CRYAB, CSE1L, CSTA, CTNNA1, CTSD, CTSG, CYB5R1, DCLK1, DCN, DDX1, DDX17, DDX39B, DDX5, DHRS2, DHX15, DHX9, DPP3, DSP, ECHS1, ECI1, EEF1D, EEF2, EFHD1, EFTUD2, EHD2, EIF2AK2, EIF4A1, EIF4A3, ENOPH1, EPHX1, EPRS, ESYT2, EZR, F13A1, F2, FABP4, FAH, FASN, FBL, FBLN1, FBLN2, FBN1, FGA, FGB, FGG, FKBP4, FLAD1, FMOD, FTL, GAPDH, GC, GDI1, GLUL, GOT2, GPD1, GPD2, GPX3, GSTK1, GSTM3, H2AFY, HADH, HBB, HBD, HDLBP, HIST1H4A, HMGB1, HNRNPA2B1, HNRNPAB, HNRNPD, HNRNPK, HNRNPL, HNRNPM, HNRNPR, HNRNPU, HP, HRG, HSP90AA1, HSP90AB1, HSP90B1, HSPA12A, HSPA5, HSPA8, HSPA9, HSPB1, HSPD1, HSPG2, HSPH1, IARS2, IGFALS, ILF2, ILF3, ILK, ITIH4, KHDRBS1, KNG1, KRT18, LAMC1, LAP3, LBP, LCP1, LGALS3BP, LMAN2, LMNB1, LRG1, LRP1, LRPPRC, LRRC59, LTF, MAOA, MAT2A, MCAM, MDH2, ME1, MYH11, MYH9, MYL9, MYO1C, NAP1L1, NCL, NID2, NONO, NPM1, NUMA1, OGN, ORM1, P4HB, PARP1, PARVA, PCBP1, PCYOX1, PDHA1, PDIA4, PDIA6, PEBP1, PGK1, PGM1, PHB, PHGDH, PKM, PLG, PLIN1, PLIN4, PNP, PON1, POSTN, PPIA, PRDX1, PRDX2, PRDX4, PRKAR2B, PRKDC, PRPF8, PSME1, PSME2, PTBP1, PTGIS, PTPN6, RBMX, RBP4, RETSAT, RNPEP, RPL13, RPL18, RPL4, RPL6, RPL7A, RPLP2, RPS3, RPS9, RPSA, RRBP1, RTCB, RTRAF, RUVBL1, RUVBL2, SARS, SELENBP1, SEPT11, SERPINA4, SERPINC1, SERPIND1, SERPINF2, SERPING1, SFPQ, SLC25A1, SLC25A13, SLC4A1, SLC9A3R1, SND1, SNRNP200, SORBS1, SORD, SPTBN1, SRSF2, SRSF6, SRSF7, STAT1, STIP1, SYNCRIP, THBS1, TNS1, TNXB, TPM1, TRAP1, TTLL12, TUBB, TUBB4B, TUBB6, TXNDC5, TYMP, U2AF2, UGDH, UGP2, USP5, VARS, VDAC1, VDAC3, XRCC6*

Supplementary File 2E. Predicted protein interactive networks of the differentially expressed proteins identified in the MLN x MNT tissues' comparison (IPA analysis).

Network	Top Diseases and Functions	Score	Focus Molecules	Molecules in Network
1	Developmental Disorder, Hematological Disease, Hereditary Disorder	42	29	Actin, ALDOA, CALR, CANX, CAT, DDX17, DHX9, EIF2AK2, EIF4A3, FBL, FGA, FGB, FGG, GAPDH, HNRNPU, ILK, KHDRBS1, LTF, MHC Class I (complex), NCL, NFkB (complex), NPM1, PARVA, RNA polymerase II, Rnr, RPS3, RPS9, RPSA, RUVBL1, RUVBL2, SERPING1, SLC4A1, SND1, SRSF6, Tap
2	Cancer, Organismal Injury and Abnormalities, Reproductive System Disease	38	27	Akt, c-Src, CAV1, Collagen Alpha1, CSE1L, CSTA, CTSD, DCN, DSP, FBN1, GOT2, Gsk3, HIST1H4A, HNRNPD, HNRNPM, Hsp27, Hsp70, Hsp90, HSP90AA1, HSP90AB1, HSPA8, HSPA9, ILF2, ILF3, LCP1, MCAM, p85 (pik3r), PCBP1, PRKAR2B, PTPN6, RPL6, STIP1, SYNCRIP, TUBB6, TUBB4B
3	Cancer, Organismal Injury and Abnormalities, Reproductive System Disease	30	23	26s Proteasome, AGT, Alpha tubulin, APCS, BCR (complex), C1S, caspase, CBX3, CLTC, CLU, CNN1, COL1A1, COL1A2, CP, CRYAB, CTNNA1, ERK, FASN, H2AFY, Histone h3, Histone h4, HNRNPK, Mek, NUMA1, PARP1, PDGF BB, PRKDC, RBMX, RPA, RPL4, STAT1, Tgf beta, Top2, TUBB, XRCC6

Network #1

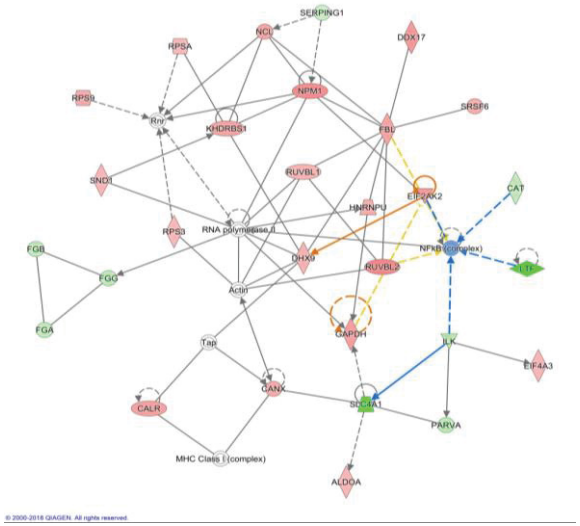

Network #2

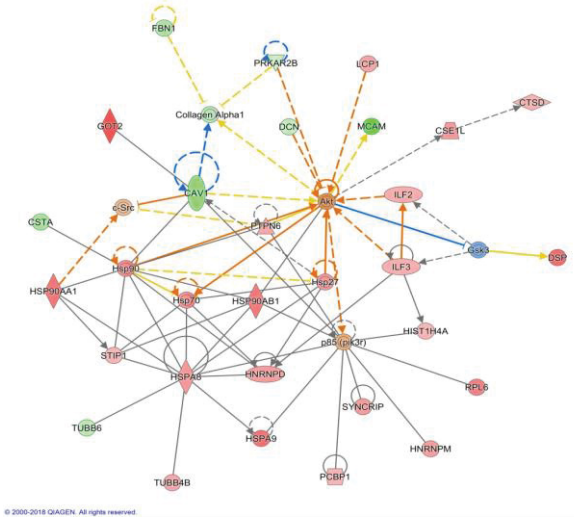

Network #3

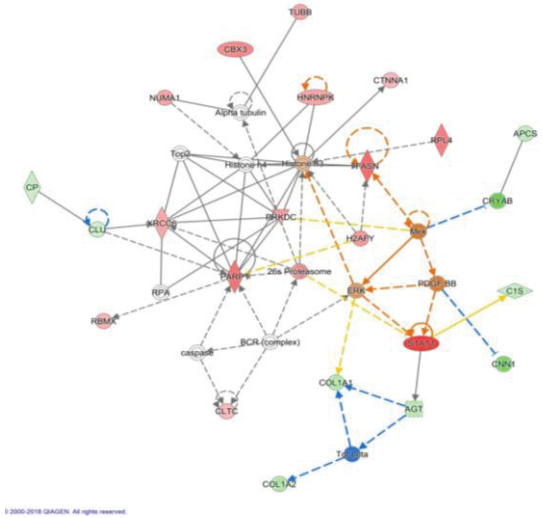

Supplementary File 2F. Main upstream regulators analysis of the differentially expressed proteins identified in the MLN x MNT tissues' comparison (IPA analysis).

Upstream Regulator	Molecule Type	z-score	p-value	Target molecules in dataset
HSF1	transcription regulator	-1.615	2.17E-10	*CBX3, CLU, COL18A1, CRYAB, DHRS2, FASN, FBLN1, HSP90AA1, HSP90AB1, HSPA8, HSPB1, HSPH1, MAT2A, PGK1*
TCR	complex	1.462	1.36E-09	*ALDOA, APOA4, APOD, APOE, FBL, HADH, HSPA9, HSPD1, LMNB1, MDH2, PGK1, PHB, PHB2, RPL4, RPL6, RPS3, RPSA, STAT1, VDAC3*
LONP1	peptidase	-1.501	3.58E-09	*ACADS, ECI1, HNRNPA2B1, HSPA9, HSPB1, HSPD1, MDH2, P4HB, SARS, TRAP1, VDAC1*
IL6	cytokine	-2.295	7.00E-09	*AGT, APOB, CLU, DCN, FGA, FGB, FGG, HP, HSPA5, LBP, ORM1, PHB, PLG, THBS1*
MYC	transcription regulator	1.938	1.20E-07	*CAV1, CLU, COL1A1, EZR, FASN, FBL, FMOD, GAPDH, HNRNPU, HSP90AA1, HSPB1, HSPD1, HSPH1, NAP1L1, NCL, NPM1, PHB*
CST5	other	-1.308	1.99E-07	*ANXA3, CAV1, DHX9, DSP, EEF1D, EZR, HNRNPA2B1, HNRNPU, LAMC1, MYL9, NCL, NUMA1, PCBP1, PRDX1, PRDX2, PRPF8, VARS, VDAC1*
PCGEM1	other	0.896	2.65E-05	*ALDOA, FASN, GAPDH, PDHA1, PGK1, PKM*
SYVN1	transporter	1.897	3.20E-05	*CAVIN1, FASN, HNRNPM, HSPB1, LGALS3BP, MCAM, PCBP1, PTBP1, RPL18, USP5*
HSPA5	enzyme	-0.243	6.38E-05	*ACADM, CLU, FASN, HSP90B1, HSPA8*
HIF1A	transcription regulator	-0.494	7.32E-05	*AGT, ALDOA, ALDOC, APOE, CAV1, GAPDH, HP, HSPB1, NPM1, PKM, PTGIS, THBS1*
miR-122-5p (miRNAs w/seed GGAGUGU)	mature microrna	-1.455	1.21E-04	*ALDOA, HMGB1, P4HB, PKM, PRDX2, PSME1*
EGFR	kinase	2.587	1.80E-04	*CAV1, FASN, HNRNPA2B1, HSP90B1, HSPA5, PKM, POSTN, PPIA*
IL15	cytokine	0.818	1.80E-04	*ALDOA, ALDOC, BPGM, GAPDH, GPD2, PGK1, PGM1, PKM*
NEUROG1	transcription regulator	-0.816	2.70E-04	*ASS1, C1S, CFH, DSP, LCP1, THBS1*
NFE2L2	transcription regulator	-1.067	3.09E-04	*CAT, FTL, ME1, PHGDH, PRDX1*
XBP1	transcription regulator	0.784	4.36E-04	*CAT, HSP90B1, HSPA5, PDIA4, XRCC6*
LDL	complex	-0.577	5.40E-04	*APOE, CD36, FABP4, HSP90B1, HSPA5*
ATF6	transcription regulator	0.832	5.64E-04	*HSP90B1, HSPA5, PDIA4, PRDX2*
TNF	cytokine	1.411	6.13E-04	*AGT, ALDH2, APOE, CAT, CFB, CNN1, COL1A2, FGG, GPD2, HSPG2, LBP, MCAM, PHGDH, PKM, PSME2, STAT1, TYMP*
PLA2R1	transmembrane receptor	1	6.54E-04	*ALDH2, CTSD, LAP3, PEBP1*
FOXA1	transcription regulator	0	7.80E-04	*AGR2, ALDH6A1, COL18A1, EFHD1, EPHX1, FKBP4*
Lh	complex	0.378	1.20E-03	*COL18A1, EZR, ILK, KRT18, PGK1, PRKAR2A, STAT1, STIP1, THBS1, TPM1*
MYOCD	transcription regulator	-0.492	1.25E-03	*CNN1, COL1A1, COL1A2, MYH11, TPM1*
PGR	ligand-dependent nuclear receptor	0.728	1.41E-03	*ACSL1, AK4, EZR, GLUL, GSTM3, KRT18, SLC9A3R1, SRSF7*
MAPK1	kinase	-1.066	1.47E-03	*ACO1, C1S, CFB, EIF2AK2, HBB, LAP3, LGALS3BP, PSME2, STAT1*
mir-122	microrna	-0.749	1.53E-03	*ALDOA, CACYBP, CSRP1, KHDRBS1, LAMC1, PKM*
IL13	cytokine	-2.404	1.72E-03	*CD36, COL1A2, F13A1, FABP4, GPX3, MAOA, SEPT11, THBS1, TNS1*
IgG	complex	-1.89	1.81E-03	*CALR, CRABP2, DSP, EZR, HSPA5, HSPB1, KRT18*
SATB1	transcription regulator	0.551	2.44E-03	*CTNNA1, CTSD, HBB, HSP90AA1, HSPA8, ILF3*
STAT3	transcription regulator	-1	2.75E-03	*AGT, COL1A1, FGG, HNRNPD, HP, LBP, PHB, STAT1*
PPARG	ligand-dependent nuclear receptor	-0.042	2.87E-03	*CAV1, COL1A1, COL1A2, FABP4, PLIN1*
miR-146a-5p (and other miRNAs w/seed GAGAACU)	mature microrna	2	4.15E-03	*CAT, CFH, LBP, LTF*
FGF8	growth factor	-1	5.26E-03	*COL18A1, CRYAB, NAP1L1, TNXB*
ESR1	ligand-dependent nuclear receptor	0.923	6.67E-03	*AGT, ASS1, CAV1, CP, CRABP2, CTSD, DDX17, FKBP4, HNRNPD, LGALS3BP, SFPQ, TPM1*
AR	ligand-dependent nuclear receptor	1.067	8.19E-03	*CAV1, FKBP4, GDI1, HSPH1, MAOA, NAP1L1, STAT1, THBS1*
MAPK9	kinase	0.283	9.18E-03	*CAV1, FASN, GAPDH, LGALS3BP*
IL1B	cytokine	0.716	1.00E-02	*APOB, APOE, CAT, COL1A1, FGG, LBP, LCP1, ORM1*
TP53	transcription regulator	-1.436	1.09E-02	*APOE, CAT, CAV1, CLU, COL18A1, CRYAB, CTSD, FASN, HMGB1, HSPA8, ME1, PHGDH, PTPN6, SFPQ, SORBS1, SRSF3, THBS1, TUBB*
CEBPA	transcription regulator	-1	1.09E-02	*A2M, ACSL1, CTNNA1, EPHX1, H1FX, LTF*
CIP2A	other	2	1.17E-02	*CFB, CRYAB, DCN, NCL*
PI3K (family)	group	2.219	1.23E-02	*CAT, CTSD, FASN, HSPA5, PKM*
EGLN	group	0.447	1.40E-02	*ALDOC, CAVIN1, FTL, GAPDH, PGM1*
SMARCA4	transcription regulator	-2.236	1.51E-02	*A2M, AGR2, AGT, ALDH2, CALB2, CP, FGG, GAPDH, HBB, KRT18, PARVA, TPM1, TUBB*
FSH	complex	0	2.03E-02	*COL18A1, EZR, ILK, KRT18, PGK1, STAT1, STIP1, THBS1, TPM1*
MGEA5	enzyme	0.707	2.07E-02	*ALDOC, CAV1, FBLN1, GLUL, MCAM, PDHA1, PRDX4, THBS1*
TP63	transcription regulator	0.939	2.12E-02	*CSTA, FASN, FBN1, GAPDH, POSTN, PRPF8, THBS1, TPM1*
WT1	transcription regulator	-0.391	2.31E-02	*AHCY, APRT, HSP90B1, THBS1, TRAP1*
TGFB1	growth factor	-2.141	3.19E-02	*ASPN, COL18A1, COL1A1, COL1A2, FASN, FBN1, ILK, THBS1, TPM1, TYMP*
CLDN7	other	0.277	3.53E-02	*AGT, ANXA3, APOE, C1S, PHGDH*
ERK1/2	group	0.651	4.21E-02	*CALR, CAT, EZR, HSPA5, PKM*
CCND1	transcription regulator	-1.982	4.01E-01	*HSPB1, RPL13, TUBB, TYMP*

Supplementary File 3A. Differentially expressed proteins into the log2 fold change values identified for MPT x MNT tissues' comparison according to the ANOVA's test.
LFQ intensities were log2-transformed and normalized by width adjustment in Perseus v. 1.5.6.0. Fold changes were presented in log2 values (up-regulated and down-regulated proteins were highlighted in red and green, respectively).

Protein Name	Gene Symbol	MNT LFQ_mean	MPT LFQ_mean2	MLN LFQ_mean	MPT x MNT fold change	ANOVA p-value
Alpha-1B-glycoprotein	*A1BG*	2.1274	0.4713	0.4517	-1.6561	1.65E-03
Alpha/beta hydrolase domain-containing protein 14B	*ABHD14B*	0.5174	-1.6124	-1.2778	-2.1298	8.50E-06
3-ketoacyl-CoA thiolase, mitochondrial	*ACAA2*	1.2126	-0.8760	-0.8970	-2.0886	5.97E-06
Acetyl-CoA carboxylase 2	*ACACB*	0.7338	-3.8072	-3.7810	-4.5410	2.57E-04
Medium-chain specific acyl-CoA dehydrogenase, mitochondrial	*ACADM*	0.4431	-1.9845	-1.0689	-2.4277	5.06E-05
Short-chain specific acyl-CoA dehydrogenase, mitochondrial	*ACADS*	1.0767	-2.8929	-2.5097	-3.9696	1.53E-06
Short/branched chain specific acyl-CoA dehydrogenase, mitochondrial	*ACADSB*	-1.6947	0.2021	0.4542	1.8968	5.96E-07
Cytoplasmic aconitate hydratase	*ACO1*	1.3932	-0.1895	-0.4186	-1.5827	5.34E-06
Acyl-coenzyme A thioesterase 1	*ACOT1*	1.8228	-0.9927	-0.0417	-2.8155	8.08E-06
Long-chain-fatty-acid--CoA ligase 1	*ACSL1*	3.5536	-2.4079	-2.4161	-5.9615	2.22E-06
Alcohol dehydrogenase class-3	*ADH5*	0.4225	-1.5999	-1.2975	-2.0224	3.39E-04
Adipocyte enhancer-binding protein 1	*AEBP1*	-0.8130	0.9414	0.2247	1.7544	6.59E-05
Afamin	*AFM*	0.8953	-1.0592	-1.6164	-1.9545	4.64E-05
Anterior gradient protein 2 homolog	*AGR2*	-2.1493	1.1504	1.0164	3.2997	6.05E-06
Angiotensinogen	*AGT*	1.4353	-0.1363	-0.9917	-1.5716	2.63E-07
Alpha-2-HS-glycoprotein	*AHSG*	1.1837	-1.4220	-3.9872	-2.6057	4.35E-07
Adenylate kinase 4, mitochondrial	*AK4*	0.3137	-2.2435	-3.2467	-2.5572	8.26E-04
Retinal dehydrogenase 1	*ALDH1A1*	1.9275	0.3203	0.1418	-1.6072	8.89E-08
Aldehyde dehydrogenase, mitochondrial	*ALDH2*	3.6553	1.5342	0.9643	-2.1212	4.99E-07
Methylmalonate-semialdehyde dehydrogenase [acylating], mitochondrial	*ALDH6A1*	0.1925	-2.4772	-2.3352	-2.6698	2.46E-04
Fructose-bisphosphate aldolase A	*ALDOA*	2.8319	4.5608	4.3895	1.7289	6.19E-06
Annexin	*ANXA3*	0.1418	-2.6747	-2.6454	-2.8164	2.46E-04
AP-1 complex subunit gamma-1	*AP1G1*	-2.5762	-0.9982	-1.1089	1.5780	3.20E-05
Apolipoprotein B-100	*APOB*	3.1646	1.3936	0.1567	-1.7710	1.65E-07
Apolipoprotein D	*APOD*	1.0605	-0.9834	-2.1300	-2.0439	1.42E-05
Apolipoprotein E	*APOE*	0.8823	-0.7092	-0.9790	-1.5915	1.12E-04
Adenine phosphoribosyltransferase	*APRT*	-1.8936	-0.3706	0.0113	1.5230	1.73E-06
Coatomer subunit delta	*ARCN1*	-2.2693	-0.3386	-0.1878	1.9306	2.51E-04
Aspartyl/asparaginyl beta-hydroxylase	*ASPH*	0.8701	-0.6635	-1.7129	-1.5336	7.73E-05
Argininosuccinate synthase	*ASS1*	0.5685	-4.5490	-4.9874	-5.1176	3.82E-07
Flavin reductase (NADPH)	*BLVRB*	2.4902	0.3637	0.3085	-2.1264	5.31E-07
Bisphosphoglycerate mutase	*BPGM*	1.0392	-4.1536	-4.4148	-5.1928	2.52E-08
Complement C1s subcomponent	*C1S*	-1.2571	-3.0649	-3.3103	-1.8078	1.90E-04
Complement C5	*C5*	0.5269	-2.2444	-3.1069	-2.7713	1.94E-05
Carbonic anhydrase 1	*CA1*	5.0484	1.7324	1.7200	-3.3160	1.22E-07
Carbonic anhydrase 2	*CA2*	3.0463	0.4364	2.3018	-2.6099	3.57E-07
Calcyclin-binding protein	*CACYBP*	-1.0595	1.2460	1.5421	2.3055	1.09E-07
Calretinin	*CALB2*	0.6328	-4.4251	-4.8767	-5.0579	9.60E-06
Cullin-associated NEDD8-dissociated protein 1	*CAND1*	1.3116	2.8206	2.6251	1.5090	1.42E-06
Macrophage-capping protein	*CAPG*	-0.7206	1.4330	1.6238	2.1535	6.80E-08
Catalase	*CAT*	3.6991	1.5582	1.5014	-2.1409	2.46E-07
Caveolin-1	*CAV1*	2.2061	-1.8566	-1.9755	-4.0627	4.11E-06
Chromobox protein homolog 3	*CBX3*	-2.2486	-0.2631	0.2724	1.9855	1.19E-04
Platelet glycoprotein 4	*CD36*	3.3264	-3.9301	-3.6375	-7.2565	5.27E-08
Liver carboxylesterase 1	*CES1*	1.9947	-1.2855	-1.8148	-3.2802	3.14E-06
Complement factor H	*CFH*	1.8955	0.2190	-1.3321	-1.6765	4.35E-06
Cytoskeleton-associated protein 4	*CKAP4*	-0.1520	1.4944	1.1412	1.6463	2.90E-06
Creatine kinase B-type	*CKB*	1.2992	-1.6374	-1.7731	-2.9366	1.57E-05
Tetranectin	*CLEC3B*	0.6369	-1.1834	-1.7043	-1.8203	5.86E-05
Calponin-1	*CNN1*	2.3538	-0.0842	-2.7271	-2.4380	8.57E-06
Collagen alpha-1(XII) chain	*COL12A1*	2.2517	4.7556	3.0561	2.5039	8.88E-09
Collagen alpha-1(XVIII) chain	*COL18A1*	0.8185	-1.4648	-2.5465	-2.2833	4.24E-08
Coatomer subunit beta	*COPB1*	-0.9751	0.8973	1.1246	1.8724	4.49E-06
Coatomer subunit gamma-1	*COPG1*	-1.4863	0.6920	0.8275	2.1783	1.40E-05
Mast cell carboxypeptidase A	*CPA3*	1.9123	0.3349	-3.2596	-1.5774	2.90E-08
Cellular retinoic acid-binding protein 2	*CRABP2*	-1.4784	1.4132	0.2527	2.8915	1.75E-03
Alpha-crystallin B chain	*CRYAB*	2.5615	-3.3989	-3.3540	-5.9603	3.25E-07
Exportin-2	*CSE1L*	0.9154	2.7027	3.1500	1.7873	4.46E-06
Cystatin-A	*CSTA*	0.0320	-3.3106	-3.3851	-3.3426	2.34E-04
Cathepsin D	*CTSD*	1.3822	3.0030	3.0946	1.6208	2.78E-06
NADH-cytochrome b5 reductase 1	*CYB5R1*	-0.2302	1.4042	2.1158	1.6344	2.82E-08
Probable ATP-dependent RNA helicase DDX17	*DDX17*	-0.7879	1.1929	1.4026	1.9808	2.08E-03
Spliceosome RNA helicase DDX39B	*DDX39B*	0.3976	1.9550	2.2677	1.5574	4.92E-07
Probable ATP-dependent RNA helicase DDX5	*DDX5*	-2.3036	-0.1424	0.4547	2.1612	5.14E-04
Dehydrogenase/reductase SDR family member 2, mitochondrial	*DHRS2*	-2.7286	-1.1462	1.6987	1.5824	1.28E-05
Pre-mRNA-splicing factor ATP-dependent RNA helicase DHX15	*DHX15*	-1.6481	0.0145	0.1670	1.6626	2.62E-04
Dipeptidyl peptidase 3	*DPP3*	-1.2255	0.3189	0.6763	1.5444	1.47E-05
Desmoplakin	*DSP*	-2.3338	0.2624	0.9284	2.5962	3.44E-04
Enoyl-CoA hydratase, mitochondrial	*ECHS1*	1.9860	0.0975	0.2648	-1.8885	5.13E-05
Enoyl-CoA delta isomerase 1, mitochondrial	*ECI1*	-1.5809	0.2388	0.3379	1.8197	4.40E-05
Elongation factor 1-delta	*EEF1D*	0.2986	1.8765	2.3384	1.5779	1.03E-05
EF-hand domain-containing protein D1	*EFHD1*	-1.6095	0.5111	1.0039	2.1205	1.05E-05
116 kDa U5 small nuclear ribonucleoprotein component	*EFTUD2*	-1.6382	0.2547	0.0454	1.8929	5.81E-04
EH domain-containing protein 2	*EHD2*	4.3360	1.4223	1.2143	-2.9137	9.59E-08
Electron transfer flavoprotein subunit beta	*ETFB*	0.9740	-1.0932	-0.3484	-2.0672	3.12E-05
Ezrin	*EZR*	-2.1635	-0.0784	0.6321	2.0851	7.20E-03
Prothrombin	*F2*	0.8241	-1.3182	-1.6662	-2.1423	4.02E-08
Fatty acid-binding protein, adipocyte	*FABP4*	4.4484	-1.4501	-1.6527	-5.8985	2.84E-07
Fumarylacetoacetase	*FAH*	1.3862	-1.7393	-2.1171	-3.1256	1.01E-05
Redox-regulatory protein FAM213A	*FAM213A*	1.5102	-2.4306	-1.6723	-3.9408	8.36E-06
Fatty acid synthase	*FASN*	5.0826	7.0661	8.2690	1.9835	8.32E-08
rRNA 2-O-methyltransferase fibrillarin	*FBL*	-1.0720	1.1000	0.8973	2.1720	8.03E-06
Fibrillin-1	*FBN1*	3.1729	0.9808	0.1689	-2.1921	3.59E-05
Fibrinogen gamma chain	*FGG*	4.8085	3.2972	2.4295	-1.5113	5.40E-07
Peptidyl-prolyl cis-trans isomerase FKBP4	*FKBP4*	0.0301	3.1529	4.0059	3.1227	3.46E-10
Fibromodulin	*FMOD*	0.7103	-2.1584	-4.1646	-2.8687	1.78E-05

Fibronectin	*FN1*	3.2214	4.7464	3.3456	1.5250	3.57E-07
Glyceraldehyde-3-phosphate dehydrogenase	*GAPDH*	3.4778	5.5608	5.5527	2.0830	1.56E-05
Glycine--tRNA ligase	*GARS*	-1.9288	-0.3239	-0.6221	1.6050	3.31E-05
Rab GDP dissociation inhibitor alpha	*GDI1*	-1.1212	0.6636	0.6986	1.7849	1.59E-04
Glutamine synthetase	*GLUL*	-1.2067	1.8061	2.0885	3.0128	4.64E-06
Aspartate aminotransferase, mitochondrial	*GOT2*	-1.1021	1.9629	2.6586	3.0650	1.24E-06
Glycerol-3-phosphate dehydrogenase [NAD(+)], cytoplasmic	*GPD1*	4.2765	-3.6608	-3.2919	-7.9373	2.36E-05
Glycerol-3-phosphate dehydrogenase, mitochondrial	*GPD2*	-1.4381	0.0917	0.6423	1.5298	7.14E-07
Glutathione peroxidase	*GPX3*	0.3461	-1.4208	-1.4885	-1.7669	8.68E-07
Histone H1.0	*H1F0*	-2.2492	-0.0541	-2.0838	2.1950	5.98E-05
Core histone macro-H2A.1	*H2AFY*	0.7714	2.6676	2.9392	1.8961	6.84E-06
Hydroxyacyl-coenzyme A dehydrogenase, mitochondrial	*HADH*	1.5491	-0.7814	-0.8059	-2.3306	2.56E-07
Hemoglobin subunit delta	*HBD*	4.0726	0.6782	0.4969	-3.3944	4.39E-07
Vigilin	*HDLBP*	-0.5045	1.1435	1.2119	1.6480	1.68E-06
Histone H1.4	*HIST1H1E*	1.3525	3.1284	2.7652	1.7759	2.69E-05
Heterogeneous nuclear ribonucleoproteins A2/B1	*HNRNPA2B1*	1.7605	3.6290	4.0310	1.8684	2.21E-06
Heterogeneous nuclear ribonucleoprotein A/B	*HNRNPAB*	-2.0178	-0.0618	0.6043	1.9560	7.64E-07
Heterogeneous nuclear ribonucleoprotein D0	*HNRNPD*	-0.4755	1.1953	1.6322	1.6709	6.21E-06
Heterogeneous nuclear ribonucleoprotein K	*HNRNPK*	1.2137	2.7245	3.1825	1.5108	8.03E-09
Heterogeneous nuclear ribonucleoprotein L	*HNRNPL*	-2.2217	-0.0321	0.6497	2.1896	9.81E-03
Heterogeneous nuclear ribonucleoprotein M	*HNRNPM*	-0.0239	1.7429	2.1221	1.7668	3.55E-07
Heterogeneous nuclear ribonucleoprotein R	*HNRNPR*	-1.0986	0.7117	0.9358	1.8102	6.04E-08
Heterogeneous nuclear ribonucleoprotein U	*HNRNPU*	0.9576	2.5463	2.7393	1.5887	1.34E-05
Haptoglobin	*HP*	2.5337	0.5639	-0.3585	-1.9698	6.22E-05
Histidine-rich glycoprotein	*HRG*	2.2502	0.6469	0.0558	-1.6033	1.39E-07
Heat shock protein HSP 90-alpha	*HSP90AA1*	3.2094	5.3977	6.1426	2.1883	3.26E-06
Heat shock protein HSP 90-beta	*HSP90AB1*	2.2352	4.4685	5.1209	2.2333	2.57E-07
Heat shock 70 kDa protein 12A	*HSPA12A*	0.3873	-3.8718	-3.9580	-4.2591	5.67E-05
78 kDa glucose-regulated protein	*HSPA5*	2.5182	4.1380	4.8827	1.6198	1.80E-08
Heat shock cognate 71 kDa protein	*HSPA8*	3.5477	5.2105	5.7345	1.6628	3.01E-07
Stress-70 protein, mitochondrial	*HSPA9*	1.3598	3.5990	4.4452	2.2392	3.73E-08
Heat shock protein beta-1	*HSPB1*	2.9881	4.6570	5.1939	1.6689	2.16E-06
60 kDa heat shock protein, mitochondrial	*HSPD1*	2.2468	4.3677	5.0749	2.1209	4.36E-07
Basement membrane-specific heparan sulfate proteoglycan core protein	*HSPG2*	3.9165	1.4272	0.4487	-2.4893	2.95E-07
Heat shock protein 105 kDa	*HSPH1*	-2.6217	0.4290	0.7817	3.0507	1.14E-06
Hypoxia up-regulated protein 1	*HYOU1*	-1.1388	0.4269	0.3379	1.5657	6.12E-05
Insulin-like growth factor-binding protein complex acid labile subunit	*IGFALS*	-1.8546	-3.4785	-4.2654	-1.6240	5.87E-05
Ig heavy chain V-III region JON;Ig heavy chain V-III region WEA;Ig heavy chain V-III region TRO	*IGHV3-21*	0.8715	-1.1872	0.3057	-2.0587	9.84E-05
Ig kappa chain V-III region B6	*IGKV3D-20*	2.3964	0.8633	0.7732	-1.5330	6.33E-05
Interleukin enhancer-binding factor 2	*ILF2*	-0.0556	1.6223	1.7105	1.6779	6.24E-05
Interleukin enhancer-binding factor 3	*ILF3*	-0.7598	0.8074	0.9704	1.5672	4.65E-05
Integrin-linked protein kinase	*ILK*	-0.5639	-2.4023	-3.1419	-1.8384	7.20E-06
Inter-alpha-trypsin inhibitor heavy chain H4	*ITIH4*	2.3430	0.7080	-0.1934	-1.6350	7.94E-07
KH domain-containing, RNA-binding, signal transduction-associated protein 1	*KHDRBS1*	-2.9218	-1.3215	-0.9233	1.6003	1.64E-03
Kininogen-1	*KNG1*	2.2146	0.5840	-0.3921	-1.6305	2.87E-07
Keratin, type I cytoskeletal 18	*KRT18*	-1.9253	2.4561	2.8070	4.3813	7.92E-06
Kinectin	*KTN1*	-1.8219	-0.1174	-0.4225	1.7045	1.84E-05
Laminin subunit gamma-1	*LAMC1*	2.8354	-0.4616	-1.9305	-3.2971	8.64E-06
Lipopolysaccharide-binding protein	*LBP*	-2.1570	-3.8189	-4.1528	-1.6619	1.28E-04
L-lactate dehydrogenase B chain	*LDHB*	3.1512	1.6243	2.0426	-1.5269	7.66E-05
Vesicular integral-membrane protein VIP36	*LMAN2*	-2.4150	-0.7556	-0.7202	1.6593	4.38E-04
Lamin-B1	*LMNB1*	-1.0286	0.7844	0.9896	1.8130	6.51E-05
Leucine-rich alpha-2-glycoprotein	*LRG1*	-0.4564	-2.7778	-3.7323	-2.3214	4.42E-04
Prolow-density lipoprotein receptor-related protein 1	*LRP1*	-0.9453	-2.5693	-3.5181	-1.6239	6.13E-05
Leucine-rich PPR motif-containing protein, mitochondrial	*LRPPRC*	0.3761	1.8887	2.5998	1.5126	1.87E-10
Leucine-rich repeat-containing protein 59	*LRRC59*	-1.9319	1.2951	1.4037	3.2270	6.57E-08
Lactotransferrin	*LTF*	2.3578	-3.6759	-5.4587	-6.0336	3.20E-07
Amine oxidase [flavin-containing] A	*MAOA*	1.9006	-3.1677	-3.0711	-5.0683	1.85E-07
Cell surface glycoprotein MUC18	*MCAM*	1.8194	-3.9521	-4.5274	-5.7715	3.32E-06
Methylcrotonoyl-CoA carboxylase beta chain, mitochondrial	*MCCC2*	-1.4150	0.4662	-1.1181	1.8812	2.71E-05
Malate dehydrogenase, mitochondrial	*MDH2*	2.1562	3.7563	3.7478	1.6001	5.20E-06
NADP-dependent malic enzyme	*ME1*	-0.2062	-1.7249	-1.9242	-1.5187	1.01E-05
C-1-tetrahydrofolate synthase	*MTHFD1*	1.2189	-0.5599	-0.1058	-1.7789	4.45E-06
Myosin-11	*MYH11*	3.4640	1.9041	-0.0918	-1.5598	1.29E-07
Myosin-9	*MYH9*	3.9996	5.8962	5.5984	1.8966	4.16E-07
Unconventional myosin-Ic	*MYO1C*	3.3706	1.2130	0.8485	-2.1576	3.90E-08
Nidogen-2	*NID2*	2.3346	-1.9316	-2.7235	-4.2663	1.17E-06
Nicotinamide N-methyltransferase	*NNMT*	-2.0795	0.0543	-1.6304	2.1338	1.50E-04
NAD(P) transhydrogenase, mitochondrial	*NNT*	-0.1145	-1.8029	-1.0699	-1.6884	4.51E-04
Non-POU domain-containing octamer-binding protein	*NONO*	-1.3830	0.3358	0.3498	1.7188	8.54E-06
Nucleophosmin	*NPM1*	-1.1842	1.0085	1.3060	2.1928	4.53E-06
Vesicle-fusing ATPase	*NSF*	-0.9276	0.7123	0.5402	1.6399	1.11E-04
Nuclear mitotic apparatus protein 1	*NUMA1*	-1.4829	0.1777	0.5041	1.6606	5.85E-06
Mimecan	*OGN*	5.0148	2.9127	0.7526	-2.1022	1.43E-06
Alpha-1-acid glycoprotein 1	*ORM1*	3.2234	1.1875	0.8735	-2.0358	1.46E-04
Protein disulfide-isomerase	*P4HB*	2.3651	4.0196	4.0523	1.6545	1.59E-06
Poly [ADP-ribose] polymerase 1	*PARP1*	-0.3357	2.1042	2.6797	2.4399	6.65E-06
Alpha-parvin	*PARVA*	0.8488	-1.3354	-1.7643	-2.1842	9.40E-07
Poly(rC)-binding protein 1	*PCBP1*	-0.6968	0.8153	0.9208	1.5121	2.25E-06
Prenylcysteine oxidase 1	*PCYOX1*	1.7375	0.1072	-0.6672	-1.6304	7.10E-07
Pyruvate dehydrogenase E1 component subunit alpha, somatic form, mitochondrial	*PDHA1*	-0.2887	-2.3811	-2.1680	-2.0924	9.57E-06
Protein disulfide-isomerase A3	*PDIA3*	2.2440	4.0449	3.6608	1.8008	5.01E-06
Phosphoglucomutase-1	*PGM1*	1.7556	0.1862	0.0038	-1.5695	7.01E-05
Prohibitin	*PHB*	1.2827	2.8465	3.0430	1.5638	9.47E-07
D-3-phosphoglycerate dehydrogenase	*PHGDH*	1.9678	-0.8964	-1.5676	-2.8642	7.46E-08
Pyruvate kinase PKM	*PKM*	2.9453	5.0940	4.9225	2.1487	1.63E-07
Plasminogen	*PLG*	1.9108	-0.4885	-1.9213	-2.3993	3.06E-05
Perilipin-1	*PLIN1*	4.4659	-2.8982	-2.4433	-7.3640	1.49E-10
Perilipin-4	*PLIN4*	3.6374	-5.2592	-5.7818	-8.8965	1.50E-07
Serum paraoxonase/arylesterase 1	*PON1*	0.6889	-1.6059	-3.2990	-2.2948	1.87E-07
Periostin	*POSTN*	2.6870	6.3962	6.6599	3.7092	1.29E-08
Peroxiredoxin-1	*PRDX1*	2.6855	4.1870	4.4239	1.5015	9.18E-07
Peroxiredoxin-2	*PRDX2*	3.9749	2.1224	2.2232	-1.8525	3.80E-06

Prolargin	*PRELP*	4.8785	3.2139	3.8117	-1.6646	1.15E-05
cAMP-dependent protein kinase type II-alpha regulatory subunit	*PRKAR2A*	2.1199	-0.1883	-0.5626	-2.3082	1.65E-02
cAMP-dependent protein kinase type II-beta regulatory subunit	*PRKAR2B*	0.8785	-1.4201	-1.0323	-2.2986	9.31E-07
Protein kinase C delta-binding protein	*PRKCDBP*	0.4444	-1.5609	-2.9268	-2.0053	8.29E-03
DNA-dependent protein kinase catalytic subunit	*PRKDC*	-0.1922	1.5011	1.9272	1.6933	1.03E-04
Pre-mRNA-processing-splicing factor 8	*PRPF8*	-1.8677	-0.2932	-0.2698	1.5745	3.78E-06
Proteasome activator complex subunit 1	*PSME1*	0.4624	2.3759	2.9383	1.9134	3.27E-07
Proteasome activator complex subunit 2	*PSME2*	-0.9478	0.7647	1.1228	1.7125	4.25E-05
Polypyrimidine tract-binding protein 1	*PTBP1*	-0.8922	1.3677	1.6058	2.2599	2.40E-07
Prostacyclin synthase	*PTGIS*	-0.6168	-4.2204	-3.8418	-3.6036	1.48E-08
Polymerase I and transcript release factor	*PTRF*	3.8445	0.8655	0.3079	-2.9790	2.45E-07
RNA-binding motif protein, X chromosome	*RBMX*	-1.5038	0.2185	0.1336	1.7223	1.68E-04
Retinol-binding protein 4	*RBP4*	-1.8033	-4.7505	-5.3913	-2.9472	7.58E-04
All-trans-retinol 13,14-reductase	*RETSAT*	-0.0800	-3.0121	-3.2020	-2.9321	1.44E-05
Aminopeptidase B	*RNPEP*	-1.4811	0.5614	1.6734	2.0426	3.98E-05
60S ribosomal protein L13	*RPL13*	-1.6845	-0.0528	0.7723	1.6317	2.54E-05
60S ribosomal protein L18	*RPL18*	-1.7992	0.6932	1.0535	2.4924	5.01E-05
60S ribosomal protein L3	*RPL3*	-1.3728	0.5731	-0.2382	1.9459	2.98E-06
60S ribosomal protein L4	*RPL4*	-0.7083	1.9934	2.0225	2.7017	2.82E-07
60S ribosomal protein L6	*RPL6*	-2.1260	1.2614	0.6111	3.3874	8.39E-06
60S ribosomal protein L7a	*RPL7A*	-0.7041	1.2934	0.8960	1.9975	2.36E-02
40S ribosomal protein S9	*RPS9*	0.1508	1.8094	1.9852	1.6586	5.55E-06
Ribosome-binding protein 1	*RRBP1*	-1.5699	0.3034	1.2376	1.8733	1.41E-04
tRNA-splicing ligase RtcB homolog	*RTCB*	-1.2926	0.2525	0.5822	1.5451	1.29E-03
RuvB-like 2	*RUVBL2*	-1.7026	0.4851	0.9080	2.1877	4.56E-06
Selenium-binding protein 1	*SELENBP1*	3.0459	1.1404	0.8430	-1.9055	1.28E-09
Heparin cofactor 2	*SERPIND1*	1.7438	-0.8025	-1.5065	-2.5463	5.39E-08
Alpha-2-antiplasmin	*SERPINF2*	0.4205	-2.2801	-2.6577	-2.7006	1.11E-03
SH3 domain-binding glutamic acid-rich-like protein	*SH3BGRL*	-0.6334	0.9192	0.8442	1.5526	2.74E-06
Tricarboxylate transport protein, mitochondrial	*SLC25A1*	0.9369	-0.7725	-0.8359	-1.7094	3.68E-05
Band 3 anion transport protein	*SLC4A1*	3.5527	-1.7120	-3.0736	-5.2647	5.09E-07
Na(+)/H(+) exchange regulatory cofactor NHE-RF1	*SLC9A3R1*	-2.8018	0.4771	1.0017	3.2788	8.36E-06
U5 small nuclear ribonucleoprotein 200 kDa helicase	*SNRNP200*	-2.3850	-0.4099	-0.0059	1.9751	1.57E-04
Sorbin and SH3 domain-containing protein 1	*SORBS1*	1.1217	-3.3356	-4.0979	-4.4572	9.33E-06
Sorbitol dehydrogenase	*SORD*	-1.4568	2.1199	1.3943	3.5766	2.76E-07
Spectrin beta chain, non-erythrocytic 1	*SPTBN1*	2.9910	1.4154	1.4726	-1.5756	1.72E-06
Serine/arginine-rich splicing factor 2	*SRSF2*	-2.0185	-0.2075	-0.3944	1.8110	3.80E-04
Serine/arginine-rich splicing factor 3	*SRSF3*	-1.9598	0.1341	0.3935	2.0939	3.90E-05
Serine/arginine-rich splicing factor 6	*SRSF6*	-1.7539	-0.2338	0.0059	1.5201	1.43E-02
Serine/arginine-rich splicing factor 7	*SRSF7*	-1.9797	-0.4400	-0.2969	1.5397	1.43E-03
Signal transducer and activator of transcription 1-alpha/beta	*STAT1*	-1.6160	1.9952	2.7418	3.6113	1.49E-06
Heterogeneous nuclear ribonucleoprotein Q	*SYNCRIP*	0.0641	1.8336	2.2367	1.7695	1.16E-06
Thrombospondin-1	*THBS1*	0.7646	3.1334	2.2863	2.3688	3.12E-07
Tenascin	*TNC*	0.5871	2.5731	0.8763	1.9860	3.48E-07
Tensin-1	*TNS1*	1.5678	-1.8431	-2.3624	-3.4109	4.31E-08
Tenascin-X	*TNXB*	1.3189	-3.6676	-4.6270	-4.9865	8.76E-07
Heat shock protein 75 kDa, mitochondrial	*TRAP1*	-2.5908	-0.9483	-0.5966	1.6426	3.99E-02
Tubulin--tyrosine ligase-like protein 12	*TTLL12*	-1.1334	1.1320	2.8059	2.2654	5.08E-09
Tubulin beta chain	*TUBB*	2.1900	3.8437	4.1848	1.6537	3.64E-05
Tubulin beta-4B chain	*TUBB4B*	3.5757	5.2204	5.4828	1.6447	3.52E-06
Thymidine phosphorylase	*TYMP*	-1.3742	1.9053	1.9692	3.2796	5.10E-05
Splicing factor U2AF 65 kDa subunit	*U2AF2*	-2.9283	-0.2138	-0.2659	2.7145	4.00E-04
UDP-glucose 6-dehydrogenase	*UGDH*	-0.2996	1.5473	1.7181	1.8469	6.22E-05
UTP--glucose-1-phosphate uridylyltransferase	*UGP2*	2.4714	0.8641	0.7377	-1.6073	1.08E-07
Valine--tRNA ligase	*VARS*	-1.6652	0.1034	1.1202	1.7686	1.90E-05

Supplementary File 3B. Functional annotation of the differentially expressed proteins identified in the MPT x MNT tissues' comparison. According to the functional classification of the PANTHER system v. 13.1, based on the gene ontology (GO) terms: A. Protein class; B. Molecular function; C. Biological process. According to the functional enrichment analysis of the DAVID v. 6.8 database: D. Top enriched biological processes (GO terms, p<0.05); E. Top enriched KEGG pathways (p<0.05).

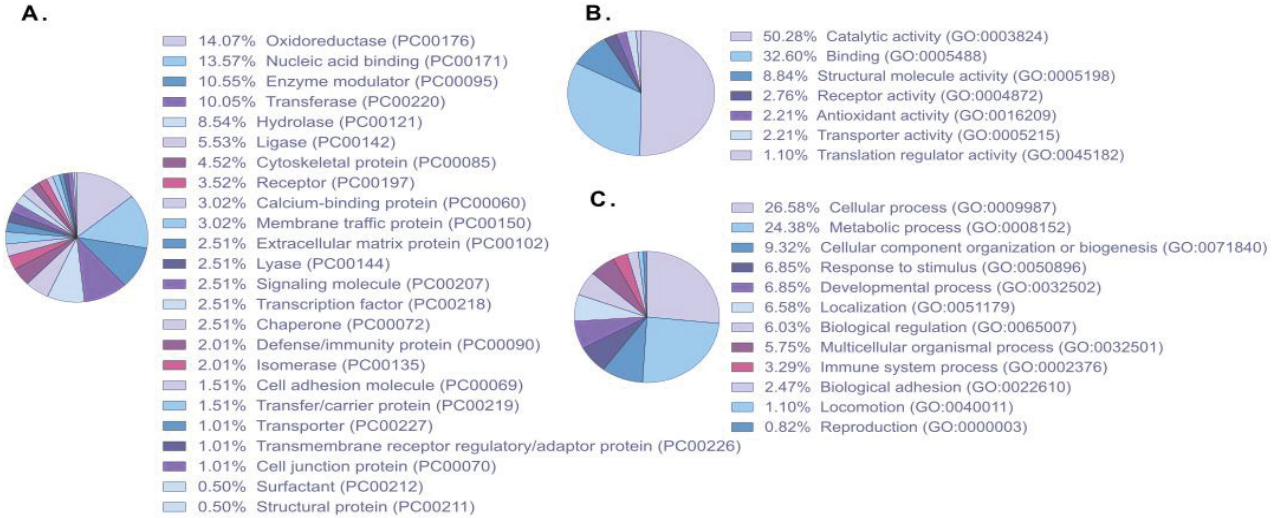

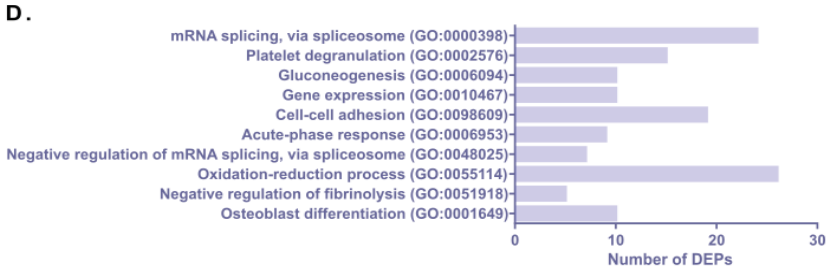

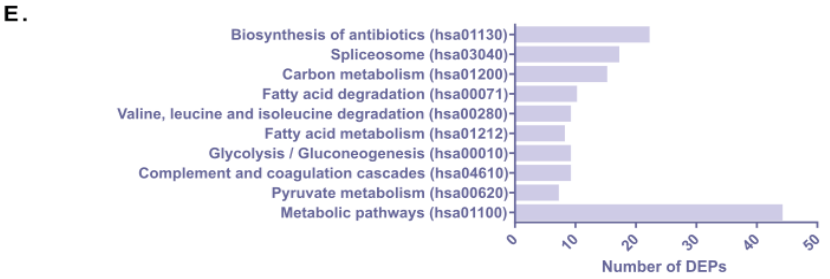

Supplementary File 3C. Main upstream regulators analysis of the differentially expressed proteins identified in the MPT x MNT tissues' comparison. (IPA analysis).

Upstream regulator	Molecule type	z-score	p-value	Gene symbol (target DEPs)
5-fluorouracil	Chemical drug	-3.4	1.36E-13	*ALDOA, ECHS1, FBL, GAPDH, GARS, GOT2, HNRNPA2B1, HNRNPAB, HSP90AB1, HSPA8, ILF2, NNT, PCBP1, PKM, PSME1, PSME2, RBMX, RPL18, RPL6, RPL7A, SRSF2, THBS1*
Dexamethasone	Chemical drug	-3.619	1.80E-09	*ACSL1, AGT, ALDH1A1, AP1G1, APOD, ASPH, C5, CAT, CAV1, CES1, CRABP2, CRYAB, CTSD, EZR, FABP4, FGG, FKBP4, FN1, GAPDH, GLUL, HNRNPAB, HSPA5, ILF2, ILF3, LBP, LRP1, MAOA, ME1, ORM1, POSTN, RBP4, SLC25A1, SPTBN1, STAT1, THBS1, TNC, VARS*
MYC	Transcription regulator	3.133	1.35E-08	*ASS1, CAV1, CSE1L, EZR, FASN, FBL, FMOD, FN1, GAPDH, HNRNPU, HSP90AA1, HSPA9, HSPB1, HSPD1, HSPH1, MTHFD1, NPM1, PHB, PKM, RPL6, RUVBL2, TRAP1*
Phytohemagglutinin	Chemical drug	-2.5	7.20E-08	*ADH5, AGT, AHSG, ALDH2, C5, CAT, COL18A1, FBN1, GPD1, GPD2, HSP90AA1, ITIH4, LBP, MAOA, PCYOX1, SLC4A1, STAT1*
Sirolimus	Chemical drug	-3.153	2.14E-07	*ACADM, ASS1, FASN, FN1, HNRNPU, HSP90AA1, HSP90AB1, HSPD1, LDHB, MYH11, NPM1, PKM, PLIN1, RPL18, RPL3, RPL7A, RPS9, SRSF3, STAT1*
CEBPB	Transcription regulator	-2.779	2.74E-06	*AGT, ALDH1A1, APOB, FABP4, HP, HSPD1, KRT18, LBP, ORM1, PLG, PRKAR2B*
Tretinoin	Chemical - endogenous mammalian	-2.012	3.68E-06	*ACSL1, ALDH1A1, APOD, APOE, CA2, CD36, CES1, CRABP2, CSE1L, DHX15, DSP, EEF1D, FN1, GARS, HNRNPD, HNRNPK, HSPB1, HSPD1, ILF3, KRT18, LTF, MYH9, NID2, NPM1, POSTN, PRDX2, PTGIS, RPL6, RUVBL2, STAT1, THBS1, TNC*
CD3	Complex	-3.729	8.45E-05	*ACADS, FBL, GAPDH, H2AFY, HNRNPA2B1, HNRNPR, HSP90AA1, HSPA8, ILF2, MDH2, NPM1, OGN, PCYOX1, PHB, RPL6, SRSF7, STAT1, THBS1*
Methotrexate	Chemical drug	-2.158	1.18E-04	*ACAA2, ACACB, ACADM, C5, CFH, ECHS1, LBP, LRP1, THBS1*
CD 437	Chemical drug	-3.162	1.39E-04	*ALDOA, HSP90AA1, HSPA8, ILF2, NPM1, PCBP1, PDIA3, RBMX, RPL13, SRSF3*
IFNG	Cytokine	2.959	3.17E-04	*AGT, ASS1, CAT, CD36, CSE1L, CTSD, DDX5, FAH, FASN, FN1, HSP90AB1, HSPA8, HSPG2, PHGDH, PRDX2, PRPF8, PSME1, PSME2, STAT1, THBS1, TYMP*
AR	Nuclear receptor	2.213	6.32E-04	*CAV1, CKAP4, FKBP4, GDI1, HSPA5, HSPH1, MAOA, SORD, STAT1, THBS1*
PI3K (family)	Group	2.433	9.56E-04	*CAT, CTSD, FASN, HSPA5, PKM, TNC*
PDGF BB	Complex	2.184	4.80E-03	*CNN1, FASN, MYH11, RPL13, SRSF7, THBS1, TNC*
CD28	Transmembrane receptor	-2.985	5.21E-03	*FBL, GAPDH, H2AFY, HSPA8, ILF2, PCYOX1, PHB, RPL6, THBS1*
SMARCA4	Transcription regulator	-2	7.27E-02	*AGR2, AGT, ALDH2, CALB2, FGG, FN1, GAPDH, KRT18, PARVA, TUBB*

Supplementary File 4A. Differentially expressed proteins into the log2 fold change values identified for MPT x MLN tissues' comparison according to the ANOVA's test.

LFQ intensities were log2-transformed and normalized by width adjustment in Perseus v. 1.5.6.0. Fold changes were presented in log2 values (up-regulated and down-regulated proteins were highlighted in red and green, respectively).

Protein Name	Gene Symbol	MNT LFQ_mean	MPT LFQ_mean2	MLN LFQ_mean	MPT x MLN fold change	ANOVA p-value
Alpha-2-HS-glycoprotein	*AHSG*	1.1837	-1.4220	-3.9872	2.5652	4.35E-07
Asporin	*ASPN*	3.6409	2.6202	0.4874	2.1328	2.14E-07
Carbonic anhydrase 2	*CA2*	3.0463	0.4364	2.3018	-1.8654	3.57E-07
Calreticulin	*CALR*	-0.2689	0.1178	1.7525	-1.6347	5.77E-05
Complement factor H	*CFH*	1.8955	0.2190	-1.3321	1.5511	4.35E-06
Chymase	*CMA1*	1.0482	-0.2228	-4.4853	4.2625	4.19E-05
Calponin-1	*CNN1*	2.3538	-0.0842	-2.7271	2.6429	8.57E-06
Collagen alpha-1(XII) chain	*COL12A1*	2.2517	4.7556	3.0561	1.6995	8.88E-09
Collagen alpha-1(XIV) chain	*COL14A1*	3.7213	3.8950	1.7020	2.1930	2.88E-06
Mast cell carboxypeptidase A	*CPA3*	1.9123	0.3349	-3.2596	3.5946	2.90E-08
Cathepsin G	*CTSG*	0.7956	-0.5105	-3.6005	3.0900	1.15E-06
Dehydrogenase/reductase SDR family member 2, mitochondrial	*DHRS2*	-2.7286	-1.1462	1.6987	-2.8449	1.28E-05
Fibromodulin	*FMOD*	0.7103	-2.1584	-4.1646	2.0062	1.78E-05
Histone H1.0	*H1F0*	-2.2492	-0.0541	-2.0838	2.0296	5.98E-05
Lactotransferrin	*LTF*	2.3578	-3.6759	-5.4587	1.7829	3.20E-07
Methylcrotonoyl-CoA carboxylase beta chain, mitochondrial	*MCCC2*	-1.4150	0.4662	-1.1181	1.5843	2.71E-05
Myosin-11	*MYH11*	3.4640	1.9041	-0.0918	1.9960	1.29E-07
Nicotinamide N-methyltransferase	*NNMT*	-2.0795	0.0543	-1.6304	1.6847	1.50E-04
Mimecan	*OGN*	5.0148	2.9127	0.7526	2.1600	1.43E-06
Phosphatidylethanolamine-binding protein 1	*PEBP1*	1.9676	2.0091	3.7814	-1.7723	1.79E-05
Purine nucleoside phosphorylase	*PNP*	1.3906	1.7133	3.3444	-1.6311	1.07E-07
Serum paraoxonase/arylesterase 1	*PON1*	0.6889	-1.6059	-3.2990	1.6931	1.87E-07
Tenascin	*TNC*	0.5871	2.5731	0.8763	1.6968	3.48E-07
Tubulin--tyrosine ligase-like protein 12	*TTLL12*	-1.1334	1.1320	2.8059	-1.6739	5.08E-09
Thioredoxin domain-containing protein 5	*TXNDC5*	-1.5932	-0.7872	1.4591	-2.2464	2.88E-06

Supplementary File 4B. Functional annotation of the differentially expressed proteins identified in the MPT x MLN tissues' comparison. According to the functional classification of the PANTHER system v. 13.1, based on the gene ontology (GO) terms: A. Protein class; B. Molecular function; C. Biological process. According to the functional enrichment analysis of the DAVID v. 6.8 database: D. Top enriched biological processes (GO terms, p<0.05); E. Top enriched KEGG pathways (p<0.05).

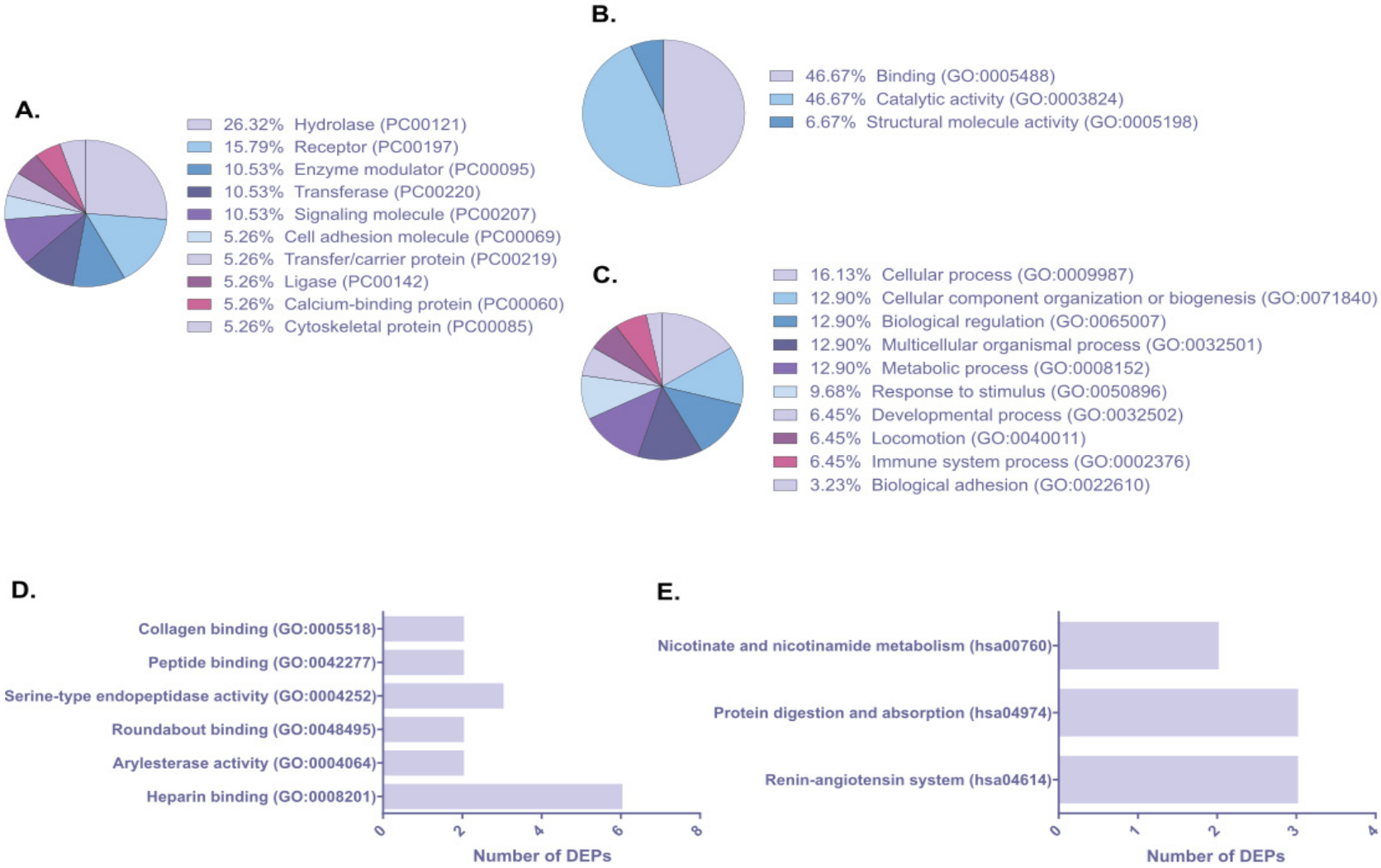

Supplementary File 4C. Main upstream regulators analysis of the differentially expressed proteins identified in the MPT x MLN tissues' comparison. (IPA analysis).

Upstream regulator	Molecule type	p-value	Gene symbol (target DEPs)
IGFBP2	Other	1.05E-03	*COL14A1, POSTN*
miR-146a-5p (and other miRNAs w/seed GAGAACU)	Mature microRNA	1.48E-03	*CFH, LTF*
MYOCD	Transcription regulator	2.22E-03	*CNN1, MYH11*
OLFM2	Other	3.88E-03	*MYH11*
HEY2	Transcription regulator	3.88E-03	*MYH11*
NKX2-3	Transcription regulator	5.17E-03	*MYH11*
HEYL	Transcription regulator	5.17E-03	*MYH11*
SBDS	Other	5.39E-03	*COL14A1, TNC*
PDGFRB	Kinase	6.46E-03	*MYH11*
CPXM1	Peptidase	7.75E-03	*COL14A1*
HEY1	Transcription regulator	9.03E-03	*MYH11*
MEMO1	Other	1.03E-02	*CA2*
ELF4	Transcription regulator	2.05E-02	*CA2*

Supplementary File 5A. Reproducibility of the technical replicates from MPT x FPT tissues' comparison.

A. Pearson correlation analysis between the primary breast tumor tissues of the male and female patients based on LFQ intensity values of the 1,340 identified proteins. **B.** Hierarchical clustering analysis from differentially expressed proteins of these group of samples (n= 447).

Legend: MPT - male primary tumor; FPT - female primary tumor.

I.

Technical Replicates	FPT_1	FPT_2	FPT_3
MPT_1	0.7300	0.7358	0.7316
MPT_2	0.7138	0.7185	0.7207
MPT_3	0.7152	0.7213	0.7233

Pearson's coefficient average= 0.7233

II.

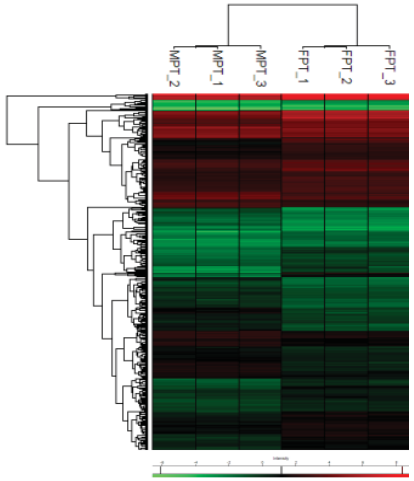

Supplementary File 5B. Differentially expressed proteins identified for MPT x FPT tissues' comparison according to the ANOVA's test.
LFQ intensities were log2-transformed and normalized by width adjustment in Perseus v. 1.5.6.0. Fold changes were presented in log2 values (up-regulated and down-regulated proteins were highlighted in red and green, respectively).
* Fold change values of the common DEPs among the MPT x FPT tissues' comparison and the groups of samples of the MBC case.

Protein Name	Gene Symbol	MPT LFQ_mean	FPT LFQ_mean2	MPT X FPT fold change	DEPs in the MPT x MNT group' comparison*	DEPs in the MPT x MLN group' comparison*	Student's T-test p-value
Alpha-2-macroglobulin	*A2M*	5.0161	4.3416	0.6745	-	-	1.40E-04
ATP-binding cassette sub-family F member 1	*ABCF1*	-2.5187	-0.6231	-1.8956	-	-	3.90E-04
Alpha/beta hydrolase domain-containing protein 11	*ABHD11*	-1.2856	-0.0770	-1.2086	-	-	4.84E-03
3-ketoacyl-CoA thiolase, mitochondrial	*ACAA2*	-0.3140	0.6086	-0.9226	-	-	1.22E-02
Short/branched chain specific acyl-CoA dehydrogenase, mitochondrial	*ACADSB*	0.9559	-0.6869	1.6428	1.8968	-0.2522	4.95E-03
Acetyl-CoA acetyltransferase, mitochondrial	*ACAT1*	1.5971	0.8435	0.7537	-	-	9.44E-04
ATP-citrate synthase	*ACLY*	1.8925	0.8409	1.0516	-	-	8.34E-04
Cytoplasmic aconitate hydratase	*ACO1*	0.2616	0.7040	-0.4424	-	-	8.92E-03
Peroxisomal acyl-coenzyme A oxidase 1	*ACOX1*	-1.1355	-0.0136	-1.1219	-	-	1.32E-03
Peroxisomal acyl-coenzyme A oxidase 3	*ACOX3*	0.3391	-1.7828	2.1219	-	-	2.07E-04
Alpha-actinin-1	*ACTN1*	4.7825	4.5063	0.2762	-	-	1.34E-02
Alpha-adducin	*ADD1*	-1.0680	-1.7314	0.6634	-	-	1.01E-02
Alcohol dehydrogenase 1B	*ADH1B*	1.4832	3.6222	-2.1390	-	-	2.38E-05
AFG3-like protein 2	*AFG3L2*	-2.5840	-1.5950	-0.9890	-	-	1.59E-02
Anterior gradient protein 2 homolog	*AGR2*	2.0072	0.4975	1.5097	3.2997	-	7.53E-04
Neuroblast differentiation-associated protein AHNAK	*AHNAK*	4.2724	5.9618	-1.6893	-0.3570	-	2.64E-06
Alcohol dehydrogenase [NADP(+)]	*AKR1A1*	0.4031	1.7732	-1.3701	-	-	1.27E-03
Aldehyde dehydrogenase X, mitochondrial	*ALDH1B1*	0.3832	-0.9418	1.3250	-	-	1.52E-02
Aldehyde dehydrogenase, mitochondrial	*ALDH2*	2.3017	2.7839	-0.4822	-	-	4.92E-03
Methylmalonate-semialdehyde dehydrogenase [acylating], mitochondrial	*ALDH6A1*	-1.7514	-0.8398	-0.9115	-	-	1.92E-03
Alpha-aminoadipic semialdehyde dehydrogenase	*ALDH7A1*	-0.1528	0.6992	-0.8520	-	-	6.48E-03
4-trimethylaminobutyraldehyde dehydrogenase	*ALDH9A1*	2.4366	1.6649	0.7717	-	-	1.27E-04
THO complex subunit 4	*ALYREF*	-0.3014	-0.6667	0.3653	-	-	8.15E-03
Aminopeptidase N	*ANPEP*	-0.1256	-1.2830	1.1574	-	-	9.37E-03
Membrane primary amine oxidase	*AOC3*	-0.7897	0.8172	-1.6069	-	-	3.74E-03
AP-1 complex subunit gamma-1	*AP1G1*	-0.3119	-0.8034	0.4915	-	-	9.09E-03
Apoptosis inhibitor 5	*API5*	-0.5896	0.0004	-0.5900	-	-	8.02E-04
Adipocyte plasma membrane-associated protein	*APMAP*	1.2874	1.8894	-0.6020	-	-	1.93E-03
NAD(P)H-hydrate epimerase	*APOA1BP*	-0.4482	-0.9260	0.4777	-	-	1.61E-02
Apolipoprotein D	*APOD*	-0.0080	-1.0230	1.0150	-	-	1.80E-03
Adenine phosphoribosyltransferase	*APRT*	0.4931	-0.5676	1.0607	-	-	2.87E-04
Rho GDP-dissociation inhibitor 1	*ARHGDIA*	3.4667	2.5785	0.8882	-	-	2.59E-03
Rho GDP-dissociation inhibitor 2	*ARHGDIB*	1.5445	2.5443	-0.9999	-	-	8.29E-04
Actin-related protein 2/3 complex subunit 3	*ARPC3*	-0.3667	0.4675	-0.8342	-	-	7.15E-04
Asporin	*ASPN*	3.4383	4.2753	-0.8370	-	-	1.67E-03
Argininosuccinate synthase	*ASS1*	-3.3604	-4.2398	0.8794	-	-	1.44E-02
Atlastin-3	*ATL3*	-0.0113	-0.2795	0.2682	-	-	1.55E-02
Sodium/potassium-transporting ATPase subunit alpha-1	*ATP1A1*	0.6741	-0.9141	1.5882	0.4076	-	1.06E-03
Sarcoplasmic/endoplasmic reticulum calcium ATPase 2	*ATP2A2*	-0.2748	0.0934	-0.3682	-	-	1.24E-02
ATP synthase subunit O, mitochondrial	*ATP5O*	1.6865	1.2763	0.4102	-	-	1.84E-02
V-type proton ATPase catalytic subunit A	*ATP6V1A*	0.9713	0.5839	0.3874	-	-	1.77E-02
V-type proton ATPase subunit C 1	*ATP6V1C1*	-1.7687	-1.4007	-0.3680	-	-	1.24E-02
B-cell receptor-associated protein 31	*BCAP31*	-1.1236	-3.5070	2.3834	-	-	1.34E-02
Biglycan	*BGN*	4.3799	6.0987	-1.7188	-0.5469	-	6.25E-06
3(2),5-bisphosphate nucleotidase 1	*BPNT1*	0.2579	-0.8002	1.0581	-	-	1.20E-03
Basic leucine zipper and W2 domain-containing protein 2	*BZW2*	-2.7607	-2.1848	-0.5758	-	-	1.01E-02
Complement C1q subcomponent subunit B	*C1QB*	-0.3905	0.0357	-0.4262	-	-	1.24E-02
Complement component C8 beta chain	*C8B*	-1.7498	-0.3261	-1.4236	-	-	8.16E-05
Carbonic anhydrase 1	*CA1*	2.4413	3.0933	-0.6520	-	-	4.92E-03
Calcyclin-binding protein	*CACYBP*	1.9023	0.2008	1.7014	2.3055	-0.2961	7.55E-05
Caldesmon	*CALD1*	2.1620	0.8959	1.2661	-	-	9.22E-05
Calreticulin	*CALR*	1.2215	2.3227	-1.1012	-	-	3.76E-05
Cullin-associated NEDD8-dissociated protein 1	*CAND1*	3.3795	2.5571	0.8225	-	-	1.03E-04
Calnexin	*CANX*	3.3149	2.6058	0.7091	-	-	6.58E-04
Adenylyl cyclase-associated protein 1	*CAP1*	2.1937	3.1861	-0.9924	-	-	7.13E-04
Calpain-2 catalytic subunit	*CAPN2*	-2.7287	-1.9845	-0.7442	-	-	1.77E-02
Carbonyl reductase [NADPH] 1	*CBR1*	1.0447	2.3642	-1.3195	-	-	2.81E-05
T-complex protein 1 subunit eta	*CCT7*	1.5647	0.8969	0.6678	-	-	4.12E-03
T-complex protein 1 subunit theta	*CCT8*	2.2690	2.6367	-0.3677	-	-	6.25E-03
Platelet glycoprotein 4	*CD36*	-2.9145	-0.2444	-2.6701	-7.2565	-	1.18E-02
CD44 antigen	*CD44*	0.0490	-0.7356	0.7847	-	-	1.07E-02
HLA class II histocompatibility antigen gamma chain	*CD74*	-1.1122	-0.5013	-0.6108	-	-	1.18E-02
Liver carboxylesterase 1	*CES1*	-1.3149	-2.9707	1.6558	-3.2802	0.5293	9.54E-03
Cofilin-1	*CFL1*	3.5838	4.8224	-1.2386	-	-	8.59E-04
Cold-inducible RNA-binding protein	*CIRBP*	-1.4318	0.2266	-1.6584	-	-	1.72E-03
Cytoskeleton-associated protein 4	*CKAP4*	2.4716	1.4232	1.0483	-	-	6.92E-03
Creatine kinase B-type	*CKB*	-1.2395	0.0712	-1.3108	-	-	3.49E-04
Chloride intracellular channel protein 1	*CLIC1*	2.5736	3.3415	-0.7678	-	-	1.76E-03
Collagen alpha-1(XII) chain	*COL12A1*	5.5918	4.5204	1.0714	-	-	1.25E-04
Collagen alpha-1(XIV) chain	*COL14A1*	4.5810	4.8660	-0.2849	-	-	1.88E-03
Collagen alpha-1(I) chain	*COL1A1*	2.4567	3.4756	-1.0189	-	-	2.12E-03
Collagen alpha-1(VI) chain	*COL6A1*	5.9465	6.8503	-0.9038	-	-	1.57E-03
Collagen alpha-2(VI) chain	*COL6A2*	5.0524	5.9200	-0.8676	-	-	1.99E-04
Collagen alpha-3(VI) chain	*COL6A3*	7.8317	8.7937	-0.9620	-	-	5.66E-04
Collagen alpha-6(VI) chain	*COL6A6*	-2.9252	-0.3331	-2.5921	-	-	7.65E-04
Coatomer subunit beta	*COPB2*	0.9255	0.1337	0.7918	-	-	1.91E-02
Coatomer subunit epsilon	*COPE*	0.5003	-0.2799	0.7803	-	-	9.98E-03
Coatomer subunit gamma-1	*COPG1*	1.3479	0.7284	0.6195	-	-	1.04E-02
Coatomer subunit zeta-1	*COPZ1*	-0.5457	-1.5883	1.0426	-	-	6.87E-03
Coronin-1B	*CORO1B*	-1.1713	0.0029	-1.1742	-	-	1.35E-02
Cytochrome c oxidase subunit 7A2, mitochondrial	*COX7A2*	-3.9441	-0.5258	-3.4183	-	-	8.16E-04
Ceruloplasmin	*CP*	2.7502	2.5904	0.1598	-	-	1.31E-02
Mast cell carboxypeptidase A	*CPA3*	1.1203	1.8109	-0.6906	-	-	2.62E-03
Copine-1	*CPNE1*	-1.0016	1.2576	-2.2592	-	-	1.19E-05
Cellular retinoic acid-binding protein 2	*CRABP2*	2.3338	1.7138	0.6199	-	-	3.56E-03
Cysteine-rich protein 2	*CRIP2*	0.5834	-0.6666	1.2500	-	-	2.75E-04
Alpha-crystallin B chain	*CRYAB*	-2.7753	-0.6785	-2.0967	-5.9603	-	1.82E-02
Cystatin-B	*CSTB*	0.7728	2.3550	-1.5822	-	-	5.57E-04
Catenin beta-1	*CTNNB1*	0.0831	-0.8898	0.9729	-	-	1.54E-03
Cathepsin G	*CTSG*	0.3942	-0.4691	0.8633	-	-	8.75E-03
Src substrate cortactin	*CTTN*	-0.4857	0.2003	-0.6861	-	-	1.23E-03
Cullin-4B	*CUL4B*	-2.7455	-3.6434	0.8979	-	-	1.52E-03
Cytochrome b5	*CYB5A*	1.8156	-0.7702	2.5857	-0.7213	0.5819	3.79E-04
NADH-cytochrome b5 reductase 1	*CYB5R1*	1.6114	-0.4381	2.0495	1.6344	-0.7116	2.09E-03
Aspartate--tRNA ligase, cytoplasmic	*DARS*	1.2667	0.4790	0.7877	-	-	1.59E-03
Decorin	*DCN*	4.2853	5.9114	-1.6261	-1.2872	0.9312	2.23E-04
L-xylulose reductase	*DCXR*	1.4109	-1.0453	2.4562	-	-	9.30E-04
N(G),N(G)-dimethylarginine dimethylaminohydrolase 2	*DDAH2*	0.0616	1.3349	-1.2733	-	-	4.30E-03
Nucleolar RNA helicase 2	*DDX21*	-1.8092	-0.2328	-1.5763	-	-	1.05E-06
Spliceosome RNA helicase DDX39B	*DDX39B*	2.7164	3.3799	-0.6634	-	-	1.48E-03
2,4-dienoyl-CoA reductase, mitochondrial	*DECR1*	0.7701	0.1629	0.6072	-	-	3.09E-04

Dehydrogenase/reductase SDR family member 2, mitochondrial	*DHRS2*	0.0103	2.2650	-2.2547	1.5824	-2.8449	2.32E-04
Dehydrogenase/reductase SDR family member 7	*DHRS7*	0.0148	-1.2321	1.2468	-	-	3.71E-03
Pre-mRNA-splicing factor ATP-dependent RNA helicase DHX15	*DHX15*	0.9471	1.8420	-0.8949	-	-	2.14E-03
Dihydrolipoyllysine-residue succinyltransferase component of 2-oxoglutarate dehydrogenase complex, ı	*DLST*	-0.1809	1.2664	-1.4473	-	-	1.89E-03
Dynamin-2	*DNM2*	0.3911	1.2330	-0.8420	-	-	5.38E-03
Dihydropyrimidinase-related protein 2	*DPYSL2*	2.3827	3.1678	-0.7851	-	-	4.85E-04
Dihydropyrimidinase-related protein 3	*DPYSL3*	2.7350	2.0078	0.7273	-	-	5.42E-04
Destrin	*DSTN*	0.7585	0.1710	0.5875	-	-	9.47E-03
E3 ubiquitin-protein ligase DTX3L	*DTX3L*	-3.6787	-4.7596	1.0809	-	-	6.15E-03
Cytoplasmic dynein 1 heavy chain 1	*DYNC1H1*	1.9115	2.5631	-0.6516	-	-	4.54E-03
Delta(3,5)-Delta(2,4)-dienoyl-CoA isomerase, mitochondrial	*ECH1*	0.0951	1.6037	-1.5086	-1.1853	-	3.54E-04
Elongation factor 1-gamma	*EEF1G*	2.7371	2.9948	-0.2577	-	-	9.71E-03
Elongation factor 2	*EEF2*	3.8856	4.3989	-0.5134	-	-	1.10E-03
EF-hand domain-containing protein D1	*EFHD1*	1.0735	-0.6262	1.6996	2.1205	-0.4928	4.21E-05
EH domain-containing protein 1	*EHD1*	0.0093	0.8366	-0.8274	-	-	1.49E-03
EH domain-containing protein 2	*EHD2*	1.7961	2.6708	-0.8748	-	-	2.30E-05
Interferon-induced, double-stranded RNA-activated protein kinase	*EIF2AK2*	-0.9141	-1.5391	0.6250	-	-	1.98E-02
Eukaryotic translation initiation factor 3 subunit A	*EIF3A*	0.4733	0.9435	-0.4702	-	-	8.97E-03
Eukaryotic translation initiation factor 3 subunit B	*EIF3B*	0.2926	1.3951	-1.1025	-	-	1.02E-02
Eukaryotic translation initiation factor 3 subunit G	*EIF3G*	-1.2738	-0.8864	-0.3875	-	-	1.05E-02
Eukaryotic translation initiation factor 3 subunit H	*EIF3H*	-1.2980	-2.5674	1.2694	-	-	2.61E-05
Eukaryotic translation initiation factor 3 subunit M	*EIF3M*	-0.0406	-1.3673	1.3266	-	-	7.06E-03
Eukaryotic initiation factor 4A-I	*EIF4A1*	3.5104	4.0940	-0.5836	-	-	3.29E-03
EMILIN-1	*EMILIN1*	0.8079	1.9785	-1.1706	-	-	6.06E-04
Alpha-enolase	*ENO1*	4.9531	5.8646	-0.9115	-	-	1.34E-04
Enolase-phosphatase E1	*ENOPH1*	-1.3233	-0.9466	-0.3767	-	-	6.88E-03
Endoplasmic reticulum aminopeptidase 1	*ERAP1*	-1.0289	-0.3242	-0.7047	-	-	6.66E-03
Erlin-2	*ERLIN2*	0.0901	1.6844	-1.5943	-0.9866	-	8.38E-04
Endoplasmic reticulum resident protein 29	*ERP29*	1.1437	1.8840	-0.7404	-	-	2.03E-03
Epithelial splicing regulatory protein 1	*ESRP1*	-2.0513	-2.5133	0.4620	-	-	1.43E-02
Ezrin	*EZR*	0.5910	1.4527	-0.8618	-	-	1.05E-02
Coagulation factor XIII A chain	*F13A1*	1.2220	1.8292	-0.6072	-	-	1.70E-03
Fatty acid-binding protein, adipocyte	*FABP4*	-0.8351	2.6886	-3.5237	-5.8985	-	3.01E-06
Fumarylacetoacetase	*FAH*	-1.4730	-2.4528	0.9798	-	-	1.11E-02
Acylpyruvase FAHD1, mitochondrial	*FAHD1*	-1.8658	-0.8957	-0.9700	-	-	3.55E-04
rRNA 2-O-methyltransferase fibrillarin	*FBL*	1.8225	1.2525	0.5700	-	-	2.36E-03
Fibulin-1	*FBLN1*	1.6389	1.1659	0.4730	-	-	1.63E-02
Fibulin-2	*FBLN2*	0.4642	-0.8255	1.2897	-	-	8.12E-04
Fibrillin-1	*FBN1*	1.6378	2.2162	-0.5784	-	-	4.20E-04
NADPH:adrenodoxin oxidoreductase, mitochondrial	*FDXR*	-1.2093	-2.8484	1.6391	-	-	9.27E-04
Fermitin family homolog 3	*FERMT3*	-1.3385	-0.5198	-0.8187	-	-	1.41E-02
Fumarate hydratase, mitochondrial	*FH*	1.6351	0.7240	0.9111	-	-	5.52E-03
Peptidyl-prolyl cis-trans isomerase FKBP3	*FKBP3*	-0.3816	-1.4602	1.0786	-	-	1.67E-02
Filamin-B	*FLNB*	4.0044	3.3944	0.6101	-	-	2.54E-03
Flotillin-1	*FLOT1*	-2.4609	0.9676	-3.4285	-	-	4.20E-05
Flotillin-2	*FLOT2*	-1.9891	0.3401	-2.3292	-	-	5.15E-04
Ferritin light chain	*FTL*	3.4154	2.3343	1.0811	-	-	8.39E-03
Glucose-6-phosphate 1-dehydrogenase	*G6PD*	2.4957	1.9337	0.5620	-	-	5.99E-04
Glycine--tRNA ligase	*GARS*	0.0397	0.4277	-0.3880	-	-	7.37E-03
Vitamin D-binding protein	*GC*	2.4064	2.7817	-0.3754	-	-	8.84E-03
Glutamate--cysteine ligase catalytic subunit	*GCLC*	-2.9280	-2.6076	-0.3204	-	-	2.01E-02
Rab GDP dissociation inhibitor alpha	*GDI1*	1.3717	0.1883	1.1834	-	-	1.62E-03
Rab GDP dissociation inhibitor beta	*GDI2*	3.1020	3.6392	-0.5373	-	-	9.00E-04
GTPase IMAP family member 4	*GIMAP4*	-2.2395	-0.0522	-2.1873	-	-	2.26E-03
Lactoylglutathione lyase	*GLO1*	-0.5944	1.0580	-1.6524	-0.6878	-0.7245	1.40E-03
Glutaredoxin-3	*GLRX3*	-1.6201	-0.9033	-0.7168	-	-	8.22E-03
Mannose-1-phosphate guanyltransferase beta	*GMPPB*	-0.9291	-1.8160	0.8869	-	-	6.36E-05
Guanine nucleotide-binding protein-like 1	*GNL1*	-2.9649	-1.4900	-1.4749	-	-	6.13E-03
Vesicle transport protein GOT1B	*GOLT1B*	-2.3833	-3.9432	1.5599	1.3264	-	1.05E-03
Glycerol-3-phosphate dehydrogenase [NAD(+)], cytoplasmic	*GPD1*	-1.4401	0.5090	-1.9491	-7.9373	-	3.08E-03
Glycerol-3-phosphate dehydrogenase 1-like protein	*GPD1L*	-1.3591	-2.1787	0.8196	-	-	3.37E-03
Glycerol-3-phosphate dehydrogenase, mitochondrial	*GPD2*	0.7261	-0.4451	1.1712	-	-	6.71E-05
Growth factor receptor-bound protein 2	*GRB2*	-0.2404	0.6368	-0.8772	-	-	8.53E-03
Glyoxylate reductase/hydroxypyruvate reductase	*GRHPR*	0.8515	-0.0754	0.9269	-	-	1.06E-03
Gelsolin	*GSN*	3.5548	3.1387	0.4161	-	-	1.10E-02
Glutathione S-transferase kappa 1	*GSTK1*	1.4627	0.8212	0.6415	-	-	1.57E-03
Glutathione S-transferase omega-1	*GSTO1*	0.3938	1.0464	-0.6527	-	-	1.17E-02
Glutathione S-transferase P	*GSTP1*	2.6552	3.2842	-0.6290	-	-	2.04E-03
Histone H1x	*H1FX*	0.5312	1.0121	-0.4808	-	-	1.28E-02
Very-long-chain (3R)-3-hydroxyacyl-CoA dehydratase 3	*HACD3*	0.6071	-1.3897	1.9969	0.9497	-	7.37E-05
Hydroxyacyl-coenzyme A dehydrogenase, mitochondrial	*HADH*	0.0437	1.0027	-0.9590	-	-	2.33E-03
Hydroxyacylglutathione hydrolase, mitochondrial	*HAGH*	-1.2344	-2.1359	0.9015	-	-	6.61E-03
Hemoglobin subunit alpha	*HBA1*	6.3265	7.8108	-1.4843	-	-	2.11E-04
Hemoglobin subunit delta	*HBD*	1.1664	3.1624	-1.9960	-3.3944	-	1.99E-04
Vigilin	*HDLBP*	1.8893	0.7358	1.1534	-	-	2.77E-03
HEAT repeat-containing protein 6	*HEATR6*	-6.4921	-5.2735	-1.2186	-	-	7.01E-03
Heme-binding protein 1	*HEBP1*	0.8179	-1.8237	2.6415	-	-	9.57E-04
Protein HID1	*HID1*	-1.4451	-2.9985	1.5534	-	-	3.29E-03
Histidine triad nucleotide-binding protein 2, mitochondrial	*HINT2*	-1.1288	-2.0250	0.8962	-	-	1.75E-02
Histone H1.4	*HIST1H1E*	3.6823	4.5532	-0.8709	-	-	1.76E-03
Histone H4	*HIST1H4A*	6.5573	8.2004	-1.6431	1.3973	-	2.86E-04
Hexokinase-1	*HK1*	1.8817	2.5936	-0.7118	-	-	3.29E-05
HLA class II histocompatibility antigen, DR alpha chain	*HLA-DRA*	-0.1484	1.0750	-1.2234	-	-	4.69E-03
High mobility group protein B2	*HMGB2*	-1.0060	-2.2201	1.2141	-	-	4.50E-03
Heterogeneous nuclear ribonucleoproteins A2/B1	*HNRNPA2B1*	4.3954	4.7191	-0.3236	-	-	7.24E-03
Heterogeneous nuclear ribonucleoprotein A3	*HNRNPA3*	2.4569	3.1470	-0.6900	-	-	1.24E-02
Heterogeneous nuclear ribonucleoprotein A/B	*HNRNPAB*	0.7106	1.3091	-0.5984	-	-	5.04E-03
Heterogeneous nuclear ribonucleoprotein M	*HNRNPM*	2.5827	3.3492	-0.7665	-	-	2.29E-03
Heterochromatin protein 1-binding protein 3	*HP1BP3*	0.7390	1.6605	-0.9215	-	-	6.74E-03
Hemopexin	*HPX*	1.9109	4.0340	-2.1231	-	-	9.33E-04
Histidine-rich glycoprotein	*HRG*	1.4133	2.1202	-0.7069	-	-	5.54E-04
Very-long-chain 3-oxoacyl-CoA reductase	*HSD17B12*	-0.8248	0.0593	-0.8840	-	-	1.73E-02
Heat shock protein HSP 90-alpha	*HSP90AA1*	4.9491	4.4529	0.4963	-	-	5.02E-04
Endoplasmin	*HSP90B1*	4.6255	4.8662	-0.2408	-	-	3.18E-04
Heat shock-related 70 kDa protein 2	*HSPA2*	-0.5653	-2.8865	2.3211	0.5626	-	2.62E-05
Heat shock 70 kDa protein 4	*HSPA4*	0.9691	0.0839	0.8853	-	-	3.08E-03
78 kDa glucose-regulated protein	*HSPA5*	4.8443	5.2348	-0.3905	-	-	7.90E-03
Stress-70 protein, mitochondrial	*HSPA9*	4.3471	3.3963	0.9508	-	-	1.09E-03
Heat shock protein beta-1	*HSPB1*	5.4058	4.0873	1.3186	-	-	1.23E-04
60 kDa heat shock protein, mitochondrial	*HSPD1*	5.1710	4.6922	0.4788	-	-	7.52E-03
Heat shock protein 105 kDa	*HSPH1*	1.3000	0.3542	0.9458	-	-	1.45E-03
Hypoxia up-regulated protein 1	*HYOU1*	1.0004	1.7578	-0.7574	-	-	5.62E-04
Isoleucine--tRNA ligase, mitochondrial	*IARS2*	1.7856	-0.2877	2.0733	1.3510	-1.1017	5.48E-04
Intercellular adhesion molecule 1	*ICAM1*	-2.7569	-0.9822	-1.7747	-	-	1.58E-03
Interferon-induced protein with tetratricopeptide repeats 1	*IFIT1*	0.0735	-1.5665	1.6400	-	-	1.04E-03
Insulin-like growth factor-binding protein complex acid labile subunit	*IGFALS*	-2.7145	-1.8051	-0.9094	-	-	1.75E-04
Ig gamma-4 chain C region	*IGHG4*	2.3908	4.3171	-1.9263	-1.4879	0.8844	1.19E-03
Ig kappa chain C region	*IGKC*	4.9988	5.5486	-0.5499	-	-	1.74E-03

Interleukin enhancer-binding factor 2	*ILF2*	2.2380	3.5718	-1.3338	-	-	1.50E-03
Interleukin enhancer-binding factor 3	*ILF3*	1.4978	2.7417	-1.2439	-	-	1.36E-04
Inverted formin-2	*INF2*	-4.4475	-4.0507	-0.3968	-	-	1.37E-02
Type II inositol 3,4-bisphosphate 4-phosphatase	*INPP4B*	-1.7958	-3.9699	2.1741	-	-	1.10E-04
Importin-4	*IPO4*	-2.2897	-0.0808	-2.2089	-	-	9.36E-05
Importin-5	*IPO5*	-0.0041	0.2329	-0.2370	-	-	5.74E-03
Isochorismatase domain-containing protein 2, mitochondrial	*ISOC2*	-0.5641	-3.1321	2.5680	0.8023	-0.7554	3.33E-04
Inositol-3-phosphate synthase 1	*ISYNA1*	-2.2436	-1.4688	-0.7748	-	-	7.56E-04
Inter-alpha-trypsin inhibitor heavy chain H1	*ITIH1*	1.6454	3.4690	-1.8236	-0.6891	-0.3507	3.10E-04
Inter-alpha-trypsin inhibitor heavy chain H2	*ITIH2*	2.1574	2.8819	-0.7244	-	-	3.82E-04
BTB/POZ domain-containing protein KCTD12	*KCTD12*	0.6244	1.4348	-0.8104	-	-	2.72E-03
Far upstream element-binding protein 2	*KHSRP*	-0.1110	1.2768	-1.3878	-	-	6.82E-03
Importin subunit beta-1	*KPNB1*	0.7714	1.4630	-0.6915	-	-	6.14E-04
Kinectin	*KTN1*	0.3494	-1.0971	1.4464	-	-	7.73E-03
Laminin subunit alpha-5	*LAMA5*	-2.9345	-2.0937	-0.8408	-	-	7.57E-03
Laminin subunit beta-1	*LAMB1*	-1.8390	-0.5084	-1.3306	-	-	4.50E-03
Laminin subunit gamma-1	*LAMC1*	0.2735	1.0656	-0.7921	-	-	1.17E-02
Lysosome-associated membrane glycoprotein 2	*LAMP2*	-1.3820	-0.3759	-1.0061	-	-	4.87E-04
Cytosol aminopeptidase	*LAP3*	3.2417	3.6837	-0.4420	-	-	1.03E-02
Plastin-2	*LCP1*	3.2706	5.0824	-1.8118	0.9455	-1.0239	1.22E-04
Galectin-1	*LGALS1*	2.7285	3.8070	-1.0785	-	-	1.13E-03
Galectin-3-binding protein	*LGALS3BP*	1.8023	0.4221	1.3802	-	-	3.18E-04
Hormone-sensitive lipase	*LIPE*	-4.5201	-2.5547	-1.9654	-	-	1.89E-04
Vesicular integral-membrane protein VIP36	*LMAN2*	0.0269	-1.6200	1.6470	1.6593	-	3.04E-04
LIM and cysteine-rich domains protein 1	*LMCD1*	-0.5599	-1.1397	0.5798	-	-	4.10E-03
Lamin-B2	*LMNB2*	1.6408	2.0218	-0.3810	-	-	2.10E-03
Leucine-rich repeat-containing protein 47	*LRRC47*	0.1146	-1.1910	1.3056	-	-	1.21E-02
U6 snRNA-associated Sm-like protein LSm4	*LSM4*	-3.6809	-1.9939	-1.6869	-	-	1.45E-02
Leukotriene A-4 hydrolase	*LTA4H*	-0.3271	0.8830	-1.2102	-	-	1.19E-03
Lumican	*LUM*	5.7124	7.6723	-1.9599	-0.4729	0.4100	1.78E-04
Melanoma-associated antigen D2	*MAGED2*	0.4622	-0.9588	1.4210	-	-	4.10E-04
Amine oxidase [flavin-containing] B	*MAOB*	0.5870	-0.4767	1.0637	-	-	8.38E-03
Microtubule-associated protein RP/EB family member 1	*MAPRE1*	0.3237	-0.8793	1.2030	-	-	1.16E-03
S-adenosylmethionine synthase isoform type-2	*MAT2A*	-0.1524	-0.8521	0.6997	-	-	3.15E-03
Methylcrotonoyl-CoA carboxylase beta chain, mitochondrial	*MCCC2*	1.1976	-1.2210	2.4187	1.8812	1.5843	7.27E-04
DNA replication licensing factor MCM7	*MCM7*	-2.1827	-1.4562	-0.7265	-	-	1.15E-02
Microsomal glutathione S-transferase 1	*MGST1*	0.7456	-0.1799	0.9255	-	-	1.20E-02
Macrophage migration inhibitory factor	*MIF*	0.5912	3.2137	-2.6225	-	-	4.51E-05
C-type mannose receptor 2	*MRC2*	-2.5560	-1.6755	-0.8804	-	-	1.62E-02
RNA-binding protein Musashi homolog 2	*MSI2*	-1.6609	-2.2601	0.5993	-	-	1.23E-02
Moesin	*MSN*	3.0626	3.7406	-0.6780	-	-	4.82E-03
Major vault protein	*MVP*	2.5716	1.1437	1.4279	-	-	3.38E-03
Myb-binding protein 1A	*MYBBP1A*	-3.2834	-1.4580	-1.8254	-	-	2.41E-03
Myosin-10	*MYH10*	0.3283	-0.4661	0.7944	-	-	1.74E-02
Myosin-11	*MYH11*	2.4111	1.4264	0.9847	-	-	1.51E-03
Myosin light polypeptide 6	*MYL6*	3.2217	3.5965	-0.3748	-	-	5.67E-03
Unconventional myosin-Ib	*MYO1B*	-2.4063	-3.1032	0.6968	-	-	1.67E-02
Unconventional myosin-Ic	*MYO1C*	1.7962	2.2503	-0.4540	-	-	1.21E-04
Unconventional myosin-VI	*MYO6*	1.1341	-0.7369	1.8710	-	-	3.95E-04
Sialic acid synthase	*NANS*	0.3406	1.1899	-0.8494	-	-	1.02E-02
Alpha-soluble NSF attachment protein	*NAPA*	0.6784	-0.4962	1.1746	-	-	2.69E-03
Nck-associated protein 1	*NCKAP1*	-2.6760	-3.2131	0.5371	-	-	8.75E-05
Nucleolin	*NCL*	3.6149	4.3590	-0.7441	-	-	3.32E-04
Protein NDRG1	*NDRG1*	0.1174	-1.8684	1.9858	-	-	7.90E-03
NADH dehydrogenase [ubiquinone] 1 alpha subcomplex subunit 9, mitochondrial	*NDUFA9*	-1.1008	-0.5974	-0.5034	-	-	2.18E-03
Negative elongation factor B	*NELFB*	-5.4219	-4.0042	-1.4176	-	-	6.86E-03
Nidogen-2	*NID2*	-0.6810	0.1636	-0.8446	-	-	2.99E-04
NAD(P) transhydrogenase, mitochondrial	*NNT*	-0.8273	-1.8392	1.0119	-	-	9.72E-03
Nucleolar and coiled-body phosphoprotein 1	*NOLC1*	0.1261	5.1124	-4.9862	-	-	1.39E-02
Non-POU domain-containing octamer-binding protein	*NONO*	0.9915	1.6669	-0.6754	-	-	5.84E-04
Vesicle-fusing ATPase	*NSF*	1.6490	-0.0551	1.7041	1.6399	-	1.76E-03
Nuclear pore complex protein Nup155	*NUP155*	-2.7349	-2.3557	-0.3792	-	-	6.48E-03
Nuclear transport factor 2	*NUTF2*	-1.7343	-0.8731	-0.8612	-	-	1.98E-02
Mimecan	*OGN*	4.1033	7.1633	-3.0599	-2.1022	2.1600	2.13E-06
Olfactomedin-like protein 1	*OLFML1*	-2.1217	-0.2228	-1.8989	-	-	4.01E-03
Alpha-1-acid glycoprotein 1	*ORM1*	2.1804	3.3065	-1.1261	-	-	1.16E-03
Ubiquitin thioesterase OTUB1	*OTUB1*	1.9658	1.3198	0.6460	-	-	4.41E-04
Protein disulfide-isomerase	*P4HB*	4.6745	4.3509	0.3236	-	-	5.62E-03
Proliferation-associated protein 2G4	*PA2G4*	0.1517	1.1207	-0.9690	-	-	1.63E-03
Palladin	*PALLD*	1.1876	-0.3743	1.5618	1.4748	0.3718	1.98E-04
Poly [ADP-ribose] polymerase 1	*PARP1*	2.6625	1.7573	0.9052	-	-	1.39E-02
Poly(rC)-binding protein 1	*PCBP1*	1.6553	2.3071	-0.6518	-	-	2.23E-03
Phosphoenolpyruvate carboxykinase [GTP], mitochondrial	*PCK2*	-0.4471	0.9325	-1.3796	-	-	5.74E-04
Proliferating cell nuclear antigen	*PCNA*	0.3166	1.4645	-1.1479	-	-	7.17E-04
Programmed cell death protein 6	*PDCD6*	-0.4946	-0.8337	0.3391	-	-	1.56E-02
Programmed cell death 6-interacting protein	*PDCD6IP*	2.1547	1.3694	0.7854	-	-	5.07E-04
Protein disulfide-isomerase A4	*PDIA4*	2.4330	3.3994	-0.9664	-	-	3.39E-03
Protein disulfide-isomerase A6	*PDIA6*	2.5872	3.2019	-0.6147	-	-	1.32E-03
Pyridoxal-dependent decarboxylase domain-containing protein 1	*PDXDC1*	0.4430	-0.5254	0.9683	-	-	1.79E-03
Pyridoxal kinase	*PDXK*	-0.7275	0.1895	-0.9170	-	-	2.86E-03
ATP-dependent 6-phosphofructokinase, liver type	*PFKL*	0.7309	1.7343	-1.0034	-	-	2.65E-03
Profilin-1	*PFN1*	2.8038	4.4528	-1.6491	0.6366	-	4.81E-05
6-phosphogluconate dehydrogenase, decarboxylating	*PGD*	2.0258	2.9043	-0.8786	-	-	7.91E-05
Phosphoglycerate kinase 1	*PGK1*	5.2569	5.6828	-0.4259	-	-	3.29E-04
6-phosphogluconolactonase	*PGLS*	1.0441	1.7637	-0.7197	-	-	6.77E-04
Phosphoglucomutase-1	*PGM1*	0.9263	0.3894	0.5369	-	-	4.11E-04
Prohibitin	*PHB*	3.7259	3.0640	0.6619	-	-	3.55E-03
Prohibitin-2	*PHB2*	3.3014	2.5926	0.7088	-	-	5.13E-04
D-3-phosphoglycerate dehydrogenase	*PHGDH*	-0.1505	1.4755	-1.6261	-2.8642	0.6712	3.98E-05
Plectin	*PLEC*	4.6501	4.2411	0.4090	-	-	1.56E-02
Perilipin-1	*PLIN1*	-0.5113	1.5714	-2.0827	-7.3640	-0.4549	6.65E-03
Purine nucleoside phosphorylase	*PNP*	2.4730	1.8265	0.6465	-	-	8.23E-04
Serine/threonine-protein phosphatase 2A 65 kDa regulatory subunit A alpha isoform	*PPP2R1A*	0.9321	1.5283	-0.5963	-	-	7.62E-06
Lysosomal Pro-X carboxypeptidase	*PRCP*	-4.1008	-2.5469	-1.5539	-	-	6.37E-03
Peroxiredoxin-1	*PRDX1*	4.9711	4.6477	0.3234	-	-	2.36E-04
Peroxiredoxin-2	*PRDX2*	2.9288	3.5377	-0.6089	-	-	4.94E-04
Thioredoxin-dependent peroxide reductase, mitochondrial	*PRDX3*	2.2241	1.4052	0.8190	-	-	6.29E-04
Peroxiredoxin-4	*PRDX4*	1.3394	0.0735	1.2659	-	-	3.67E-03
Peroxiredoxin-5, mitochondrial	*PRDX5*	1.4343	2.3146	-0.8802	-	-	6.99E-04
Peroxiredoxin-6	*PRDX6*	4.2584	3.6548	0.6036	-	-	1.75E-03
Prolargin	*PRELP*	3.8360	5.0968	-1.2608	-	-	3.34E-03
Phosphatidylinositol 3,4,5-trisphosphate-dependent Rac exchanger 1 protein	*PREX1*	0.5417	-2.0682	2.6099	-	-	3.54E-04
Glucosidase 2 subunit beta	*PRKCSH*	0.4205	1.5991	-1.1786	-	-	1.11E-03
DNA-dependent protein kinase catalytic subunit	*PRKDC*	2.4480	4.0590	-1.6110	1.6933	-	9.56E-05
Pre-mRNA-processing factor 19	*PRPF19*	-0.3784	0.2675	-0.6459	-	-	3.09E-03
Pre-mRNA-processing factor 40 homolog A	*PRPF40A*	-2.8519	-1.6169	-1.2349	-	-	1.06E-02
26S protease regulatory subunit 6A	*PSMC3*	-0.6115	0.3288	-0.9403	-	-	3.69E-03
26S proteasome non-ATPase regulatory subunit 3	*PSMD3*	0.1434	-0.6757	0.8191	-	-	1.16E-03

26S proteasome non-ATPase regulatory subunit 5	*PSMD5*	-0.5591	0.0272	-0.5863	-	-	8.33E-03
Proteasome activator complex subunit 1	*PSME1*	3.0662	4.3039	-1.2377	-	-	1.43E-04
Proteasome activator complex subunit 2	*PSME2*	1.5963	2.7401	-1.1438	-	-	1.70E-03
Prostacyclin synthase	*PTGIS*	-3.1416	-0.6804	-2.4612	-3.6036	-0.3787	1.21E-03
Prostaglandin reductase 1	*PTGR1*	-1.6833	-3.0809	1.3975	-	-	7.63E-04
Tyrosine-protein phosphatase non-receptor type 6	*PTPN6*	-1.2336	-0.5445	-0.6891	-	-	4.35E-03
Transcriptional activator protein Pur-alpha	*PURA*	-0.7149	-1.2377	0.5228	-	-	1.06E-02
Glutamine--tRNA ligase	*QARS*	-0.1372	-0.7230	0.5859	-	-	1.42E-03
Ras-related protein Rab-10	*RAB10*	-1.2062	-2.4212	1.2150	-	-	4.71E-04
Ras-related protein Rab-7a	*RAB7A*	1.7375	0.5861	1.1514	-	-	8.79E-06
Ras-related protein Rab-8A	*RAB8A*	-1.7160	-2.1427	0.4267	-	-	1.19E-02
Ras-related protein Rap-1A	*RAP1A*	2.0609	1.4358	0.6251	-	-	2.07E-03
Arginine--tRNA ligase, cytoplasmic	*RARS*	1.8054	0.2763	1.5291	-	-	3.12E-04
Protein RCC2	*RCC2*	-1.1127	-0.6524	-0.4603	-	-	1.65E-02
Retinol dehydrogenase 13	*RDH13*	-4.1484	-2.8013	-1.3471	-	-	1.56E-03
60S ribosomal protein L12	*RPL12*	1.6658	1.0697	0.5961	-	-	1.67E-03
60S ribosomal protein L23	*RPL23*	-1.3517	0.6730	-2.0247	-	-	1.22E-04
60S ribosomal protein L3	*RPL3*	1.3243	0.5648	0.7596	-	-	4.89E-03
60S ribosomal protein L30	*RPL30*	-2.6438	-0.3398	-2.3040	-	-	2.06E-03
60S ribosomal protein L35	*RPL35*	-1.0932	-2.6959	1.6026	-	-	7.43E-04
60S ribosomal protein L36	*RPL36*	-1.1263	-0.1673	-0.9590	-	-	5.52E-04
60S ribosomal protein L6	*RPL6*	2.0942	1.2756	0.8186	-	-	1.12E-02
60S ribosomal protein L7	*RPL7*	1.5951	2.6157	-1.0207	-	-	4.45E-03
60S acidic ribosomal protein P2	*RPLP2*	-0.7787	1.0729	-1.8516	-	-	4.61E-04
Dolichyl-diphosphooligosaccharide--protein glycosyltransferase subunit 2	*RPN2*	2.3158	2.0184	0.2974	-	-	1.12E-02
40S ribosomal protein S12	*RPS12*	-1.3264	-0.6046	-0.7218	-	-	1.62E-02
40S ribosomal protein S15	*RPS15*	-2.2259	-1.6276	-0.5984	-	-	4.59E-03
40S ribosomal protein S19	*RPS19*	1.0031	0.4284	0.5747	-	-	8.30E-03
40S ribosomal protein S2	*RPS2*	1.8521	1.3000	0.5521	-	-	1.37E-02
40S ribosomal protein S25	*RPS25*	0.3141	1.0812	-0.7671	-	-	1.34E-02
40S ribosomal protein S7	*RPS7*	0.1310	-0.1657	0.2967	-	-	1.79E-02
40S ribosomal protein S8	*RPS8*	1.6164	2.1685	-0.5521	-	-	6.41E-03
40S ribosomal protein SA	*RPSA*	2.8031	3.3727	-0.5696	-	-	2.63E-03
Ribosomal L1 domain-containing protein 1	*RSL1D1*	-0.9366	0.2162	-1.1528	-	-	5.01E-06
RuvB-like 1	*RUVBL1*	1.2807	0.4469	0.8338	-	-	6.79E-03
RuvB-like 2	*RUVBL2*	1.0146	0.4119	0.6027	-	-	9.94E-03
Protein S100-A10	*S100A10*	-1.5560	0.8012	-2.3572	-	-	1.40E-02
Protein S100-A4	*S100A4*	0.3326	1.4087	-1.0761	-	-	3.66E-03
Deoxynucleoside triphosphate triphosphohydrolase SAMHD1	*SAMHD1*	2.4038	3.1888	-0.7850	-	-	5.91E-04
Sec1 family domain-containing protein 1	*SCFD1*	-0.5775	0.5056	-1.0831	-	-	3.94E-03
Protein scribble homolog	*SCRIB*	-1.4489	-2.8106	1.3618	-	-	2.43E-03
Succinate dehydrogenase [ubiquinone] iron-sulfur subunit, mitochondrial	*SDHB*	-1.4024	-0.1433	-1.2591	-	-	5.33E-04
Protein transport protein Sec31A	*SEC31A*	0.9255	-0.2277	1.1532	-	-	6.82E-03
Translocation protein SEC63 homolog	*SEC63*	-0.7103	-2.2640	1.5537	0.9846	-	3.50E-03
Septin-9	*SEPT9*	0.9382	1.5747	-0.6365	-	-	9.80E-03
Kallistatin	*SERPINA4*	-0.7923	0.5419	-1.3342	-	-	4.99E-04
Leukocyte elastase inhibitor	*SERPINB1*	1.5539	2.5313	-0.9775	-	-	4.39E-03
Serpin B6	*SERPINB6*	0.5586	1.5812	-1.0226	-	-	1.78E-03
Serpin B9	*SERPINB9*	-2.2324	0.7892	-3.0217	-	-	1.29E-05
Antithrombin-III	*SERPINC1*	2.9658	3.6816	-0.7157	-	-	3.95E-04
Heparin cofactor 2	*SERPIND1*	-0.2495	1.5455	-1.7950	-2.5463	0.7040	5.04E-05
Pigment epithelium-derived factor	*SERPINF1*	2.9810	3.2276	-0.2466	-	-	8.08E-03
Plasma protease C1 inhibitor	*SERPING1*	2.2555	2.5661	-0.3106	-	-	1.16E-03
Serpin H1	*SERPINH1*	3.8463	3.3332	0.5131	-	-	1.95E-03
SH3 domain-binding glutamic acid-rich-like protein	*SH3BGRL*	1.6886	-0.0278	1.7164	1.5526	-	9.65E-05
Mitochondrial dicarboxylate carrier	*SLC25A10*	-0.7371	-1.6041	0.8669	-	-	1.42E-03
Calcium-binding mitochondrial carrier protein SCaMC-1	*SLC25A24*	-1.9389	1.0513	-2.9903	-	-	3.90E-04
4F2 cell-surface antigen heavy chain	*SLC3A2*	-0.6195	-0.0451	-0.5744	-	-	1.88E-02
Band 3 anion transport protein	*SLC4A1*	-1.0871	0.2559	-1.3430	-	-	2.57E-03
Na(+)/H(+) exchange regulatory cofactor NHE-RF1	*SLC9A3R1*	1.1481	-0.7538	1.9019	3.2788	-	7.81E-04
Small nuclear ribonucleoprotein Sm D3	*SNRPD3*	-0.3577	1.0134	-1.3711	-	-	6.07E-05
Sorting nexin-3	*SNX3*	-0.1125	-1.6178	1.5054	-	-	9.56E-04
Extracellular superoxide dismutase [Cu-Zn]	*SOD3*	-1.8878	1.3966	-3.2844	-	-	1.11E-03
Sorbitol dehydrogenase	*SORD*	2.8848	-1.8654	4.7502	3.5766	0.7255	3.11E-05
Sepiapterin reductase	*SPR*	-0.7473	-2.0268	1.2795	-	-	1.21E-02
Spectrin alpha chain, non-erythrocytic 1	*SPTAN1*	2.1239	2.5604	-0.4365	-	-	2.12E-04
Spectrin beta chain, erythrocytic	*SPTB*	-5.7627	-3.5939	-2.1688	-	-	2.12E-03
Spectrin beta chain, non-erythrocytic 1	*SPTBN1*	1.8119	2.1804	-0.3685	-	-	4.54E-03
Signal recognition particle 14 kDa protein	*SRP14*	-0.4287	0.3701	-0.7988	-	-	9.31E-03
Serine/arginine-rich splicing factor 1	*SRSF1*	0.8749	1.2053	-0.3304	-	-	1.33E-02
Single-stranded DNA-binding protein, mitochondrial	*SSBP1*	-0.1478	-0.9119	0.7641	-	-	1.22E-02
Translocon-associated protein subunit delta	*SSR4*	-0.1461	0.4041	-0.5502	-	-	1.46E-02
FACT complex subunit SSRP1	*SSRP1*	0.0294	0.9383	-0.9089	-	-	5.46E-04
PCTP-like protein	*STARD10*	-0.3574	-1.1051	0.7477	-	-	8.29E-04
Stomatin-like protein 2, mitochondrial	*STOML2*	-2.0558	-1.4653	-0.5906	-	-	3.99E-03
Succinyl-CoA ligase [GDP-forming] subunit beta, mitochondrial	*SUCLG2*	0.0472	0.5494	-0.5022	-	-	4.19E-04
Transgelin	*TAGLN*	4.3480	3.0404	1.3076	-	-	2.40E-04
Transgelin-2	*TAGLN2*	3.3209	2.1410	1.1799	-	-	7.77E-04
Transaldolase	*TALDO1*	1.7731	2.2881	-0.5150	-	-	1.61E-03
Antigen peptide transporter 2	*TAP2*	-1.8405	-1.1001	-0.7403	-	-	3.99E-03
TAR DNA-binding protein 43	*TARDBP*	-1.7159	-2.5892	0.8733	-	-	1.95E-02
Threonine--tRNA ligase, cytoplasmic	*TARS*	0.3155	0.8323	-0.5167	-	-	8.90E-04
Serotransferrin	*TF*	4.9653	6.6243	-1.6590	-0.8474	0.5147	1.06E-04
Transforming growth factor-beta-induced protein ig-h3	*TGFBI*	3.3410	3.7941	-0.4531	-	-	7.14E-03
Thrombospondin-1	*THBS1*	4.0665	1.5728	2.4937	2.3688	0.8471	2.04E-04
THO complex subunit 6 homolog	*THOC6*	-3.8006	-3.3799	-0.4207	-	-	4.30E-03
Mitochondrial import inner membrane translocase subunit TIM44	*TIMM44*	-3.0074	-2.2011	-0.8064	-	-	1.16E-02
Transketolase	*TKT*	3.9051	3.2735	0.6316	-	-	5.51E-03
Transmembrane and coiled-coil domain-containing protein 1	*TMCO1*	-1.6837	-3.3929	1.7091	-	-	6.90E-03
Transmembrane emp24 domain-containing protein 10	*TMED10*	0.9672	0.4368	0.5304	-	-	9.48E-05
Tenascin	*TNC*	3.3005	5.0245	-1.7240	1.9860	1.6968	2.35E-05
Transportin-3	*TNPO3*	-4.3370	-3.7462	-0.5908	-	-	1.62E-02
Tenascin-X	*TNXB*	-2.2074	-0.0595	-2.1479	-4.9865	0.9594	3.32E-04
DNA topoisomerase 1	*TOP1*	-0.8958	0.0503	-0.9460	-	-	9.58E-03
Tumor protein D54	*TPD52L2*	-0.0349	0.2607	-0.2956	-	-	1.89E-03
Triosephosphate isomerase	*TPI1*	4.5354	3.8163	0.7191	-	-	9.26E-03
Tropomyosin alpha-1 chain	*TPM1*	1.0174	0.5473	0.4701	-	-	4.13E-03
Transformer-2 protein homolog alpha	*TRA2A*	-2.7149	-1.5017	-1.2133	-	-	7.59E-03
Heat shock protein 75 kDa, mitochondrial	*TRAP1*	-0.0066	0.9584	-0.9649	-	-	1.79E-02
Transcription intermediary factor 1-beta	*TRIM28*	2.2034	3.1644	-0.9611	-	-	2.85E-06
60 kDa SS-A/Ro ribonucleoprotein	*TROVE2*	0.2238	-0.3770	0.6008	-	-	1.87E-02
Translin	*TSN*	-0.3144	-1.4786	1.1642	-	-	1.99E-03
Tubulin--tyrosine ligase-like protein 12	*TTLL12*	1.8751	0.1683	1.7068	2.2654	-1.6739	4.34E-04
Transthyretin	*TTR*	2.6024	4.1766	-1.5742	-0.9912	0.3103	6.04E-05
Tubulin beta chain	*TUBB*	4.6650	5.2282	-0.5632	-	-	6.12E-03
Tubulin beta-3 chain	*TUBB3*	1.9310	0.1963	1.7347	-	-	3.08E-04
Tubulin beta-4B chain	*TUBB4B*	5.9746	6.7288	-0.7542	-	-	1.02E-03
Elongation factor Tu, mitochondrial	*TUFM*	3.2311	3.6925	-0.4614	-	-	4.36E-03

Twinfilin-1	*TWF1*	-0.2051	-1.3279	1.1228	-	-	4.04E-03
Ubiquitin-conjugating enzyme E2 N	*UBE2N*	1.0336	1.5541	-0.5205	-	-	8.95E-03
E3 UFM1-protein ligase 1	*UFL1*	-0.1857	-1.1610	0.9753	-	-	4.23E-04
Cytochrome b-c1 complex subunit 2, mitochondrial	*UQCRC2*	2.2081	1.3022	0.9060	-	-	1.76E-03
General vesicular transport factor p115	*USO1*	0.9581	-1.0775	2.0356	1.0570	-	1.46E-03
Ubiquitin carboxyl-terminal hydrolase 5	*USP5*	1.9255	0.0957	1.8297	1.3369	-0.7031	2.89E-04
Vesicle-associated membrane protein-associated protein B/C	*VAPB*	0.7592	-1.0209	1.7801	1.4288	-	1.63E-03
Valine--tRNA ligase	*VARS*	0.5402	1.4403	-0.9001	-	-	1.26E-03
Prefoldin subunit 3	*VBP1*	-3.6872	-2.8850	-0.8022	-	-	4.34E-03
Versican core protein	*VCAN*	1.6056	3.9702	-2.3646	-	-	1.87E-05
Voltage-dependent anion-selective channel protein 1	*VDAC1*	3.8396	2.6532	1.1865	-	-	4.35E-06
Voltage-dependent anion-selective channel protein 3	*VDAC3*	2.6086	1.5929	1.0157	-	-	3.00E-04
Vimentin	*VIM*	7.7022	8.0754	-0.3732	-	-	1.21E-02
Vacuolar protein sorting-associated protein 26A	*VPS26A*	-1.9639	-0.9524	-1.0115	-	-	2.86E-03
Vacuolar protein sorting-associated protein 35	*VPS35*	1.3684	1.5629	-0.1945	-	-	9.42E-04
von Willebrand factor A domain-containing protein 1	*VWA1*	-1.8005	-2.9238	1.1233	-	-	5.32E-03
WD repeat-containing protein 1	*WDR1*	2.7330	2.2251	0.5079	-	-	1.66E-02
Exportin-5	*XPO5*	-4.1165	-2.8327	-1.2837	-	-	3.76E-04
X-ray repair cross-complementing protein 5	*XRCC5*	2.4682	3.0233	-0.5550	-	-	6.99E-03
X-ray repair cross-complementing protein 6	*XRCC6*	3.1947	3.7476	-0.5529	-	-	1.82E-03
14-3-3 protein theta	*YWHAQ*	0.7696	1.5810	-0.8115	-	-	9.56E-04
CAAX prenyl protease 1 homolog	*ZMPSTE24*	-3.7610	-1.3514	-2.4095	-	-	2.12E-03

Supplementary File 5C. Functional annotation of the differentially expressed proteins in the MPT x FPT tissues' comparison. According to the functional classification of the PANTHER system v. 13.1, based on the gene ontology (GO) terms: A. Protein class; B. Molecular function; C. Biological process. According to the functional enrichment analysis of the DAVID v. 6.8 database: D. Top enriched biological processes (GO terms, p<0.05); E. Top enriched KEGG pathways (p<0.05).

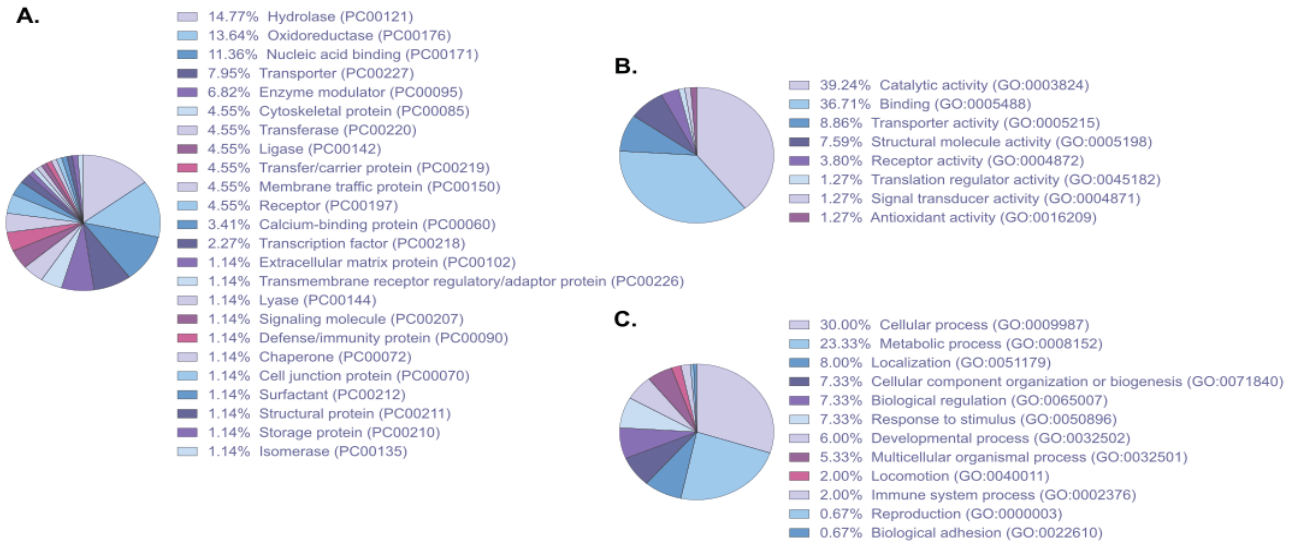

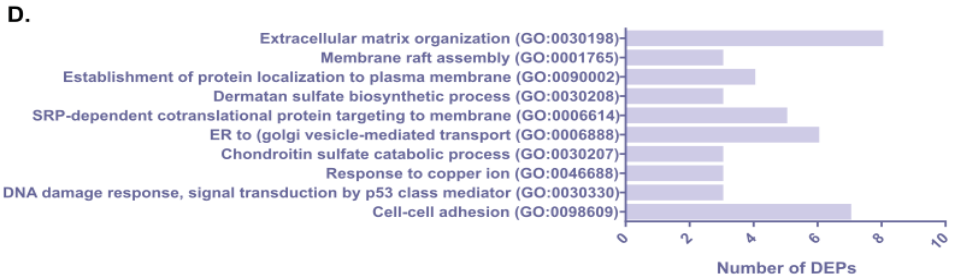

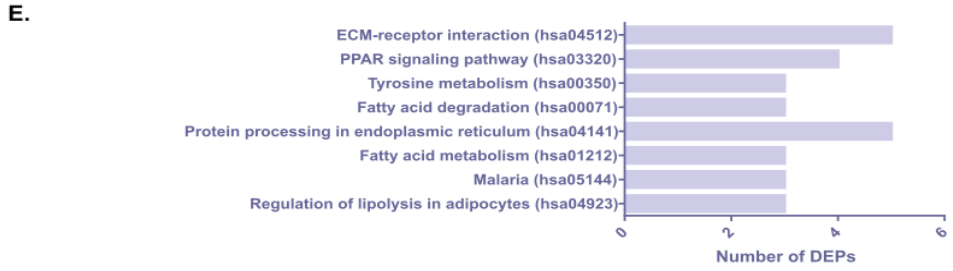

Supplementary File 5D. Functional enrichment analysis (p>0.05) through DAVID analysis of the main up-regulated and down-regulated proteins identified in the MPT x FPT tissues' comparison.

Gene Symbol	MPT X FPT fold change	GOTERM_BP_DIRECT	GOTERM_CC_DIRECT	GOTERM_MF_DIRECT	KEGG_PATHWAY
SORD	4.75	GO:0006006~glucose metabolic process,GO:0006062~sorbitol catabolic process,GO:0006970~response to osmotic stress,GO:0009725~response to hormone,GO:0019640~glucuronate catabolic process to xylulose 5-phosphate,GO:0030317~sperm motility,GO:0031667~response to nutrient levels,GO:0042493~response to drug,GO:0046370~fructose biosynthetic process,GO:0046686~response to cadmium ion,GO:0046688~response to copper ion,GO:0051160~L-xylitol catabolic process,GO:0051164~L-xylitol metabolic process,GO:0055114~oxidation-reduction process	GO:0005615~extracellular space,GO:0005829~cytosol,GO:0016020~membrane,GO:0031514~motile cilium,GO:0031966~mitochondrial membrane,GO:0070062~extracellular exosome	GO:0003939~L-iditol 2-dehydrogenase activity,GO:0008270~zinc ion binding,GO:0016491~oxidoreductase activity,GO:0030246~carbohydrate binding,GO:0042802~identical protein binding,GO:0046526~D-xylulose reductase activity,GO:0051287~NAD binding	hsa00040:Pentose and glucuronate interconversions,hsa00051:Fructose and mannose metabolism,hsa01100:Metabolic pathways
CYB5A	2.59	GO:0019852~L-ascorbic acid metabolic process,GO:0046686~response to cadmium ion,GO:0055114~oxidation-reduction process,GO:1902600~hydrogen ion transmembrane transport	GO:0005737~cytoplasm,GO:0005741~mitochondrial outer membrane,GO:0005789~endoplasmic reticulum membrane,GO:0016020~membrane,GO:0016021~integral component of membrane,GO:0043231~intracellular membrane-bounded organelle,GO:0070062~extracellular exosome	GO:0004033~aldo-keto reductase (NADP) activity,GO:0004129~cytochrome-c oxidase activity,GO:0019899~enzyme binding,GO:0020037~heme binding,GO:0046872~metal ion binding	
ISOC2	2.57	GO:0008152~metabolic process,GO:0031648~protein destabilization	GO:0005634~nucleus,GO:0005737~cytoplasm	GO:0003824~catalytic activity,GO:0005515~protein binding	
THBS1	2.49	GO:0000187~activation of MAPK activity,GO:0001666~response to hypoxia,GO:0001937~negative regulation of endothelial cell proliferation,GO:0001953~negative regulation of cell-matrix adhesion,GO:0002040~sprouting angiogenesis,GO:0002544~chronic inflammatory response,GO:0002576~platelet degranulation,GO:0002581~negative regulation of antigen processing and presentation of peptide or polysaccharide antigen via MHC class II,GO:0002605~negative regulation of dendritic cell antigen processing and presentation,GO:0006954~inflammatory response,GO:0006955~immune response,GO:0006986~response to unfolded protein,GO:0007050~cell cycle arrest,GO:0007155~cell adhesion,GO:0008284~positive regulation of cell proliferation,GO:0009612~response to mechanical stimulus,GO:0009749~response to glucose,GO:0010595~positive regulation of endothelial cell migration,GO:0010596~negative regulation of endothelial cell migration,GO:0010748~negative regulation of plasma membrane long-chain fatty acid transport,GO:0010751~negative regulation of nitric oxide mediated signal transduction,GO:0010754~negative regulation of cGMP-mediated signaling,GO:0010757~negative regulation of plasminogen activation,GO:0010759~positive regulation of macrophage chemotaxis,GO:0010763~positive regulation of fibroblast migration,GO:0016477~cell migration,GO:0016525~negative regulation of angiogenesis,GO:0018149~peptide cross-linking,GO:0030194~positive regulation of blood coagulation,GO:0030198~extracellular matrix organization,GO:0030335~positive regulation of cell migration,GO:0030511~positive regulation of transforming growth factor beta receptor signaling pathway,GO:0030823~regulation of cGMP metabolic process,GO:0032026~response to magnesium ion,GO:0032570~response to progesterone,GO:0032695~negative regulation of interleukin-12 production,GO:0032914~positive regulation of transforming growth factor beta1 production,GO:0033574~response to testosterone,GO:0034605~cellular response to heat,GO:0034976~response to endoplasmic reticulum stress,GO:0036066~protein O-linked fucosylation,GO:0040037~negative regulation of fibroblast growth factor receptor signaling pathway,GO:0042327~positive regulation of phosphorylation,GO:0042493~response to drug,GO:0042535~positive regulation of tumor necrosis factor biosynthetic process,GO:0043032~positive regulation of macrophage activation,GO:0043066~negative regulation of apoptotic process,GO:0043154~negative regulation of cysteine-type endopeptidase activity involved in apoptotic process,GO:0043536~positive regulation of blood vessel endothelial cell migration,GO:0043537~negative regulation of blood vessel endothelial cell migration,GO:0043652~engulfment of apoptotic cell,GO:0045727~positive regulation of translation,GO:0045766~positive regulation of angiogenesis,GO:0048266~behavioral response to pain,GO:0048661~positive regulation of smooth muscle cell proliferation,GO:0050921~positive regulation of chemotaxis,GO:0051592~response to calcium ion,GO:0051895~negative regulation of focal adhesion assembly,GO:0051897~positive regulation of protein kinase B signaling,GO:0051918~negative regulation of fibrinolysis,GO:0071356~cellular response to tumor necrosis factor,GO:0071363~cellular response to growth factor stimulus,GO:1902043~positive regulation of extrinsic apoptotic signaling pathway via death domain receptors,GO:2000353~positive regulation of endothelial cell apoptotic process,GO:2000379~positive regulation of reactive oxygen species metabolic process,GO:2001027~negative regulation of endothelial cell chemotaxis,GO:2001237~negative regulation of extrinsic apoptotic signaling pathway	GO:0005576~extracellular region,GO:0005577~fibrinogen complex,GO:0005615~extracellular space,GO:0005783~endoplasmic reticulum,GO:0005788~endoplasmic reticulum lumen,GO:0009897~external side of plasma membrane,GO:0009986~cell surface,GO:0016529~sarcoplasmic reticulum,GO:0030141~secretory granule,GO:0031012~extracellular matrix,GO:0031091~platelet alpha granule,GO:0031093~platelet alpha granule lumen,GO:0070062~extracellular exosome	GO:0001786~phosphatidylserine binding,GO:0001948~glycoprotein binding,GO:0001968~fibronectin binding,GO:0005178~integrin binding,GO:0005509~calcium ion binding,GO:0005515~protein binding,GO:0008201~heparin binding,GO:0017134~fibroblast growth factor binding,GO:0030169~low-density lipoprotein particle binding,GO:0042802~identical protein binding,GO:0043236~laminin binding,GO:0043394~proteoglycan binding,GO:0050431~transforming growth factor beta binding,GO:0050840~extracellular matrix binding,GO:0070051~fibrinogen binding,GO:0070052~collagen V binding	hsa04015:Rap1 signaling pathway,hsa04115:p53 signaling pathway,hsa04145:Phagosome,hsa04151:PI3K-Akt signaling pathway,hsa04350:TGF-beta signaling pathway,hsa04510:Focal adhesion,hsa04512:ECM-receptor interaction,hsa05144:Malaria,hsa05205:Proteoglycans in cancer,hsa05206:MicroRNAs in cancer,hsa05219:Bladder cancer
MCCC2	2.42	GO:0006552~leucine catabolic process,GO:0006768~biotin metabolic process,GO:0009083~branched-chain amino acid catabolic process,GO:0015936~coenzyme A metabolic process,GO:0051291~protein heterooligomerization	GO:0002169~3-methylcrotonyl-CoA carboxylase complex, mitochondrial,GO:0005739~mitochondrion,GO:0005759~mitochondrial matrix,GO:0005829~cytosol,GO:1905202~methylcrotonoyl-CoA carboxylase complex	GO:0004485~methylcrotonoyl-CoA carboxylase activity,GO:0005515~protein binding,GO:0005524~ATP binding,GO:0016874~ligase activity	hsa00280:Valine, leucine and isoleucine degradation,hsa01100:Metabolic pathways
HSPA2	2.32	GO:0006986~response to unfolded protein,GO:0007140~male meiosis,GO:0007141~male meiosis I,GO:0007283~spermatogenesis,GO:0007286~spermatid development,GO:0009408~response to heat,GO:0009409~response to cold,GO:0031662~positive regulation of cyclin-dependent protein serine/threonine kinase activity involved in G2/M transition of mitotic cell cycle,GO:0042026~protein refolding,GO:0070194~synaptonemal complex disassembly,GO:0090084~negative regulation of inclusion body assembly,GO:1901896~positive regulation of calcium-transporting ATPase activity	GO:0000795~synaptonemal complex,GO:0001673~male germ cell nucleus,GO:0005634~nucleus,GO:0005739~mitochondrion,GO:0005829~cytosol,GO:0009986~cell surface,GO:0016020~membrane,GO:0036128~CatSper complex,GO:0043209~myelin sheath,GO:0070062~extracellular exosome,GO:0072562~blood microparticle,GO:0072687~meiotic spindle	GO:0005515~protein binding,GO:0005524~ATP binding,GO:0019899~enzyme binding,GO:0051082~unfolded protein binding,GO:0051861~glycolipid binding	hsa03040:Spliceosome,hsa04010:MAPK signaling pathway,hsa04141:Protein processing in endoplasmic reticulum,hsa04144:Endocytosis,hsa04612:Antigen processing and presentation,hsa04915:Estrogen signaling pathway,hsa05134:Legionellosis,hsa05145:Toxoplasmosis,hsa05162:Measles,hsa05164:Influenza A
IARS2	2.07	GO:0006418~tRNA aminoacylation for protein translation,GO:0006428~isoleucyl-tRNA aminoacylation,GO:0006450~regulation of translational fidelity	GO:0005737~cytoplasm,GO:0005739~mitochondrion,GO:0005759~mitochondrial matrix,GO:0005829~cytosol,GO:0016021~integral component of membrane	GO:0000049~tRNA binding,GO:0002161~aminoacyl-tRNA editing activity,GO:0004822~isoleucine-tRNA ligase activity,GO:0005524~ATP binding	hsa00970:Aminoacyl-tRNA biosynthesis

CYB5R1	2.05	GO:0002576~platelet degranulation,GO:0015701~bicarbonate transport,GO:0016126~sterol biosynthetic process,GO:0055114~oxidation-reduction process,GO:1903955~positive regulation of protein targeting to mitochondrion	GO:0005739~mitochondrion,GO:0005789~endoplasmic reticulum membrane,GO:0005886~plasma membrane,GO:0016020~membrane,GO:0016021~integral component of membrane,GO:0031092~platelet alpha granule membrane,GO:0070062~extracellular exosome	GO:0004128~cytochrome-b5 reductase activity, acting on NAD(P)H,GO:0005515~protein binding,GO:0016491~oxidoreductase activity,GO:0071949~FAD binding	hsa00520:Amino sugar and nucleotide sugar metabolism
USO1	2.04	GO:0006886~intracellular protein transport,GO:0006888~ER to Golgi vesicle-mediated transport,GO:0007030~Golgi organization,GO:0045056~transcytosis,GO:0048208~COPII vesicle coating,GO:0048211~Golgi vesicle docking,GO:0048280~vesicle fusion with Golgi apparatus,GO:0061025~membrane fusion,GO:0098609~cell-cell adhesion	GO:0000139~Golgi membrane,GO:0005730~nucleolus,GO:0005783~endoplasmic reticulum,GO:0005794~Golgi apparatus,GO:0005795~Golgi stack,GO:0005829~cytosol,GO:0005913~cell-cell adherens junction,GO:0012507~ER to Golgi transport vesicle membrane,GO:0016020~membrane,GO:0030133~transport vesicle,GO:0048471~perinuclear region of cytoplasm	GO:0005515~protein binding,GO:0008565~protein transporter activity,GO:0044822~poly(A) RNA binding,GO:0098641~cadherin binding involved in cell-cell adhesion	
HACD3	2.00	GO:0007249~I-kappaB kinase/NF-kappaB signaling,GO:0007257~activation of JUN kinase activity,GO:0007264~small GTPase mediated signal transduction,GO:0007266~Rho protein signal transduction,GO:0016601~Rac protein signal transduction,GO:0030148~sphingolipid biosynthetic process,GO:0030497~fatty acid elongation,GO:0042761~very long-chain fatty acid biosynthetic process,GO:0043547~positive regulation of GTPase activity,GO:0045070~positive regulation of viral genome replication,GO:0046726~positive regulation by virus of viral protein levels in host cell	GO:0005737~cytoplasm,GO:0005739~mitochondrion,GO:0005783~endoplasmic reticulum,GO:0005925~focal adhesion,GO:0016021~integral component of membrane,GO:0030176~integral component of endoplasmic reticulum membrane,GO:0031965~nuclear membrane	GO:0005096~GTPase activator activity,GO:0005515~protein binding,GO:0018812~3-hydroxyacyl-CoA dehydratase activity,GO:0019899~enzyme binding,GO:0102344~3-hydroxy-behenoyl-CoA dehydratase activity,GO:0102345~3-hydroxy-lignoceroyl-CoA dehydratase activity	hsa00062:Fatty acid elongation,hsa01040:Biosynthesis of unsaturated fatty acids,hsa01212:Fatty acid metabolism
SLC9A3R1	1.90	GO:0003096~renal sodium ion transport,GO:0006461~protein complex assembly,GO:0007191~adenylate cyclase-activating dopamine receptor signaling pathway,GO:0007605~sensory perception of sound,GO:0008285~negative regulation of cell proliferation,GO:0008360~regulation of cell shape,GO:0008361~regulation of cell size,GO:0010642~negative regulation of platelet-derived growth factor receptor signaling pathway,GO:0014067~negative regulation of phosphatidylinositol 3-kinase signaling,GO:0016055~Wnt signaling pathway,GO:0019933~cAMP-mediated signaling,GO:0022612~gland morphogenesis,GO:0030033~microvillus assembly,GO:0030036~actin cytoskeleton organization,GO:0030336~negative regulation of cell migration,GO:0030643~cellular phosphate ion homeostasis,GO:0032415~regulation of sodium:proton antiporter activity,GO:0032416~negative regulation of sodium:proton antiporter activity,GO:0032782~bile acid secretion,GO:0034635~glutathione transport,GO:0035414~negative regulation of catenin import into nucleus,GO:0040023~establishment of nucleus localization,GO:0044062~regulation of excretion,GO:0045198~establishment of epithelial cell apical/basal polarity,GO:0045859~regulation of protein kinase activity,GO:0045930~negative regulation of mitotic cell cycle,GO:0051683~establishment of Golgi localization,GO:0051898~negative regulation of protein kinase B signaling,GO:0060088~auditory receptor cell stereocilium organization,GO:0060158~phospholipase C-activating dopamine receptor signaling pathway,GO:0070293~renal absorption,GO:0070373~negative regulation of ERK1 and ERK2 cascade,GO:0090002~establishment of protein localization to plasma membrane,GO:0097291~renal phosphate ion absorption,GO:2001244~positive regulation of intrinsic apoptotic signaling pathway	GO:0001726~ruffle,GO:0005634~nucleus,GO:0005737~cytoplasm,GO:0005813~centrosome,GO:0005886~plasma membrane,GO:0005902~microvillus,GO:0012505~endomembrane system,GO:0015629~actin cytoskeleton,GO:0016020~membrane,GO:0016324~apical plasma membrane,GO:0030175~filopodium,GO:0031526~brush border membrane,GO:0031528~microvillus membrane,GO:0031982~vesicle,GO:0032426~stereocilium tip,GO:0043231~intracellular membrane-bounded organelle,GO:0045121~membrane raft,GO:0048471~perinuclear region of cytoplasm,GO:0070062~extracellular exosome,GO:0071944~cell periphery,GO:0097225~sperm midpiece	GO:0005102~receptor binding,GO:0005515~protein binding,GO:0008013~beta-catenin binding,GO:0017081~chloride channel regulator activity,GO:0019902~phosphatase binding,GO:0030165~PDZ domain binding,GO:0031698~beta-2 adrenergic receptor binding,GO:0032403~protein complex binding,GO:0032947~protein complex scaffold,GO:0043621~protein self-association,GO:0050780~dopamine receptor binding,GO:0070851~growth factor receptor binding	
USP5	1.83	GO:0006511~ubiquitin-dependent protein catabolic process,GO:0016579~protein deubiquitination,GO:0032436~positive regulation of proteasomal ubiquitin-dependent protein catabolic process,GO:0071108~protein K48-linked deubiquitination	GO:0005764~lysosome	GO:0004197~cysteine-type endopeptidase activity,GO:0004843~thiol-dependent ubiquitin-specific protease activity,GO:0005515~protein binding,GO:0008270~zinc ion binding,GO:0043130~ubiquitin binding	
VAPB	1.78	GO:0006874~cellular calcium ion homeostasis,GO:0006888~ER to Golgi vesicle-mediated transport,GO:0006987~activation of signaling protein activity involved in unfolded protein response,GO:0007029~endoplasmic reticulum organization,GO:0019048~modulation by virus of host morphology or physiology,GO:0030148~sphingolipid biosynthetic process,GO:0030968~endoplasmic reticulum unfolded protein response,GO:0044790~negative regulation by host of viral release from host cell,GO:0044791~positive regulation by host of viral release from host cell,GO:0044828~negative regulation by host of viral genome replication,GO:0044829~positive regulation by host of viral genome replication,GO:0044830~modulation by host of viral RNA genome replication,GO:0045070~positive regulation of viral genome replication,GO:0046725~negative regulation by virus of viral protein levels in host cell,GO:0090114~COPII-coated vesicle budding,GO:0098609~cell-cell adhesion	GO:0000139~Golgi membrane,GO:0005737~cytoplasm,GO:0005783~endoplasmic reticulum,GO:0005789~endoplasmic reticulum membrane,GO:0005794~Golgi apparatus,GO:0005913~cell-cell adherens junction,GO:0016021~integral component of membrane,GO:0070971~endoplasmic reticulum exit site	GO:0005515~protein binding,GO:0008017~microtubule binding,GO:0019899~enzyme binding,GO:0033149~FFAT motif binding,GO:0042803~protein homodimerization activity,GO:0046982~protein heterodimerization activity,GO:0048487~beta-tubulin binding,GO:0098641~cadherin binding involved in cell-cell adhesion	
SH3BGRL	1.72	GO:0009967~positive regulation of signal transduction	GO:0005615~extracellular space,GO:0005634~nucleus,GO:0005737~cytoplasm,GO:0070062~extracellular exosome	GO:0005070~SH3/SH2 adaptor activity,GO:0017124~SH3 domain binding	
TTLL12	1.71	GO:0006464~cellular protein modification process		GO:0005524~ATP binding,GO:0016874~ligase activity	

NSF	1.70	GO:0001921~positive regulation of receptor recycling,GO:0006813~potassium ion transport,GO:0006886~intracellular protein transport,GO:0006887~exocytosis,GO:0006888~ER to Golgi vesicle-mediated transport,GO:0006890~retrograde vesicle-mediated transport, Golgi to ER,GO:0006891~intra-Golgi vesicle-mediated transport,GO:0016192~vesicle-mediated transport,GO:0017157~regulation of exocytosis,GO:0035494~SNARE complex disassembly,GO:0043001~Golgi to plasma membrane protein transport,GO:0045026~plasma membrane fusion,GO:0045732~positive regulation of protein catabolic process,GO:0048208~COPII vesicle coating,GO:0048211~Golgi vesicle docking	GO:0000139~Golgi membrane,GO:0005737~cytoplasm,GO:0005765~lysosomal membrane,GO:0005795~Golgi stack,GO:0005829~cytosol,GO:0005886~plasma membrane,GO:0014069~postsynaptic density,GO:0043198~dendritic shaft,GO:0043209~myelin sheath,GO:0070062~extracellular exosome	GO:0000149~SNARE binding,GO:0005515~protein binding,GO:0005524~ATP binding,GO:0016887~ATPase activity,GO:0017075~syntaxin-1 binding,GO:0017137~Rab GTPase binding,GO:0019901~protein kinase binding,GO:0030165~PDZ domain binding,GO:0032403~protein complex binding,GO:0035255~ionotropic glutamate receptor binding,GO:0042623~ATPase activity, coupled,GO:0046872~metal ion binding	hsa04721:Synaptic vesicle cycle,hsa04727:GABAergic synapse,hsa04962:Vasopressin-regulated water reabsorption
CACYBP	1.70	GO:0007568~aging,GO:0045740~positive regulation of DNA replication,GO:0055007~cardiac muscle cell differentiation,GO:0060416~response to growth hormone,GO:0060548~negative regulation of cell death,GO:0071277~cellular response to calcium ion	GO:0005641~nuclear envelope lumen,GO:0005654~nucleoplasm,GO:0005737~cytoplasm,GO:0030877~beta-catenin destruction complex,GO:0043005~neuron projection,GO:0044297~cell body,GO:0070062~extracellular exosome	GO:0005515~protein binding,GO:0042803~protein homodimerization activity	hsa04310:Wnt signaling pathway
EFHD1	1.70	GO:0031175~neuron projection development	GO:0005743~mitochondrial inner membrane,GO:0070062~extracellular exosome	GO:0005509~calcium ion binding	
CES1	1.66	GO:0006695~cholesterol biosynthetic process,GO:0006805~xenobiotic metabolic process,GO:0008152~metabolic process,GO:0009636~response to toxic substance,GO:0030855~epithelial cell differentiation,GO:0051791~medium-chain fatty acid metabolic process,GO:0090122~cholesterol ester hydrolysis involved in cholesterol transport	GO:0005615~extracellular space,GO:0005788~endoplasmic reticulum lumen,GO:0005829~cytosol	GO:0004771~sterol esterase activity,GO:0047374~methylumbelliferyl-acetate deacetylase activity,GO:0052689~carboxylic ester hydrolase activity	hsa00983:Drug metabolism - other enzymes,hsa01100:Metabolic pathways
LMAN2	1.65	GO:0006888~ER to Golgi vesicle-mediated transport,GO:0006890~retrograde vesicle-mediated transport, Golgi to ER,GO:0007029~endoplasmic reticulum organization,GO:0007030~Golgi organization,GO:0015031~protein transport,GO:0050766~positive regulation of phagocytosis	GO:0000139~Golgi membrane,GO:0005615~extracellular space,GO:0005789~endoplasmic reticulum membrane,GO:0005793~endoplasmic reticulum-Golgi intermediate compartment,GO:0005794~Golgi apparatus,GO:0005887~integral component of plasma membrane,GO:0009986~cell surface,GO:0016020~membrane,GO:0030134~ER to Golgi transport vesicle,GO:0033116~endoplasmic reticulum-Golgi intermediate compartment membrane,GO:0070062~extracellular exosome	GO:0001948~glycoprotein binding,GO:0005537~mannose binding,GO:0030246~carbohydrate binding,GO:0031072~heat shock protein binding,GO:0046872~metal ion binding	hsa04141:Protein processing in endoplasmic reticulum
ACADSB	1.64	GO:0006631~fatty acid metabolic process,GO:0009083~branched-chain amino acid catabolic process,GO:0033539~fatty acid beta-oxidation using acyl-CoA dehydrogenase,GO:0055088~lipid homeostasis	GO:0005739~mitochondrion,GO:0005759~mitochondrial matrix,GO:0070062~extracellular exosome	GO:0000062~fatty-acyl-CoA binding,GO:0003995~acyl-CoA dehydrogenase activity,GO:0009055~electron carrier activity,GO:0050660~flavin adenine dinucleotide binding,GO:0052890~oxidoreductase activity, acting on the CH-CH group of donors, with a flavin as acceptor	hsa00071:Fatty acid degradation,hsa00280:Valine, leucine and isoleucine degradation,hsa01100:Metabolic pathways,hsa01212:Fatty acid metabolism
ATP1A1	1.59	GO:0002026~regulation of the force of heart contraction,GO:0002028~regulation of sodium ion transport,GO:0006883~cellular sodium ion homeostasis,GO:0008217~regulation of blood pressure,GO:0010107~potassium ion import,GO:0010248~establishment or maintenance of transmembrane electrochemical gradient,GO:0015991~ATP hydrolysis coupled proton transport,GO:0016311~dephosphorylation,GO:0030007~cellular potassium ion homeostasis,GO:0031947~negative regulation of glucocorticoid biosynthetic process,GO:0034220~ion transmembrane transport,GO:0036376~sodium ion export from cell,GO:0042493~response to drug,GO:0045822~negative regulation of heart contraction,GO:0045823~positive regulation of heart contraction,GO:0045989~positive regulation of striated muscle contraction,GO:0055119~relaxation of cardiac muscle,GO:0060048~cardiac muscle contraction,GO:0060081~membrane hyperpolarization,GO:0071260~cellular response to mechanical stimulus,GO:0071383~cellular response to steroid hormone stimulus,GO:0086002~cardiac muscle cell action potential involved in contraction,GO:0086004~regulation of cardiac muscle cell contraction,GO:0086009~membrane repolarization,GO:0086013~membrane repolarization during cardiac muscle cell action potential,GO:0086064~cell communication by electrical coupling involved in cardiac conduction,GO:1903416~response to glycoside,GO:1903779~regulation of cardiac conduction,GO:1990573~potassium ion import across plasma membrane	GO:0005768~endosome,GO:0005783~endoplasmic reticulum,GO:0005794~Golgi apparatus,GO:0005886~plasma membrane,GO:0005890~sodium:potassium-exchanging ATPase complex,GO:0005901~caveola,GO:0014069~postsynaptic density,GO:0014704~intercalated disc,GO:0016020~membrane,GO:0016021~integral component of membrane,GO:0016323~basolateral plasma membrane,GO:0016324~apical plasma membrane,GO:0030315~T-tubule,GO:0042383~sarcolemma,GO:0042470~melanosome,GO:0043209~myelin sheath,GO:0043231~intracellular membrane-bounded organelle,GO:0043234~protein complex,GO:0070062~extracellular exosome,GO:1903561~extracellular vesicle	GO:0000166~nucleotide binding,GO:0005391~sodium:potassium-exchanging ATPase activity,GO:0005515~protein binding,GO:0005524~ATP binding,GO:0016791~phosphatase activity,GO:0019901~protein kinase binding,GO:0019904~protein domain specific binding,GO:0030506~ankyrin binding,GO:0030955~potassium ion binding,GO:0031402~sodium ion binding,GO:0043531~ADP binding,GO:0043548~phosphatidylinositol 3-kinase binding,GO:0046872~metal ion binding,GO:0051087~chaperone binding,GO:1990239~steroid hormone binding	hsa04022:cGMP-PKG signaling pathway,hsa04024:cAMP signaling pathway,hsa04260:Cardiac muscle contraction,hsa04261:Adrenergic signaling in cardiomyocytes,hsa04911:Insulin secretion,hsa04918:Thyroid hormone synthesis,hsa04919:Thyroid hormone signaling pathway,hsa04960:Aldosterone-regulated sodium reabsorption,hsa04961:Endocrine and other factor-regulated calcium reabsorption,hsa04964:Proximal tubule bicarbonate reclamation,hsa04970:Salivary secretion,hsa04971:Gastric acid secretion,hsa04972:Pancreatic secretion,hsa04973:Carbohydrate digestion and absorption,hsa04974:Protein digestion and absorption,hsa04976:Bile secretion,hsa04978:Mineral absorption
PALLD	1.56	GO:0003334~keratinocyte development,GO:0003382~epithelial cell morphogenesis,GO:0007010~cytoskeleton organization,GO:0016477~cell migration,GO:0030036~actin cytoskeleton organization	GO:0001726~ruffle,GO:0002102~podosome,GO:0005634~nucleus,GO:0005737~cytoplasm,GO:0005739~mitochondrion,GO:0005884~actin filament,GO:0005886~plasma membrane,GO:0005925~focal adhesion,GO:0015629~actin cytoskeleton,GO:0030018~Z disc,GO:0030027~lamellipodium,GO:0030424~axon,GO:0030426~growth cone	GO:0003779~actin binding,GO:0005515~protein binding,GO:0051371~muscle alpha-actinin binding	

GOLT1B	1.56	GO:0007165~signal transduction,GO:0015031~protein transport,GO:0016192~vesicle-mediated transport,GO:0043123~positive regulation of I-kappaB kinase/NF-kappaB signaling	GO:0000139~Golgi membrane,GO:0005783~endoplasmic reticulum,GO:0016020~membrane,GO:0016021~integral component of membrane	GO:0004871~signal transducer activity	
SEC63	1.55	GO:0001889~liver development,GO:0006612~protein targeting to membrane,GO:0006614~SRP-dependent cotranslational protein targeting to membrane,GO:0006620~posttranslational protein targeting to membrane,GO:0006807~nitrogen compound metabolic process,GO:0010259~multicellular organism aging,GO:0036498~IRE1-mediated unfolded protein response,GO:0072001~renal system development	GO:0005622~intracellular,GO:0005783~endoplasmic reticulum,GO:0005789~endoplasmic reticulum membrane,GO:0005829~cytosol,GO:0016020~membrane,GO:0016021~integral component of membrane	GO:0004872~receptor activity,GO:0005515~protein binding,GO:0044822~poly(A) RNA binding	hsa03060:Protein export,hsa04141:Protein processing in endoplasmic reticulum
AGR2	1.51	GO:0010628~positive regulation of gene expression,GO:0010811~positive regulation of cell-substrate adhesion,GO:0030154~cell differentiation,GO:0034976~response to endoplasmic reticulum stress,GO:0045742~positive regulation of epidermal growth factor receptor signaling pathway,GO:0048546~digestive tract morphogenesis,GO:0048639~positive regulation of developmental growth,GO:0060480~lung goblet cell differentiation,GO:0060548~negative regulation of cell death,GO:0070254~mucus secretion,GO:0090004~positive regulation of establishment of protein localization to plasma membrane,GO:1903896~positive regulation of IRE1-mediated unfolded protein response,GO:1903899~positive regulation of PERK-mediated unfolded protein response	GO:0005615~extracellular space,GO:0005739~mitochondrion,GO:0005783~endoplasmic reticulum	GO:0002162~dystroglycan binding,GO:0005154~epidermal growth factor receptor binding,GO:0005515~protein binding,GO:0042803~protein homodimerization activity	
ECH1	-1.51	GO:0006635~fatty acid beta-oxidation,GO:0008152~metabolic process,GO:0009062~fatty acid catabolic process	GO:0005739~mitochondrion,GO:0005777~peroxisome,GO:0016020~membrane,GO:0070062~extracellular exosome	GO:0003824~catalytic activity,GO:0005102~receptor binding,GO:0005515~protein binding,GO:0016853~isomerase activity	hsa04146:Peroxisome
TTR	-1.57	GO:0001523~retinoid metabolic process,GO:0006144~purine nucleobase metabolic process,GO:0006810~transport,GO:0030198~extracellular matrix organization,GO:0042572~retinol metabolic process,GO:0044267~cellular protein metabolic process,GO:0070327~thyroid hormone transport	GO:0005576~extracellular region,GO:0005615~extracellular space,GO:0005737~cytoplasm,GO:0043234~protein complex,GO:0070062~extracellular exosome	GO:0005179~hormone activity,GO:0005515~protein binding,GO:0042562~hormone binding,GO:0042802~identical protein binding,GO:0046982~protein heterodimerization activity,GO:0070324~thyroid hormone binding	
ERLIN2	-1.59	GO:0008203~cholesterol metabolic process,GO:0018108~peptidyl-tyrosine phosphorylation,GO:0030433~ER-associated ubiquitin-dependent protein catabolic process,GO:0032933~SREBP signaling pathway,GO:0045541~negative regulation of cholesterol biosynthetic process,GO:0045717~negative regulation of fatty acid biosynthetic process	GO:0005737~cytoplasm,GO:0005783~endoplasmic reticulum,GO:0005789~endoplasmic reticulum membrane,GO:0005886~plasma membrane,GO:0016021~integral component of membrane,GO:0043234~protein complex,GO:0045121~membrane raft,GO:0070062~extracellular exosome	GO:0004713~protein tyrosine kinase activity,GO:0005515~protein binding,GO:0015485~cholesterol binding,GO:0031625~ubiquitin protein ligase binding	
PRKDC	-1.61	GO:0001756~somitogenesis,GO:0001933~negative regulation of protein phosphorylation,GO:0002326~B cell lineage commitment,GO:0002328~pro-B cell differentiation,GO:0002360~T cell lineage commitment,GO:0002638~negative regulation of immunoglobulin production,GO:0002684~positive regulation of immune system process,GO:0006302~double-strand break repair,GO:0006303~double-strand break repair via nonhomologous end joining,GO:0006464~cellular protein modification process,GO:0007420~brain development,GO:0007507~heart development,GO:0008283~cell proliferation,GO:0008630~intrinsic apoptotic signaling pathway in response to DNA damage,GO:0010332~response to gamma radiation,GO:0014823~response to activity,GO:0016233~telomere capping,GO:0018105~peptidyl-serine phosphorylation,GO:0031648~protein destabilization,GO:0032481~positive regulation of type I interferon production,GO:0032869~cellular response to insulin stimulus,GO:0033077~T cell differentiation in thymus,GO:0033152~immunoglobulin V(D)J recombination,GO:0033153~T cell receptor V(D)J recombination,GO:0035234~ectopic germ cell programmed cell death,GO:0042752~regulation of circadian rhythm,GO:0043065~positive regulation of apoptotic process,GO:0043066~negative regulation of apoptotic process,GO:0045944~positive regulation of transcription from RNA polymerase II promoter,GO:0048146~positive regulation of fibroblast proliferation,GO:0048511~rhythmic process,GO:0048536~spleen development,GO:0048538~thymus development,GO:0048639~positive regulation of developmental growth,GO:0048660~regulation of smooth muscle cell proliferation,GO:0072431~signal transduction involved in mitotic G1 DNA damage checkpoint,GO:0097681~double-strand break repair via alternative nonhomologous end joining,GO:2000773~negative regulation of cellular senescence,GO:2001229~negative regulation of response to gamma radiation	GO:0000784~nuclear chromosome, telomeric region,GO:0005654~nucleoplasm,GO:0005667~transcription factor complex,GO:0005730~nucleolus,GO:0005829~cytosol,GO:0005958~DNA-dependent protein kinase-DNA ligase 4 complex,GO:0016020~membrane,GO:0031012~extracellular matrix,GO:0070419~nonhomologous end joining complex	GO:0003690~double-stranded DNA binding,GO:0004672~protein kinase activity,GO:0004674~protein serine/threonine kinase activity,GO:0004677~DNA-dependent protein kinase activity,GO:0005515~protein binding,GO:0005524~ATP binding,GO:0008134~transcription factor binding,GO:0016301~kinase activity,GO:0019899~enzyme binding,GO:0044822~poly(A) RNA binding	hsa03450:Non-homologous end-joining,hsa04110:Cell cycle
PHGDH	-1.63	GO:0006541~glutamine metabolic process,GO:0006544~glycine metabolic process,GO:0006564~L-serine biosynthetic process,GO:0006566~threonine metabolic process,GO:0007420~brain development,GO:0009070~serine family amino acid biosynthetic process,GO:0009448~gamma-aminobutyric acid metabolic process,GO:0010468~regulation of gene expression,GO:0019530~taurine metabolic process,GO:0021510~spinal cord development,GO:0021782~glial cell development,GO:0021915~neural tube development,GO:0031175~neuron projection development,GO:0055114~oxidation-reduction process,GO:0070314~G1 to G0 transition	GO:0005829~cytosol,GO:0043209~myelin sheath,GO:0070062~extracellular exosome	GO:0004617~phosphoglycerate dehydrogenase activity,GO:0009055~electron carrier activity,GO:0051287~NAD binding	hsa00260:Glycine, serine and threonine metabolism,hsa01100:Metabolic pathways,hsa01130:Biosynthesis of antibiotics,hsa01200:Carbon metabolism,hsa01230:Biosynthesis of amino acids
DCN	-1.63	GO:0001822~kidney development,GO:0001890~placenta development,GO:0006469~negative regulation of protein kinase activity,GO:0007519~skeletal muscle tissue development,GO:0007568~aging,GO:0009612~response to mechanical stimulus,GO:0009887~organ morphogenesis,GO:0010508~positive regulation of autophagy,GO:0010596~negative regulation of endothelial cell migration,GO:0014068~positive regulation of phosphatidylinositol 3-kinase signaling,GO:0016239~positive regulation of macroautophagy,GO:0016525~negative regulation of angiogenesis,GO:0019221~cytokine-mediated signaling pathway,GO:0019800~peptide cross-linking via chondroitin 4-sulfate glycosaminoglycan,GO:0022617~extracellular matrix disassembly,GO:0030198~extracellular matrix organization,GO:0030203~glycosaminoglycan metabolic process,GO:0030206~chondroitin sulfate biosynthetic process,GO:0030207~chondroitin sulfate catabolic process,GO:0030208~dermatan sulfate biosynthetic process,GO:0032496~response to lipopolysaccharide,GO:0042060~wound healing,GO:0045944~positive regulation of transcription from RNA polymerase II promoter,GO:0046426~negative regulation of JAK-STAT cascade,GO:0051901~positive regulation of mitochondrial depolarization,GO:0090141~positive regulation of mitochondrial fission,GO:1900747~negative regulation of vascular endothelial growth factor signaling pathway	GO:0005576~extracellular region,GO:0005589~collagen type VI trimer,GO:0005615~extracellular space,GO:0005737~cytoplasm,GO:0005796~Golgi lumen,GO:0031012~extracellular matrix,GO:0043202~lysosomal lumen	GO:0004860~protein kinase inhibitor activity,GO:0005515~protein binding,GO:0005518~collagen binding,GO:0005539~glycosaminoglycan binding,GO:0044822~poly(A) RNA binding,GO:0047485~protein N-terminus binding,GO:0050840~extracellular matrix binding	hsa04350:TGF-beta signaling pathway,hsa05205:Proteoglycans in cancer
HIST1H4A	-1.64	GO:0000183~chromatin silencing at rDNA,GO:0006303~double-strand break repair via nonhomologous end joining,GO:0006334~nucleosome assembly,GO:0006335~DNA replication-dependent nucleosome assembly,GO:0006336~DNA replication-independent nucleosome assembly,GO:0006352~DNA-templated transcription, initiation,GO:0016233~telomere capping,GO:0031047~gene silencing by RNA,GO:0032200~telomere organization,GO:0034080~CENP-A containing nucleosome assembly,GO:0044267~cellular protein metabolic process,GO:0045653~negative regulation of megakaryocyte differentiation,GO:0045814~negative regulation of gene expression, epigenetic,GO:0045815~positive regulation of gene expression, epigenetic,GO:0051290~protein heterotetramerization,GO:1904837~beta-catenin-TCF complex assembly	GO:0000228~nuclear chromosome,GO:0000784~nuclear chromosome, telomeric region,GO:0000786~nucleosome,GO:0005576~extracellular region,GO:0005634~nucleus,GO:0005654~nucleoplasm,GO:0016020~membrane,GO:0031012~extracellular matrix,GO:0043234~protein complex,GO:0070062~extracellular exosome	GO:0003677~DNA binding,GO:0005515~protein binding,GO:0019904~protein domain specific binding,GO:0042393~histone binding,GO:0044822~poly(A) RNA binding,GO:0046982~protein heterodimerization activity	hsa05034:Alcoholism,hsa05203:Viral carcinogenesis,hsa05322:Systemic lupus erythematosus

PFN1	-1.65	GO:0001843~neural tube closure,GO:0010634~positive regulation of epithelial cell migration,GO:0030036~actin cytoskeleton organization,GO:0030837~negative regulation of actin filament polymerization,GO:0030838~positive regulation of actin filament polymerization,GO:0032232~negative regulation of actin filament bundle assembly,GO:0032233~positive regulation of actin filament bundle assembly,GO:0032781~positive regulation of ATPase activity,GO:0045944~positive regulation of transcription from RNA polymerase II promoter,GO:0050434~positive regulation of viral transcription,GO:0050821~protein stabilization,GO:0051054~positive regulation of DNA metabolic process,GO:0051496~positive regulation of stress fiber assembly,GO:0051497~negative regulation of stress fiber assembly,GO:0060071~Wnt signaling pathway, planar cell polarity pathway,GO:0071363~cellular response to growth factor stimulus,GO:0098609~cell-cell adhesion,GO:1900029~positive regulation of ruffle assembly	GO:0005634~nucleus,GO:0005737~cytoplasm,GO:0005829~cytosol,GO:0005856~cytoskeleton,GO:0005913~cell-cell adherens junction,GO:0005925~focal adhesion,GO:0005938~cell cortex,GO:0016020~membrane,GO:0043005~neuron projection,GO:0045202~synapse,GO:0070062~extracellular exosome,GO:0072562~blood microparticle	GO:0000774~adenyl-nucleotide exchange factor activity,GO:0003779~actin binding,GO:0003785~actin monomer binding,GO:0005102~receptor binding,GO:0005515~protein binding,GO:0005546~phosphatidylinositol-4,5-bisphosphate binding,GO:0017048~Rho GTPase binding,GO:0044822~poly(A) RNA binding,GO:0070064~proline-rich region binding,GO:0098641~cadherin binding involved in cell-cell adhesion	hsa04015:Rap1 signaling pathway,hsa04810:Regulation of actin cytoskeleton,hsa05131:Shigellosis,hsa05132:Salmonella infection
GLO1	-1.65	GO:0005975~carbohydrate metabolic process,GO:0006090~pyruvate metabolic process,GO:0006357~regulation of transcription from RNA polymerase II promoter,GO:0006749~glutathione metabolic process,GO:0009438~methylglyoxal metabolic process,GO:0030316~osteoclast differentiation,GO:0043066~negative regulation of apoptotic process	GO:0005737~cytoplasm,GO:0005829~cytosol,GO:0070062~extracellular exosome	GO:0004462~lactoylglutathione lyase activity,GO:0008270~zinc ion binding	hsa00620:Pyruvate metabolism
TF	-1.66	GO:0001895~retina homeostasis,GO:0002576~platelet degranulation,GO:0006879~cellular iron ion homeostasis,GO:0031647~regulation of protein stability,GO:0033572~transferrin	GO:0005576~extracellular	GO:0005515~protein binding,GO:0008198~ferrous	hsa04066:HIF-1 signaling
AHNAK	-1.69	GO:0043484~regulation of RNA splicing,GO:0051259~protein oligomerization,GO:0098609~cell-cell adhesion,GO:1901385~regulation of voltage-gated calcium channel activity	GO:0005634~nucleus,GO:0005737~cytoplasm,GO:0005765~lysosomal membrane,GO:0005829~cytosol,GO:0005886~plasma membrane,GO:0005913~cell-cell adherens junction,GO:0005925~focal adhesion,GO:0015629~actin cytoskeleton,GO:0016020~membrane,GO:0019013~viral nucleocapsid,GO:0030315~T-tubule,GO:0031982~vesicle,GO:0042383~sarcolemma,GO:0043034~costamere,GO:0044291~cell-cell contact zone,GO:0045121~membrane raft,GO:0070062~extracellular exosome	GO:0005515~protein binding,GO:0044548~S100 protein binding,GO:0044822~poly(A) RNA binding,GO:0097493~structural molecule activity conferring elasticity,GO:0098641~cadherin binding involved in cell-cell adhesion	
BGN	-1.72	GO:0001974~blood vessel remodeling,GO:0006469~negative regulation of protein kinase activity,GO:0019221~cytokine-mediated signaling pathway,GO:0019800~peptide cross-linking via chondroitin 4-sulfate glycosaminoglycan,GO:0030198~extracellular matrix organization,GO:0030203~glycosaminoglycan metabolic process,GO:0030206~chondroitin sulfate biosynthetic process,GO:0030207~chondroitin sulfate catabolic process,GO:0030208~dermatan sulfate biosynthetic process,GO:0046426~negative regulation of JAK-STAT cascade	GO:0005576~extracellular region,GO:0005578~proteinaceous extracellular matrix,GO:0005737~cytoplasm,GO:0005796~Golgi lumen,GO:0009986~cell surface,GO:0030133~transport vesicle,GO:0031012~extracellular matrix,GO:0042383~sarcolemma,GO:0043202~lysosomal lumen,GO:0070062~extracellular exosome	GO:0004860~protein kinase inhibitor activity,GO:0005201~extracellular matrix structural constituent,GO:0005539~glycosaminoglycan binding,GO:0050840~extracellular matrix binding	
TNC	-1.72	GO:0001649~osteoblast differentiation,GO:0007155~cell adhesion,GO:0007162~negative regulation of cell adhesion,GO:0007528~neuromuscular junction development,GO:0008284~positive regulation of cell proliferation,GO:0009611~response to wounding,GO:0009612~response to mechanical stimulus,GO:0010628~positive regulation of gene expression,GO:0014012~peripheral nervous system axon regeneration,GO:0030198~extracellular matrix organization,GO:0042060~wound healing,GO:0042127~regulation of cell proliferation,GO:0042475~odontogenesis of dentin-containing tooth,GO:0045471~response to ethanol,GO:0060447~bud outgrowth involved in lung branching,GO:0060739~mesenchymal-epithelial cell signaling involved in prostate gland development,GO:0060740~prostate gland epithelium morphogenesis,GO:0071300~cellular response to retinoic acid,GO:0071305~cellular response to vitamin D,GO:0071774~response to fibroblast growth factor,GO:0071799~cellular response to prostaglandin D stimulus	GO:0005576~extracellular region,GO:0005604~basement membrane,GO:0005614~interstitial matrix,GO:0005615~extracellular space,GO:0005925~focal adhesion,GO:0016020~membrane,GO:0031012~extracellular matrix	GO:0045545~syndecan binding	hsa04151:PI3K-Akt signaling pathway,hsa04510:Focal adhesion,hsa04512:ECM-receptor interaction,hsa05206:MicroRNAs in cancer
SERPIND1	-1.79	GO:0006935~chemotaxis,GO:0007596~blood coagulation,GO:0008218~bioluminescence,GO:0010951~negative regulation of endopeptidase activity	GO:0005576~extracellular region,GO:0005615~extracellular space,GO:0070062~extracellular exosome	GO:0004866~endopeptidase inhibitor activity,GO:0004867~serine-type endopeptidase inhibitor activity,GO:0008201~heparin binding	hsa04610:Complement and coagulation cascades
LCP1	-1.81	GO:0002286~T cell activation involved in immune response,GO:0010737~protein kinase A signaling,GO:0016477~cell migration,GO:0022617~extracellular matrix disassembly,GO:0031100~organ regeneration,GO:0033157~regulation of intracellular protein transport,GO:0044319~wound healing, spreading of cells,GO:0051017~actin filament bundle assembly,GO:0051639~actin filament network formation,GO:0051764~actin crosslink formation,GO:0071803~positive regulation of podosome assembly	GO:0001725~stress fiber,GO:0001726~ruffle,GO:0001891~phagocytic cup,GO:0002102~podosome,GO:0005615~extracellular space,GO:0005737~cytoplasm,GO:0005829~cytosol,GO:0005884~actin filament,GO:0005886~plasma membrane,GO:0005925~focal adhesion,GO:0015629~actin cytoskeleton,GO:0030175~filopodium,GO:0032432~actin filament bundle,GO:0032587~ruffle membrane,GO:0070062~extracellular exosome	GO:0003779~actin binding,GO:0005509~calcium ion binding,GO:0042802~identical protein binding,GO:0051015~actin filament binding,GO:0051020~GTPase binding	
ITIH1	-1.82	GO:0010951~negative regulation of endopeptidase activity,GO:0030212~hyaluronan metabolic process	GO:0005576~extracellular region,GO:0070062~extracellular exosome,GO:0072562~blood microparticle	GO:0004867~serine-type endopeptidase inhibitor activity,GO:0005509~calcium ion binding	
IGHG4	-1.93	GO:0006508~proteolysis,GO:0006910~phagocytosis, recognition,GO:0006911~phagocytosis, engulfment,GO:0006956~complement activation,GO:0006958~complement activation, classical pathway,GO:0038096~Fc-gamma receptor signaling pathway involved in phagocytosis,GO:0042742~defense response to bacterium,GO:0045087~innate immune response,GO:0050853~B cell receptor signaling pathway,GO:0050871~positive regulation of B cell activation	GO:0005576~extracellular region,GO:0005615~extracellular space,GO:0009897~external side of plasma membrane,GO:0042571~immunoglobulin complex, circulating,GO:0070062~extracellular exosome,GO:0072562~blood microparticle	GO:0003823~antigen binding,GO:0004252~serine-type endopeptidase activity,GO:0034987~immunoglobulin receptor binding	

GPD1	-1.95	GO:0006094~gluconeogenesis,GO:0006127~glycerophosphate shuttle,GO:0006654~phosphatidic acid biosynthetic process,GO:0019432~triglyceride biosynthetic process,GO:0045821~positive regulation of glycolytic process,GO:0046168~glycerol-3-phosphate catabolic process,GO:0046486~glycerolipid metabolic process,GO:0071320~cellular response to cAMP,GO:0071356~cellular response to tumor necrosis factor	GO:0005739~mitochondrion,GO:0005829~cytosol,GO:0009331~glycerol-3-phosphate dehydrogenase complex,GO:0070062~extracellular exosome	GO:0004367~glycerol-3-phosphate dehydrogenase [NAD+] activity,GO:0004368~glycerol-3-phosphate dehydrogenase activity,GO:0042803~protein homodimerization activity,GO:0051287~NAD binding	hsa00564:Glycerophospholipid metabolism
LUM	-1.96	GO:0007409~axonogenesis,GO:0007601~visual perception,GO:0014070~response to organic cyclic compound,GO:0018146~keratan sulfate biosynthetic process,GO:0030198~extracellular matrix organization,GO:0030199~collagen fibril organization,GO:0032914~positive regulation of transforming growth factor beta1 production,GO:0042340~keratan sulfate catabolic process,GO:0045944~positive regulation of transcription from RNA polymerase II promoter,GO:0051216~cartilage development,GO:0070848~response to growth factor	GO:0005576~extracellular region,GO:0005578~proteinaceous extracellular matrix,GO:0005583~fibrillar collagen trimer,GO:0005615~extracellular space,GO:0005796~Golgi lumen,GO:0031012~extracellular matrix,GO:0043202~lysosomal lumen,GO:0070062~extracellular exosome	GO:0005201~extracellular matrix structural constituent,GO:0005515~protein binding,GO:0005518~collagen binding	hsa05205:Proteoglycans in cancer
HBD	-2.00	GO:0007596~blood coagulation,GO:0015671~oxygen transport	GO:0005829~cytosol,GO:0005833~hemoglobin complex,GO:0072562~blood microparticle	GO:0005344~oxygen transporter activity,GO:0005506~iron ion binding,GO:0005515~protein binding,GO:0019825~oxygen binding,GO:0020037~heme binding	
PLIN1	-2.08	GO:0006629~lipid metabolic process,GO:0016042~lipid catabolic process	GO:0005783~endoplasmic	GO:0008289~lipid binding	hsa03320:PPAR signaling
CRYAB	-2.10	GO:0001666~response to hypoxia,GO:0002088~lens development in camera-type eye,GO:0006457~protein folding,GO:0006936~muscle contraction,GO:0007021~tubulin complex assembly,GO:0007517~muscle organ development,GO:0007568~aging,GO:0010629~negative regulation of gene expression,GO:0010941~regulation of cell death,GO:0030308~negative regulation of cell growth,GO:0031109~microtubule polymerization or depolymerization,GO:0032355~response to estradiol,GO:0032387~negative regulation of intracellular transport,GO:0042542~response to hydrogen peroxide,GO:0043066~negative regulation of apoptotic process,GO:0043154~negative regulation of cysteine-type endopeptidase activity involved in apoptotic process,GO:0051260~protein homooligomerization,GO:0051403~stress-activated MAPK cascade,GO:0060561~apoptotic process involved in morphogenesis,GO:0071480~cellular response to gamma radiation,GO:1900034~regulation of cellular response to heat,GO:2000378~negative regulation of reactive oxygen species metabolic process	GO:0005634~nucleus,GO:0005654~nucleoplasm,GO:0005737~cytoplasm,GO:0005739~mitochondrion,GO:0005794~Golgi apparatus,GO:0005829~cytosol,GO:0009986~cell surface,GO:0014069~postsynaptic density,GO:0015630~microtubule cytoskeleton,GO:0030018~Z disc,GO:0030424~axon,GO:0031430~M band,GO:0032432~actin filament bundle,GO:0043197~dendritic spine,GO:0043204~perikaryon,GO:0043209~myelin sheath,GO:0070062~extracellular exosome,GO:0097060~synaptic membrane,GO:0097512~cardiac myofibril	GO:0005212~structural constituent of eye lens,GO:0005515~protein binding,GO:0008017~microtubule binding,GO:0042802~identical protein binding,GO:0042803~protein homodimerization activity,GO:0046872~metal ion binding,GO:0051082~unfolded protein binding	hsa04141:Protein processing in endoplasmic reticulum
TNXB	-2.15	GO:0007155~cell adhesion,GO:0030036~actin cytoskeleton organization,GO:0030199~collagen fibril organization,GO:0032963~collagen metabolic process,GO:0048251~elastic fiber assembly	GO:0005578~proteinaceous extracellular matrix,GO:0005583~fibrillar collagen trimer,GO:0005615~extracellular space,GO:0005622~intracellular,GO:0031012~extracellular matrix,GO:0070062~extracellular exosome	GO:0005178~integrin binding,GO:0005201~extracellular matrix structural constituent,GO:0005515~protein binding,GO:0008201~heparin binding	hsa04151:PI3K-Akt signaling pathway,hsa04510:Focal adhesion,hsa04512:ECM-receptor interaction,hsa05206:MicroRNAs in cancer
DHRS2	-2.25	GO:0008207~C21-steroid hormone metabolic process,GO:0008285~negative regulation of cell proliferation,GO:0009636~response to toxic substance,GO:0034599~cellular response to oxidative stress,GO:0043011~myeloid dendritic cell differentiation,GO:0043066~negative regulation of apoptotic process,GO:0055114~oxidation-reduction process	GO:0005634~nucleus,GO:0005635~nuclear envelope,GO:0005737~cytoplasm,GO:0005739~mitochondrion,GO:0005759~mitochondrial matrix,GO:0070062~extracellular exosome	GO:0004090~carbonyl reductase (NADPH) activity,GO:0005515~protein binding,GO:0016491~oxidoreductase activity	
PTGIS	-2.46	GO:0001516~prostaglandin biosynthetic process,GO:0006690~icosanoid metabolic process,GO:0006769~nicotinamide metabolic process,GO:0007566~embryo implantation,GO:0019371~cyclooxygenase pathway,GO:0032088~negative regulation of NF-kappaB transcription factor activity,GO:0035360~positive regulation of peroxisome proliferator activated receptor signaling pathway,GO:0045019~negative regulation of nitric oxide biosynthetic process,GO:0045766~positive regulation of angiogenesis,GO:0046697~decidualization,GO:0050728~negative regulation of inflammatory response,GO:0055114~oxidation-reduction process,GO:0071347~cellular response to interleukin-1,GO:0071354~cellular response to interleukin-6,GO:0071456~cellular response to hypoxia,GO:0097190~apoptotic signaling pathway,GO:1900119~positive regulation of execution phase of apoptosis	GO:0005615~extracellular space,GO:0005634~nucleus,GO:0005783~endoplasmic reticulum,GO:0005789~endoplasmic reticulum membrane,GO:0005901~caveola,GO:0016021~integral component of membrane	GO:0004497~monooxygenase activity,GO:0005506~iron ion binding,GO:0005515~protein binding,GO:0008116~prostaglandin-I synthase activity,GO:0016705~oxidoreductase activity, acting on paired donors, with incorporation or reduction of molecular oxygen,GO:0020037~heme binding	hsa00590:Arachidonic acid metabolism,hsa01100:Metabolic pathways
CD36	-2.67	GO:0000122~negative regulation of transcription from RNA polymerase II promoter,GO:0001954~positive regulation of cell-matrix adhesion,GO:0002479~antigen processing and presentation of exogenous peptide antigen via MHC class I, TAP-dependent,GO:0002576~platelet degranulation,GO:0002755~MyD88-dependent toll-like receptor signaling pathway,GO:0006629~lipid metabolic process,GO:0006898~receptor-mediated endocytosis,GO:0006910~phagocytosis, recognition,GO:0006955~immune response,GO:0007155~cell adhesion,GO:0007166~cell surface receptor signaling pathway,GO:0007204~positive regulation of cytosolic calcium ion concentration,GO:0007263~nitric oxide mediated signal transduction,GO:0007596~blood coagulation,GO:0010744~positive regulation of macrophage derived foam cell differentiation,GO:0010886~positive regulation of cholesterol storage,GO:0019915~lipid storage,GO:0019934~cGMP-mediated signaling,GO:0030194~positive regulation of blood coagulation,GO:0030299~intestinal cholesterol absorption,GO:0030301~cholesterol transport,GO:0031623~receptor internalization,GO:0032735~positive regulation of interleukin-12 production,GO:0032755~positive regulation of interleukin-6 production,GO:0032760~positive regulation of tumor necrosis factor production,GO:0033993~response to lipid,GO:0034197~triglyceride transport,GO:0034381~plasma lipoprotein particle clearance,GO:0034383~low-density lipoprotein particle clearance,GO:0035634~response to stilbenoid,GO:0038124~toll-like receptor TLR6:TLR2 signaling pathway,GO:0042953~lipoprotein transport,GO:0042992~negative regulation of transcription factor import into nucleus,GO:0043123~positive regulation of I-kappaB kinase/NF-kappaB signaling,GO:0043277~apoptotic cell clearance,GO:0044130~negative regulation of growth of symbiont in host,GO:0044539~long-chain fatty acid import,GO:0050702~interleukin-1 beta secretion,GO:0050731~positive regulation of peptidyl-tyrosine phosphorylation,GO:0050830~defense response to Gram-positive bacterium,GO:0050892~intestinal absorption,GO:0050909~sensory perception of taste,GO:0055096~low-density lipoprotein particle mediated signaling,GO:0060100~positive regulation of phagocytosis, engulfment,GO:0060907~positive regulation of macrophage cytokine production,GO:0070374~positive regulation of ERK1 and ERK2 cascade,GO:0070508~cholesterol import,GO:0070542~response to fatty acid,GO:0070543~response to linoleic acid,GO:0071221~cellular response to bacterial lipopeptide,GO:0071222~cellular response to lipopolysaccharide,GO:0071223~cellular response to lipoteichoic acid,GO:0071404~cellular response to low-density lipoprotein particle stimulus,GO:0071447~cellular response to hydroperoxide,GO:0071726~cellular response to diacyl bacterial lipopeptide,GO:1900227~positive regulation of NLRP3 inflammasome complex assembly,GO:1990000~amyloid fibril formation,GO:2000121~regulation of removal of superoxide radicals,GO:2000334~positive regulation of blood microparticle formation,GO:2000379~positive regulation of reactive oxygen species metabolic process,GO:2000505~regulation of energy homeostasis	GO:0005581~collagen trimer,GO:0005615~extracellular space,GO:0005794~Golgi apparatus,GO:0005886~plasma membrane,GO:0005887~integral component of plasma membrane,GO:0009897~external side of plasma membrane,GO:0009986~cell surface,GO:0016020~membrane,GO:0016021~integral component of membrane,GO:0016324~apical plasma membrane,GO:0030666~endocytic vesicle membrane,GO:0031092~platelet alpha granule membrane,GO:0031526~brush border membrane,GO:0045121~membrane raft,GO:0045177~apical part of cell,GO:0045335~phagocytic vesicle,	GO:0005041~low-density lipoprotein receptor activity,GO:0005515~protein binding,GO:0008035~high-density lipoprotein particle binding,GO:0008289~lipid binding,GO:0030169~low-density lipoprotein particle binding,GO:0050431~transforming growth factor beta binding,GO:0070053~thrombospondin receptor activity,GO:0070892~lipoteichoic acid receptor activity,GO:0071813~lipoprotein particle binding	hsa03320:PPAR signaling pathway,hsa04145:Phagosome,hsa04152:AMPK signaling pathway,hsa04512:ECM-receptor interaction,hsa04640:Hematopoietic cell lineage,hsa04920:Adipocytokine signaling pathway,hsa04931:Insulin resistance,hsa04975:Fat digestion and absorption,hsa05144:Malaria

OGN	-3.06	GO:0007409~axonogenesis,GO:0018146~keratan sulfate biosynthetic process,GO:0035385~Roundabout signaling pathway,GO:0042340~keratan sulfate catabolic process,GO:0048662~negative regulation of smooth muscle cell proliferation,GO:0048846~axon extension involved in axon guidance,GO:0050770~regulation of axonogenesis	GO:0005576~extracellular region,GO:0005578~proteinaceous extracellular matrix,GO:0005615~extracellular space,GO:0005783~endoplasmic reticulum,GO:0005796~Golgi lumen,GO:0031012~extracellular matrix,GO:0043202~lysosomal lumen,GO:0070062~extracellular exosome,GO:1903561~extracellular vesicle	GO:0005515~protein binding,GO:0008083~growth factor activity,GO:0008201~heparin binding,GO:0048495~Roundabout binding	
FABP4	-3.52	GO:0001816~cytokine production,GO:0006469~negative regulation of protein kinase activity,GO:0006810~transport,GO:0019433~triglyceride catabolic process,GO:0042632~cholesterol homeostasis,GO:0045892~negative regulation of transcription, DNA-templated,GO:0050727~regulation of inflammatory response,GO:0050729~positive regulation of inflammatory response,GO:0050872~white fat cell differentiation,GO:0050873~brown fat cell differentiation,GO:0071285~cellular response to lithium ion,GO:0071356~cellular response to tumor necrosis factor	GO:0005634~nucleus,GO:0005737~cytoplasm,GO:0005811~lipid particle,GO:0005829~cytosol,GO:0070062~extracellular exosome	GO:0005215~transporter activity,GO:0005504~fatty acid binding	hsa03320:PPAR signaling pathway,hsa04923:Regulation of lipolysis in adipocytes

ANEXO 1 – TERMO DE CONSENTIMENTO LIVRE E ESCLARECIDO

TERMO DE CONSENTIMENTO LIVRE E ESCLARECIDO

Concordo em participar livremente deste estudo, entendo que serei entrevistado e submetido a uma avaliação laboratorial. E, entendo que os riscos de minha participação nesta pesquisa são mínimos.

Entendo que minha participação é inteiramente voluntária, podendo me recusar a responder qualquer questão ou retirar o meu consentimento em participar neste estudo a qualquer hora, sem nenhum prejuízo ao meu tratamento atual ou futuro.

Eu,_____, após ter lido e entendido todas as informações e esclarecido todas as minhas dúvidas referentes a este estudo, concordo voluntariamente em participar do mesmo. Atesto também o recebimento das "Informações ao doador", necessário para a minha compreensão do estudo.

Data:____/____/_____

_____

Assinatura (do doador ou responsável) ou impressão datiloscópica

Eu, Prof. Dr. Iglenir João Cavalli, declaro que forneci todas as informações referentes ao estudo ao doador.

_____Data:____/____/_____

Prof. Dr. Iglenir João Cavalli